AN INVESTIGATION INTO THE THERMAL DEGRADATION OF

SEVERAL CHLORINATED POLYMER SYSTEMS AND POLY-

(ETHYLENE OXIDE) : SALT BLENDS.

By

EDITH JANE MILLAN

A Thesis for the Degree of

Doctor of Philosophy.

Supervisor: Dr. I.C. McNeill.

Chemistry Department
University of Glasgow.   April 1990.

To my Mother and Father,

with much gratitude.

"Man succeeded because the evolutionary processes which

moulded him developed four inter-related characteristics of

unestimable value : highly manipulative hands to fashion what

his structure lacks : a large and imaginative brain to devise

things for his hands to make : an insatiable curiosity to

explore, to question and to find out : and the power of speech

permitting easy transmission and collective accumulation of

knowledge and concepts".

Anon.

ACKNOWLEDGEMENTS.

SUMMARY

Polymer degradation is a complex branch of chemistry. A general outline of the major types of process which can occur during thermal decomposition is given in Chapter 1. In addition, a brief summary of the degradation of polymers in the presence of additives along with a more detailed acount of the decomposition of several chlorine-containing polymers are presented. The chapter concludes with a short section on the importance of polymer degradation.

The thermal analysis techniques employed in this research are described in depth in Chapter 2 together with the additional analytical methods used in identifying and quantifying degradation products.

The experimental work is described in Chapters 3, 4 and 5. Chapter 3 is concerned with the synthesis and thermal degradation of chlorinated poly(ethylene oxide). As a basis the decomposition of poly(ethylene oxide) (PEO) is first investigated and it is observed that the polymer thermally degrades in a random fashion, initiated by C-O and C-C bond scission, which yields a variety of degradation products. The synthesis of chlorinated poly(ethylene oxide) in both air and in an atmosphere of nitrogen are described. Chlorinated polymers can be obtained with chlorine contents 60.96% and 71.75% which correspond to the substitution of approximately 2 and 3 chlorine atoms respectively per ethylene oxide repeat unit. Degradation results show that chlorination destabilises poly(ethylene oxide) to heating. The mechanism of decomposition is similar to that for the unchlorinated polymer in that it is a

random process. Chlorine-containing compounds are produced including hydrogen chloride, phosgene and chlorinated acetyl chlorides. Quantitative analysis indicates that in trichlorinated poly(ethylene oxide) approximately one molecule of HCl is evolved per four monomer units and this figure is increased to roughly one molecule of HCl produced per three monomer units in dichlorinated poly(ethylene oxide). Chain fragments in both cases amount to about 60% by weight of products evolved.

Chapter 4 details the degradation of several chlorine-containing polystyrenes, in which the chlorine substituent is either on the ring or in the polymer backbone, and compares the results with those obtained for polystyrene. The position of chlorine within the macromolecule has a pronounced effect on the breakdown mechanism of the polymer. Poly-p-chlorostyrene and poly-o-chlorostyrene show similar thermal properties to polystyrene with depolymerisation being the major process occurring during degradation. In ring-chlorinated polystyrene however, the polymer is thermally destabilised and displays a two stage decomposition. These observations are attributed to a small amount of chain-chlorination which occurs simultaneously with ring-chlorination. Thus the initial degradation is due to the elimination of HCl which is followed subsequently by depolymerisation and chain transfer processes, which account for the bulk of the decomposition products. A destabilised two stage degradation is also observed with chain-chlorinated polystyrene (30.19% Cl). The two stage decomposition arises from dehydrochlorination, in which all available chlorine is

eliminated, and chain fragmentation.   It has also been possible to prepare chain-chlorinated polystyrenes with chlorine contents which correspond to an approximately di- and tri-substituted styrene unit (41.56% Cl and 49.07% Cl respectively). In these highly chlorinated polymers a two stage degradation is less easily distinguished.   However, increased yields of HCl (31.78%) and residual char (10.48%) are produced on decomposition.   To account for these observations, a mechanism is proposed in which, following HCl elimination from the polymer main-chain, dehydrochlorination continues via a cyclisation reaction involving the chlorinated polyene backbone and its phenyl side groups.   The second dehydrochlorination is favoured as it restores aromaticity.

The thermal degradation of several poly(ethylene oxide)-salt blends of low (10:1 EO:salt) and high (2:1 EO:salt) salt concentrations are discussed in Chapter 5.   The decomposition of PEO in the presence of some transition metal, alkaline earth and alkali metal salts is detailed. $ZnBr_2$, $CoBr_2$ and $CaBr_2$ reduce the thermal stability of PEO and dramatically alter the mechanism of degradation of PEO as seen by the multistage decomposition process (as opposed to the single stage in pure PEO) and the formation of additional degradation products.   The most significant of these new decomposition products is dioxane. Product distribution also changes during the various stages of degradation in hgih salt content blends, with dioxane production being a major process in the early stages of decomposition, but ceasing during the second stage of degradation.   In these blends the first decomposition stage is a result of the degradation

of PEO-salt complex and the second stage due to degradation of uncomplexed PEO. It is proposed that dioxane is produced as a direct consequence of the complexation between the cations and non-adjacent ether oxygen atoms, via a cyclisation reaction.

The presence of $ZnCl_2$ also destabilises PEO to heating and results in a two stage decomposition which is, however, rather different to that of the above blends producing unstable degradation products. The difference in decomposition behaviour of PEO-$ZnCl_2$ blends is attributed to a difference in complex structure in which Zn^{2+} is coordinated between two adjacent ether oxygen atoms.

NaSCN and $LiClO_4$ both thermally destabilise PEO. NaSCN-PEO blends show a single stage degradation at high salt content and evolve additional decomposition products (H_2S, HCN) whereas $LiClO_4$-PEO blends exhibit a two-stage degradation and produce decomposition products as for pure PEO.

ZnO and $CaCl_2$ were found to have no effect on the thermal degradation of PEO. On the other hand, NaBr has a slight stabilising influence.

The final chapter, Chapter 6, gives a summary of conclusions reached and mechanisms proposed during this research and ends with some suggestions for future work.

CONTENTS

CHAPTER ONE - INTRODUCTION

1.1 INTRODUCTION

Throughout the evolution of mankind, the significance of materials for human society is emphasised by the fact that the various ages of our history have been named after the material used at that time i.e:

The Stone Age

The Bronze Age and

The Iron Age

This trend has continued up to the present time whereupon we are now in the era of the "Polymer Age".

Although synthetic polymeric compounds were known about in the early nineteenth century[1], it was not until the 1930's that the science of high polymers began to emerge, and the major growth of polymer technology came even later. Before the beginning of World War II, relatively few such materials were available for the manufacture of articles required for a civilised life. The rapid increase in the range of manufactured products following World War II resulted directly from the development of a wide variety of polymers in the form of fibres, plastics, elastomers, adhesives and resins. The trend of replacing conventional materials with polymeric substitutes is still increasing and thus it is important to understand the chemical and physical properties of such macromolecules in order to tailor them to our needs. A major contribution to understanding is the science of polymer degradation.

1.2 Polymer Degradation.

Polymer degradation is the collective term used to describe various processes which cause a deterioration in the physical or chemical properties of polymers or their outward appearance. These reactions may be induced by a variety of energy transfer agencies including heat, light, radiation and mechanical impact in addition to chemical attack. Degradation may occur during every phase of the life of a polymer i.e. during its synthesis, processing, fabrication and use. All of the bonds in a polymer molecule may be sites for polymer degradation. The bond energies are manifold and depend not only on the type of atoms connected by the bond but also on the chemical and physical environment surrounding the bond. Tertiary and allylic bonds are usually weaker than primary or secondary ones. In polymers containing only primary or secondary carbon atoms such as PVC, the presence of such bonds is undesirable as they form weak sites which are very readily attacked. These bonds may be formed during polymerisation and processing. The method of polymerisation can be of vital importance in the avoidance of such weak links. A polymer prepared by radical initiated polymerisation may be more prone to degradation than if prepared by ionic means due to the termination steps in radical polymerisation for example disproportionation, producing an unsaturated end group or head-to-head combination which may result in a site of weakness. Therefore, the main factor affecting polymer stability is the dissociation energy of the various bonds in the polymer which, in common polymers, range from[2] around 65 k cal mol^{-1} (C-Cl) to 108 k cal mole^{-1} (C-F) the C-C bond energy range being intermediate at 75-85 k cal mol^{-1}. Thermal

degradation begins with the scission of the weakest bond present.

The initial step then usually determines the course of the

degradation process. Other components of the chemical structure

such as steric factors, stability of the intermediates, or the

possibility of their resonance stabilisation, may also have great

influence on the degradation.

1.2.1 Classification of Polymer Degradation.

Classification of polymer degradation can be based upon the

main factors responsible for degradation, e.g. thermal, photo,

radiation, biological, chemical or mechanical degradation.

Alternatively, the major processes occurring during degradation may be

used as a classification system. This includes random main chain

scission, depolymerisation, cross-linking, substituent elimination and

substituent cyclisation reactions. As the aim of this work is to

investigate the thermal degradation of certain polymer systems, the

possible processes taking place during thermal degradation are

detailed below.

The thermal degradation of polymers may be broadly divided into

two classes[3] - namely main chain scission and substituent reactions.

1) Main chain scission - is characterised by the cleavage of a bond in

the polymer backbone resulting in the formation of macroradicals

containing distinguishable monomer units.

$$\text{\textasciitilde CH}_2 - \overset{\displaystyle X}{\underset{\displaystyle Y}{C}} - CH_2 - \overset{\displaystyle X}{\underset{\displaystyle Y}{C}} - \text{\textasciitilde} \quad \xrightarrow[\text{scission}]{\text{C-C}} \quad \text{\textasciitilde} CH_2 - \overset{\displaystyle X}{\underset{\displaystyle Y}{C}}\cdot + \cdot CH_2 - \overset{\displaystyle X}{\underset{\displaystyle Y}{C}} - \text{\textasciitilde}$$
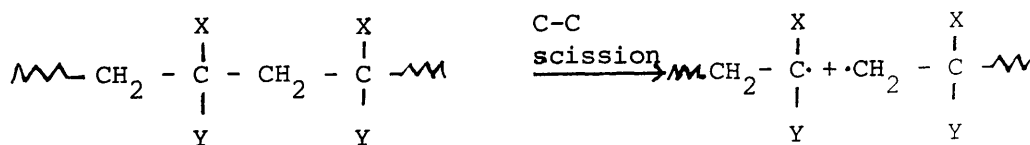
The macroradicals may then undergo a number of reactions which include "random" degradation processes and ordered depolymerisation reactions. It should be noted that in this context the word "random" is of rather loose definition as in all degradation processes the decomposition is defined, as previously described, by bond strength and/or environment. Thus, the use of the terms is as follows:

a) Random degradation processes - in these types of reactions a wide range of chain fragments of different lengths may be produced. This is the case in the degradation of polyethylene. The macroradicals formed participate in hydrogen abstraction or disproportionation reactions yielding hydrocarbon chain fragments having 1 to 70 carbon atoms.[3]

b) Depolymerisation - this, in essence, is a reversal of polymerisation resulting in monomer formation. Depolymerisation is favoured if the substituents X and Y on the polymer are capable of stabilising the intermediate radical produced. This can be done by an electron withdrawing effect, as is seen in polystyrene (X = H, Y = Ph), or by means of steric crowding observed in poly(methyl methacrylate) (X = CH_3, Y = $COOCH_3$). Poly(methyl methacrylate) degrades via a depolymerisation reaction, "unzipping" to produce almost 100% yields of methyl methacrylate.[4] The depolymerisation of polystyrene, however, is not so simple due to the presence of an active α-hydrogen atom. These easily undergo hydrogen abstraction by macroradicals in an intramolecular "back-biting" reaction producing dimer, trimer, tetramer and pentamer (see Chapter 4). This "unbuttoning" of oligomeric fragments is in competition with the depolymerisation process and thus the monomer yield from polystyrene is considerably

less than 100%.   If the α-hydrogen is replaced with a methyl group as in poly(α-methyl styrene) monomer yield increases to approximately 100%.[5]

2) <u>Substituent reactions</u> - these will occur as dominating processes in a polymer system only if they can be initiated at temperatures lower than that at which main chain scission takes place.   Thus substituent reactions are normally observed at relatively low temperatures (i.e. < 250°C).   These substituent reactions can be classified into three main groups:

a) Elimination - the classic example of an elimination reaction is the dehydrochlorination of poly(vinyl chloride).

$$\text{\textasciitilde}\underset{H}{\overset{H}{C}} - \underset{H}{\overset{Cl}{C}} - \underset{H}{\overset{H}{C}} - \underset{H}{\overset{Cl}{C}} \text{\textasciitilde} \quad \xrightarrow[\text{elimination}]{\text{HCl}} \quad \text{\textasciitilde} CH = CH - CH = CH \text{\textasciitilde}$$
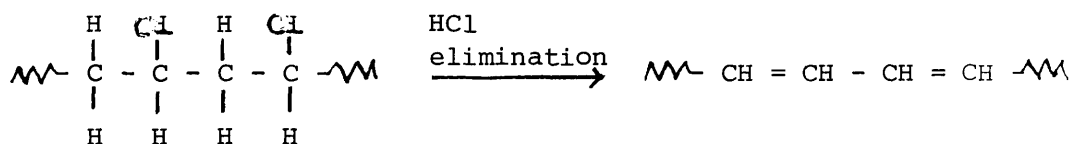
The mechanism of elimination of HCl however, even after extensive research,[6,7] is still a matter of controversy although there is a general consensus over the major features.   The details of the thermal degradation of PVC are discussed later in this chapter.

b) Cyclisation - reactions which result in the formation of cyclic structures being incorporated into the polymer backbone may occur between adjacent substituent groups along the polymer chain.   These reactions can be associated with the elimination of small, volatile,

molecules although this is not always the case.   Polyacrylonitrile

for example, begins to discolour at 150°C,[8] due to conjugation

arising from the polymerisation of sequences of neighbouring nitrile

groups.
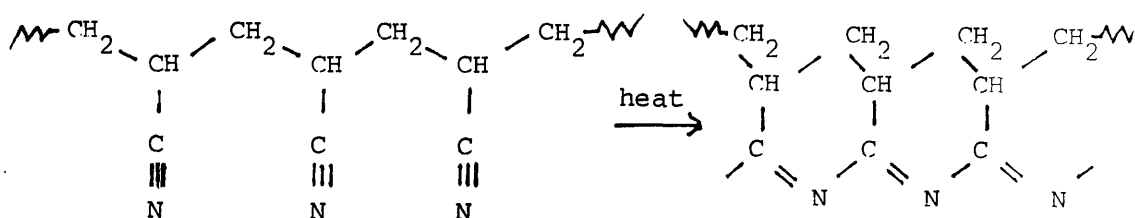
This reaction is of practical importance in the formation of carbon

fibres.   In contrast, poly(methacrylic acid) on heating between

$200-300^{\circ}$C cyclises via an intramolecular dehydration reaction forming

anhydride rings[9] with the elimination of water.
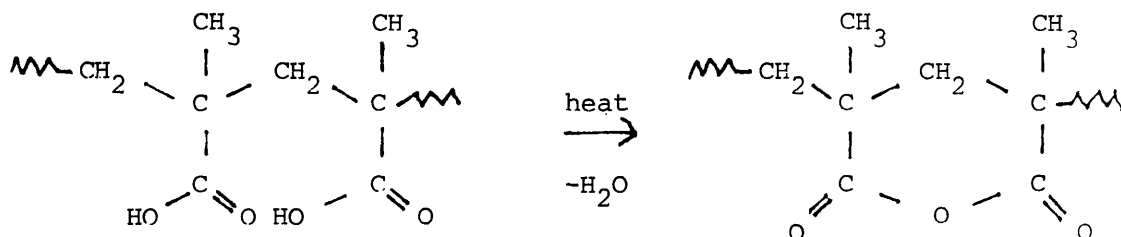
Intermolecular dehydration may also occur resulting in cross-linking

between polymer chains.

c) Ester decomposition – these reactions result in the formation of a carboxylic acid and an alkene.   Depending on polymer structure, the alkene may be liberated and the acid left as repeat units in the polymer chain backbone or the acid may be evolved and olefinic double bonds appear in the polymer backbone.   The former example is typified by the thermal degradation of poly(t-butyl methacrylate).   The intramolecular mechanism involved[9] is via an interaction between the carbonyl group and a hydrogen atom on the β-carbon atom of the ester group.
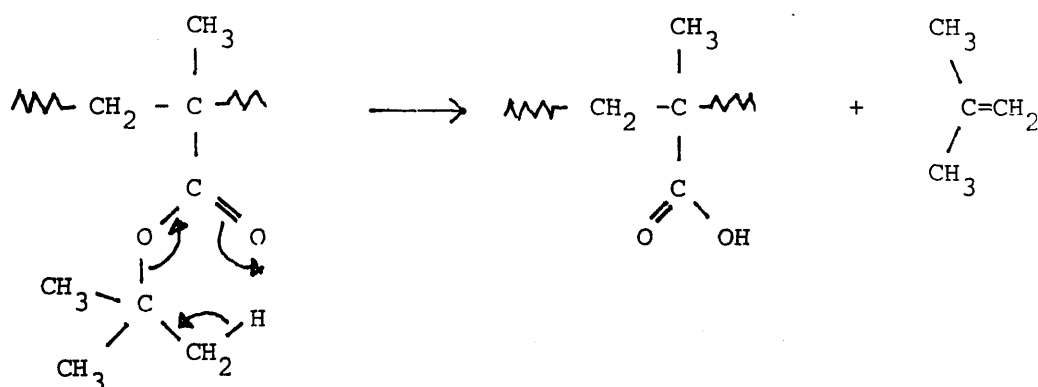
The reaction is favoured by the labile hydrogen atom and the formation of a stable six membered ring intermediate.

Poly(vinyl esters) for example poly(vinyl acetate) also exhibit ester decomposition.   However in this class of compound, carboxylic acid is released and the alkene double bond forms the polymer backbone.[10]

$$\sim\!\!\sim\!\!CH - CH\!\!\sim\!\!\sim \qquad\qquad \sim\!\!\sim\!\!CH = CH\!\!\sim\!\!\sim$$

$$\begin{array}{c} O \quad\; H \\ | \\ CH_3 - C = O \end{array} \xrightarrow{\text{heat}} \begin{array}{c} + \\ CH_3 - C \underset{OH}{\overset{O}{<\!\!\!<}} \end{array}$$
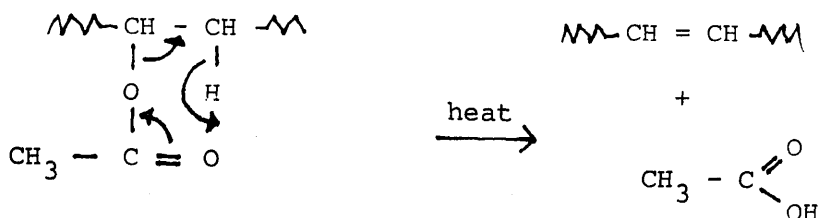
Once initiated by the scission of a C-O bond and consequently the removal of a carboxylic acid molecule, the process is activated by the formation of double bonds resulting in a conjugated polyene sequence.

Although the variety of substituents incorporated into polymers results in an equal variety of reaction mechanisms there are features which substituent reactions have in common. They often occur at temperatures below those of which depolymerisation begins.   If allowed to continue to a marked degree they will inhibit depolymerisation due to the formation of structures which prevent depropagation.   This results in products being structurally dissimilar to the parent polymer. Conjugated unsaturated structures frequently lead to colouration of higher long chain fragment degradation products and residue. At higher temperatures (i.e. $> 500^{\circ}C$), the final product is usually a carbonaceous residue similar to graphite and arises from the dehydrogenation of the initially formed cyclic or cross-linked structures which have not completely volatilised.

1.3 DEGRADATION OF POLYMERS IN THE PRESENCE OF ADDITIVES

In order to expand the range of useful polymeric materials the chemical and physical properties of polymers can be modified by the use of additives. These additives can take a wide variety of forms ranging from organic polymers to small inorganic compounds. In the field of commercial plastics, polymers are commonly blended with plasticisers, stabilisers, fillers and reinforcing agents. Thus it is of importance to have some insight into the effects of additives on the degradation of the associated polymer.

As there is a wide range of additive types, for the purpose of this general introduction the degradation of polymer-additive systems is reviewed in three classes - binary polymer blends, fire-retardent compounds and polymer-salt blends.

1.3.1 Binary Polymer Blends.

Binary polymer blends form almost exclusively heterogeneous mixtures. Such blends can be envisaged as consisting of a continuous phase of one polymer into which is dispersed the other polymer so that there exist domains of a single pure polymer separated from the domains of the second polymer by a phase boundary. As a result of the two-phase nature of the polymer blend system, the possible interactions which may occur during degradation can be grouped as either reactions which occur in the bulk of either domain or else reactions occurring at phase boundaries. The probability of bulk reactions taking place within a polymer phase will be much greater than that for reactions across a boundary surface because the surface to volume ratio is small. Six processes[11] appear

to be feasible.   The possible interactions occurring in bulk
are:

       small molecule + macromolecule

       small radical + macromolecule

       small molecule + macroradical

       2 small molecules (product interaction)

while those occurring at phase boundaries include:

       macroradical + macromolecule

       2 macromolecules

       Investigations into the thermal degradation of several
polymer blend systems over the last twenty years, and in particular
work carried out in the laboratories at the University of Glasgow,
have enabled some general patterns of behaviour to be distinguished.
In some cases it has been shown that the interaction processes
occurring result in destabilisation of either or both of the polymeric
components while in other cases blending improves thermal stability.
The three major polymers which have been studied are polystyrene (PS),
poly(vinyl chloride) (PVC) and poly(methyl methacrylate) (PMMA).
Some examples of the effect of different polymeric environments on
the degradation behaviour of these polymers are detailed below:

a) PS Blends

i) PS-Poly(α-methyl styrene) and PS-Polyoxyethylene glycol.

       Richards and Satter[12] observed that styrene in the presence
of P$_A$MS produced significant amounts of styrene at temperatures where
monomer production from pure PS is negligable (i.e. between 260° and
280^OC).   It was also noted that styrene evolution increased as the
molecular weight of PAMS used was decreased.   The destabilising

effect of PAMS can be explained by the monomer radicals produced in the depolymerisation of PAMS chains migrating into the PS phase and abstracting tertiary hydrogen atoms.   Consequent chain scission may result in polystyryl radical formation which can then give rise to styrene monomer.   The molecular weight effect of PAMS on styrene production can be accounted for by the fact that the lower the molecular weight of PAMS, the higher will be the concentration of PAMS monomer radicals in the sample available for the initiation of PS chain scission.

A similar destabilising effect is seen in PS-POEG blends.[13] When PS was heated isothermally along with low molecular weight POEG (mwt = 4000) at higher temperatures (350°-385°C), the degradation of PS accelerated as POEG concentration and temperature increased.   POEG degrades initially under these conditions via random chain scission generating small POEG radicals which are capable of diffusing into the PS zone and abstracting active hydrogen atoms initiating chain scission followed by styrene formation in a similar fashion to the scheme proposed by Richards and Satter for PS-PAMS blends.   The mechanism for the radical induced degradation in PS-POEG blends is illustrated below:

$$\sim O - CH_2-CH_2 - O - CH_2-CH_2 \sim \xrightarrow[\text{scission}]{\text{chain}} \sim O - CH_2-\dot{C}H_2 + \dot{O}-CH_2-CH_2\sim$$

i) H abstraction
ii) PS scission

$$\sim O - CH_2-\dot{C}H_2$$

or

$$\sim CH_2-CH_2-\dot{O}$$

$$+ \sim CH_2 - \overset{\overset{\displaystyle H}{|}}{C} - CH_2-CH-CH_2\sim \longrightarrow \sim CH_2 - \overset{+}{C} = CH_2 + \dot{C}H-CH_2\sim$$

$$\sim CH_2-CH_2-OH$$
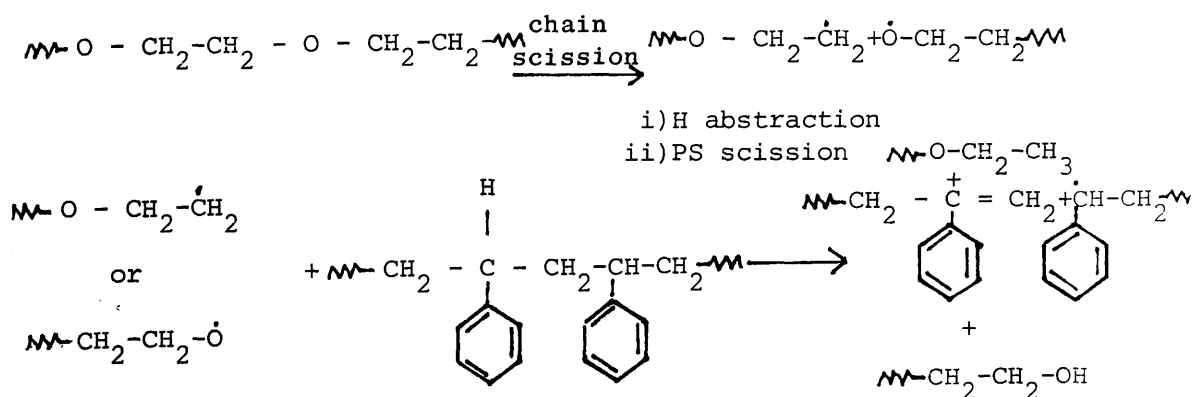
ii) PS-Poly(vinyl chloride), PS-Poly(vinyl acetate) and PS-Polyacrylonitrile.

When PS-PVC[14] or PS-PVA[15] blends are degraded two affects are noted on the degradation of PS. Firstly PS undergoes more rapid chain scission resulting in a drop in molecular weight and secondly the evolution of styrene occurs at slightly higher temperatures indicating a stabilising effect on PS volatilisation. The fall in molecular weight may be explained by small radicals (Cl$\cdot$ or CH$_3$COO$\cdot$) diffusing across the phase boundary into the PS phase to participate in initiating chain scission as in the previous examples. In contrast to the small radical - macromolecule interactions, the stabilisation in styrene formation is thought to arise from macroradical-macromolecule interactions occurring at phase boundaries (unless the "macro" radical is small enough to diffuse into the second polymer phase). The macro-molecules involved are the conjugated polyene residues from PVC or PVA degradation. Their function is that of radical scavengers.

When PS-PAN blends are degraded, the stabilisation of PS is easily observed from thermal volatilisation analysis (TVA) studies[16]. The conjugated nitrile oligomer structure obtained from the decomposition of PAN acts as a scavenger for PS radicals. In contrast to the above cases, however, PAN does not provide radical species on degradation which could initiate chain scission in the PS phase and thus the rate of chain scission is reduced.

iii) PS - Poly(Methyl methacrylate)

This is an example in which the degradation of either polymer has no apparant effect on the degradation of the other.

b) <u>PVC Blends</u>.

i) PVC - Poly(vinyl acetate) and PVC - Alloprene.

The major degradation products from PVC and PVA are HCl and acetic acid respectively.   The dehydrochlorination of PVC occurs at lower temperatures than the deacetylation of PVA.   When PVC is degraded in the presence of PVA,   acetic acid production begins coincidently with the formation of HCl.   The HCl evolution however occurs at slightly lower temperatures than observed for pure PVC indicating that both polymers are destabilised.   This destabilisation is brought about by acid catalysis.   HCl from the initial PVC degradation diffuses into the PVA phase to catalyse loss of acetic acid.   The acetic acid produced then diffuses into the PVC phase to catalyse loss of HCl.   The reactions continue due to allylic activation by double bond formation.   The acid catalysis mechanisms are illustrated below:
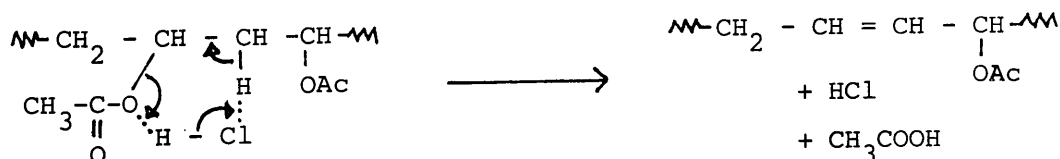
and
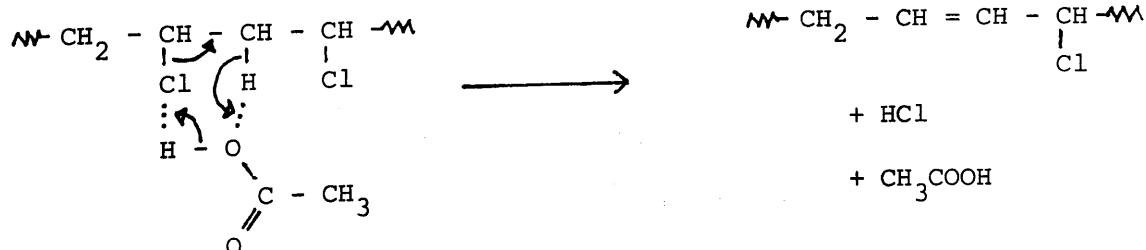
Both mechanisms are similar to that proposed by Braun and Bender[18] for the autocatalysis in the degradation of PVC, although it is also possible that small radical species may be involved in the decomposition process.

Radiotracer degradation experiments involving labelled PVC - Alloprene(commercial chlorinated natural rubber) blends[19] reveal a similar destabilisation in PVC, presumably catalysed by HCl evolved from the thermally less stable Alloprene.

ii)   PVC-Poly(methyl acrylate), PVC-Poly(methyl methacrylate), PVC-Polystyrene and PVC-Poly(α-methyl styrene).

TVA experiments have shown that in the presence of PMA, PMMA PS and PAMS, PVC is stabilised.[16]   Chain scission occurs in the accompanying polymers which may be followed by their depolymerisation. These observations are accounted for by the following explanation. Cl· radicals evolved on the degradation of PVC migrate to the second polymer phase where they initiate chain scission by means of H abstraction.   The diffusion of some Cl· radicals from the PVC phase results, however, in them not being available to participate in the dehydrochlorination of PVC, thus PVC is stabilised.

iii) PVC - Polyacrylamide and PVC - Poly(n-butyl methacrylamide).

PAM and PBMAM decompose at low temperatures (approximately 240°C) evolving ammonia and butylamine respectively.   As a result of this, when mixtures of PVC with these polymers are degraded PVC is destabilised.   This destabilisation is brought about by the diffusion of ammonia or butylamine into the PVC phase and initiates HCl elimination.   Product interaction is also observed in these systems as ammonium chloride and butylamine hydrochloride are

formed.

iv) PVC - Polyacrylonitrile

On heating PVC with PAN[16] it is seen that PVC is destabilised. It has been proposed[16] that in this case destabilisation is due to physical effects rather than chemical ones. The physical state of the blend hinders HCl release thereby increasing the importance of autocatalysis.

c) PMMA Blends.

i) PMMA - Poly(vinyl chloride) and PMMA - Poly(vinyl acetate)

When blends of PMMA with PVC are degraded two effects on the production of MMA monomer are apparent[20] - the earlier production of MMA monomer (approximately $100^{\circ}C$ lower than in pure MMA) which occurs simultaneously with the dehydrogenation of PVC and the evolution of MMA monomer $30^{\circ}C$ higher than for PMMA alone. Therefore PVC has both a destabilising and stabilising affect on PMMA. This is explained[21] by two interactive processes. The first is the attack on PMMA by Cl· radicals, produced on PVC degradation, initiating chain scission and unzipping of monomer. The second process is the reaction of HCl with pendant ester groups. This results in the formation of anhydride rings which act as blocking groups reducing the zip length of depolymerisation and thus destabilising the chain. Similar affects are noted in PMMA-PVA blends[22] however the destabilisation is less effective as PVA is more stable than PVC.

ii) PMMA - Polyacrylonitrile

PMMA is stabilised when heated in the presence of PAN.[23] The ammonia released on the degradation of PAN reacts with the

ester groups in PMMA to produce cyclic structures which block depolymerisation thus stabilising the polymer.

1.3.2 FIRE-RETARDANT COMPOUNDS.

The science of fire-retardants in polymers is an extremely complex field.   A variety of commercial fire-retardant chemicals are available which may function in a number of ways.   In order to understand these processes it is first necessary to have some insight into the events which occur during the combustion of a polymer.   The combustion of a polymer, or any solid, can be described by two consecutive chemical processes - decomposition and combustion.   On the addition of heat to a polymer, the polymer decomposes and any resultant flammable degradation products on entering the flame zone, undergo combustion to form combustion products with the simultaneous evolution of heat.   Part of this heat reaches the polymer surface and can initiate further degradation thus yielding more combustible products.   This series of events is known as the combustion cycle and is illustrated below:

$$\text{polymer + heat} \xrightarrow[\text{degradation}]{\text{thermal}} \text{degradation products}$$

flame + O_2

combustion products

+

heat transfer   heat
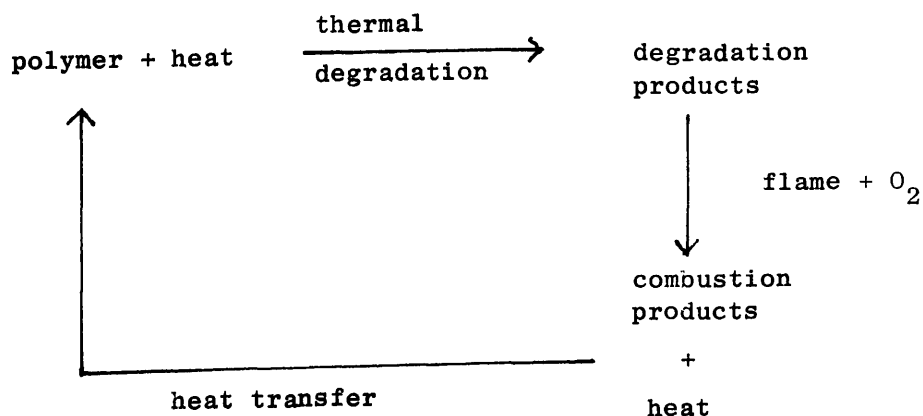
Scheme : Combustion Cycle of a Polymer (adapted from reference 24).

In addition to the fire hazard induced by the flammability of products evolved and the rate and amount of heat released during decomposition, there is also a health hazard which results from smoke generation.   It has been shown, however, that as the amount of char after combustion increases, the level of smoke production should decrease.[25]

In a fire retarded polymer composition, the combustion cycle must be interrupted at some stage.   This may be achieved by one or more of the following:

i) altering the decomposition of the polymer to produce less flammable degradation products.

ii) interfering with flame reactions.

iii) reducing thermal feedback to the polymer.

Many, if not most, fire retardants may function simultaneously by several different mechanisms which also can depend on the nature of the substrate polymers.   Thus it is more systematic to deal with individual classes of additive, according to the principal element they contain, and explain their mode of action rather than to discuss in depth the different mechanisms by which a fire retardant may operate.   However, some examples to demonstrate the types of interaction encountered are given in this section.

The major elements used in fire retardants are aluminium and boron (Group III), phosphorous and antimony (Group V) and chlorine and bromine (Group VII).   They may be incorporated into

fire retardant polymer compositions either as additives or reactives.   Additive fire retardants are compounds which are physically mixed with the polymer.   This is distinct from reactive fire retardants which are chemically bound to the polymer forming an integral part of the repeating structural unit.

More than one fire retardant may be used in a polymer system.   When the combined effect of two or more fire retardants is greater than the sum of the effects of each of the individual compounds, synergism is said to occur.   This is commonly found in phosphorous-halogen compounds and for this reason halogenated compounds are usually used in combination with antimony oxide.

a) Aluminium and Boron

Alumina trihydrate (ATH) at present is the compound used in greatest quantities[26] as a fire retardant for organic polymers. ATH is added to polymers as an inert filler.   It owes its fire retardant properties to a number of factors.   Firstly, ATH is a heat sink absorbing thermal energy from the flame due to its high heat capacity, so reducing heat transfer back to the polymer.   In addition, its decomposition to anhydrous alumina is endothermic. Furthermore, the water of hydration evolved acts as an inert dilutent for the flammable polymer degradation products and also cools the flame.   Finally the alumina residue acts as a protective covering on the surface of the polymer.   Thus $Al_2O_3.3H_2O$ is a very effective fire retardant.   One disadvantage is however that relatively high loadings[27] of ATH are required in order for it to function as a satisfactory fire retardant.   This restricts its

use to polymer systems, such as carpet upholstery back coatings which will not chemically or physically deteriorate at such high filler concentrations.

Boron containing compounds used in fire retardants include boric acid and hydrated boric salts.   These are frequently used together as mixtures of boric acid and borax $(Na_2B_4O_7.10H_2O)$. The mode of action in this case is fourfold:

i) the formation of inorganic glassy deposits on the surface of the polymer which may act as intumescent coatings.

ii) the promotion of char formation with hydroxylated polymers, due to the formation of borate esters, rather than the production of flammable gaseous products.

iii) the liberation of water from hydrated compounds and/or ammonia from ammonium borates which act both as a heat sink and as a dilutent in the gas phase of the combustable fuel.

iv) the chemical inhibition by free-radical scavengers of oxidation reactions at the gas-solid interface.

b) <u>Phosphorous and Antimony</u>.

Phosphorous containing fire retardants are associated with changing the thermal degradation processes in polymers.   An example of this is the effect of ammonium polyphosphate (APP) on the thermal degradation of polyurethanes[28].   The factor responsible for the alteration in decomposition mechanism is the reaction of the polyurethane with polyphosphoric acid (PPA) which is formed by the elimination of ammonia and water from APP at temperatures below degradation threshold of the polymer.   The

acid catalysed reaction results in the formation of less flammable volatile products and more char. This char will serve to protect underlying polymer. Similar observations are seen in APP-polyether-urethane blends.[29,30]

When APP is blended with PMMA, the degradation mechanism of PMMA is greatly altered. Once more PPA is involved and its interaction with PMMA produces cyclic anhydride structures which restrict the normal depolymerisation process of PMMA, reducing the yield of the monomer, and allow chain scission and fragmentation reactions to compete effectively.[31]

c) **Chlorine and Bromine**

Chlorine containing compounds are well known as fire retardants both as additives and reactives. Additives may be introduced using chlorinated compounds such as chlorinated high molecular weight paraffins (chlorinated wax) or hexachlorocyclo-pentadiene derivatives.[32] Alternatively, chlorine may be incorporated into the structure of the polymer either by copolymerisation of monomers including chlorostyrene, chlorinated alkenes and chlorinated oligomers such as chlorinated ethers[3] or by direct substitution of hydrogen atoms by chlorine in an existing polymer. The latter reactions include the formation of chlorinated PVC and chlorinated polyethylene.

Due to the different methods of including chlorine as a fire retardant, the fire retardant may operate in a variety of ways. Chlorine, when introduced as an integral part of the

polymer structure will directly affect the products and rate of the thermal degradation of the polymer. Although less is understood about the mode of interaction of chlorinated additives, what is clear is that both type of fire retardant compound evolve HCl, either on decomposition of the retardant or on its interaction with the polymer. This HCl then may enter the flame where complex free radical reactions occur. The HCl serves to quench the major primary reactions responsible for propagating combustion within the flame : the oxidation of hydrogen radicals which produces more highly reactive radicals, and the oxidation of carbon monoxide to carbon dioxide which is an extermely exothermic reaction.

These reactions are reproduced[3] below:

$$H\cdot + O_2 \longrightarrow \cdot OH + \cdot O\cdot$$

$$\cdot OH + CO \longrightarrow \cdot H + CO_2$$
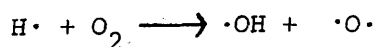
In the presence of HCl, however, the following reactions occur:

$$\cdot H + HCl \longrightarrow H_2 + Cl\cdot$$

$$\cdot OH + HCl \longrightarrow H_2O + Cl\cdot$$
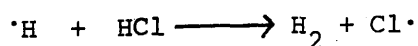
Thus less reactive Cl· radicals are generated which eventually reform HCl.

Bromine containing fire retardants function in an analogous manner liberating HBr. Nevertheless, bromine is much more effective than chlorine as a fire retarding element in both additives and reactives. Bromine-containing additives[3] in general are

aromatic and include compounds such as brominated biphenyls and biphenyl ethers. Brominated m°nomers may be used as reactives[3] in several polymer systems. In the preparation of poly(ethylene teraphthalate), for example, tetrabromophthalic acid and a suitable brominated diol can partially replace teraphthalic acid and ethylene glycol. Another example is the copolymerisation of brominated acrylic monomers such as 2-bromoethyl methacrylate to permit the introduction of bromine into acrylic polymers.

1.3.3 POLYMER-SALT BLENDS

Previous investigations into the thermal degradation of polymer-salt blends have concentrated on polymers having structures which contain pendent groups. Investigations into the thermal decomposition of poly(methylacrylate) (PMA) and of methylacrylate-methylmethacrylate (MA-MMA) copolymers in the presence of zinc chloride indicate the formation of degradation products not associated with the pure polymer and an alteration in product distribution when common products are evolved. Kochneva et al[33] studying $ZnCl_2$-PMA blends found that $ZnCl_2$ affects both free-radical stages in the degradation of PMA producing methanol and hydrogen as a result of the formation of a complex between $ZnCl_2$ and the ester carbonyl group of PMA. $ZnCl_2$ also alters the degradation mechanism of MA-MMA copolymers. Kopylova and co-workers[34] discovered that in the presence of $ZnCl_2$ methanol, carbon dioxide, carbon monoxide and water production are increased whilst the formation of MA and MMA is decreased relative to the decomposition of the pure copolymer.

Jamieson[35] reviewing the thermal degradation behaviour of several polymer systems containing silver acetate demonstrated that the presence of AgAc can result in various effects, of different extent, on the decomposition of the polymer. In PMMA-AgAc blends[36], the depolymerisation of PMMA is greatly increased due to an interaction between the polymer and salt during degradation. Results for blends in the ratio 10:1 by weight of polymer to acetate demonstrate most clearly the effect of AgAc in inducing early decomposition of the polymer. During the degradation of AgAc the major volatile products evolved are acetic acid, acetic anhydride, water, CO_2 and ketene. These are produced following the formation of free radical intermediates which initiate rapid depolymerisation of PMMA in the polymer-salt blends. A suggested mechanism is that of radical attack at the carbonyl group of the methacrylate ester forming an unsaturated chain end and a macroradical which can readily undergo depolymerisation.

A similar process is observed in poly(n-butyl methacrylate)-AgAc blends[35] although to a lesser extent. This mechanism also holds for poly(vinyl acetate)-AgAc mixtures as an increase in the rate of deacetylation is noted as is the greater production of highly volatile products from the decomposition of the resultant polyene residue. In contrast, the depolymerisation of PS and PAMS and, the dehydrochlorination of PVC and Alloprene are unaffected by AgAc.

Investigations into the thermal degradation of PMMA-$ZnBr_2$ and PVA-$ZnBr_2$ blends by McGuiness[37] revealed that the additive has a profound effect on the thermal decomposition of the polymer involved.

In PMMA-ZnBr$_2$ blends, the effect of ZnBr$_2$ on the degradation of PMMA, through the formation of a co-ordination complex is to weaken bonds in the MMA unit which would not normally break resulting in products other than those from pure PMMA. The complex formation involves the zinc atom coordinating to the lone pairs of electrons on the oxygen carbonyl of adjacent ester groups resulting in a 2:1 monomer: salt complex. Alternatively, each ester group can act as a bidentate ligand.
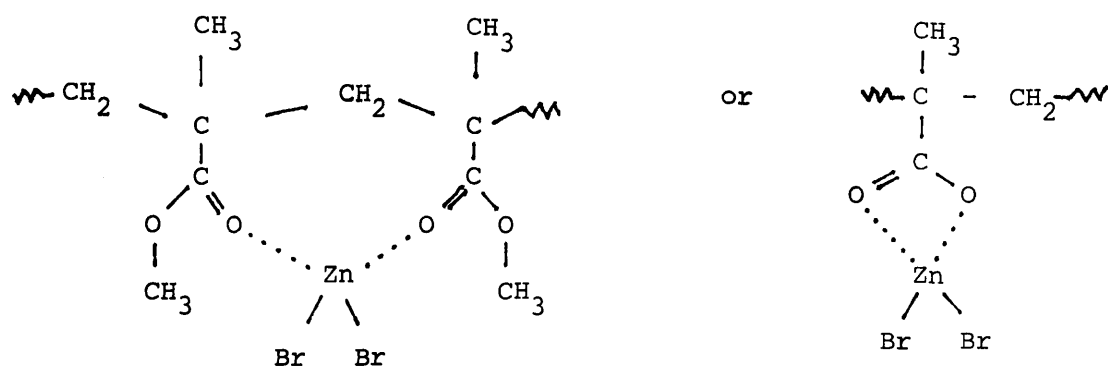
The decomposition occurs in three stages. The first of these consists of a number of competing reactions which result in the formation of organic salt and anhydride structures. At this point there is the simultaneous evolution of small volatile molecules including carbon monoxide, bromomethane and methanol. The second stage in the blend degradation arises from the decomposition of anhydride rings formed in the first stage accompanied by the degradation of any uncomplexed monomer units. Depolymerisation of regions of any uncoordinated polymer chains also may occur. The main process occuring in the final stage is the decomposition of organic salt units. The residue, consisting of polymeric sequencies of conjugated double bonds or possible cross-linked sections, also

breaks down at this stage.

Similar complexes between PVA and $ZnBr_2$ in PVA-$ZnBr_2$ blends are formed.   The effect of $ZnBr_2$ on the thermal degradation of PVA is to lower the activation energy for acetic acid production.

More recently,[38] a detailed study has been carried out by Liggat into the effect of transition metal chelates on the thermal degradation of a number of polymer and copolymer systems.   It was observed that in contrast to the TVA behaviour of poly(methyl methacrylate)(PMMA) alone, Co(acac)$_3$-PMMA blends have two degradation steps below 200°C.   These result from the decomposition of the chelate:

$$Co(acac)_3 \longrightarrow Co(acac)_2 + acac\cdot$$
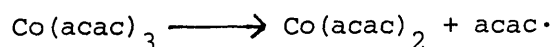
The first degradation peak (with maximum at approximately 135°C) arises from the decomposition of the π-type complex formed between Co(acac)$_3$ and the unsaturated sites at the chain-ends.   The complex may decompose in such a way as to (a) generate a macroradical and Co(acac)$_2$ or (b) maintain unsaturated chain ends and produce acac$\cdot$radical plus Co(acac)$_2$.   This is illustrated below:
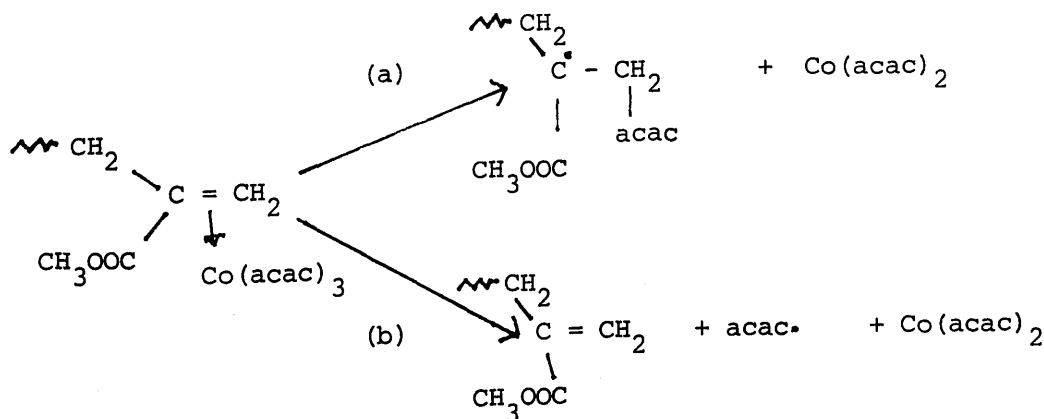
In reaction (a) depolymerisation of the macroradical leads to the loss of unsaturated sites as shown in reaction (c). Alternatively the acac. radical formed in reaction (b) can abstract a hydrogen atom from the polymer backbone to regenerate acetylacetone. This process (illustrated in reaction (d)) not only preserves the original unsaturated chain-ends but generates more in addition to forming depolymerisable macroradicals.
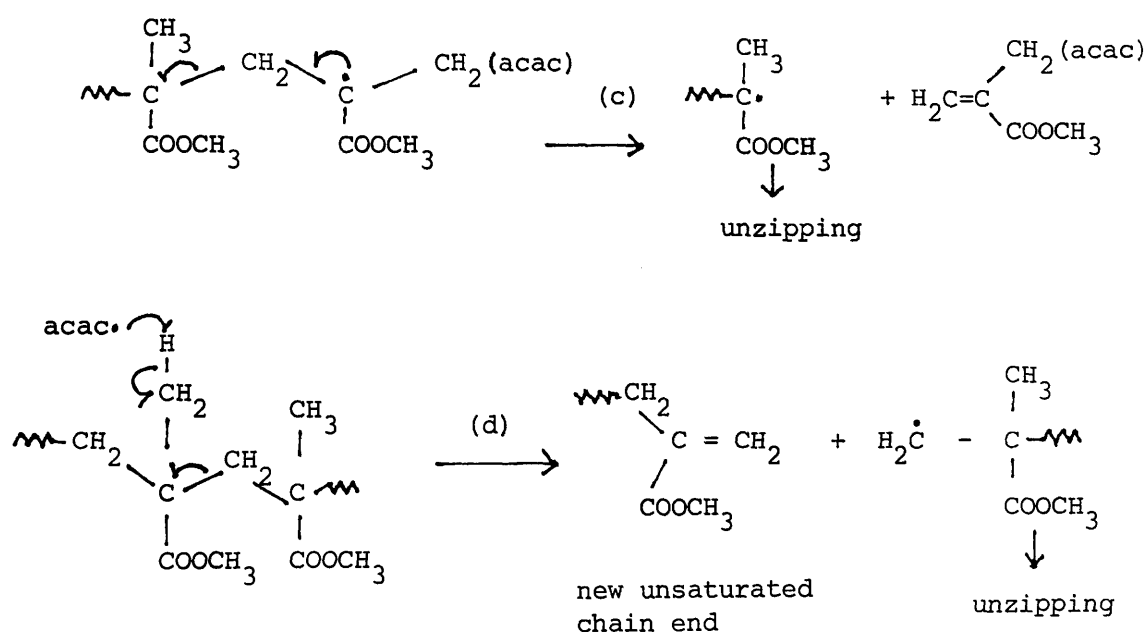
The evidence from TVA experiments indicates that routes (a)/(c) and (b)/(d) both occur.

The second decomposition peak results from the normal decomposition of the $Co(acac)_3$ dispersed throughout the remainder of the polymer matrix. The acac. radical generated leads to the production of monomer as described for the first degradation peak. Furthermore, $Co(acac)_2$ produced complexes with the ester groups and induces side chain scission and double bond formation.

The major peak in the TVA trace is obtained above $220^{\circ}C$. The degradation in this temperature region is characterised by the formation of cobalt carboxylate and anhydride structures which act to block and thus reduce the depolymerisation process.   The carboxylate structures are formed in the following reaction:
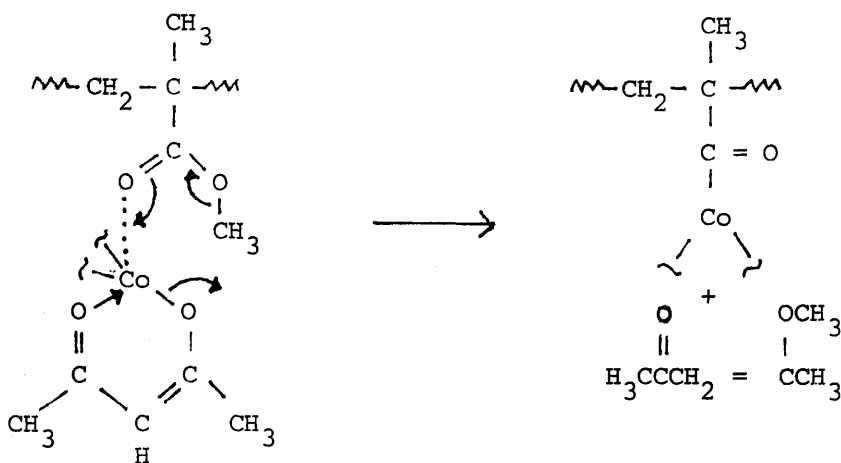
If this reaction is repeated then polymer chains may become crosslinked by cobalt dicarboxylate bridges.

Anhydride structures are produced from the attack on pendant ester groups by a small radical R.   The anhydride cyclisation process is illustrated below:
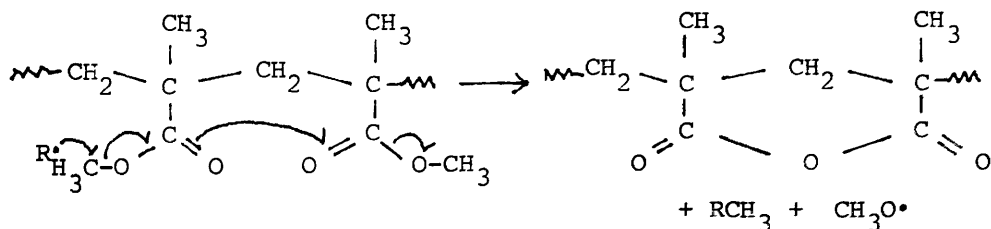
Three radicals initiate the formation of anhydride rings. $CH_3\overset{\bullet}{C}O$ produced on the decomposition of $Co(acac)_3$, produces acetone as the major by-product (RCH_3) in the above reaction.   Similar minor

reactions are observed with $CH_3O\overset{\bullet}{C}O$ and $CH_3O\bullet$ radicals which produce methyl acetate and dimethyl ether respectively as the by-product.

The final process which occurs in the degradation of $Co(acac)_3$-PMMA blends is fragmentation of the above structures in the polymer backbone and remaining polymer chains.

Investigations into $Mn(acac)_3$-PMMA blends show an additional third low temperature (i.e. $< 250^\circ C$) decomposition step, which can be accounted for by $Mn(acac)_3$ being able to associate with both unsaturated chain ends and ester groups of the polymer at room temperature whereas $Co(acac)_3$ only forms a complex with the unsaturated groups under the same conditions. The processes occuring during the degradation of $Mn(acac)_3$-PMMA blends are very similar to those in $Co(acac)_3$-PMMA blends. Carboxylate and anhydride structures are produced in addition to acetylacetone and acetone, however, the enhancement in their production is reflected in the greater interaction of $Mn(acac)_3$ with the polymer in earlier stages of the degradation.

Blends of $Co(acac)_3$ and $Mn(acac)_3$ with MAA-MMA copolymers were also studied by Liggat. In these systems, the presence of methacrylic acid groups in the chain have important consequences in that the interaction with the methacrylic acid groups is stronger than that with the ester groups. As a result of this the ligand scission reactions occur at lower temperature on the copolymer blends than in those with PMMA. Also, the stronger interaction of the bis chelates with the acid structures inhibits sublimation and encourages further formation of depolymerisation blocking structures, thus enhancing the

effects of the chelates on the latter stages of degradation which are otherwise much the same as those of the PMMA blends.

In $Cu(acac)_2$-PMMA blends, decomposition promoted by π-complexation of $Cu(acac)_2$ at chain ends is not very significant. Ester interaction promotes decomposition as shown by the production of acetylacetone at relatively low temperature and acac·radicals produced by chelate decomposition initiate depolymerisation. The copper metal concurrently formed during degradation of the chelate has no effect on PMMA. In addition, as there is no formation of unsaturated sites along the backbone, the presence of $Cu(acac)_2$ does not lead to fragmentation of the polymer. Thus, the influence of $Cu(acac)_2$ on PMMA is limited to acac·radical initiated decomposition.

In contrast to the minor influence $Cu(acac)_2$ has on the thermal degradation of PMMA, the chelate has a marked effect on the degradation behaviour of a MAA-MMA copolymer. Initially, the decomposition of the chelate, by interaction mainly with acid groups (but also with ester groups) in the polymer produces acac·radicals which initiate depolymerisation. Subsequently the copper metal produced in the first stage catalyses decarboxylation at the acid side groups producing radicals which initiate depolymerisation. In addition, newly created "weak links" in the polymer act as sites for further unzipping.

The effects of $Co(acac)_3$, $Mn(acac)_3$, $Co(acac)_2$ and $Cu(acac)_2$ on the thermal degradation of poly(vinyl acetate) (PVAc) were also investigated. It was observed that in these systems, influence of

the chelates is slight. $Co(acac)_3$ and $Cu(acac)_2$ have no effect on the deacetylation of PVAc but both $Mn(acac)_3$ and $Co(acac)_2$ reduce the onset temperature of deacetylation. $Mn(acac)_3$ and $Co(acac)_3$ introduce low temperature ($< 200^{\circ}$C) degradation steps arising from the reduction of the chelates. As a consequence of this reduction, ketone groups are formed on the polymer backbone. With $Cu(acac)_2$ the most thermally stable of the chelates studied, no effect on the decomposition of PVAc can be detected.

$Mn(acac)_3$, $Co(acac)_3$ and $Cu(acac)_2$, on the basis of TVA results, have little or no effect on the degradation of polystyrene.

In the presence of $Cu(acac)_2$, the TVA behaviour of PVC is unchanged. With $Co(acac)_3$-PVC blends, however, two low temperature degradation peaks are observed at 159°C and 190°C due to the evolution of acetyl acetone. This can be attributed to chelate decomposition. The acac·radicals abstract an α hydrogen atom and the macroradical produced serves as an initiation site for the dehydrochlorination process. This accounts for the marked reduction in both onset and maximum rate temperatures for dehydrochlorination in the blend.

Surprisingly, although $Mn(acac)_3$ would be expected to introduce unsaturated sites along the polymer backbone, the chelate seems to have little effect on the TVA behaviour of PVC.

1.4 DEGRADATION OF CHLORINE CONTAINING POLYMERS.

Chlorine containing polymers, such as polyvinyl chloride (PVC), polychloroprene rubber (CR), chlorinated butyl rubber (CBR) and chlorinated polyethylene (CPE) etc. are widely used in a variety of applications including wire and cable jacketing, paints, printing inks, adhesives and fire retardant additives due to their attractive physical, mechanical and chemical properties. Unfortunately, most of these materials exhibit rather poor thermal and/or thermooxidative stabilities. As a result of this, sustained efforts have been made by academic and industrial research groups to elucidate the degradation and stabilisation of these polymers. However, in spite of intensive research, there remain certain essential details of the degradation mechanisms which are obscure. Processes occuring during the thermal degradation of chlorine containing polymers depend upon:

(a) the site of chlorine attachment within the polymer

(b) structural irregularities and defects

(c) end groups

The structural irregularities within and terminal groups on a polymer are in turn dependent on preparative method and post treatment procedures.

In general, when heated in an atmosphere of inert gas or in air, polymers with hydrocarbon chain structures containing chlorine undergo thermal or oxidative degradation processes, sometimes associated with cross-linking. Hydrogen chloride evolution initiated at low temperatures may be distinctly separated from polymer

chain degradation.   High temperatures cause accelerated dehydrochlorination, with simultaneous formation of unsaturated bonds in the hydrocarbon chains, followed by chain scission.   In the degradation process, volatile products and a non-volatile residue are formed.

The thermal degradation of several chlorine and bromine containing polymers has recently been reviewed[39] by McNeill.   The following section comprises a summary of the thermal decomposition behaviour of the major classes of chlorine-containing polymers with examples of common representatives of each group detailed.

1.4.1 VINYL POLYMERS

(a) Poly(vinyl chloride) (PVC).

A characteristic feature of PVC is its abnormally low thermal stability.   It is common knowledge that the low stability of PVC is caused essentially by the presence within the macromolecules of labile groups.   The exact nature of initiation of and mechanism of breakdown however is still open to debate.   The issue is further complicated as the decomposition is sensitive to several variables. The degradation is affected by sample form[38] as in thicker samples HCl release is hindered which enhances the autocatalytic dehydro-chlorination process.   Degradation atmosphere is also important as PVC degrades faster when heated in oxygen[40,41] than when heated in an inert atmosphere or in vacuo.   Thermal stability is also influenced by the method of polymerisation[41] (suspension, bulk) and the rate of heating.[41]

Investigations using thermograviometry, TG,[39] and TVA[42,43] indicate that the thermal degradation occurs in two stages. The first stage is essentially due to dehydrochlorination of the polymer chain which gives near quantitative loss of HCl, however, a little benzene and traces of ethylene are also observed. The second stage in the degradation arises from fragmentation of the unsaturated backbone produced in the first reaction. The average polyene length decreases as HCl loss increases and finally reaches a limited constant value[40] of approximately 6 to 10 double bonds in conjugation. This is explained by secondary processes such as cyclisation of polyenes,[44] and crosslinking of dehydrochlorinated polymer chains. The secondary products are low volatility, coloured materials collected as cold ring fractions in TVA studies and a high volatility fraction which includes aliphatic, aromatic and mixed aromatic-aliphatic compounds as confirmed by pyrolysis gas chromatography-mass spectrometry (GC-MS)[45] experiments. A black carbonaceous char residue remains after heating to $500^{\circ}C$.

The dehydrochlorination of PVC begins around $205^{\circ}C$ as determined by TVA[38] and reaches a maximum rate in the range 268-304 $^{\circ}C$ with a shoulder appearing on the peak attributed to dehydrochlorination at approximately $310^{\circ}C$. Fragmentation of the resultant unsaturated backbone commences at $370^{\circ}C$ with a rate maximum at roughly $450^{\circ}C$.

Although the degradation of PVC has been the focus of considerable research[6,7] the mechanism of dehydrochlorination has not been determined with any certainty, however, there is general agreement over the major features involved[8]. It is agreed that

the dehydrochlorination is initiated at defect sites along the polymer backbone. These structural abnormalities include β-chloroallyl groups[40], carbonylallyl (oxovinylene) groups[46] and tertiary chlorines:[40]

$$-CH = CHCHCl -, \qquad \underset{\underset{\displaystyle}{\overset{\displaystyle O}{\overset{\|}{}}}}{-C}CH = CH -, \qquad -CH_2-\underset{\underset{\displaystyle Cl}{|}}{\overset{\overset{\displaystyle R}{|}}{C}}-$$
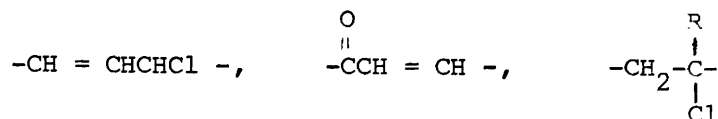
Although there is still controversy with regard to the relative importance, as labile moieties, of the various irregular structures that PVC contains, it is becoming accepted that the β-chloroallylic groups[47] are of major importance.

Three mechanisms have been suggested[48] for the thermal dehydrochlorination of PVC which are based on different active centres, namely radical, ionic and molecular. The radical mechanism was initially proposed many years ago[49] and it has been confirmed by a large number of experimental studies[50] especially by the application of ESR[51] for the detection of radicals. Dean et al[48] using conductimetric and u.v./visible spectral methods observed that the rate of thermal dehydrochlorination of PVC increased linearly with the concentration of allylic Cl atoms. Initiation of thermal decomposition is thought to occur as follows:

$$\text{\textasciitilde}\text{\textasciitilde}- CH = CH - \underset{\underset{\displaystyle Cl}{|}}{CH} - CH_2 - \underset{\underset{\displaystyle Cl}{|}}{CH}\text{\textasciitilde}\text{\textasciitilde} \overset{\Delta}{\longrightarrow} \text{\textasciitilde}\text{\textasciitilde}-CH = CH - \underset{\overset{\displaystyle \bullet}{}}{CH} - CH_2 - \underset{\underset{\displaystyle Cl}{|}}{CH} \text{\textasciitilde}\text{\textasciitilde}$$

$$P_1^{*} \hspace{6cm} P_1^{\bullet} + \cdot Cl$$
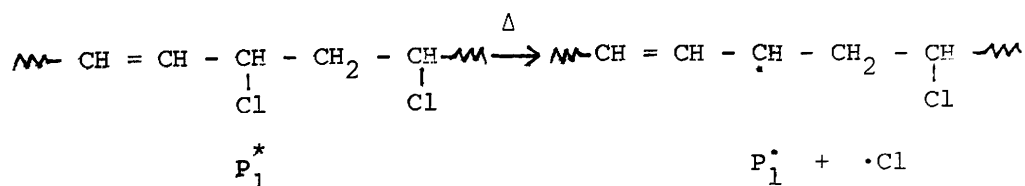
The reaction continues, forming polyene sequences and eliminating HCl.

$$\text{WW—CH} = \text{CH} - \underset{\bullet}{\text{CH}} - \text{CH}_2 - \underset{|}{\text{CH}}\text{—WW} \quad + \cdot \text{Cl} \xrightarrow{\Delta} \text{WW— CH} = \text{CH} - \text{CH} = \text{CH} - \underset{|}{\text{CH}}\text{—WW}$$

$$\underset{\text{Cl}}{} \qquad\qquad\qquad\qquad\qquad\qquad\qquad\qquad \underset{\text{Cl}}{}$$

$$\overset{\bullet}{P_1} \qquad\qquad\qquad\qquad\qquad\qquad\qquad \overset{*}{P_2} \qquad\qquad + \text{HCl}$$
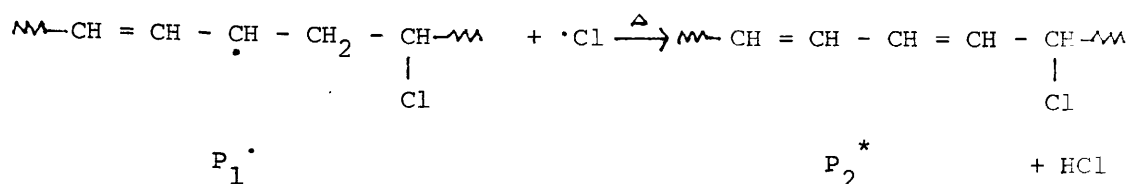
The structure $\overset{*}{P_2}$ is also active and thermally decomposes as

for $\overset{*}{P_1}$ continuing the dehydrochlorination process.   The resultant

polyenes formed have polyene sequences containing 6 to 10 conjugated

double bonds.   The length of polyene sequences is limited by

certain groups in the polymer chain such as tail to tail structures

or branches

$$\text{WW— (CH=CH)}\underset{n-1}{\overline{}} \overset{\bullet}{\text{CH}} - \text{CH}_2 - \underset{|}{\text{CH}}\text{—WW} \quad +\cdot\text{Cl} \xrightarrow{\Delta} \text{WW—(CH=CH)}\underset{n-1}{\overline{}} \text{CH=CH} - \underset{|}{\text{CH}}\text{—WW}$$

$$\qquad\qquad\qquad\qquad\qquad \text{R} \qquad\qquad\qquad\qquad\qquad\qquad\qquad \text{R + HCl}$$

$$\overset{\bullet}{\text{P}}\text{n-1} \qquad\qquad\qquad\qquad\qquad\qquad\qquad \text{Pn}$$
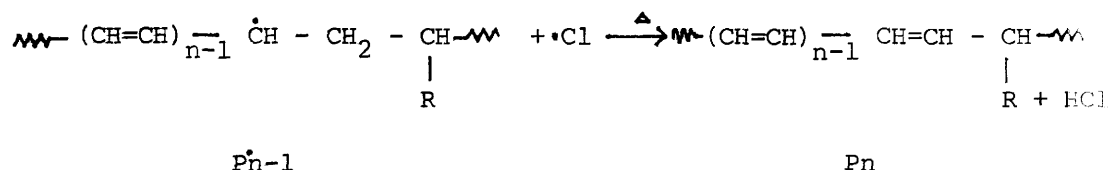
where $R=H$, $-CH_2Cl$, $-CH_2-CH_2Cl$ or other long branch groups and Pn is a

stable polyene sequence .

This radical mechanism however, fails to explain autocatalytic

dehydrochlorination.   It is probable, therefore, that elimination

of HCl via a 4-centred transition state (reaction 1) and HCl-catalyzed

elimination via a 6-centred transition state (reaction 2) occurs

simultaneously with the free radical route.[39]   These molecular

mechanisms are shown below:

$$\text{HCl +}$$

$$\text{WW— CH}_2\text{CH} \rightleftarrows \text{CHCHCl—WW} \longrightarrow \text{WW— CH}_2\text{CH=CHCHCl—WW} \qquad (1)$$

$$\text{2HCl +}$$

$$\text{WW—CH}_2\text{CH} \rightleftarrows \text{CHCHCl—WW} \longrightarrow \text{WW— CH}_2\text{CH = CHCHCl—WW} \quad (2)$$
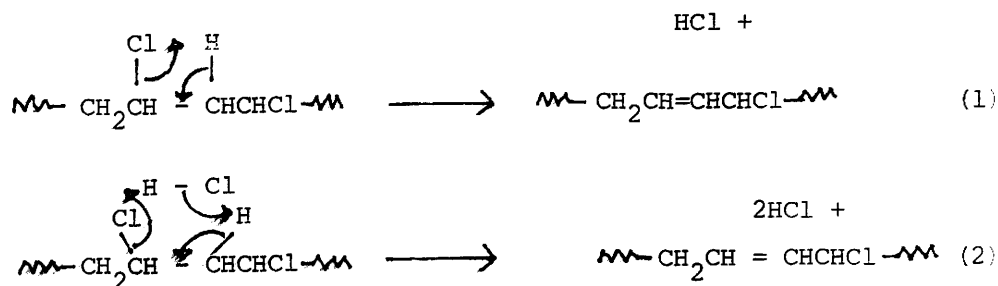
Secondary degradation products such as benzene and other aromatic compounds, as well as the carbonaceous residue obtained at high temperatures, are formed as a result of intramolecular cyclisation reactions.[45] The crosslinking which takes place during HCl loss, occurs by means of a Diels-Alder type reaction as this crosslinking may be reversed or prevented by heating the polymer with maleic anhydride.[5]

b) Chlorinated Poly(vinyl chloride) (CPVC)

Investigations using TG have revealed that chlorination of PVC, to give chlorinated polyvinyl chlorides (CPVC's) having chlorine contents of 67-75% w/w, results in polymers with increased thermal stability.[51] This is attributed to long internal (CHCl) sequences which appear as a consequence of the chlorination reaction. Degradation, as for PVC, occurs in two stages corresponding to the elimination of HCl followed by, in the case of CPVC, the decomposition of the resultant chlorinated polyene residue. The maximum rate of weight loss for the first reaction occurs at approximately 295°C for PVC and is elivated to roughly 330°C for CPVC (Cl content 67%, heating rate 10° min^{-1} under N_2). The second high temperature degradation step is at approximately 450°C for all systems. There is also an increase in weight % residue remaining after heating to 500°C under N_2 with CPVC (32-39% residue) as compared to PVC (21%).

Pyrolysic-GLC indicated that whereas PVC produced essentially aromatic hydrocarbon compounds including naphthalene on degradation, CPVC yielded chlorinated aromatics namely mono- and dichlorobenzenes and negligable naphthalene species.

Chlorination of PVC leads to the production of materials which have exceptionally good fire properties.[52]   Flammability is decreased as is smoke production tendancy of the polymers while there is a substantial increase in the char remaining after combustion.

c) Poly(vinylidene chloride)(PVDC)

PVDC thermally degrades in a similar fashion to CPVC liberating HCl and chlorinated aromatic compounds.[50]   The latter degradation products, however, are not produced in similar analagous mono:dichlorobenzene ratios as in CPVC. PVDC is somewhat less stable than PVC.   This can be attributed to the presence of $-CCl_2$ units along the polymer backbone which are more thermally labile than the -CHCl structures present in PVC.   PVDC degrades at $120-220^{\circ}C$ to give only HCl, yielding one molecule of HCl per vinylidene chloride repeat unit, and at temperatures above $250^{\circ}C$ chlorinated aromatic compounds are also produced.   Autocatalysis is observed after 15% reaction and a free radical dehydrochlorination mechanism, initiated at the chain ends and proceeding along the chains has been proposed.[53]

1.4.2 CHLORINATED RUBBER

a) Chlorinated Rubber (CR)

Natural rubber is chlorinated by a process which involves both substitution and addition reactions[54] to give a final commercial product with 65-68% chlorine content.   The structure of CR is complex and Dodson and McNeill[55] investigating the thermal

degradation of CR, have proposed an alternative polymer structure
and decomposition mechanism to that previously reported.[56]   The
recent study reveals that gaseous degradation products are evolved
in two distinct temperature regions.   CR begins to degrade at $200^{\circ}C$
and the initial decomposition process reaches a maximum rate at
$300^{\circ}C$.   During this stage a weight loss of approximately 67%
of the original weight is observed.   Most of this (95%) is due to
the elimination of HCl although small amounts of carbon dioxide and
carbon monoxide as well as traces of methane and ethylene are also
formed.   The second decomposition occurs between 400° and $500^{\circ}C$.
In this stage about 3% weight loss is recorded and methane, ethylene,
HCl (traces) and hydrogen are detected as degradation products.
The remaining 30% by weight remains as a char residue.
Discolouration of the polymer at only 1% dehydrochlorination indicates
that conjugation develops along the chain as in PVC degradation.
CR readily looses $^{5}/_{7}$ of the total available HCl.   If the
predominant structure type in CR is that illustrated below:

I
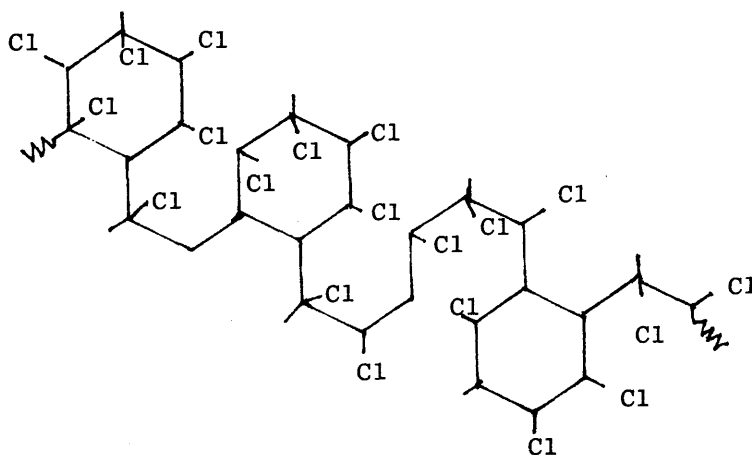
then loss of HCl from cyclic structure (I) can be envisaged as occuring as shown in equation 1.

$$\text{I} \longrightarrow \text{II} \longrightarrow \text{III} \tag{1}$$
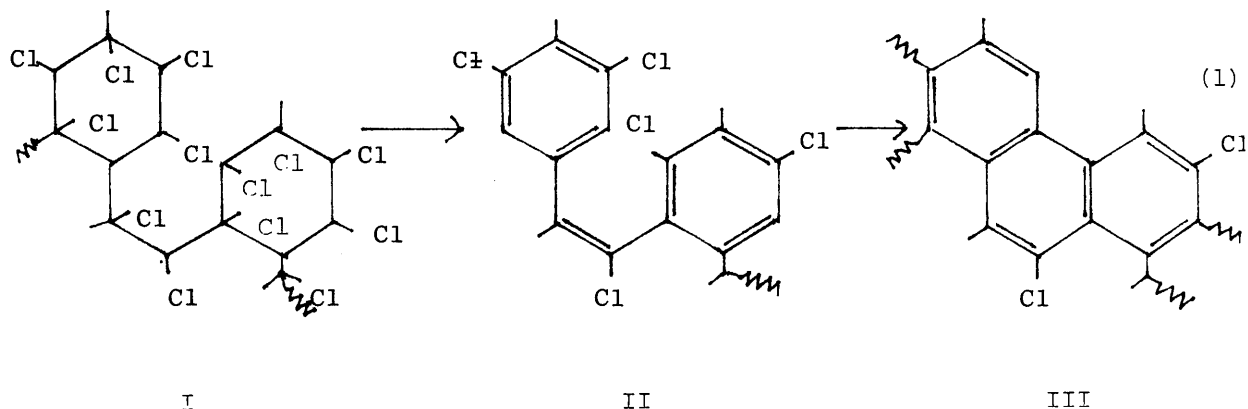
Dehydrochlorination from adjacent units along the polymer chain could produce structure II with long conjugated sequences. In this reaction 4 molecules of HCl per 2 isoprene units are lost i.e. $4/7$ or 57% of total HCl. Further loss of HCl in a cyclisation reaction produces cyclic structure III which would account for the evolution o f $5/7$ or 71% of total HCl. The remainder of the HCl produced at higher temperatures, is formed as a result of Diels-Alder type reactions between adjacent fused systems.

b) Chlorobutyl Rubber (CBR)

In the halogenation (Cl_2, Br_2) of butyl rubber, several structures[46] are formed within the macromolecules which are distinguished by the position of the halogen atom with respect to the $\diagdown C = C \diagup$ bond, principally:

exo-(a_1) endo-(a_2) Di X-(a_n)
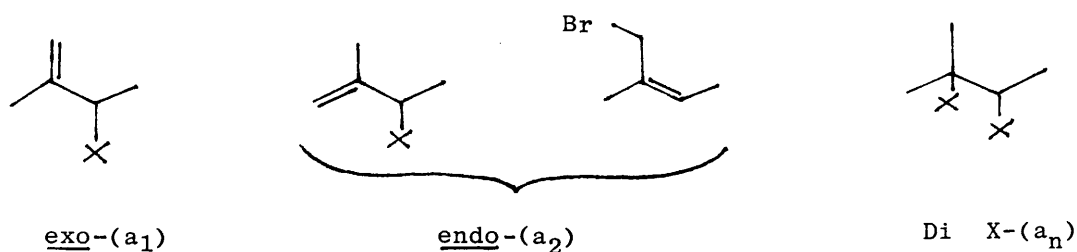
During the halogenation of butyl rubber, there is a decrease of 10-30% in the unsaturation of the molecules and simultaneous isomerization of part of the internal $\ce{>C=C<}$ bonds into neighbouring exo groups.   The proportion of exo and endo-methylene structure is dependent upon the halogen : it is greater in chlorobuty rubber than in bromobutyl rubber (6:1 in CBR cf 1:1 in BBR).

Experimental data on the dehydrochlorination of CBR[46] indicate that both these labile groups (exo-and endo-) are responsible for the decomposition of the polymer.   It is important that the stability of the endo- structure (a_2), in which the chlorine atom is in the β-position with respect to the internal $\ce{>C=C<}$ bond, appears to be more than an order lower than that of the exo- structure (a_1), in which the chlorine atom is in the β-position to the external $\ce{>C=C<}$ bond.   In spite of the content of endo-structures (a_2) in CBR being 7-9 times lower than that of the exo-structures (a_1), the high rate of dehydrochlorination in the initial stages of thermal degradation of CBR is determined by this essentially unstable endo-structure (a_2).

c) Polychloroprene(PC)

The processes which occur during the degradation of poly-chloroprene (PC) comprise the elimination of HCl and other minor gaseous decomposition products followed by decomposition of the resultant residue to yield hydrocarbons as for PVC.   Dehydro-chlorination takes place less readily than in PVC unless oxygen is

present and in the absence of air the elimination of HCl is not
autocatalytic.   The polymer is very sensitive to the presence of
small concentrations of impurity structures, formed on the reaction
with oxygen during or after polymerisation, which considerably reduce
its thermal stability.

TG experiments[57] indicate that a two stage weight loss occurs
during the degradation of PC with the maximum rate of weight loss in
the range $357^{\circ}-365^{\circ}C$.   This initial decomposition is attributed
to dehydrochlorination however comparison of weight loss and evolved
gas analysis data for HCl evolution from PC clearly show the presence
of additional products.   Approximately 90% of the chlorine in PC
is lost as HCl.   The second decomposition occurs in the range
$400^{\circ}-550^{\circ}C$.

Product analysis following degradation in a TVA system[58] has
revealed that below $400^{\circ}C$, in addition to HCl, small amounts of
ethylene and a trace of chloroprene are evolved.   Above $400^{\circ}C$
methane and smaller amounts of hydrogen, ethylene and trace amounts
of propylene are produced.

A complex liquid fraction[57] is obtained in addition to the
gaseous products which contains two dichloro-4-vinylcyclohexene
isomers.   The less volatile liquid components contain aromatic
structures with 1,2-disubstitution predominating.   The involatile
residue of partial degradation of PC differs from that obtained in
PVC in that the extent of conjugation in PC residues is much less
than in PVC.   In PC, UV studies indicate that the major absorptions
are characteristic of trienes.   This is to be expected if random

loss of HCl occurs by the nonradical mechanism illustrated below in equation (1), as opposed to the "unzipping" radical chain process observed in the dehydrohalogenation of PVC.   PC does not accelerate PMMA degradation in PC-PMMA blends[57-59] which is also consistent with a nonradical loss of HCl.

(1)
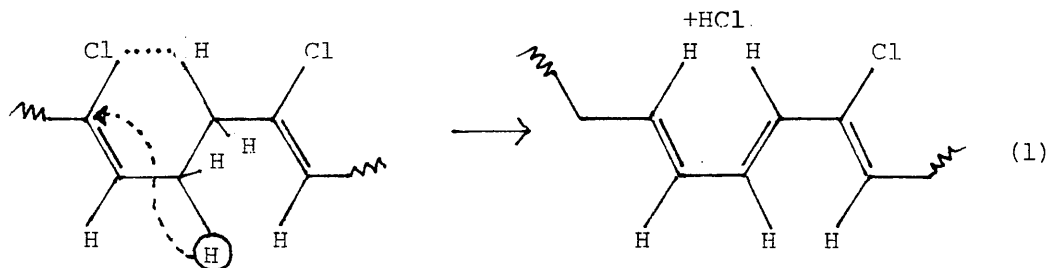
Recent spectroscopic studies on the initial stages of thermal degradation of low molecular weight PC suggest that decomposition is initiated following allylic rearrangement[58] of defect structures within the polymer.   The possible structural irregularities i.e. 1,2 unit, 3,4 unit and isomerized 1,2 unit are illustrated below:
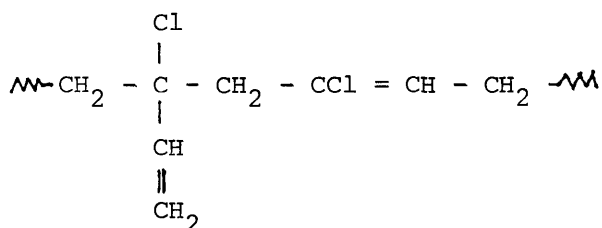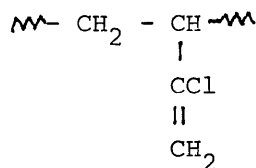
1,2 unit -1,4 unit   3,4 unit
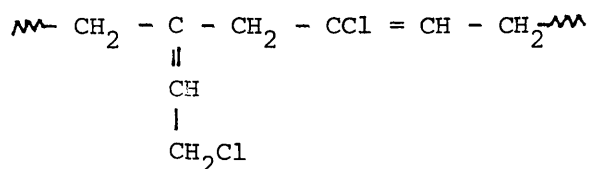
isomerized 1,2 - 1,4 unit

Of the structural irregularities, isomerized 1,2 unit is not initially present in the polymer and the 1,4 unit dominates.[60] The first stage reaction during thermal degradation of PC is allylic rearrangement of a 1,2 unit and this process is finished within 30 minutes at 150°C. The extent of HCl loss is proportioned to the decrease of isomerized 1,2 unit thus it is proposed that the second stage of thermal degradation is dehydrochlorination of the isomerized 1,2 unit which contains the most labile chlorine atom. The mechanism suggested for this reaction[60] is via a back-biting process involving a six-membered transition state yielding cyclic structures within the polymer back bone. The major (structure I) and minor (structure II) decomposition products, are shown below.

$$\text{W}-CH_2-CCl=CH-CH_2-CH_2-\underset{\underset{\underset{CH_2Cl}{|}}{\overset{\overset{CH}{\|}}{}}{C}-CH_2-CCl=CH_2-CH_2-\text{W}$$

$$\text{W}-CH=CH \overset{CH_2-CH_2}{\underset{CH_2-CH}{\diagdown \diagup}} C-CH_2-CCl=CH-CH_2-\text{W} \quad +$$

(I)

$$\text{W}-CH_2-CCl=CH-CH_2-\underset{CH-CH_2}{\overset{CH=CCl}{C}}{C}\overset{CH=CCl}{\underset{CH-CH_2}{\diagup \diagdown}}CH-CH_2-\text{W}$$
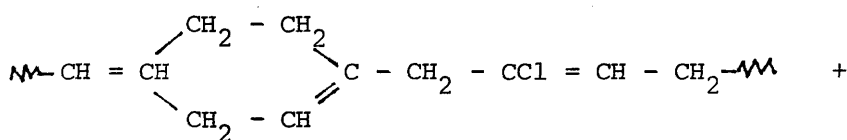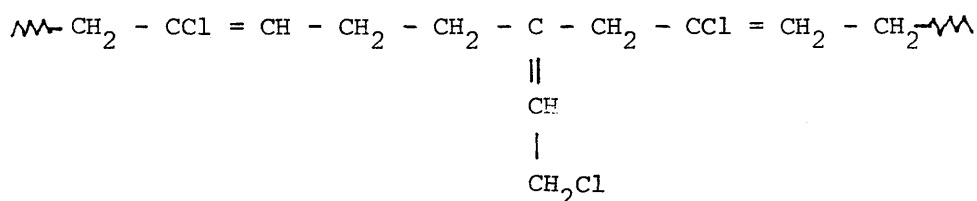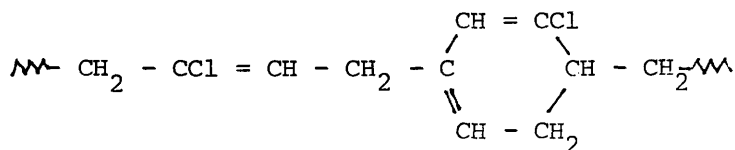
(II)

1.4.3 CHLORINATED POLYOLEFINS AND PARAFFINS

a) Chlorinated Polyethylene (CPE)

Three pentad type structures are present within chlorinated polyethylene (CPE) polymer chains, namely, AABAA, AABAB and BABAB, where A and B represent CH_2 and CHCl groups respectively. The labile groups in CPE (which is one of the least stable halogen containing elastomers) are saturated and non-terminal and may have the following structures[46]: $- C(O)-CH_2-CHCl-$, $- CH(OH)-CHCl-CH_2^-$ $- CHCl-CHCl-$ and $- \overset{|}{\underset{|}{C}} - Cl$.   Kinetic degradation experiments on CPE with chlorine contents ranging from 2 to 40% weight and which have no hydroxyl and an insignificant amount of carbonyl groups, have revealed that a correlation is obtained between the rate of HCl evolution and the content of chlorines at tertiary carbons.[61] Thus, the low stability of CPE is caused by the presence of labile $- \overset{|}{\underset{|}{C}} - Cl$ groups within macromolecules.   This fact also accounts for the marked differences between the characteristics of CPE degradation and those of vinyl chloride polymers and CBR.

Thermogravimetric results[62] show that the degradation of CPE occurs in two stages.   The first stage is associated mainly with HCl evolution and occurs in the temperature range $230^{\circ}-410^{\circ}C$ (maximum rate of weight loss at $330^{\circ}C$).   Chain decomposition accounts for the second degradation stage at $410^{\circ}-525^{\circ}C$, and this process reaches a maximum rate of weight loss at $490^{\circ}C$.

b) Chlorinated Ethylene-Propylene Copolymer (CEPC)

Chlorinated ethylene-propylene copolymer (CEPC), like CPE, evolves HCl on heating.   CEPC samples with chlorine contents up

to 40% weight, like PVC, do not contain geminal chlorines (as verified by the absence of the band at 530 cm^{-1} in IR spectra).[51] Kinetic data[46] on the thermal degradation of CEPC reveals that there is no correlation between either the quantity of carbonyl and unsaturated groups or the vicinal and other chlorine containing non-branched structures and the number of labile groups.   The best relationship has been achieved between the results of the quantitative estimation of the labile group content and the tertiary carbons with chlorines at the branching points
$$- \overset{\overset{\textstyle CH_3}{|}}{C} Cl - CH_2 -$$
Thus, as for CPE, the thermal stability is determined by the presence of saturated branched chlorine-containing structures
$$- \overset{|}{\underset{|}{C}} - Cl$$
within macromolecules.

c) Chloroparaffin (CP)

        Camino and Costa, using several thermoanalytical techniques, have studied the thermal degradation[63] and mechanism of action[64,65] of a highly chlorinated paraffin (CP) used as a fire retardant additive for polymers.   The linear CP ($\overline{M}n$ = 1400) consists of sequences of CHCl units, isolated or very short sequences of CH_2 and isolated CCl_2 units, and terminated by methyl groups.   TG results indicate that the thermal degradation of CP is a two stage process. The first stage occurs between 275° and 400°C, with the weight loss due to decomposition being approximately 70%.   The second stage occurs over a broader temperature range starting above 450°C. By 800°C, a further 10% of weight has been lost in the second step, but the residue is still volatilizing although at a very low rate. Analysis of the dehydrochlorination reaction reveals that on heating

above 250°C the CP eliminates about 60-70% of its chlorine as HCl

initially in an apparant zero order reaction, however the amount of

HCl evolved at higher temperatures tends to a lower limit which suggests

that some hindrance to the formation of HCl develops in the product as

dehydrochlorination progresses and could be evidence for side reactions.

After the elimination of HCl, the initially white powder is

transformed to a charred residue containing 35% by weight of chlorine.

This is more stable than the original CP and degrades above 300°C

although still gives HCl as the major decomposition product.   On

heating in the range 300° to 800°C, the residue decomposes to give

two peaks in the TVA trace at 350° and 700°-800°C respectively.

The first peak is mainly associated with the production of HCl.

Formation of volatiles non-condensable at -196°C partially overlaps

HCl evolution but becomes the predominant degradation process above

500°C.

Dehydrochlorination of CP is likely to be initiated at allylic

chlorine atoms formed after preliminary partial elimination of HCl

(initiated by labile Cl atoms).   Once initiated, dehydrochlorination

proceeds along the molecule with the formation of conjugated double

bonds as in PVC.   Complete dehydrochlorination of CP is, however,

restrained by the greater stability of Cl atoms in vinyl structures

created by elimination of HCl as shown below:[63]

$\text{\textasciitilde\textasciitilde\textasciitilde} CHCl - CHCl - CH = CH(Cl) - CHCl - CHCl - CHCl - CH_2 \text{\textasciitilde\textasciitilde\textasciitilde} \xrightarrow{-3HCl}$

$\text{\textasciitilde\textasciitilde} CCl = CH - CH = CH(Cl) - CH = CCl - CH = CH \text{\textasciitilde\textasciitilde}$
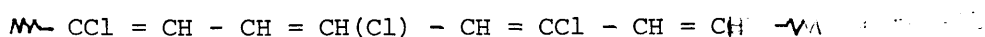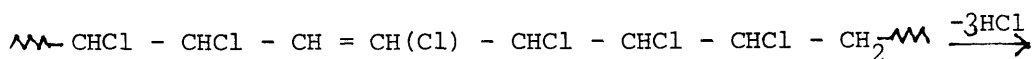
Cross-linked chlorinated residue could arise from an inter-molecular addition reaction between double bonds. Thus the thermal degradation of CP can be compared to that of PVCC as in both cases the main dehydrochlorination process leading to a more stable residue is preceded by a limited loss of HCl eliminated from labile structures. The main difference between the thermal decomposition of the two polymers, however, is the transformation of PVCC to an almost completely insoluble product at early stages of dehydro-chlorination (after 10% weight loss)[66].

1.4.4 CHLORINATED POLYACRYLONITRILE AND CHLORINE CONTAINING ACRYLATE POLYMERS.

a) Chlorinated Polyacrylonitrile (CPAN)

Polyacrylonitrile may be chlorinated in the solid state at $130^\circ C$ and $140^\circ C$ in the presence of NaCl to yield products with chlorine contents of 20.82% and 42.11%.[67] These values correspond to chlorinated polyacrylonitrile (CPAN) which contains one chlorine atom per either two or one repeat unit respectively. IR spectroscopy reveals that the chlorinated polymer consists mainly of α,β-dichlorinated units. The differential thermal analysis (DTA) curve for CPAN gives broad, single exothermic peaks as in the cases of poly α-chloroacrylonitrile (PCAN) and acrylonitrile – CAN copolymers.[68] Thermal dehydrochlorination of CPAN starts at about the onset temperature of the exothermic reaction. The mode resembles that in PCAN and acrylonitrile-CAN copolymers, which indicates that even in CPAN the initiation of polymerisation of cyano groups takes place as a side effect of the thermal dehydrochlorination.[68] On the

other hand, dehydrochlorination in CPAN occurs at a lower temperature

than in PCAN (DTA peak maximum for CPAN 1 (20.82% Cl), CPAN 2 (42.11%

Cl), PCAN and PAN being approximately 150°, 170°, 215° and 270°C

respectively).[67] This indicates that β-substituted chlorine

atoms are more easily dehydrochlorinated at lower temperature than

α-chlorine atoms. Thus it appears that α,β-dichlorinated units

result from the addition of chlorine to the double bonds produced by

dehydrochlorination after β-chlorination. By 300°C dehydro-

genation is almost completed in both PCAN and slightly chlorinated

CPAN (20.82% Cl) but not in highly chlorinated CPAN (42.11% Cl).

This observation may be explained if the α,β-dichlorinated unit is

considered as a chlorinated moiety.[67] The chlorinated moiety can be

easily dehydrochlorinated as illustrated below:

$$\text{\scriptsize M\!\!V\!\!V}\!\!- CH_2 - \underset{\underset{Cl}{|}}{C}(C\equiv N) - \underset{\underset{Cl}{|}}{CH} - CH(C\equiv N)\text{\scriptsize -\!\!V\!\!V\!\!V} \longrightarrow$$

$$\text{\scriptsize M\!\!V\!\!V}\!\!- CH = C(C\equiv N) - CH = C(C\equiv N)\text{\scriptsize -\!\!V\!\!V\!\!V} +2HCl$$
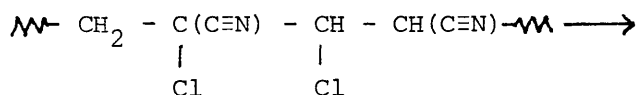
Complete dehydrochlorination is difficult in highly chlorinated CPAN

due to the presence of Cl atoms not subjected to intramolecular

dehydrochlorination such as chlorine atom (I) or (II) in

$$\text{\scriptsize M\!\!V\!\!V}\!\!- CH_2 - \underset{\underset{Cl}{|}}{C}(C\equiv N) - \underset{\underset{\underset{(I)}{Cl}}{|}}{CH} - CH(C\equiv N) - \underset{\underset{\underset{(II)}{Cl}}{|}}{CH} - \underset{\underset{Cl}{|}}{C}(C\equiv N)\text{\scriptsize -\!\!V\!\!V\!\!V}$$
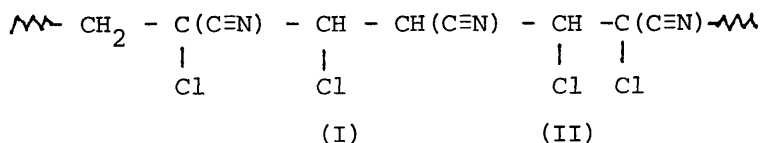
b) <u>Chlorine-Containing Acrylate Polymers.</u>

Rao et al[69] have investigated the thermal degradation of several chlorine-containing acrylate polymers and their copolymers with methyl methacrylate (MMA) using TG and gas chromatography-mass spectrometry (GC-MS).

i) <u>Poly(chloroethyl methacrylate)</u> (PCEMA)

The TG curve of poly(chloroethyl methacrylate) (PCEMA) shows that weight loss begins at approximately $250^{\circ}C$ with a maximum rate at $314^{\circ}C$.   Decomposition is complete by $445^{\circ}C$.   From GC-MS analysis the most abundant non-chlorinated products are CO_2 and acetaldehyde. Among the chlorinated products are vinyl chloride, ethyl chloride and monomer (CEMA).   Vinyl chloride may be formed by the decomposition of ester groups which occurs via a six-membered ring intermediate involving β-hydrogen atoms.[70]
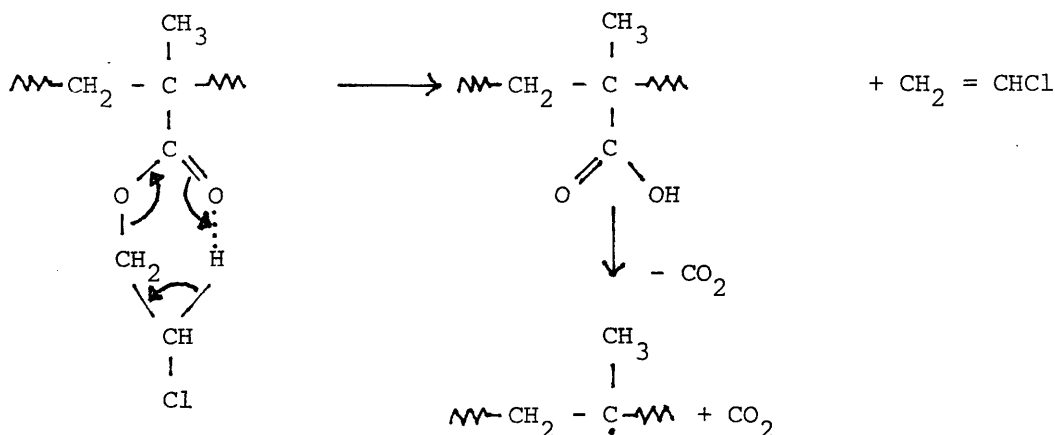
This process also generates CO_2.   Monomer is produced as a result of random chain scission followed by depolymerisation.   The propagating radical formed during the depolymerisation reaction may

undergo intra- and intermolecular reactions liberating ethyl

chloride as shown below:[69]

a) intramolecular

$ClCH_2CH_2$ $- O$
$C = O$
$C - CH_3$
$CH_3 - \overset{\cdot}{C} \diagdown CH_2$ $CH_2 -\!\!\!\wedge\!\!\!\wedge$
$COOCH_2CH_2Cl$

$ClCH_2CH_2^{\cdot}$

$+$

$O - C \diagup\!\!\diagup O$
$CH_3 \diagup \overset{|}{C} \diagdown CH_2 \overset{|}{C} - CH_3$
$CH_2 -\!\!\!\wedge\!\!\!\wedge$
$COOCH_2CH_2Cl$

b) intermolecular

$\wedge\!\!\!\wedge\!\!- CH_2 - \overset{\overset{\displaystyle CH_3}{|}}{\underset{|}{C}} - CH_2 -\!\!\!\wedge\!\!\!\wedge$
$O = C$
$O - CH_2CH_2Cl$
$CH_3 - \overset{\cdot}{C} - CH_2 -\!\!\!\wedge\!\!\!\wedge$
$COOCH_2CH_2Cl$

$\longrightarrow$

$\wedge\!\!\!\wedge\!\!- CH_2 - \overset{\overset{\displaystyle CH_3}{|}}{\underset{|}{C}} - CH_2 -\!\!\!\wedge\!\!\!\wedge$
$C = O$
O
$CH_3 - C - CH_2 -\!\!\!\wedge\!\!\!\wedge$
$COOCH_2CH_2Cl$

$+ \cdot CH_2CH_2Cl$
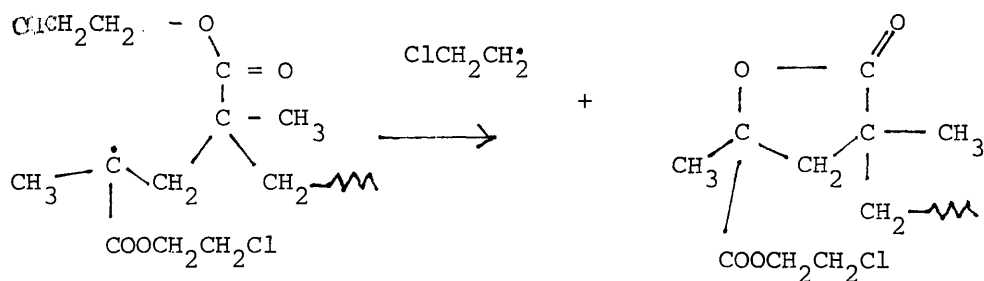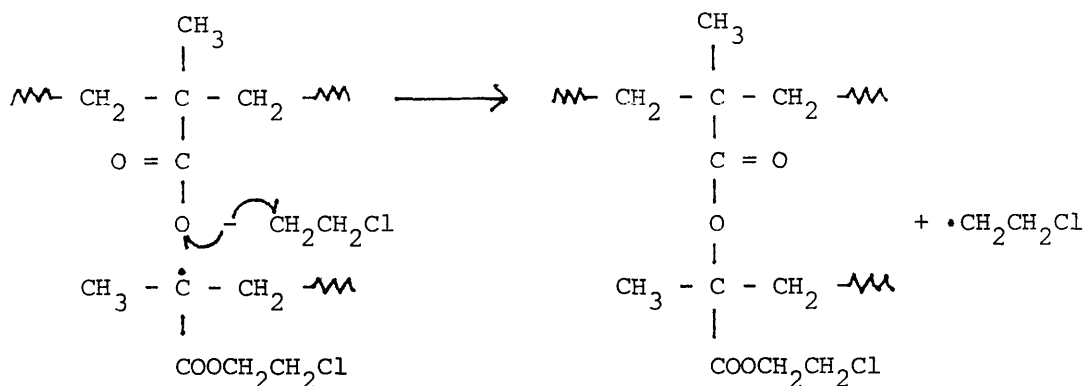
Acetaldehyde is produced via decomposition of the chloroethoxide

radical which is evolved during the formation of anhydride rings as

illustrated overleaf:

$$\cdots C(CH_3)(C=O)(O\cdot) - CH_2 - C(CH_3)(C=O)(O-CH_2CH_2Cl) \cdots \longrightarrow \cdots C(CH_3) - CH_2 - C(CH_3) \cdots + \cdot OCH_2CH_2Cl$$

$$\cdot OCH_2CH_2Cl \longrightarrow \left[CH_2 \overset{O}{-} CH_2 \right] \longrightarrow CH_3CHO$$
$$+$$
$$\cdot Cl$$
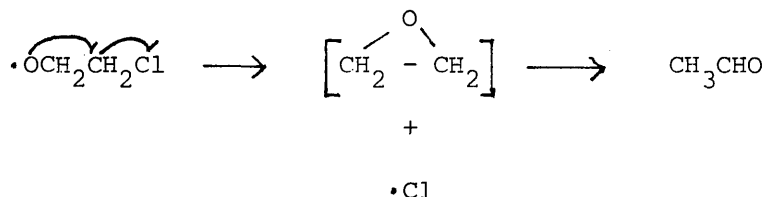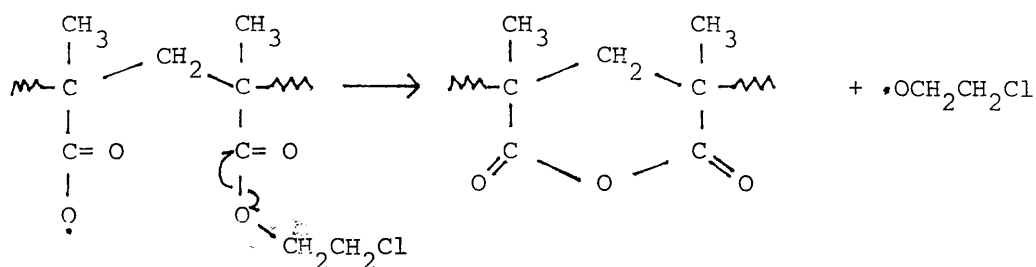
ii) Methyl methacrylate-chloroethyl methacrylate copolymers

Thermolysis of poly (72 MMA-$\underline{co}$-28 CEMA) produces CO_2, propene

ethylchloride, acetaldehyde and vinyl chloride as a result of ester

decomposition.[69] In addition, MMA is produced which is not

unexpected considering that the copolymer contains sequences of MMA

interspersed with CEMA units.   The lack of CEMA monomer however,

suggests that decomposition of CEMA units occurs more readily than

depolymerisation in these co-polymers.

iii) Poly(2,2,2-trichloroethyl methacrylate)(PTCEMA)

The TG curve for poly(2,2,2-trichloroethyl methacrylate)(PTCEMA)

shows a two stage weight loss, having onset temperatures of the first

and second decomposition steps at 195° and 275°C respectively.[69]

The initial stage of degradation is attributed to dissociation of the

bulky CCl_3 group which accounts for 40% weight loss.   The principal

degradation products are vinylidene chloride, CO_2 and propene with

vinyl chloride as a minor product.   The absence of monomer suggests

that ester decomposition is an important pathway for degradation,

probably facilitated by the polar CCl_3 groups and stability of the

$\cdot CCl_3$ radical.   The major pyrolysis product, vinylidene chloride,

is most likely to be produced by the elimination of the stable

$CCl_3CH_2\cdot$ radical, which is assisted by the electron withdrawing

effect of the CCl_3 group:
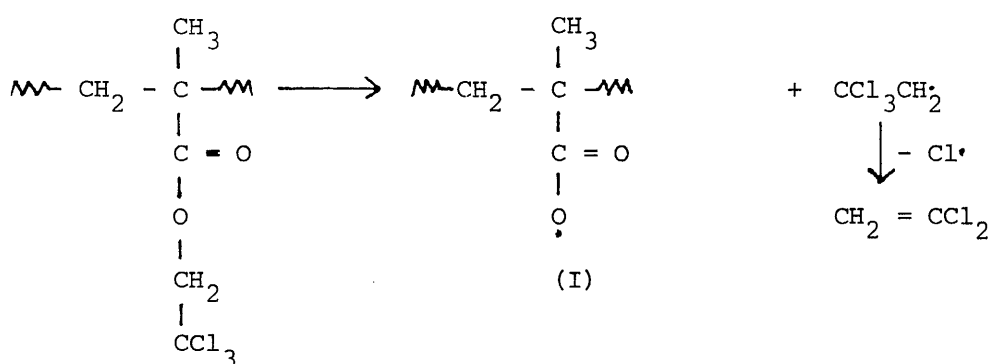
Decarboxylation of the carboxylate radical (I) and subsequent

processes can produce the other products mentioned.

(iv) <u>Methyl methacrylate – trichloroethyl methacrylate copolymers</u>

Thermal degradation of poly(76 MMA-<u>co</u>-24 TCEMA) yields in

addition to the products for PTCEMA, dichloroacetaldehyde and MMA.[69]

Dichloroacetaldehyde is produced in the ester decomposition reaction

illustrated below:
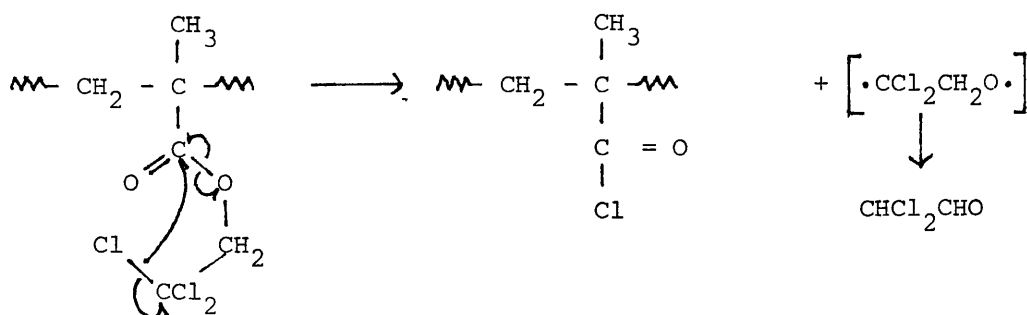
The fact that dichloroacetaldehyde is not observed in the

decomposition of the homopolymer is attributed to the steric

hindrance of the CCl_3 group inhibiting the formation of the cyclic

transition state postulated above.

v) Poly(methyl-α-chloroacrylate)(PMCA)

TG results show poly(methyl-α-chloroacrylate)(PMCA) to be

appreciably more stable than PCEMA or PTCEMA.[69]   Although weight

loss commences at 225°C, the rate of degradation is much slower than in

PCEMA or PTCEMA.   Also, a substantial amount (~20%) of carbonaceous

char remains at 475°C.   The major decomposition products are CO_2,

CH_3Cl and MCA monomer with trace amounts of propene.   Whereas

production of HCl might have been expected from the initial weight

loss of ~30% and the appearance of an olefinic absorption band at

1625 cm^{-1} in the IR spectrum of the residue obtained on heating

PMCA to 175°C, the volatile product is in fact CH_3Cl, which may be

explained by the acidolysis of PMCA.[69]

The production of monomer will result from random scission

of main chains.   This is conceivable considering the high

polarization of C-C back-bone bonds by the chlorine atom attached to

one of the carbons.   GC-MS analysis of the products of pyrolysis

obtained from poly(62 MMA-co-38 MCA) differ from that of the

homopolymer of MCA only in that MMA is produced instead of MCA.

However, due to the similarlity in retention times of the two monomers,

it is not easy to separate small amounts of MCA from MMA.

Therefore, the degradation processes for PMCA and copolymers

of MCA (i.e. elimination reactions prevailing) are distinctly different

from those of those of the other two forementioned polymers with Cl

in the pendant groups in which both ester decomposition and main

chain scission occur with the former taking the dominant role.

vi) Poly(acryloyl chloride)(PAC)

Diab and coworkers[71] have quantitatively analysed the products

of thermal degradation of poly(acryloyl chloride)(PAC) and copolymers

of acryloyl chloride with methyl methacrylate (AC- MMA) using thermal

analysis, IR spectroscopy and gas-liquid chromatography.

On heating PAC to 500°C, the major gaseous degradation

products evolved are HCl and CO. The liquid fraction comprises

acrylic acid, acryloyl chloride (monomer) and chain fragments

(C_6-C_{15}), some of which contain pyrone structures. Traces of

water are also observed. It appears that as is normal for

polyacrylates, the mechanism of degradation is dominated by side-

group reactions and chain transfer to give short fragments, rather

than unzipping to monomer as for the polymethacrylates. The

formation of HCl is probably due to elimination of a chlorine atom

followed by hydrogen abstraction:
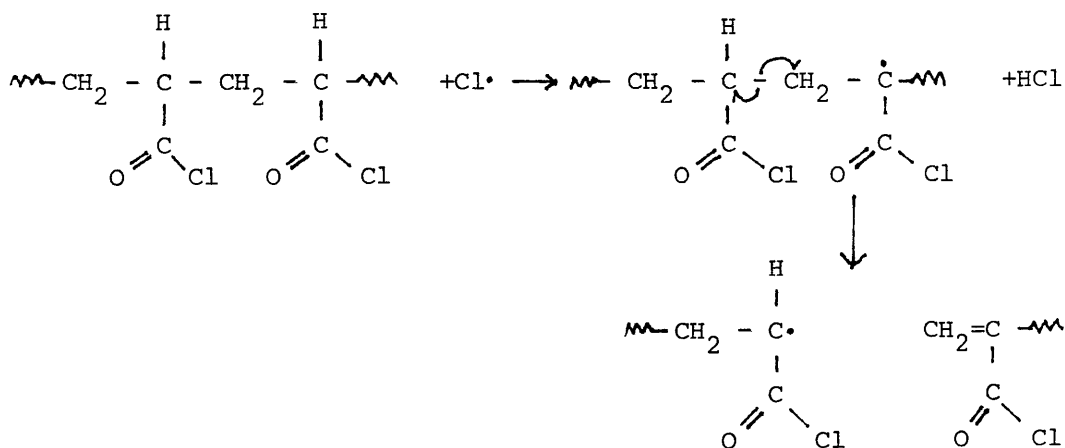
In addition, HCl may possibly be formed by elimination of two
adjacent AC units in the polymer chain, forming 3,5-(6 chloro-2-
pyrone) and its fragments as shown below:
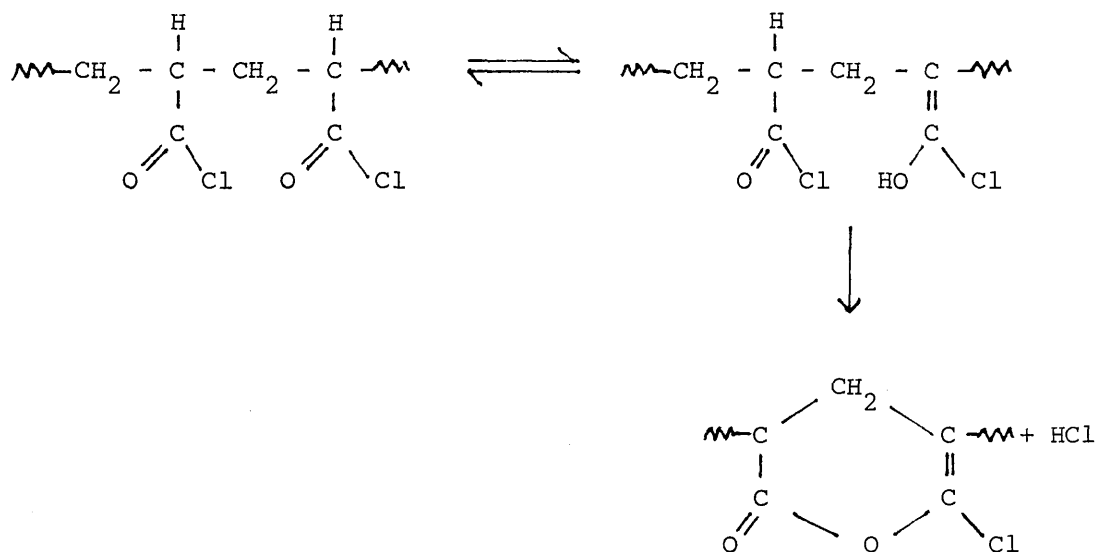
These kinds of sequences will increase the yield of chain fragments
which account for 65 mol % of the degradation products of PAC.

vii) <u>Acrylolyl chloride methyl-methacrylate copolymers</u>

In addition to the products formed during the
decomposition of PAC, the thermal degradation of AC-MMA copolymers results
in the formation of methyl chloride, MMA monomer and chain fragments
which contain anhydride structures.[71]   It is suggested that the
mechanism for the production of methyl chloride involves protonation
of the methoxide group on the pendant ester chain by liberated HCl,
resulting in six membered ring intermediate which finally degrades
evolving methyl chloride and yielding an anhydride structure in the
polymeric residue:

$$HCl + \quad \text{CH}_2 - \overset{\overset{\text{CH}_3}{|}}{\underset{|}{\text{C}}} - \text{CH}_2 - \overset{\overset{\text{CH}_3}{|}}{\underset{|}{\text{C}}} \longrightarrow \quad \text{CH}_2 - \overset{\overset{\text{CH}_3}{|}}{\underset{|}{\text{C}}} - \text{CH}_2 - \overset{\overset{\text{CH}_3}{|}}{\underset{|}{\text{C}}}$$

$$O = C - O \quad O = C - O \qquad\qquad O = C - O \qquad C \overset{+}{-} O - H$$

$$\underset{\text{CH}_3}{|} \qquad \underset{\text{CH}_3}{|} \qquad\qquad \underset{\text{CH}_3}{|} \qquad \underset{\text{CH}_3}{|}$$

$$+ \; Cl^-$$

$$\text{CH}_2 - \overset{\overset{\text{CH}_3}{|}}{\underset{|}{\text{C}}} - \text{CH}_2 - \overset{\overset{\text{CH}_3}{|}}{\underset{|}{\text{C}}} \longrightarrow \quad \text{CH}_2 - \overset{\overset{\text{CH}_3}{|}}{\underset{|}{\text{C}}} - \text{CH}_2 - \overset{\overset{\text{CH}_3}{|}}{\underset{|}{\text{C}}}$$

$$O = C \qquad\qquad C = O \qquad\qquad O = C \qquad C = O$$

$$\overset{+}{\underset{|}{O}} \qquad\qquad\qquad O$$

$$\underset{\text{CH}_3}{|}$$

$$+ \; CH_3OH + Cl^- \qquad\qquad\qquad + \; CH_3Cl$$
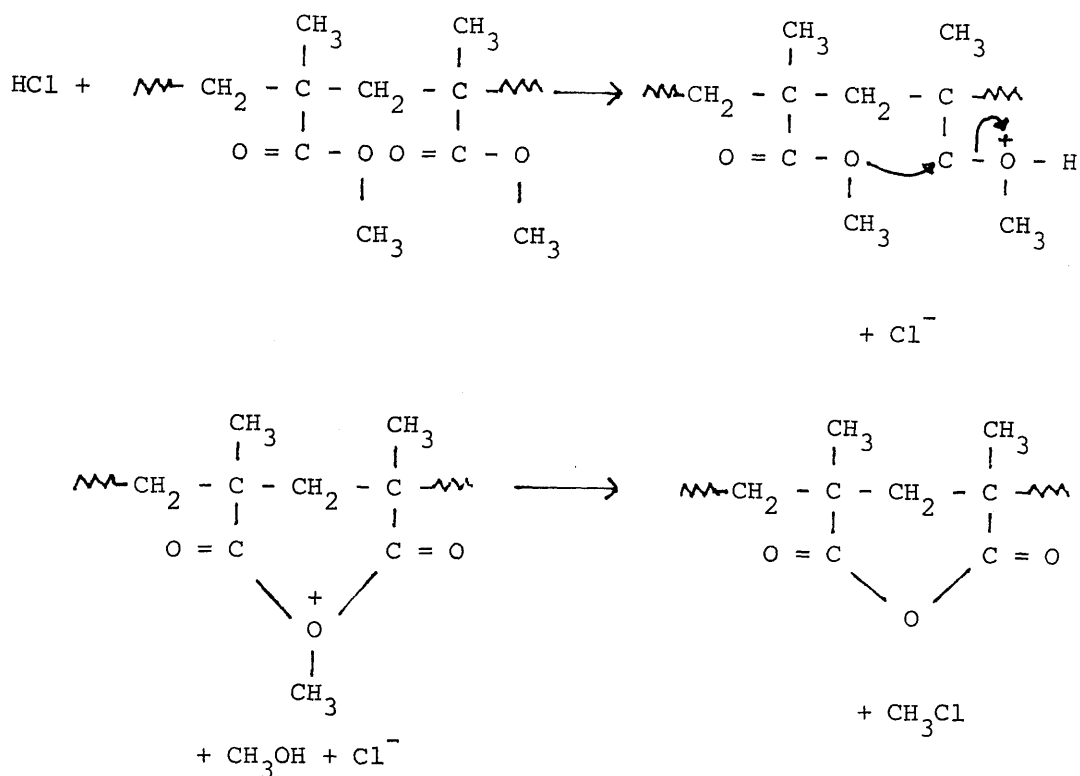
This mechanism explains the relative yields of CH_3Cl (5.2 mol %

maximum) and HCl (7.2 mol % maximum) in the degradation of AC-MMA

copolymers (poly(35AC-co-65MMA)).

1.4.5 POLYEPICHLOROHYDRIN ELASTOMERS AND CHLORAL POLYMERS

a) Poly(epichlorohydrin)(PECH)

The thermal degradation of polyepichlorohydrin (PECH) and

of the 1:1 copolymer of epichlorohydrin and ethylene oxide, both in

the uncompounded and compounded form, has been studied in air and

nitrogen using TG.[72]   The structures of both polymers are shown

below:

$$\left[CH_2 - \underset{\underset{CH_2Cl}{|}}{CH} - O \right]_n \qquad\qquad \left[CH_2 - \underset{\underset{CH_2Cl}{|}}{CH} - O - CH_2 - CH_2 - O \right]_n$$
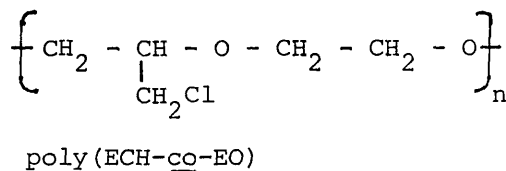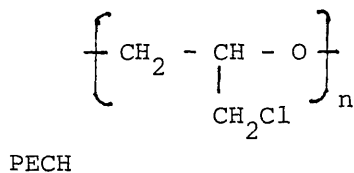
PECH   poly(ECH-co-EO)

TG results indicate that for both the homopolymer and copolymer, degradation (based on weight loss) occurs in one stage in air or nitrogen.   In uncompounded and compounded PECH and poly(ECH-co-EO), weight loss is first detected above 200°C and the rate increases rapidly at temperatures greater than 250°C.   HCl evolution begins, in all cases, at temperatures greater than 290°C and proceeds at a rapid rate in the temperature range 310-330°C.   The final HCl yield at 400°C amounts to 30-35% of that available for practically all the samples.   Relatively little difference ($\sim$10°C) is observed between the plots of % available HCl as a function of temperature for uncompounded and compounded homopolymer samples in either air or nitrogen.   This is also true for copolymer samples with the exception of the uncompounded sample, which appears to be rather more stable in nitrogen.

The production of HCl from PECH is a result of an elimination reaction occurring between the Cl atom in the pendant group and the tertiary hydrogen atom in the polymer backbone.   The reaction mechanism, forming unsaturated side groups, as adapted from reference 73 is illustrated below:

$$\text{\scriptsize \raisebox{0pt}{$\sim\!\!\!\!\sim$} CH}_2 - \text{CH} - \text{O} - \text{CH}_2 - \text{CH} - \text{O}\!\!\sim\!\!\!\sim \longrightarrow \sim\!\!\!\!\sim \text{CH}_2 - \text{CH} - \text{O} - \text{CH}_2 - \text{C} - \text{O} \sim\!\!\!\sim$$

$$\qquad\qquad | \qquad\qquad\qquad | \qquad\qquad\qquad\qquad\qquad | \qquad\qquad\quad \|$$

$$\qquad\quad CH_2Cl \qquad\qquad CH_2Cl \qquad\qquad\qquad\quad CH_2Cl \qquad\quad CH_2 \quad + HCl$$
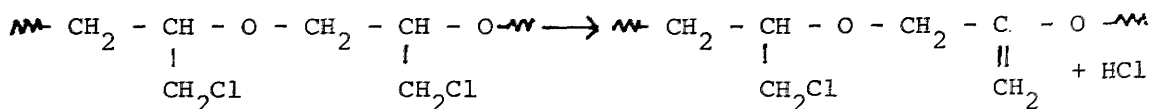
b) <u>Polychloral</u>

The thermal stability of polychloral depends strongly on the type of initiator[74] used in synthesis (i.e. whether it is anionic

or cationic polymerisation), which in turn determines the end groups present in the polymer, and on the post-treatment procedure (e.g. PCl_5 or acetylchloride) or end capping agents applied.[74]

Anionic Initiation Mechanism

Anionic initiators which are effective in the polymerisation of chloral may be divided into two groups:

(i) initiators which contain, or can produce in situ, a chloride anion which initiates polymerisation by adding to a monomer molecule:

$$Cl^- + \begin{array}{c} CCl_3 \\ | \\ C = O \\ | \\ H \end{array} \rightleftharpoons \begin{array}{c} CCl_3 \\ | \\ Cl - C - O^- \\ | \\ H \end{array} \qquad \text{(counter ion omitted)}$$
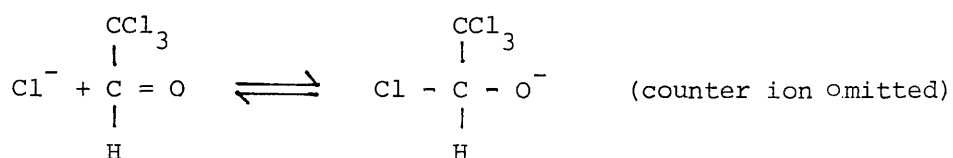
Examples of this group include stable organic salts containing Cl^- anion such as carbenium chlorides, sulphonium chloride and ammonium chloride, and also some inorganic salts e.g. lithium chloride.

(ii) salts which initiate polymerisation by the addition of an alkoxide ion:

$$\underset{\sim}{t} - BuO^- Li^+ + \begin{array}{c} CCl_3 \\ | \\ C = O \\ | \\ H \end{array} \rightleftharpoons \underset{\sim}{t} - Bu - O - \begin{array}{c} CCl_3 \\ | \\ C - O^- \\ | \\ H \end{array} Li^+$$
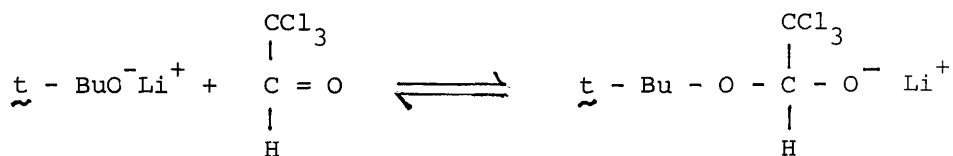
The most effective initiator in this group is tertiary butyl lithium.   Thus, depending on the choice of anionic initiator, it is possible to obtain chloral polymers containing known determined end groups at the beginning of the chain.   This is illustrated

below:

$$Cl - \underset{\underset{H}{|}}{\overset{\overset{CCl_3}{|}}{C}} - O \left(\underset{\underset{H}{|}}{\overset{\overset{CCl_3}{|}}{C}} - O \right)_n \text{~~~} \quad \text{or} \quad R - O - \underset{\underset{H}{|}}{\overset{\overset{CCl_3}{|}}{C}} - O \left(\underset{\underset{H}{|}}{\overset{\overset{CCl_3}{|}}{C}} - O \right)_n \text{~~~}$$
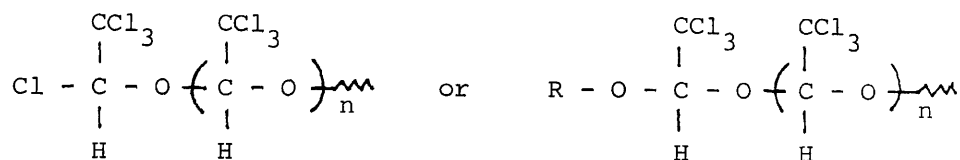
Cationic Initiation Mechanisms

Chloral can be polymerised by protonic acids.   Initiation involves protonation of the carbonyl oxygen of the monomer molecule:

$$H^+ A^- \; + \; O = \underset{\underset{H}{|}}{\overset{\overset{CCl_3}{|}}{C}} \; \rightleftharpoons \; H - \overset{+}{O} = \underset{\underset{H}{|}}{\overset{\overset{CCl_3}{|}}{C}} \quad A^-$$
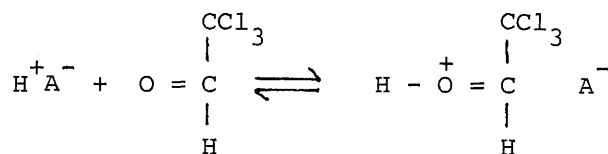
Thus cationic polymerisation results in the hydroxy-terminated structure

$$HO - \underset{\underset{H}{|}}{\overset{\overset{CCl_3}{|}}{C}} \left(O - \underset{\underset{H}{|}}{\overset{\overset{CCl_3}{}}{C}} \right)_n \text{~~~}$$
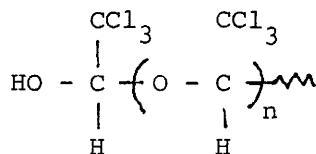
Post-treatment Procedures

In addition to the use of different initiators to produce specific initial end groups in polychloral, there are post-treatment procedures using end capping agents to produce the terminal end groups.   These end capping agents include PCl_5, and acetylchloride, which may act as either an acetylating or chlorinating species.   Post treatment usually leads to stabilisation of the polymer.

Thermal Degradation of Polychloral

The thermal degradation of polychloral is very similar to that of other polyacetals[75] in that the decomposition is initiated at the chain ends followed by depropagation to monomer. The DTG curves for a number of polychloral samples prepared by cationic or anionic polymerisation show peak maxima in one, or more than one, of four temperature regions [74] namely:

$170 \pm 15°C$, $\quad$ $210 \pm 15°C$, $\quad$ $300 \pm 15°C$, $\quad$ $340 \pm 15°C$

These temperature maxima are characteristic for specific types of end group which initiate degradation. The $170°C$ peak is dominant in samples prepared with tertiary butyllithium. Thus instability is associated with the $-CH(CCl_3)-O^-$ end group. The $210°C$ peak is present in all anionic preparations and cationic synthesized polymers initiated with H_2SO_4. The peak decreases with acetylchloride treatment (which produces an additional peak at $300°C$), and totally disappears to leave only a peak at $300°C$ on treatment with PCl_5. The disappearance of the sharp peak at $210°C$ in polymers prepared by a cationic mechanism together with the appearance of a peak at $300°C$ on treatment with acetyl chloride or PCl_5 indicates two points. Firstly decomposition at $210°C$ is due to the presence of hydroxyl end groups such as $-CH(CCl_3)-OH$ and secondly PCl_5 and acetyl chloride are acting as stabilising agents by replacing the less stable hydroxy terminal groups with $-Cl$ or $-CH(CCl_3)-OCOR$ groups which increases the degradation temperature to $300°C$. With acetyl chloride treatment however, incomplete stabilisation is obtained. The peak maximum at $300°C$ is also

indicative of the presence of $-CH(CCl_3)-OR$ end groups formed during

anionic polymerisation.   Further stabilisation of polychloral can be

achieved if the polymer is prepared using Ph_3P as initiator and

subjected to post treatment with PCl_5 in CCl_4.   This results in a

peak maximum at approximately $340^O C$ which is attributed to

$-CH(CCl_3)-Cl$ terminal groups.   A similar high temperature maximum

(about $350^O C$) is obtained for polymers synthesised using $SbCl_5$ as

initiator.   Thus it appears that polychloral containing chlorine

end groups is more resistant towards thermal degradation than polychloral

containing tertiary butyl ether, ester or hydroxyl end groups.

1.5   IMPORTANCE OF POLYMER DEGRADATION

In general, polymer degradation is thought of as a harmful

process which should be avoided or prevented as it results in the

deterioration in the properties of the polymer.   In the rubber

industry for instance, problems of "ageing" or oxidation of rubber

samples were restricting the use of rubber until the development of

suitable anti-oxidant systems.   A problem encountered in the

use of some synthetic vinyl polymers is that above a so-called

"ceiling" temperature the polymerisation process is reversed and

depolymerisation occurs resulting in the production of monomer.

In other cases low molecular weight decomposition products are

evolved.   This seriously limits the use of polymers such as

poly(methyl methacrylate) or polystyrene at high temperatures and

has thus encouraged investigations into the design of heat resistant

polymer structures.   One such polymer is poly(phenylene ether ether

ketone) or PEEK, illustrated below,
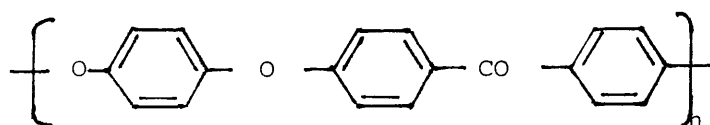
applications of which include high performance composites in the aerospace industry.[76]

The most devastating and destructive effect of polymer degradation concerns polymers in a fire situation. In some cases the polymeric substitutes are more flammable than the conventional materials they replace. The increased destructive capability due to flammability is exacerbated by the production of toxic gases and dense smoke. The use of polymers, particularly polyurethane foams, in the upholstry industry has resulted in numerous tragedies. Thus in a fire situation the cost of polymer degradation can be very high both in terms of loss of property and more importantly loss of human life. As a consequence intensive studies have been carried out into developing flame retardants and fire retarded polymers such as described earlier in this chapter, although much research is still required to understand fully the complex processes which occur in both the gaseous and condensed phases.

It must be noted, however, that polymer degradation is not always a disadvantage and is sometimes encouraged. This is typified by the aesthetically and environmentally unpleasing problem of plastic litter, whether it is on an industrial, commercial or domestic scale. It is due to the very nature of commercial packing material i.e. their water impermeability and non-biodegradable properties which limits, if not totally prevents degradation. In some cases it is possible to recycle polymer waste if the polymer readily depolymerises to give a high yield of monomer as was previously mentioned in the case of the thermal degradation of

poly(methyl methacrylate) and polystyrene.   Frequently, however, the waste consists of a number of polymeric components of which the majority do not undergo depolymerisation.   Nevertheless, as the importance of and emphasis on "environmentally friendly" products increases, the recycling of some polymer waste has become commercially viable.[77-79]   From an environmentalists point of view, polymers used for commercial packaging materials should ideally "self-destruct", that is to say eventually completely degrade when subjected to various environmental factors such as UV radiation and micro-organisms.   This has resulted in the development of commercial plastics with limited but reproducable life-times.

These biodegradable and environmentally degradable polymers are important in several agricultural, horticultural and medical applications which work on the basis of "time-controlled" degradation.   In the medical field this phenomenum is used in surgical sutures[80] and in controlled-release drugs.[80]   The major agricultural and horticultural function for these polymer based products is in short term crop protective films (mulching films). In mulch films, time-controlled degradation is brought about by additives which act both as antioxidants and photoactivators.   An example of such a compound is ferric dibutyldithiocarbamate (Fe(III) DBC)[81] which is used in conjunction with low density polyethylene.

Other instances in which polymer degradation is favoured include the manufacture of monomers.   Depolymerisation leading to high purity monomer may be exploited for practical production of these materials. The degradation of a polymeric material can also be used to produce compounds which have specific properties such as electrical

conductivity. Pyrolysis of several polymers, noteably phthalonitrile resins[82] results in environmentally stable, highly conductive materials which do not require the addition of external chemical dopants. The conductivity of these compounds can be varied and controlled as a function of both the pyrolytic temperature and annealing time. Carbon fibres have been industrially produced from poly(acrylonitrile)(PAN) and pitches.[83] PAN gives carbon fibres with excellent mechanical strength and low carbon yield.[84] Carbon fibres may also be prepared from syndiotactic 1,2-polybutadiene (s-PB).[85]

In conclusion, polymer degradation plays an important role in every life phase of a polymer, namely synthesis, processing, use and disposal. It also has marked effects on man and his environment. Thus the importance of studying its mechanism and relationships is evident.

CHAPTER 2 : THERMAL AND ANALYTICAL TECHNIQUES

2.1 THERMAL ANALYSIS

Experimental methods used to follow the progress of polymer
degradation reactions usually involve the direct measurement of loss
in weight or of the evolution of volatile degradation products.
Various commercial instruments are available which measure these
or certain other properties of polymers as they are heated
isothermally or under linear programmed temperature conditions.
These experimental techniques can be grouped together under the
description "thermal analysis".

When polymers degrade, a complex mixture of products results
in which a variety of different types of product can be distinguished.
Products may be volatile enough not to be condensed at liquid
nitrogen temperature ($-196^{\circ}C$), volatile at degradation temperature
but condensed at or below ambient temperature, or take the form of
involatile residues.   Reactions may also occur within the polymer
as a result of which no volatile material is produced.   Due to the
wide range of products formed, more than one technique has been used
to study the degradation of polymers in this research.   Most
emphasis is given to thermal volatilisation analysis as this is the
most versatile of the techniques employed and also allows study of
all the product fractions produced during degradation.

2.1.1   Thermal Volatilisation Analysis

Thermal volatilisation analysis (TVA) is a versatile
thermoanalytical technique which was devised and developed by McNeill
and has subsequently been the subject of a number of publications.[86-90]

The basic principle of TVA is the measurement of the pressure of volatile products produced during the degradation of a polymer sample which is being heated either at a constant rate, or isothermally. The sample, either in the form of a fine powder or a thin film cast upon the base of the degradation tube, is heated in a continuously pumped high vacuum system. As the polymer degrades, a pressure develops due to the evolution of volatile products as they distil from the sample to a cold trap some distance away. The change in pressure is measured by a Pirani gauge and recorded as a function of time or temperature, producing a measure of the rate of volatilisation of polymer. The system is shown diagramatically in Figure 2.1.

```
            ┌──────────┐
            │ Pirani   │
            │ Gauge    │
            └────┬─────┘
                 │
                 │
┌──────────┐     │      ┌──────────┐     Vacuum
│ Heated   │     │      │ Cold     │ ──▶  Pumps
│ Sample   ├─────┴──────┤ Traps    │
└──────────┘            └──────────┘
```
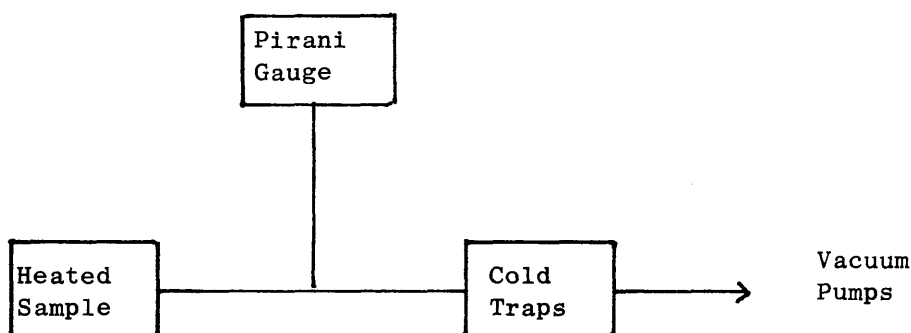
Figure 2.1   Principle of TVA System.

Differential Condensation TVA

In order to gain further information about the degradation products, the apparatus is modified to include a second cold trap B. This second trap is at a higher temperature than that of the original trap A and is placed between the sample and the Pirani gauge. Now

it is possible for degradation products, due to a difference in their volatilities, to condense differentially between the two traps.   This type of TVA is known as Differential Condensation TVA and is depicted in Figure 2.2.

$$T_B > T_A$$

Cold Trap A = $-196^{\circ}C$

Cold Trap B = 0°, -45°, -75° or $-100^{\circ}C$
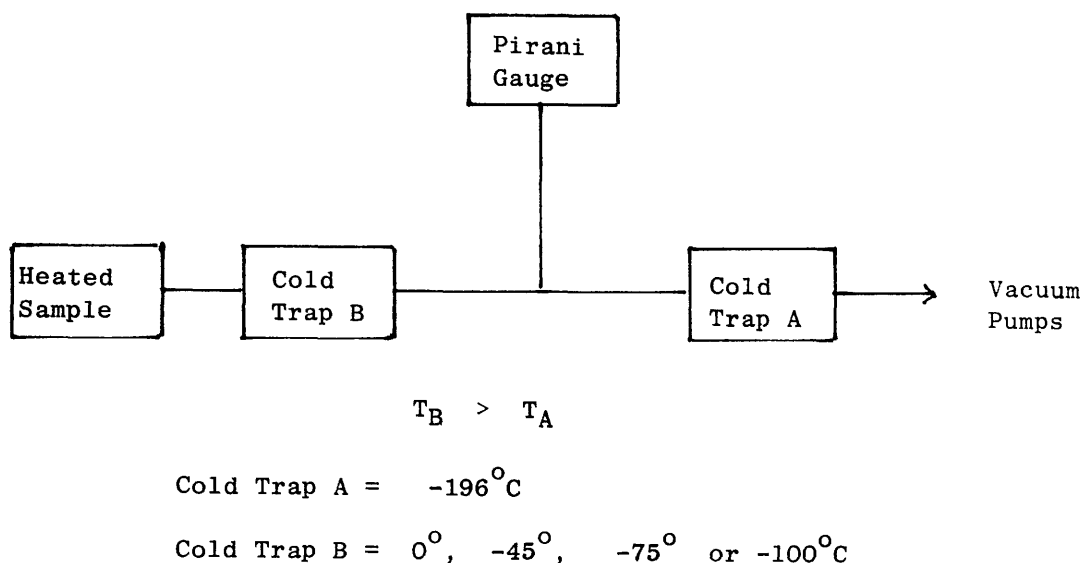
Figure 2.2   Principle of Differential Condensation TVA.

In practice a four parallel limb system is constructed in which the initial cold trap temperature in each line is different; the temperatures used in this work were 0°, -45°, -75° and $-100^{\circ}C$. Immediately following the cold traps are Pirani gauges which measure the pressure of condensable products which are not condensed out at these temperatures.   The four limbs then go through a main trap at $-196^{\circ}C$ and a Pirani gauge situated after this trap indicates the presence of any non-condensable products.   If the path lengths are equal, then equal amounts of volatile products enter each limb. Thus, if the Pirani gauges are matched, any deviation from

coincident read-out is due to differential condensation of the degradation products.

The TVA system used in these investigations is shown schematically and pictorially in Figures 2.3 and 2.4.

Details of TVA System

The sample heating assembly comprising oven, degradation tube and tube head is illustrated in Figure 2.5.   The oven used was a Perkin Elmer F11 oven coupled with a linear temperature programmer which allows the sample to be heated from ambient temperature to approximately $500^{\circ}C$ at heating rates from 1° to 40° min^{-1}.   Alternatively, the oven can be used isothermally.   In these studies, both heating modes were used and when the programmed mode was in operation, a heating rate of 10° min^{-1} was employed.

Oven temperatures were measured using a Type K thermocouple touching the external base of the degradation tube and having a 0° reference.   A Leeds-Northrup Speedomax W multipoint chart recorder was used to record the thermocouple millivolt output as well as that of the Pirani gauges.   Conversion of millivolt output to temperature was done using standard tables.

Due to the insulating effect of the Pyrex glass tube base, sample temperatures had to be obtained from temperature calibration curves plotted for each degradation tube.   In order to calibrate a degradation tube, a second Type K thermocouple was inserted via the calibration port until it was in good contact with the base of the tube.   The system was evacuated and continuously pumped to high vacuum, then heated as for TVA conditions whilst the oven and the

A:sample

B:stopcocks

C:cold trap
(0°,-45°,-75°,-100°C)

D:Pirani gauge

E:cold trap
(-196°C)

F:product
take-off point

vacuum
pumps
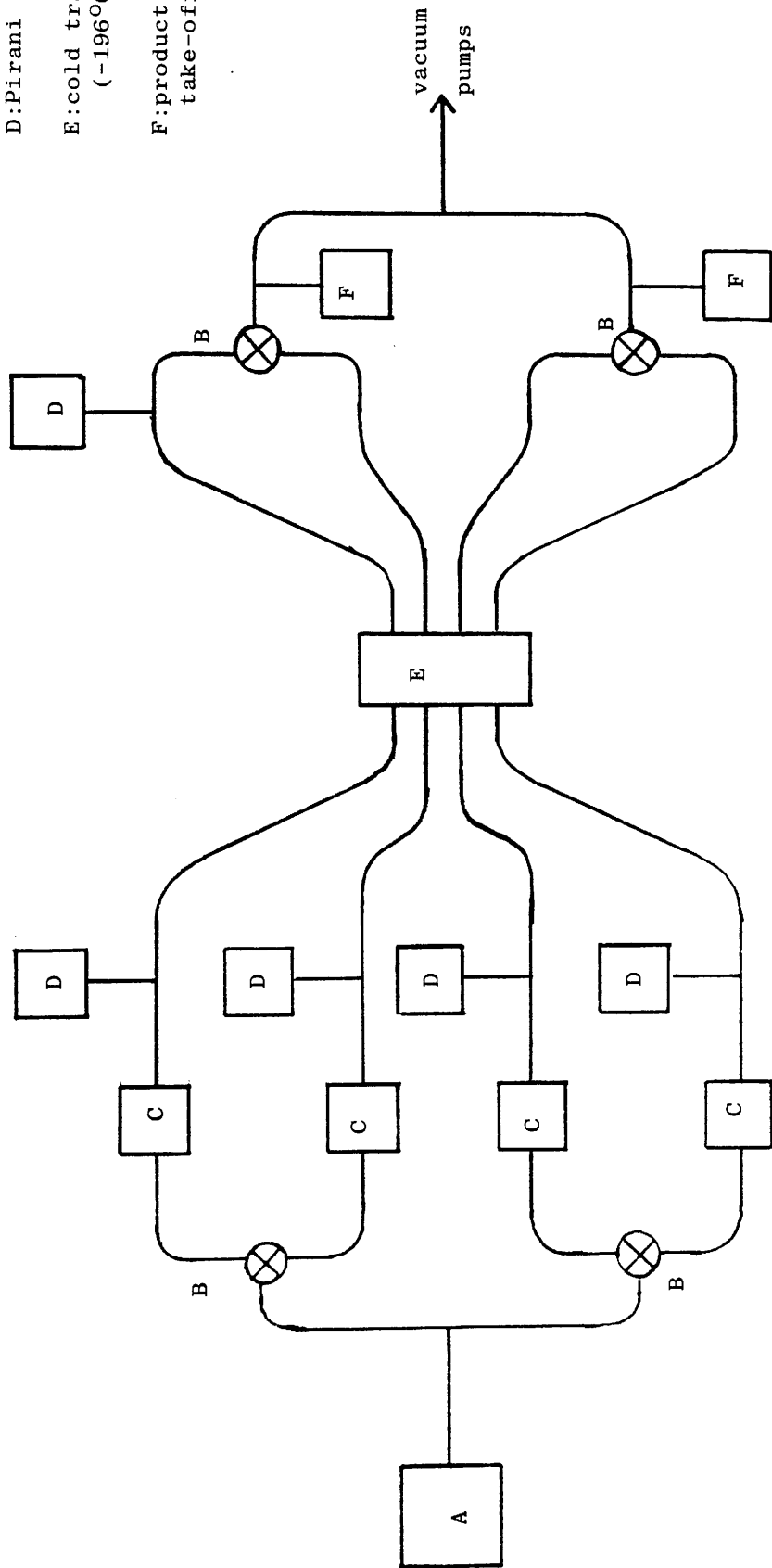
Figure 2.3   Parallel Limb Differential Condensation TVA System.
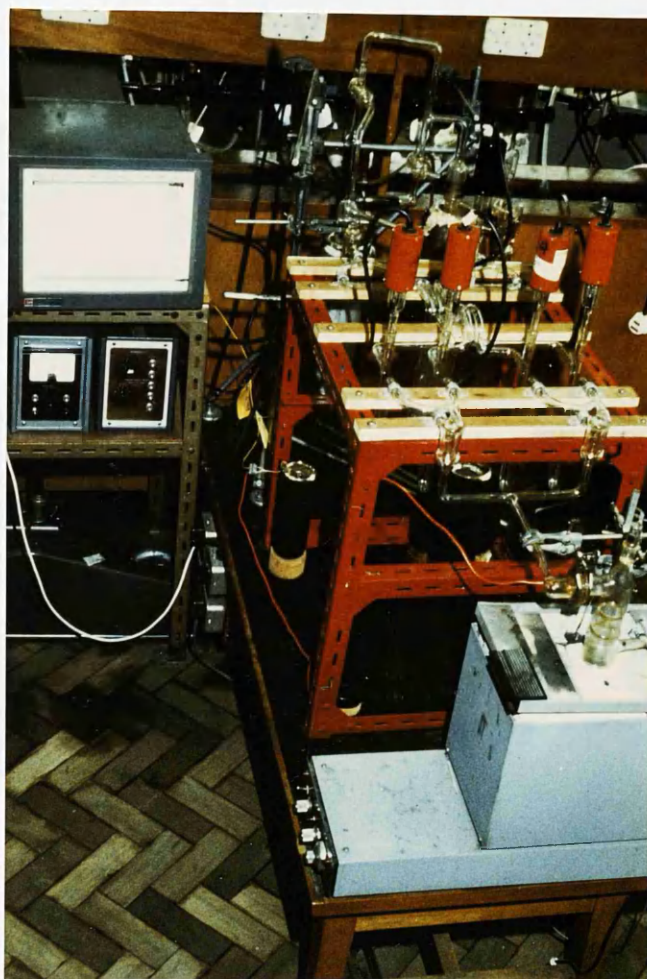
Figure 2.4a : Differential Condensation TVA System
illustrating parallel limbs.
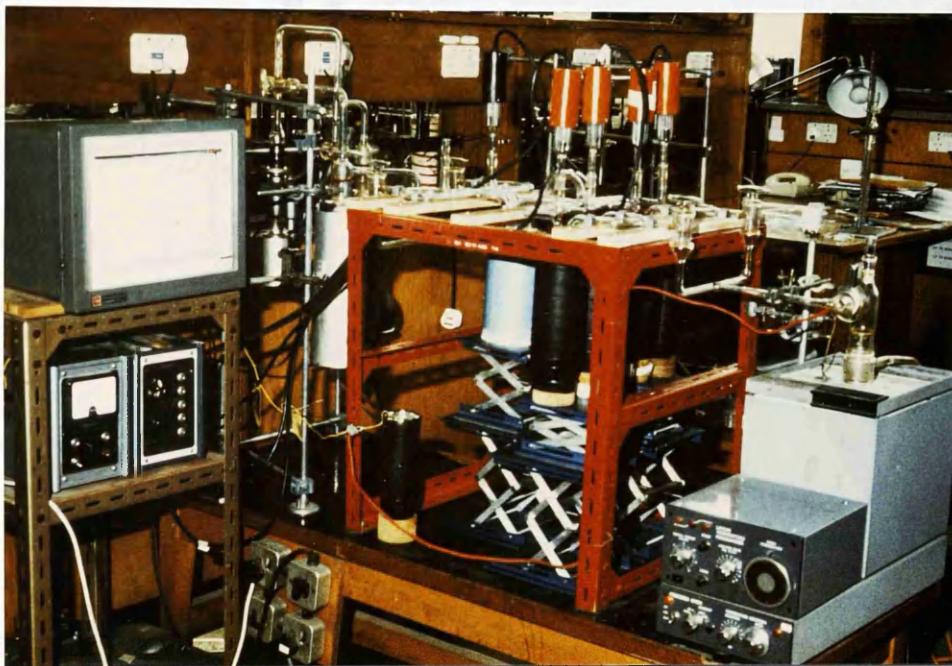
Figure 2.4b : Parallel Limb Differential Condensation
TVA System as in operation.

A:port for
   calibration
   thermocouple

B:ground glass
   flange joint

C:TVA tube head

D:B40 ground
   glass joint

E:water cooled
   jacket
   "cold ring"

F:oven thermocouple

G:oven

H:TVA tube

I:fan

J:temperature
   programmer
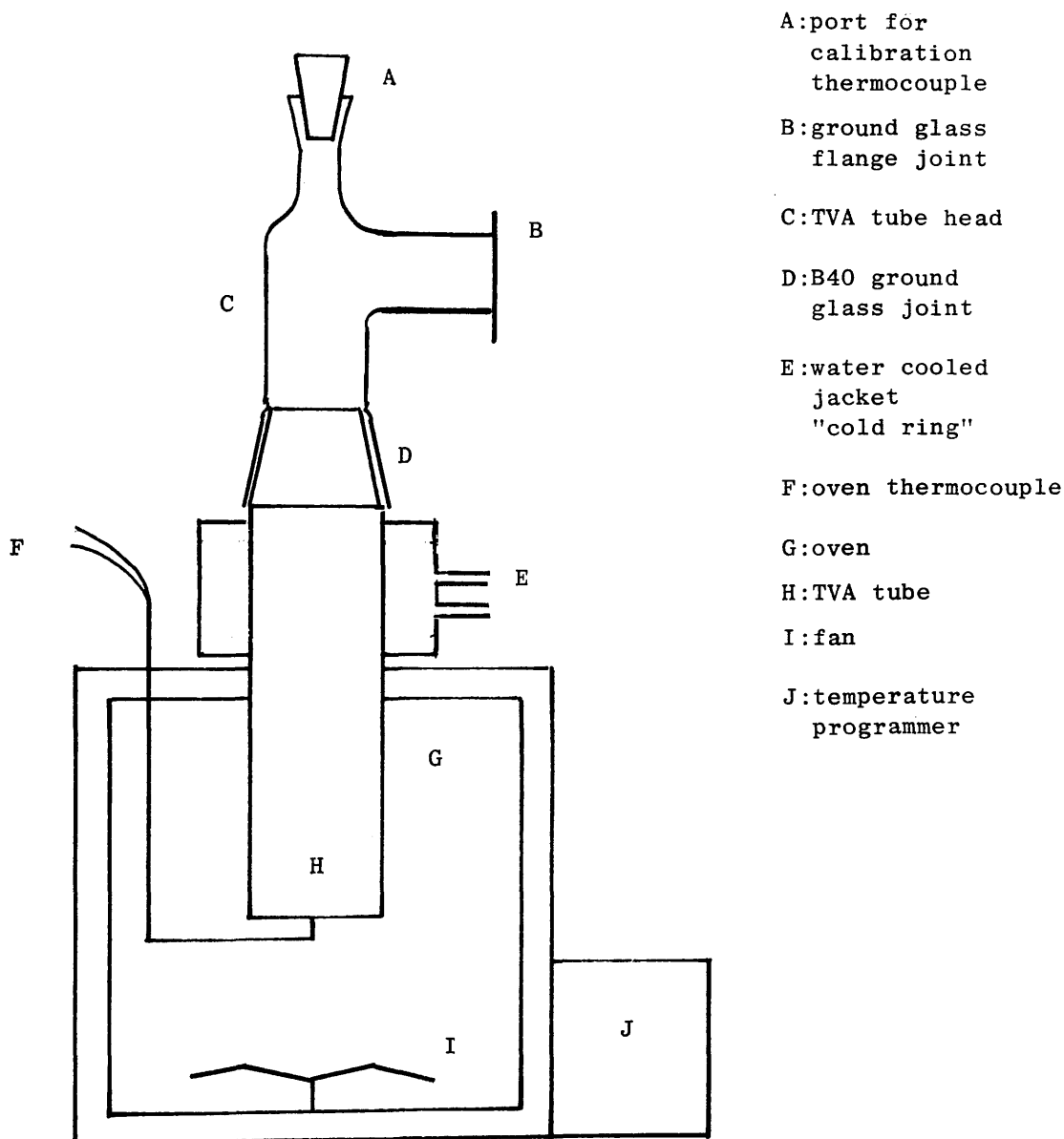
Figure 2.5 Oven and Degradation Tube Assembly.

tube base temperatures were simultaneously recorded. A typical calibration curve is shown in Figure 2.6. The temperature differential across the tube base was found to be approximately $25^{O}C$. Typical TVA tube base temperatures compared to oven temperatures when heated at a rate of 10° min^{-1} are reproduced in Table 2.1. Since the polymer samples were spread very thinly over the base of the tube, sample temperature can be taken as being equal to that of the internal tube base.

The TVA head assembly consists of a B40 ground glass joint into which fits the cone of the degradation tube, a B19 socket which acts as a port for the calibration thermocouple (and which is stoppered during TVA experiments) and finally a ground glass flange joint which connects with the parallel limb and pumping system. This tube head can be used for most samples, however for those that are hygroscopic a modified system had to be constructed. The replacement of the B19 socket with an SP10 single pump stopcock allows sample preparation to be carried out in a dry-box and subsequent transfer of the sample to the vacuum system to be made without contact with atmospheric moisture. A modified degradation tube head is illustrated in Figure 2.7.

As it is impossible to calibrate a degradation tube using the modified tube head arrangement, the modified tube head had to be built so that there was no alteration in the position of the degradation tube within the oven from that with the conventional tube head, once the assembly was connected.

Pressures were measured using Edwards G5C-2 Pirani gauge heads with Pirani 14 meter units. The output from each of the
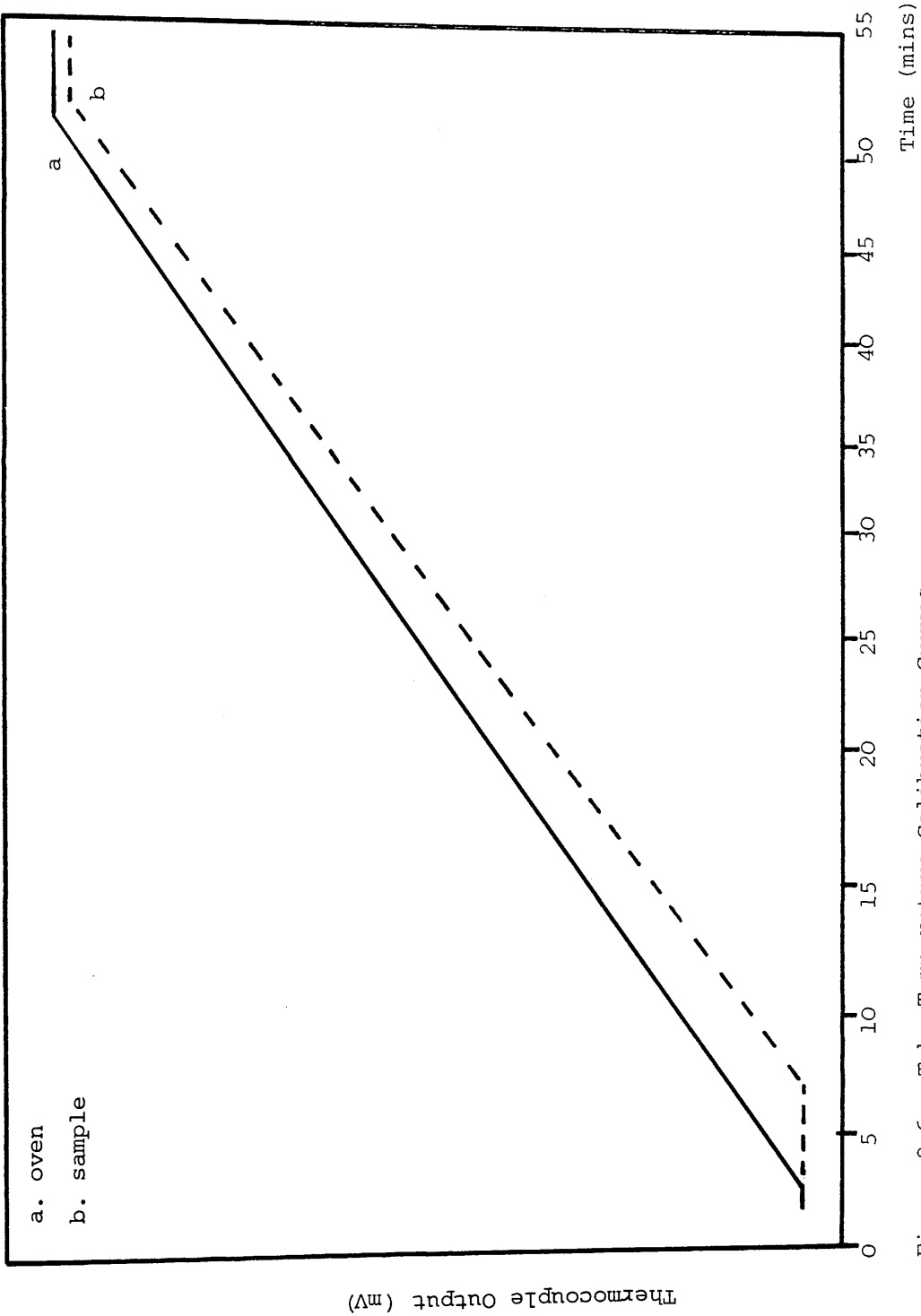
Figure 2.6 : Tube Temperature Calibration Curves

Pirani Output x 2.5 (mv)	Temperature (^oC)	Pirani Output x 2.5 (mv)	Temperature (^oC)
OVEN	OVEN	TVA TUBE	TVA TUBE
0.80	20	0.80	20
2.02	50	1.05	27
3.05	75	1.63	41
4.10	100	2.48	61
6.13	150	4.63	113
8.13	200	6.85	168
10.16	250	8.95	221
12.21	300	11.08	273
14.29	350	13.13	322
16.40	400	15.28	374
18.51	450	17.45	425
19.58	475	18.60	452
20.01	485	19.45	472
20.43	495	20.15	489

Table 2.1 Comparison of Oven Temperatures and TVA Tube base Temperatures at a heating rate of 10° min^{-1}.
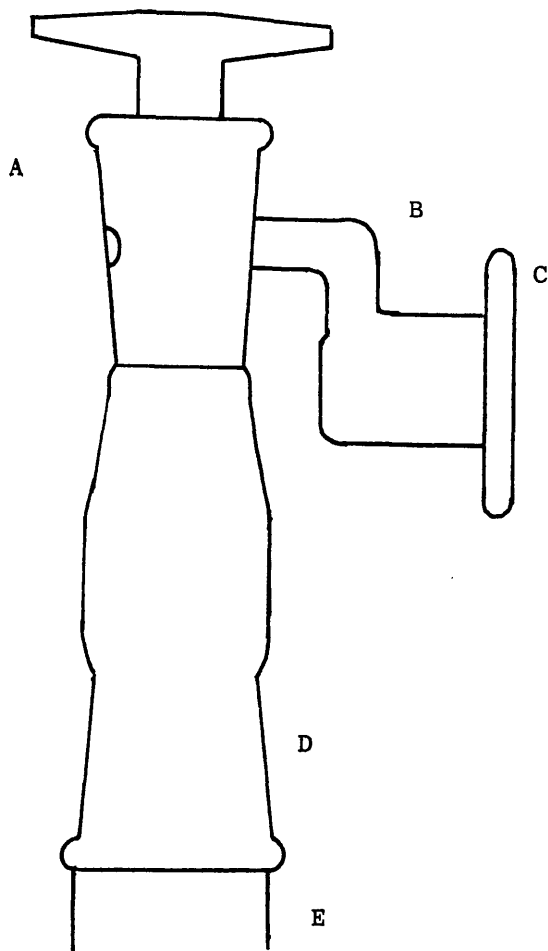
A: SP10 single pump stopcock

B: glass connected to maintain tube height

C: ground glass flange joint

D: B40 ground glass joint

E: degradation tube

Figure 2.7 Modified Degradation Tube Head

five Pirani gauges in the TVA system had to be matched, thus the gauges were cross calibrated in the following manner.

The line was thoroughly evacuated and cold traps were put in place as for a normal TVA experiment. Once under high vacuum (as indicated by a vacustat gauge), the line was isolated from the pumping system and dry nitrogen was introduced. The line was re-opened to the pumps until a pressure reading of approximately half full scale output (the maximum usually achieved during a degradation) was recorded whereupon the line was once more isolated from the pumps. The outputs of the Pirani gauges were brought into coincidence using variable resistances. The line was then evacuated in stages with the coincidence being checked at each step. A test run was carried out in which a sample of potassium permanganate was degraded. The volatile product evolved is oxygen which, in small amounts and under these highly evacuated conditions, is non-condensable at -196°C. Thus the oxygen passes through all five cold traps and the five Pirani gauge outputs should be coincident.

The TVA system is not well suited for quantitative analysis as the Pirani gauge response is only linear over a range of 0-1.5mv while a normal 35-50mg sample gives a Pirani output of 4-5mv on degradation. In addition, the output depends upon the compound produced. However, important qualitative results and insight into the number of degradation processes involved are obtained. The information obtained from a TVA curve includes the onset temperature of evolution of volatile products, T(onset), the temperature of the maximum rate of evolution of volatile products,

T(max), and some idea of the nature of the products produced via the comparison of the behaviour of the various individual Pirani traces. One valuable feature is the ability to indicate a change in product composition during degradation. Furthermore, provided there is sufficient temperature difference or resolution between subsequent peaks, a TVA curve can indicate multistage degradation processes.

TVA Product Analysis

The products arising from the degradation of a sample in the TVA apparatus fall into two main categories viz:

(a) involatile residue

(b) volatile products

The volatile degradation products can be sub-divided into three classes namely:-

(1) Products volatile at the temperature of degradation but involatile at ambient temperature. These collect on the portion of the degradation tube outside the oven which is cooled by the water-jacket. This class of product is referred to as the cold ring fraction or CRF.

(2) Products volatile at degradation and ambient temperatures but condensable at -196°C. These are referred to as condensables.

(3) Products volatile at -196°C. These products are referred to as non-condensables.

The residue may be removed from the base of the tube and analysed by infra-red spectroscopy. This may be done by dissolving the residue in a suitable solvent if possible and obtaining an infra-red spectrum either as a solution or as a film cast onto a salt plate.

Alternatively, insoluble residue can be scraped off the tube base and ground to a fine powder prior to forming a Nujol mull or KBr disc.   If there is insufficient residue or the residue is difficult to remove, then previously ground KBr can be added to the residue and the two ground together in the degradation tube.

The CRF usually consists of high boiling chain fragments of low volatility which may take the form of oils, tars or waxes.   In some systems, crystalline material may be deposited by sublimation. Depending on its nature, the CRF may be directly removed for analysis by scraping with a spatula then smearing onto a NaCl plate, or, if the sample is solid, making a KBr disc.   Alternatively, the region of the tube may be wiped with a tissue moistened with a suitable volatile solvent, from which the CRF may be deposited on a salt plate.

Volatile products which are condensable at -196°C may be collected by closing the taps to the pumps after degradation and distilling the products into a suitable collection vessel (attached at point F in Figure 2.3).   The total condensable products can then be analysed by infra-red spectroscopy, mass spectrometry or gas chromatography.   For infra-red spectroscopy a gas cell, shown in Figure 2.8 is used.   Figure 2.8 ii) illustrates a gas cell in which less volatile liquid products collected in the side arm can be removed.   The condensable products can also be separated by subambient TVA for further examination, as discussed below.

Non-condensable products, typically hydrogen, oxygen, carbon monoxide and methane, which cannot be isolated in liquid nitrogen,

i)

A

B

C   C

D
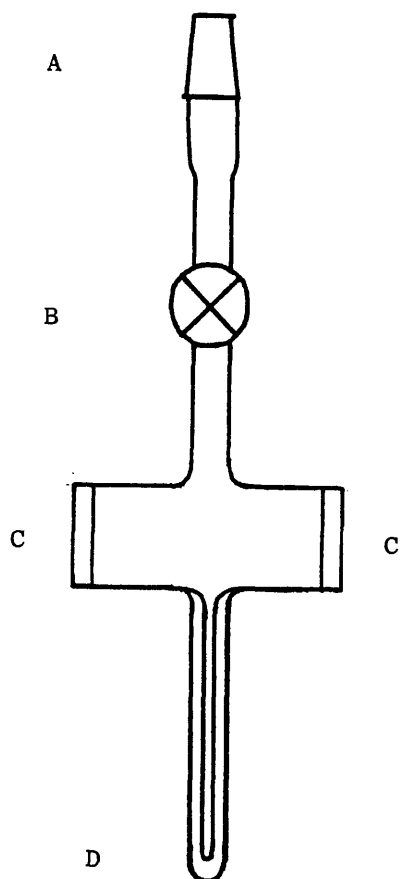
A: B14 cone

B: stopcock

C: NaCl window

D: collection finger

ii)

A

B

E

C

D
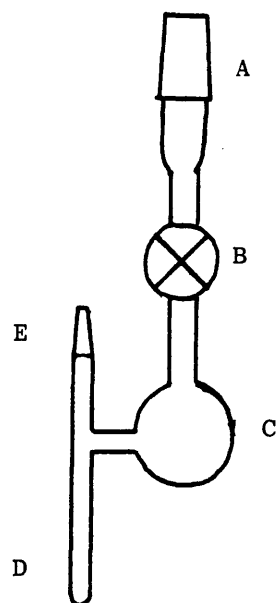
E: B10 cone to allow access to
   liquid products

Figure 2.8   Gas cell used for IR analysis of
              i) highly volatile gaseous products and
              ii) less volatile liquid products

may be collected if the degradation is carried out in a closed

system.   In these experiments a cross-tube is used.   This is

illustrated in Figure 2.9.   Samples are introduced, in either

powdered form or in solution to limb A.   Care has to be taken

not to leave any traces of sample in the construction at the top

of the limb as this would degrade on sealing the tube resulting in

gaseous product contamination and could possibly also prevent a

complete seal being formed.   With liquid samples, the solvent is

very gently removed under suction, then the cross-tube evacuated

to a pressure of $10^{-4} - 10^{-5}$ Torr, and finally sealed under high

vacuum.   The sample is now ready for degradation.   Degradation

is carried out using a TVA oven which has been modified to allow

a degradation tube to enter horizontally.   Thus, limb A of the

cross-tube is placed in the oven and the temperature monitored

directly using a Type K thermocouple connected to a Comark Digital

Thermometer Model 5000.   In order to remove condensable products,

a cold trap $(-196^{o}C)$ is placed around limb B before degradation

commences.   After degradation, the cross-tube and cold trap are

removed to a vacuum line onto which is incorporated a Topler

pumping system.   This pump is used in conjunction with the

Edwards speedivac EO1 Oil Diffusion Pump and Edwards speedivac

ED100 Rotary Pump present (which are in operation in the TVA system)

and its function is for the transferal of gaseous compounds from

one evacuated region to another.   Attached to the Topler pump is

a gas cell (at socket C in Figure 2.10) for the collection of non-

condensable gas.   The closed system containing the non-condensable

gas is connected via the cone indicated.   The Topler pumping

assembly is shown in Figure 2.10.
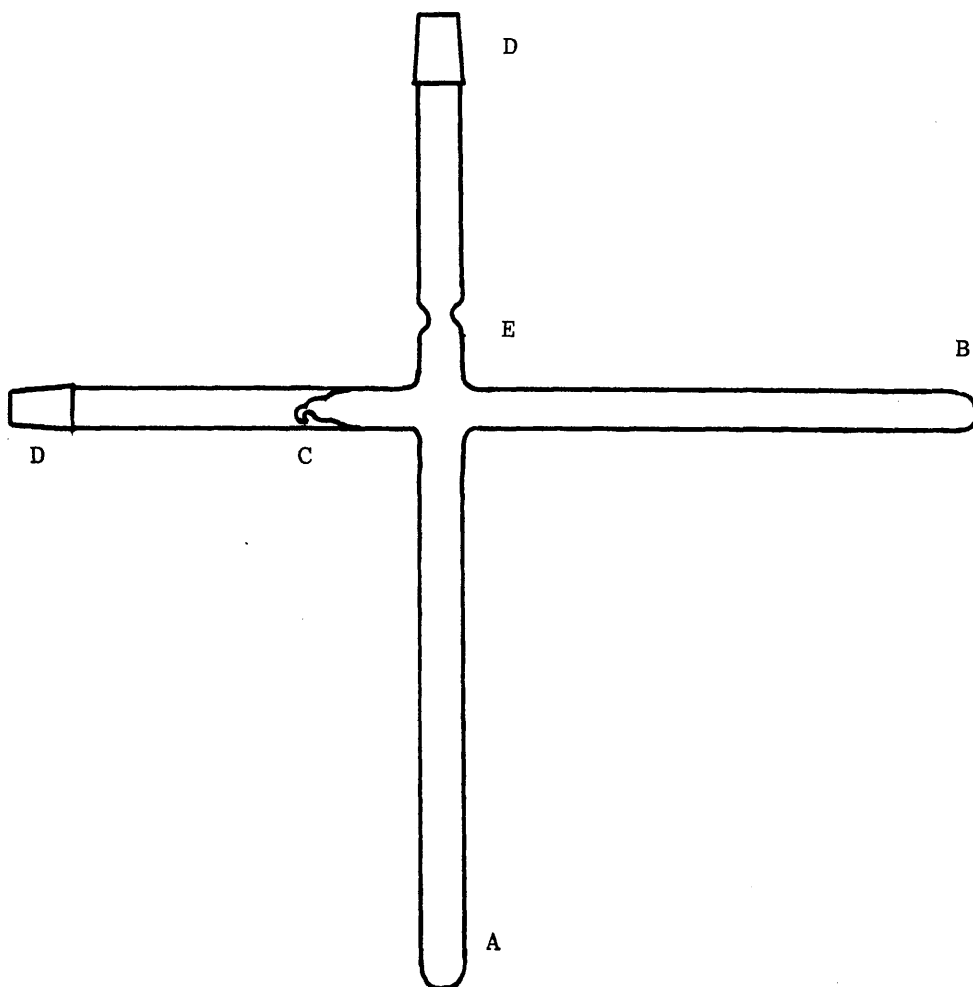
A: sample limb

B: condensable product limb

C: break-seal

D: B14 cone

E: glass constriction

Figure 2.9   Cross-tube for closed system degradations.

A,a1-a6 : stopcocks

B: B14 socket for attachment of
    cross-tube

C: B14 socket for attachment of
    gas cell.

D: double oblique tap

E: mercury reservoir

F: pumping chamber

G: gas cell

H: Pirani gauge

I: valve
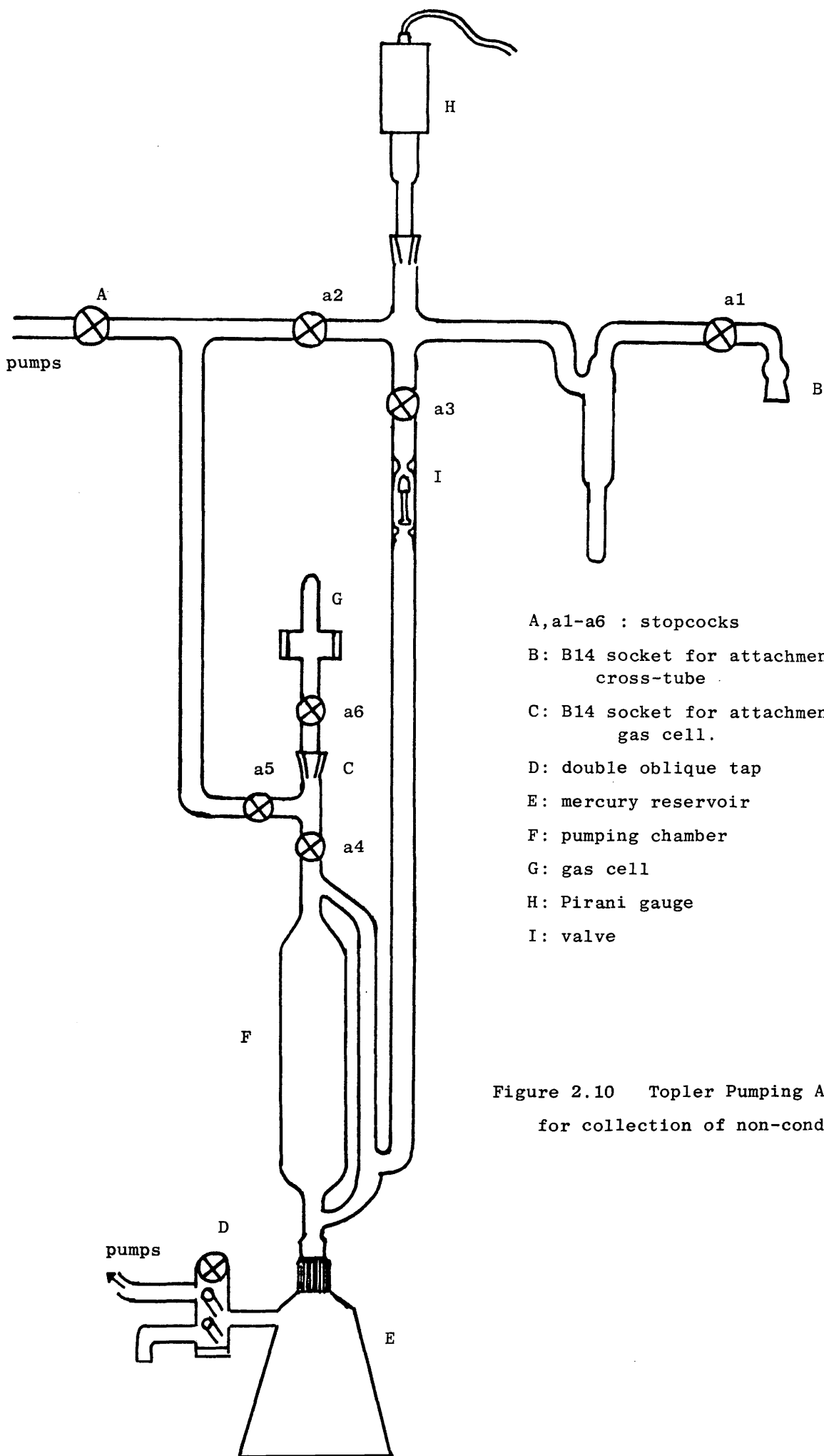
Figure 2.10   Topler Pumping Assembly
for collection of non-condensable ga

Before the break-seal is broken, the gas cell and Topler pump must be fully evacuated. This is done by opening all stopcocks and having the double oblique tap open to the rotary pumps. Once the assembly system has been evacuated, it is isolated from the pumps by closing stopcock A, and the double oblique tap. Stopcocks A_2 and A_5 are also closed to reduce the volume into which the non-condensable gas will be released. Mercury is then pushed into the pumping chamber by carefully opening the double oblique tap to the atmosphere. The sealed cross-tube can now be opened via the break-seal. The gas evolved is drawn into the pumping chamber by lowering the mercury, which is done by opening the double oblique tap to the pumps. After closing stopcock A_3, the non-condensable products are forced into the gas cell on raising the mercury. The stopcock on the gas cell (A_6) is closed to prevent removal of the gaseous products and the cycle repeated a minimum of three times to ensure transfer of material. The gas cell can then be removed and the contents analysed by infra-red spectroscopy or mass spectrometry.

A less time consuming method which can also be used to detect and identify non-condensable (and condensable) products is to bleed the gas, as it is evolved, into a quadrupole mass-spectrometer attached to the TVA line via a T-junction between the main traps and pumping system. This arrangement is extremely useful for multistage degradations, however, due to technical difficulties with the quadrupole instrument, this option was not always available, thus the previously described system was mainly used.

2.1.2 Subambient TVA (SATVA)

During a TVA experiment, the degradation products can be separated into residue, cold-ring fraction, condensable and non-condensable products. Valuable information on the mechanism of degradation may be obtained by identifying all the condensable products. However, if the total condensable products are examined there can be difficulties in product identification due to the overlap in spectral bands of different compounds. In order to overcome these limitations, a method has been devised to separate condensable products. Developed independently by McNeill et al[91] and Ackermann and McGill,[92-94] the technique is based on the separation of a frozen mixture using differences in component volatilities as the compounds are warmed in a controlled manner from $-196^{\circ}C$ to ambient temperature under continuously pumped vacuum conditions. The process is known as subambient thermal volatilisation analysis or SATVA. The main features of a SATVA system are illustrated in Figure 2.11
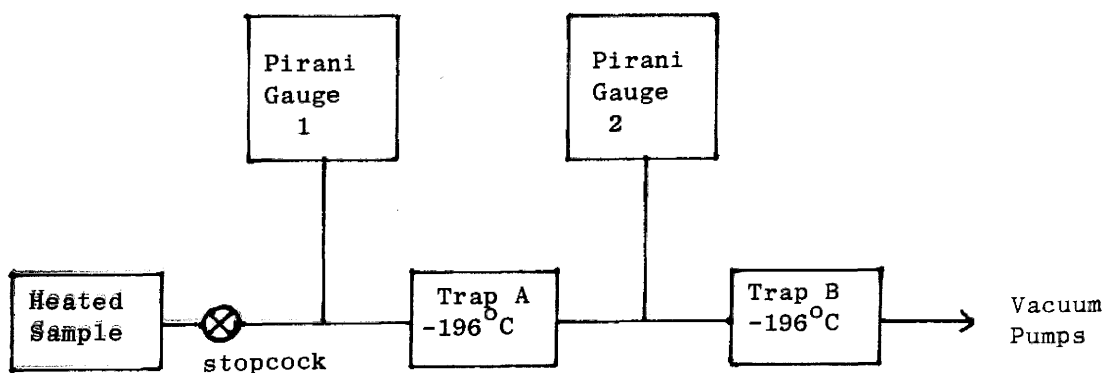
Figure 2.11   Principle of SATVA System.

During a SATVA separation of the condensable products obtained in a TVA experiment, the system is also continuously evacuated.   Trap A, referred to as the subambient trap, is cooled to -196°C.   The trap (shown in Figure 2.12) consists of a U-tube and is surrounded by glass beads contained in a Pyrex glass vessel which is submerged in liquid nitrogen.

Once the subambient trap is at a temperature of -196°C, the Pirani gauges are at zero response (high vacuum).   The pressure of condensable volatile products as they evolve on degradation can be monitored using Pirani gauge 1.   When the condensable products have been collected, the stopcock (Figure 2.11) is closed, Pirani gauge 1 switched off and the liquid nitrogen is removed from the subambient trap and placed around trap B.   The subambient trap then warms up to ambient temperature.   It must be noted that the rate of warming is not linear but is reproducable for a subambient trap provided that the glass beads are not altered. As the trap warms up, products distil from the trap into trap B as the temperature becomes high enough for each product to vaporize.   The pressure response in Pirani gauge 2 during distillation and the subambient trap temperature are recorded as a function of time. Resolution of distillation peaks may be enhanced by increasing warm-up time.   This can be done by placing a chilled Dewar flask around the subambient trap.   However in some cases peak overlap is unavoidable.   Furthermore, a single peak may be due to simultaneous evolution of several materials of similar volatility.   Despite these possible limitations, the technique is extremely useful and experimentally simple and convenient.

sample

pumps
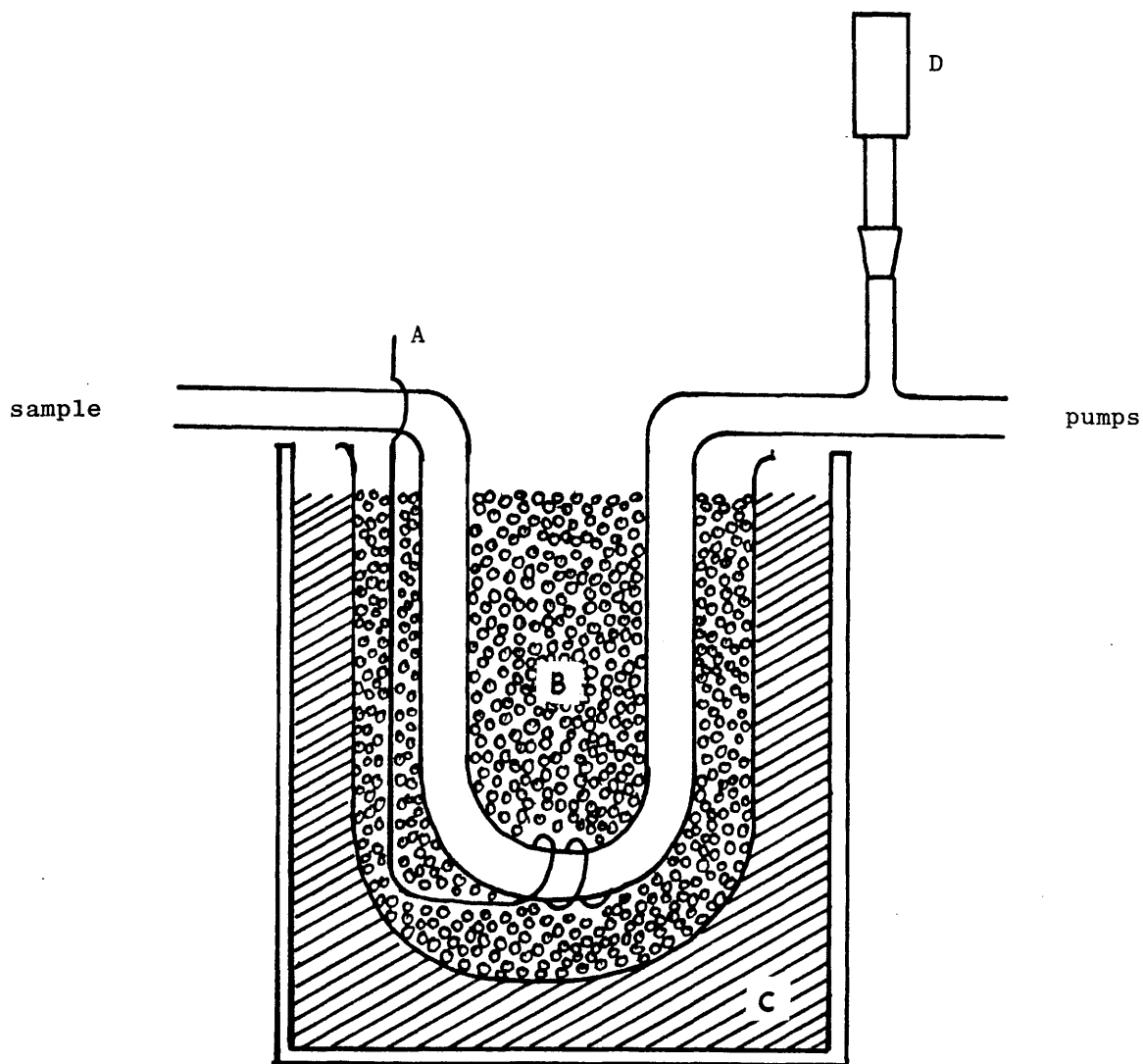
A: type K thermocouple

B: 2.5mm glass beads in pyrex flask

C: liquid nitrogen

D: Pirani gauge

Figure 2.12   Subambient Trap.

Products giving individual SATVA peaks may be isolated by use of a parallel limb system represented in Figure 2.13. In this arrangement, stopcocks A-C are closed after collection of the total condensable products. Product(s) responsible for the first SATVA peak are distilled onto the -196°C trap. At the minimum point of the trough between subsequent SATVA peaks, stopcock C is opened to allow the collection of the second SATVA peak and stopcocks d and h closed to isolate the degradation product(s) of the first peak. This process is repeated in each limb. The products are collected by distillation into suitable vessels-gas cells (Figure 2.8) for the more volatile products of the first peaks and cold fingers (Figure 2.14) for the later, less volatile components (liquid fraction). The separated condensable products can then be removed for analysis by infra-red spectroscopy, mass spectrometry or gas liquid chromatography-mass spectrometry.

Quantitative Analysis of Cold Ring Fraction and Hydrogen Chloride.

The quantity of CRF and, in the case of chlorinated samples, HCl evolved were estimated after certain TVA experiments. The CRF was removed by swabbing the area covered in the TVA tube using a piece of tissue dampened with a suitable solvent. The tissue was then rinsed thoroughly into a previously weighed sample bottle. The solvent was removed firstly by blowing in a gentle stream of dry nitrogen and finally under vacuum until a constant weight for the bottle plus CRF was obtained. From this the weight % CRF produced per mg polymer degraded could be estimated.

HCl production was determined quantitatively during SATVA
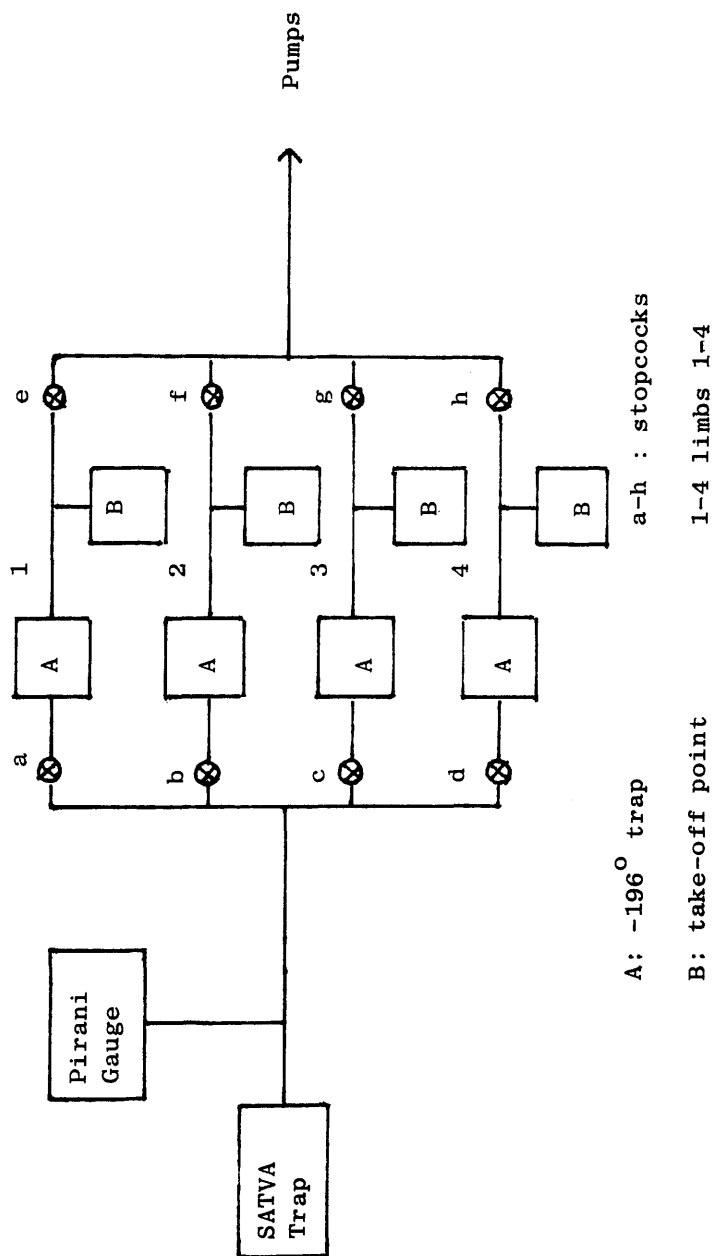
Figure 2.13 Parallel-Limb System used in isolation of products by SATVA

A: -196° trap

B: take-off point

a-h : stopcocks

1-4 limbs 1-4
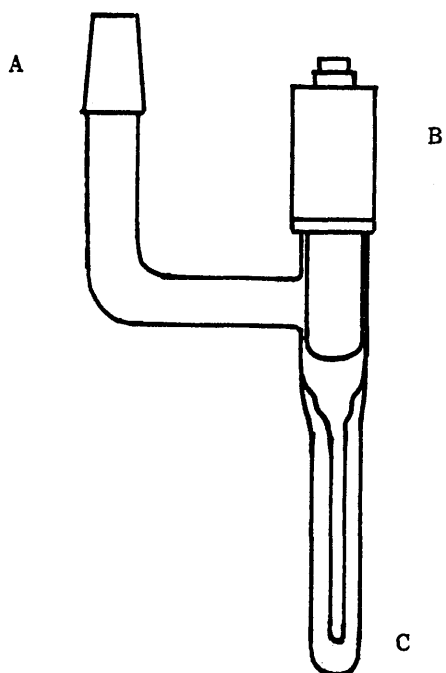
A: B14 cone for connection to SATVA system

B: rota flow tap

C: capillary tube

Figure 2.14 Cold Finger for collection of Liquid Fraction.

experiments in which the fraction containing HCl was condensed into a suitable medium and removed for subsequent titration. It was found that the first fraction in the SATVA trace for chlorinated poly(ethylene oxide) consisted of HCl and CO_2. Prior to degradation, 10ml 0.5-2N KOH solution were degassed on the SATVA line by repeated freeze-thawing cycles. The degradation was carried out as usual, however the HCl fraction was distilled into the KOH solution contained in a vessel submerged in liquid nitrogen. Once distillation was complete, the vessel was closed by means of a rota flow tap, the contents allowed to thaw at room temperature, mixed thoroughly and the solution complete with washings transferred to a volumetric flask. From this standard solution aliquots were taken, added to 50ml iso-propyl alcohol and neutralized with 0.5M HNO_3 using bromophenyl blue indicator. The solution was then made slightly acidic by the addition of 0.05M HNO_3, diphenylcarbazone solution was introduced as indicator and the solution was finally titrated with mercuric nitrate. Thus the chloride content present in the original solution was determined by the quantity of mercuric halide formed rather than from HCl/KOH titration.

2.1.3 <u>Thermogravimetry (TG)</u>.

In thermogravimetry (TG) the weight of a sample is recorded as a function of time or temperature. The TG curve obtained can give information on sample composition, (eg water of crystallisation) thermal stability and thermal decomposition. TG studies can be carried out in a variety of atmospheres, usually air or nitrogen, however moderate vacuum conditions are also available. This is useful for comparison with TVA results, but unlike TVA which only

records products volatile enough to reach the Pirani gauge, in a

TG experiment the weight loss is recorded from all volatile

products evolved from the sample pan.   TG used in conjunction

with TVA can thus be very useful in revealing chain fragmentation

without volatile product formation.

In some cases where multistage degradation occurs, it is

difficult to distinguish the various steps.   This can be

facilitated if a derivative of the TG curve is included.   The

technique yielding the first derivative of the TG curve is referred

to as differential thermogravimetry (DTG) and a DTG peak allows

the temperature at the maximum rate of weight loss to be obtained.

The system used in this research consisted of a DuPont 951

Thermobalance coupled to a DuPont 990 Thermal Analyser.   With this

arrangement both TG and DTG curves could be recorded simultaneously.

Degradations were carried out, usually under nitrogen, at a flow

rate of 50ml min^{-1} and heating from ambient temperature to $500^{o}C$

at 10° min^{-1}.   TG _in vacuo_ was also carried out for comparison

with TVA work.   The samples, 5-10mg, were in powder form when

pure polymers were investigated.   For studies of polymer-salt

blends, films were cast directly onto the sample pan from methanol.

Due to the hygroscopic nature of these films, preheat runs were

performed then the sample cooled prior to the full TG experiment.

The whole process was carried out in dynamic nitrogen.

2.1.4 Differential Scanning Calorimetry (DSC).

Whenever a material undergoes a change in physical state

such as melting or transition from one crystalline form to another,

or whenever it reacts chemically, heat is either absorbed or liberated. Many such processes can be initiated simply by raising the temperature of the material.

A differential scanning calorimeter is designed to determine the enthalpies of these processes by measuring the differential heat flow required to maintain a sample of material and a reference at the same temperature. Differential scanning calorimetry (DSC) involves heating a sample and an inert reference at a controlled rate. During heating, any process involving a change in energy of the sample will result in a difference in temperature between the sample and reference. The sample and reference are kept at the same temperature by the addition of heat to the cooler component. The difference in power input required to thermally equilibrate the system is recorded as a function of time and a DSC curve of dH/dT versus time, where H is the amount of energy supplied, can be obtained. In an endothermic reaction, the sample temperature lags behind that of the reference. This results in a negative deviation from the thermally equilibrated straight line trace. If an exothermic reaction occurs, a positive deviation is observed due to the relative increase in sample temperature.

The instruments used in this work consisted of a DuPont 910 Differential Scanning Calorimeter in connection with a DuPont 990 Thermal Analyser. The operating conditions used were heating at a rate of 10° min^{-1} from ambient temperature to $500^{\circ}C$ under a nitrogen flow of 50ml min^{-1}. Powder and film samples were prepared and used as for TG analysis.

2.1.5 <u>Definition of Terms used in discussing TVA, DSC and TG Data.</u>

In TVA, DSC and TG/DTG curves the temperatures of interest are the onset temperature of degradation, T(onset), and the temperature at which the maximum rate of degradation occurs, T(max). As there are different approaches possible in determining the above temperatures[95] the methods employed in this work are detailed below. However, although T(max) is clearly definable, T(onset) is always an approximate value since the onset of change is normally very gradual.

<u>TVA Curves</u>

The onset temperature in a TVA curve corresponds to the temperature at which volatile products begin to evolve on degradation. This is characterised by the elevation of one or more of the individual TVA traces from the base line. The peak maximum indicates the maximum rate of evolution of volatiles at that stage of degradation and from this T(max) can easily be obtained. When more than one degradation step occurs, the T(onset) of subsequent stages is taken as the turning point between consecutive peaks. A simplified single TVA trace (shown in Figure 2.15) illustrates these points. It should be noted however, depending upon the resolution between peaks, the T(onset) of any subsequent peak may not truly represent the temperature at which compounds begin to evolve in that stage.

Apart from degradation temperatures, information can be obtained about the nature of the volatile products in a TVA experiment from the differential condensation indicated by Pirani responses. A typical TVA curve is shown in Figure 2.16. The designations for the

RELATIVE RATE

Temperature (^{o}C)
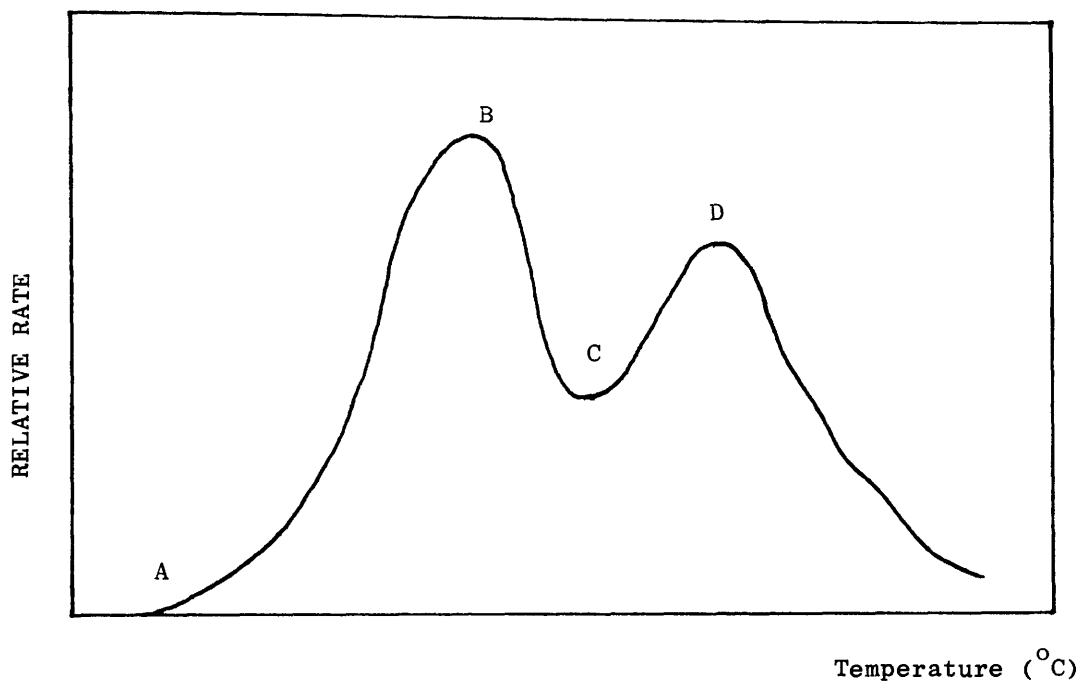
A: T(onset) of peak 1

B: T(max) of peak 1

C: T(onset) of peak 2

D: T(max) of peak 2

Figure 2.15 Single TVA Curve illustrating T(onset) and T(max)
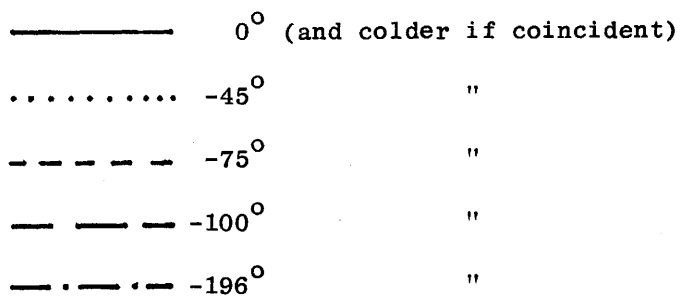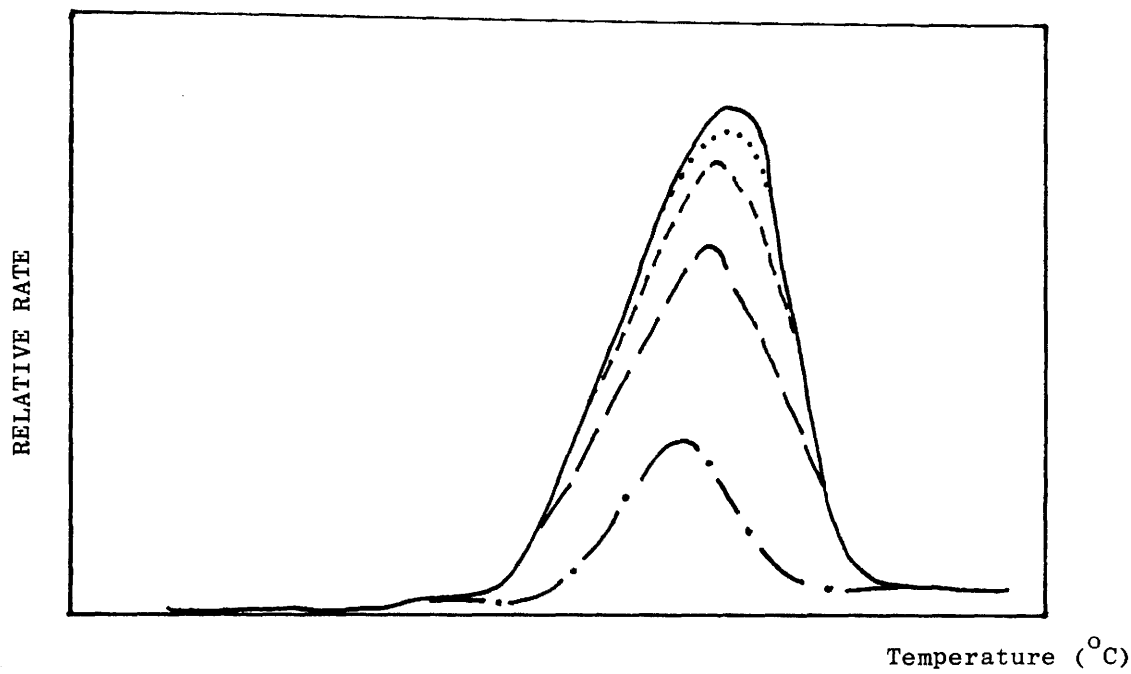
Figure 2.16 Typical TVA Curve

individual trap traces of the TVA curve illustrated are used throughout this thesis.

DSC Curves

Several methods can be used to evaluate the temperature onset in DSC curves.[95] The approach employed throughout this work is simply to define T(onset) as the temperature at which the curve deviates from the baseline. The peak maximum, T(max) and peak minimum, T(min) of exothermic and endothermic peaks can easily be obtained. This is illustrated in Figure 2.17.

TG/DTG Curves

The onset temperature obtained from a TG curve can be detected when the sample initially begins to lose weight. It can be designated as the point where the curve falls away from the 100% weight base line.

The maximum rate of weight loss is obtained from the peak maximum in the DTG curve. The TG-DTG curves of a two stage degradation process, defining the appropriate T(onset) and T(max) temperatures are presented in Figure 2.18.

2.2   ANALYTICAL TECHNIQUES

In conjunction with and in addition to the thermal analytical techniques employed, a number of other analytical techniques used are mentioned below.
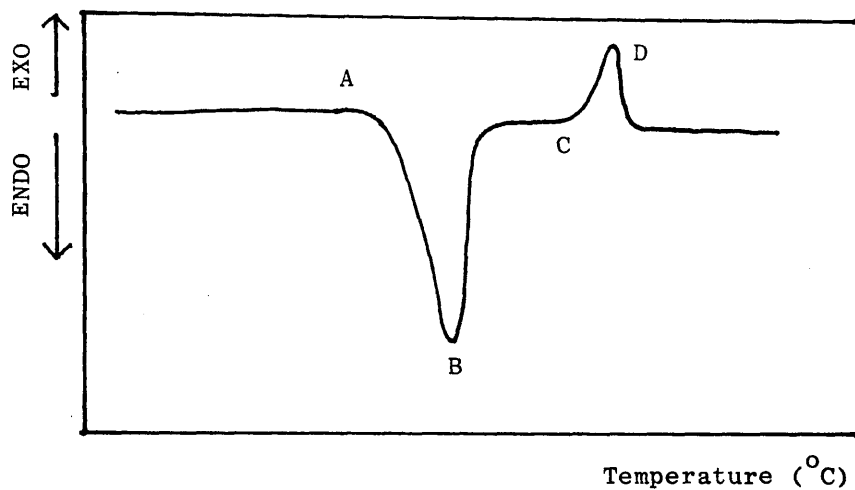
A; T(onset) of endothermic peak

B: T(min)   "

C: T(onset) of exothermic peak

D: T(max)   "

Figure 2.17   Typical DSC/DTA Curve illustrating T(onset), T(max)

and T(min).
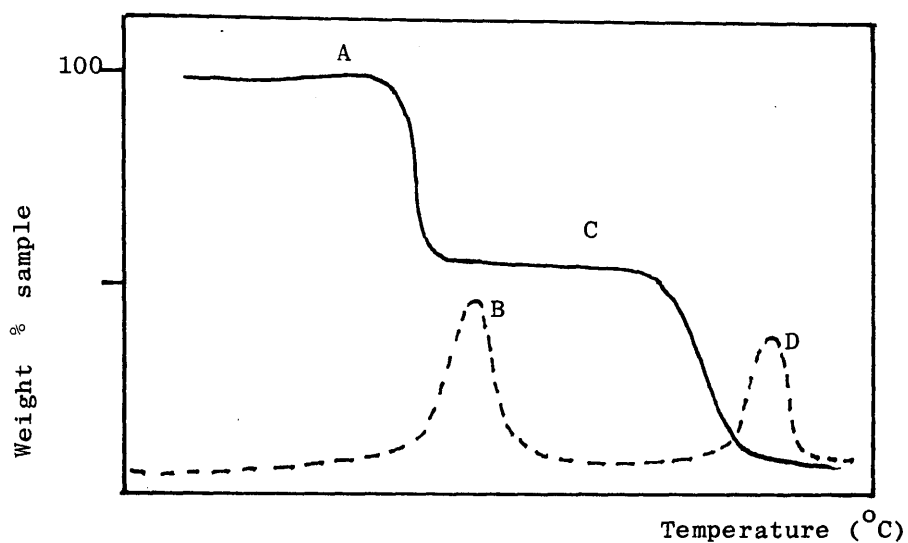
A: T(onset) of 1st weight loss

B: T(max)   "

C: T(onset) of 2nd weight loss

D: T(max)   "

Figure 2.18 Typical TG(-) and DTG (--) Curves illustrating T(onset)

and T(max).

2.2.1 Infra-Red Spectroscopy

Infra-red (IR) spectra were mostly obtained using a Perkin Elmer Model 257 grating spectrophotometer with range $4000-600cm^{-1}$. However, in some of the blend studies a wider range of infra-red frequencies was necessary for product identification.   In these cases a Perkin-Elmer Model 577 grating spectrophotometer having a range of $4000-200cm^{-1}$ was employed.

The undegraded polymer, CRF and residue were analysed by the KBr technique or as a film.   The KBr technique involves grinding a mixture of 2-3mg of sample with 300mg KBr (finely divided) and compressing it to form a circular disc.   Using a pressure of 8 tons per square inch, a disc of 13mm diameter and 1.5mm thick is obtained.   Films of the dissolved samples were cast onto NaCl or CsI_2 discs and the solvent allowed to evaporate.

Volatile gaseous products of degradation were studied using gas cells as shown in Figure 2.8.   Liquid degradation products separated by SATVA were collected in cold fingers (Figure 2.14) and examined as a film between sodium chloride plates.

After the assignment of infra-red absorption bands, the identification of degradation products was carried out, whenever possible, by comparison with spectra of authentic samples. Reference gas phase spectra were obtained from Weltis' book[96] and the paper by Pierson, Fletcher and Gantz.[97]   Solid and liquid phase organic reference spectra were obtained via the Aldrich[98] and Sadtler[99] catalogues of IR spectra.   The book by Nyguist and Kagel[100] was used as a source of reference spectra of inorganic compounds.

2.2.2 Mass Spectrometry

Two instruments were available for mass spectral analysis. The more convenient (unfortunately, however, less frequently available) instrument, a VG MicroMass QX200 quadrupole mass spectrometer, was coupled directly to a TVA-SATVA system. During degradation, (TVA process), non-condensable products could be bled into the mass spectrometer.   After separation by SATVA, samples of each condensable product fraction could be admitted to the spectrometer.   This method allowed the analysis of compounds with molecular weight of less than 150 a.m.u.

More commonly, separated fractions were removed from the SATVA line and analysed using a Kratos M512 single focusing mass spectrometer in conjunction with a DS55C data system.   Degradation products were identified where possible by comparison with reference spectra.[101,102]   Although the majority of fractions analysed consisted of a mixture of products, the reference spectra were of use in giving an indication of the relative importance of fragmentation ions and were of importance in showing whether a parent peak would be expected to be seen.

2.2.3 Elemental Analysis.

Chlorinated polymer samples (5-10mg) were characterised from elemental analysis performed on a Carlo Erba Model 1106 Elemental Analyser.   By this method weight percentage carbon, hydrogen and chlorine were calculated and the number of chlorine atoms per polymer repeat unit, X, was evaluated using the equations given below, based on the atomic weight of $Cl = 35.453$ and the formula

weight of each repeat unit, 44.053 for PEO and 104.150 for PS, as follows:

$$3545.3\chi = X(44.053 + 34.445\chi)$$

for chlorinated poly(ethylene oxide) and

$$3545.3\chi = X(104.150 + 34.445\chi)$$

for chlorinated polystyrene where:

X = weight % chlorine obtained by elemental analysis

χ = number of chlorine atoms per polymer repeat unit.

Elemental analysis was also carried out on some CRF and residue samples in conjunction with quantitative analysis in order to determine the chlorine distribution throughout those degradation products. A sample calculation for the estimation of the weight percentage chlorine present in CRF expressed per mg polymer sample is as follows:

total weight of Cl in CRF = mg CRF produced per 100mg polymer

X mg Cl per 100mg CRF x polymer sample weight

$$\text{weight of Cl in CRF per 100mg polymer} = \frac{\text{total weight of Cl in CRF x 100}}{\text{polymer sample weight.}}$$

2.2.4 Gas Chromatography - Mass Spectrometry

Liquid fractions obtained by SATVA were further separated after treatment when necessary (see chapter 3) using gas chromatography. This was carried out using a Perkin Elmer F11 Gas Chromatograph equipped with a 1.83m x 6.35mm O.D. coil glass column packed with 15% FFAP (free fatty acid phase) coated on gas chrom $\emptyset$

(mesh 100-120).   Nitrogen was used as a carrier gas with a flow rate of 40ml min^{-1}.   Samples were heated at a rate of 5° min^{-1} from 50°C to 220°C.   A flame ionisation detector was employed.

Compounds were identified by comparison of observed retention times to those of standard compounds, or from mass spectra obtained for each component.   This was made possible by using a LKB 9000 combined Gas Chromatograph-Mass Spectrometer (GC-MS) fitted with a DB-1 fuse silica capillary column (60m x 0.32mm 1D) and a solid injection system.   Helium was used both as carrier and make up gas, 7ml min^{-1} and 25ml min^{-1} respectively.   Mass spectra were recorded at 22 e.v. using an accelerating voltage of 3.5kv, a filament current of 4A and a trap current of 60mA.   The source and separator temperatures were both 270°C.   The column operating conditions were as reported.   It must be noted however that the solid injection system on the GC-MS was not best suited to the liquid samples introduced as low molecular weight compounds may have been lost on injection.   Nevertheless numerous minor and also major peaks were obtained in the GC-MS trace which could not have been separated by SATVA alone.

CHAPTER 3 : CHLORINATED POLY(ETHYLENE OXIDE)

3.1 INTRODUCTION

Before considering the effect of altering the chemical structure of poly(ethylene oxide) (PEO) by chlorination, it is important as a basis to understand the thermal behaviour of the pure unchlorinated polymer. Thus, initial investigations were carried out on the thermal degradation of PEO.

3.2 THERMAL DEGRADATION OF POLY(ETHYLENE OXIDE) - M.wt 100,000

3.2.1 Introduction

Ethylene oxide polymers are divided into two classes which are defined by molecular weight.[103] These molecular weights cover a broad range - from several hundreds to several million. Compounds in the lower molecular weight region i.e. with an average molecular weight of 200 - 200,000 are called poly(ethylene glycols) (PEG). Polymers with molecular weight of 1×10^5 - 5×10^6 are termed poly(ethylene oxide) (PEO). The division is somewhat arbitrary and is based on preparative method, commercial nomenclature, physical and chemical properties and uses of the polymer. PEG samples may take the form of viscous liquids up to hygroscopic solids. They are good lubricants and are used in metal working, urethanes, rubber chemicals, electronics, ceramics, pharmaceuticals and cosmetics. PEO samples are solids and are used in applications where water solubility and high viscosity are desired such as denture adhesives, lubricants, friction reduction, flocculation, packaging films and acid cleaners.

The thermal degradation and stability of polymeric derivatives

of ethylene oxide have been the subject of previous studies.

Madorsky and Straus[104] examined products of degradation, activation

energies and rates of degradation using PEG of molecular weight

9000 - 10000.   Bortel et al[105] on the other hand investigated the

degradation of high molecular weight PEO (m.wt. 1-3 x 10^6).   More

recently work has been carried out in our own laboratories by

Grassie and Mendosa[106] studying the thermal degradation of PEG of

molecular weight 1000 and 1500.   In each case it has been concluded

that the mode of degradation is via a radical chain mechanism; the

products of degradation of PEG and PEO are accounted for in terms

of, in the first instance, random C-O and C-C scission.   However,

in order to compare the effect of reactives (Cl substituents) and

additives (salts) on the thermal degradation behaviour of PEO and

also the possible effect of chain length on the thermal degradation

of PEO as compared with previous TVA/SATVA studies on PEG, a further

more detailed study has been undertaken, which is reported below.

3.2.2   Experimental

Purification of PEO.

The polymer used in the present investigations was a commercial

Aldrich sample of PEO with molecular weight 100,000 which before

purification was in the form of a free-flowing white powder.   PEO

was purified by dissolving in warm toluene followed by precipitation

from petroleum ether (b.pt 60-80°C).   This procedure was repeated

three times and the white solid was dried in vacuo at 40°C for 48

hours before subsequent analysis.   The PEO so obtained was not

so amenable to the grinding which would be necessary in the formation

of certain PEO-additive blends.   Thus the studies were made on both

purified and unpurified polymer samples.

Thermal Analysis of Poly(ethylene oxide) M.wt 100,000

TG, DSC, TVA and SATVA investigations were performed on appropriate sample sizes (4 - 100mg) of PEO.

TG

Thermogravimetry (TG) was carried out heating from ambient temperature to $500^{\circ}C$ at a programmed rate of 10° min^{-1}. Analysis was performed under a dynamic nitrogen atmosphere with a flow rate of 50 ml min^{-1} and also, in order for direct comparison of degradation temperatures with TVA results, in vacuo. The TG curves obtained are illustrated in Fig. 3.1. The TG curves indicate that in each case weight loss occurs in a single step during thermal degradation. Under nitrogen, weight loss begins around $314^{\circ}C$ for polymer samples prior to and after purification with the maximum rate of evolution of volatile products in both cases occurring at approximately $383-385^{\circ}C$. The residue after heating each sample to $500^{\circ}C$ is small, about 1.75 - 2.08% of the total weight of polymer sample degraded. When thermogravimetric experiments were carried out in vacuo similar degradation temperatures were again observed for both samples viz. $374^{\circ}C$ and $371^{\circ}C$ for the temperature of the maximum rate of weight for pre-purified and purified PEO respectively, some 10° lower than under nitrogen. However, degradation onset temperatures appeared to be slightly elevated in vacuo i.e. 324° and 321° accordingly.
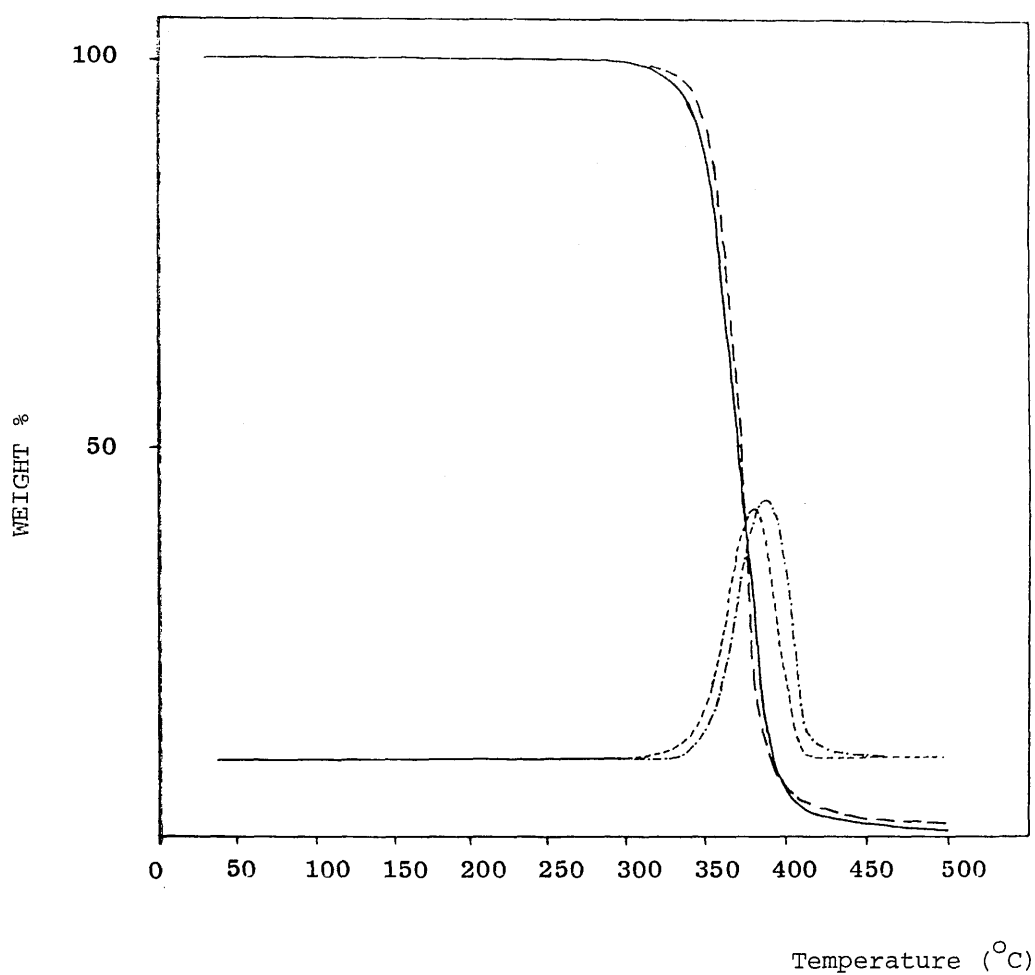
Fig. 3.1 TG Curves for PEO under nitrogen (-) and in vacuo (--) and
DTG curves for PEO under nitrogen (--) and in vacuo (-.-.)
at heating rate of 10° min^{-1}

DSC

The differential scanning calorimetry (DSC) curves exhibit two endothermic transitions as shown in Fig. 3.2. The peak temperatures occur at 68°C and 389°C (average) and can be assigned to melting point, T_m, and the maximum rate of degradation of the polymer, T_{max}, respectively. As for the TG results, differences between the original and reprecipitated samples were minimal.

TVA

The thermal volatilisation analysis (TVA) curve in Fig. 3.3 obtained for a 50 mg powder sample shows that during the thermal degradation of PEO, the evolution of volatile products commences at 310°C and continues to form a single peak with a maximum value corresponding to the temperature at the maximum rate of product evolution at 372°C (average).

The individual TVA trace based on the responses of the gauges after the traps at 0°, -45°, -75° and -100°C were non-coincident indicating the evolution of a mixture of products of different volatilities. The presence of non-condensable products is indicated by the -196°C trace rising from the baseline. On the water cooled region of the TVA tube was collected a viscous pale yellow cold-ring fraction (CRF). The formation of CRF began around 360°C. Occasionally, at the highest temperatures during a TVA experiment, the oily CRF ran down the walls of the TVA tube and was further degraded. To prevent confusion of primary and secondary degradation products, heating was discontinued immediately after the evolution of volatile materials had ceased ($\sim$ 450°C). The
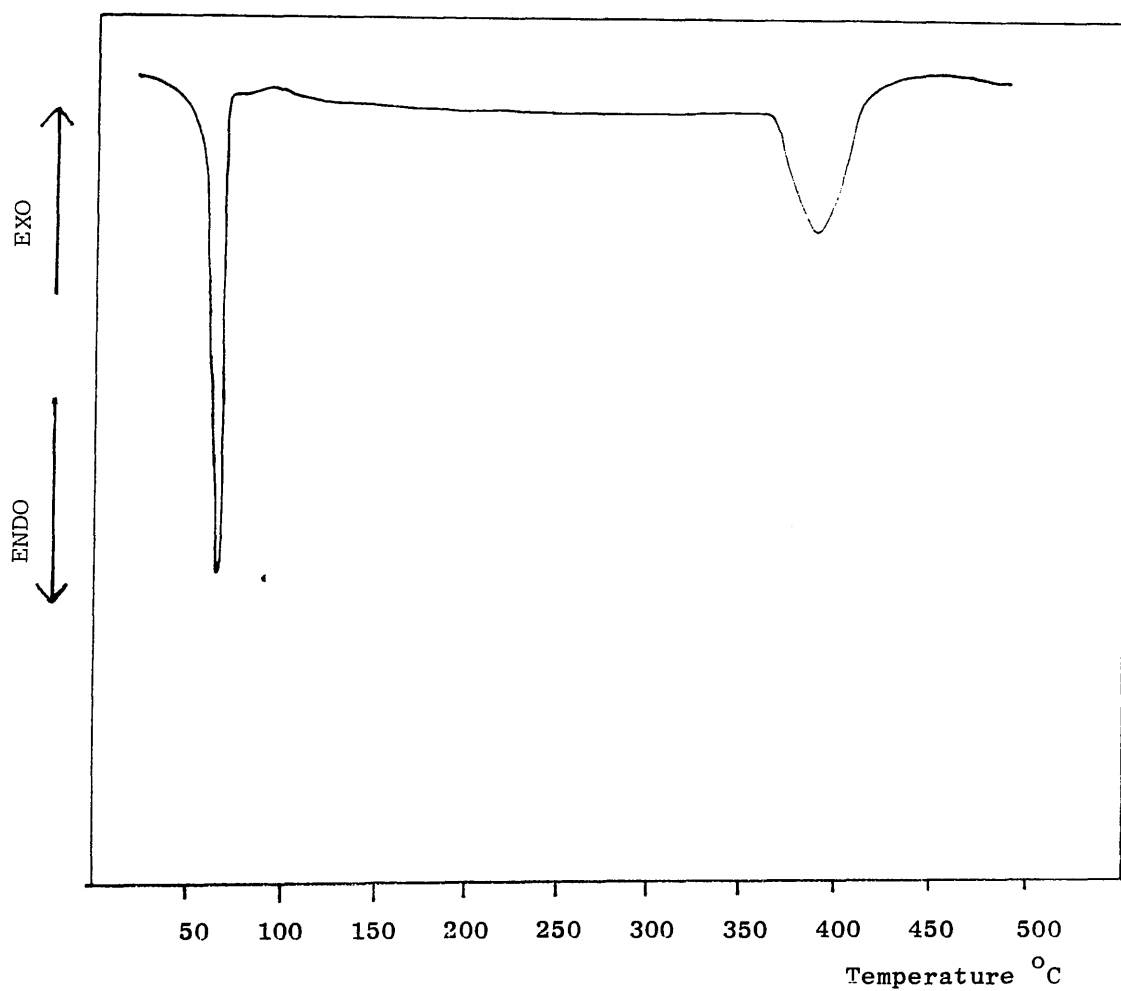
Fig. 3.2 DSC curve for PEO under nitrogen at a heating rate of 10° min^{-1}
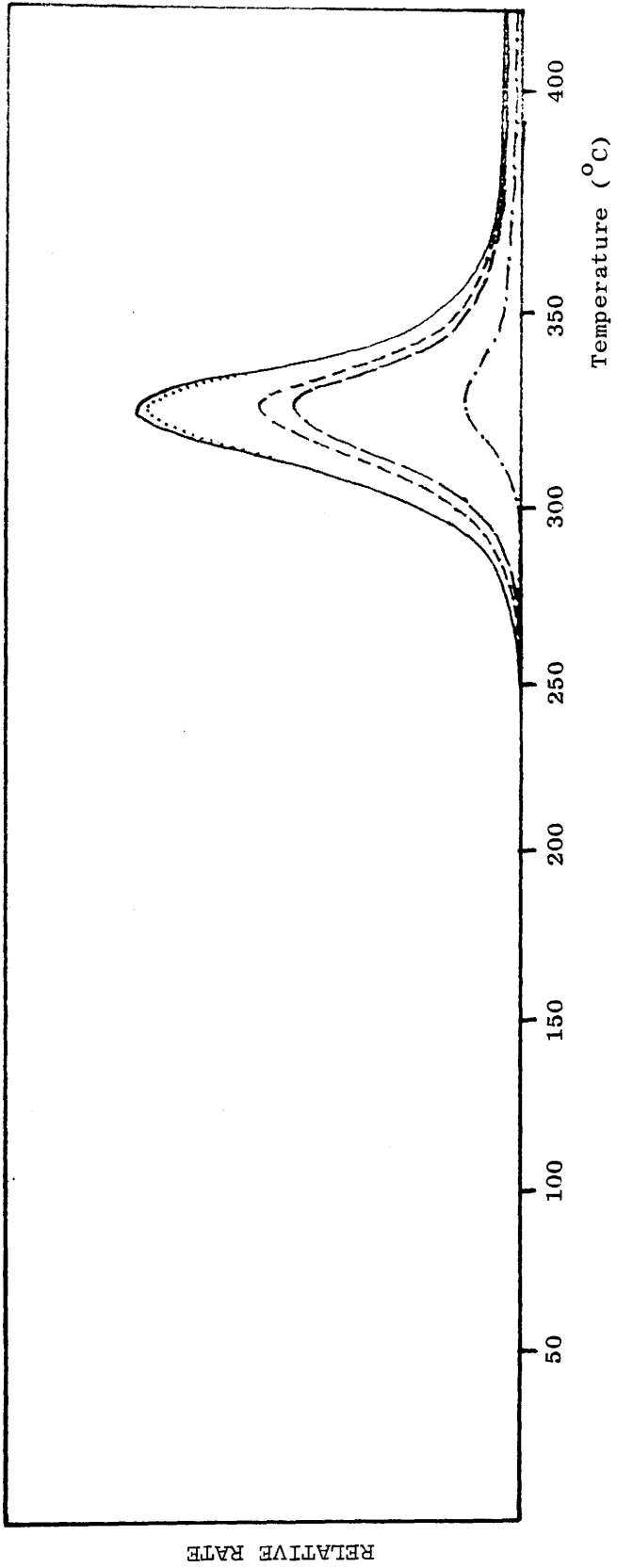
Fig 3.3 TVA curve for PEO using 50 mg powder sample.
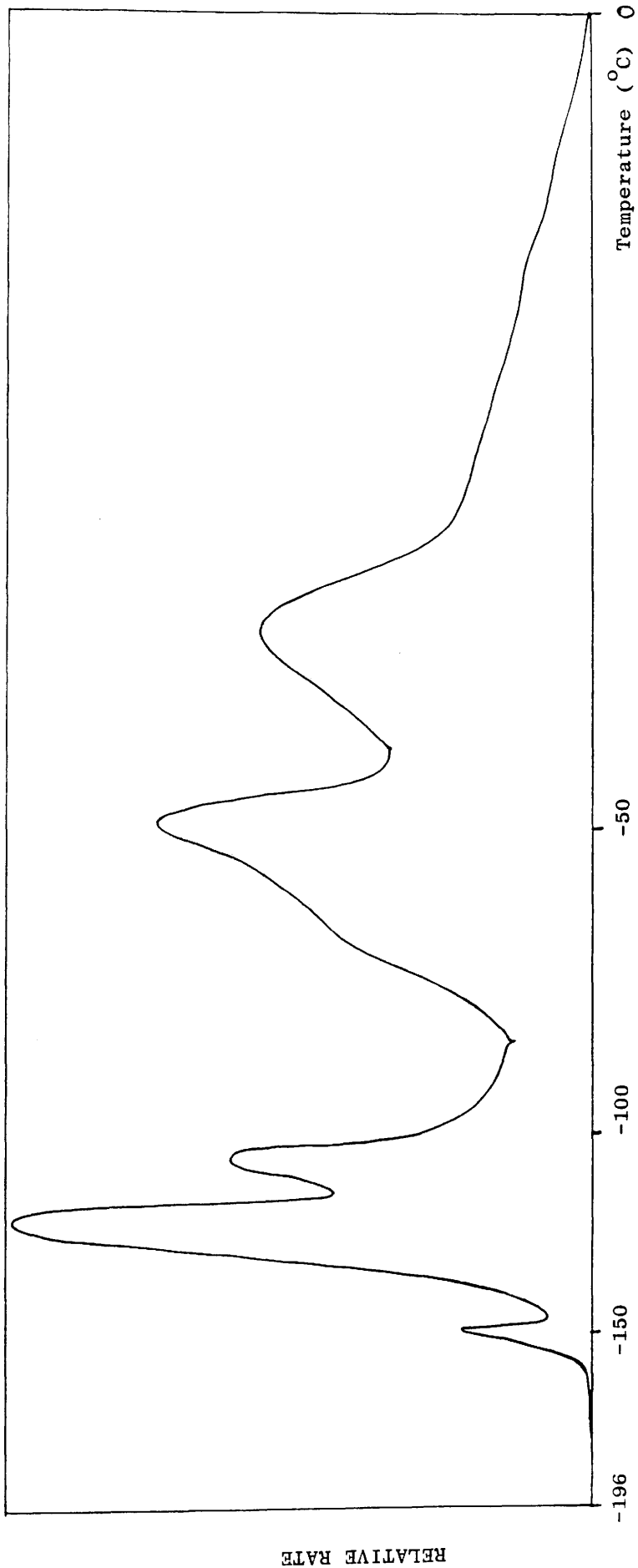
Fig. 3.4   SATVA trace for condensable volatile degradation products of PEO after heating to 500°C.

CRF when left at ambient temperature solidified to a wax.   The
residue left in the bottom of the TVA tube was a carbonaceous char.

SATVA Separation of Condensable Degradation Products.

The condensable volatile products of degradation were
separated using subambient thermal volatilisation analysis
(SATVA) and identified using IR spectroscopy and mass spectrometry.
In these experiments powder samples of between 60-150 mg were used.
With smaller sample sizes greater resolution is obtained between
peaks however in order to identify the less abundant products and
gain enough material for spectroscopic investigation of the final
low volatile fractions, larger sample sizes were used.   The
SATVA trace obtained for the condensable volatile products after
heating PEO to 500°C, illustrated in Fig. 3.4, indicates five
major fractions.   The boundary selected for each fraction is
illustrated in the diagrammatic representation of the SATVA trace
for PEO in Fig. 3.5 below:
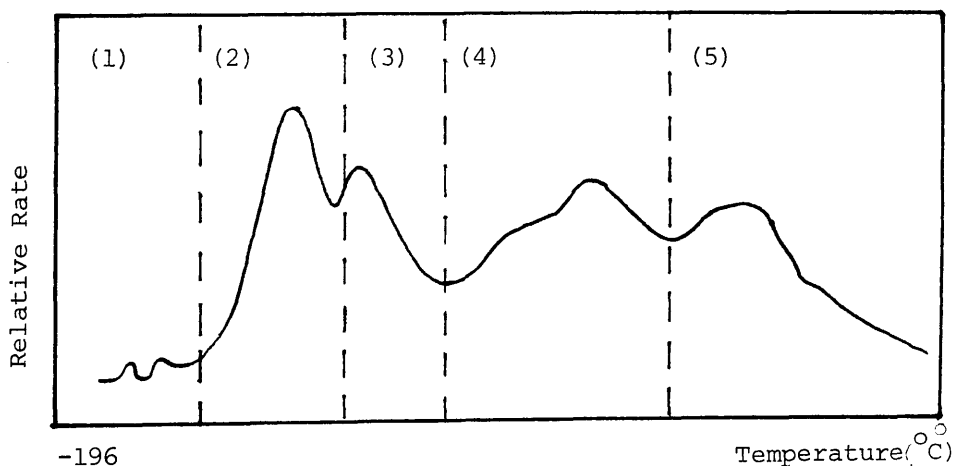
Fig. 3.5: Diagrammatic SATVA trace for PEO indicating fraction
           boundaries.

Due to the small quantities of component present, materials giving both of the first peaks were taken to comprise fraction (1). The compounds present were found to be CO_2 as seen from an absorption band at 2320 cm^{-1} in the IR spectrum (see Fig. 3.6) and from the molecular ion peak at $^m/e$ = 44 (100%) in the mass spectrum of the fraction, ethene with IR absorption bands at 950 cm^{-1}, 1443 cm^{-1} and 1890 cm^{-1} and a peak at $^m/e$ = 28 (36 %) in the mass spectrum and finally a trace of ketene as seen by a doublet in the IR spectrum at 2160 cm^{-1} and 2130 cm^{-1} and a peak in the mass spectrum at $^m/e$ = 42.   Ethyne was also present in trace amounts.

Formaldehyde was identified in fraction (2) from the characteristic winged absorption bands at 1745 cm^{-1} and 1505 cm^{-1} together with the C-H absorption bands in the region 2750-2900 cm^{-1} of the IR spectrum (see Fig. 3.7).   A base peak (100%) of $^m/e$ = 29 and molecular ion peak at $^m/e$ = 30 in the mass spectrum confirms the above interpretation.   However traces of methyl ethyl ether were suggested by the presence of a weak molecular ion peak at $^m/e$ = 60 and other peaks at $^m/e$ = 59, 45 and 31.   A white insoluble solid was also collected in the cold finger of the gas cell, which was attributed to paraformaldehyde[106].

The major component of fraction (3) was acetaldehyde with the additional absorption in the IR spectrum (see Fig. 3.8) at 1615 cm^{-1} and 1205 cm^{-1} arising due to an overlap with the fourth fraction.   The characteristic base peak of an aldehyde at $^m/e$ = 29 was seen in the mass spectrum as well as peaks at $^m/e$ = 44, 43 and 15 due to acetaldehyde.

The fourth fraction consisted of two poorly resolved peaks.
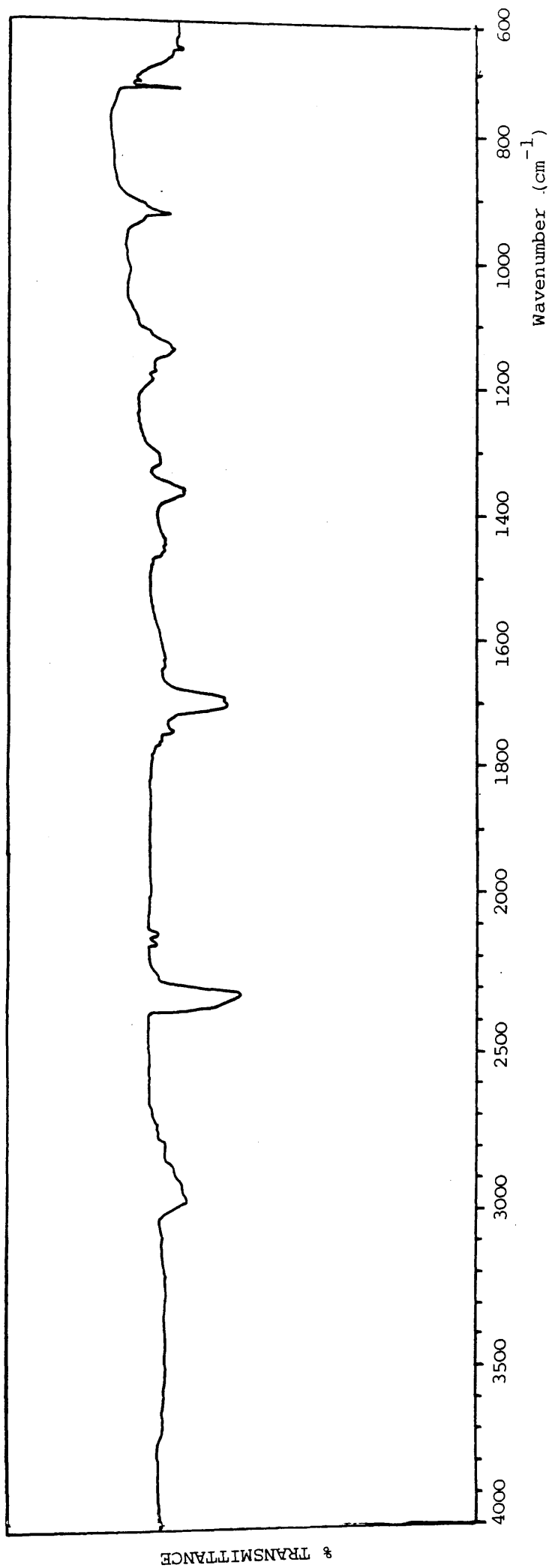
Fig. 3.6   IR spectrum of degradation products in Fraction (1) of SATVA trace for PEO.
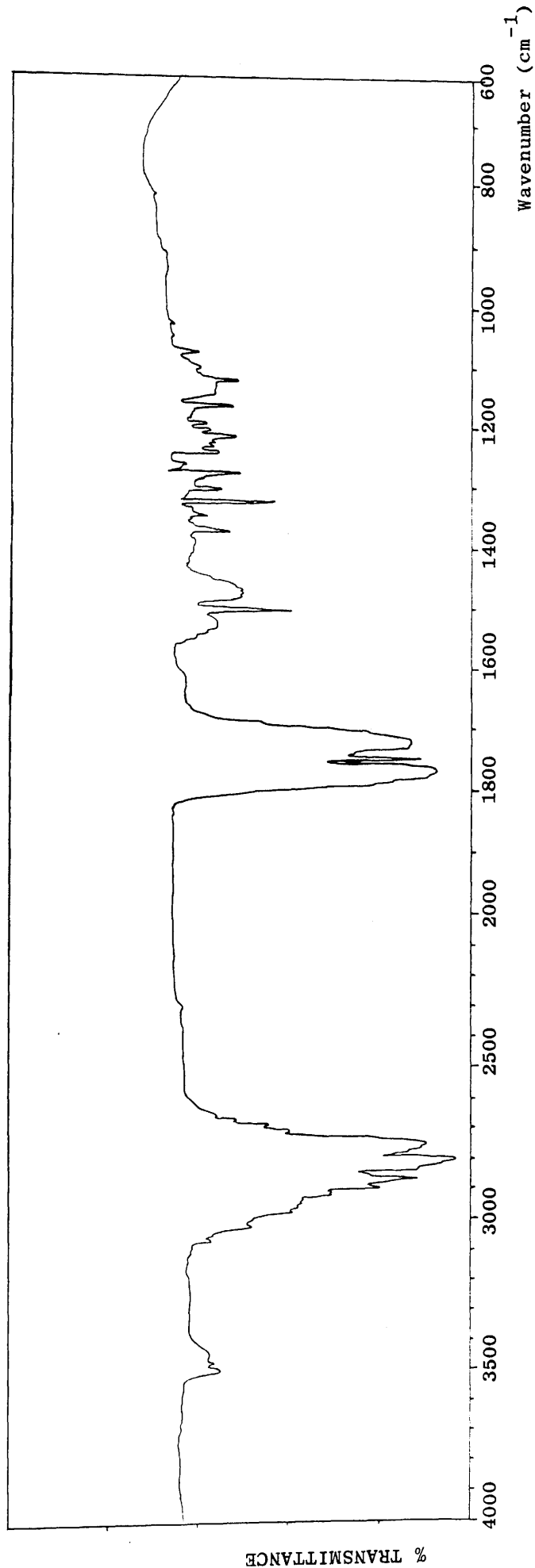
Fig 3.7   IR spectrum of degradation products in Fraction (2) of SATVA trace for PEO.

% TRANSMITTANCE
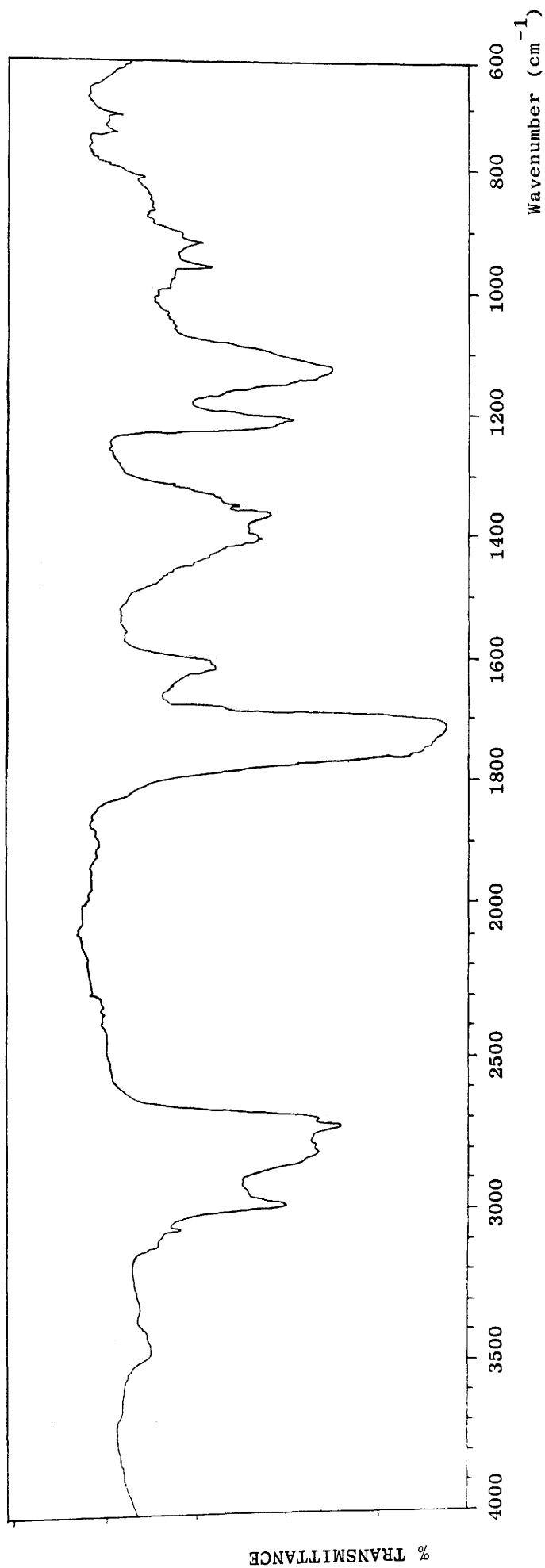
Fig 3.8   IR spectrum of degradation products in Fraction (3) of SATVA trace for PEO.

The IR spectrum of this fraction, illustrated in Fig. 3.9a, shows strong absorption bands at 2980 cm^{-1} and 2800 cm^{-1} attributed to CH_3 and CH_2 stretching vibrations, an absorption at 1212 cm^{-1} from CH_2 twisting and a strong band at 1140 cm^{-1} due to C-O stretching. The presence of unsaturated compounds was indicated by the strong absorption at 1620 cm^{-1} and weak bands at 3130 cm^{-1} and 816 cm^{-1}. Aldehydic compounds also feature but to a lesser extent as indicated by the weak carbonyl absorption band at 1775 cm^{-1} and a very weak C-H stretching vibration at 2740 cm^{-1} and 2700 cm^{-1}. Thus the fraction consists of a complex mixture of saturated and unsaturated ethers and aldehydes. Previous work by Grassie and Mendosa[106] on the thermal degradation of PEG has shown methoxy and ethoxy-acetaldehyde to be formed. In the current investigation, when the degradation of PEG 1500 was carried out, the gas phase IR spectrum obtained for the fraction containing these compounds (excluding the hydroxyl band) matched exactly that obtained for PEO 100,000 fraction (4) (see Fig. 3.9b). The mass spectrum of the fourth fraction from PEO degradation suggests the presence of the following compounds: diethyl ether, ethyl vinyl ether, divinyl ether, vinyloxyacetaldehyde, methoxyacetaldehyde and ethoxyacetaldehyde. The relevant peaks in the mass spectrum used for product identification are given in Table 3.1. The parent molecular ion used for identification is listed first followed by the major peaks in decreasing intensity as reported in reference spectra.[101,102] Where reference spectra were not available, the peaks are listed in order of decreasing molecular weight.

The final fraction was collected as a pale yellow liquid.
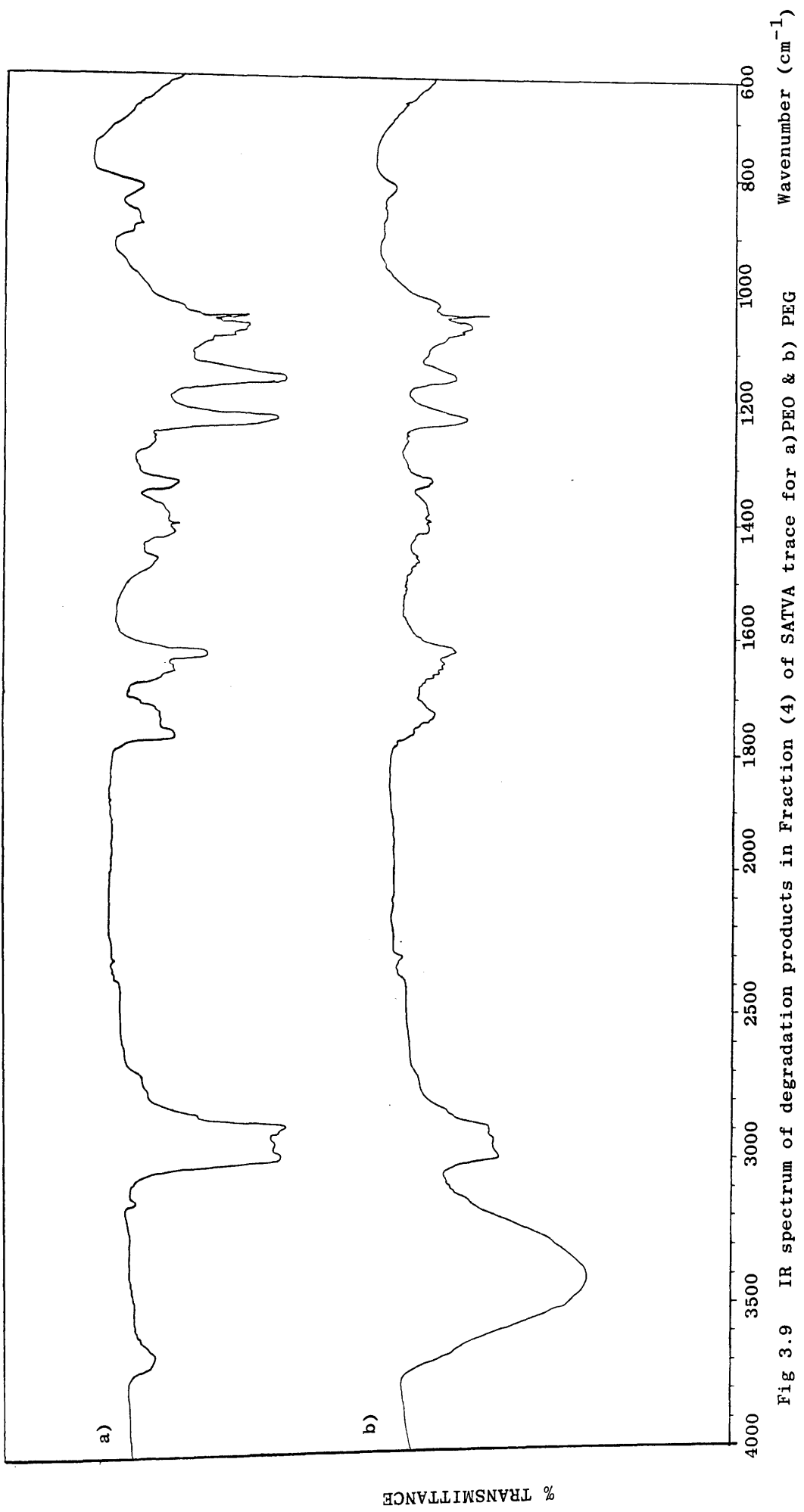
Fig 3.9   IR spectrum of degradation products in Fraction (4) of SATVA trace for a)PEO & b) PEG

$^m/e$	% Base	Compound
31	100	
45	59	
29	38.8	$CH_3CH_2OCH_2CH_3$
59	10	
74	0.7	
72	2.3	
44	85	
43	19.0	
29	38.8	$CH_3CH_2OCH=CH_2$
15	16.6	
57	2.0	
70	0.8	
43	19	
42	5.0	$CH_2=CHOCH=CH_2$
44	8.5	
27	17.6	
86	1.0	
59	10.0	
27	17.6	
43	19.0	$CH_2=CHOCH_2CHO$
29	38.8	
57	2.0	
74	0.7	
31	100.	
29	38.8	
59	10.0	
57	2.0	CH_3OCH_2CHO
43	19.0	
45	59.0	
15	14.6	
88	0.4	
29	38.8	
31	100	
59	10.0	$CH_3CH_2OCH_2CHO$
73	7.4	
43	19.0	
15	14.6	

Table 3.1 : Mass Spectral Data for PEO Degradation Products in
Fraction (4) of the SATVA.

The main absorption bands in the IR spectrum (reproduced in Fig. 3.10) indicate hydroxyl, ether and unsaturated structures. Identification was limited by the overlap of the absorption bands in the IR spectrum and the complicated mass spectrum obtained, however traces of water, ethanol and ethylene glycol are indicated and vinyl oxyethanol may also be present. The mass spectral data for the final fraction are shown in Table 3.2. From this, the largest chain fragment in the final fraction $^m/e = 117$, contains two repeat units and is terminated by an ethyl end group. The CRF was investigated by IR spectroscopy using either a smear of the compound on a NaCl plate or a thin film cast onto a salt plate from CH_2Cl_2. The spectrum obtained for the CRF is illustrated in Fig. 3.11. The CRF took the form of a yellow viscous liquid and was found to consist of low molecular weight fragments of PEO having alkyl end groups and only a trace of hydroxyl end groups. There was no indication in the spectrum, however, of the presence of carbonyl compounds such as aldehydic terminal groups. An absorption band at 1620 cm^{-1} suggests unsaturation in the structure although conformation of this from C=C-H absorption bands in the region 850 cm^{-1} - 1000 cm^{-1} cannot be made due to the strong bands at 842 cm^{-1} and 950 cm^{-1} due to the asymmetric and symmetric CH rocking modes of the oligomeric backbone.

The residue was also analysed by IR spectroscopy. Once the CRF and any grease at the top of the tube had been removed, KBr was added directly to the sample in the TVA tube and ground in situ to maximise recovery of the small amount of residue obtained. The main absorption band observed in the IR spectrum
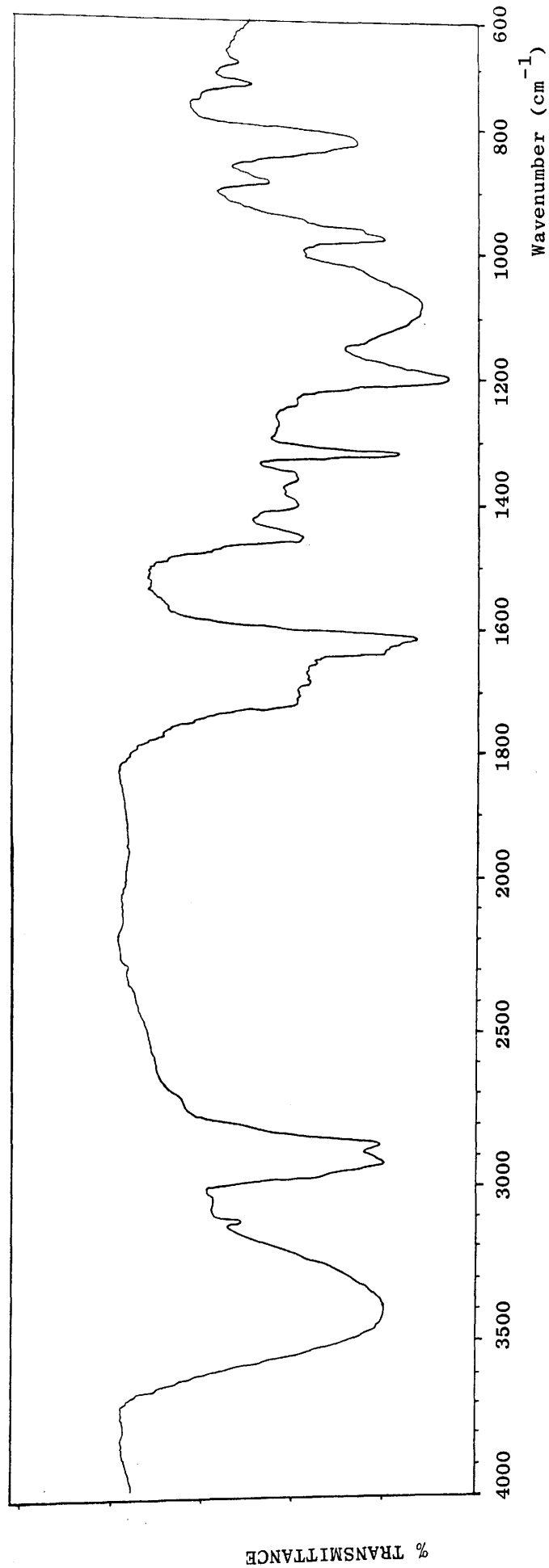
Fig 3.10   IR spectrum of degradation products in Fraction (5) of SATVA trace for PEO.

$^m/e$	% Base	Compound
45	83.2	
73	79.5	
89	3.4	
33	2.0	
86	2.6	
88	0.9	$H_2C=CHOCH_2CH_2OH$
71	2.4	
59	30.8	
43	58.8	
31	40.0	
46	2.4	
45	83.2	
29	72.4	CH_3CH_2OH
17	1.7	
18	7.7	
17	1.7	H_2O
62	0	
45	83.2	$HOCH_2CH_2OH$
31	40.0	
117	0.7	
103	1.4	
89	3.4	
73	79.5	
59	30.8	$CH_3CH_2OCH_2CH_2OCH_2CH_2^{\bullet}$
45	83.2	
44	19.0	
29	72.4	
28	100	

Table 3.2 : Mass Spectral Data for PEO Degradation Products in Fraction (5) of the SATVA Separation.
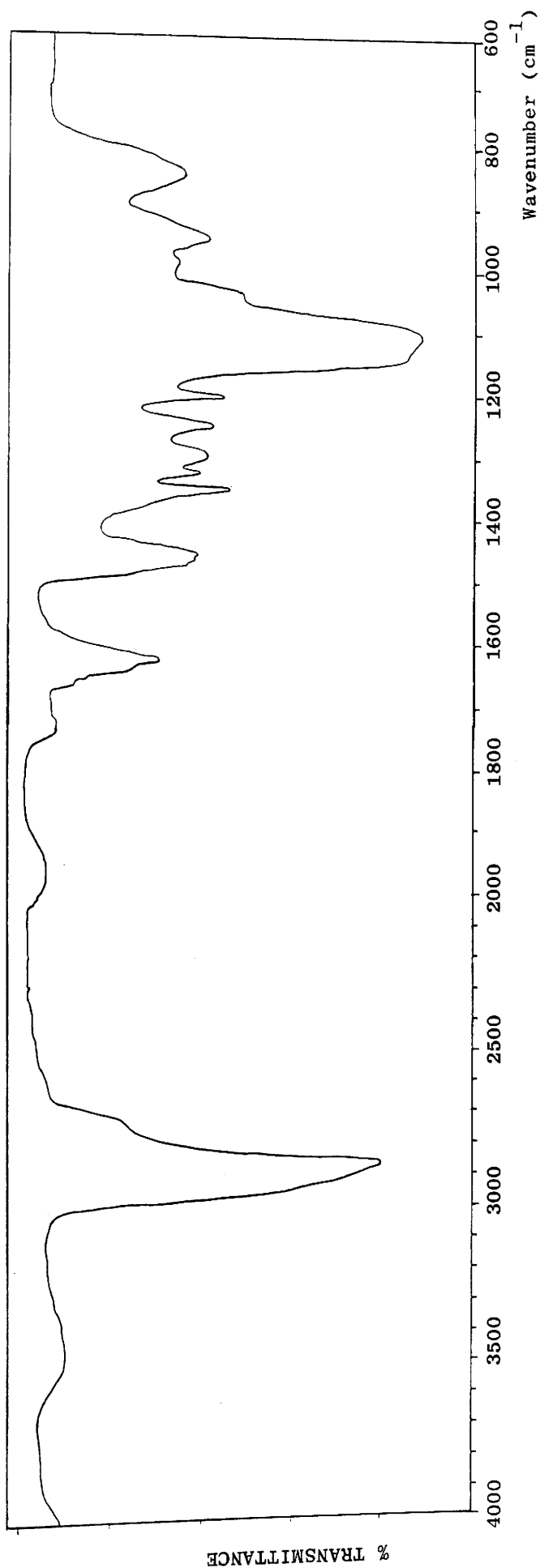
Fig 3.11   IR spectrum of CRF obtained on heating PEO to 500°C run as liquid film.

was in the C-O stretching region (1100 cm^{-1}).

In the case of the non-condensable products, the thermal degradation was carried out in an evacuated closed system and the products were transferred into a gas cell using the Topler pump (see Chapter 2) for IR analysis and mass spectrometry. The products thus identified were carbon monoxide, methane and ethane. The IR spectrum for the non-condensable products evolved on the degradation of PEO is shown in Fig. 3.12.

The degradation products from PEO identified after separation by SATVA experiments are summarised in Table 3.3.

Product Fraction	Compound(s)
Non-condensable products	CO, CH_4, CH_3CH_3
SATVA Fraction (1)	CO_2, H_2CCO, $CH_2=CH_2$, $HC\equiv CH$
SATVA Fraction (2)	$HCHO$, $CH_3OCH_2CH_3$
SATVA Fraction (3)	CH_3CHO
SATVA Fraction (4)	$CH_3CH_2OCH_2CH_3$, $CH_3CH_2OCH=CH_2$ $CH_2=CHOCH=CH_2$, $CH_2=CHOCH_2CHO$ CH_3OCH_2CHO, $CH_3CH_2OCH_2CHO$
SATVA Fraction (5)	H_2O, CH_3CH_2OH, $HOCH_2CH_2OH$ $H_2C=CHOCH_2CH_2OH$
CRF	oligomeric polyether
Residue	Carbonaceous char

Table 3.3 : Products from Thermal Degradation of PEO on heating to 490°C.

% TRANSMITTANCE

Wavenumber (cm^{-1})
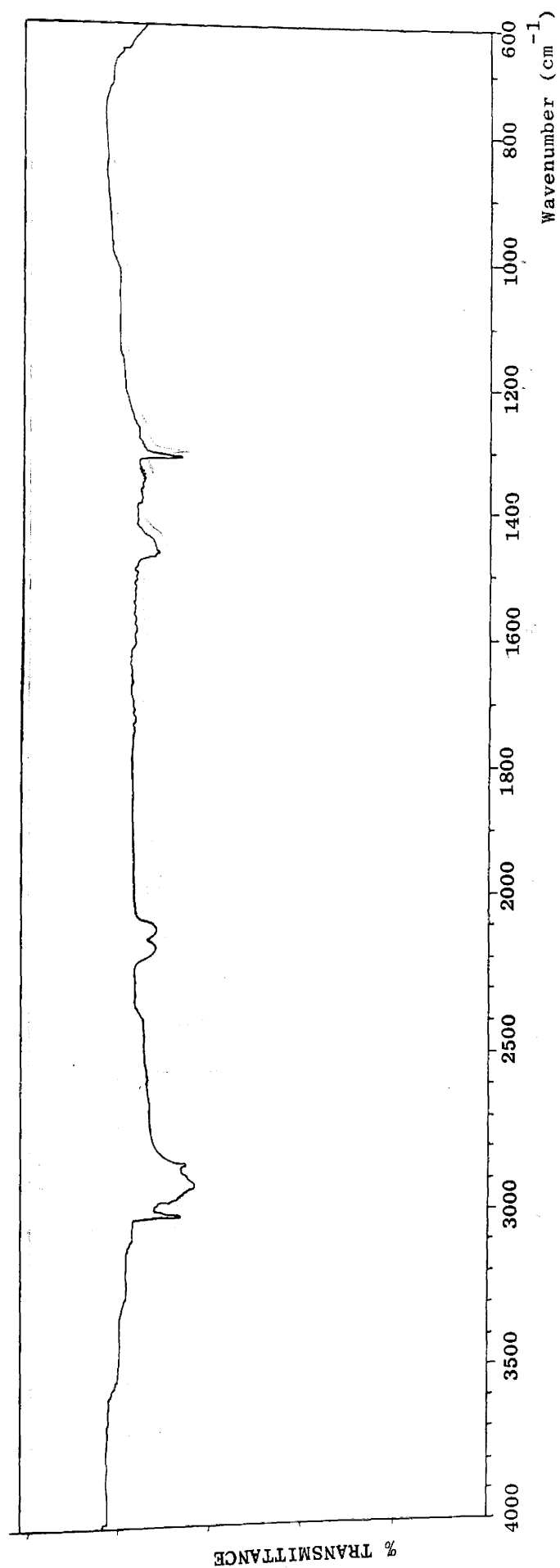
Fig 3.12   IR spectrum of non-condensable products obtained on heating PEO to 500°C.

3.2.3 Discussion

The onset temperatures of evolution of volatile products $(T_{(onset)})$ and the temperatures at which the degradation process occurs at a maximum rate $T_{(max)}$ obtained by each analytical method are in general agreement. The $T_{(max)}$ temperatures recorded in vacuo (TVA, TG) are lower than those measured under nitrogen (TG, DSC) as small volatile degradation products, will diffuse more readily from the polymer bulk in a continuously evacuated system. As the differences in degradation temperatures observed between the polymer as supplied and after purification were negligible and from the apparent purity of the commercial compound as seen by IR analysis, it was considered feasible to use the latter for the preparation of blends. The observed thermal behaviour was comparable to that found by Grassie and Mendosa[106] for PEG 1500 (TVA onset and maximum temperatures 325°C and 366°C respectively), with the exception of the DSC traces where PEG has a lower Tm and an additional endothermic peak at 110°C.

The TG and TVA curves indicate that during the thermal degradation of PEO, weight loss (evolution of volatile compounds) occurs in a single step over a relatively narrow temperature range. The behaviour of the individual TVA traces indicates the presence of a variety of degradation products. This is verified in the SATVA product separation. On considering the degradation products, the number of compounds and the lack of monomer implies that the thermal degradation of PEO is not due to a simple depolymerisation process. Instead, it suggests random chain scission without depolymerisation. An important factor for

random degradation is that the participating chemical bonds must be equivalent i.e. they must have approximately the same bond dissociation energy. Thus it seems unlikely that the degradation process would be initiated by the scission of a C-H bond[105] since the C-O and C-C bonds are more easily broken (average bond enthalpies at 298 K in kJ mol^{-1}[107]: C-H = 412, C-O = 360, C-C = 348). As previously mentioned, it has been claimed[104-6] that the thermal degradation of PEO takes place by a radical chain mechanism initiated at random along the length of the chain. The degradation products obtained in this examination of high molecular weight PEO are similar to those observed by Grassie and Mendosa, working on low molecular weight PEG, who have proposed a detailed degradation mechanism. Formaldehyde, acetaldehyde, methane, ethane, carbon monoxide, ethylene glycol, methoxy and ethoxyacetaldehyde were products common to both investigations. The present work reveals the presence of unsaturated compounds hitherto unreported although Bornmaun[108] has observed unsaturated aldehydes containing up to six carbon atoms on the thermal decomposition of an epoxy resin. Some differences in product formation between PEG and PEO were that with PEO, water and ethylene glycol were less important products. In high molecular weight polymers, since the proportion of end groups per unit mass of sample decreases with increasing molecular weight, reactions at end groups will become less important. This may account for only traces of ethanol being present if the formation of ethanol is via a chain terminal reaction as illustrated below:

$$\text{\textasciitilde} O-CH_2-CH_2-O-CH_2CH_2-OH \xrightarrow{\text{C-O scission}} \text{\textasciitilde} O-CH_2CH_2-O^\bullet$$

$$+ \quad {}^\bullet CH_2CH_2-OH$$

$$\big\downarrow \text{disproportionation}$$

$$\text{\textasciitilde} O-CH_2CH=O + CH_3CH_2-OH$$
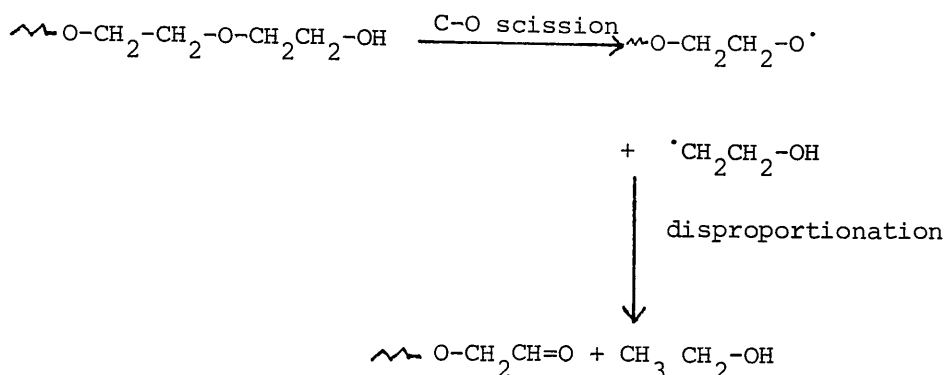
A similar reaction scheme could account for the formation of small amounts of ethylene glycol and water. It should also be noted that this reaction leads to the formation of unsaturated end groups which can in turn give rise to the production of unsaturated compounds observed. The absence of ethylene oxide monomer as a product may be accounted for by the scission fragment $\cdot CH_2CH_2O\cdot$ preferentially rearranging to CH_3CHO (a major product) rather than cyclising to form a strained three membered ring. In the mechanism of degradation proposed for high molecular weight PEO a number of processes can occur following the initial random C-C or C-O bond cleavage. Formaldehyde may be formed by the breaking of a bond in the α position relative to the terminal carbon or oxygen radical as shown below:

$$\text{\textasciitilde} O-CH_2-CH_2-O\overset{a}{|}CH_2\overset{b}{|}CH_2-O\text{\textasciitilde}$$

C-O scission /a   b \ C-C scission

$$\text{\textasciitilde} O-\dot{C}H_2-CH_2-O^\bullet + \cdot CH_2CH_2-O\text{\textasciitilde} \qquad 2\cdot CH_2-O-CH_2-CH_2\text{\textasciitilde}$$

$$\big\downarrow \qquad\qquad \big\downarrow \qquad\qquad \big\downarrow$$

$$\text{\textasciitilde} O-\dot{C}H_2 + CH_2O \qquad CH_2=CH_2 + \dot{O}\text{\textasciitilde} \qquad 2 CH_2O + 2\dot{C}H_2CH_2\text{\textasciitilde}$$

Ethene can also be formed following C-O scission (see above)
but since only a trace of this product was present, it may be
that the $\cdot CH_2CH_2O$—$\wedge\wedge$ radical preferentially participates in
intra- or intermolecular hydrogen transfer.   With intra-
molecular hydrogen transfer this can involve stabilised
transition states with four to six membered rings.   Methoxy and
ethoxyacetaldehyde are formed via a back-biting reaction
involving terminal carbon radicals and a five and six membered
ring transition state respectively followed by the scission of
a C-O bond.   This reaction scheme, as suggested by Grassie
and Mendosa[106] is reproduced below:

Similar cyclic reactions may be involved in the formation of the
hydrocarbons methane and ethane, however, in these cases bond
cleavage is such that a carbonyl end group is formed on the
macromolecule which is a precursor for the formation of
acetaldehyde (see below).   Mechanisms proposed in the
present study for the production of acetaldehyde are as follows:

$$HC\overset{\displaystyle O}{\underset{\displaystyle |}{\diagdown}} CH_2 \qquad \xrightarrow[\text{H transfer}]{\text{intramolecular}} \qquad \text{w-OCH}_2 - \overset{\cdot}{C}H - \overset{\frown}{O} \overset{\frown}{\smile} CH_3$$

$$\text{w-OCH}_2$$

$$\downarrow \text{ C-O scission}$$

$$\text{w-O} - CH_2CHO + \cdot CH_3$$

$$\text{w-CH}_2CH_2 - O - CH_2CHO + \cdot CH_3 \qquad \xrightarrow[\text{H transfer}]{\text{intramolecular}} \text{w-CH}_2\overset{\cdot}{C}H - \overset{\frown}{O}\overset{\frown}{\smile}CH_2CHO + CH_4$$

$$\downarrow \quad \begin{array}{l}\text{i)C-O scission}\\ \text{ii)H abstraction}\end{array}$$

$$CH_3CHO + \quad CH_2CHO$$

$$OCH_2 - \overset{\displaystyle O}{\underset{\displaystyle |}{CH}} \overset{\diagup\diagdown}{\qquad} CH_2 \qquad \xrightarrow[\text{H transfer}]{\text{intramolecular}} \text{w-OCH}_2\overset{\cdot}{C}H - O - CH_2CH_3$$

$$\overset{|}{H} \qquad \cdot CH_2$$

$$\downarrow \quad \text{C-O scission}$$

$$\text{w-OCH}_2CHO + \cdot CH_2CH_3$$

$$\text{w-CH}_2CH_2 - O - CH_2CHO + \cdot CH_2CH_3 \qquad \xrightarrow[\text{H transfer}]{\text{intermolecular}} \text{w-CH}_2\overset{\cdot}{C}H - \overset{\frown}{O}\overset{\frown}{\smile}CH_2CHO + CH_3CH_3$$

$$\downarrow \quad \begin{array}{l}\text{i) C-O scission}\\ \text{ii) H abstraction}\end{array}$$

$$CH_3CHO + \text{w-CH}_2CHO$$

Alternatively acetaldehyde may be formed by splitting out of $\cdot CH_2CH_2O\cdot$ in a type of pseudo depolymerisation process, which (as previously mentioned) rearranges to give acetaldehyde.

The presence of ethanol may result from intramolecular hydrogen transfer involving a terminal oxygen radical followed by C-O cleavage. Depending upon the position of the C-O scission

ethanol or vinyloxyethanol may be formed as illustrated below:

$$
\begin{array}{c}
\text{CH}_2 \quad\text{O}\quad \text{CH} - \text{CH}_2 - \text{O} \sim\!\!\sim \\
| \qquad\qquad \text{H} \\
\text{CH}_2 \\
\quad\quad\text{O}\cdot
\end{array}
$$

↓ intramolecular H transfer

$$\text{HOCH}_2\text{CH}_2 - \text{O} - \overset{\cdot}{\text{CH}} - \text{CH}_2 - \text{O} \sim\!\!\sim$$

↓   ↓

$$\text{HOCH}_2\overset{\cdot}{\text{CH}}_2 \qquad\qquad \text{HOCH}_2\text{CH}_2\text{OCH}=\text{CH}_2$$

↓ H abstraction

$$\text{HOCH}_2\text{CH}_3$$
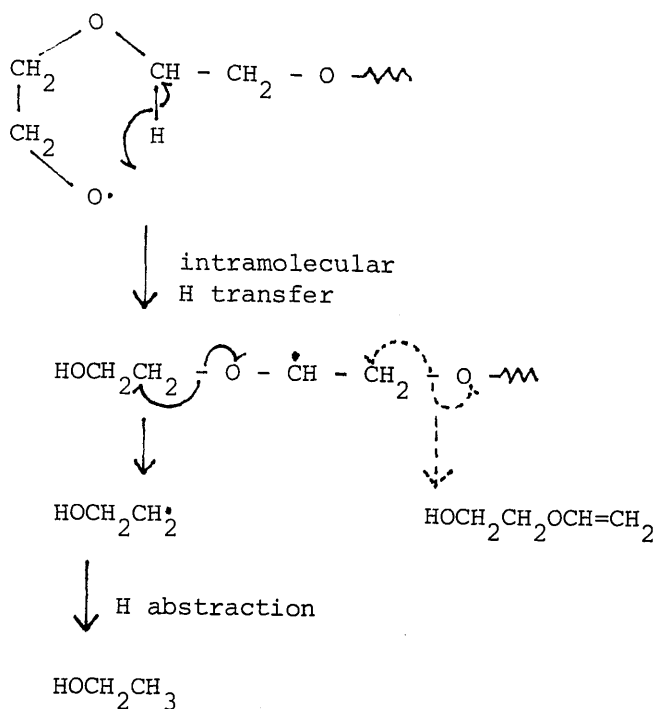
The processes mentioned so far have involved intramolecular reactions followed by intermolecular reactions. The formation of methyl ether and diethyl ether are due to simple intermolecular hydrogen abstraction.

$$\sim\!\!\sim\text{CH}_2\text{OCH}_2\text{CH}_2\text{O}\overset{\cdot}{\text{CH}}_2 \xrightarrow{\text{H abstraction}} \sim\!\!\sim\text{CH}_2\text{O} \quad \text{CH}_2\text{CH}_2\text{OCH}_3$$

↓ i) C-O scission
  ii) H abstraction

$$\text{CH}_3\text{CH}_2\text{OCH}_3 + \overset{\cdot}{\text{O}}\text{CH}_2\!\!\sim\!\!\sim$$

$$\sim\!\!\sim\text{CH}_2\text{CH}_2\text{OCH}_2\text{CH}_2\text{OCH}_2\overset{\cdot}{\text{CH}}_2 \xrightarrow{\text{H abstraction}} \sim\!\!\sim\text{CH}_2\text{CH}_2\text{O} \quad \text{CH}_2\text{CH}_2\text{OCH}_2\text{CH}_3$$

↓ i) C-O scission
  ii) H abstraction

$$\text{CH}_3\text{CH}_2\text{OCH}_2\text{CH}_3 + \overset{\cdot}{\text{O}}\text{CH}_2\!\!\sim\!\!\sim$$
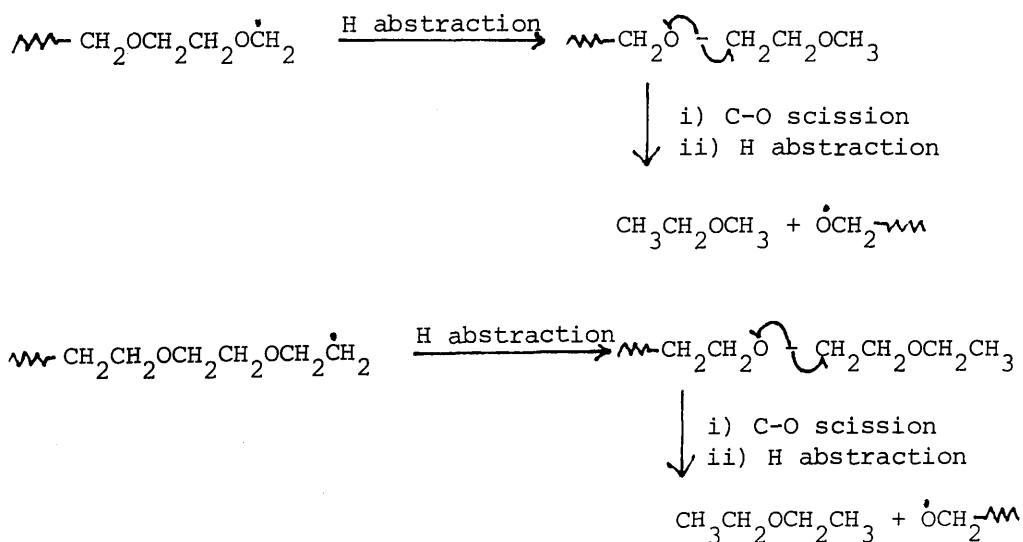
The fate of the macroradicals produced by intermolecular hydrogen abstraction has not yet been discussed.   There are two possibilities - either C-O scission, resulting in a carbonyl terminated macromolecule which can then undergo further chain scission and transfer or abstraction reactions to form aldehydic products, or C-O cleavage forming unsaturated end groups from which compounds such as ethyl vinyl ether, divinyl ether and vinyl oxyacetaldehyde may be produced.   This reaction scheme is shown below:

$\text{\Large\textasciitilde} OCH_2CH_2 - O - \dot{C}H - \dot{C}H_2 - O - CH_2CH_2O \text{\Large\textasciitilde}$

1) $\downarrow$ or   2) $\downarrow$

$\text{\Large\textasciitilde} OCH_2\dot{C}H_2 + O = CHCH_2 \text{\Large\textasciitilde}$

   aldehydes

$\text{\Large\textasciitilde} CH_2CH_2 - O - CH_2CH_2 - O - CH = CH_2 + \dot{O}CH_2 \text{\Large\textasciitilde}$

  $\downarrow$ i) C-O scission   loss H·

  $\downarrow$ ii) H abstraction

    $CH_3CH_2OCH = CH_2$

       $\text{\Large\textasciitilde} CH_2\dot{C}H_2 - O - \dot{C}HCH_2 - O - CH = CH_2$

            $\downarrow$ C-O scission

       $\text{\Large\textasciitilde} CH_2\dot{C}H_2 + O=CHCH_2 - O - CH=CH_2$
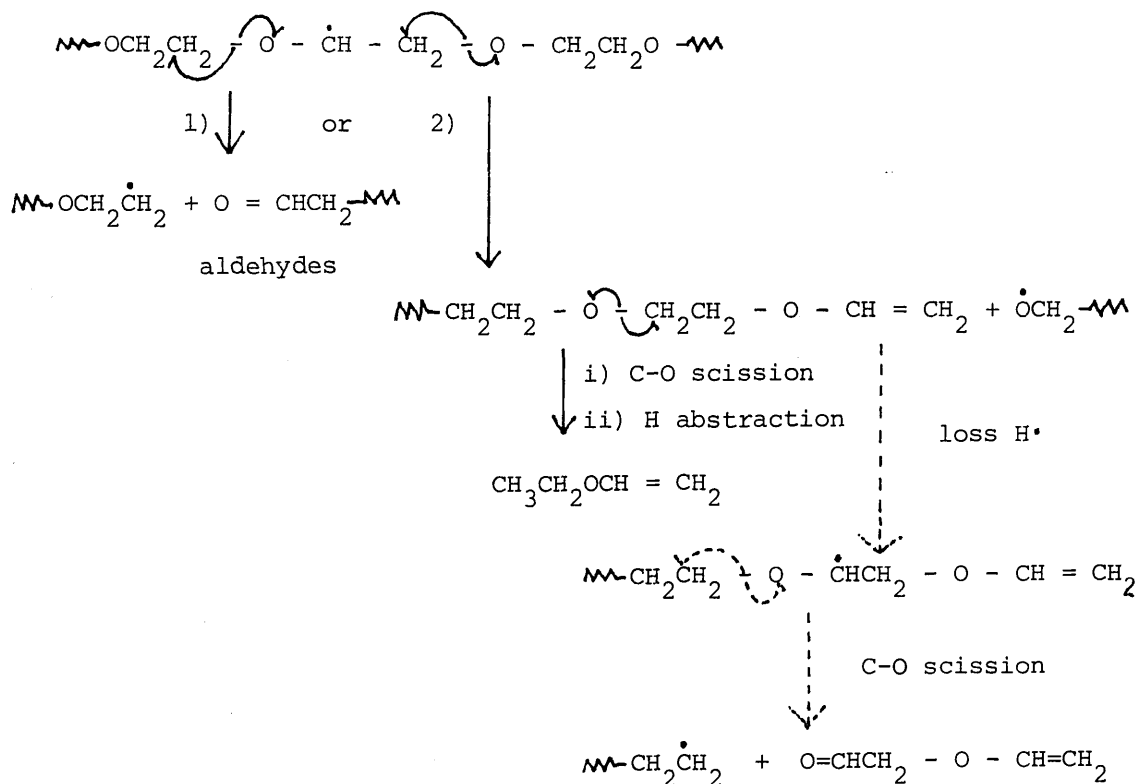
The presence of unsaturation in the CRF products may also be explained in this way.   As the MW falls and the temperature rises, it becomes possible for larger fragments to vapourise to the cold ring.   The production of CO can be explained by the break

down of a CH_2O unit:

$$\text{↜ } CH_2CH_2OCH_2 \text{ — } CH_2O \text{ — } CH_2CH_2\text{↝}$$

$$\downarrow$$

$$CO + H_2$$
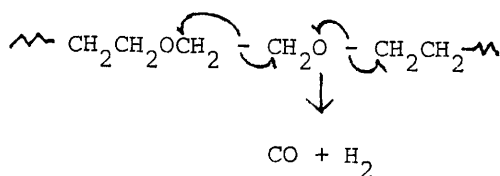
In this process hydrogen[109] is simultaneously produced and will be present in the non-condensable fraction.

Ketone could be formed in an elimination type reaction following hydrogen abstraction from an oxygen-terminated macro-radical in the mechanism outlined below:

$$\text{↜ } OCH_2 - \overset{}{\underset{H}{CH}} - \dot{O} \xrightarrow{\text{H abstraction}} \ \ \ \ \ \ \ \ \ \ \ \ \ \ \ \text{↜}OH + \overset{O}{\underset{CH_2}{\overset{\|}{C}}}$$
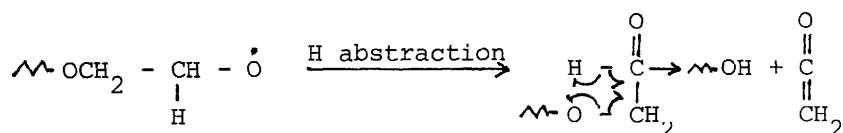
3.3 SYNTHESIS OF CHLORINATED POLY(ETHYLENE OXIDE)

Preparation

The preparation of chlorinated poly(ethylene oxide) (CPEO) was carried out in air, under nitrogen and in vacuo. For reactions carried out in an atmosphere of nitrogen, the apparatus illustrated in Fig. 3.13 was assembled and the following procedure adopted:

To approximately 1 g PEO was added 80 ml CCl_4 (a chlorine resistant solvent) and the solution was warmed until all the PEO had dissolved. The solution was then purged with dry nitrogen during which time a solution of chlorine in CCl_4 was prepared. The chlorine concentration of the solution was determined by removing 1 ml portions, adding 5 ml (excess) 1M KI solution and titrating with aqueous 0.1M NaS_2O_3. Depending on the number of hydrogen atoms required to be substituted, the appropriate volume of chlorine solution was added to give approximately 45, 63 or 72% chlorine by weight corresponding on average to mono-, di-, or tri-substitution of the ethylene oxide units, respectively. The chlorine solution was introduced dropwise at ambient temperature whilst the reaction vessel was being irradiated with U.V. light from a Hanovia mercury vapour lamp (264 and 365 nm radiation) in an atmosphere of nitrogen. Once the chlorine colour had disappeared, the solution was purged with nitrogen gas for an hour to remove HCl produced in the substitution reaction. The solution volume was reduced by rotary evaporation then the polymer was isolated by precipitation into Analar grade methanol and dried under vacuum for two days prior to elemental analysis.

A: PEO/CCl$_4$ solution in 3 necked
              r.b. flask.

B: Cl$_2$/CCl$_4$ solution in dropping
              funnel

C: N$_2$ inlet

D: silica glass window

E: drying tube containing CaCl$_2$

F: magnetic stirrer
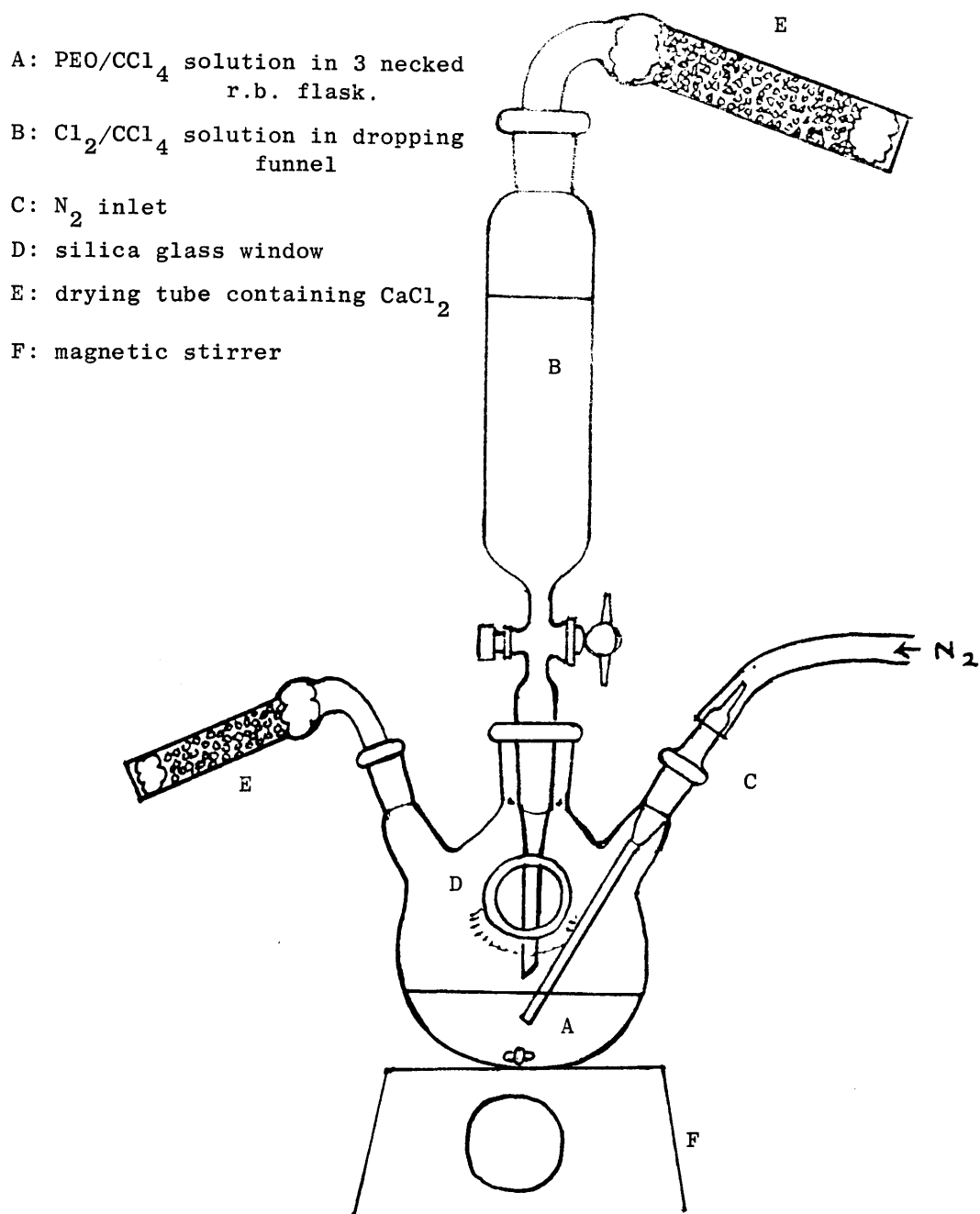
Fig 3.13   Apparatus for chlorination of PEO under nitrogen.

The effect of reacting the polymer in air was investigated in a similar manner by replacing the nitrogen inlet with a third drying tube.

Chlorination was also attempted in vacuo. A PEO solution in chloroform (0.6771g/70 ml) was degassed to a pressure of 6×10^{-3} torr and chlorine was condensed at $-196^{\circ}C$ into the PEO solution from a bulb of known volume which had been flushed with Cl_2 at atmospheric pressure. The solution was irradiated as before and allowed to warm to room temperature. The solution took ten minutes to decolourise after which time it was bubbled with nitrogen for an hour and the solvent then removed in vacuo resulting in a colourless fruity-smelling oil. There was also present a very small amount of a white compound which was found to be insoluble in CH_2Cl_2.

To investigate possible prevention of chain scission during chlorination, ionic chlorination was attempted. PEO (0.5g) was dissolved in 50 ml distilled water and chlorine was bubbled slowly through the solution for forty minutes. The solution was purged with nitrogen for ten minutes to remove excess chlorine and then extracted with four 50 ml portions of CH_2Cl_2. The extract was dried over $MgSO_4$ and the solvent removed in vacuo leaving a little colourless solid. An IR spectrum obtained from a film of the product cast from CH_2Cl_2 indicated that chlorination had not taken place. Details of experimental conditions are presented in Table 3.4.

Table 3.4   Experimental Conditions for Chlorination of PEO.

Sample.	Atmosphere	Reaction Time (mins)	Molar Ratio of Reactions Cl_2:EO	Molar Ratio in Products. Cl:EO
2CPEO (n)	N_2	35	2.57 : 1	2.02 : 1
2CPEO (a)	air	80	2.00 : 1	1.86 : 1
3CPEO (n)	N_2	35	4.02 : 1	2.94 : 1
3CPEO (a)	air	60	3.06 : 1	2.70 : 1

Polymer Characterisation.

The trichlorinated (3CPEO) and dichlorinated (2CPEO) poly
(ethylene oxide)s synthesised in air and under nitrogen were
characterised by elemental analysis, IR spectrocopy and molecular
weight determination.   Number average ($\overline{M}n$), weight average ($\overline{M}w$)
z-average ($\overline{M}z$) and p-average ($\overline{M}p$) molecular weights were obtained
using gel-permeation chromatography (GPC).   The distribution in
molecular weight (D) was also calculated.   This was performed
through the services of PSCC, Rapra Technology Limited.   The
system used to carry out this work was calibrated using the Mark-
Houwink parameters for polystyrene, hence the molecular weight
average of PEO and its chlorinated derivatives are expressed as their
"polystyrene equivalents".   The solvent used in each case was
THF.

The elemental compositions (wt. % based on repeat unit) of
the chlorinated polymers are shown in Table 3.5.   The IR spectra
of the polymers together with that for pure PEO are illustrated in
Figures 3.14 - 3.17 whilst absorption bands and their assignments
are given in Table 3.6.   The final computed GPC traces for each
sample are reproduced in Figures 3.18 - 3.22 and the molecular
weight averages and distributions tabulated in Table 3.7.

Results and Discussion
─────────────────────

The chlorine content for the chlorinated PEO prepared either under nitrogen or in air corresponds approximately to the theoretical value expected for a di-substituted (62.78%) or tri-substituted (72.16%) EO unit.   Shimizu et al[110] have found that there is an upper unit of chlorination, 75% which is a limit of the chlorination process rather than due to hydrogen content. In the polymers synthesised in this investigation, the upper chlorination limit was not reached even when an excess of Cl_2 was added (see 3CPEO(a) Table 3.5).   A higher chlorine content might have been obtained, however, if the reaction had been allowed to continue for a longer period of time.

The chlorinated polymers, after purification were in the form of white powders.   When synthesis was carried out to prepare the mono-chlorinated derivative, however, the main product was an oil which was unsuitable for analysis by the main techniques employed, namely TVA, SATVA and TG.   By this method of preparation, the maximum degree of chlorination obtainable is an average of three chlorine atoms per EO repeat unit.

The rate of reaction is dependent on the atmosphere as the reactions carried out in air proceeded at a slower rate.'   This may be due to oxygen acting as a radical scavenger.

Comparison of the IR spectra of PEO (Fig. 3.14) and chlorinated PEO (2CPEO) (Fig. 3.15) reveals the appearance on the latter of a strong absorption band at 750 cm^{-1}, attributed to C-Cl stretching, together with reductions in the CH_2 stretching and bending absorptions at 2950 cm^{-1} and 1460 cm^{-1}, respectively.

Table 3.5   Elemental Analysis for Chlorinated Poly(ethylene oxide).

Sample.	Wt.% C	obs (cal)	Wt.% H	obs (cal)	Wt.% Cl	obs. (cal)
*2 CPEO (n)**	19.85	(21.27)	1.17	(1.78)	62.98	(62.78)
2 CPEO (a)	21.35	(16.50)	1.62	(1.78)	60.96	(62.78)
3 CPEO (n)	17.10	(16.30)	0.40	(0.68)	71.75	(72.16)
3 CPEO (a)	17.24	(16.30)	0.69	(0.68)	71.26	(72.16)

*

approximate number of Cl atoms per repeat unit.

**

atmosphere during synthesis i.e. nitrogen (n) or air (a)
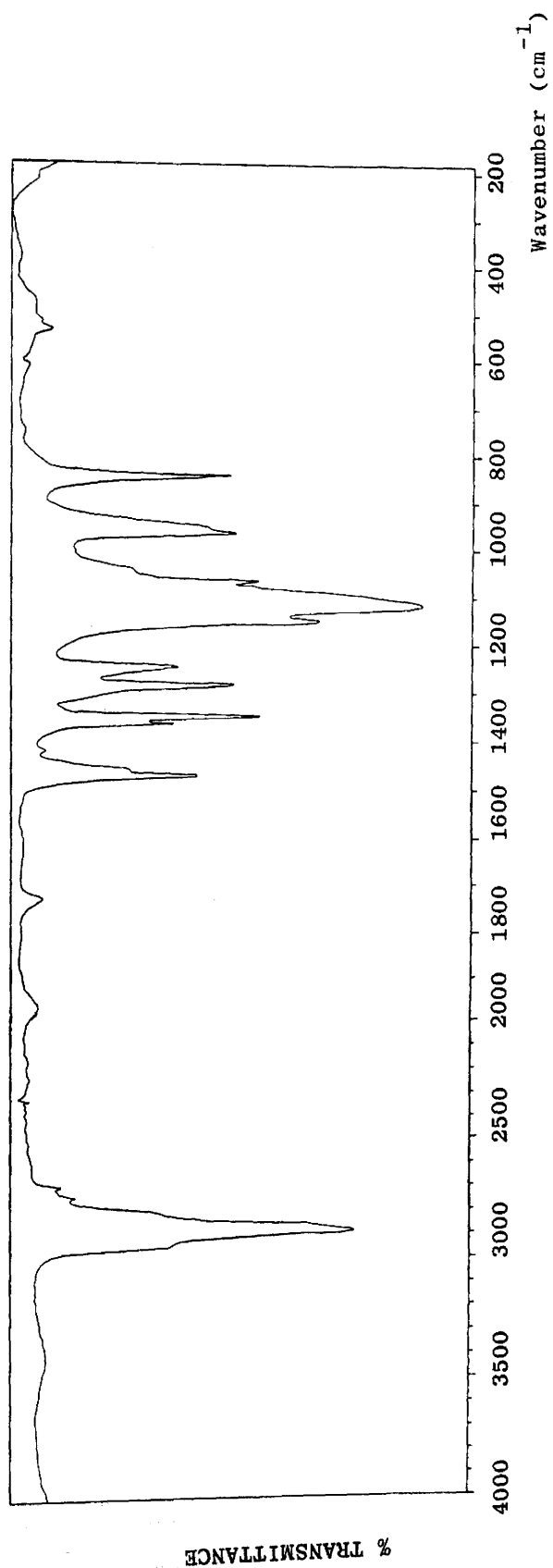
Fig 3.14   IR spectrum of PEO run as film cast from CH_2Cl_2 on CsI plate
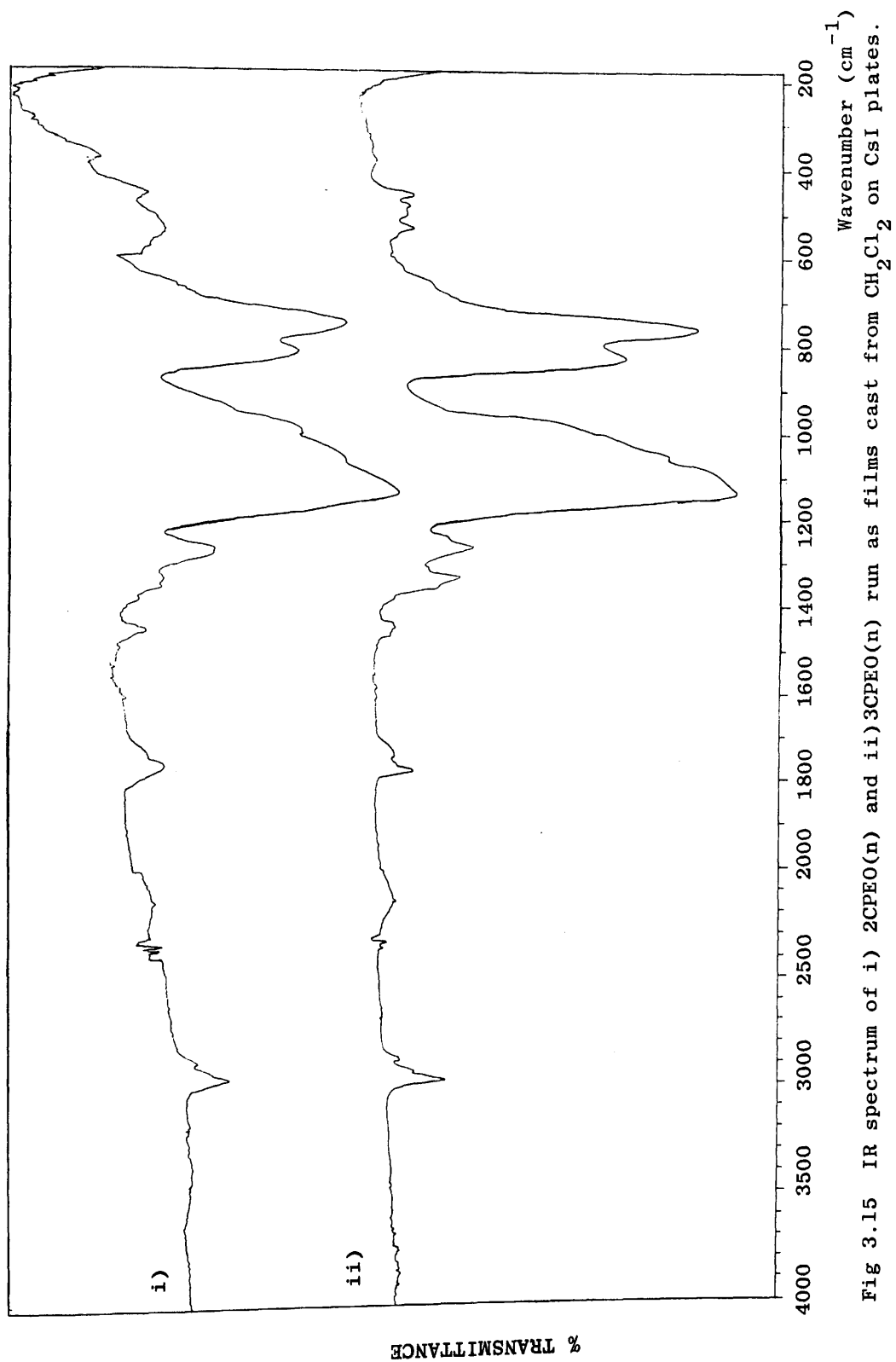
Fig 3.15 IR spectrum of i) 2CPEO(n) and ii) 3CPEO(n) run as films cast from CH_2Cl_2 on CsI plates.

These changes are also evident in the spectrum of more highly chlorinated PEO (3CPEO) (Figures. 3.16, 3.17). The C-H absorptions in 2CPEO and 3CPEO are too weak to be definitive, but it appears that the dichlorinated polymer may contain a mixture of $-CH_2-CCl_2O-$ and $-CHCl-CHClO-$structural units rather than a uniform $(-CH_2-CCl_2O-)_n$ repeat structure.

The mechanism for the chlorination of PEO can be described by the following reactions. Chlorine radicals initiated in the homolysis of Cl_2 by UV irradiation (reaction i) abstract a hydrogen atom from PEO (reaction ii) The polymer radical can then react either with the newly produced Cl radical or more probably a molecule of Cl_2 to produce chlorinated PEO and a chlorine radical (reaction iii).

$$Cl_2 \xrightarrow{h\nu} 2Cl\cdot \qquad (i)$$

$$\sim\!CH_2CH_2O\!\sim + Cl\cdot \longrightarrow \sim\!CH_2\overset{\cdot}{C}HO\!\sim + HCl \qquad (ii)$$

$$\sim\!CH_2\overset{\cdot}{C}HO\!\sim + Cl_2 \longrightarrow \sim\!CH_2\overset{\overset{\textstyle Cl}{|}}{C}HO\!\sim + Cl\cdot \qquad (iii)$$
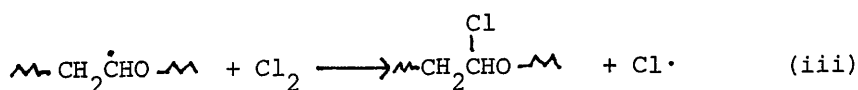
The chlorine radicals formed in reactions (i) and (iii) can continue the chlorination process by abstracting hydrogen either from the substituted carbon atom (reaction (iv)) or its unsubstituted neighbour (reaction (v)). Subsequent reactions between the polymer radicals and chlorine result in the dichlorinated polymer (reactions (vi) and (vii)). Repetition of the process yields the trichlorinated polymer (reactions viii -xi).
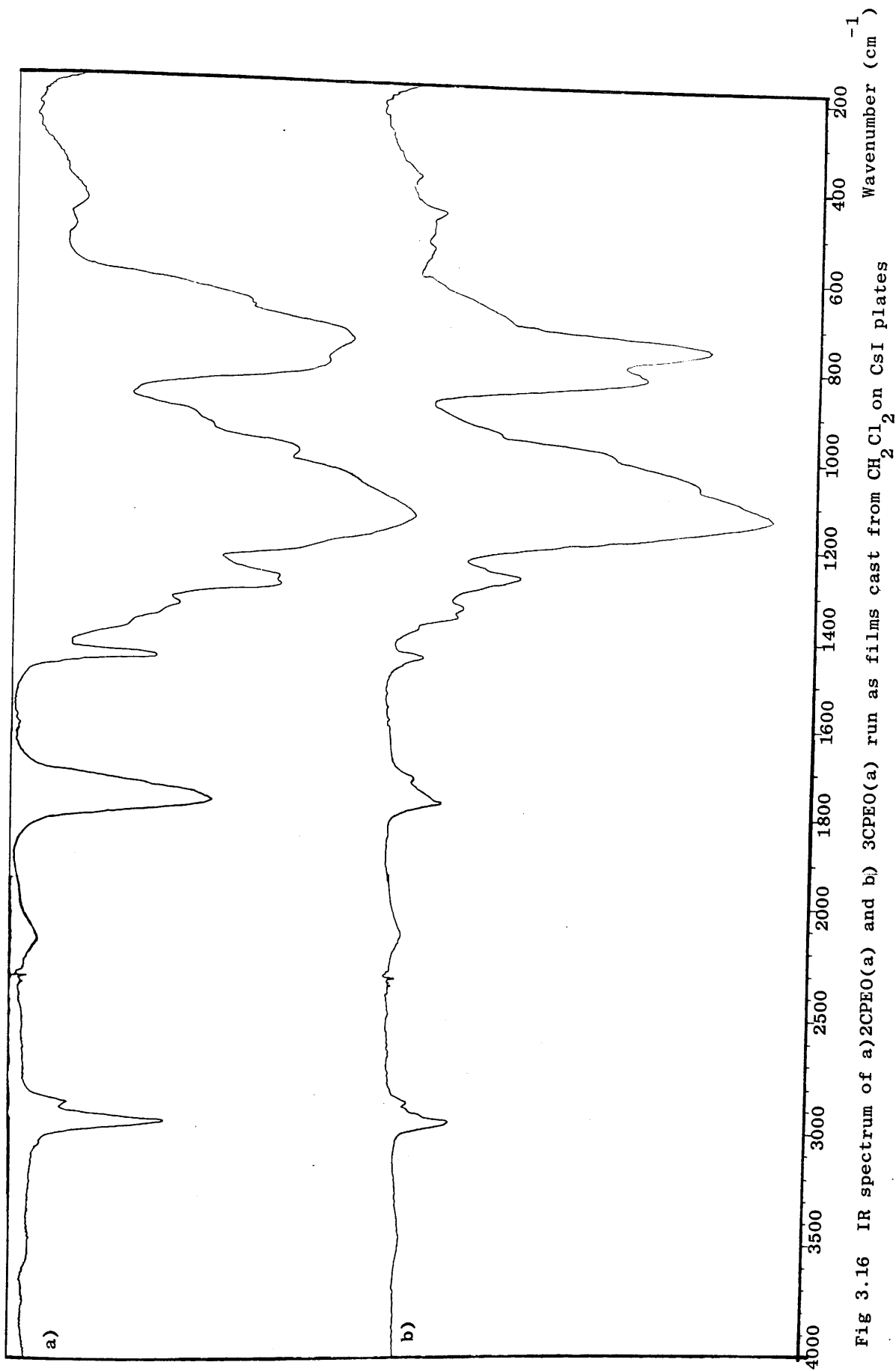
Fig 3.16 IR spectrum of a)2CPEO(a) and b) 3CPEO(a) run as films cast from CH_2Cl_2 on CsI plates

Fig 3.17   IR spectrum of 3CPEO(n) run as i) KBr disc and ii) film cast from CH_2Cl_2 on CsI plate

% TRANSMITTANCE

Wavenumber(cm^{-1})
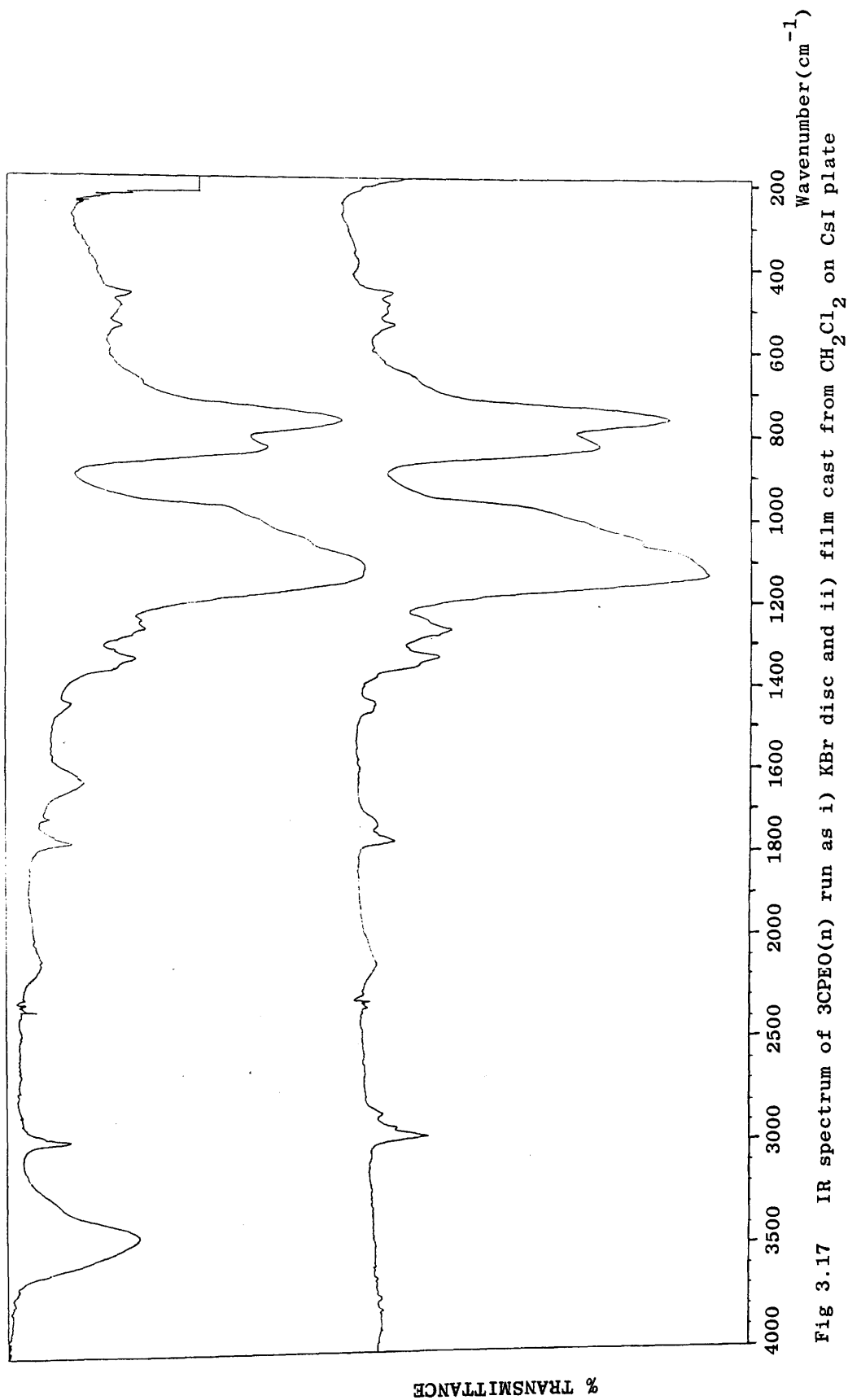
Table 3.6   IR Absorption frequencies and assignments for PEO, di-chlorinated PEO (2CPEO) and tri-chlorinated PEO (3CPEO).

PEO	3CPEO(n)	3CPEO(a)	2CPEO(n)	2CPEO(a)	Assignments
	2970 (w)	2970 (w)	2950 (w)	2950 (w)	CH_2 asym. stretch
2890 (s)	2930 (vw)	2930 (vw)			CH_2 sym stretch
	2870 (vw)	2870 (vw)	2870 (vw)	2870 (vw)	CH stretch
	1770 (w)	1770 (w)	1770 (w)	1770 (m)	acid halide carbonyl
	1725 (w)	1725 (w)	1720 (w)		aldehyde carbonyl
1468 (m)	1440 (vw)	1445 (w)	1445 (w)	1445 (m)	CH_2 bending
1360 (m)					CH_2 wagging sym
1343 (s)					CH_2 wagging asym.
	1330 (m)	1330 (w)	1330 (vw)	1340 (vw)	C-H bending
1282 (m)					CH_2 twisting
	1260 (m)	1260 (m)	1260 (m)	1275 (m)	C-O-C epoxide
1150 (m)					CO-C asym stretch
1100 (s)	1130 (s)	1128 (s)	1125 (s)	1130 (s)	C-O-C asym stretch
1060 (m)	1050 (sh)	1055 (sh)	1055 (sh)	1055 (sh)	C-O-C symm
962 (m)		985 (sh)	980 (sh)	980 (m)	CH_2 rocking
945 (m)					CH_2 rocking
843 (m)					CH_2 rocking asym.
	825 (s)	815 (s)	810 (s)	790 (s)	C-Cl stretch
	760 (s)	750 (s)	745 (s)	740 (s)	C-Cl stretch
530 (vw)	535 (vw)	535 (vw)			OCC bending
	460 (w)	458 (w)	460 (vw)	450 (vw)	C-Cl in acid halide.

$$\text{W}-CH_2 - \overset{\overset{\displaystyle Cl}{|}}{CH} - O - \text{W} \quad + Cl\cdot$$

(iv) ⟋ or ⟍ (v)

$$HCl + \text{W}CH_2 - \overset{\bullet}{C}ClO-\text{W} \qquad\qquad \text{W}\overset{\bullet}{C}H - CClHO-\text{W} \quad + HCl$$

(vi) $\downarrow$ Cl_2 or $Cl_2 \downarrow$ (vii)

$$Cl\cdot \quad + \text{W} CH_2 - CCl_2O-\text{W} \qquad\qquad \text{W} CClH - CClHO-\text{W} + Cl\cdot$$

(viii) $\downarrow$ or $\downarrow$ (ix)

$$HCl + \text{W}\overset{\bullet}{C}H - CCl_2O-\text{W} \qquad\qquad \text{W}CClH - \overset{\bullet}{C}ClO-\text{W} \quad + HCl$$

(x) $\downarrow$ Cl_2 or $Cl_2 \downarrow$ (xi)

$$Cl\cdot + \text{W}CClH - CCl_2O-\text{W} \qquad\qquad \text{W}CClH - CCl_2O-\text{W} + Cl\cdot$$
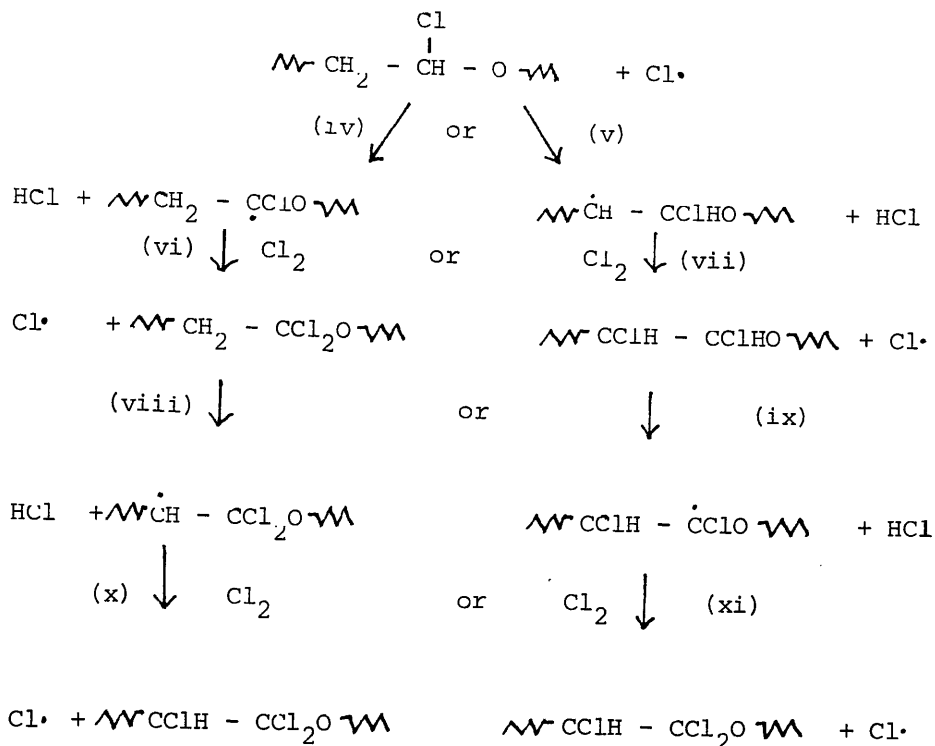
The free radical chlorination mechanism leads to some chain
scission as a side reaction during synthesis. This is
indicated by the presence of a weak absorption band at 1770 cm^{-1}
which is attributed to an acid halide carbonyl stretch, together
with the C-Cl absorption bond at 460 cm^{-1}. A weak absorption
at 1725 cm^{-1} can be assigned to an aldehydic carbonyl stretch
with the corresponding single C-H stretch (together with isolated
C-H absorptions from the polymer backbone) appearing at 2870 cm^{-1}
as a very weak absorption. Aldehydic end groups are produced
as a result of main chain scission facilitated after the abstraction
of hydrogen by a chlorine radical as shown below:

$$\text{\textasciitilde CH}_2\text{CH}_2 - \text{O} - \text{CH}_2\text{CH}_2\text{O} \text{\textasciitilde} \quad + \cdot \text{Cl}$$

$$\downarrow$$

$$\text{\textasciitilde CH}_2\overset{\bullet}{\text{CH}} - \text{O} - \text{CH}_2\text{CH}_2\text{O} \text{\textasciitilde} \quad + \text{HCl}$$

$$\downarrow \quad \text{C-O scission}$$

$$\text{\textasciitilde CH}_2\text{CHO} \quad + \quad \overset{\bullet}{\text{CH}}_2\text{CH}_2\text{O} \text{\textasciitilde}$$
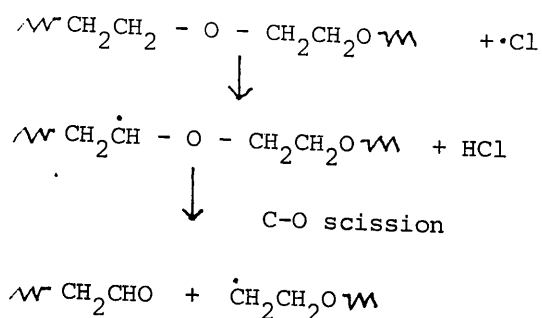
A similar reaction occurs once chlorine has been incorporated into the polymer structure, leading to the formation of acid halide end groups as illustrated below:

$$
\begin{array}{c}
\text{Cl} \\
| \\
\text{\textasciitilde CH}_2 - \text{C} - \text{O}\text{\textasciitilde} \\
| \\
\text{H}
\end{array}
$$

$$\downarrow \cdot \text{Cl}$$

$$
\begin{array}{c}
\text{Cl} \\
\nwarrow \\
\text{\textasciitilde CH}_2 - \underset{\bullet}{\text{C}} - \text{O}\text{\textasciitilde} \quad + \text{HCl}
\end{array}
$$

$$\downarrow \quad \text{C-O scission}$$

$$
\begin{array}{c}
\text{Cl} \\
| \\
\text{\textasciitilde CH}_2 - \text{C} = \text{O} \quad + \quad \cdot\text{CH}_2\text{CH}_2\text{O}\text{\textasciitilde}
\end{array}
$$
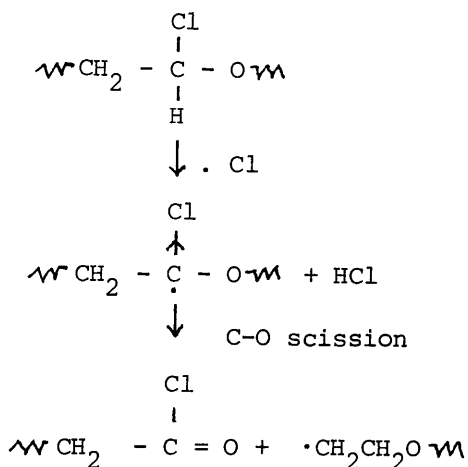
These chain scission reactions are in competition with the chlorination reaction. From the IR data, under conditions where there is a high chlorine content in solution, main chain scission is a minor reaction whilst chlorination proceeds preferentially. The relative intensities of these end groups absorptions (acid halide stronger) suggest that the latter reaction is more important than aldehydic end formation, due to

the electron withdrawing inductive effect of the chlorine atom enhancing chain scission. Main chain scission proved especially awkward, however, when attempts were made to prepare the monochlorinated derivative as the products obtained in these cases were oils.

When the reaction was carried out in air, the IR spectra showed no significant increases in the carbonyl stretching absorption (1775 cm^{-1}) relative to that for the ether C-O-C asymmetric stretching band (1120 cm^{-1}). This suggests that under these experimental conditions oxygen does not enhance chain scission via the formation of carbonyl compounds. Kagiya et al[111] investigating radiation induced degradation of PEO in the atmosphere of chlorine compounds observed the appearance of a variety of carbonyl absorption bands in the IR spectrum when PEO powder was subjected to γ radiation in air. These included ester type carbonyl (1750 cm^{-1}), aldehydic (1733 cm^{-1}), ketonic (1721 cm^{-1}), and carbonyl (1715 cm^{-1}) absorptions. In addition, hydroxyl bands were observed (3400 cm^{-1}). Similar oxidative degradation occurred when UV radiation was employed. In similar experiments in CCl_4 little change in the IR spectrum was noted apart from the appearance of an acid chloride absorption. Chlorine appeared to have the greatest effect on the degradation of PEO when the polymer was irradiated with UV light. This was seen by the decrease in molecular weight and the presence of IR bands at 1760 cm^{-1} and 800 cm^{-1} due to acid chloride and C-Cl ansorptions respectively in the irradiated product. Also it was noted that when UV irradiation of PEO was carried out in vacuum, cross linking took place. Thus the results obtained in the present investigation

are in agreement with the Japanese workers.   The apparent lack

of oxidation products is due to the dilution effect of the solvent

and Cl_2 on the atmospheric oxygen and also the less severe

conditions employed (35-80 minutes irradiation c.f. 4 hours).

Oxygen, however, slightly hinders the chlorination reaction.

Initial IR spectra for the synthesised chlorinated polymers

were obtained as KBr discs (to prevent the complications of any

residual chloroalkane solvent peaks in the assignments of the

polymer absorptions).   This however led to the appearance of

OH absorptions which were attributed to traces of water in the

KBr as when IR spectra were obtained using films cast from CH_2Cl_2,

the broad absorption bands at 3440 cm^{-1} and 1630 cm^{-1} disappeared

(see Figure 3.17).

Prior to discussion of the results of the molecular weight

measurements, it should be noted that GPC is a relative technique,

in this case based on polystyrene.   The resultant molecular

weights may therefore vary considerably from the actual molecular

weight of the polymer.   This in fact was noticed as the $\overline{Mn}$ value

of 1000 received from Rapra Technology Limited for PEO is

considerably lower than the suppliers stated molecular weight of

100,000.   It is possible that this difference may arise from

polar PEO interacting with the gel phase in the GPC and thus being

retained in the column, mimicking the behaviour of low molecular

weight compounds.   The separation mechanism in GPC is based on

porous beads within the gel phase which separates by size.   Thus

larger molecules which cannot penetrate the pores are eluted first

whilst smaller molecules are retained in the pores resulting in a

greater elution time.   The experimental curve produced by a

GPC instrument is a differential weight distribution of

retention volumes which is subsequently, by means of numerical

computation, converted to a molar mass distribution.   Polar

molecules of PEO, although they are large in size, may be held

by the porous beads and eluted at a later stage than would be

expected for their molecular weight.   Thus $\overline{M}n$ appears at a

lower value.   This factor may contribute to the peak obtained

in the molecular weight distribution curves at lower molecular

weights and account for the high value produced for the distribution

of molecular weights in the PEO sample (D = 18.3).

On considering the $\overline{M}n$ values for chlorinated PEO, the

trend observed is that upon chlorination, both in nitrogen and in

air, the molecular weight increases.

CALIBRATION : THF.7.88
RUN NO./NAME: A207 SAMPLE A   (7459)   1147 080788

PEAK START: 1430   MN: 9.12E+02
PEAK FINISH: 2050

                                 MW: 1.67E+04
BASELINE START: 1430
BASELINE FINISH: 2400   MZ: 4.37E+04

FLOW CORRECTION: .996   MP: 1.98E+04

KP: 1.200X10^{-4}
                                 D: 18.301
AP: .710

Fig 3.18   GPC trace for PEO.

10^ 1   10^ 8

MOLECULAR   WEIGHT
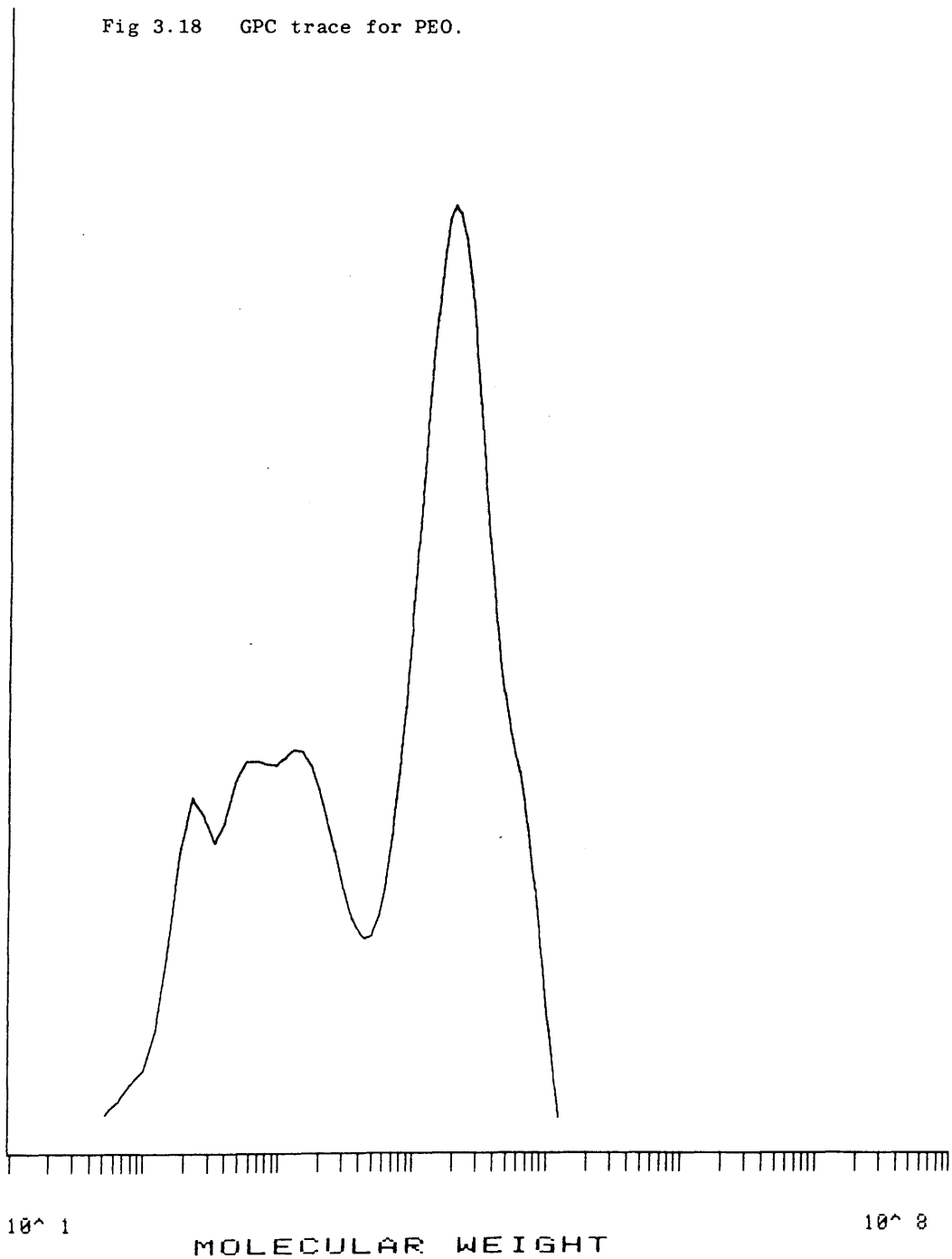
CALIBRATION : THF.7.88
RUN NO./NAME: A204 SAMPLE B (7460)   0941 080788

PEAK START: 1490   MN: 2.36E+03
PEAK FINISH: 2050

                                  MW: 1.14E+04
BASELINE START: 1490
BASELINE FINISH: 2400   MZ: 2.00E+04

FLOW CORRECTION: .995   MP: 1.36E+04

KP: 1.200X10^{-4} D: 4.835
AP: .710

Fig 3.19   GPC trace for 2CPEO(n)

10^ 1   10^ 8

MOLECULAR WEIGHT
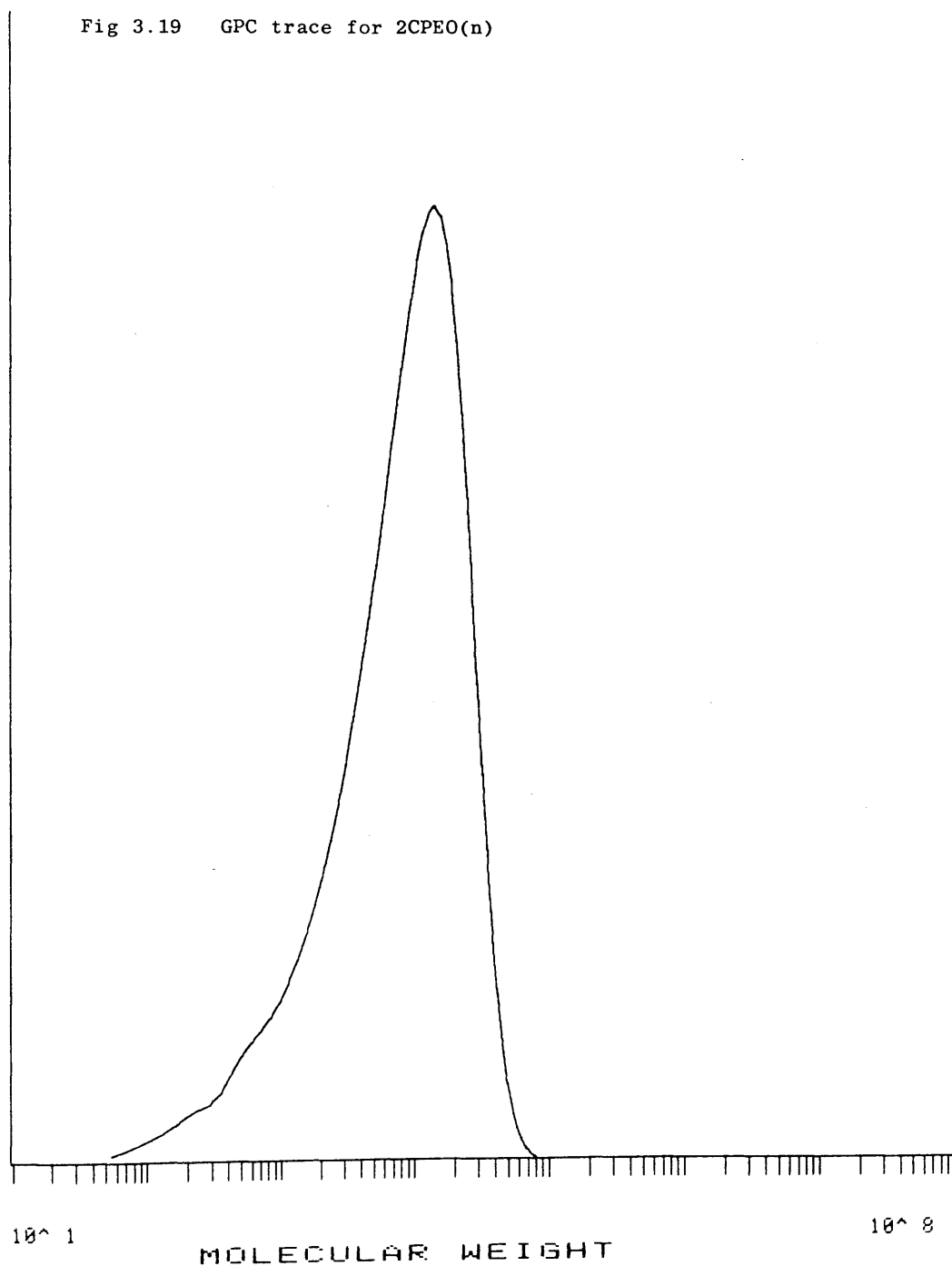
CALIBRATION : THF.7.88
RUN NO./NAME: A203   SAMPLE C   (7461)   9859 080788

PEAK START: 1520   MN: 1.77E+03
PEAK FINISH: 2050

                                     MW: 3.33E+03

BASELINE START: 1520
BASELINE FINISH: 2400   MZ: 1.55E+04

FLOW CORRECTION: .995   MP: 1.00E+04

KP: 1.200×10^{-4} D: 4.701
AP: .710

Fig 3.20   GPC trace for 2CPEO(n)

10^ 1   10^ 8
        MOLECULAR   WEIGHT
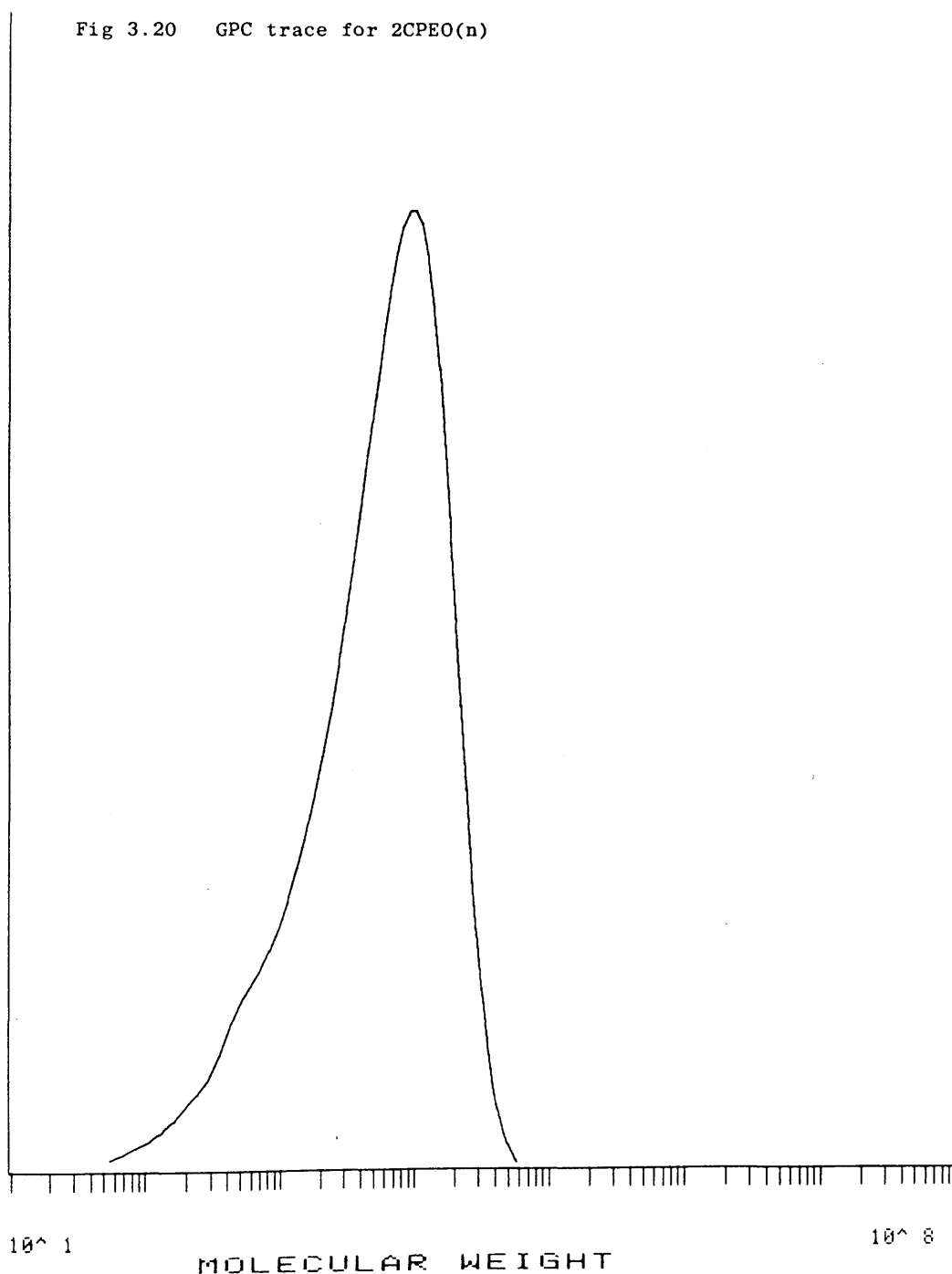
CALIBRATION : THF.7.88
RUN NO./NAME: A209 SAMPLE D (7462)   1324 080788

PEAK START: 1490   MN: 4.02E+03
PEAK FINISH: 2030

                                 MW: 1.34E+04
BASELINE START: 1490
BASELINE FINISH: 2400   MZ: 1.91E+04

FLOW CORRECTION: .997   MP: 1.32E+04

KP: 1.200X10^{-4} D: 3.324
AP: .710

Fig 3.21   GPC trace for 2CPEO(a)

10^ 1   MOLECULAR WEIGHT   10^ 8
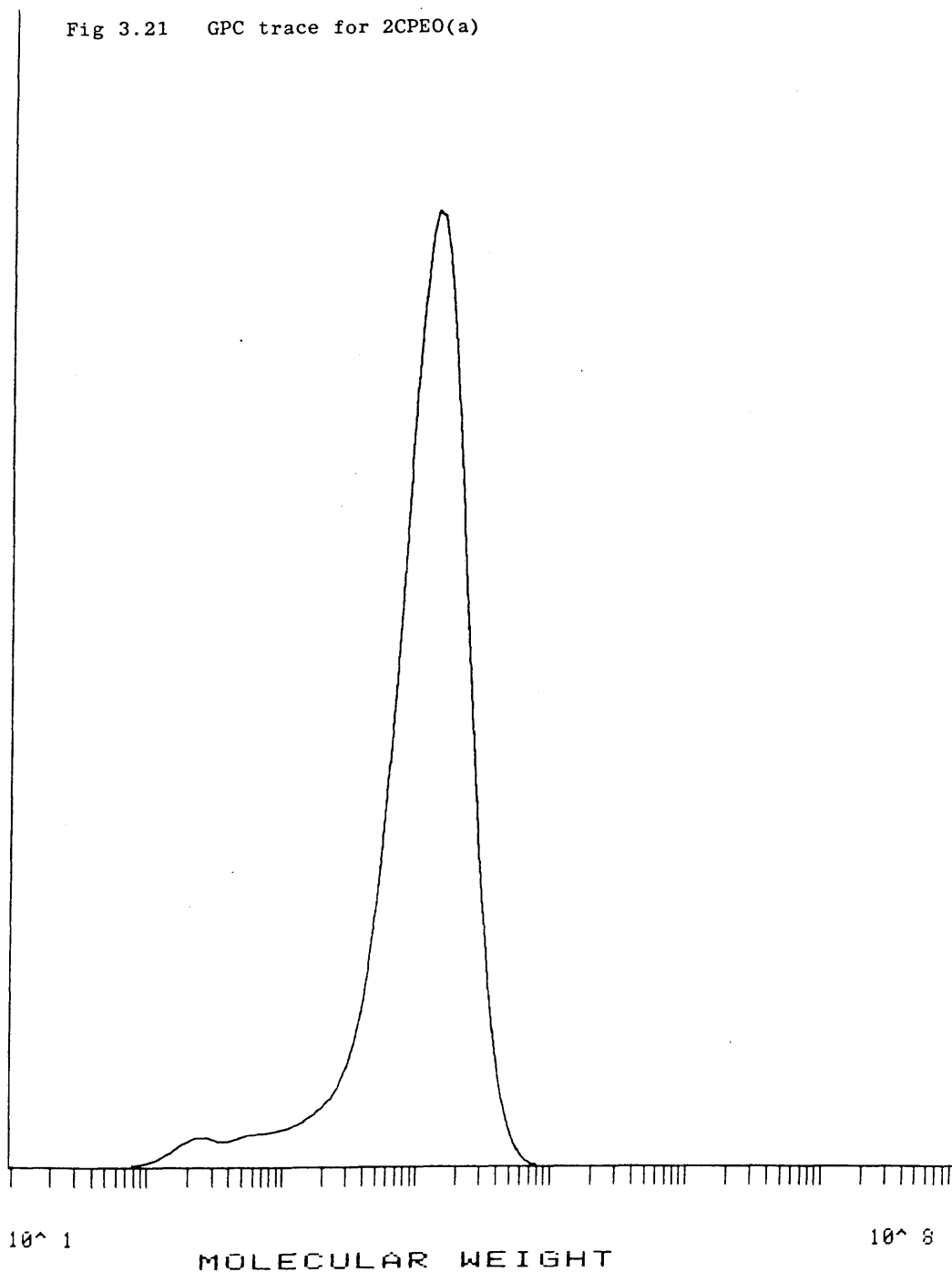
CALIBRATION : THF.7.88
RUN NO./NAME: A208 SAMPLE E (7463)   1228 080788

PEAK START: 1450   MN: 1.73E+03
PEAK FINISH: 2050

                                   MW: 1.08E+04
BASELINE START: 1450
BASELINE FINISH: 2400   MZ: 2.18E+04

FLOW CORRECTION: 1.000   MP: 1.02E+04

KP: 1.200×10^{-4} D: 6.250
AP: .710

Fig 3.22   GPC trace for 3CPEO(a)

10^1 10^8
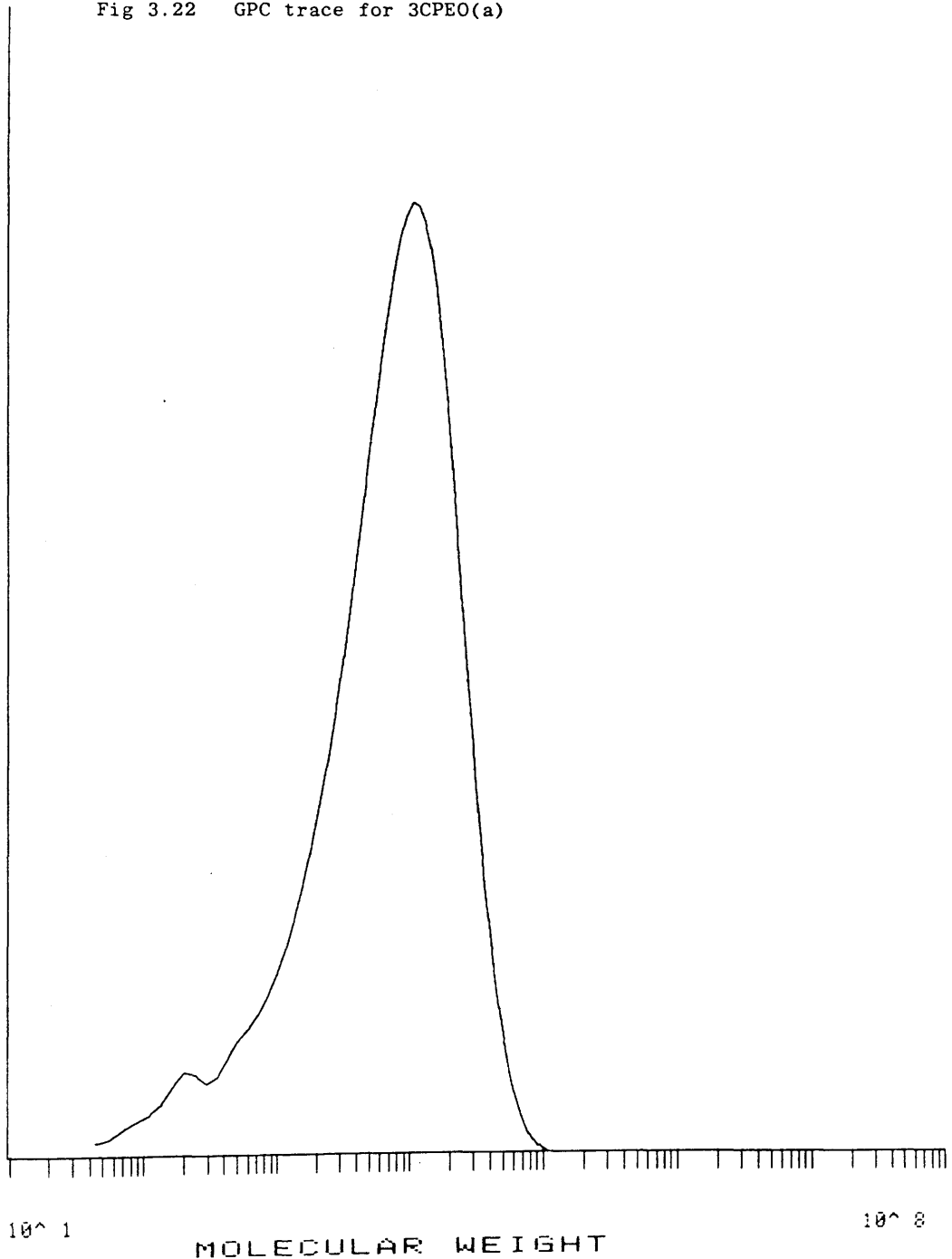
MOLECULAR WEIGHT

Table 3.7   Molecular Weight Averages expressed as "polystyrene equivalents" and Molecular Weight Distribution (D), for PEO, di-chlorinated PEO (2CPEO) and tri-chlorinated PEO (3CPEO)

Sample.	$\overline{M}n$ (10^{+3})	$\overline{M}w$ (10^{+4})	$\overline{M}z$ (10^{+4})	$\overline{M}p$ (10^{+4})	D
PEO	0.91	1.67	4.37	1.98	18.30
PEO	1.00	1.90	4.35	2.25	18.90
2CPEO(n)	2.01	1.10	1.98	1.37	5.48
2CPEO(n)	2.36	1.14	2.00	1.36	4.84
3CPEO(n)	1.77	8.33	1.55	1.00	4.70
3CPEO(n)	1.81	8.47	1.59	0.95	4.69
2CPEO(a)	1.73	1.08	2.18	1.02	6.25
2CPEO(a)	1.50	1.06	2.19	1.02	7.04
3CPEO(a)	3.72	1.32	1.89	1.32	3.54
3CPEO(a)	4.02	1.34	1.91	1.32	3.32

3.4 THERMAL DEGRADATION OF CHLORINATED POLY(ETHYLENE OXIDE)

3.4.1 Experimental

Thermal Analysis of Chlorinated Poly(ethylene oxide)

TG   Thermogravimetry was performed under nitrogen.   In all cases, irrespective of the conditions of synthesis or degree of chlorination, weight loss occurred in a single stage.   Typical TG and DTG curves for chlorinated PEO are illustrated in Figure 3.23.   The onset temperatures (T_{onset}) and temperatures of the maximum rate of degradation (T_{max}) for the various chlorinated samples are shown together with values obtained for PEO in Table 3.8.

Weight loss for CPEO prepared under nitrogen begins at approximately 240°C for both di- and tri-chlorinated samples. The onset temperatures for the polymers prepared in air are not so consistant however, being 251°C for the dichlorinated compound and 227°C for the trichlorinated compound.   When T_{max} values are also considered, it is apparent that the polymers made in air are less stable than those prepared under nitrogen, whether one or two Cl atoms are present per monomer unit.   Extent of chlorination also affects the temperatures of the maximum rate of degradation as, irrespective of being prepared in air or under nitrogen, the trichlorinated polymer appears to be slightly less stable than the dichlorinated compound.   The residue in each case after heating to 500°C is negligible, accounting for less than 1% of the original polymer weight.

On comparing the temperatures of onset of weight loss and maximum rate of weight loss of the chlorinated compounds to those
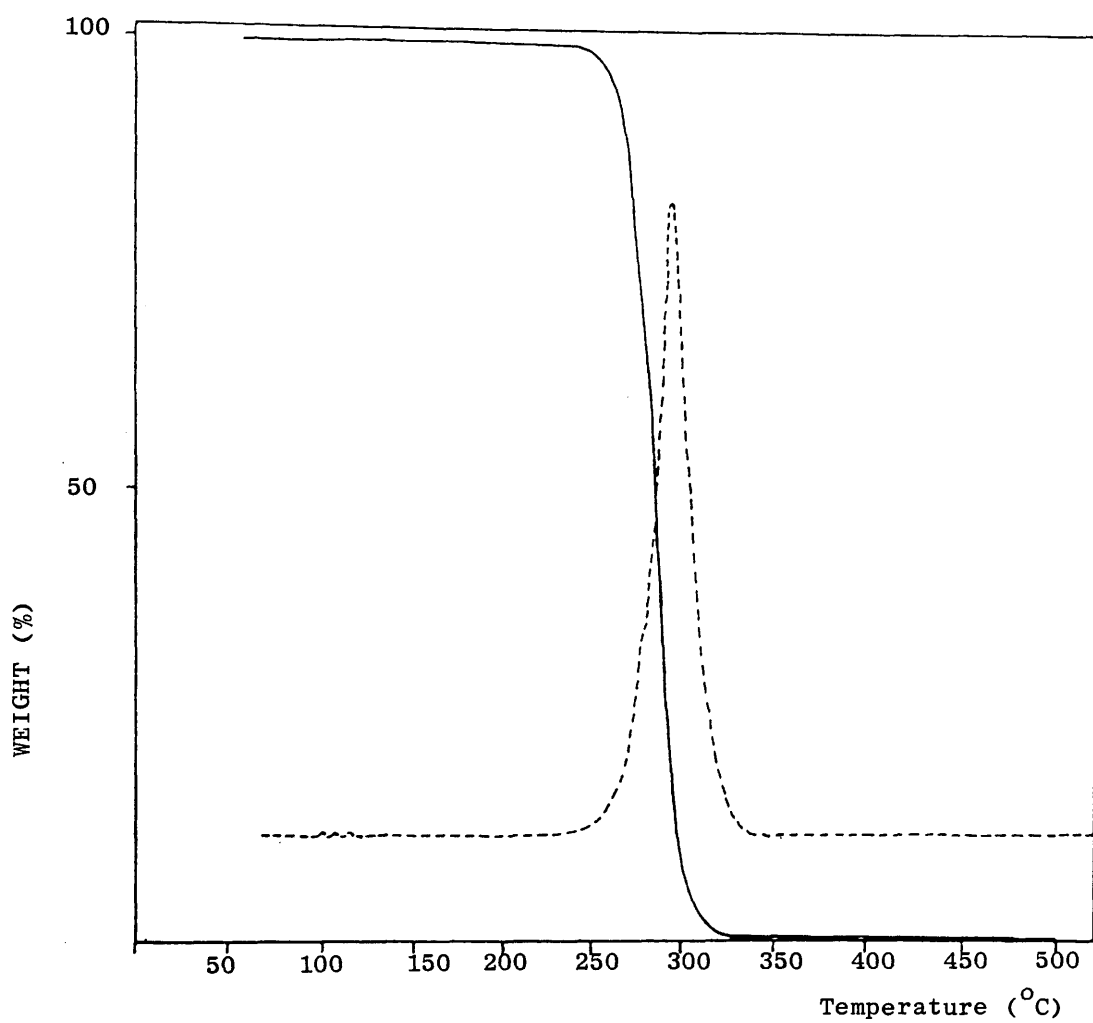
Fig 3.23   TG(-) and DTG (---) curves for 3CPEO under nitrogen at a heating rate of 10° min^{-1}
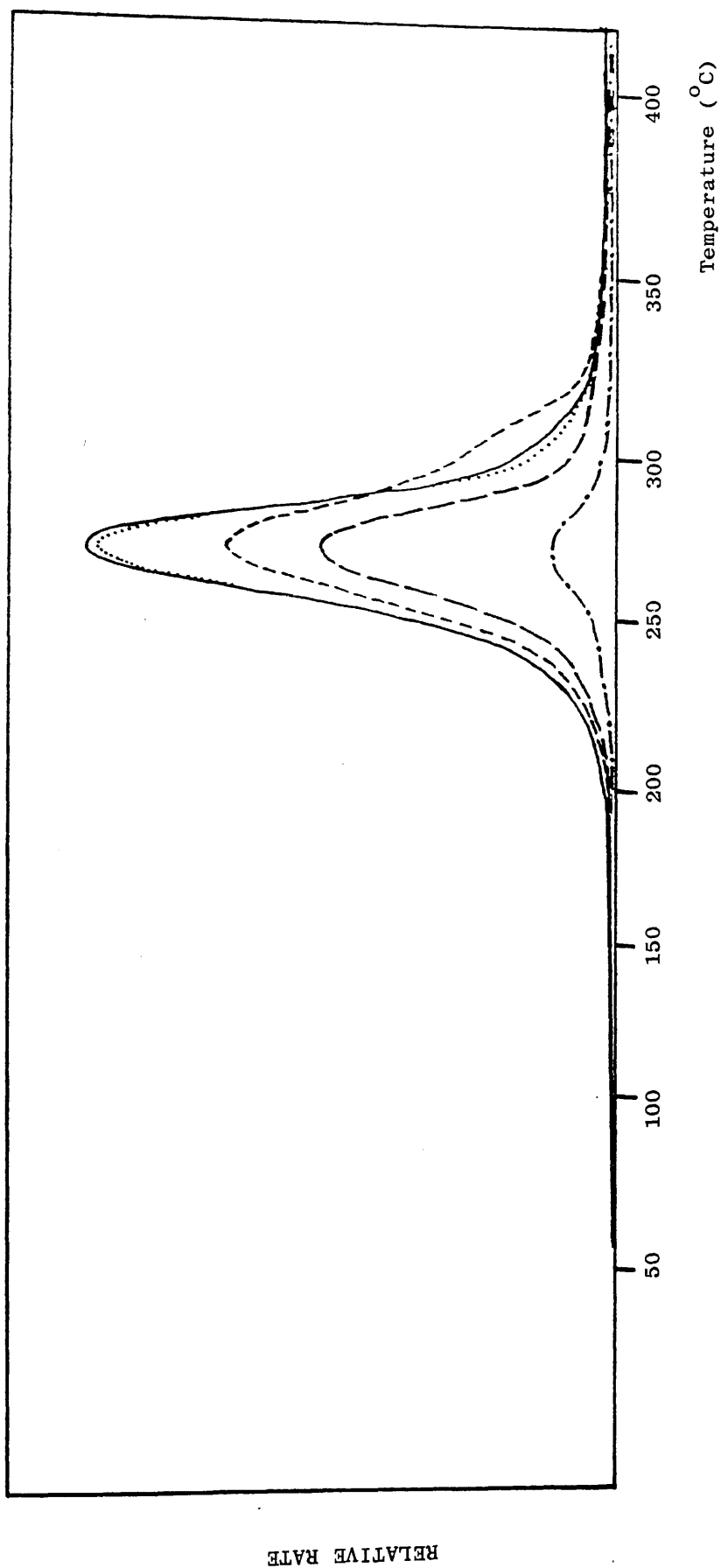
Fig 3.24 TVA curve for 3CPEO(n) using 43 mg powder sample.

obtained for pure PEO, it can be seen that chlorination

destabilises PEO to heating.

TVA

   The TVA curves for all the chlorinated polymers were

similar in appearance and a typical TVA curve for CPEO is

reproduced in Figure 3.24.   As in the case of PEO, a single

degradation peak was observed.   The onset of evolution of

volatile products occurs in the range 190-210°C and reaches a

maximum between 265 and 270°C.   The behaviour of the individual

TVA traces indicate a variety of compounds being evolved including

non-condensable products.   A notable difference is in the

appearance of a slight plateau in the -75°C trace following the

main degradation peak.   This type of behaviour is known as a

"limiting rate effect",[91]   and has been observed in several polymer

systems.[92]   The limiting rate effect occurs when a substance

condenses in the initial trap (0, 45, -75,-100°C) of a TVA system

but is sufficiently volatile to distil slowly from this trap to

the main trap (-196°C).   The TVA behaviour of CPEO, showing

this effect, is illustrated diagramatically in Figure 3.25.
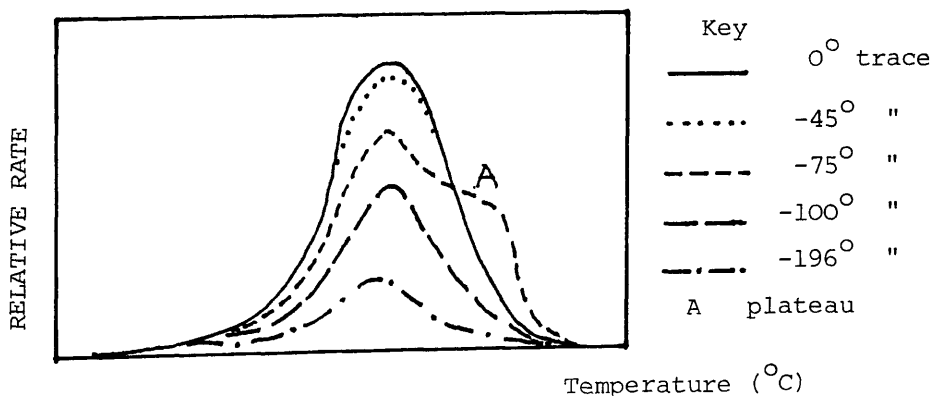
Fig 3.25 Diagramatic Representation of TVA Curve for CPEO
          illustrating the limiting rate effect in -75° trace.

Table 3.8 Onset temperatures and temperatures of maximum rate
          of degradation of chlorinated PEO obtained from TG
          and DTG under nitrogen with a heating rate of 10° min^{-1}.

Sample.	T_{onset} ($^{\circ}$C)	T_{max} ($^{\circ}$C)	Weight % Residue.
2[*]CPEO(n)[**]	190	277	1.0
2CPEO(a)	207	270	0.8
3CPEO(n)	190	261	0.75
3CPEO(a)	175	240	0.5
PEO	314	383	1.75

[*] approximate number of Cl atoms per EO unit.

[**] atmosphere during synthesis i.e. nitrogen(n) or air(a)

Table 3.9   Onset temperatures and temperatures of maximum rate
          of degradation of chlorinated PEO obtained from TVA.

Sample	T_{onset} ($^{\circ}$C)	T_{max} ($^{\circ}$C)
2CPEO(n)	213	271
2CPEO(a)	200	267
3CPEO(n)	217	271
3CPEO(a)	192	266
PEO	310	374

These limiting rate effects are very temperature dependent and
any slight variation in trap temperature may cause the effect to
disappear.   In the chlorinated PEO system however, the limiting
rate effect was found to be reproducible.

The results obtained by TVA for onset and rate maximum
temperatures for each chlorinated polymer sample and including
pure PEO for comparison are shown in Table 3.9.   The values
produced from TVA experiments are comparable to those obtained
by TG.   Although under TVA conditions there is no difference
in temperature, at the maximum rate of degradation, between the
di- and tri-chlorinated compounds prepared under nitrogen, this
temperature is once again lower for the samples prepared in air.
The TVA traces also demonstrate the thermal destabilising effect
chlorine has since in the pure polymer the degradation peak begins
at approximately 310°C and reaches a maximum at 374°C which is
roughly 100°C higher than the degradation temperatures of CPEO.

SATVA Separation of Condensable Degradation Products.

Chlorinated PEO samples of approximately 75 mg were heated
to 450°C at a rate of 10° min^{-1} and the volatile degradation
products were separated by SATVA and identified using gas or
liquid phase IR spectroscopy.   The SATVA traces for all
chlorinated samples indicated three major fractions as illustrated
in Figures 3.26 and 3.27.

In the case of the dichlorinated polymers the final two
SATVA peaks are poorly resolved and the materials present were
collected as a single fraction.   With the trichlorinated

Fig 3.26 SATVA trace for condensable volatile degradation products on heating 50 mg 2CPEO(n) to 450°C
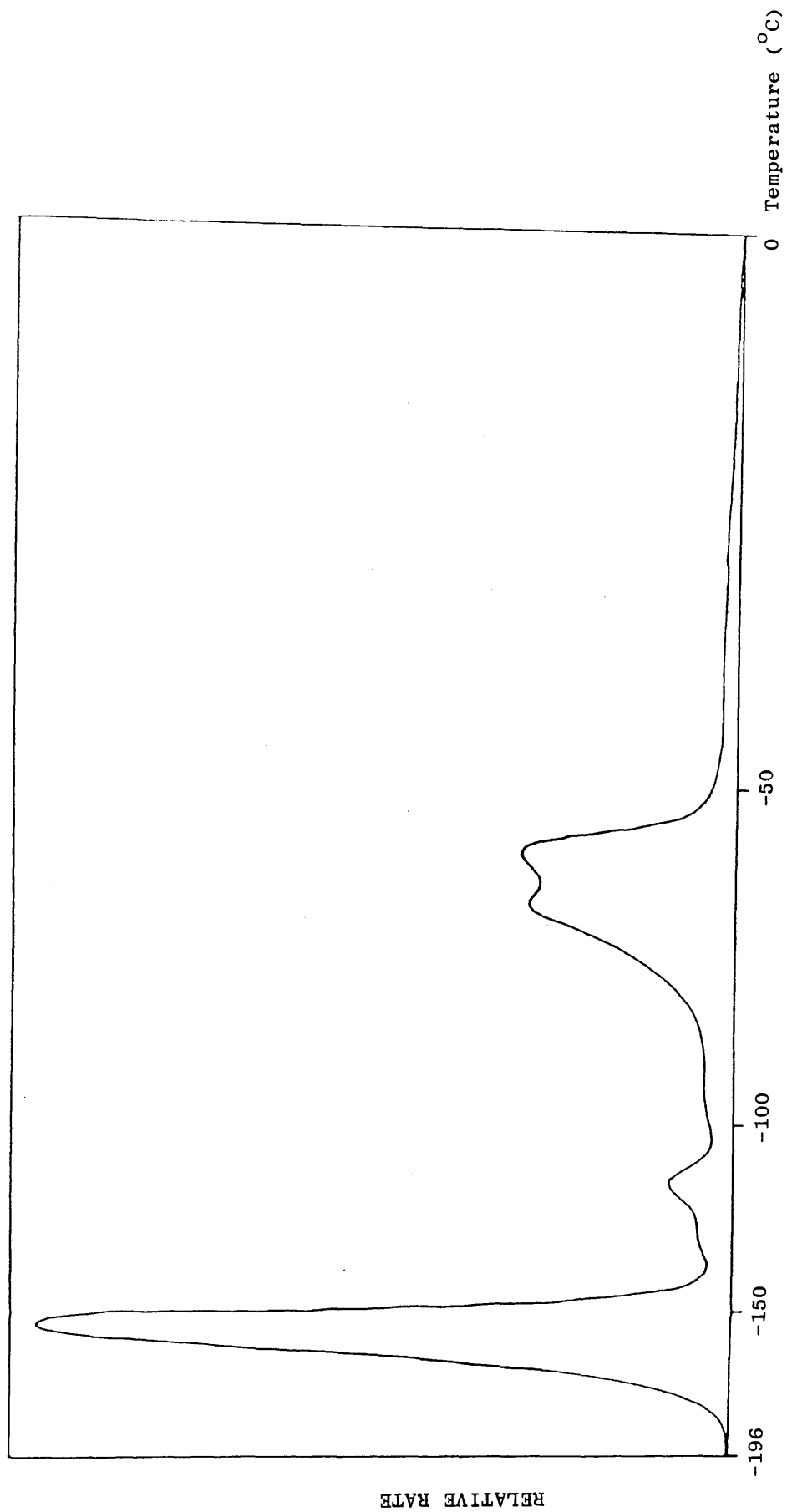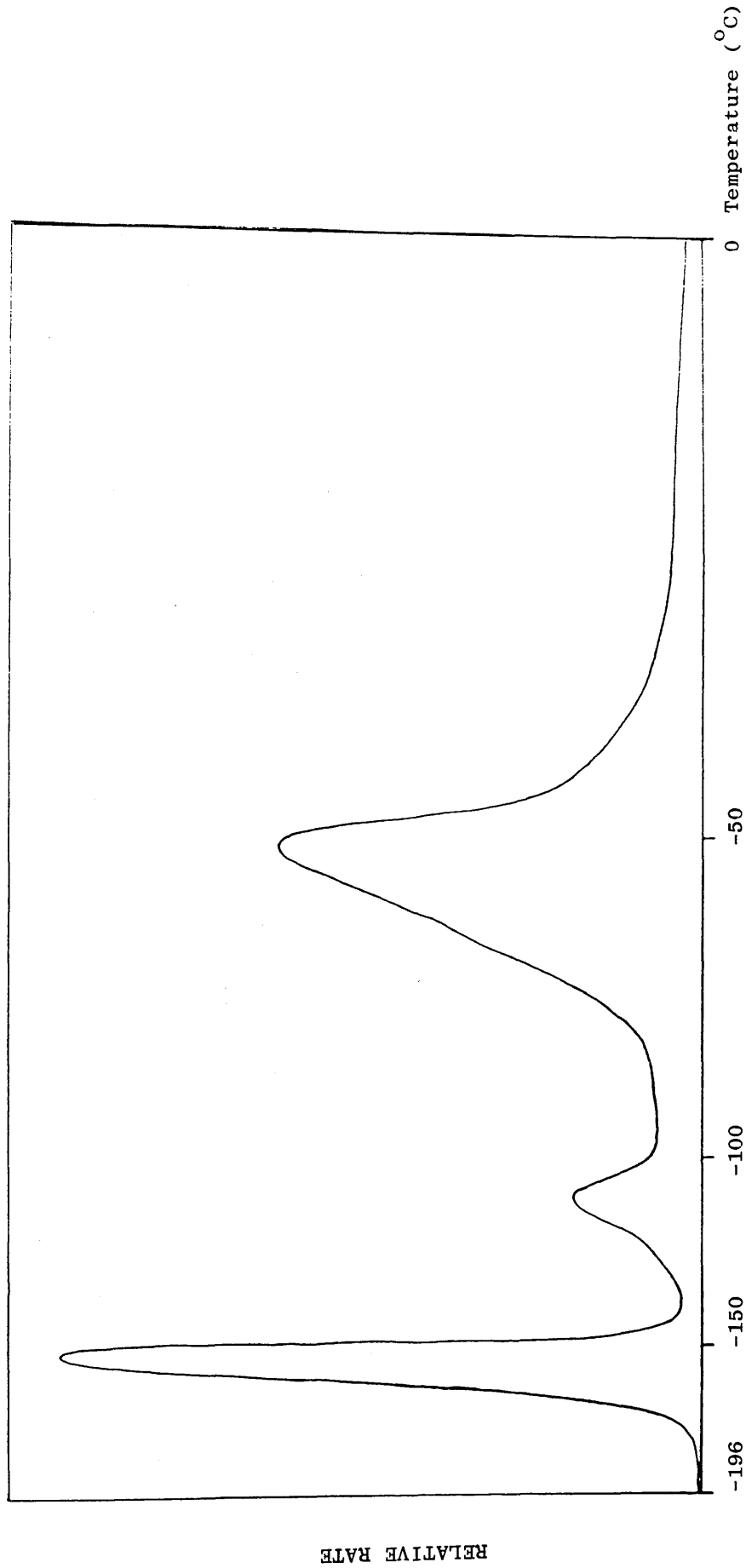
Fig. 3.27 SATVA trace for condensable volatile degradation products on heating 77 mg 3CPEO(n) to 450°C

compounds, the first peak in the final fraction appeared as a

shoulder. These features as well as the fraction boundaries

are diagramatically shown in Figure 3.28.
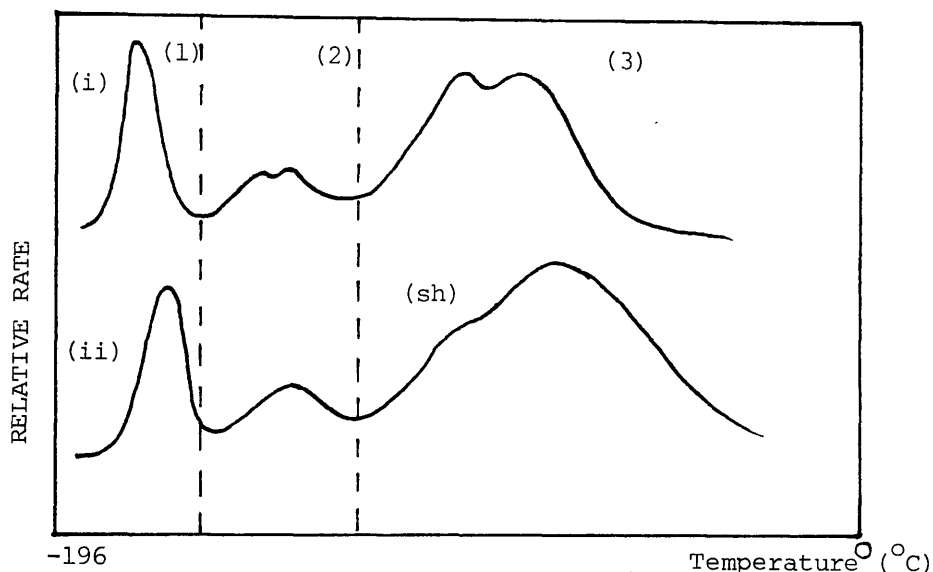
Figure 3.28 : SATVA trace for condensable volatile degradation
products of (i) 2CPEO and (ii) 3CPEO indicating
peak shoulder (sh) and product fraction
boundaries (----)

The products obtained on thermal degradation were the

same irrespective of the atmosphere under which the polymers

were prepared or their degree of chlorination. The first

fraction was found to consist of HCl and CO_2. The gas phase

IR spectrum of the degradation products in Fraction (1) of the

SATVA trace for CPEO is reproduced in Figure 3.29. The

second fraction was mainly due to phosgene (see Figure 3.30)

however traces of CCl_4 (solvent) and an unidentified unsaturated

compound were also observed. The final fraction, a colourless

liquid with a pungent odour was found to be a complex mixture

of chlorinated acetyl chlorides, with some aldehydic and
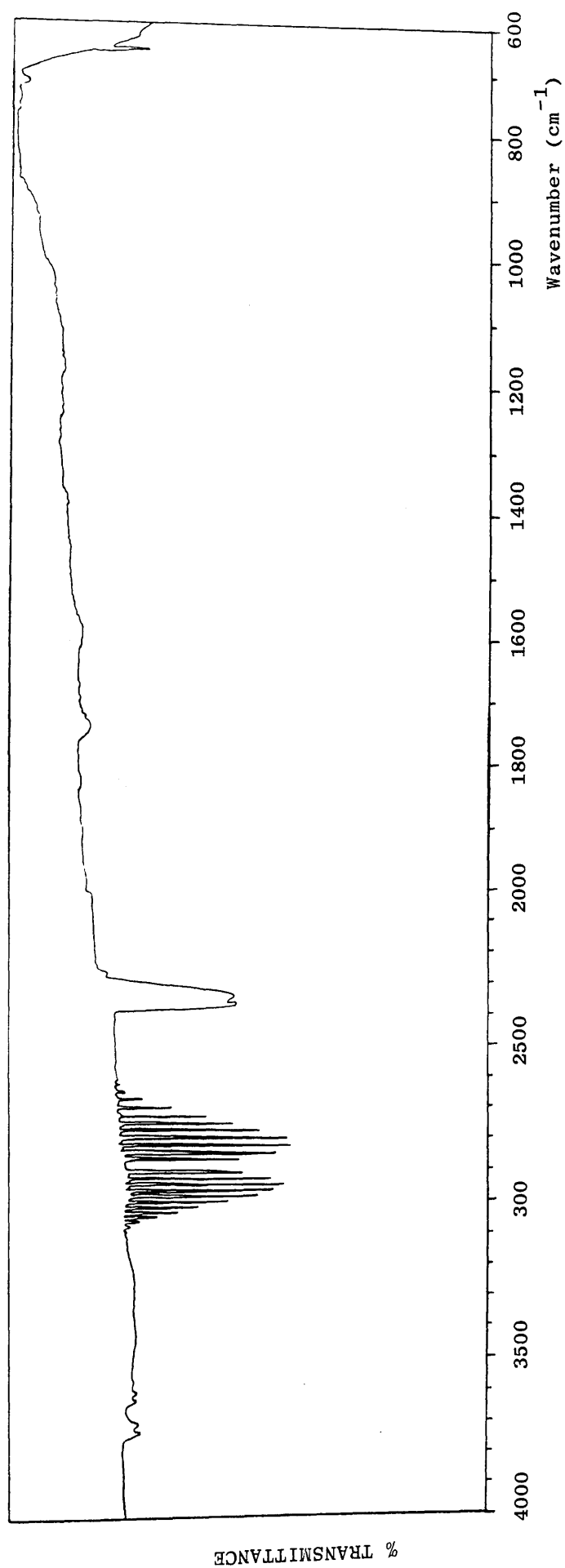
Fig 3.29 IR spectrum of degradation products in Fraction (1) of SATVA trace of CPEO.
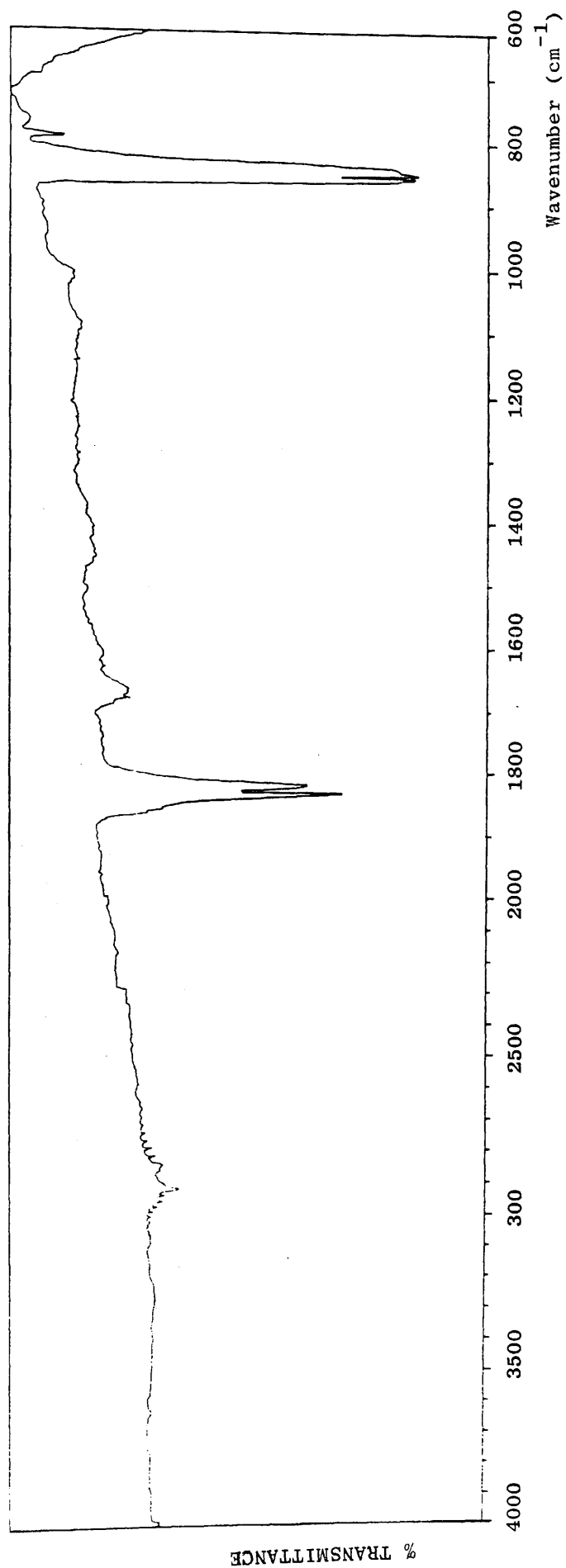
Fig 3.30   IR spectrum of degradation products in Fraction (2) of SATVA trace of PEO.

unsaturated compounds also present.   The liquid phase IR spectrum

for the final fraction is shown in Figure 3.31.   In both types

of chlorinated polymer mono-, di- and trichloroacetyl chlorides

were found to be present but in different amounts.   The main

component was dichloroacetyl chloride.   Traces of chloroacetyl

chloride were found after degradation of the trichlorinated

polymer, but IR absorptions suggested that this material was

more abundant from the dichlorinated polymer.   The IR absorption

frequencies of all the degradation products from CPEO as separated

by SATVA together with the corresponding assignments are listed in

Table 3.10.

Due to the overlap of absorption bands in the IR spectra

of the chlorinated acetyl chlorides, the identification of chloro-

acetyl chloride was verified using coupled gas-liquid chromatography

and mass spectrometry (GC-MS).   For this experiment, initially a

sample of products from degradation of the more highly chlorinated

PEO, 3CPEO(a) was analysed as only trace amounts of chloroacetyl

chloride had been indicated by the IR spectrum.   Approximately

100 mg of polymer was degraded under the usual TVA conditions

and the volatile products were separated by SATVA.   The final

fraction was removed for GC-MS analysis but prior to injecting

the sample, ethyl acetate (solvent) was added then the solution

was treated with methanol to convert the acid chlorides present

to their corresponding esters and thus ensure their removal from

the GC column.   The reaction is as follows:
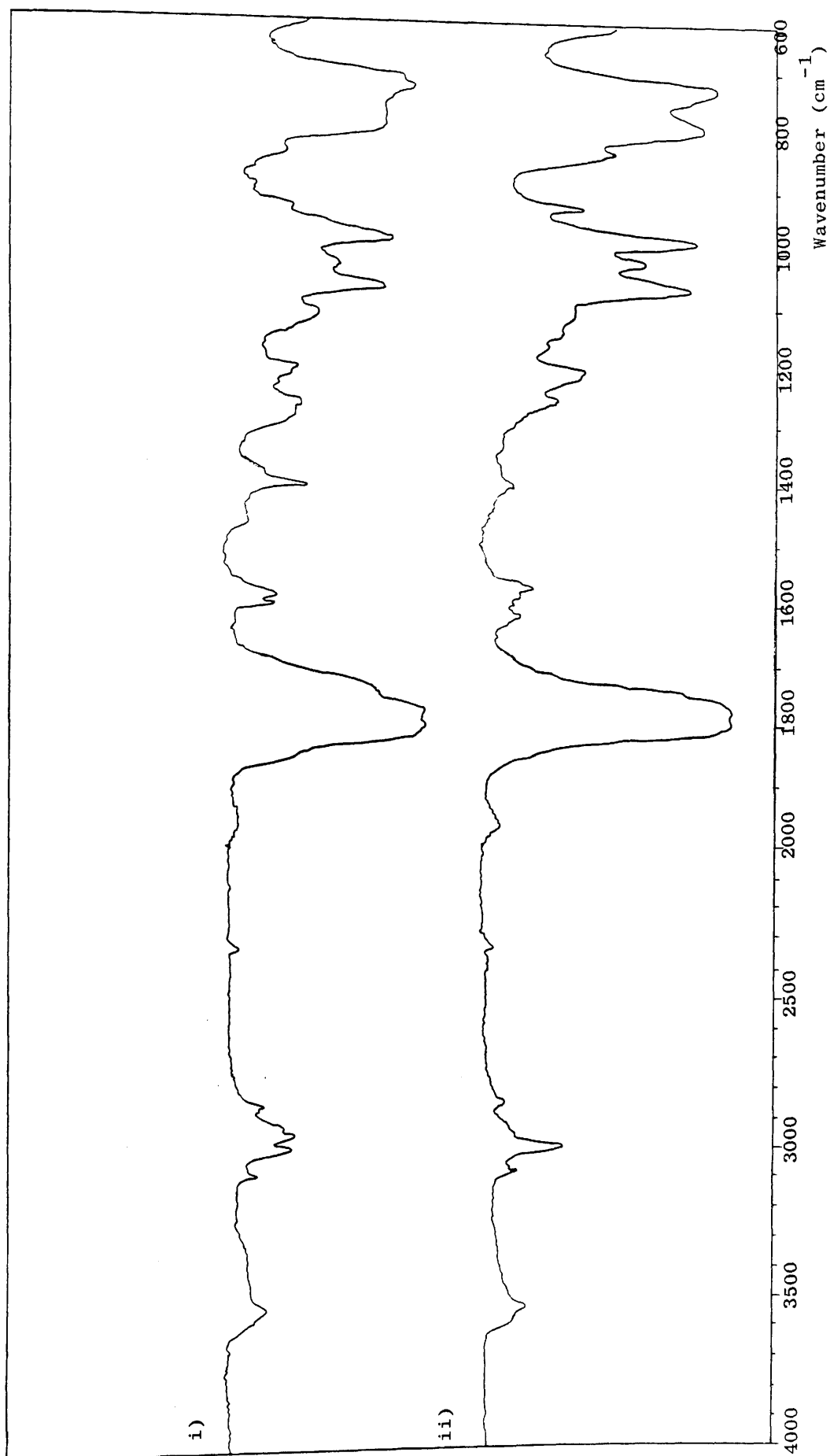
Fig 3.31 Liquid phase IR spectrum of degradation products on Fraction (3) of SATVA trace of PEO.

Table 3.10a - IR Spectrum for Fraction (1) of SATVA trace
for 2CPEO and 3CPEO degradation products.

Absorbance Frequency (cm^{-1})	Product or Band Assignment
3720 (m), 3700 (m) 3630 (m), 3590 (m)	CO_2
2920 (s), 2820 (s)	HCl
2330 (s), 719 (w), 665 (w)	CO_2

Table 3.10b - IR Spectrum for Fraction (2) of SATVA trace
for 2CPEO and 3CPEO degradation products.

Absorbance Frequency (cm^{-1})	Product or Band Assignment
1833 (s), 1820 (s) 856 (s), 850 (s)	$COCl_2$
2920 (w) 2870 (w)	HCl (trace overlap)
2118 (w) 2170 (w) 1680 (w) 1666 (w) 1600 (w)	unidentified
795 (w)	CCl_4 (trace, solvent)

Table 3.10c — IR Spectrum for Fraction (3) of SATVA trace
for 2CPEO degradation products.

Absorbance Frequency (cm^{-1})	Product or Band Assignment
3570 (w) 3530 (w)	CCl_3COCl
3080 (w)	$\rangle C=CH_2$
3000 (m) 2950 (m)	$CHCl_2COCl$
2930 (w), 2860 (w), 2850 (w)	CH_2, CH
2332 (w)	CO_2 (trace overlap)
1960 (w)	unidentified
1796 (s)	CCl_3COCl, $CHCl_2COCl$, $CH_2ClCOCl$
1772 (s)	$CHCl_2COCl$
1745 (sh)	$CHCl_2CHO$
1740 (sh)	CCl_3COCl
1735 (sh)	CH_2ClCHO
1595 (m), 1580 (m)	$\rangle C=C\langle$
1396 (m)	$CH_2ClCOCl$, $CHCl_2CHO$
1260 (m)	$CH_2ClCOCl$, $CHCl_2COCl$
1200 (m)	$CHCl_2CHO$
1112 (m)	unidentified
1065 (s), 985 (s), 730 (s)	$CHCl_2COCl$
1036 (m), 970 (sh) 896 (w) 716 (sh)	$CH_2ClCOCl$
1026 (m), 840 (m), 730 (s)	CCl_3COCl
930 (m)	unidentified
795 (s)	$CHCl_2COCl$, CCl_3COCl, $CHCl_2CHO$
756 (sh)	$CHCl_2COCl$, CH_2ClCHO

Table 3.10d -   IR Spectrum for Fraction (3) of SATVA trace
for 3CPEO degradation products.

Absorbance Frequency (cm^{-1})	Product or Band Assignment
3580 (w), 3530 (w)	CCl_3COCl
3520 (w)	$CHCl_2COCl$
3080 (w), 3060 (w)	$>C=C<^H_H$
3000 (m)	$CHCl_2COCl$, $CH_2ClCOCl$
2848 (w)	CH
2330 (w)	CO_2 (trace, overlap)
2020 (vw)	CCl_3COCl
1965 (w)	unidentified
1795 (s), 1775 (s)	$CHCl_2COCl$
1746 (sh)	CCl_2HCHO
1735 (sh)	CH_2ClCHO
1614 (w), 1568 (w)	$>C=C<$
1396 (w)	$CH_2ClCOCl$, $CHCl_2CHO$
1365 (vw)	$CHCl_2CHO$
1253 (w), 1203 (m), 1065 (s) 986 (s)	$CHCl_2COCl$
1020 (s)	CCl_3COCl
930 (m)	unidentified
797 (s)	$CHCl_2COCl$
795 (s)	CCl_3COCl, $CHCl_2CHO$
752 (sh) 728 (s)	$CHCl_2COCl$, CH_2ClCHO
728 (s)	CCl_3COCl

$$CCl_3C(=O)Cl$$

$$CCl_3 \overset{O}{\overset{\|}{C}} - OCH_3$$

$$HCCl_2C(=O)Cl \quad \xrightarrow{3CH_3OH} \quad HCCl_2\overset{O}{\overset{\|}{C}} - OCH_3 + 3HCl$$

$$H_2CClC(=O)Cl$$

$$H_2CCl\overset{O}{\overset{\|}{C}} - OCH_3$$
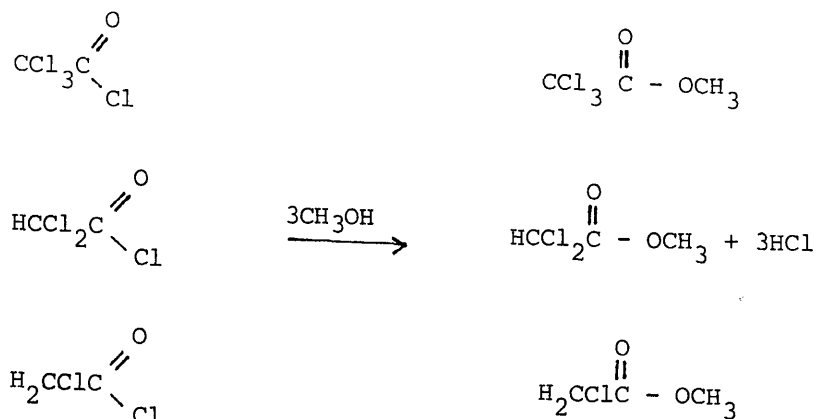
The derivatised sample was injected into a Perkin Elmer F-11 GC fitted with a 1.83m x 6.35mm O.D. column packed with 15% FFAP (free fatty acid phase) programmed from $50^{\circ}C$ at 5° min^{-1} using nitrogen as carrier gas at a flow rate of 40ml min^{-1}. The resultant chromatogram, illustrated in Figure 3.32, showed eleven peaks, the largest of which were due to ethyl acetate (solvent) and methanol. When authentic samples of methoxylated mono- and dichloroacetyl chlorides were injected it was found that the sample peak 7 corresponded to $CH_2ClCOOCH_3$, while that of peak 9 had the same retention time as $CHCl_2COOCH_3$.

GC-MS was carried out on a LKB 9000 instrument equipped with a 60 m x 0.32 m I.D. column packed with 1% FFAP programmed from $58^{\circ}C$ at $5^{\circ}C$ min^{-1} with helium as carrier gas. Under these conditions eight sample peaks were observed as shown in Figure 3.33. In this case, the highly volatile components were not

Fig 3.32 GC analysis of esterified liquid degradation products of 3CPEO obtained in Fraction (3) after SATVA separation column packed with 15% FFAP programmed from 50° to 5° min^{-1} N_2 carrier gas.

Fig 3.33   GC analysis of esterified liquid degradation products of 3CPEO obtained in Fraction (^{3}) after SATVA separation column packed with 1% FFAP programmed from 58°C at 5° min. He carrier gas.

so readily separated from the solvent peak, however four strong
peaks were distinguished and four weaker peaks were also
present.   It must be noted however that due to the nature of
the GC detector (i.e. flame ionisation detector) comparison of
peak intensity between halogenated and non-halogenated
derivatives cannot provide an accurate indication of product
distribution.   This is because the detector responds to the
amount of CO_2 and H_2O produced on combustion of the injected
compounds.   Thus a chlorinated hydrocarbon would produce less
of the above products and therefore a smaller deflection in the
chromatogram than the corresponding unchlorinated hydrocarbon.
In the case under investigation however, the major products were
all halogenated so a relative estimation could be made.

GC-MS analysis was performed on mono-, di- and trichloro-
acetyl methyl esters and by comparing the retention time and
molecular ion patterns of the standard compounds to those obtained
for the esterified degradation products, identification could be
verified.   The $^m/e$ values and assignments for the standard
compounds are given in Tables 3.11 - 3.13, and the similar
values obtained from GC-MS separation of the final SATVA fraction
from the degradation of 3CPEO are presented in Table 3.14.

By the above comparison it was found that sample peak 1
in the GC-MS chromatogram for the final SATVA fraction of 3CPEO
degradation (see Figure 3.33) was due to $CH_2ClCOOCH_3$, the large
sample peak 4 to $CHCl_2COOCH_3$ and sample peak 7 to CCl_3COOCH_3.

Table 3.11   MS $^m/e$ values and assignments for $CH_2ClCOOCH_3$

$^m/e$	Ratio of $^m/e$ values	Assignments
108, 110	3:1	$CH_2ClCOOCH_3$
77, 79	3:1	CH_2ClCO
64, 66	3:1	unidentified
59	–	$.COOCH_3$
49, 51	3:1	$.CH_2Cl$

Table 3.12   MS $^m/e$ values and assignments for $CHCl_2COOCH_3$

$^m/e$	Ratio of $^m/e$ values.	Assignments.
142, 144, 146	9:6:1 (very weak)	$CHCl_2COOCH_3$
141, 143, 145	– (very weak)	$.CCl_2COOCH_3$
127, 129, 131	9:6:1	$CHCl_2COO.$
111, 113, 115	9:6:1	$CHCl_2CO$
98, 100, 102	9:6:1	unidentified
83, 85, 87	9:6:1	$.CHCl_2$
63, 65	3:1	unidentified
59	–	$.COOCH_3$

Table 3.13 MS $^m/e$ values and assignments for CCl_3COOCH_3

$^m/e$	Ratio of $^m/e$ values	Assignments
141, 143, 145	9:6:1	$.CCl_2COOCH_3$
117, 119, 121, 123	27:27:9:1	$.CCl_3$
97, 99	2:1	unidentified
82, 84, 86	9:6:1	$.CCl_2$
63, 65	3:1	unidentified
59	–	$.COOCH_3$

Table 3.14 ^{m}/e values and assignments of GC peaks from degradation products of 3CPEO obtained in fraction (3) after SATVA separation.

GC Peak (Fig. 3.33)	^{m}/e	^{m}/e Ratio	Assignment
	108, 110	3:1	$.CHClCOOCH_3$
	84, 86	3:1	unidentified
1	77, 79	3:1	CH_2ClCO
	76, 78	3:1	unidentified
	64, 66	3:1	unidentified
	29	−	$.CHO$
	147,	−	unidentified
	120, 122	3:1	unidentified
	89, 91	2:1	unidentified
2	85	−	unidentified
	75, 77, 79	−	unidentified
	61, 63	3:1	unidentified
	147	−	unidentified
	93, 95	3:1	unidentified
3	89, 91	2:1	unidentified
	75	−	unidentified
	47	−	unidentified
	142, 144, 146	9:6:1	$CHCl_2COOCH_3$
	141, 143, 145	9:6:1	$.CCl_2COOCH_3$
	127, 129, 131	9:6:1	$CHCl_2COO.$
	111, 113, 115	9:6:1	$CHCl_2CO$
4	98, 100, 102	−	unidentified
	83, 85, 87,	9:6:1	$.CHCl_2$
	76, 79	−	unidentified
	63, 65	−	unidentified
	59	−	$.COOCH_3$

Table 3.14   contd.

	$^m/e$	$^m/e$ Ratio	Assignments
	107, 109, 111	-	unidentified
	93, 95	3:1	unidentified
5	89	-	unidentified
	79	-	unidentified
	61	-	unidentified
	156, 158	-	unidentified
	141, 143, 145	9:6:1	$.CCl_2COOCH_3$ (overlap)
	127	-	unidentified
	111, 113, 115	9:6:1	$CHCl_2CO$ (overlap)
6	93	-	unidentified
	83, 85, 87	9:6:1	$.CHCl_2$ (overlap)
	77, 79	3:1	CH_2ClCO
	76, 78	-	unidentified
	65	-	unidentified
	59	-	$.COOCH_3$ (overlap)
	41	-	unidentified
	141, 143, 145	9:6:1	$.CCl_2COOCH_3$
	117, 119, 121, 123	27:27:9:1	$.CCl_3$
	97, 99, 101	-	unidentified
7	82, 84, 86	9:6:1	$.CCl_2$
	63, 65	3:1	unidentified
	59	-	$.COOCH_3$
	155, 157, 159	-	unidentified
	147, 149, 151	-	unidentified
	117, 119, 121, 123	27:27:9:1	$.CCl_3$
8	111, 113	-	$CHCl_2CO$
	99, 101	-	unidentified
	83, 85, 87	9:6:1	$.CHCl_2$
	82, 84, 86	9:6:1	$.CCl_2$
	73, 61, 63	-	unidentified
	59	-	$.COOCH_3$ (overlap)

The remaining major peak, peak 6, was unassigned. Nevertheless by this technique, the presence of chloroacetyl chloride and trichloroacetyl chloride as indicated by IR spectroscopy was confirmed and, in addition, it was established that the major chlorinated degradation product in the last SATVA fraction was dichloroacetyl chloride. GC-MS analysis was also performed on dichlorinated PEO. The final degradation fraction from 2CPEO obtained from SATVA separation was treated with methanol as before and injected into the GC equipped with the 1% FFAP packed column. The resultant chromatograph was much more complex than that obtained for 3CPEO, showing numerous tightly packed peaks. This is illustrated in Figure 3.34. Due to the poor resolution between peaks it was not possible to obtain pure mass spectra of each component peak however, the data obtained for the major peaks are given in Table 3.15. The first peak in the GC chromatograph, peak A, was found to be due to methanol which had been used in the esterification reaction. Peak B, was identified as arising from chloroacetaldehyde whilst peak C was due to the ester obtained from chloroacetyl chloride. The compound(s) in peak D were unable to be identified however peak E could be attributed to dichloroacetyl chloride methyl ester. Peak F could not be assigned to any product although peak G indicated the trace amounts of trichloroacetyl chloride originally present as the mass spectrum obtained for the peak matched that for trichloroacetyl ester. Peak H was not identified and peak I gave a mass spectrum for $CCl_2=CH-\overset{\overset{\displaystyle O}{\|}}{C}-OCH_3$ which suggests the presence in trace amounts of a dichlorinated propenoic acid chloride as a degradation product. Thus GC-MS
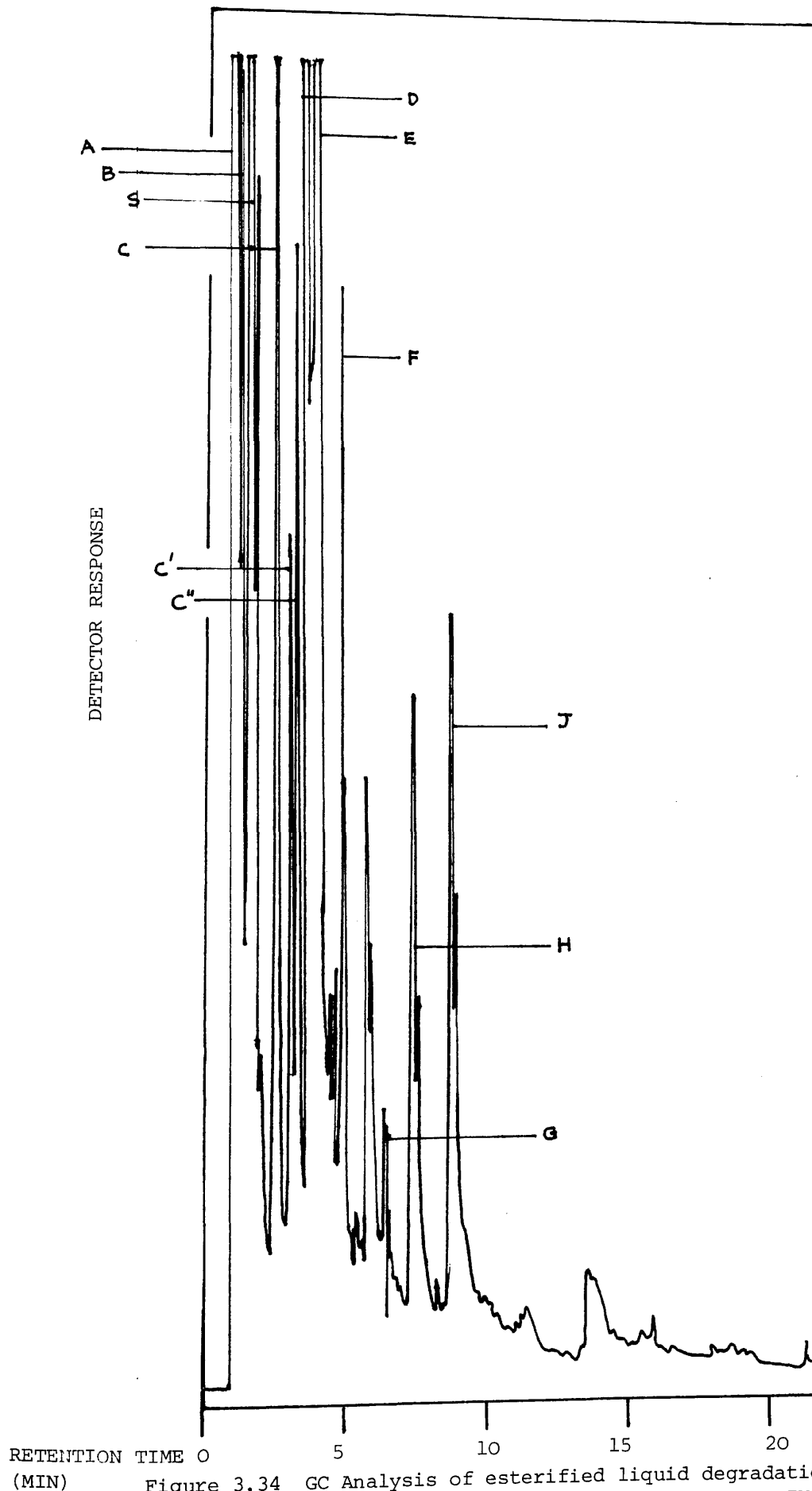
DETECTOR RESPONSE

A

B

S

C

D

E

F

C'

C"

J

H

G
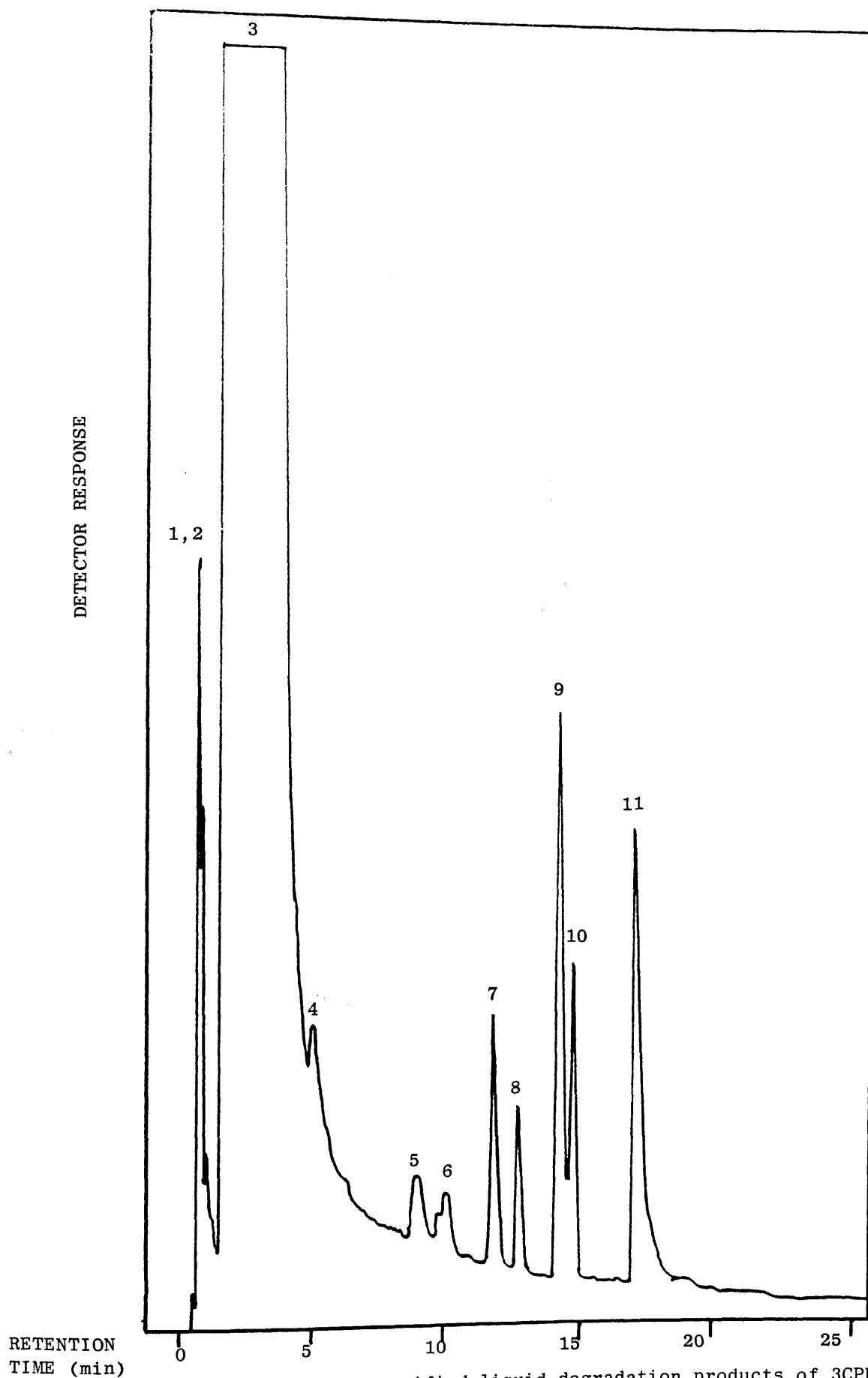
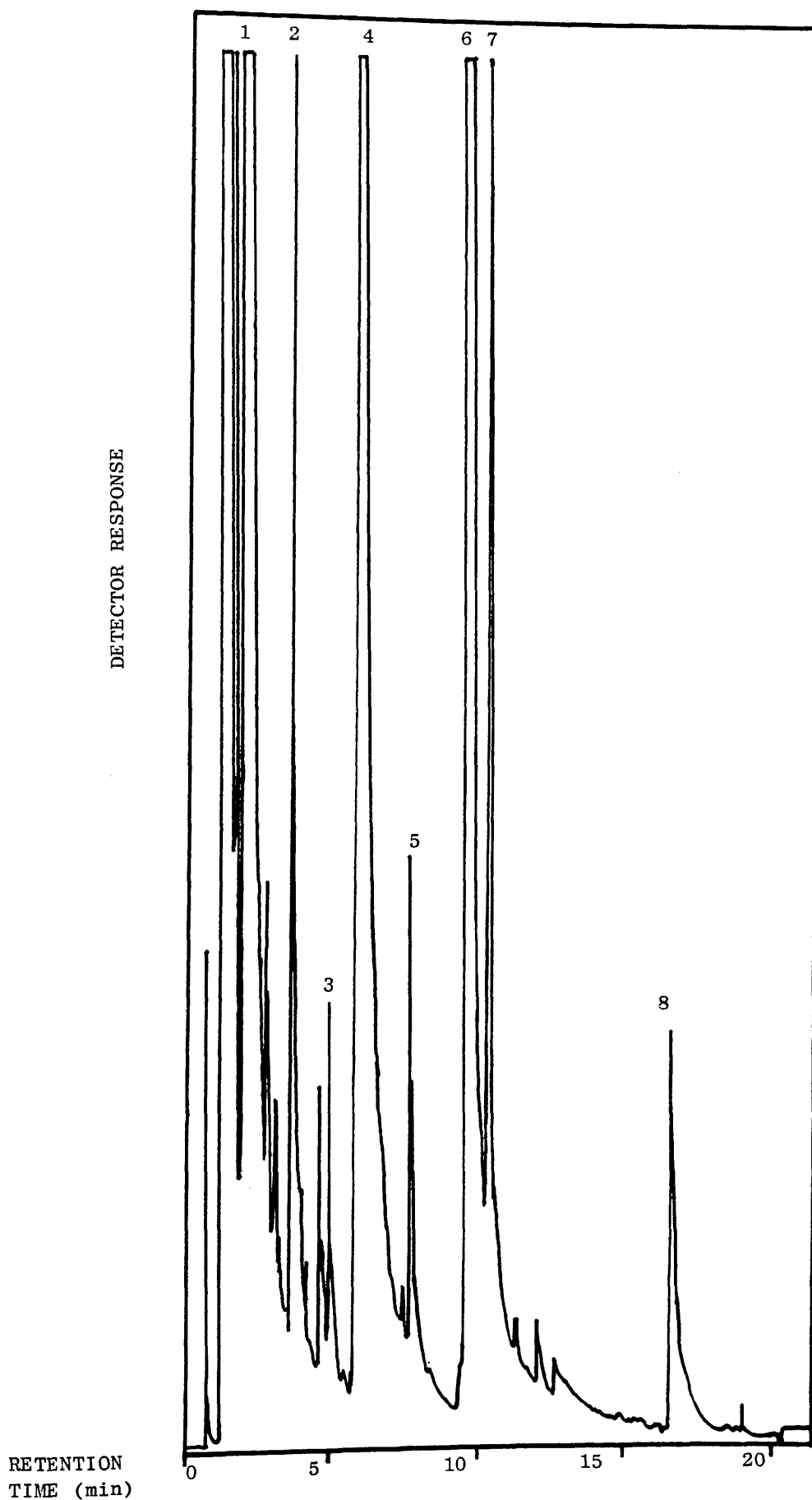RETENTION TIME 0   5   10   15   20
(MIN)

Figure 3.34   GC Analysis of esterified liquid degradation products
of 2CPEO obtained in Fraction 3 after SATVA separation.
Column packed with 1% FFAP programmed from 58°C at 5° min⁻
He carrier gas.

Table 3.15 ^{m}/e values and assignments of GC peaks from degradation products of 2CPEO obtained in Fraction (3) after SATVA separation.

GC Peak (Fig. 3.34)	^{m}/e	^{m}/e Ratio	Assignments
	29	-	unidentified
A	31 (s)	-	$CH_2=OH$
	32	-	CH_3OH
	78, 80	2:1	CH_2ClCHO
	74	-	CH_3OCH_2CHO
	50, 52 (s)	3:1	M-CO
	49, 51	5:2	$.CH_2Cl$
B	45	-	CH_3OCH
	43	-	unidentified
	29	-	.CHO
	31	-	$CH_2=OH$ (overlap)
	32	-	CH_3OH (overlap)
	108, 110	3:1	$CH_2ClCOOCH_3$
	77, 79	3:1	CH_2ClCO
C	64, 66	3:1	unidentified
	59	-	$.COOCH_3$
	49, 51	3:1	$.CH_2Cl$
	132, 134, 136	9:6:1	unidentified
	108, 110	3:1	$CH_2ClCOOCH_3$ (overlap)
	97, 99	3:2	unidentified
C'	83, 85, 87	9:6:1	$.CHCl_2$
	77, 79	5:2	CH_2ClCO (overlap)
	64, 66	3:1	unidentified
	61, 63	3:1	unidentified
	59	-	$.COOCH_3$
	49, 51	3:1	$.CH_2Cl$ (overlap)
	29	-	.CHO

Table 3.15 contd.

	$^m/e$	$^m/e$ Ratio	Assignments
	136, 138, 140	6:3:1	unidentified
	120, 122	2:1	unidentified
	108, 110	3:1	$CH_2ClCOOCH_3$ (overlap)
C"	93, 95	3:1	unidentified
	75 (s)	-	unidentified
	59	-	$.COOCH_3$ (overlap)
	47	-	unidentified
	43	-	unidentified
	118	-	unidentified
	89,	-	unidentified
	90, 92	3:1	unidentified
D	91, 93	3:1	unidentified
	62, 64	3:1	unidentified
	59	-	$.COOCH_3$
	45	-	CH_3OCH_2, CH_3CH_2O
	29	-	$.CHO$ (trace)
	111, 113, 115	9:6:1	$CHCl_2CO$
	98, 100, 102	9:6:1	unidentified
	83, 85, 87	9:6:1	$.CHCl_2$
E	79	-	unidentified
	76	-	$CH_3OCH_2CH_2OH$ (trace)
	63, 65	3:1	unidentified
	59	-	$.COOCH_3$

Table 3.15 contd.

	$^m/e$	$^m/e$ Ratio	Assignments
	124, 126	2:1	Unidentified
	107, 109	2:1	Unidentified
	93, 95	3:1	unidentified
	89 (s)	–	unidentified
F	79	–	unidentified
	78	–	unidentified
	61 (s)	–	unidentified
	59	–	$.COOCH_3$
	43	–	unidentified
	45	–	unidentified
	141, 143, 145	9:9:1	$.CCl_2COOCH_3$
	117, 119, 121, 123	27:27:9:1	$.CCl_3$
	113, 115	1:1	unidentified
G	83, 85, 87	6:6:1	$.CHCl_2$ (trace)
	82, 84, 86	9:6:1	$.CCl_2$ (trace)
	78	–	unidentified
	59	–	$.COOCH_3$
	154, 156, 158	9:6:1	$CCl_2=CHCOOCH_3$ (overlap)
	123, 125, 127 (s)	9:6:1	$CCl_2=CHCO$ (overlap)
	138, 146	2:1	unidentified
	97, 99	2:1	unidentified
H	141, 145	3:1	$.CCl_2COOCH_3$ (trace overlap)
	83, 85, 87	9:6:1	$.CHCl_2$
	78	–	unidentified
	75	–	unidentified
	61, 63, 65	6:4:1	unidentified
	59	–	$.COOCH_3$
	43	–	unidentified

Table 3.15 contd..

$^m/e$	$^m/e$ Ratio	Assignments
154, 156, 158	9:6:1	$CCl_2=CHCOOCH_3$
123, 125, 124	9:6:1	$CCl_2=CHCO$
121	–	unidentified
119	–	$.CCl=CHCOOCH_3$
95, 97, 99	9:6:1	$CCl_2=CH$
59	–	$.COOCH_3$

I

Table 3.15 $^m/e$ values and assignments of GC peaks from degradation products of 2CPEO obtained in Fraction (3) after SATVA separation.

has confirmed the presence of mono-, di- and to a much lesser extent, trichloroacetyl chloride, indicated from IR data in the degradation product of 2CPEO. From comparing peak widths in the GC trace, it may be that chloroacetyl chloride is present in slightly greater amounts than dichloroacetyl chloride although the compression in the trace makes the comparison difficult. In addition to the chlorinated acetyl chloride degradation products, the production of chlorinated acetaldehyde has also been detected by GC-MS. This supports the suggestion of aldehydic compounds in the degradation products as was indicated by the absorption on the IR spectrum of the final SATVA fraction at 2850 cm^{-1} (see Figure 3.31).

The cold ring fraction (CRF), collected on the cooled portion of the TVA tube, was in the form of an amber resin. IR spectra of each CRF sample revealed that the resin consisted of chain fragments having both acid chloride end groups, indicated by a strong absorption band at 1775 cm^{-1} and a weak absorption at 455 cm^{-1}, and aldehydic end groups shown by the strong carbonyl band at 1750 cm^{-1}. There is also evidence for the formation of unsaturated groups in the CRF, from the presence of very weak absorptions at 3090 cm^{-1} and 1650 cm^{-1}. The IR spectra for the CRF obtained after heating di- and trichlorinated PEO to 500°C are reproduced in Figure 3.35.

The residue remaining after degradation, in the case of the dichlorinated compounds, was a shiny black solid while in the case of the trichlorinated polymers, the solid was dull grey/black. In both systems the residue was found by IR analysis to be mostly
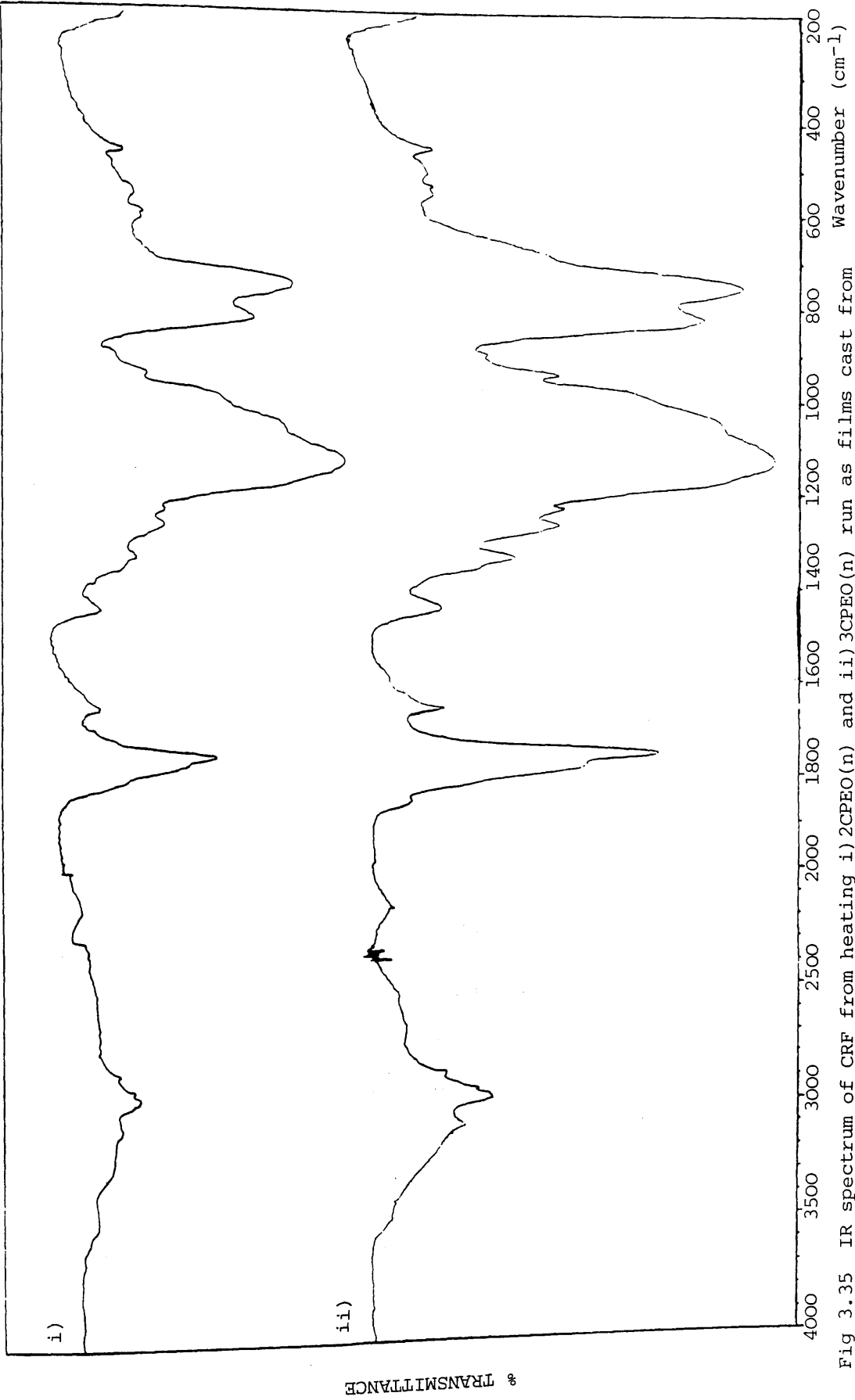
Fig 3.35 IR spectrum of CRF from heating i) 2CPEO(n) and ii) 3CPEO(n) run as films cast from CH_2Cl_2 on CsI plates

carbonaceous char although elemental analysis revealed the presence of approximately 12% by weight of Cl. The non-condensable product indicated by the $-196^{\circ}C$ trace in the TVA curve was CO.

Quantitative Analysis of HCl and CRF Production.

Quantitative analysis of the weight % HCl evolved and CRF produced on degradation in the TVA system to $500^{\circ}C$ was carried out for each chlorinated polymer sample using the methods described in Chapter 2. For each determination, a polymer sample of approximately 75 mg was used. The average value for each estimation is given in Table 3.16.

The distribution of products indicates that CRF is the major product of the degradation of CPEO as in both di- and tri-chlorinated polymers approximately 60% by weight is evolved. HCl appears to be a relatively minor product, ranging from between 5 - 10% of the original polymer weight. The quantity of HCl produced by the trichlorinated compound is less than that produced from the dichlorinated compound. The weight % HCl obtained from 3CPEO corresponds to roughly one molecule of HCl produced per four monomer units while in 2CPEO this is increased to approximately one molecule of HCl per three monomer units. The observation that as chlorine content increases HCl production decreases can simply be explained by the reduction in available hydrogen atoms. The products evolved on the thermal degradation are listed in Table 3.17 and Table 3.18. Included in these tables are chloro-acetaldehydes, which although they could not be positively identified from IR analysis, are plausable degradation products.

Table 3.16   Quantitative Analysis of Product Distribution from
              chlorinated PEO on heating to 500°C.

Polymer Sample.	No Cl atoms per EO unit.	mg HCl evolved per 100 mg polymer.	mg CRF produced per 100 mg polymer.
3CPEO(n)	2.97	5.61	58.79
2CPEO(n)	2.02	9.57	60.46
3CPEO(a)	2.70	7.68	60.65
2CPEO(a)	1.86	9.73	59.34

Table 3.17 Products obtained on the Thermal Degradation of Dichlorinated PEO (2CPEO).

Product Fraction.	Product.	Identification	Relative Importance	Assessment of Importance.
Non-condensable products	CO	IR	minor	TVA, IR
Condensable gaseous products	HCl	IR	major	quantitative analysis
	CO_2	IR	Medium	IR
	Cl_2CO	IR	minor	SATVA
Condensable liquid products	$Cl_2CHCOCl$	IR, GC-MS	major	GC, IR
	$ClCH_2COCl$	IR, GC-MS	major	GC, IR
	$ClCH_2CHO$	IR, MS	minor	GC, IR
	CCl_3COCl	IR, GC-MS	trace	GC, IR
	Cl_2CHCHO (?)	IR	trace	
	$CCl_2=CHCOCl$	MS	trace	GC
CRF	oligomeric chain fragments	IR	major	quantitative analysis
Residue	chlorinated char	IR elemental analysis.	trace	TG

Table 3.18 Products obtained on the Thermal Degradation of Trichlorinated PEO (3CPEO)

Product Fraction.	Product	Identification	Relative Importance	Assessment of Importance.
Non-condensable product	CO	IR	minor	TVA
Condensable gaseous products	HCl	IR	major	quantitative analysis
	CO_2	IR	medium	IR
	Cl_2CO	IR	minor	SATVA
Condensable liquid products	$Cl_2CHCOCl$	IR, GC-MS	major	GC, IR
	CCl_3COCl	IR, GC-MS	medium	GC, IR
	$CH_2ClCOCl$	IR, GC-MS	minor	GC, IR
	$CHCl_2CHO$ (?)	IR	trace	
	CH_2ClCHO (?)	IR	trace	
CRF	oligomeric chain fragments	IR	major	quantitative analysis
Residue	chlorinated char	IR elemental analysis	trace	TG

3.4.2 Discussion

The thermal stability of PEO is markably decreased on the introduction of chlorine into the polymer structure, as is observed from TVA and TG experiments. There appears also to be a tendancy for polymers chlorinated in the presence of air to be slightly less stable than those prepared under nitrogen. It may be that irregularities in structure due to oxidation products are responsible for this difference. The thermal behaviour of chlorinated PEO is in complete contrast to that of fluorinated PEO. When Lagow et al[112-115] reacted finely ground PEO with fluorine, an extremely stable high molecular weight per fluoropolyether was obtained which could withstand temperatures in excess of 340°C. This is approximately 100°C greater than the onset temperature of degradation in the chlorinated polymers synthesised in this investigation. This decrease in thermal stability is a reflection of the greater bond strength of C-F as compared with C-Cl.

In each chlorinated PEO sample, weight loss or evolution of volatile degradation products occurred in a single step over a relatively narrow temperature range. This suggests that there is no formation of a stable partially degraded intermediate resulting for example from the elimination of HCl, as is observed in the thermal degradation of PVC.

Consideration of the strengths of the various bonds present suggests that the degradation of chlorinated PEO may well be initiated by C-Cl scission. The most plausible events occurring during the degradation of trichlorinated PEO are first postulated.

Degradation Mechanism of Trichlorinated PEO.

Initiation of decomposition is proposed to occur by the scission of a C-Cl bond at a disubstituted carbon atom. This site is chosen due to the inductive effects of the chlorine atoms distributing electron density so as to favour C-Cl scission. The resultant macroradical can then undergo β C-O chain scission, to produce a terminal acid chloride group.

$$
\begin{array}{ccccccccccc}
 & Cl & & Cl & & Cl & & Cl & & Cl & & Cl \\
 & | & & | & & | & & | & & | & & | \\
\text{\textasciitilde} C & - & C & - O - & C & - & C & - O - & C & - & C \text{\textasciitilde} \\
 & | & & | & & | & & | & & | & & | \\
 & H & & Cl & & H & & Cl & & H & & Cl
\end{array}
$$

↓ C-Cl scission

$$
\begin{array}{ccccccccccc}
 & Cl & & Cl & & Cl & & Cl & & Cl & & Cl \\
 & | & & | & & | & & | & & | & & | \\
\text{\textasciitilde} C & - & C & - O - & C & - & C & - O - & C & - & C - O\text{\textasciitilde} \quad + Cl\cdot \\
 & | & & | & & | & & \bullet & & | & & | \\
 & H & & Cl & & H & & & & H & & Cl
\end{array}
$$

↓ C-O scission

$$
\begin{array}{ccccccccccc}
 & Cl & & Cl & & Cl & & Cl & & Cl & & Cl \\
 & | & & | & & | & & | & & | & & | \\
\text{\textasciitilde} C & - & C & - O - & C & - & C & = O \; + \cdot C & - & \cdot C - O\text{\textasciitilde} \\
 & | & & | & & | & & & & | & & | \\
 & H & & Cl & & H & & & & H & & Cl
\end{array}
$$
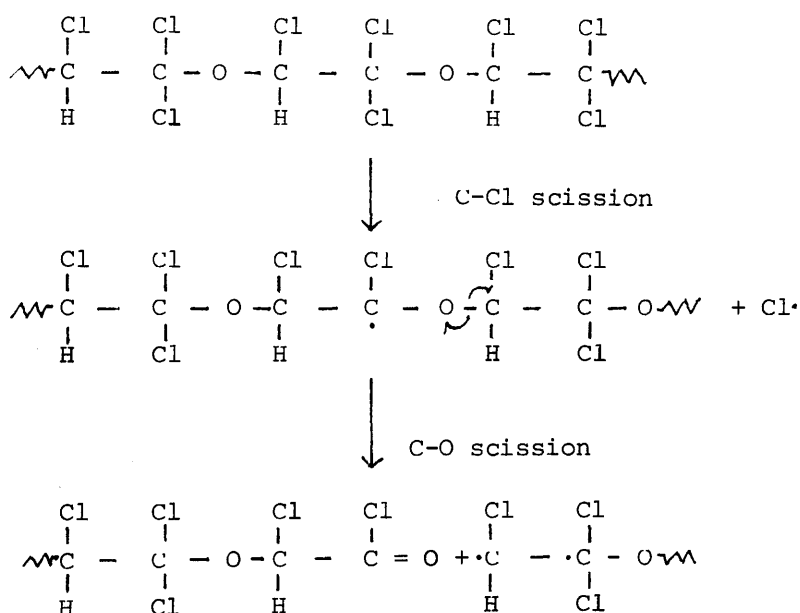
The polymer radical which was concurrently generated on chain scission can initiate "depolymerisation" by abstracting a Cl· radical from the α carbon atom on the neighbouring repeat unit of the acid chloride terminated polymer chain enhancing chain scission.

$$
\begin{array}{ccccccc}
& Cl & & Cl & & Cl & Cl \\
& | & & | & & | & | \\
\text{ww-C} & - & C & - O - & C & - & C = O \\
& | & & | & & | \\
& H & & Cl & & H
\end{array}
\quad + \quad
\begin{array}{ccc}
Cl & Cl \\
| & | \\
\cdot C & - & C - O\text{-ww} \\
| & | \\
H & Cl
\end{array}
$$

intermolecular
Cl abstraction

$$
\begin{array}{ccccccc}
Cl & & Cl & & Cl & Cl \\
| & & | & & | & | \\
\text{ww-C} & - & C & - O - & C & - & C = O \\
| & & \cdot & & | \\
H & & & & H
\end{array}
\quad + \quad
\begin{array}{ccc}
Cl & Cl \\
| & | \\
Cl - C & - & C - O\text{-ww} \\
| & | \\
H & Cl
\end{array}
$$

C—O
scission

$$
\begin{array}{ccc}
Cl & Cl \\
| & | \\
\text{ww- C} & - & C = O \\
| \\
H
\end{array}
\quad + \quad
\begin{array}{ccc}
Cl & Cl \\
| & | \\
\cdot C & - & C = O \\
| \\
H
\end{array}
$$

abstraction   Cl /   \ H   abstraction

$$
\begin{array}{ccc}
Cl & Cl \\
| & | \\
Cl - C & - C & = O \\
| \\
H
\end{array}
\qquad
\begin{array}{ccc}
Cl & Cl \\
| & | \\
H - C & - C & = O \\
| \\
H
\end{array}
$$
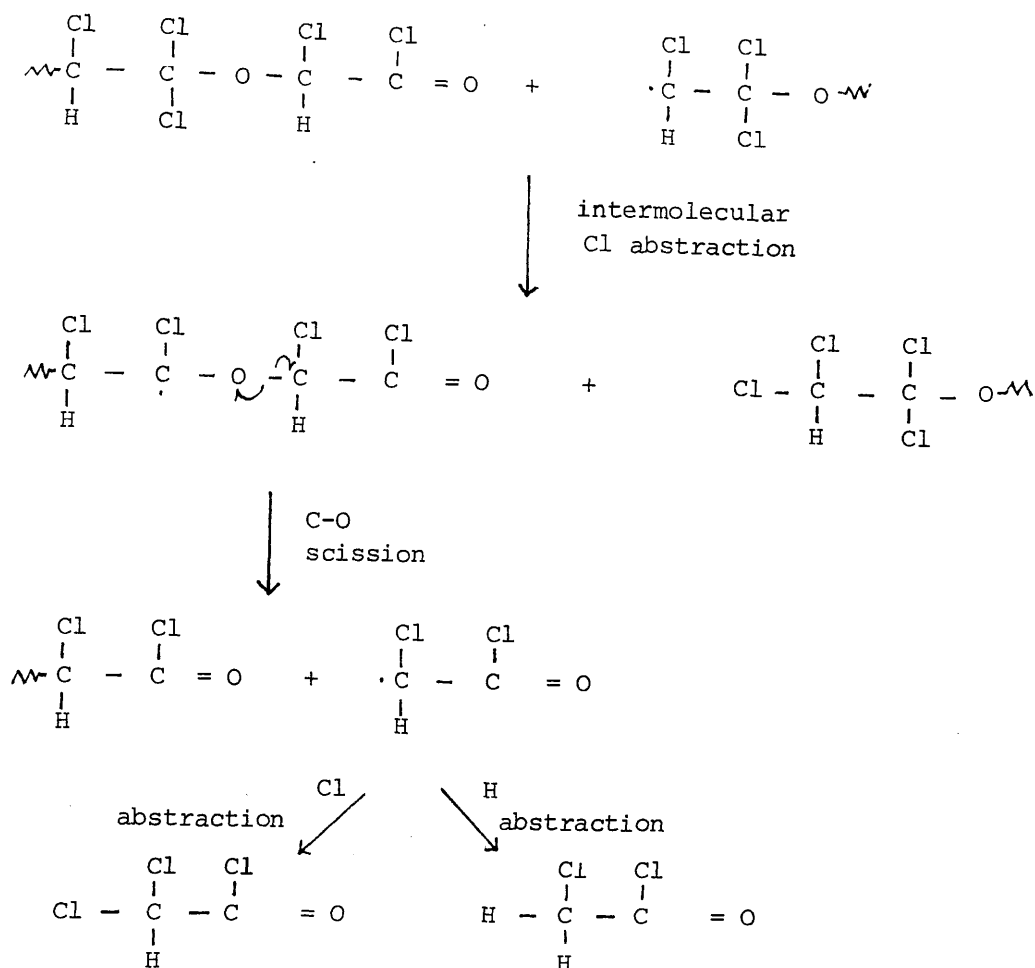
The chloroacetyl chloride radical evolved then goes to produce

dichloroacetyl chloride or chloroacetyl chloride by abstraction of

a chlorine or hydrogen radical respectively.   GC-MS analysis

indicates that dichloroacetyl chloride is the main product, therefore

Cl· abstraction is favoured.   This process of forming chloro-

acetyl chlorides may continue until interrupted, for example, by the

elimination of HCl or the production of phosgene.   The results

obtained from quantitative analysis of HCl production suggest that

it is a fairly random process which occurrs on average once in

every four monomer units.   If the mechanism for HCl production

is not via elimination of adjacent H and Cl atoms but instead

is by the abstraction of hydrogen from a macromolecule by a Cl·

radical, this provides a route for the formation of trichloroacetyl

chloride as illustrated below:

$$\begin{array}{cccc} Cl & Cl & Cl & Cl \\ | & | & | & | \\ \text{\textasciitilde}C - C - O - C - C - O \text{\textasciitilde} & & & + \; Cl\cdot \\ | & | & | & | \\ Cl & H & Cl & H \end{array}$$

i) H abstraction
ii) C-O scission

$$\begin{array}{cccc} Cl & Cl & Cl & Cl \\ | & | & | & | \\ \text{\textasciitilde}C - C - O - C - C = O & & & + \; HCl \\ | & | & | & \\ Cl & H & Cl & \end{array}$$

C-O scission

$$\begin{array}{ccc} Cl & Cl & \\ | & | & \\ \text{\textasciitilde}C - C - O\cdot & + & \cdot C - C = O \\ | & | & | \\ Cl & H & Cl \end{array}$$

Cl / abstraction   H \ abstraction

$$\begin{array}{cc} Cl & Cl \\ | & | \\ Cl - C - C = O & \qquad H - C - C = O \\ | & | \\ Cl & Cl \end{array}$$
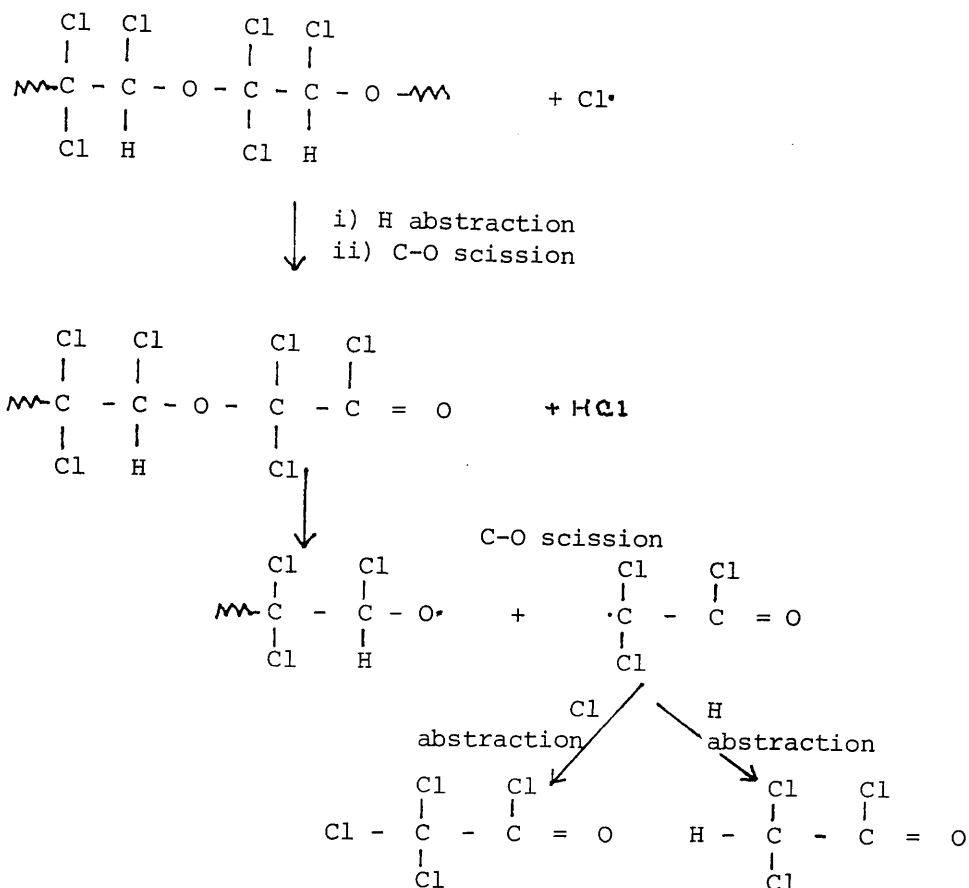
The presence of absorption bands at 3080 cm^{-1} and 1613 cm^{-1} in the

IR spectrum of the fraction containing the chlorinated acid

chlorides suggests that HCl is produced by an elimination reaction

(see Figure 3.31).

It would also appear to be plausible that chain scission

could occur within the polymer in such a way that aldehydic end

groups may be formed.   This would be the case if a monochlorinated

carbon atom underwent C-Cl scission followed by facilitated C-O

scission:

$$\underset{\substack{Cl \\ | \\ \text{\textasciitilde}C \\ | \\ Cl}}{} - \underset{\substack{Cl \\ | \\ C \\ | \\ H}}{} - O - \underset{\substack{Cl \\ | \\ C \\ | \\ Cl}}{} - \underset{\substack{Cl \\ | \\ C \\ | \\ H}}{} - O\text{\textasciitilde} \xrightarrow{-Cl \cdot} \underset{\substack{Cl \\ | \\ \text{\textasciitilde}C \\ | \\ Cl}}{} - \underset{\substack{\cdot \\ | \\ C \\ | \\ H}}{} - O \cdot \underset{\substack{Cl \\ | \\ C \\ | \\ Cl}}{} - \underset{\substack{Cl \\ | \\ C \\ | \\ H}}{} - O\text{\textasciitilde}$$

$$\downarrow \text{ C-O scission}$$

$$\underset{\substack{Cl \\ | \\ \text{\textasciitilde}C \\ | \\ Cl}}{} - \underset{\substack{| \\ C \\ | \\ H}}{} = O \quad + \quad \cdot\underset{\substack{Cl \\ | \\ C \\ | \\ Cl}}{} - \underset{\substack{Cl \\ | \\ C \\ | \\ H}}{} - O\text{\textasciitilde}.$$
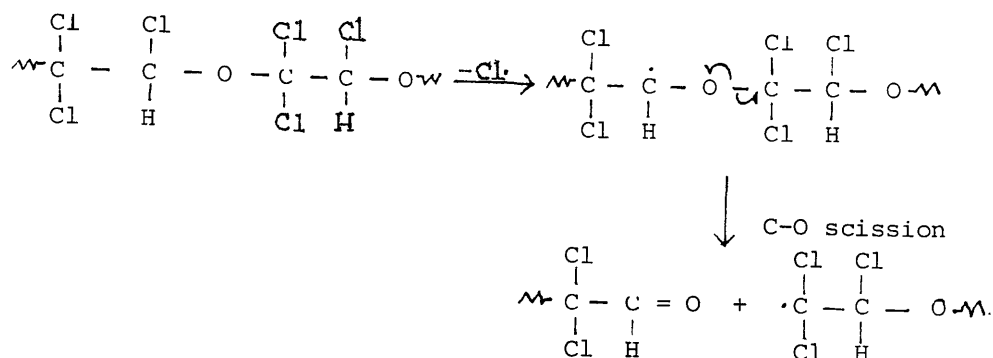
and through a series of events similar to those just described
the corresponding chlorinated aldehydes - chloroacetaldehyde,
dichloroacetaldehyde and trichloroacetaldehyde (chloral) would
be produced.   The IR spectrum of the liquid fraction (Figure
3.31) is of limited value in the identification of these
compounds due to the overlap in spectral bands of the chloro-
acetyl chlorides.   There is however evidence of the presence
of aldehydic compounds from the presence of a weak absorption at
2845 cm^{-1} which can be attributed to the isolated C-H stretch of
an aldehyde.   The breadth of the carbonyl band may indicate
a mixture of carbonyl compounds; the shoulder on the lower
wavenumber side 1748 cm^{-1} is in the region of aldehydic carbonyls.
The presence of aldehydic compounds was also suggested by the mass
spectral data obtained after GC-MS separation.   In several
fractions mass spectral peaks at $^m/e$ = 29 indicative of aldehydes
were observed.   Although positive identification of the chloro-
aldehydes could not be obtained from the experimental data
presented, they remain probable products since during the
esterification reaction the low boiling point aldehydes (85°,[116]
90°,[98] and 98°C[98] for mono-, di- and trichloroacetaldehydes
respectively as compared with 106°,[116a] 108°,[117] and 115°C[98] for the

corresponding chloroacetyl chlorides) may have evaporated.
Alternatively these reactive aldehydes may have undergone further
reactions.

At higher temperatures main chain scission becomes more
feasible.   As a result of this phosgene, although it is a
relatively minor product, is produced.

```
        Cl |  Cl        |  Cl    Cl
        |  |  |         |  |     |
  ʌʌʌ-C  +  C  - O   +  |  C  -  C -ʌʌʌ
        |  |  |         |  |     |
        H  |  Cl        |  H     Cl
```

↓ C-C and C-O scission

```
     Cl                             Cl    Cl
     |          Cl                  |     |
 ʌʌʌ-C·   +       \C=O     +       ·C  -  C -ʌʌʌ
     |          /                  |     |
     H          Cl                 H     Cl
```
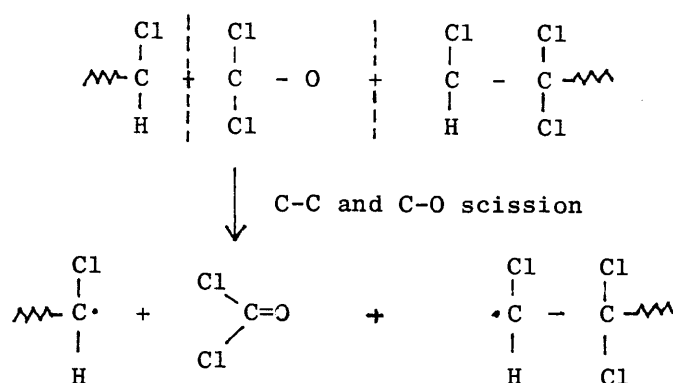
Similar chain scission at a monosubstituted carbon atom and
subsequent decomposition yields non-condensable CO and an
additional, if rather less significant, route to the formation
of HCl.

```
     Cl  Cl|      Cl| Cl
     |   | |      |  | |
 ʌʌʌ-C - C + O - C + C -ʌʌʌ
     |   | |      |  | |
     H  Cl|      H  | Cl
```

↓ i) C-C and C-O scission
   ii) decomposition

```
     Cl  Cl                      Cl
     |   |                       |
 ʌʌʌ-C - C·    + CO  +  HCl  +  ·C-ʌʌʌ
     |   |                       |
     H  Cl                       Cl
```
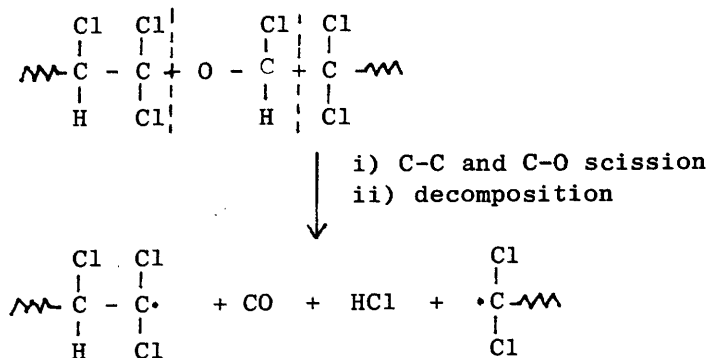
As well as the intermolecular chain transfer processes which
produce highly volatile chain fragments, larger chain fragments

may be produced via intramolecular back-biting reactions. The

radicals involved in the reaction may have arisen from side

chain enhanced chain scission in the formation of chloroacetyl

chlorides or from the higher temperature induced main chain

scission. A possible mechanism is as follows:

intramolecular
Cl transfer

C-O scission
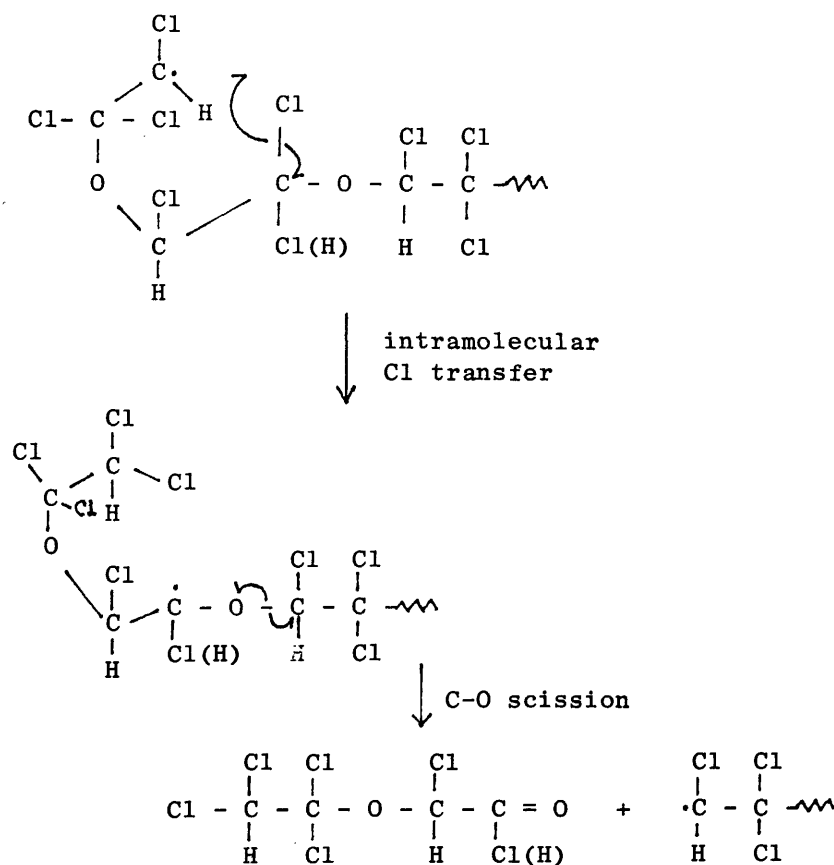
This process is favourable as it involves a six membered

transition state, the macroradical of which is additionally

stabilised by the electron withdrawing inductive effect (-I) of the

terminal chlorine atom. Following the chlorine (or hydrogen)

transfer there is cleavage of a C-O bond. By this method

oligomeric chain fragments (CRF) having either acid chloride or carbonyl end groups may be produced. Alternatively larger oligomeric chain fragments may arise via intermolecular Cl or H abstraction by macroradicals produced as a result of main chain scission.

Degradation Mechanism of Dichlorinated PEO.

The degradation of dichlorinated PEO (2CPEO) yielded all the products which were identified on the decomposition of trichlorinated PEO (3CPEO) however, the lower chlorine content in the polymer resulted in a different product distribution. From quantitative analysis of weight % HCl and CRF produced (see Table 3.16), it is seen that CRF is a major product of degradation in both di- and tri-chlorinated polymers as it accounts for approximately 60% by weight of the original polymer sample after degradation. As previously mentioned, HCl production is diminished in polymers of higher chlorine content. Phosgene and CO are minor products from both 3CPEO and 2CPEO and it is proposed that the mechanisms involved in the formation of the degradation products of dichlorinated PEO so far mentioned are similar to those described in the decomposition of trichlorinated PEO. The effect of two chlorine atoms in the polymer backbone as opposed to three is clearly reflected in the IR spectra of the liquid degradation products of 2CPEO and 3CPEO (see Figure 3.23). The IR spectrum of the compounds evolved on the degradation of the dichlorinated polymer has additional peaks to those for the trichlorinated degradation products on the aliphatic CH_2

stretching region at ~ 2950 cm^{-1} and ~ 2930 cm^{-1}. It is also evident from the moderately strong IR absorption band at 1403 cm^{-1} in the degradation products from 2CPEO that chloroacetyl chloride is produced in greater amounts from the degradation of 2CPEO than from 3CPEO. The corresponding band in the degradation products of 3CPEO appears as a weak absorption. Conversely, trichloroacetyl chloride production is decreased on the degradation of 2CPEO as is illustrated by the reduction in the absorption band at ~ 1020 cm^{-1}. There are two possible repeat unit structures for dichlorinated PEO – the polymer backbone may either contain disubstituted carbon atoms in which both chlorine atoms are attached to the same carbon atom within the repeat unit or monosubstituted carbon atoms in which the chlorine atoms are on alternate carbon atoms.

a) Disubstituted Carbon Repeat Unit.

If the disubstituted carbon structure is first considered and degradation occurs in a similar fashion to that proposed for 3CPEO, then the following processes may occur. Initiation of degradation brought about by homolysis of a C-Cl bond, is followed by β C-O scission of the resultant macroradical producing an acid halide end group and regenerating a polymer radical.

$$\text{MM-C(H)(H)}-\text{C(Cl)(Cl)}-\text{O}-\text{C(H)(H)}-\text{C(Cl)(Cl)}-\text{O}-\text{C(H)(H)}-\text{C(Cl)(Cl)}-\text{O-MM}$$

↓ C-Cl scission

$$\text{MM-C(H)(H)}-\text{C(Cl)(Cl)}-\text{O}-\text{C(H)(H)}-\overset{\cdot}{\text{C}}-\text{O} \curvearrowleft \text{C(H)(H)}-\text{C(Cl)(Cl)}-\text{O-MM}$$

↓ C-O scission

$$\text{MM-C(H)(H)}-\text{C(Cl)(Cl)}-\text{O}-\text{C(H)(H)}-\text{C(Cl)}=\text{O} \;+\; \overset{\cdot}{\text{C}}(H)(H)-\text{C(Cl)(Cl)}-\text{O-MM}$$
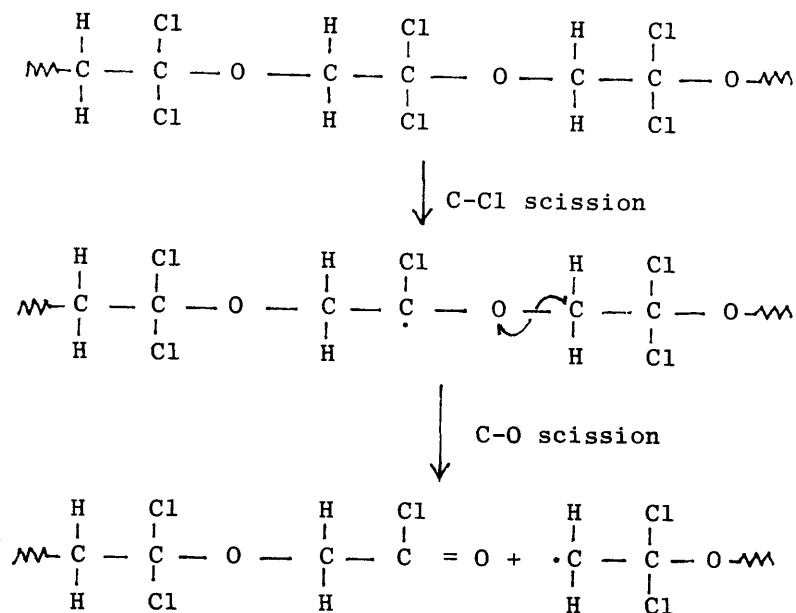
Intermolecular Cl abstraction by the macroradical promotes the "depolymerisation" process by the splitting out of $\cdot CH_2CClO$ radicals:

$$\text{MM-C(H)(H)}-\text{C(Cl)(Cl)}-\text{O}-\text{C(H)(H)}-\text{C(Cl)}=\text{O} \;+\; \overset{\cdot}{\text{C}}(H)(H)-\text{C(Cl)(Cl)}-\text{O-MM}$$

↓ intermolecular Cl abstraction

$$\text{MM-C(H)(H)}-\overset{\cdot}{\text{C}}(Cl)-\text{O} \curvearrowleft \text{C(H)(H)}-\text{C(Cl)}=\text{O} \;+\; \text{Cl}-\text{C(H)(H)}-\text{C(Cl)(Cl)}-\text{O-MM}$$

↓ C-O scission

$$\text{MM-C(H)(H)}-\text{C(Cl)}=\text{O} \;+\; \overset{\cdot}{\text{C}}(H)(H)-\text{C(Cl)}=\text{O}$$

Cl abstraction ↙   ↘ H abstraction

$$\text{Cl}-\text{C(H)(H)}-\text{C(Cl)}=\text{O} \qquad\qquad \text{H}-\text{C(H)(H)}-\text{C(Cl)}=\text{O}$$
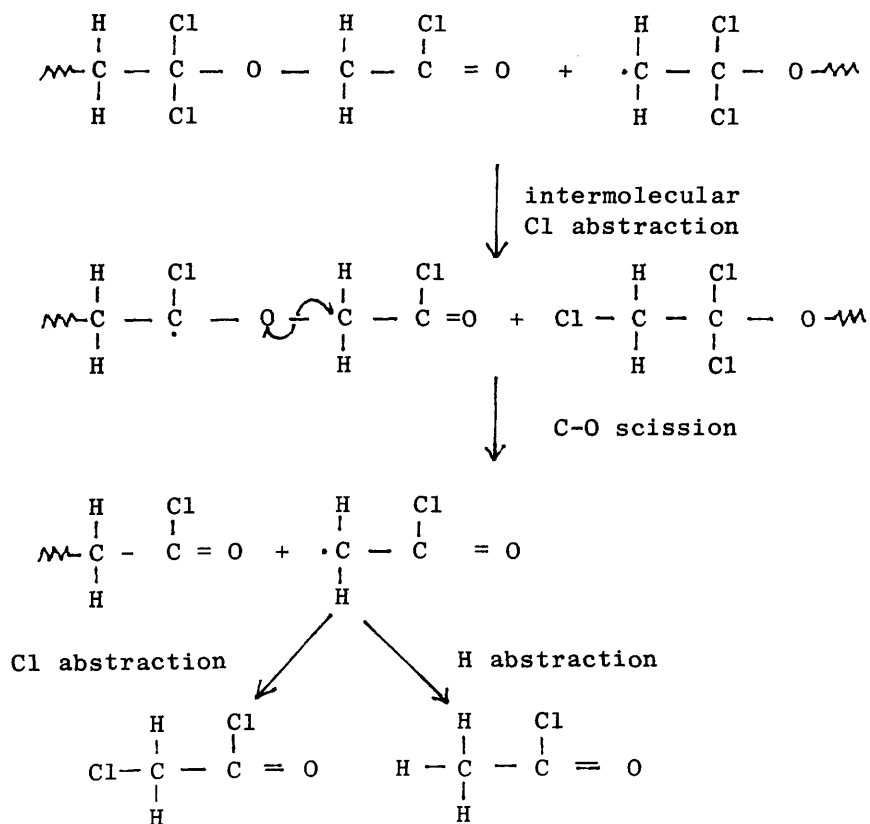
Cl abstraction by the $\cdot CH_2CClO$ radical results in the formation of chloroacetyl chloride. Alternatively, H abstraction leads to the production of acetyl chloride. Although extensive overlapping in spectral bands occurs for these compounds, the absorption bands of medium intensity at ~ 1112 cm^{-1} and 956 cm^{-1} (present as a shoulder on the strong 984 cm^{-1} band of dichloro-acetyl chloride) plus the weak bands at 1376 cm^{-1} and 1423 cm^{-1} are present only in acetyl chloride and therefore suggest the presence of this compound.

The production of phosgene and CO arises from main chain scission and further decomposition, as was the case for 3CPEO, and is illustrated below:
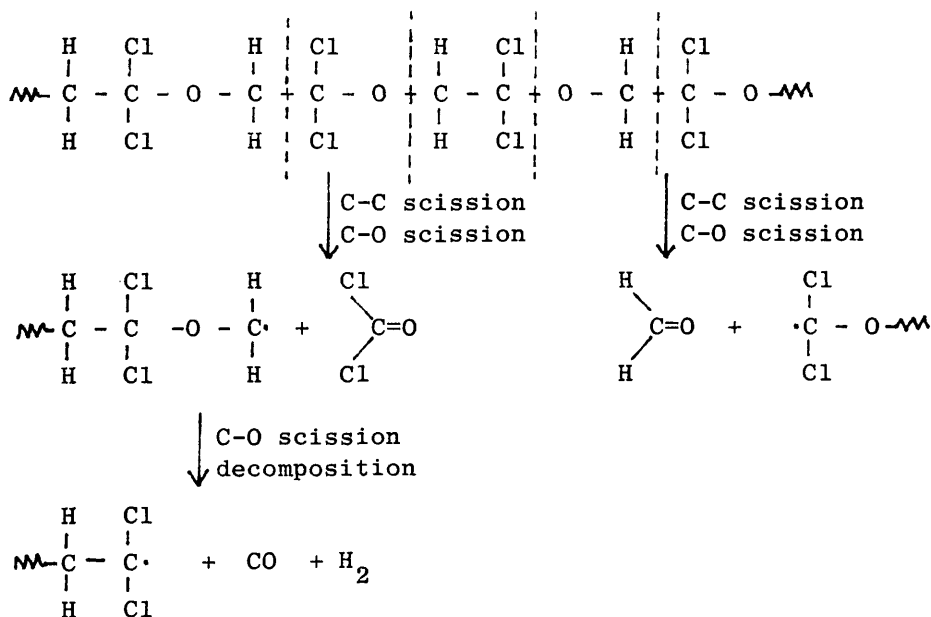
By this process it should be, in theory, possible to produce trace amounts of formaldehyde. Formaldehyde, however, was not detected in any of the gaseous product fractions from 2CPEO. This may suggest that the polymer chain predominantly consists of monosubstituted carbon atoms and that phosgene is produced from structural irregularities in which both chlorine atoms have been

substituted at the same carbon.

(b) <u>Monosubstituted Carbon Repeat Unit</u>.

On considering the monosubstituted carbon structure the following events are proposed to occur during degradation.   As before, initiation is via C-Cl bond scission:
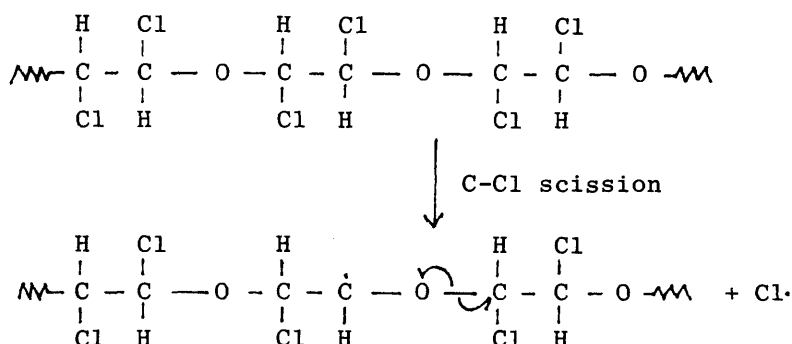
C-Cl scission

This encourages C-O scission in the bond adjacent to the carbon

radical resulting in a macromolecule terminated by an aldehydic

group.   If chain scission occurs at the C-O bond neighbouring

the newly formed end group then a chloroacetaldehyde radical

is formed which, on hydrogen abstraction, produces chloroacetaldehyde.

This may occur by disproportionation at the end of the polymer chain:
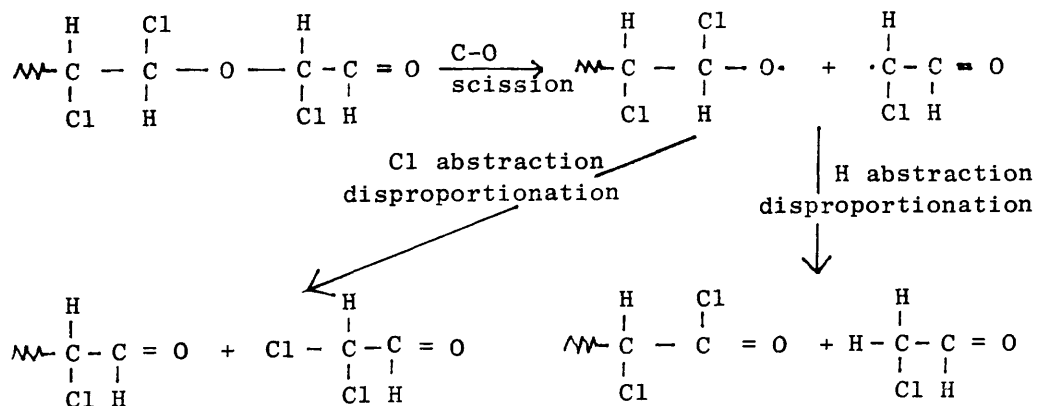
The predominance of chloroacetyl chlorides as products from the degradation of 2CPEO suggests that disproportionation which results in the formation of an acid chloride is the favoured route.

The chlorine radical produced in the initiation step, on the abstraction of hydrogen to produce HCl, provides a source of acetylchloride end groups:

$$
\begin{array}{c}
\text{M}\!\!-\!\!\underset{\underset{Cl}{|}}{\overset{\overset{H}{|}}{C}} - \underset{\underset{H}{|}}{\overset{\overset{Cl}{|}}{C}} - O - \underset{\underset{H}{|}}{\overset{\overset{H}{|}}{C}}\!\!...
\end{array}
$$

M–C(H)(Cl)–C(Cl)(H)–O–C(H)(Cl)–C(Cl)(H)–O–C(H)(Cl)–C(Cl)(H)–O–M + Cl·

↓ H abstraction

M–C(H)(Cl)–C(Cl)(H)–O–C(H)(Cl)–C·(Cl)–O C(H)(Cl)–C(Cl)(H)–O–M + HCl

↓ C–O scission

M–C(H)(Cl)–C(Cl)(H)–O–C(H)(Cl)–C(Cl)=O + ·C(H)(Cl)–C(Cl)(H)–O–M
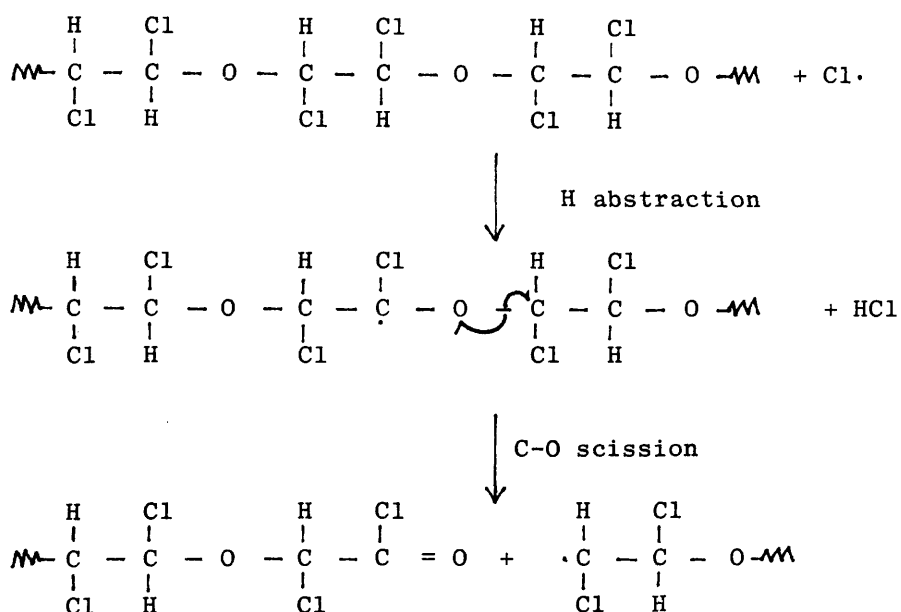
If the acid chloride terminated polymer chain undergoes β C-O scission, the resultant radicals may participate in a disproportionation reaction similar to that described for the aldehydic terminated macromolecules.   This leads to the production of mono- and dichloroacetyl chlorides as illustrated below:
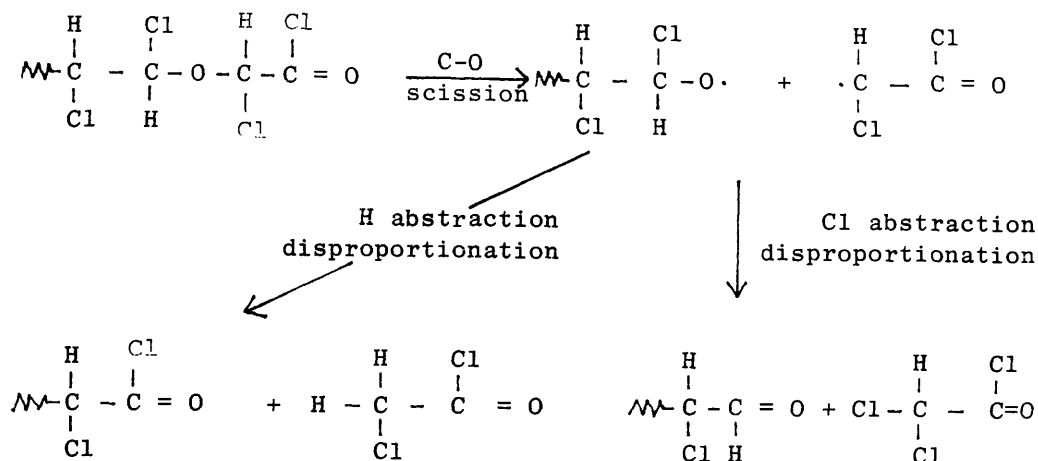
This process results in the formation of dichloroacetyl chloride, the major acid chloride product. As this compound could not be readily produced by the first degradation scheme proposed for 2CPEO (i.e. disubstituted carbon repeat unit mechanism), it seems plausible that the above process is the dominant route for degradation. This also implies that the original polymer consists of repeat units in which chlorine atoms are attached to adjacent carbon atoms. It is probable that this arrangement is sterically favoured as it will present less hindrance. As previously suggested, structural abnormalities may give rise to the production of phosgene. The indication of unsaturated compounds from the bands at ~ 1595 cm^{-1}, 1480 cm^{-1} and 3040 cm^{-1} in the IR spectrum of the liquid fraction obtained on the degradation of 2CPEO suggest that HCl is also produced by elimination of chlorine and hydrogen from adjacent carbon atoms.

CRF may arise via a similar mechanism as described for

3CPEO namely intramolecular back-biting reactions producing acid halide and aldehydic terminated oligomer chain fragments. CO is evolved by the decomposition of a $\left[-O-\overset{\displaystyle Cl}{\underset{\displaystyle H}{C}}-\right]$ section in the polymer chain as for 3CPEO.

The formation of CO_2 can result from an interaction between two macroradicals, one of which - an oxygen terminated radical, combines with a tertiary carbon radical to become grafted onto the chain:

```
      Cl      H(Cl)     Cl      H(Cl)      Cl      H(Cl)
      |        |        |        |         |        |
 ᴧᴧ-C   -   C-O  -   C   -   C - O  -    C   -   C - O -ᴧᴧ
      |        |        |        ·         |        |
      H       Cl        H                  H       Cl
```

```
                         ·
                  +      O
                         |
            (Cl) H - C - Cl
                     |
               Cl - C - H
                     ⌇
```

```
                         ↓
```

```
      Cl      H(Cl)        Cl      H(Cl)          Cl       H(Cl)
      |        |           |        |             |         |
 ᴧᴧ-C   -   C - O  -    C    -    C   -    0  -   C    -    C   -   0-ᴧᴧ
      |        |           |        |             |         |
      H       Cl           H        O             H         Cl
                                    |
                        (Cl) H   -    C  -  Cl
                                      |
                           Cl   -    C  -  H
                                      ⌇
```
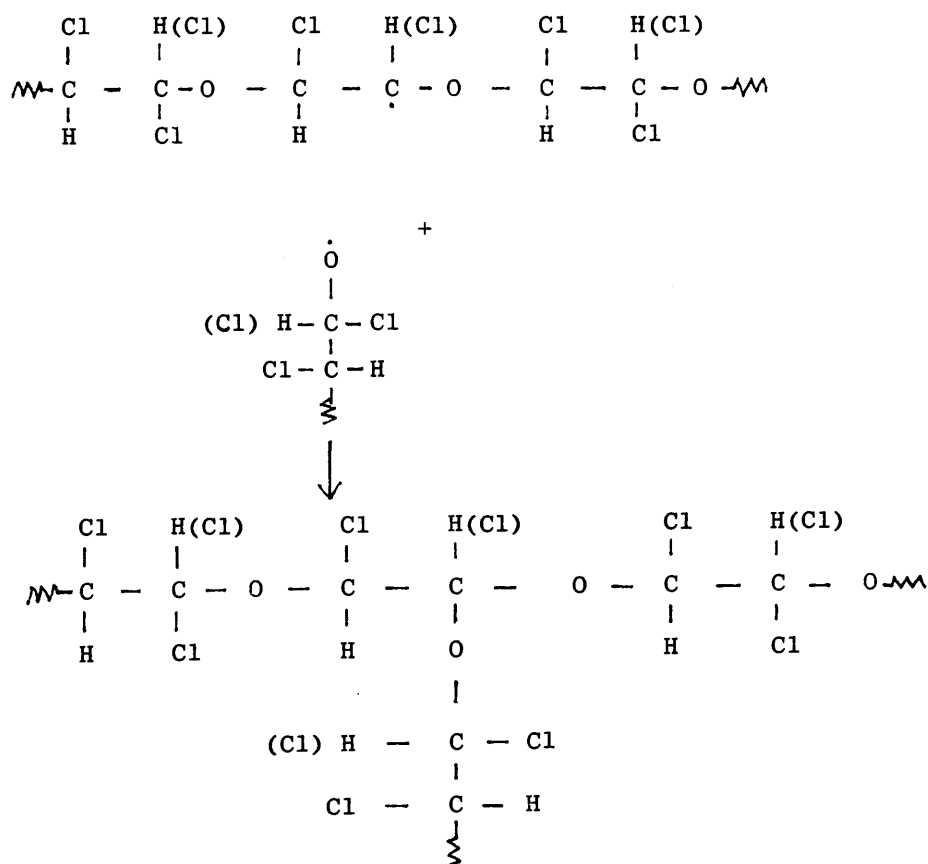
The abstraction of hydrogen (or chlorine) at the branching carbon atom will initiate C-O chain scission as indicated below with the eventual evolution of CO_2.

$$
\begin{array}{c}
\text{Cl} \qquad \text{H(Cl)} \qquad\qquad \text{Cl} \qquad\qquad\qquad \text{Cl} \qquad \text{H(Cl)} \\
| \qquad\quad | \qquad\qquad\quad | \qquad\qquad\qquad\quad | \qquad\quad | \\
\text{W\!\!-} \text{C} - \text{C} - \text{O} - \text{C} - \dot{\text{C}} - \text{O} \curvearrowright \text{C} - \text{C} - \text{O} -\text{W} \\
| \qquad\quad | \qquad\qquad\quad | \quad\ | \qquad\qquad\quad | \qquad\quad | \\
\text{H} \qquad\quad \text{Cl} \qquad\qquad \text{H} \quad \text{O} \qquad\qquad\quad \text{H} \qquad\quad \text{Cl} \\
\\
| \\
\text{(Cl)H} - \text{C} - \text{Cl} \\
| \\
\text{Cl} - \text{C} - \text{H} \\
\S
\end{array}
$$

C-O scission ↓

$$
\begin{array}{c}
\text{Cl} \qquad \text{H(Cl)} \qquad\qquad \text{Cl} \qquad\qquad\qquad \text{Cl} \qquad \text{H} \\
| \qquad\quad | \qquad\qquad\quad | \qquad\qquad\qquad\quad | \qquad\quad | \\
\text{W\!\!-} \text{C} - \text{C} - \text{O} - \text{C} \text{C} = \text{O} \quad + \quad \dot{\text{C}} - \text{C} - \text{O} -\text{W} \\
| \qquad\quad | \qquad\qquad\quad | \quad\ | \qquad\qquad\qquad \quad\ | \\
\text{H} \qquad\quad \text{Cl} \qquad\qquad \text{H} \quad \text{O} \qquad\qquad \text{(Cl)H} \quad \text{Cl} \\
\\
| \\
\text{(Cl)H} - \text{C} - \text{Cl} \\
| \\
\text{Cl} - \text{C} - \text{H} \\
\S
\end{array}
$$

2C-O scission ↓

$$
\begin{array}{c}
\text{Cl} \qquad\quad \text{H} \quad \text{Cl} \qquad\qquad \text{Cl} \qquad \text{H} \\
| \qquad\qquad | \quad\ | \qquad\qquad\quad | \qquad\quad | \\
CO_2 \ + \ \dot{\text{C}} - \text{O} - \text{C} - \text{C} -\text{W} + \ \dot{\text{C}} - \text{C} - \text{O} -\text{W} \\
| \qquad\qquad | \quad\ | \qquad\qquad\quad | \qquad\quad | \\
\text{(Cl)H} \qquad \text{Cl} \quad \text{H} \qquad\qquad \text{(Cl)H} \quad \text{Cl}
\end{array}
$$
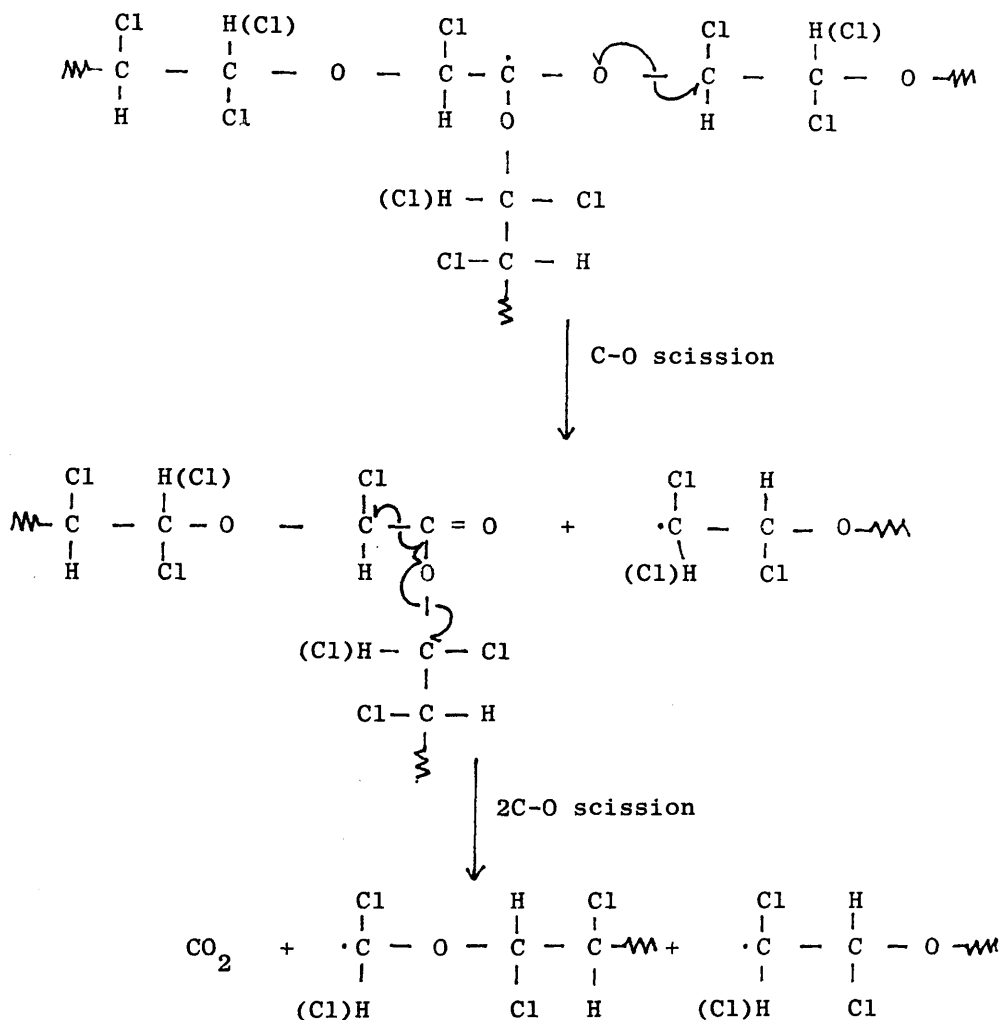
This mechanism is viable as CO_2 is a degradation product of relatively low importance and thus extensive grafting is not required.

From the experimental data obtained, it has been shown that the main products on the thermal degradation of 2CPEO are oligomeric chain fragments which comprise CRF, and

volatile products comprising dichloroacetyl chloride, mono-
chloroacetyl chloride and trichloroacetyl chloride, of which
dichloroacetylchloride is the major product and trichloroacetyl
chloride is present in trace amounts, and finally HCl.

These products as well as phosgene, CO_2 and CO were formed in
the degradation of both 2CPEO and 3CPEO.   In the dichlorinated
PEO system it was also possible to detect chloroacetaldehyde
although the presence of dichloroacetaldehyde could not be
confirmed.

3.5 CONCLUSION

Under the conditions employed in this investigation it
has been possible to chlorinate PEO such that the resultant
polymers have a chlorine content corresponding to a di-
substituted (62.78%) or trisubstituted (72.16%) EO unit.

It has been shown that chlorination of PEO thermally
destabilises the polymer.   Prior to chlorination, degradation
(as determined by TVA) of PEO commences at approximately $310^{\circ}C$
whilst the chlorinated polymers begin to degrade in the range
192° - $217^{\circ}C$.   This loss in stability is reflected in the
bond strengths present in the polymer and the formation of the
new C-Cl bonds introduces points of weakness as these bonds are
weaker than the original C-H or C-C bonds.

The thermal degradation of PEO is initiated via random
main chain scission i.e. C-O or C-C bonds resulting in a variety
of decomposition products including CO_2, formaldehyde, acetaldehyde,

methoxyacetaldehyde, ethoxyacetaldehyde, diethylether, ethanol

and alkyl terminated oligomeric chain fragments (CRF).

The thermal degradation of chlorinated PEO, after initiation
through C-Cl scission, is a random single stage process
producing various chloroacetyl chlorides in preference to their
aldehydic analogues.   In addition to mono-, di-, and tri-
chloroacetyl chloride, carbon monoxide, carbon dioxide, phosgene
and HCl are evolved as well as a substantial amount of acid
chloride and carbonyl terminated CRF.

CHAPTER 4 : <u>CHLORINATED POLYSTYRENE</u>

4.1 <u>INTRODUCTION</u>

Many types of chlorinated polymers have been synthesised in the search for improved thermal characteristics such as reduced flammability.   Thermal properties are closely associated with the microstructure of polymers, especially with the distribution of Cl atoms.

Chlorination of a polymer should obey the classical rules of organic chemistry, consequently ionic and radical chlorination should yield entirely different products.   In polystyrene (PS), there are two possible regions for chlorination - either in the aromatic ring or along the polymer backbone in the main chain (See Fig. 4.1).

a) ring-chlorination   b) chain-chlorination
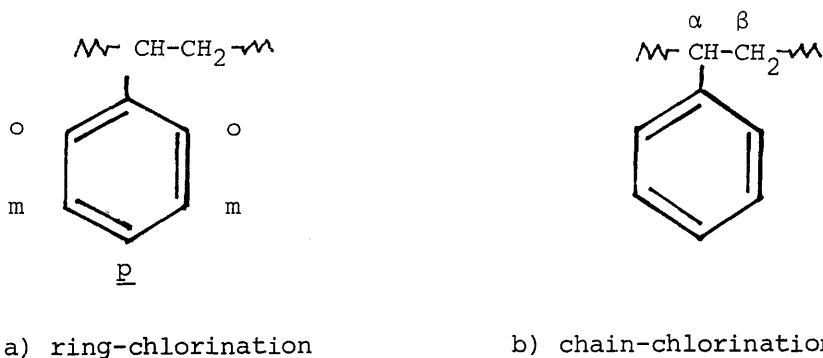
Figure 4.1 <u>Sites for Chlorination in Polystyrene.</u>

Chlorinated PS has been synthesised by both ionic and radical mechanisms[117] and structures studied by various methods. Bachmann et al[118] used thermal depolymerisation of ionically chlorinated PS to assist elucidation of the structure.   Teysse and co-workers,[119] also working on the ionic chlorination of PS, characterised structures using chemical and IR analyses.   It was observed that chlorination takes place concurrently in the aromatic ring and in the main chain.   Ring chlorination is favoured with

Cl in the para-position preferably and the ortho-position secondarily.

At higher degrees of chlorination i.e. two Cl atoms per styrene unit,

the second Cl atom substitutes at position 3 in para-chlorosytrene units

and at position 5 in ortho-chlorosytrene producing 3,4- and 2,5-

dichlorostyrene units respectively.   Investigations by pyrolysis

gas chromatography of ionically chlorinated PS, having ring

substitution of 0.1 - 1.6 Cl atoms per styrene unit, synthesised with

and without the use of iron powder catalysts, were carried out by

Okumoto et al.[120]   In both the catalysed and uncatalysed

reactions identical pyrolysis products were identified namely styrene,

p-chlorostyrene, o-chlorostyrene, 3,4-, 2,5- and 2,4- dichlorostyrene.

The reactions so far mentioned have used chlorine as one of the

reactants however chloride ions in the form of hydrochloric acid

have been used in ionic chlorinations, in the presence of hydrogen

peroxide by Auseinov and Salakhov[121] and in an electrolytic reaction

performed by Watanabe.[122]

Photochemical chlorination of PS has been carried out by

Jenkins et al[123] who investigated changes in IR spectra, glass

transition temperature and molecular weight.   In contrast to

ionic reactions, the radical chlorination proceeds mainly by

substitution at the α hydrogen position in the chain.   It was also

observed that some main chain scission took place as chlorination

proceeded.[123]   Pyrolysis GC investigations into the distribution

of Cl atoms in photo-chlorinated PS by Tsuge et al[124] suggested that

Cl atoms were first substituted for the α followed by the β hydrogens

of the main chain but that substitution occurs competitively in the

ring at the p-position even before α and β hydrogens are substituted.

The ring reaction, however, appears to be the minor process.

Thus from the above review, the method employed to chlorinate PS has a definite effect on the resultant chemical structure. In general, ionic chlorination of PS favours substitution in the aromatic ring whilst in radical chlorination main chain substitution is preferred. It must be noted however that these methods of synthesis are not mutually exclusive of either type of product and that where main chain substitution is dominant, a small amount of ring substitution will be obtained and when ring substitution is the major reaction, main chain substitution, although to a much lesser extent, will also be observed. In the case where ring substitution is the main product, the added complication arises that there is more than one site in the ring available for chlorination. The investigations outlined find that p-substitution is preferred with o-substitution secondary.

This, therefore, has been the situation for the chlorination of PS until very recently when McNeill and Coşkun synthesised ring-chlorinated PS [125] with the minimum indication of chain chlorination and also prepared chain-chlorinated PS [126] in which chlorine is almost exclusively in the polymer backbone. Ring chlorination was carried out at $-20^{\circ}C$ by the reaction of chlorine with PS in methylene chloride using iodine as catalyst. Chain-chlorinated PS was obtained from the direct reaction of chlorine with a PS solution in vacuo. The polymer structures were identified by IR spectroscopy and the degradation behaviour characterised by TVA and SATVA.

The objective of the present investigation was to determine

the effect of the position of chlorination within PS and the degree

of chlorination in PS on its thermal stability and degradation

behaviour using TVA, SATVA and TG techniques.   In order to achieve

this, it is useful first to study PS derivatives in which chlorine

is situated either exclusively in the aromatic ring or in the main

chain, if possible.   This can be done for ring-chlorinated PS if,

instead of reacting chlorine with PS, the chlorinated polymer is

prepared via the polymerisation of chlorosytrene to give poly-

(chlorostyrene).   For this study, poly(p-chlorostyrene) and poly(o-

chlorostyrene) were prepared in such a manner.   The chain-

chlorinated PS however was prepared by direct radical

chlorination.

There is interest in halogenated PS for use as a non-

flammable expanded polymer as the halogenated product is found to be

self-extinguishing.[127-129]   An important use of chlorinated PS,

or more precisely poly(chlorosytrenes), is in the production of

monomer since PS selectively chlorinated in the p-position on

degradation provides a synthetic route to p-chlorostyrene.[130,131]

This is an important raw material for the preparation of drugs,

pesticides, ion-exchange resins and polymers which are photosensitive,

have good adhesive properties and are heat resistant.   Similarly

the controlled degradation of poly(o-chlorostyrene)[130] yields a high

proportion of o-chlorostyrene.

Nomenclature

Due to the variety of chlorinated polystyrenes which can be

synthesised through numerous routes, the following abbreviations

are used throughout this thesis to describe the type of

chlorinated PS:

PoCS - poly(o-chlorosytrene) prepared by the polymerisation
of o-chlorostyrene.

PpCS - poly(p-chlorosytrene) prepared by the polymerisation
of p-chlorostyrene.

RCPS - ring-chlorinated polystyrene prepared by the iodine
catalysed chlorination of polystyrene.

CCPS - chain-chlorinated polystyrene prepared by direct
chlorination of polystyrene _in vacuo_.

4.2 THERMAL DEGRADATION OF POLYSTYRENE

4.2.1 Introduction

The thermal degradation of polystyrene (PS), has been studied in great detail.[132]   As for chlorine-containing polystyrenes, the method of preparation has an effect on the degradation behaviour of the polymer.   In radically prepared PS, degradation occurs in two stages.   The first stage occurs at relatively low temperatures (200 - 280°C) and is due to a main chain scission reaction which causes a reduction in molecular weight [133,134] but does not involve the evolution of volatile degradation products.   This process is thought to be initiated at weak links, produced during the radical polymerisation process.

The second, higher temperature degradation reaction is due to the depolymerisation of macromolecules resulting in the production of styrene monomer together with larger fragments.   Initiation of this process is believed to be mostly due to the scission of chain-end allylic links formed in the lower temperature reaction and also, to a lesser degree, by a small amount of random chain scission.[135,136] A typical degradation mechanism adapted from references (135) and (136) for PS is given in Figure 4.2.

In addition to styrene being formed, traces of benzene and toluene are produced.   Larger chain fragments such as dimer, trimer, tetramer and pentamer are also formed.   These oligomers are a result of intra-molecular transfer reactions involving active α hydrogens in a "back biting" mechanism.   This is illustrated in Figure 4.3.
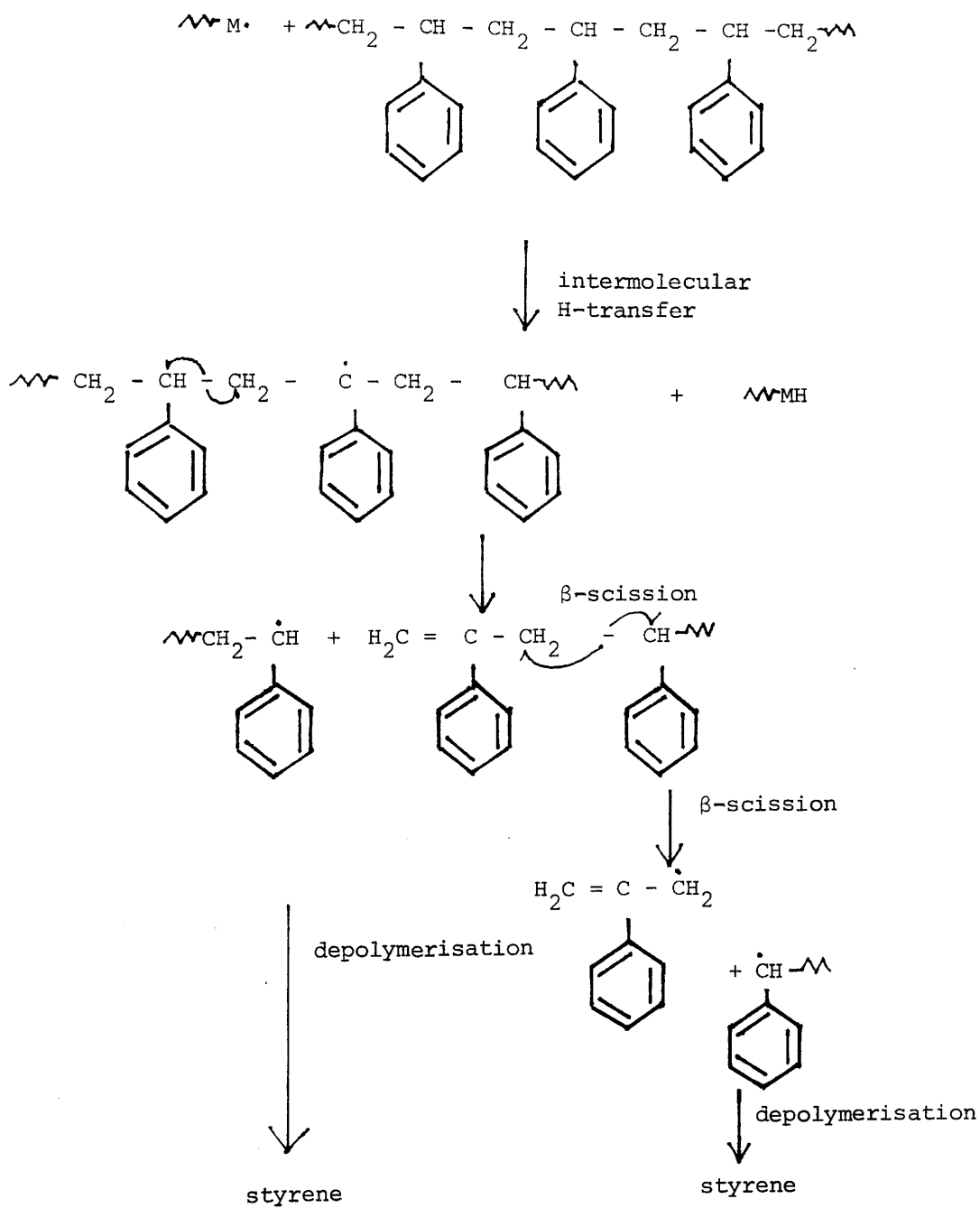
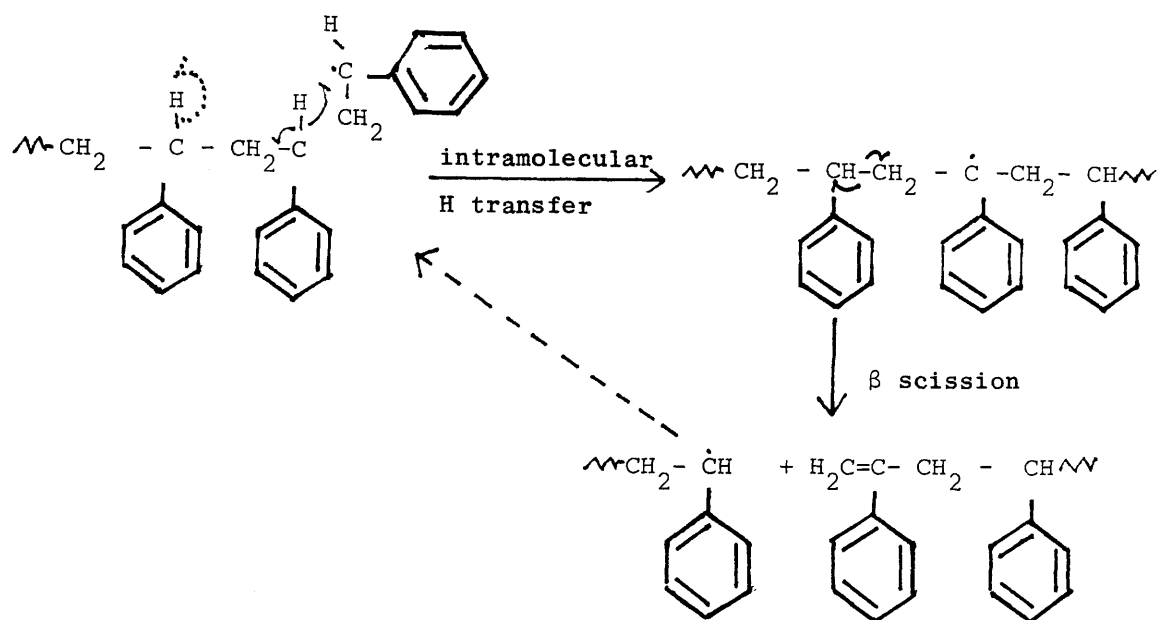Figure 4.2   Mechanism for depolymerisation of PS.

Figure 4.3   Mechanism for production of oligomer in PS.

In anionically prepared PS, the first degradation process
leading to a drop in molecular weight does not occur.   However
depolymerisation does proceed giving similar products obtained
by the degradation of radically prepared PS.

4.2.2 Experimental

Thermal Analysis of Polystyrene.

The thermal degradation behaviour of a commercial sample of PS was investigated to provide a basis for comparison with chlorinated products. The polymer used was a standard PS, supplied by the Polymer Supply and Characterisation Centre (PSCC), with weight average molecular weight ($\overline{M}w$) 3000,000 - 350,000 and PSCC reference number PS-2.

TG

Thermogravimetric (TG) curves were obtained in a dynamic nitrogen atmosphere with a flow rate of 50 ml min^{-1} and heating from ambient temperature to 500°C at 10° min^{-1}. The TG curve, illustrated in Figure 4.4 shows that weight loss occurs in a single step over a narrow temperature range, having an onset temperature of approximately 350°C. The maximum rate of weight loss occurs around 423°C and there is a negligible amount (0.8% of original polymer weight) of residue.

DSC

The DSC curve obtained for PS under nitrogen reveals two endothermic transitions. The small peak at approximately 130°C is due to the melting point of the polymer (Tm) whilst the large peak at 430°C arises from the polymer decomposing. The glass transition temperature (Tg) is not visible in the curve. The DSC curve is shown in Figure 4.5.

TVA

The TVA curve for a 50 mg sample of PS used as received without_{out}
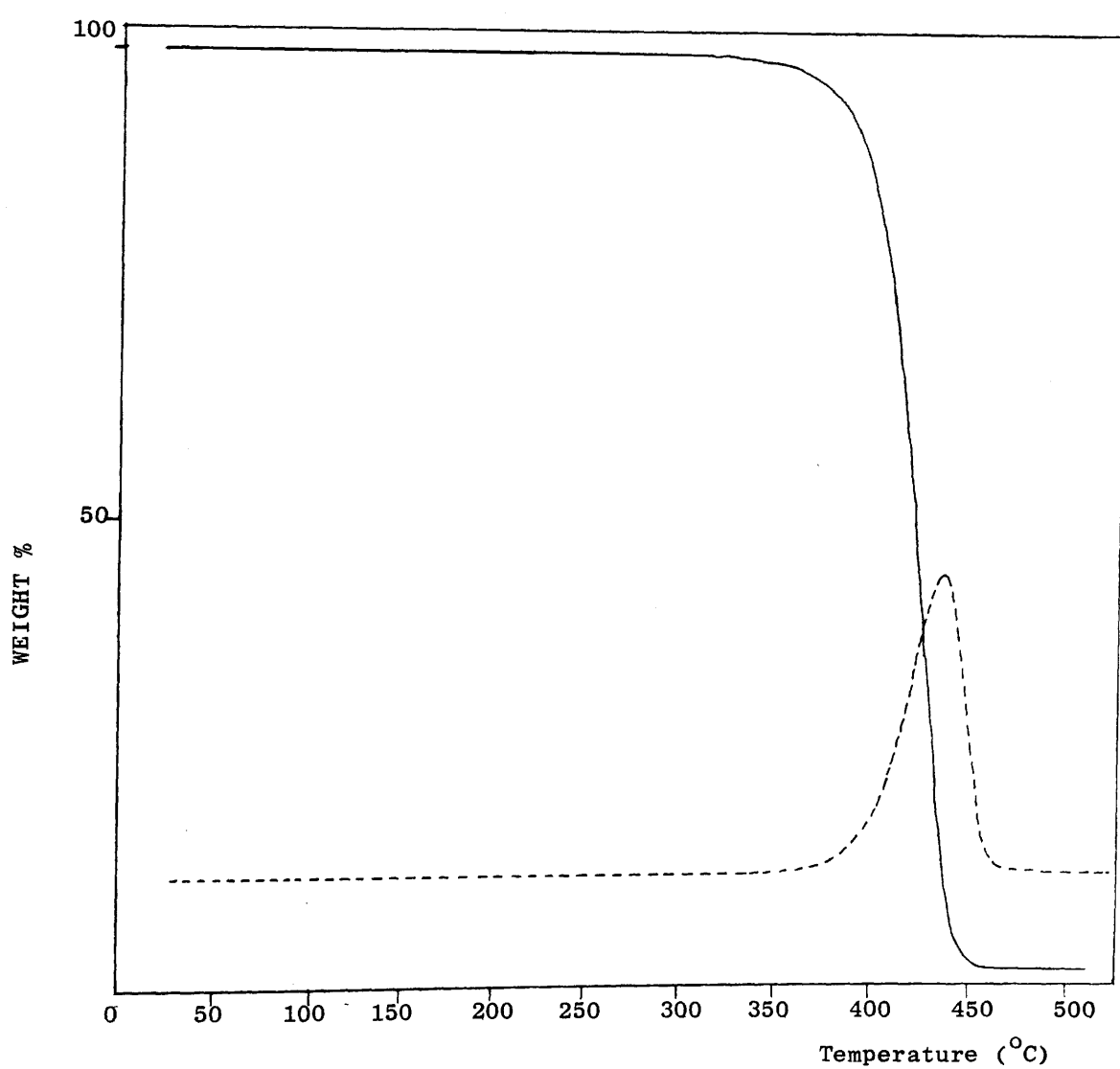The TVA curve for a 50 mg sample of PS used as received

Figure 4.4 TG(-) and DTG(---) curves for PS obtained under nitrogen at a heating rate of 10° min^{-1}.
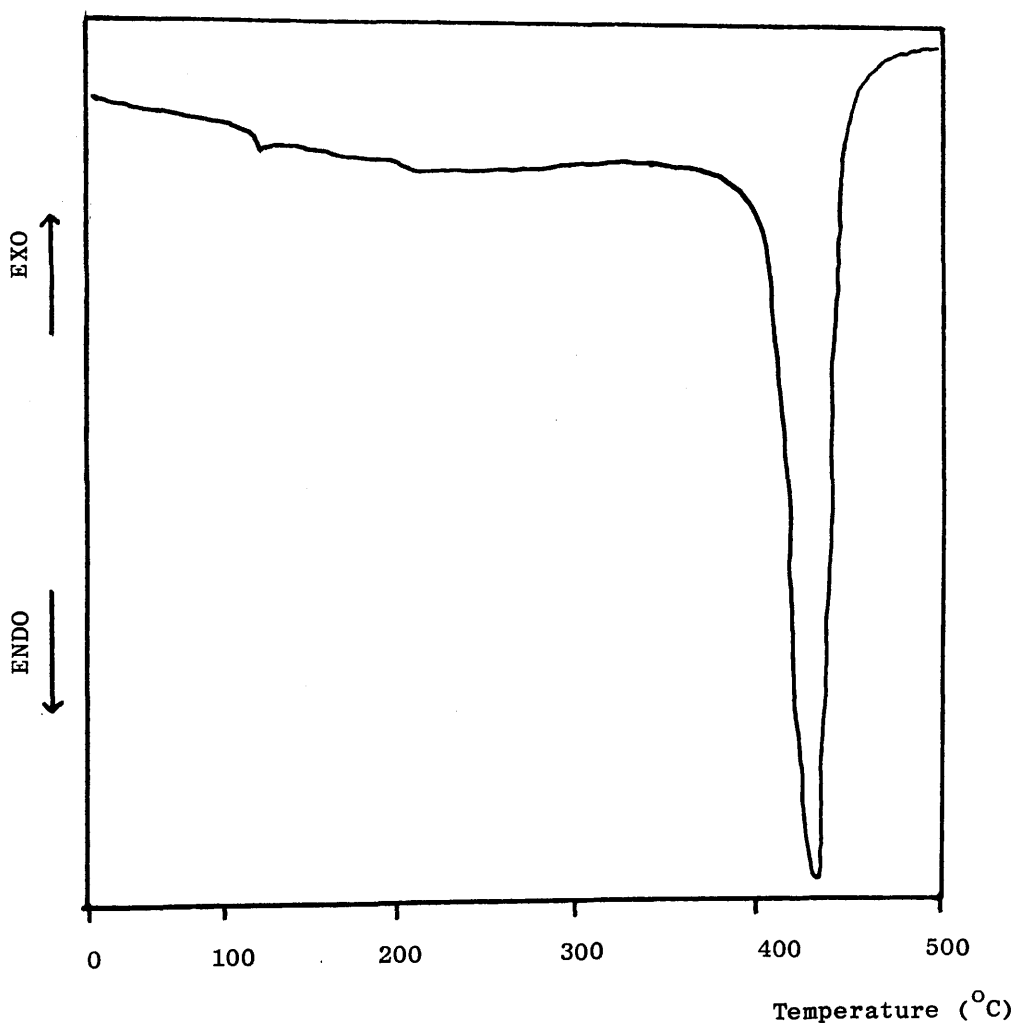
Figure 4.5   DSC trace for PS obtained under nitrogen

further purification, is reproduced in Figure 4.6. The TVA curve

illustrates the "one-stage" production of volatile compounds from

PS and is almost identical to that obtained by McNeill.[90] The

onset temperature of evolution and the maximum rate of evolution

of volatile products occur at approximately 265^OC and 400^OC,

respectively. On examining the individual trap traces it can be

seen that the 0^OC and -45^OC traces are coincident, the -75^OC trace

shows a slight limiting rate effect[90] and the -100^OC trace is

virtually coincident with the -196^OC trace which is following the

base-line indicating that no non-condensable products are produced.

These data are consistant with the main volatile product of

degradation being styrene.

SATVA Separation of Thermal Degradation Products.

The thermal degradation products of PS degraded by TVA were

separated using SATVA. A sample size of 50 mg was taken and

heated to approximately 500^OC at a rate of 10° min^{-1}. The

resultant SATVA trace on allowing the products to warm to ambient

temperature shows a large single peak (Figure 4.7). IR

spectroscopy revealed the product to be styrene.

The cold ring fraction (CRF) produced during degradation,

a colourless liquid, was removed for spectroscopic analysis. An

IR spectrum of the CRF is illustrated in Figure 4.8. The CRF was

found to consist of oligomeric chain fragments. Quantitative

analysis indicated that the CRF was approximately 36% by weight of

the initial sample. As there was no residue remaining in the

bottom of the tube after degradation, the remaining 64% can be

ascribed to styrene. This compares favourably with CRF[137] and

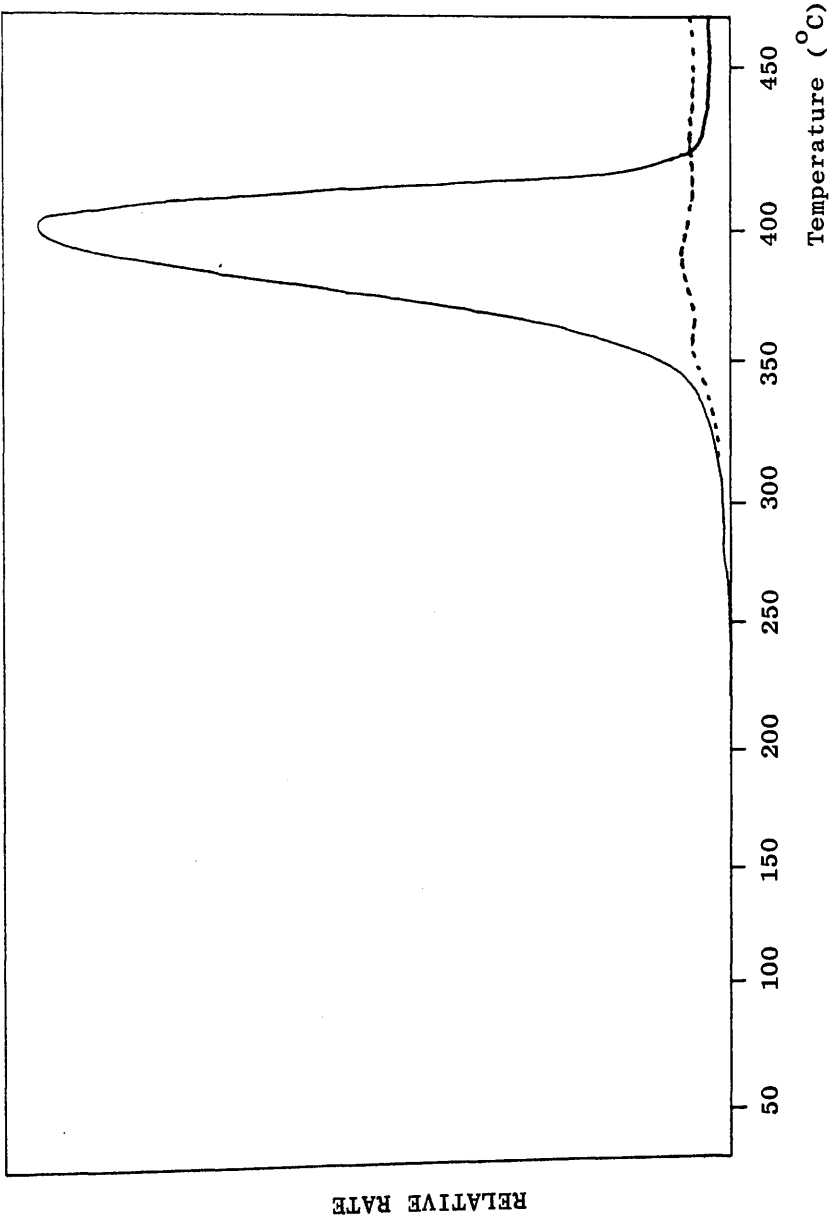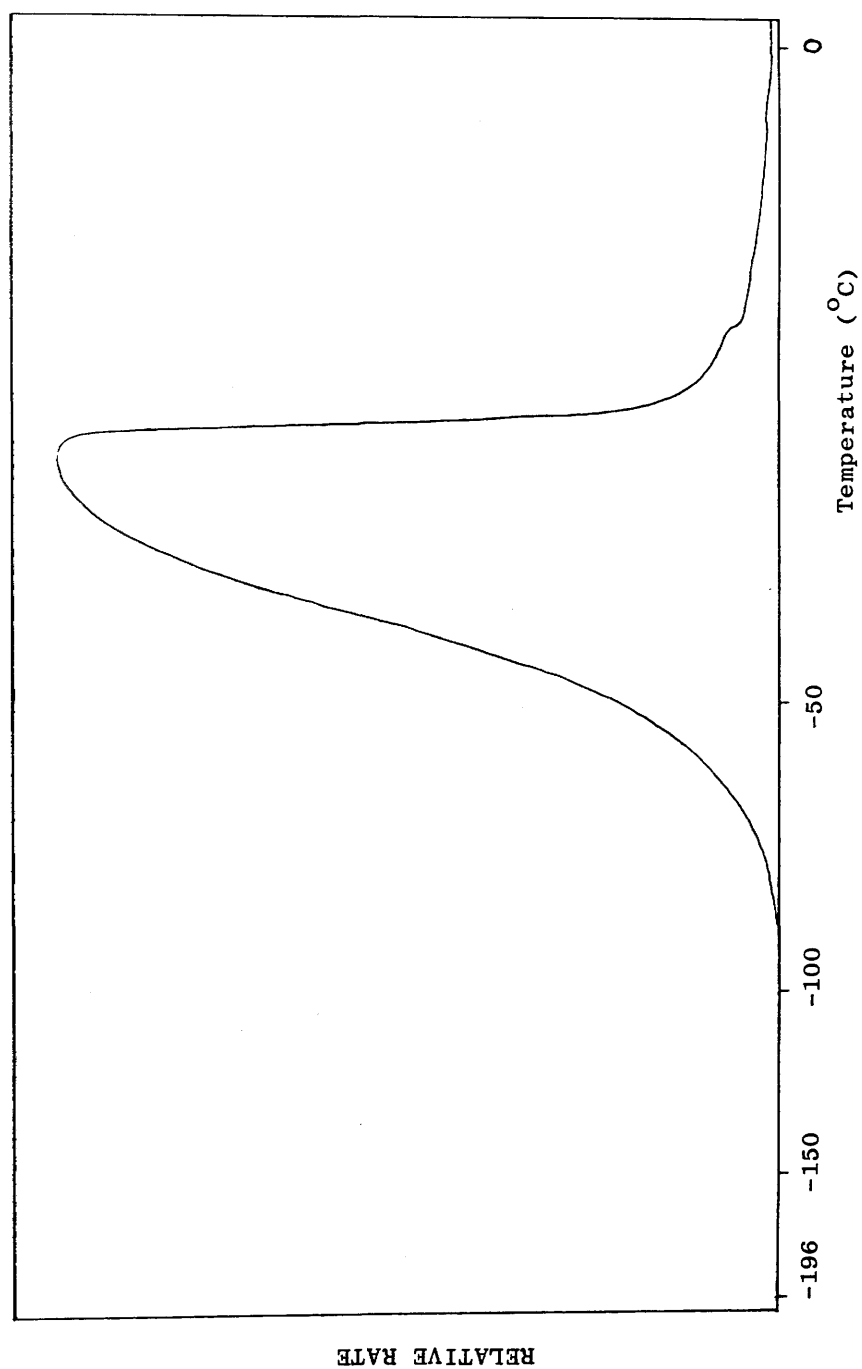Figure 4.6 TVA curve for PS using 50mg sample.

Figure 4.7   SATVA trace for condensable volatile degradation products of PS after heating to 500°C
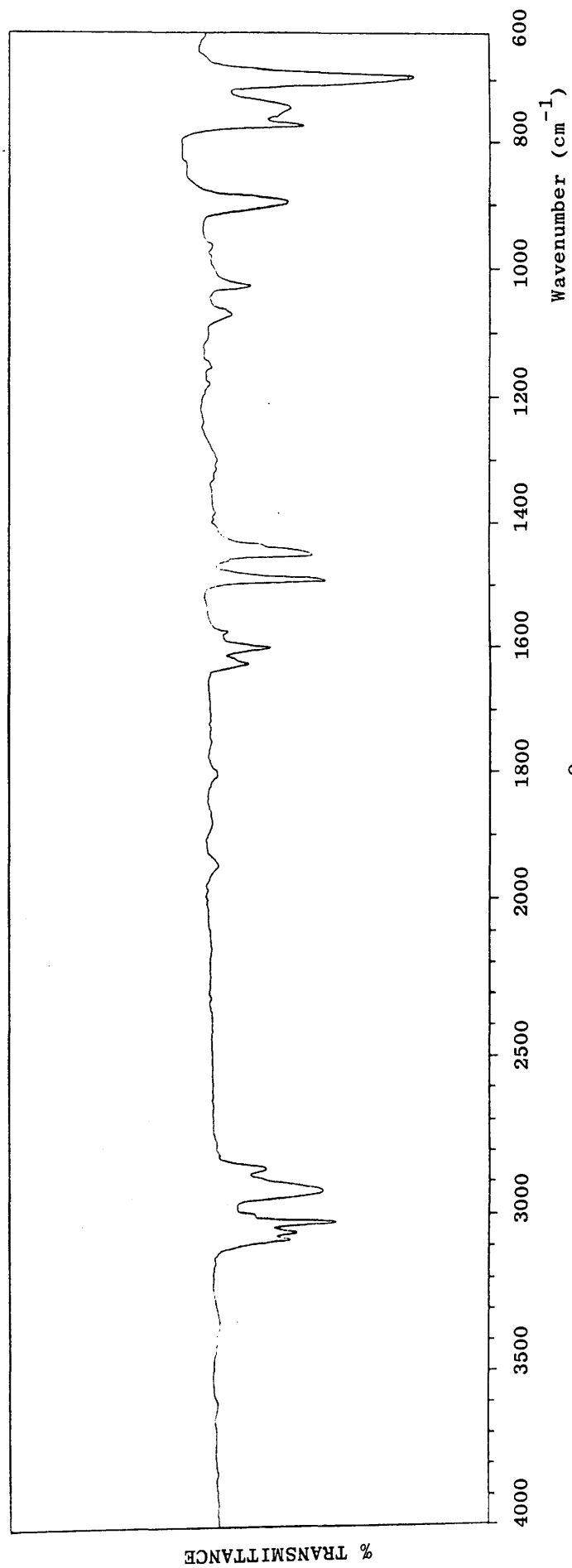
Figure 4.8 IR spectrum of CRF obtained on heating PS to 500°C run as liquid film.

styrene yields of 35% and 65% respectively as previously reported for PS under TVA conditions.

4.2.3 Discussion

From TG and TVA data it can be clearly seen that weight loss occurs in a single step during the thermal degradation of PS. The onset and rate maximum temperatures obtained by the two techniques are in good agreement.

Product analysis indicates that depolymerisation to produce styrene takes place during thermal degradation but that in addition intramolecular transfer processes produce the oligomeric fragments forming the CRF.

4.3 SYNTHESIS OF POLY(CHLOROSTYRENES)

The synthesis and degradation of poly(chlorostyrenes) were carried out in association with Anne-Marie Campbell.[138]

Ortho- and Para-chlorostyrene Monomers.

Ortho- and para-ring-chlorinated polystyrenes were prepared via the polymerisation of the respective monomers o- and p-chlorostyrene, which were supplied by Aldrich. The monomers were used without further purification but purity was checked by obtaining IR spectra. The spectra also provided a reference for comparison with the polymers formed and the products of degradation.

Polymerisation

O- and p-chlorostyrene were degassed on a vacuum line by the freeze-thaw technique and then distilled into dilatometers containing 0.01% w/v (i.e. 0.01 g per 100 ml) azodiisobutyronitrile (AIBN) initiator. The dilatometers were sealed in vacuo and polymerisation carried out at 60°C until the contraction in volume indicated 12% polymerisation. The reaction conditions are given below in Table 4.1.

Chlorostyrene	Percentage Polymerisation	Volume Contraction	Time of Polym.(mins)	Temp. of Polym.(°C)
ortho	12	0.17	250	60
para	12	0.17	340	60

Table 4.1 **Reaction conditions for polymerisation of o-chlorostyrene and p-chlorostyrene**.

Purification

The poly(o-chlorostyrene)(PoCS) and poly(p-chlorostyrene) (PpCS) prepared were isolated by precipitation in Analar methanol and purified by repeated dissolution in the minimum volume of methylene chloride followed by reprecipitation in methanol. Finally the polymers were dried for 15 hours in vacuo.

Polymer Characterisation

The synthesised poly(chlorostyrene) polymers were characterised by elemental analysis, IR spectroscopy and molecular weight determination. Number average ($\bar{M}n$), weight average ($\bar{M}w$), z-average ($\bar{M}z$) and p-average ($\bar{M}p$) molecular weights were determined

by PSCC Rapra Technology Limited as outlined for chlorinated
PEO in Chapter 3.

Results and Discussion

The chlorine content of both PoCS and PpCS was found by
elemental analysis to be 25.6% by weight, in agreement with the
theoretical value for one chlorine atom per styrene unit. The IR
spectra for PS, PpCS and PoCS are illustrated in Figure 4.9$_{a-c}$ and
the IR absorption frequencies with their corresponding assignments
are shown in Table 4.2.

The most significant differences between the IR spectrum of
PpCS (Figure 4.9b) and that of PS (Figure 4.9a) are outlined below:

i)   reduction in the intensity of the C-H aromatic stretching

        bands at 3025 - 3080 cm^{-1} relative to the aliphatic C-H

        stretching bands at 2928 cm^{-1} and 2850 cm^{-1}.

ii)   disappearance of the characteristic aromatic mono-

        substitution absorption band pattern of PS in the region

        2000 - 1650 cm^{-1} and the appearance of a new absorption at

        1890 cm^{-1} attributed to p-disubstituted aromatic ring.

iii)   reduction in the absorption band of the in-plane bending

        and stretching of the phenyl ring at 1600 cm^{-1} in PpCS.

iv)   appearance of a new absorption band at 1410 cm^{-1} in PpCS.

v)   changes in C-H in-plane bending absorptions at 1090 cm^{-1}

        and 1012 cm^{-1}, the former being particularly strong in PpCS.

vi)   a very strong absorption band at 825 cm^{-1} present only in

        PpCS due to C-H our-of-plane deformation of the p-disubstituted

        ring.

When the IR spectrum of PoCS (Figure 4.9c) is compared to the IR spectrum of PS, the following differences are noted:

i)   decrease in the intensity of the C-H aromatic stretching bands at 3068 cm^{-1} and 3020 cm^{-1} relative to the aliphatic C-H stretching bands at 2920 cm^{-1} and 2851 cm^{-1}.

ii)   appearance of o-disubstituted aromatic ring absorption pattern with bands at 1948 cm^{-1}, 1915 cm^{-1}, 1880 cm^{-1}, 1834 cm^{-1} and 1797 cm^{-1}.

iii) changes in C-H in-plane bending absorptions in the 1000 - 1200 cm^{-1} region, the strong band at 1030 cm^{-1} being attributed to C-H in-plane deformation for o-disubstituted ring.

The IR spectrum for ring chlorinated polystyrene (RCPS) prepared via the reaction between chlorine and PS by McNeill and Coskun[125] is reproduced in Figure 4.9d.   The absorption bands at 1890 cm^{-1} and 820 cm^{-1} indicate p-Cl substitution as these bands are observed in the IR spectrum of PpCS. However the weaker band in the IR spectrum at 1030 cm^{-1} suggests o-Cl substitution as this band is present in the IR spectrum of PoCS.   Unchlorinated rings are also indicated by the absorption at 690 cm^{-1}.   These comparisons confirm the conclusions of McNeill and Coskun that ring chlorination of PS gives predominantly the p-Cl product but that a small amount of o-substitution also occurs.

The GPC traces of PS, PpCS and PoCS (Figures 4.10-4.12) indicate that the chlorine-containing polymers were of somewhat higher molecular weight than the PS sample.   The results are shown in Table 4.3.
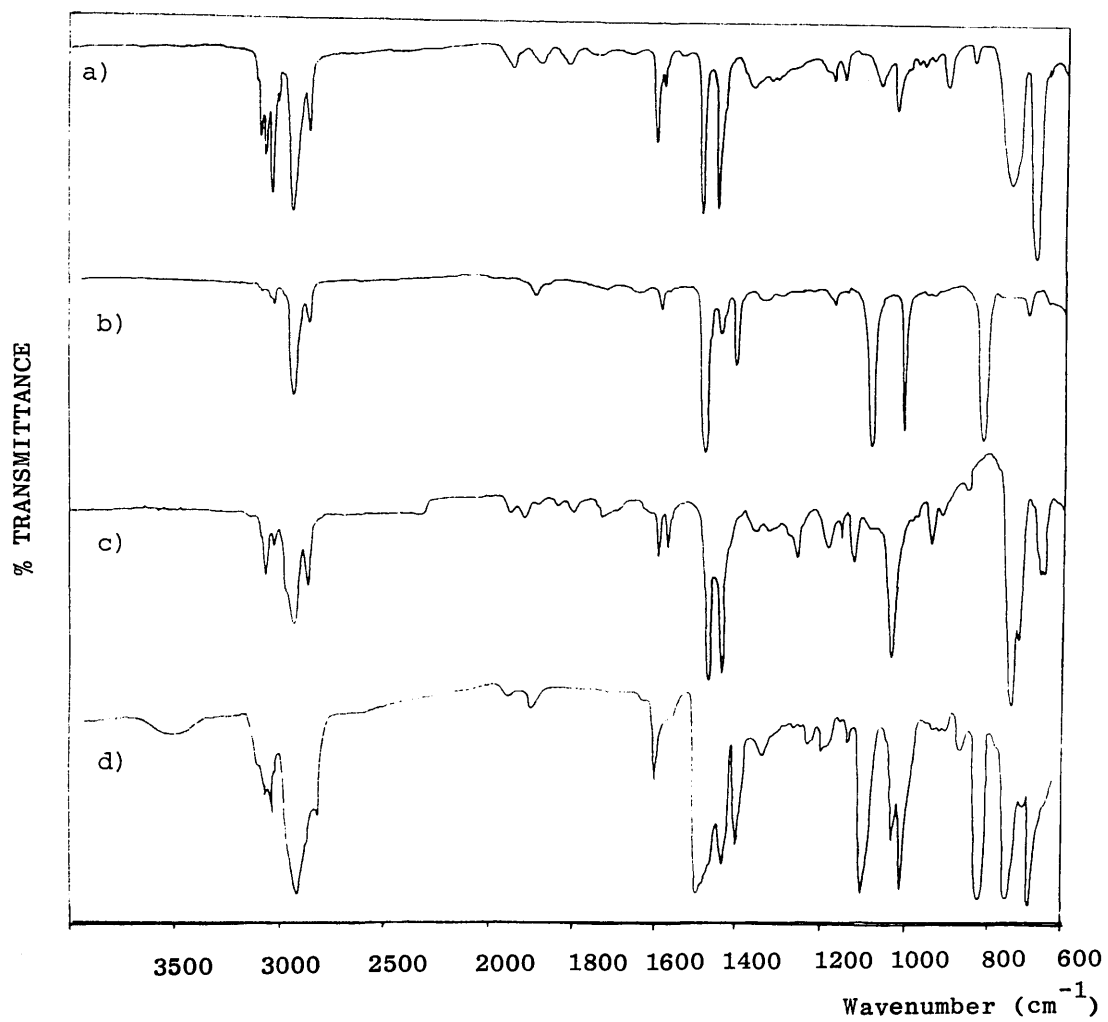
Figure 4.9 IR spectrum for a)PS b)PpCS c) PoCS and d) RCPS
films cast from CH_2Cl_2

Polystyrene Absorption (cm^{-1})	Assignment	Poly(p-chlorostyrene) Absorption (cm^{-1})	Assignment	Poly(o-chlorostyrene) Absorption (cm^{-1})	Assignment
3083(m) 3060(s), 3028(s)	aromatic C-H stretching	3025, 3040 3060, 3080	aromatic C-H stretching	3068, 3020 2952, 2920	aromatic C-H stretching
2930(s) 2850(m)	aliphatic CH stretching (CH$_2$,CH)	2928, 2850	aliphatic CH stretching(CH$_2$,CH)	2851	aliphatic CH stretch (CH$_2$CH)
1940 (w) 1870(w) 1801(w) 1744 (w) 1667(w)	Overtone and combination bands characteristic of mono substituted phenyl ring	1890, 1770 1645	Overtone and combination bands characteristic of p-disubstituted phenyl ring	1948, 1915 1880, 1834 1797	Overtone and combination bands characteristic of p-disub.phenyl ring
1602(s), 1584(w) 1494(s) 1454(s)	in plane bending stretching vibrations of phenyl ring	1594, 1485, 1447 1410	in plane bending stretching vibrations of phenyl ring	1594, 1570, 1473 1440	in plane bending stretch vibration of phenyl ring
		1090, 1013	in plane C-H bending vibration	1190 1128 1030(s)	in plane C-H bend vib. for o-disub. phenyl ring
760, 700	out of plane C-H and phenyl ring vibrations characteristic of mono substituted phenyl ring	825	out of plane C-H bending vibrations for p-disubstituted phenyl ring	749(s) 680	out of plane C-H bending vibration for o-disubstitute phenyl ring.

Table 4.2   IR absorption frequencies (cm^{-1}) and corresponding assignments for Polystyrene, poly(p-chlorostyrene) and poly(o-chlorostyrene)

CALIBRATION : THF.7.88
RUN NO./NAME: A192   SAMPLE 1   (7453)   1031 070788

PEAK START: 1140   MN: 1.38E+05
PEAK FINISH: 1720

                                   MW: 3.41E+05
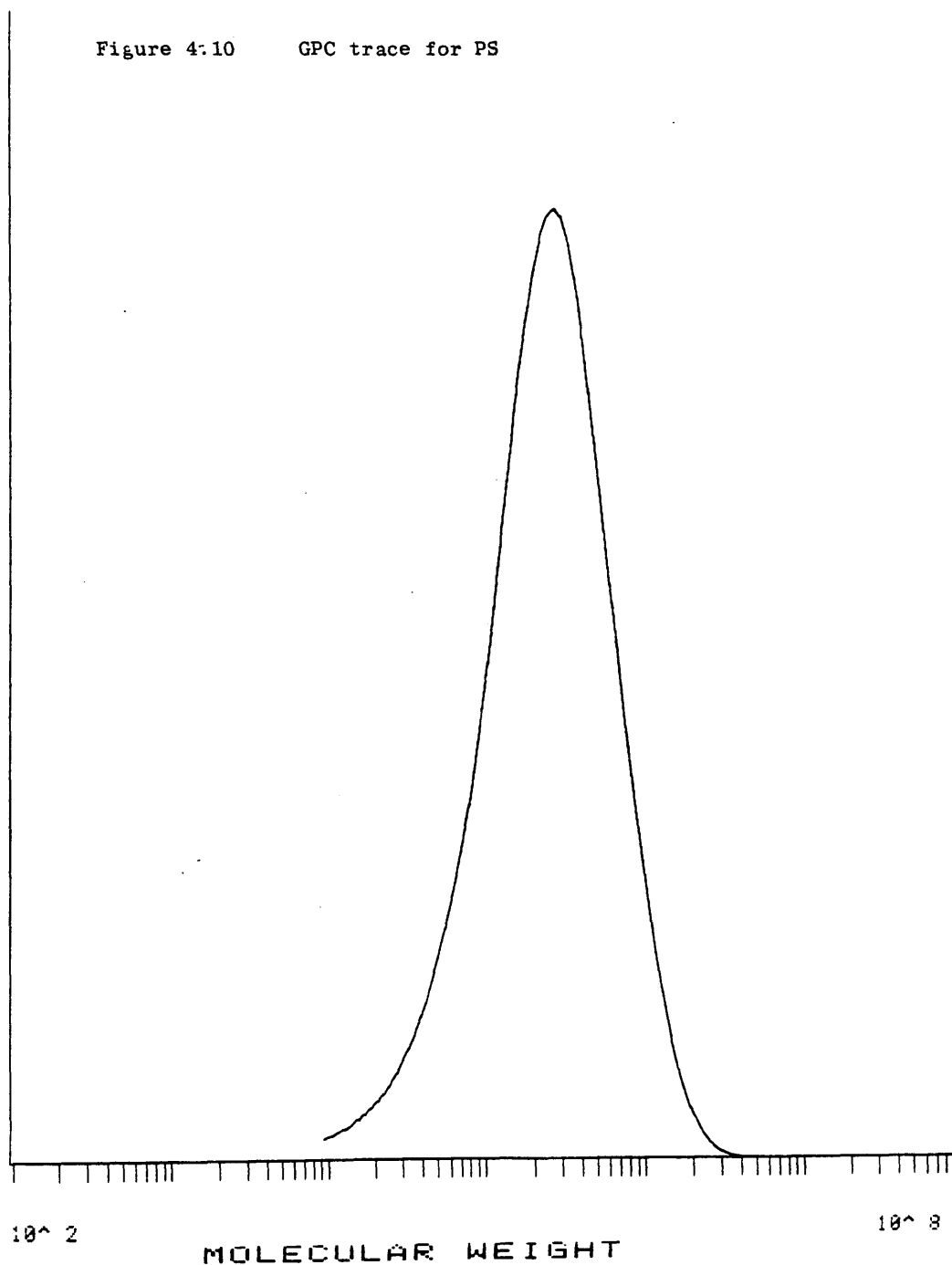BASELINE START: 1140
BASELINE FINISH: 2400   MZ: 6.62E+05

FLOW CORRECTION: 1.000   MP: 2.53E+05

KP: 1.200×10^{-4} D: 2.474
AP: .710

Figure 4.10   GPC trace for PS

10^2 10^8

MOLECULAR WEIGHT

CALIBRATION : THF.7.88
RUN NO./NAME: A198 SAMPLE 5 (7657)   1435 070788

PEAK START: 1100   MN: 3.86E+05
PEAK FINISH: 1600
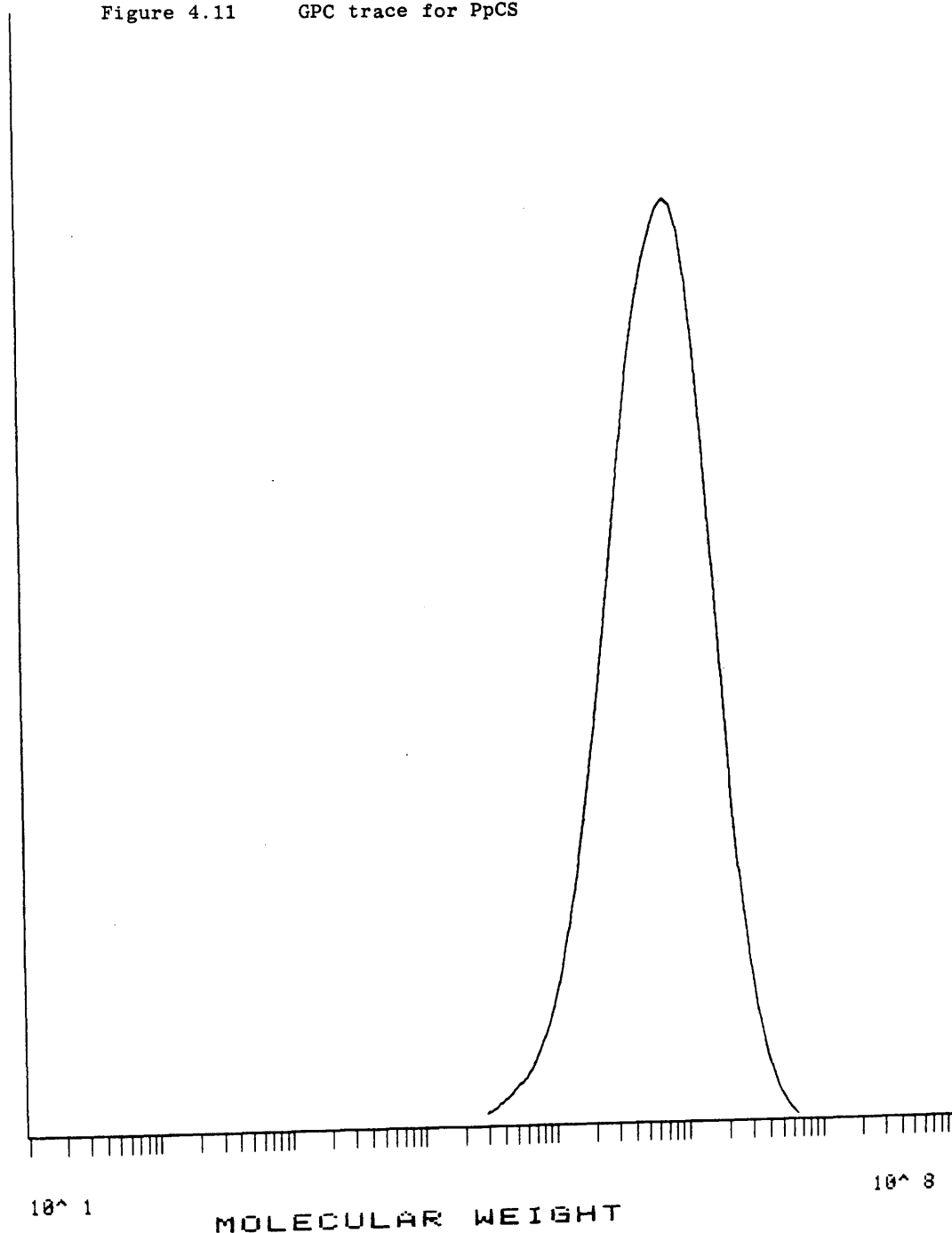   MW: 8.39E+05
BASELINE START: 1100
BASELINE FINISH: 2400   MZ: 1.49E+06

FLOW CORRECTION: 1.001   MP: 7.33E+05

KP: 1.200×10^{-4} D: 2.173
AP: .710

Figure 4.11   GPC trace for PpCS

$10^{\wedge} 1$ MOLECULAR WEIGHT $10^{\wedge} 8$

PSCC   GPC   SYSTEM

CALIBRATION : THF.7.88
RUN NO./NAME: A201   SAMPLE 6   (7458)   1635 870788

PEAK START: 1060   MN: 2.88E+05
PEAK FINISH: 1630

                                 MW: 7.10E+05

BASELINE START: 1060
BASELINE FINISH: 2400   MZ: 1.66E+06
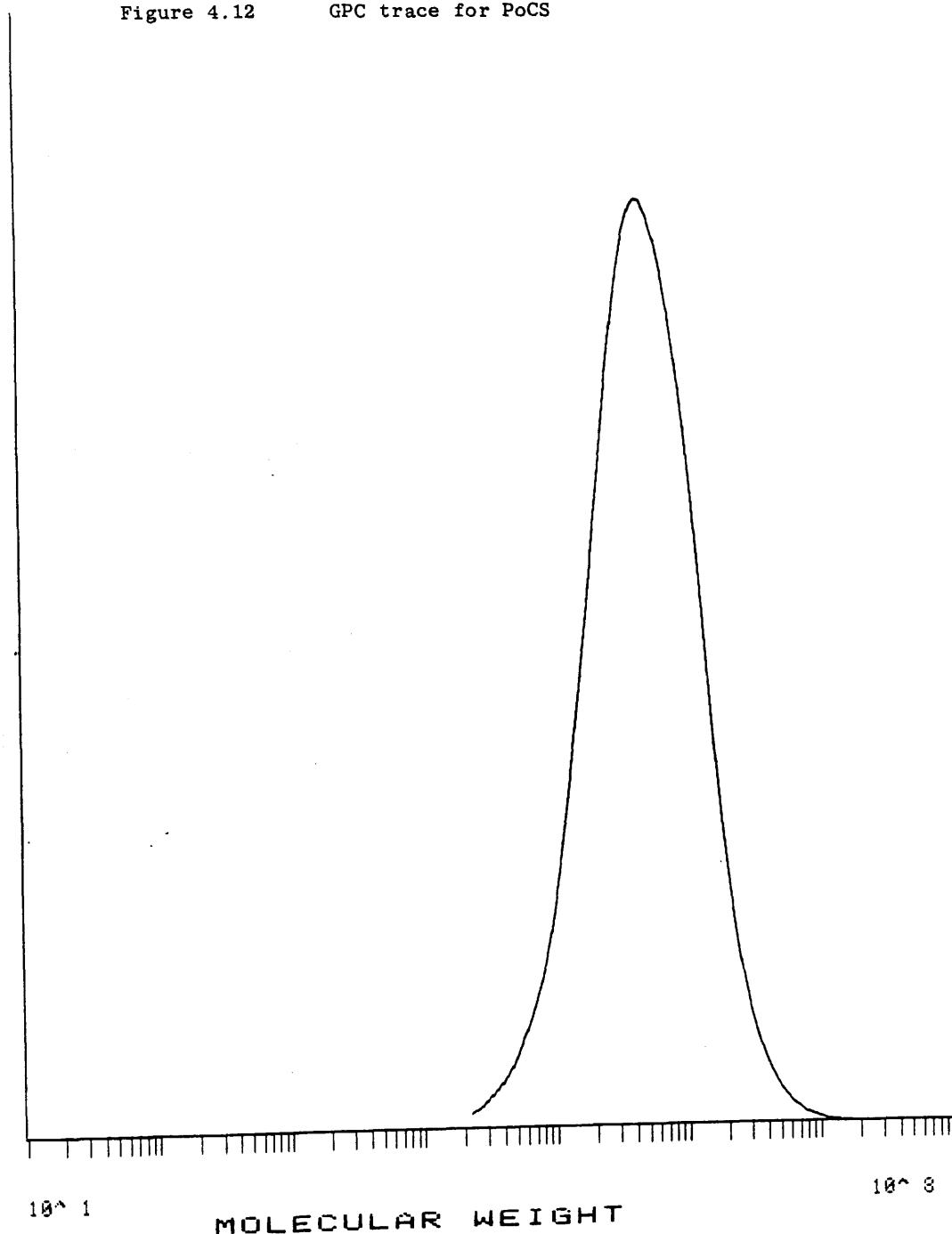
FLOW CORRECTION: 1.000   MP: 4.25E+05

KP: 1.200X10^{-4} D: 2.466
AP: .710

Figure 4.12   GPC trace for PoCS

10^ 1   MOLECULAR   WEIGHT   10^ 8

Sample.	$\overline{M}n\,(10^5)$	$\overline{M}w(10^5)$	$\overline{M}z(10^5)$	$\overline{M}p(10^5)$	D
PS	1.41	3.44	6.68	2.48	2.44
PS	1.38	3.41	6.62	2.53	2.47
PpCS	3.86	8.39	14.90	7.33	2.17
PoCS	2.90	7.22	18.40	4.13	2.49
PoCS	2.88	7.10	16.60	4.25	2.47

Table 4.3 Molecular Weight Averages expressed as "polystyrene equivalents" and Molecular Weight Distributions (D) for PS, Poly(p-chlorostyrene)(PoCS) and poly)o-chlorostyrene)(PoCS).

4.4 THERMAL DEGRADATION OF POLY(CHLOROSTYRENES)

The thermal stability and degradation behaviour of poly-o-
and poly(p-chlorostyrene) (PoCS, PpCS) prepared as described in
section 4.3 were examined by TG, TVA and SATVA.   The results
obtained were compared to those reported[125]   for ring chlorinated
polystyrene (RCPS) prepared by direct chlorination of PS and the
experimental values obtained for polystyrene in section 4.2.

4.4.1 Experimental

Thermal Analysis of Poly(chlorostyrenes).

TG

The TG curves for PoCS and PpCS illustrated in Figure 4.13
and Figure 4.14 show that in each case weight loss occurs in a single
stage, as for PS, with a threshold of degradation at approximately
$376^{\circ}C$ and $360^{\circ}C$ respectively.   The temperature of the maximum
rate of degradation is around $413^{\circ}C$ for PoCS and slightly lower at
$401^{\circ}C$ for PpCS.   The corresponding temperatures for PS, $T_{onset}=$
$350^{\circ}C$ and $T_{max} = 423^{\circ}C$ are similar to the degradation temperatures
of the poly(chlorostyrenes).

However, if the degradation temperatures for ring-chlorinated
polystyrene are included a very different picture is produced.   It
has been found that TG produces a two stage weight loss curve.[125]
In this case the onset temperature for degradation is lowered
relative to pure PS to around $230^{\circ}C$ and the maximum rate for the
main degradation occurs at $390^{\circ}C$.   The TG curve for RCPS is
reproduced in Figure 4.15.

In all the chlorinated polymers mentioned, there is very
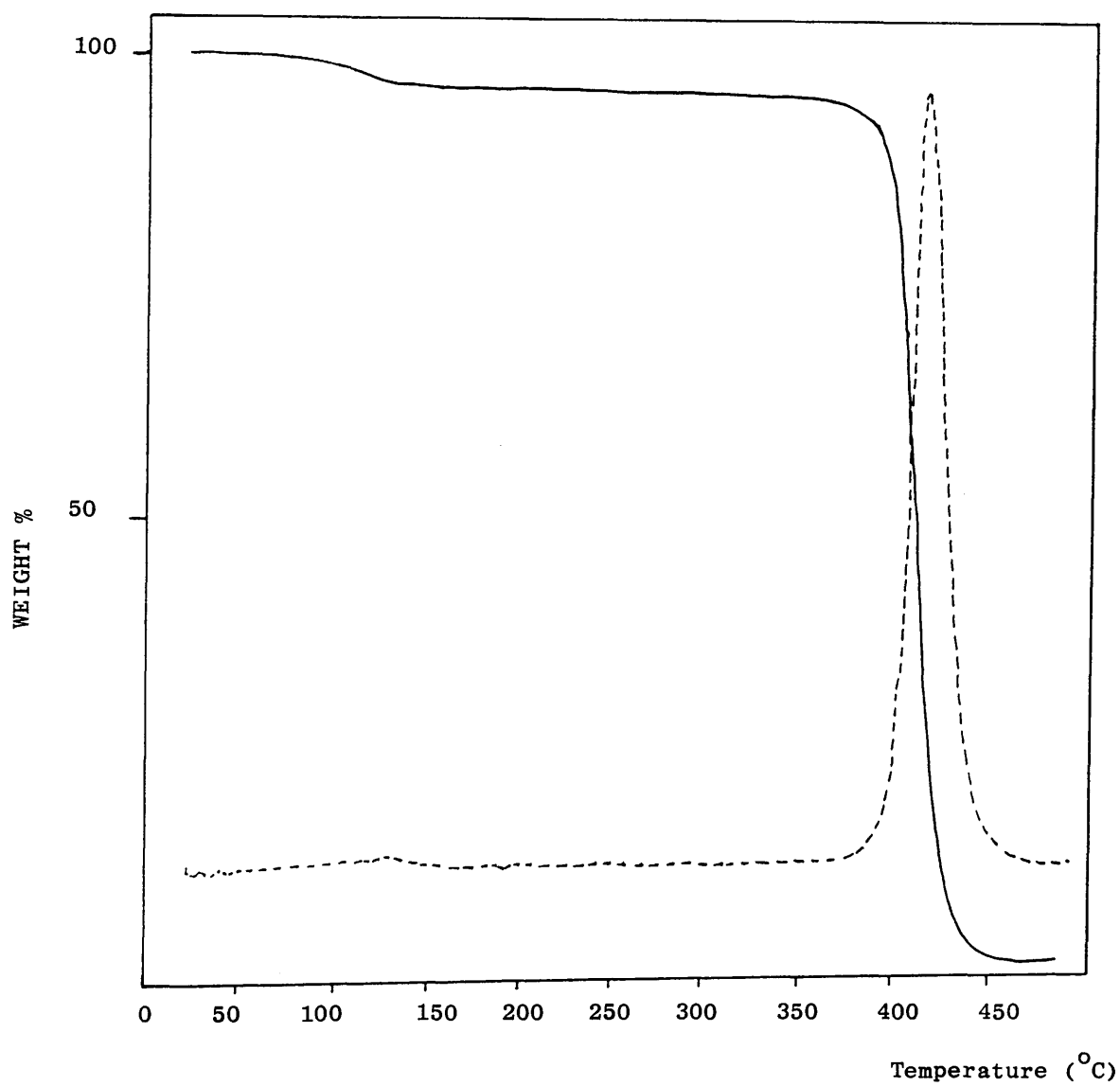
Figure 4.13   TG(-) and DTG(---) curves for PoCS obtained
under nitrogen at a heating rate of 10° min^{-1}
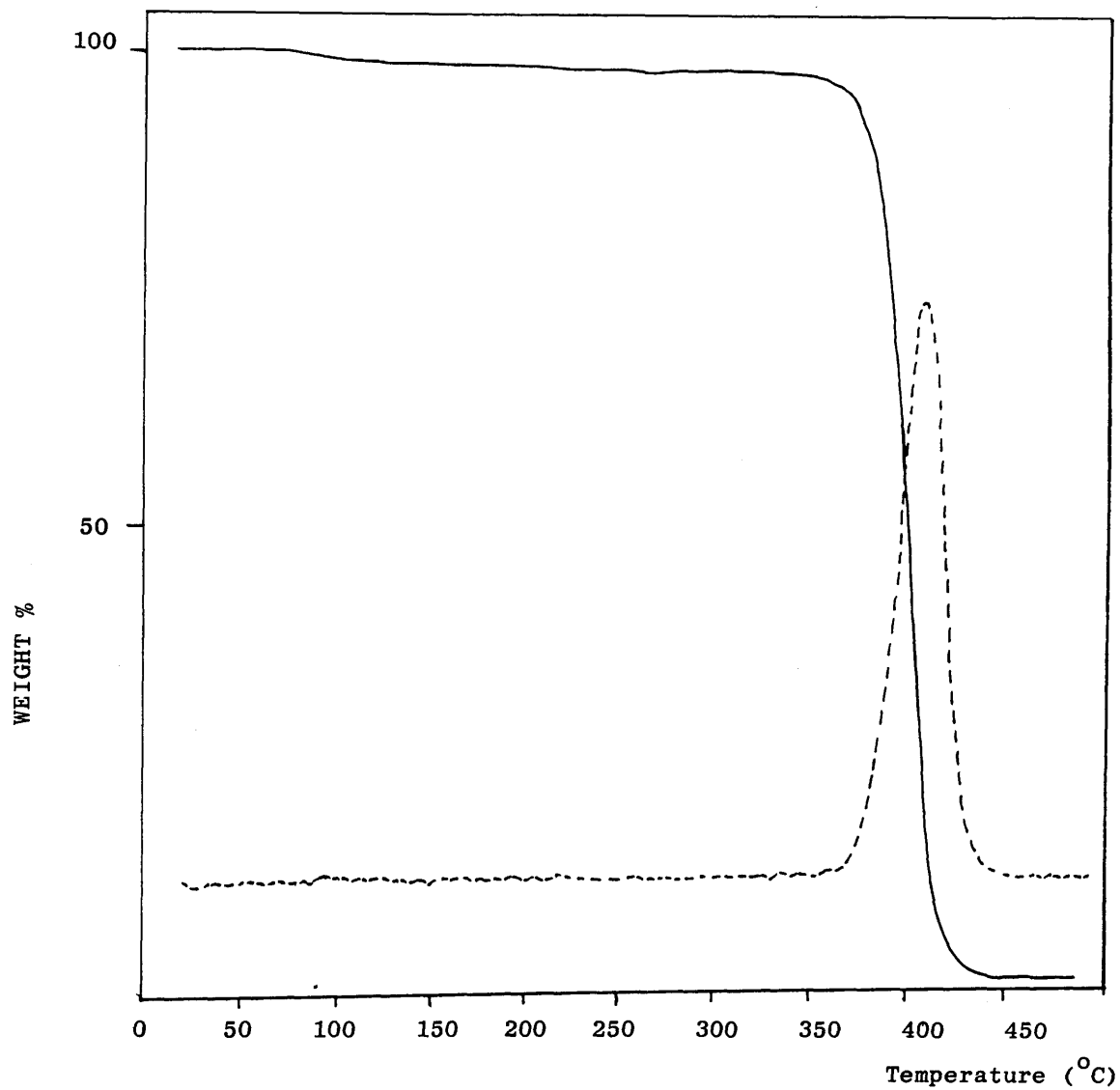
Figure 4.14 TG(-) and DTG(---) curves for PpCS obtained under
nitrogen at a heating rate of 10° min^{-1}
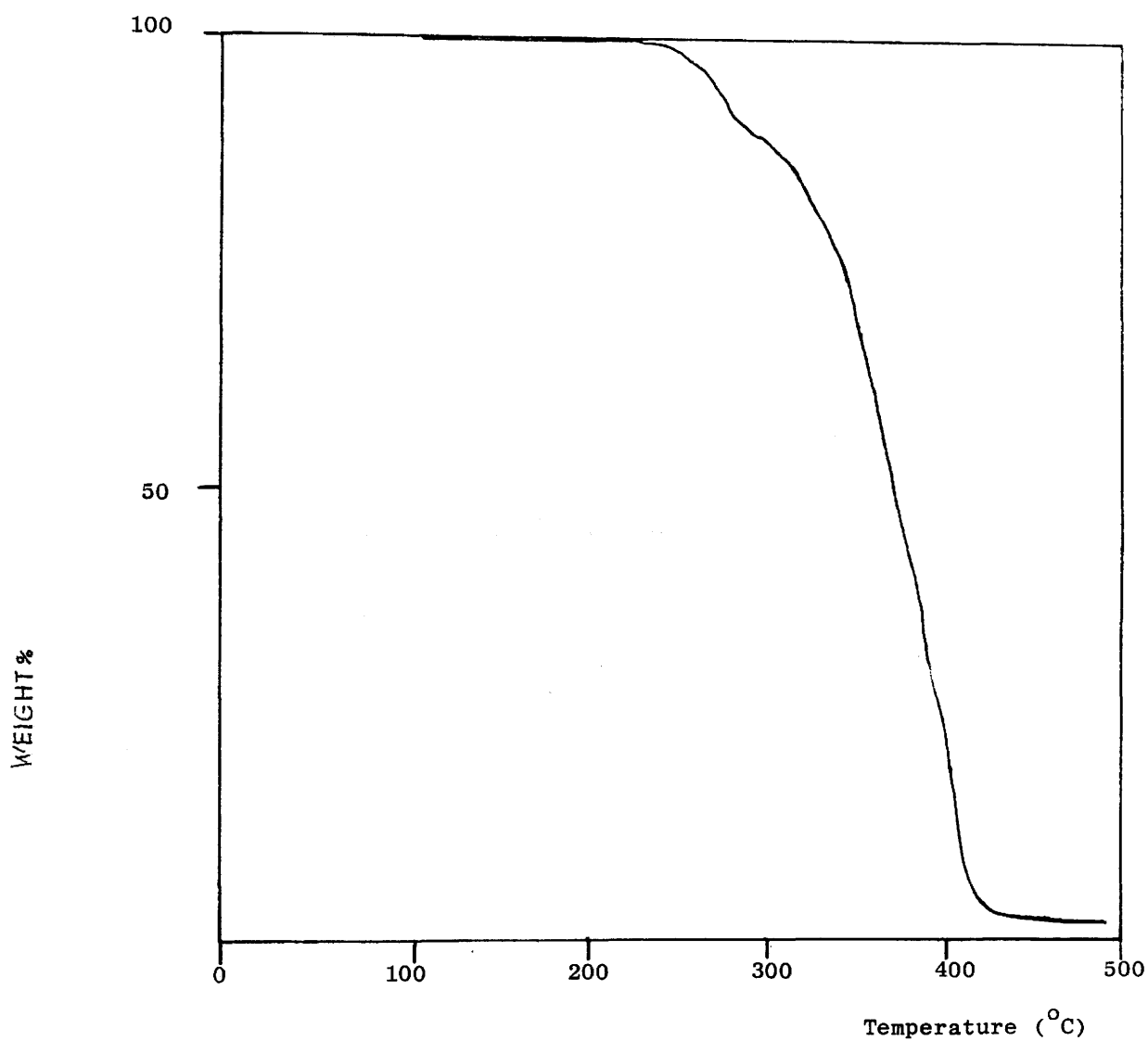
Figure 4.15 TG curve for RCPS obtained under nitrogen at a
heating rate of 10° min^{-1}

little residue remaining ($\sim$2% polymer weight) after heating to 500°C at 10° min^{-1} under a dynamic flow of nitrogen (50 ml min^{-1}). The TG results, including those for PS and RCPS are summarised in Table 4.4.

Polymer	T_{onset} ($^{\circ}$C)	T_{max} ($^{\circ}$C)	Wt % Residue
PS	350	423	0.80
PoCS	376	413	1.61
PpCS	360	401	1.45
RCPS	230	390	2.00

Table 4.4 <u>TG results for PS, PoCS, PpCS and RCPS</u>.

Polymer	T_{onset} ($^{\circ}$C)	T_{max} ($^{\circ}$C)
PS	265	400
PoCS	358	405
PpCS	351	400
RCPS	220, 340	320, 380

Table 4.5 <u>TVA degradation temperatures for PS, PoCS, PpCS and RCPS</u>.

<u>TVA</u>

TVA curves were obtained using approximately 50 mg of PoCS and PpCS which had been teased into small pieces. The samples were heated to 500°C <u>in vacuo</u> at a rate of 10° min^{-1}. The TVA curves are presented in Figures 4.16 and 4.17. The initial broad peak ranging from approximately 48°-176°C on the TVA trace
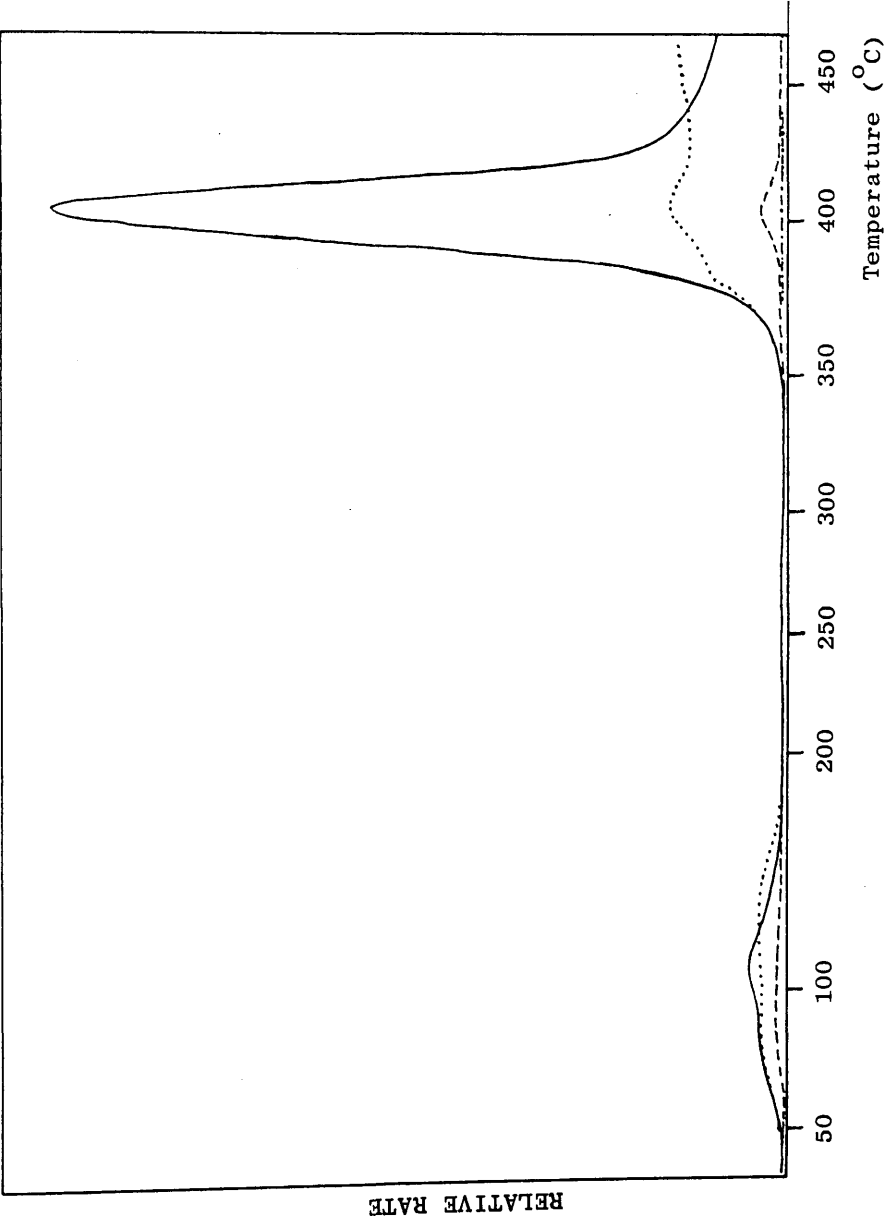
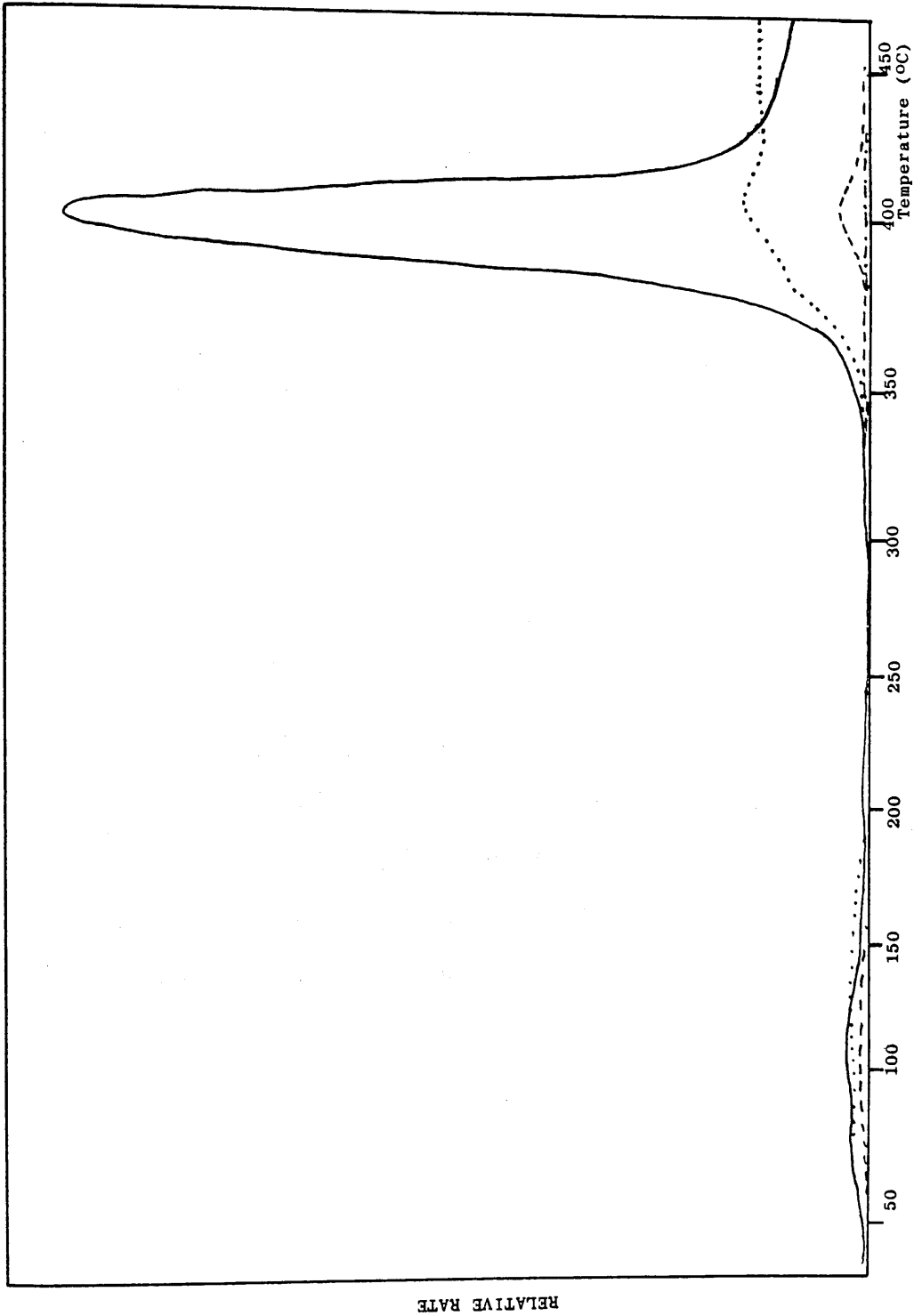Figure 4.16 TVA curve for PoCS using 50mg sample.

Figure 4.17   TVA curve for PpCs using 50 mg sample.

of PoCS is due to traces of trapped methylene chloride (solvent)
gradually being released from the polymer sample as the temperature
increases.   The evolution of volatile products on degradation
occurs in a single stage commencing at approximately 358°C and with
rate maximum around 405°C.   Most of the degradation products
are condensed between -45°C and -75°C.   The -45°C trace exhibits
a limiting rate effect and there is slight elevation of the
coincident -75°C and -100°C traces.   No non-condensable products
are produced.

The TVA curve for PpCS is vitrually identical to that for
PoCS apart from slight variations in degradation temperatures.   In
both cases, the temperatures recorded for the onset of degradation
and the maximum rate of degradation using TVA are in agreement with
those obtained from TG.

The two stage degradation observed by TG in RCPS is again
revealed by TVA (reproduced[125] in Figure 4.18).   The first stage
is due to products which are initially volatile at -100°C but
this stage overlaps with the main degradation process which results
in products of lower volatility than styrene as indicated by the
behaviour of the -45°C and -75°C traces.   The rate maximum for
the main degradation process occurs at approximately 380°C and
there are no non-condensable products.

The T_{onset} and T_{max} temperatures for PS, PoCS, PpCS and
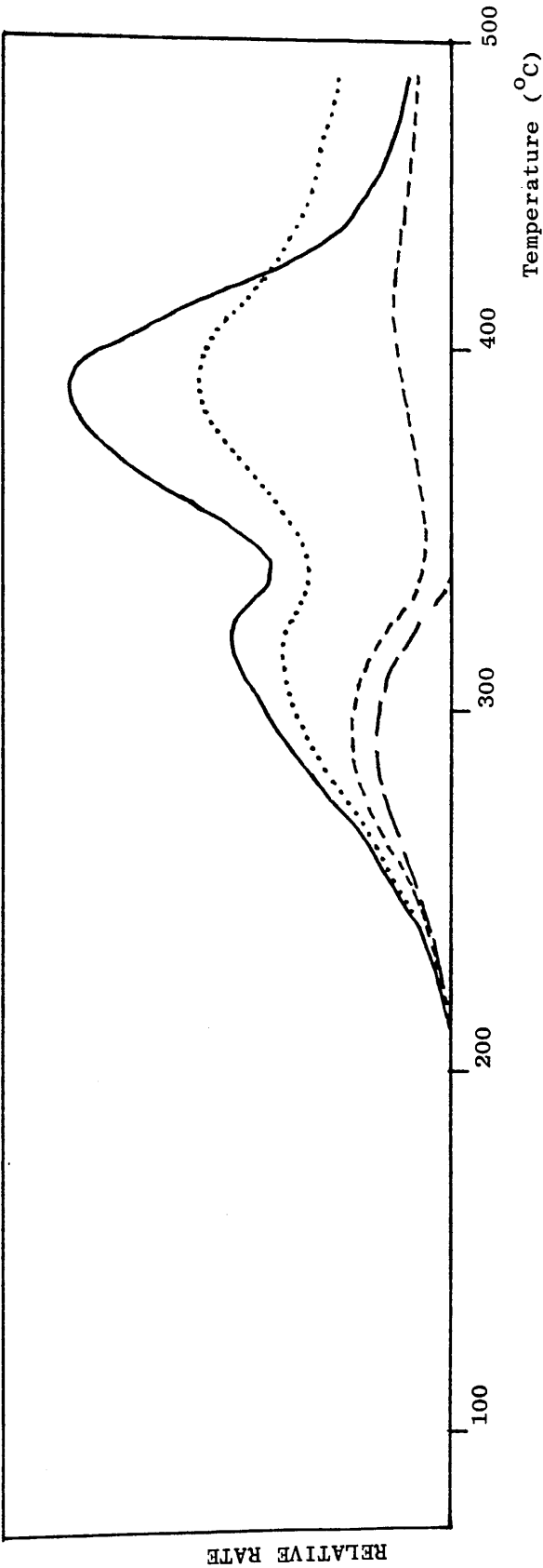RCPS as obtained under TVA conditions are given in Table 4.5.

Figure 4.18 TVA curve for RCPS using 50mg sample.

SATVA Separation of Degradation Products

Condensable degradation products evolved on heating polymer samples to 500°C followed by collection at -196°C were separated by SATVA and analysed spectroscopically. The SATVA traces for approximately 50 mg PoCS and PpCS samples in the form of small pieces are shown in Figures 4.19a and 4.19b. The SATVA trace for PoCS shows two main fractions - a small sharp initial peak due to a very small amount of highly volatile product(s) and a large broad peak, preceeded by a slight shoulder, due to material of lower volatility. The first fraction was found by IR spectroscopy to consist only of HCl, whereas the second fraction from IR and mass spectral data was found to be a partially resolved mixture comprising mainly o-chlorostyrene monomer with trace amounts of toluene and styrene.

The SATVA trace for PpCS is similar to that obtained for PoCS. However, there is a notable reduction in the height of the peak due to HCl production. Thus, PpCS when degraded to 500°C shows trace amounts of HCl and toluene products but the main degradation product is monomer, p-chlorostyrene.

The corresponding SATVA trace for RCPS has been reproduced in Figure 4.19c for comparison. Here two fractions are observed again but in this case the first fraction (HCl) is present in much greater amounts than in Figures 4.19a and 4.19b indicating greater HCl production.

The cold-ring-fractions (CRF's) for both PoCS and PpCS were pale amber tars and were structurally analysed by IR spectroscopy.
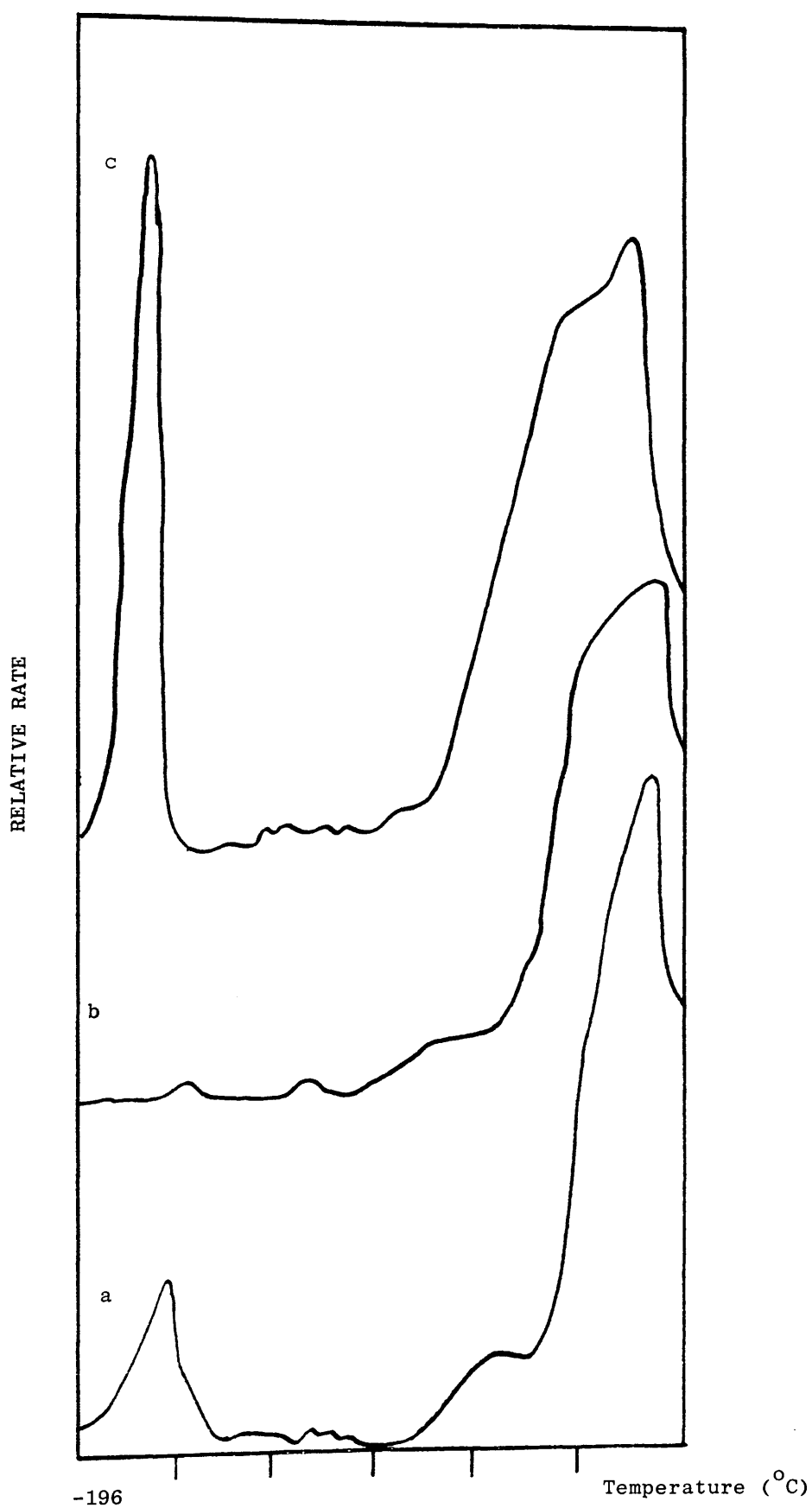
Figure 4.19   SATVA trace for condensable volatile degradation
products of a)PoCS b) PpCS and c)RCPS after heating to
500°C

In the IR spectrum of the CRF from PpCS (Figure 4.20a) new peaks appear at 1625 cm^{-1}, 960 cm^{-1} and 900 cm^{-1} indicating the presence of unsaturation. The last of these absorptions, due to vinylidene, is particularly strong and the very weak band at 960 cm^{-1} is attributed to trans disubstituted olefin. Similar absorptions are present in the spectrum of the CRF of RCPS. It seems likely therefore, that the CRF of PpCS consists of short chain fragments terminated by $H_2C = C\text{-}$ structures.

The IR spectrum of the CRF from PoCS (Figure 4.20b) indicates the presence of a new absorption band at 1730 cm^{-1} which may be due to the presence of oxidised fragments containing a carbonyl group. In addition new weak absorptions in the in-plane phenyl ring deformation region are observed at 1490 cm^{-1} and 1050 cm^{-1}. The vinylidene absorption band at 910 cm^{-1} is not as intense as the band observed in the spectrum of the CRF of PpCS. An extra band at 1455 cm^{-1} in the PoCS CRF spectrum may be attributed to CH$_3$ bending. This, in conjugation with the strong aliphatic CH$_3$ stretching absorption bands at 2929 cm^{-1}, suggest that the CRF of PoCS consists of short chain fragments terminated by saturated structures such as: $H_3C - CH$
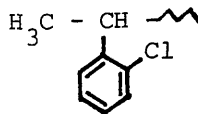
Quantitative analysis of CRF production gave yields of 14% and 16% on heating PpCS and PoCS to 500°C respectively.
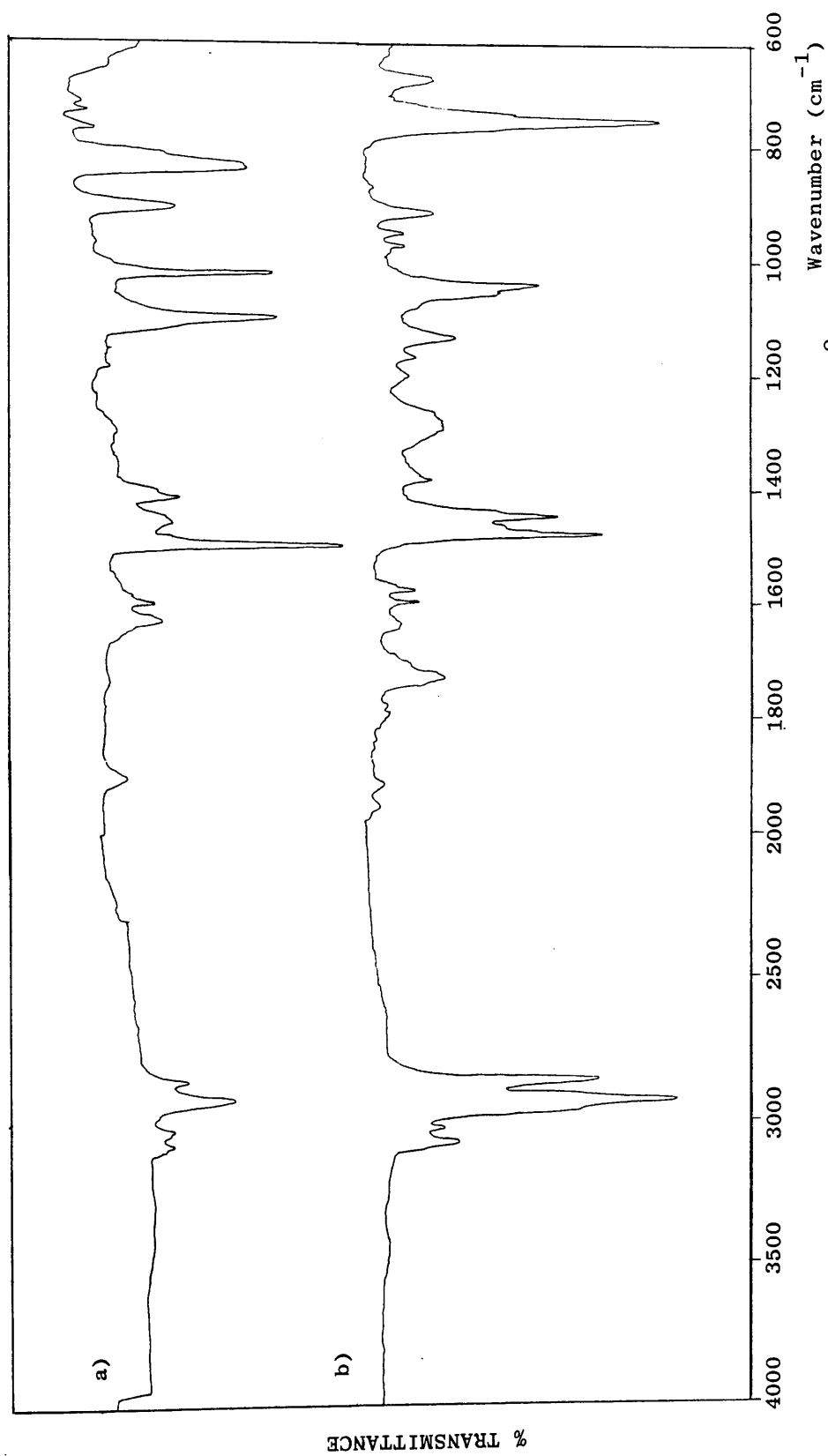
Figure 4.20 IR spectrum of CRF obtained on heating a)PpCS and b) PoCS to 500°C run as liquid film.

4.4.2 <u>Discussion</u>

The method of synthesis of polystyrene with ring chlorine substituents has a marked effect on the polymers degradation behaviour. Ring-chlorinated PS (RCPS) prepared by the substitution reaction of chlorine with PS is thermally less stable than PS. This instability however is attributed to a small amount of chain chlorination which accompanies substitution in the ring. A two stage degradation is observed by TG and TVA experiments. An early loss of HCl on heating RCPS up to approximately 300°C (temperatures typical of dehydrochlorination reactions in polymers containing Cl attached to the backbone[5]) together with spectroscopic evidence indicates that the site of HCl production is along the polymer backbone. In the main degradation, a lower threshold for the production of volatile products and CRF than for PS and a greater breadth of TVA peak are a consequence of the destabilising effect of chain unsaturation resulting from dehydrochlorination which leads to chain scission. This provides an additional mode of initiation of degradation. The production of approximately 30% by weight monomer[125] (p-, o-chlorostyrene and styrene) after HCl evolution suggests that the main degradation reaction is very similar to that for PS. Thus the depolymerisation and transfer reactions found in the thermal degradation of PS also occur in the decomposition of ring chlorinated PS.

Ring-brominated PS,[139] on the other hand, has been found to be more thermally stable than ring-chlorinated PS, having a similar thermal stability to polystyrene and degrading in the

same manner to give approximately 62% by weight of monomers

(p-bromostyrene and styrene) and a CRF with a brominated repeat

structure and terminal unsaturation.   This increase in thermal

stability of ring-brominated PS as compared to ring-chlorinated

PS can be attributed to the polymer being brominated exclusively

in the ring and thus lacking destabilising backbone halogenation.

The preparation of poly(chlorostyrenes) via the polymerisation

of p-chloro and o-chlorostyrene results in products in which

chlorination is exclusively in the ring.   These chloropolymers

exhibit similar thermal properties to those of PS.   A single

stage degradation occurring over a narrow temperature range in

the region of that for PS is observed.   The main process

taking place during the thermal degradation of poly(chlorostyrene)

is depolymerisation.   There appears to be less transfer reactions

taking place than in PS leading to the production of small chain

fragments and CRF as the weight % CRF evolved approximates to half

the value observed for PS (See Section 4.2.2).   This is the

result of terminal radicals formed in the depolymerisation steps

being stable enough not to participate in various side reactions.

The presence of chlorine on the aromatic rings of PS can stabilise

these radicals in two ways:

1) the electron-withdrawing inductive effect (-I) of chlorine

enhances resonance stabilization
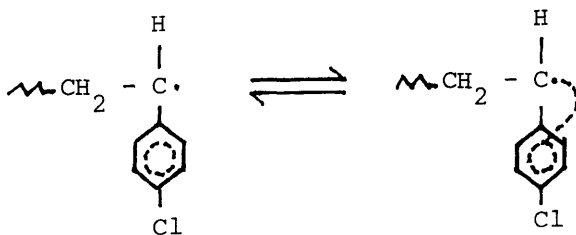
2) steric hindrance preventing chain transfer

$$CH_2 - \overset{\overset{\textstyle H}{\textstyle |}}{C}\cdot$$

(attached ring with Cl)
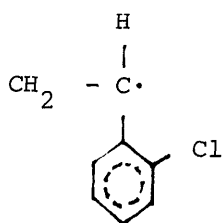
Thus the dominant reaction is depolymerisation. A typical reaction mechanism for the depolymerisation of poly(chlorostyrene) is given in Figure 4.21.
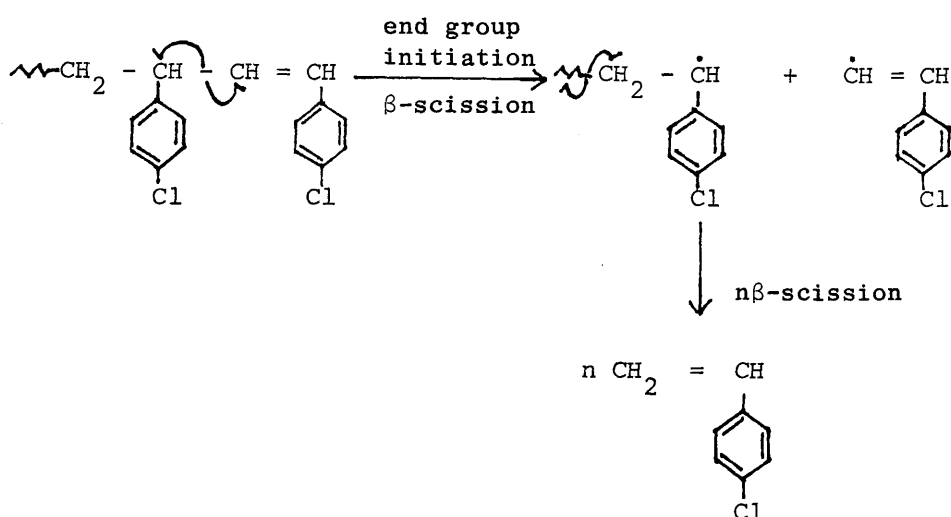
Figure 4.21 Typical depolymerisation mechanism for poly(chloro-styrene).

The production of small amounts of HCl indicates that chlorine situated in the polymer backbone is not the sole site for HCl formation and thus the ring chlorine atoms must in some way be involved in a minor HCl-producing reaction. There are two possible ways in which chlorine can be removed from the ring, either by an intermolecular reaction or an intramolecular

mechanism.   Intermolecular processes will be favoured by PpCS whereas PoCS, due to the close proximity of the ortho chlorine atoms to the aliphatic hydrogen atoms in the backbone of the polymer, will favour intramolecular interactions.   From the relative amounts of HCl produced in PpCS and PoCS as indicated by SATVA, the intramolecular reaction is preferred.   A possible reaction mechanism for the removal of HCl from PoCS involving elimination of HCl followed by hydrogen rearrangement is shown in Figure 4.22.
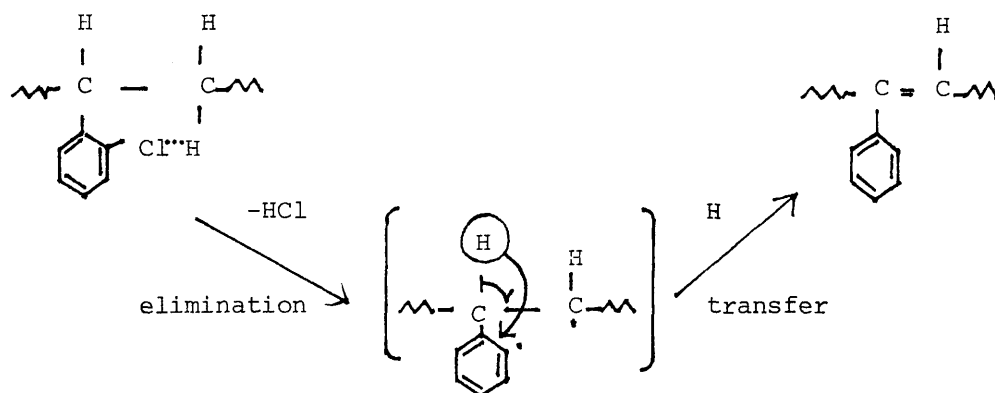
Figure 4.22   Mechanism for HCl evolution from PoCS.

4.5 SYNTHESIS OF CHAIN-CHLORINATED POLYSTYRENE

Preparation

The preparation of chain-chlorinated polystyrene (CCPS) was carried out in an evacuated system using the standard PS sample referred to in Section 4.2.2.   The procedure was similar to that of McNeill and Coşkun.[125]   Approximately 2g or 1g PS, depending on the required chlorine content of the final product, was dissolved in 100 ml warm carbon tetrachloride.   The solution was degassed in vacuo following six repeated freeze-thaw cycles and a measured quantity of chlorine transferred to the PS solution

cooled at $-196^{\circ}C$ from a bulb of known volume which had previously
been flushed with dry nitrogen followed by chlorine at atmospheric
pressure.   The chlorination apparatus is illustrated in
Figure 4.23.

Once all the chlorine had distilled into the PS solution,
the reaction vessel was sealed by closing all rotaflow taps (in the
order C_4, C_2, C_1 to prevent pressure build up in the chlorine bulb),
thawed to ambient temperature and the reaction allowed to proceed
for ten hours.   The chain-chlorinated polymer was then isolated
by precipitation from methanol, purified by a further two reprecipitations
and dried in vacuo at room temperature for two days prior to elemental
analysis.

The possibility of synthesising the trichlorinated product
was investigated firstly as described then using very similar
apparatus with a thicker-walled reaction vessel to accommodate the
pressure increase on HCl evolution during the reaction.   The
vessel was sealed by glass-blowing after chlorine transference
and left for eight days to allow the reaction to go to completion.

Polymer Characterisation

The chain-chlorinated PS samples were characterised by
elemental analysis, IR spectroscopy and molecular weight
determination as previously described.

Results and Discussion

The chlorination reaction conditions are detailed in Table
4.6.   The discrepancy between chlorine contents in the products
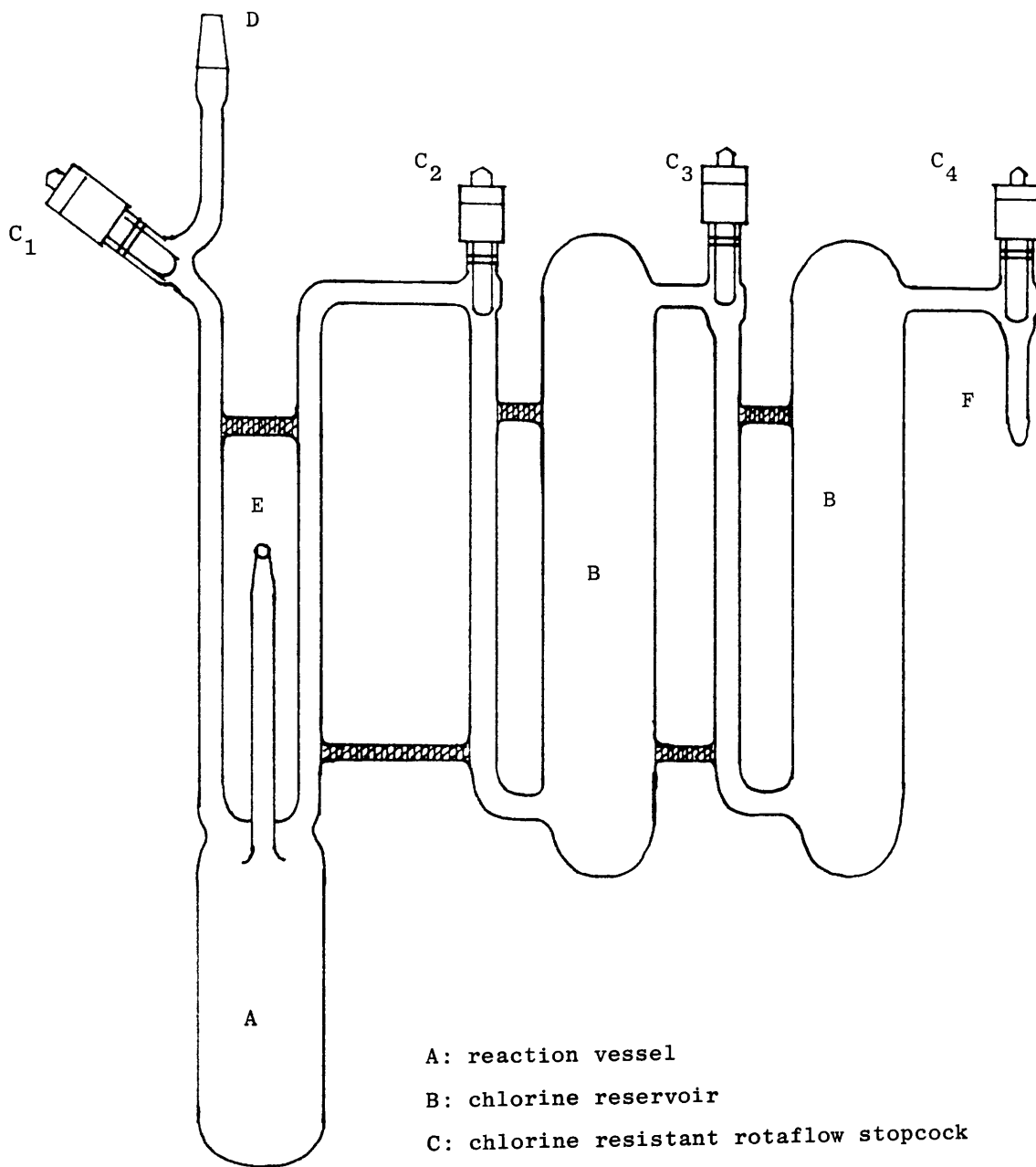
A: reaction vessel

B: chlorine reservoir

C: chlorine resistant rotaflow stopcock

D: B14 cone attachment for evacuation

E: B10 cone solution inlet

F: gas inlet

Figure 4.23 Vacuum Chlorination Apparatus

obtained when considering the molar ratio of reactants is attributed to incomplete transfer of the PS solution to the chlorination apparatus resulting in an excess of chlorine being available. This is most noticeable at high PS concentrations where the solutions are more viscous.

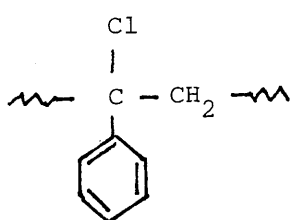The chlorine contents of mono-chain-chlorinated PS (CCPS), di-chain-chlorinated PS (2CCPS) and tri-chain-chlorinated PS (3CCPS) are given in Table 4.7. From the results it can be seen that the chlorine content of the mono- and di-chain-chlorinated polymers is in good agreement with the theoretical weight % chlorine content although the earlier attempts at synthesising tri-chain-chlorinated PS resulted in polymers in which the average number of chlorine atoms per repeat unit was approximately 2.7. In the final preparation of tri-chain-chlorinated PS, (3CCPS4), where a large excess of chlorine was added, the solution remained yellow after 12 hours and a white precipitate was observed. The polymer was found to be readily soluble in methylene chloride suggesting cross-linking had not taken place. The insolubility in the reaction mixture may be a consequence of chlorination altering the physical properties of the resultant polymer either in solubility towards carbon tetrachloride or from increased molecular weight.

The IR spectra for PS, CCPS, 2CCPS, and 3CCPS are illustrated in Figure 4.24 a-d, and the IR absorption frequencies with their corresponding assignments are shown in Table 4.8. The major difference between the spectra of chain-chlorinated PS and PS is that in the former, the methylene C-H stretch band at 2920 cm^{-1}, and especially the methine absorption band at 2850 cm^{-1} decrease in

relation to the aromatic C-H stretching absorption at 3020 cm^{-1}.
Furthermore, this decrease is found to be proportional to the amount
of chlorine substituted into the backbone of the polymer.   The
band at 1235 cm^{-1}, attributed to C-H bending in -CHCl-, which is
absent in poly(p-chlorostyrene) and poly(o-chlorostyrene) (see
Figure 4.9b,c) but present to a small extent in ring-chlorinated
polystyrene (due to some chain chlorination) (see Figure 4.9c) is
stronger in the chain-chlorinated polymers, being weakest in CCPS
which has the least number of Cl atoms per styrene unit and
strongest in 3CCPS which has the highest number of Cl atoms per
styrene unit.   These observations suggest that chlorination
occurs first at the tertiary H position and that at more than 1:1
molar ratio of Cl$_2$ to styrene units, substitution continues at the
methylene sites.   The C-Cl stretching band present at about
740 cm^{-1} is not clearly seen in the spectrum of the chain-chlorinated
polystyrenes, because it is masked by the very strong 700 and
750 cm^{-1} aromatic absorptions, and the strong band at 825 cm^{-1}
which appears in the spectrum of ring-chlorinated polystyrene due to
para-substitution is very weak in the chain-chlorinated polymers.
This indicates that ring substitution is not a significant side
reaction.   The aromatic substitution pattern in the range 2000 -
1700 cm^{-1} confirms this.   Thus, the chain-chlorinated polymers
correspond approximately to the following structures:
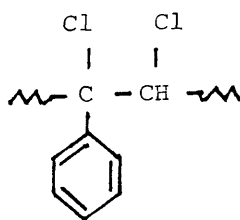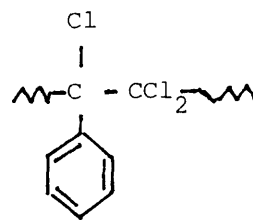
Polymer Sample	Solvent	Reaction Time (hrs)	Molar Rate of reactants Cl_2/Styrene	Wt % Cl in product	Molar ratio in product Cl/Sty.
CCPS1	CCl_4	12	1.35/1	30.19	1.25/1
CCPS2	CCl_4	12	1.35/1	34.76	1.54/1
CCPS3	CCl_4	12	1.33/1	32.57	1.39/1
CCPS4	CCl_4	12	1.33/1	34.19	1.50/1
2CCPS1	CCl_4	12	2.61/1	47.77	2.60/1
2CCPS2	CCl_4	12	2.15/1	42.62	2.14/1
2CCPS3	CCl_4	12	2.14/1	41.56	2.04/1
3CCPS1	CCl_4	12	2.57/1	49.07	2.70/1
3CCPS2	CCl_4	12	2.83/1	47.79	2.57/1
3CCPS3	CCl_4	192	2.74/1	47.84	2.63/1
3CCPS4	CCl_4	12	4.03/1	51.00	2.97/1

Table 4.6   Chain chlorination of PS in Absence of Air.

Polymer Sample	Wt % Cl observed (Theoretical)	Wt % C observed (Theoretical)	Wt % H observed (Theoretical)
CCPS1	30.19(25.58)	63.10	4.89
CCPS2	34.76 (25.58)	58.98	4.36
CCPS3	32.57(25.58)	61.90	4.70
CCPS4	34.19(25.58)	59.06	4.42
2CCPS1	47.77(40.97)	50.15	3.61
2CCPS2	42.62(40.97)	53.04	3.91
2CCPS3	41.56(40.97)	53.21	3.71
3CCPS1	49.07(51.26)	47.00	3.37
3CCPS2	47.29(51.26)	51.33	3.20
3CCPS3	47.84(51.26)	46.77	3.20
3CCPS4	51.00(51.26)	45.18	3.36

Table 4.7   Elemental Analysis of Mono-chain-chlorinated PS (CCPS) di-chain-chlorinated PS(2CCPS) and tri-chain-chlorinated PS (3CCPS)

Figure 4.24   IR spectrum for a)PS   b)CCPS   c) 2CCPS and d) 3CCPS run as KBr discs
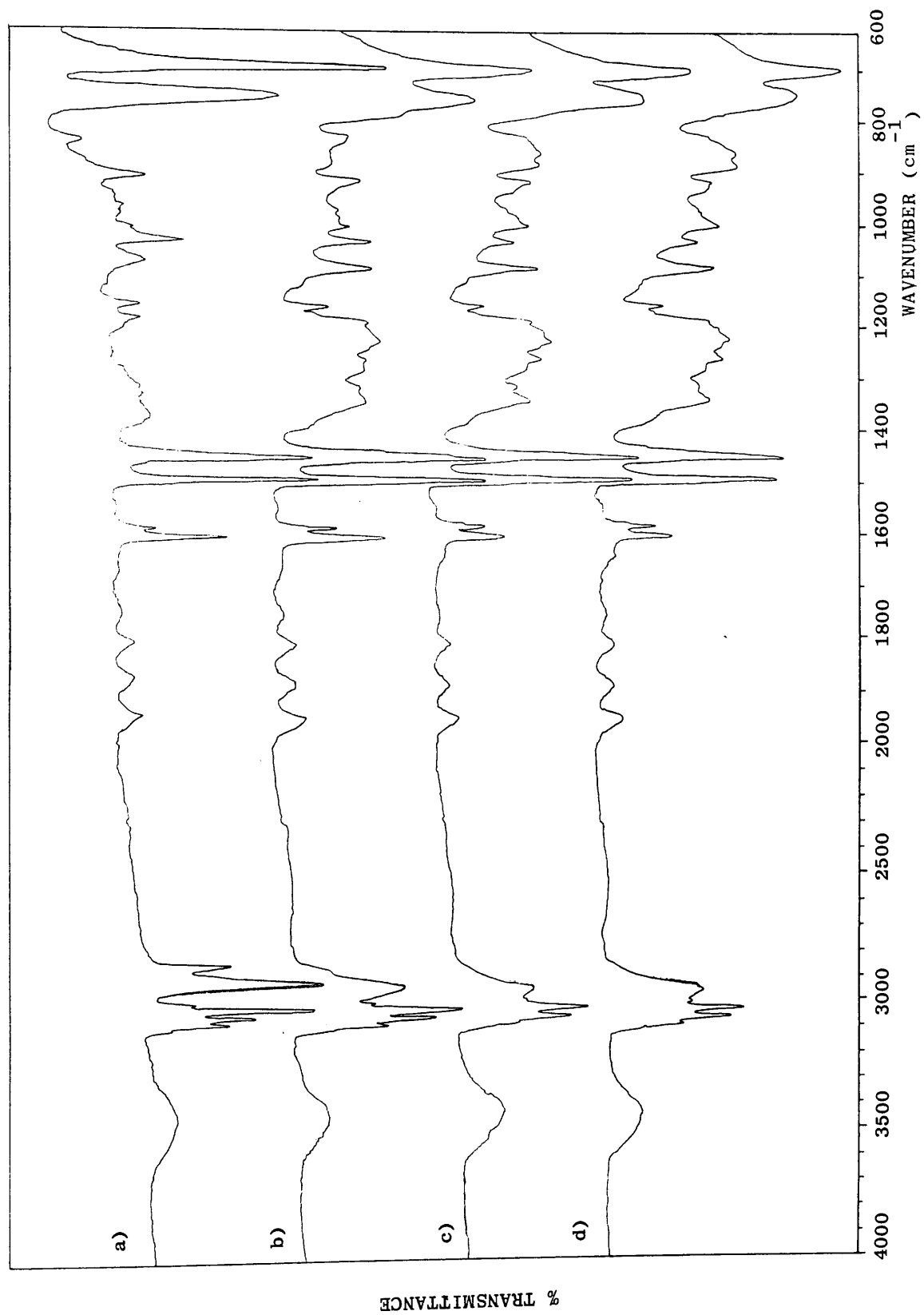
Polystyrene		Chain-Chlorinated Polystyrene	
Absorption (cm^{-1})	Assignment	Absorption (cm^{-1})	Assignment
3083(m), 3060(s)	aromatic C-H	3082(m), 3058(s)	aromatic C-H
3028(s), 3000(m)	stretching	3026(s), 3000(m)	stretching
2930(s) 2850(m)	aliphatic C-H stretching (CH_2CH)	2930(m), 2860(sh)	aliphatic C-H stretching (CH_2CH)
1940(w), 1870(w)	overtone and combination	1945(w), 1880(w)	overtone and combination
1801(w), 1744(w) 1667(w)	bands characteristic of mono substituted phenyl ring	1804(w), 1748(w) 1655(w)	bands characteristic of mono substituted phenyl ring
1602(m). 1584(w) 1494(s) 1454(s)	in plane bending,stretching vibrations of phenyl ring	1601(m), 1582(w) 1493(s), 1453(s)	in plane bending stretching vibrations of phenyl ring
760(s), 700(s)	out of plane C-H and phenyl ring vibrations characteristic of mono substituted phenyl rings	755(s) 698(s)	out of plane C-H and phenyl ring vibrations characteristic of mono substituted phenyl ring masking C-Cl stretching

Table 4.8   IR absorption frequencies (cm^{-1}) and corresponding assignments for polystyrene and chain-chlorinated polystyrene.

CALIBRATION : THF.7.88
RUN NO./NAME: A195 SAMPLE 4   (7456)   1234 970788

PEAK START: 1200   MN: 7.03E+04
PEAK FINISH: 1760

                                 MW: 1.65E+05
BASELINE START: 1200
BASELINE FINISH: 2400   MZ: 3.03E+05

FLOW CORRECTION: 1.001   MP: 1.40E+05

KP: 1.200×10^{-4} D: 2.354
AP: .710

Figure 4.27   GPC trace for 3CCPS

$10^{\wedge} 1$

$10^{\wedge} 3$

MOLECULAR WEIGHT
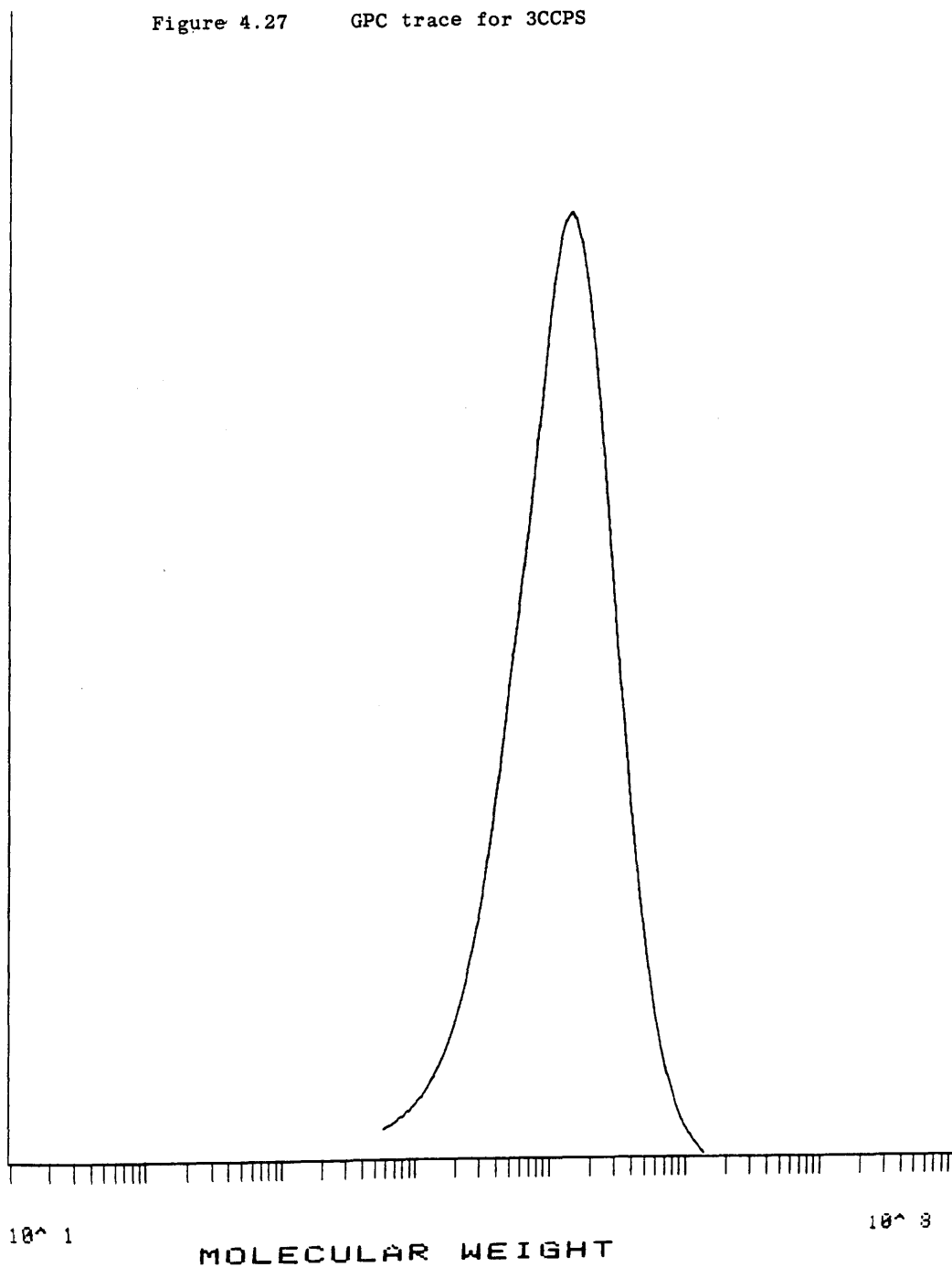
CALIBRATION : THF.7.88
RUN NO./NAME: A196   SAMPLE 3   (7455)   1313 070788

PEAK START: 1140   MN: 1.09E+05
PEAK FINISH: 1770

                                     MW: 3.06E+05
BASELINE START: 1140
BASELINE FINISH: 2400   MZ: 6.36E+05

FLOW CORRECTION: 1.000   MP: 2.08E+05

KP: 1.200X10^{-4}
AP: .710   D: 2.801

Figure 4.26   GPC trace for 2CCPS

10^1 10^8

MOLECULAR WEIGHT
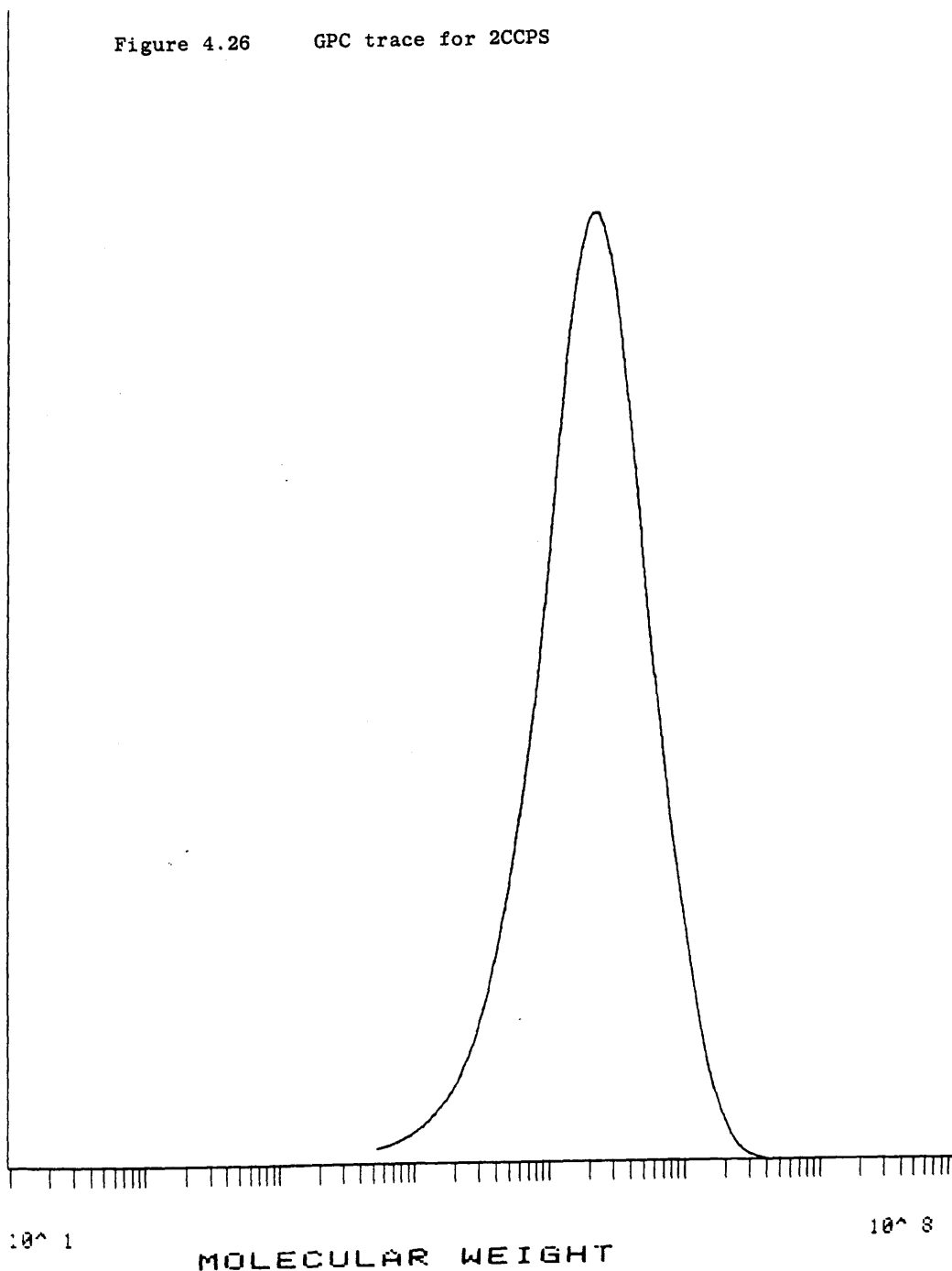
CALIBRATION : THF.7.38
RUN NO./NAME: A193 SAMPLE 2 (7454)   1112 070788

PEAK START: 1170   MN: 1.02E+05
PEAK FINISH: 1750

                               MW: 2.46E+05

BASELINE START: . 1170
BASELINE FINISH: 2400   MZ: 4.66E+05

FLOW CORRECTION: 1.000   MP: 1.89E+05

KP: 1.200X10^{-4} D: 2.405
AP: .710

Figure 4.25   GPC trace for CCPS

10^ 2   MOLECULAR WEIGHT   10^ 8
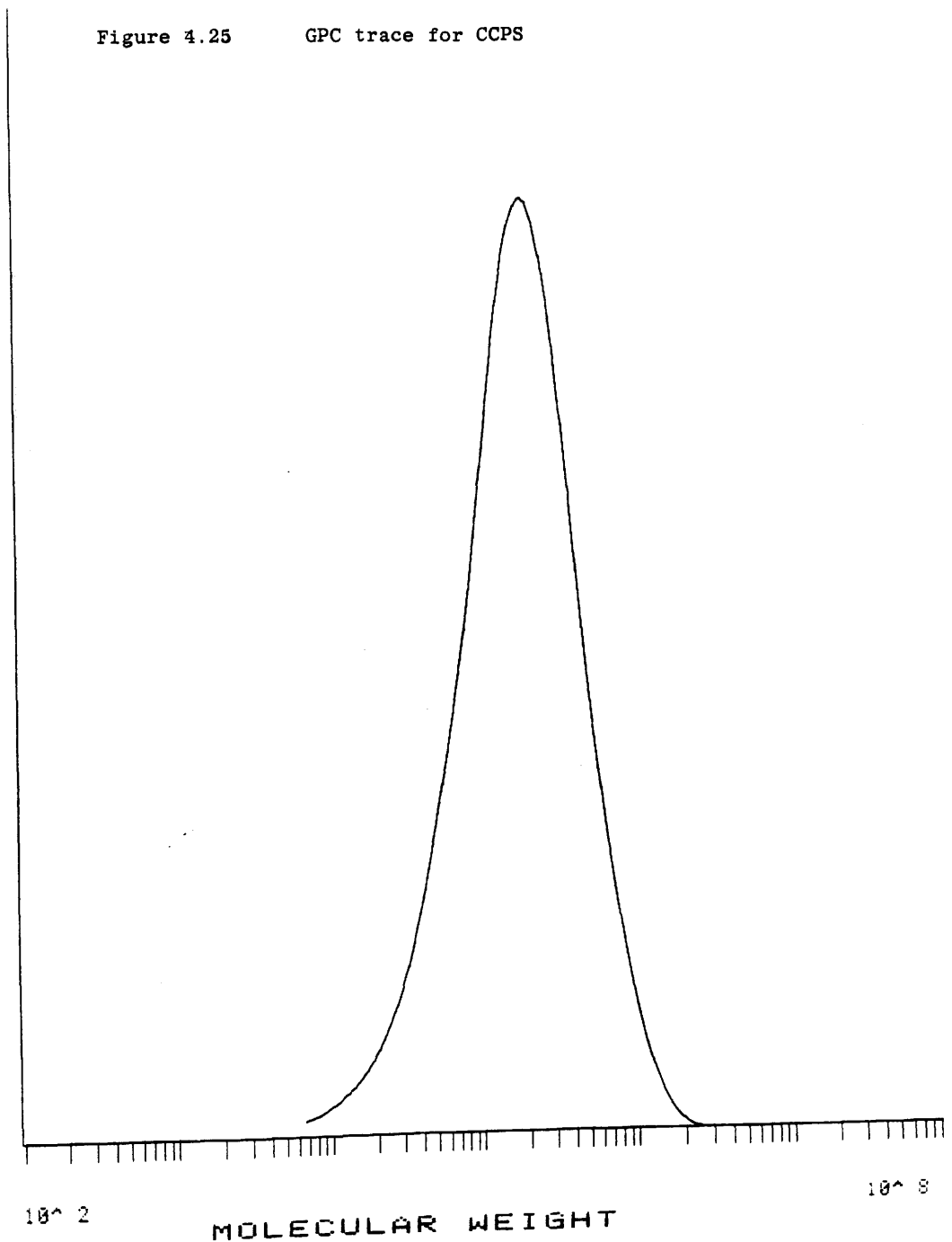
Sample	$\bar{M}n(10^5)$	$\bar{M}w(10^5)$	$\bar{M}z(10^5)$	$\bar{M}p(10^5)$	D
PS	1.41	3.44	6.68	2.48	2.44
PS	1.38	3.41	6.62	2.53	2.47
CCPS	0.96	2.37	4.52	1.89	2.45
CCPS	1.02	2.46	4.66	1.89	2.40
2CCPS	1.09	3.06	6.36	2.08	2.80
2CCPS	1.07	3.08	6.44	2.08	2.87
3CCPS	0.70	1.65	3.03	1.40	2.35
3CCPS	0.75	1.65	2.97	1.37	2.20

Table 4.9   Molecular Weight Averages expressed as "polystyrene equivalents" and Molecular Weight Distributions (D) for PS, mono-chain-chlorinated PS, di-chain-chlorinated PS and tri-chain chlorinated PS.

The possible presence of some unchlorinated styrene units however is not excluded.

The GPC traces of CCPS, 2CCPS and 3CCPS are reproduced in Figure 4.25 - Figure 4.27. The number average molecular weights $\bar{M}n$ are somewhat lower than that for PS, falling in the range 0.70 - 1.07 x 10^5. The weight average molecular weights, $\bar{M}w$, are also reduced relative to PS ranging from 1.65 x 10^5 to 3.08 x 10^5. In general the molecular weight becomes lower as the degree of chlorination increases. This is shown in Table 4.9.

4.6   THERMAL DEGRADATION OF CHAIN-CHLORINATED POLYSTYRENE

4.6.1   Experimental

Thermal Analysis of Chain-Chlorinated Polystyrene.

The thermal degradation behaviour of the synthesised chain-chlorinated PS samples was investigated using TG, DSC and TVA techniques under the conditions previously described. After purification, the chlorinated polymers could be finely ground and these studies were carried out on powdered samples.

TG

The TG curves for mono-, di- and tri-chain-chlorinated PS are shown in Figures 4.28 - 4.30. These curves, together with that for pure PS for direct comparison, are reproduced in Figure 4.31. The approximate onset temperatures of degradation (T_{onset}) and temperatures at the maximum rate of evolution of degradation products (T_{max}) are presented in Table 4.10.

On comparing the TG traces of CCPS with that for pure PS, it

Figure 4.28   TG(-) and DTG(---) curves for CCPS obtained under nitrogen at a heating rate of 10° min^{-1}
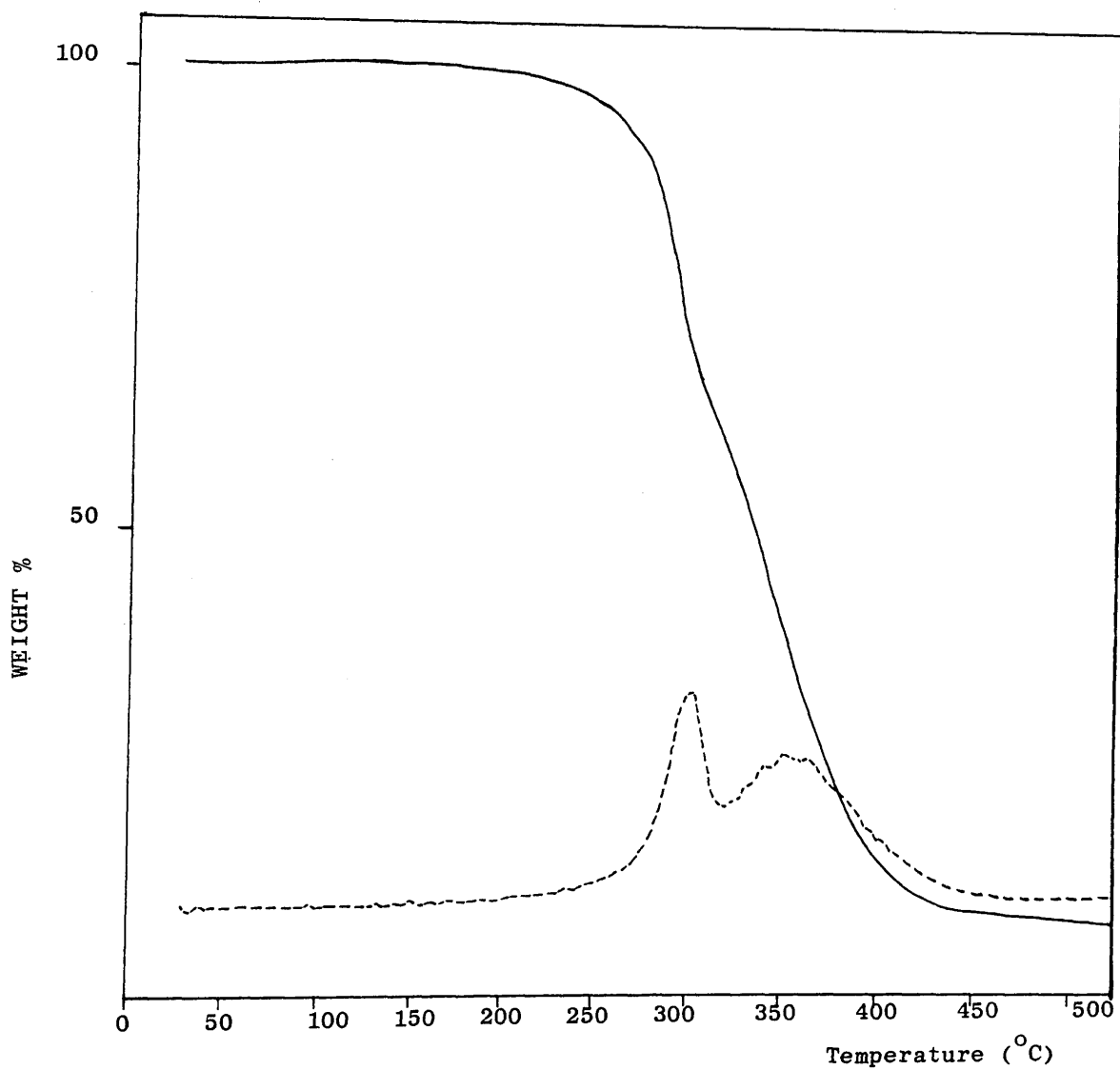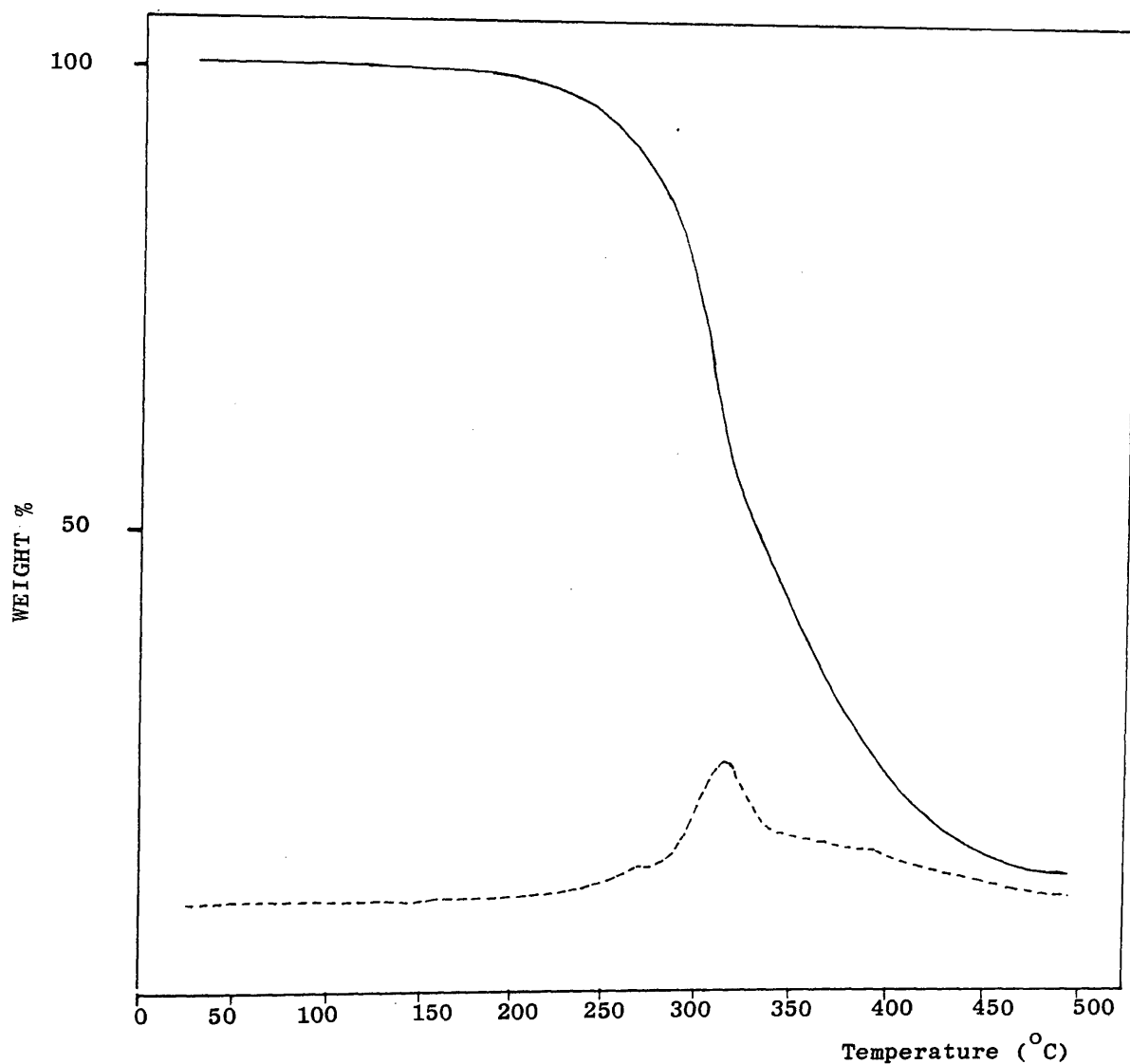
Figure 4.29 TG(-) and DTG(---) curves for 2CCPS obtained under
nitrogen at a heating rate of 10° min^{-1}
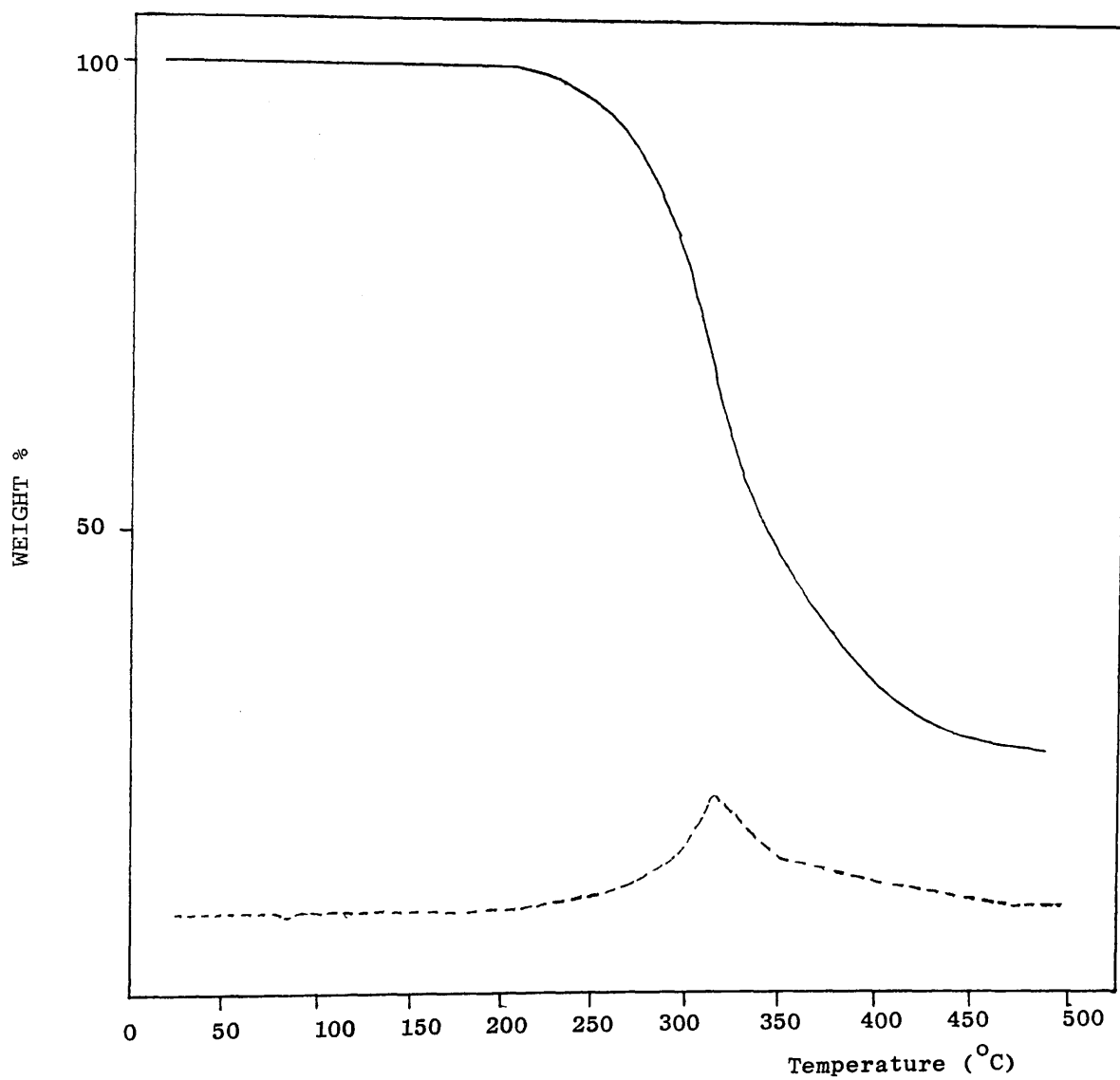
Figure 4.30   TG(-) and DTG(---) curves for 3CCPS obtained under nitrogen at a heating rate of 10° min^{-1}
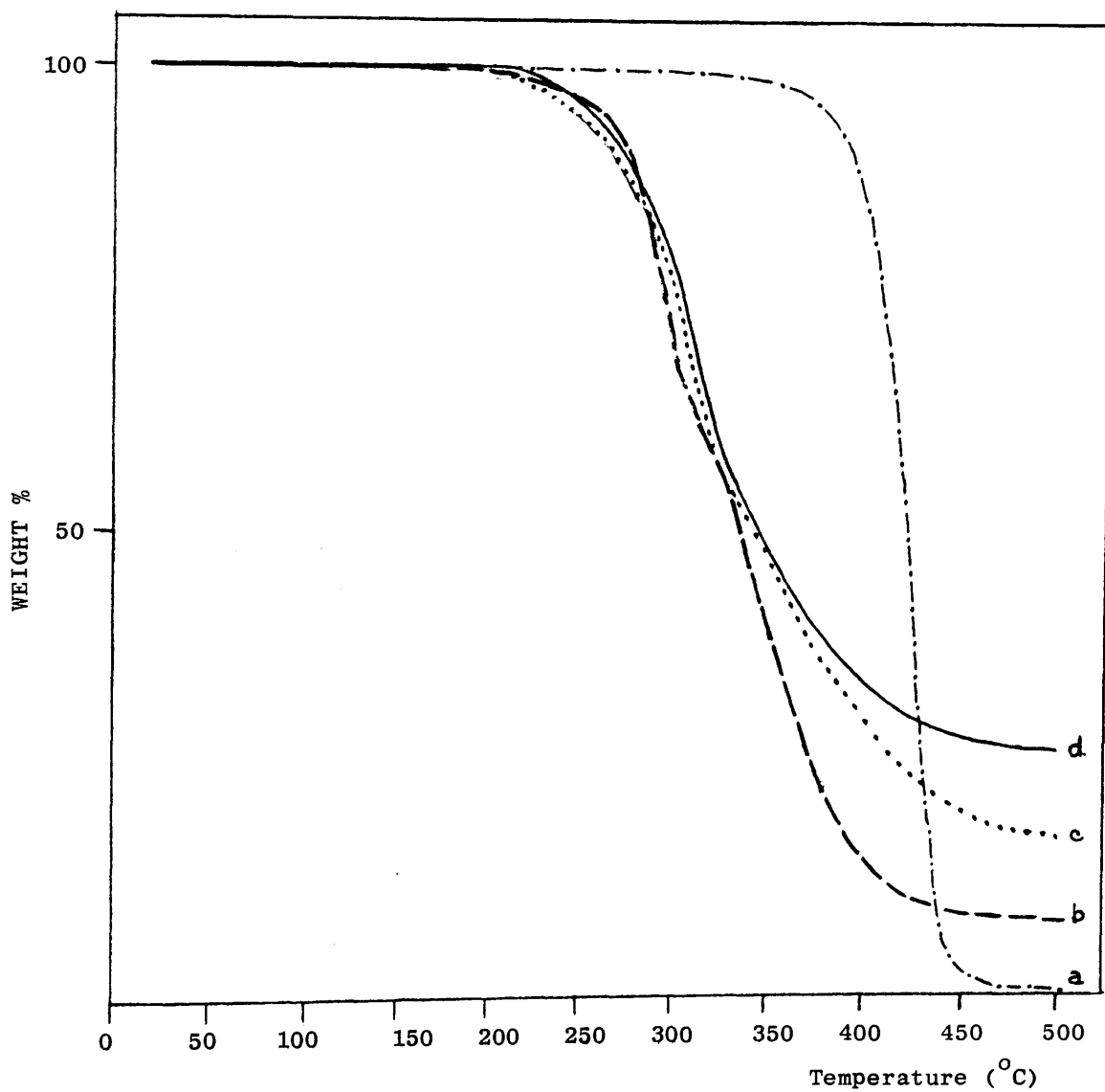
Figure 4.31 TG curves for a)PS b)CCPS c)2CCPS and d) 3CCPS obtained under nitrogen at a heating rate of 10° min^{-1}

Polymer Sample	T onset (°C)	T max(°C) Stage 1	% wt loss Stage 1	T onset Stage 2	T max(°C) Stage 2	% wt loss Stage 2	Wt % residue
CCPS1	207	291	28.5	297	355	61.5	10
CCPS2	205	300	30.5	306	350	61.6	7.9
CCPS3	203	318		indistinguishable	345	93.6*	6.4
CCPS4	202	323	30.0	302	346	62.0	8.0
2CCPS1	183	318		indistinguishable		82.0*	18.0
2CCPS2	192	316	41.0	322		41.75	17.25
2CCPS3	183	330		indistinguishable		84.4*	15.6
3CCPS1	182	336		indistinguishable		68.0	32.0
3CCPS2	192	311		indistinguishable		74.0*	26.0
3CCPS4	185	320		indistinguishable		80.5*	19.5
PS	242(350)	402(423)		single degradation		99.2	0.8

* Total weight loss.

Table 4.10   TG Onset and Maximum Degradation Temperature for mono-, di-, and tri-chain chlorinated PS on heating to 500°C under nitrogen.

Polymer Sample	T onset ($^{\circ}$C)	T max ($^{\circ}$C)	Wt. % Residue
CPS1	207	308	5.75
2CPS2	205	320	10.00
2CPS3	200	313	12.25

Table 4.11   TG Onset and maximum degradation temperature for mono-, and di-chain chlorinated PS on heating to 500°C in vacuo.

can be seen from the lowering of the threshold for weight loss that chlorination along the backbone destabilised PS to heating. The onset temperature of degradation is around 200°C for the monochlorinated samples but slightly lower at approximately 183°C in the more highly chlorinated polymers.

A close examination of the TG curves suggests that weight loss occurs in two stages for monochlorinated polymers. This is seen more clearly in the DTG traces from which the temperature at the maximum rate of degradation in each stage (308°C and 349°C average) has been recorded (see Table 4.10). The di- and tri-chlorinated compounds show no distinguishable second stage, weight loss occuring over quite a wide temperature range with T_{max} at approximately 322°C. There is an increase in the weight % residue left after heating to 500°C which amounts to just over twice that obtained for the monochlorinated sample, i.e.8%(average) compared to 19%(average)residue by weight. When TG was carried out <u>in vacuo</u>, in each case the behaviour was very similar to that obtained under nitrogen. The results are shown in Table 4.11.

<u>DSC</u>

The DSC trace (see Figure 4.32) for the monochlorinated polymer shows an endothermic peak at 292°C followed by a second endothermic peak at 350°C. In the dichlorinated polymer an exothermic peak at approximately 310°C (average) is observed between the two endothermic peaks. In neither type of sample could a melting point (indicated by a large sharp endotherm) be detected. This was confirmed when a melting point determination
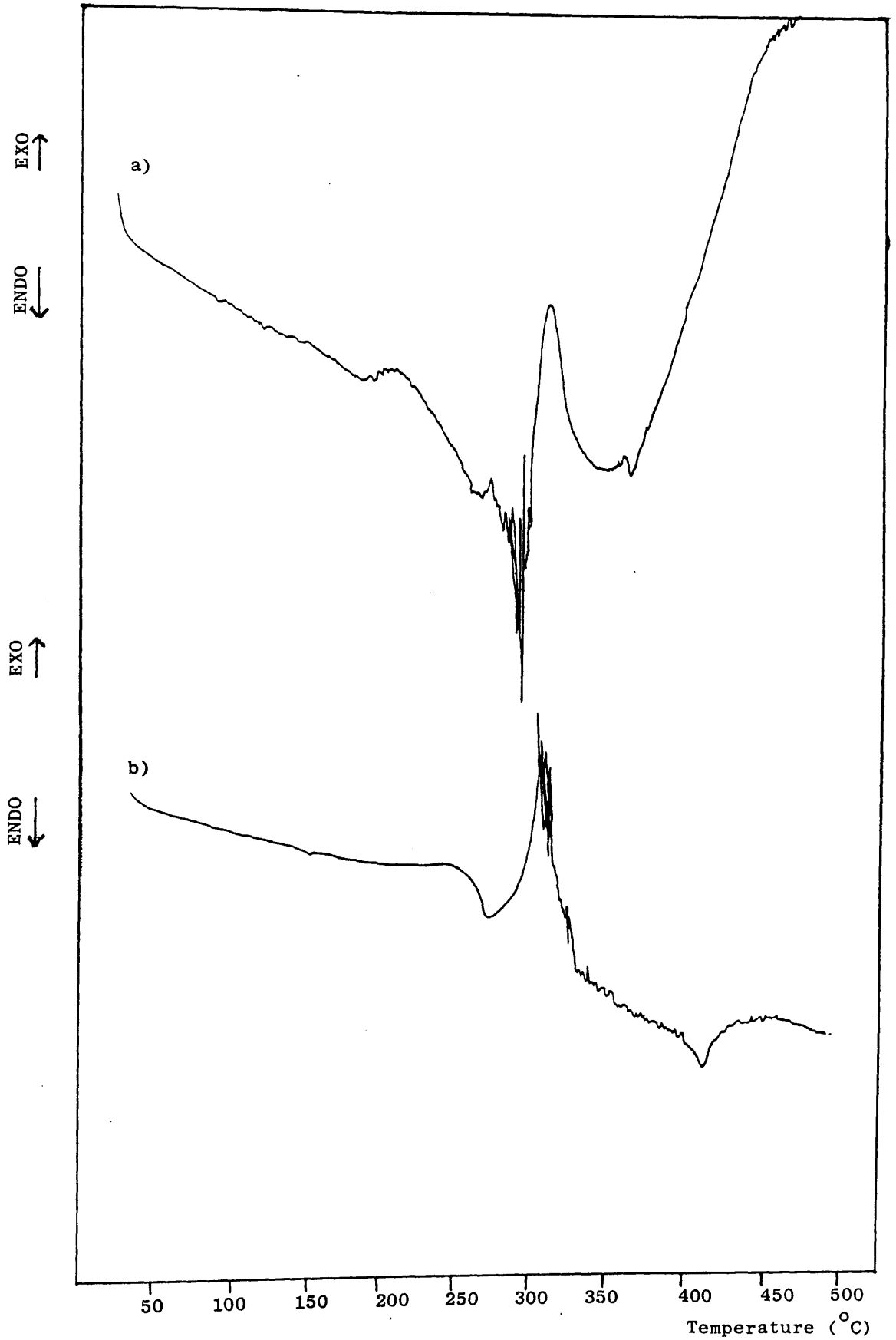
Figure 4.32   DSC curves for a) CCPS and b) 2CCPS obtained under nitroge

at a heating rate of 10° min^{-1}

was carried out on CCPS1 whereupon the sample began to decompose at 248°C. This corresponds approximately to the onset of the first endothermic peak (see Table 4.12).

TVA

The decrease in thermal stability upon chain-chlorination of PS is illustrated even more clearly from TVA traces. The TVA curves of CCPS are illustrated in Figure 4.33 - Figure 4.35. These are reproduced together with the TVA curve for PS in Figure 4.36, to demonstrate the destabilisation affect of chlorination in the backbone of PS. The T_{onset} and T_{max} temperatures obtained from TVA are presented in Table 4.13. Degradation temperatures for PS are included for comparison.

The single TVA peak for the production of volatile products from PS begins at about 261°C reaching a maximum at 400°C. However the introduction of 1-2 Cl atoms per styrene unit leads to the earlier production of volatile compounds at around 150°C with two shoulders (215°C and 274°C) preceeding the main peak at 303°C. (See Figure 4.33). During the initial stages of degradation, there is little difference in the volatility of products as the 0°C, -45°C, -75°C and -100°C limb traces are coincident. However, as the degradation proceeds, the 0°C and -45°C traces diverge rising slightly above the coincident -75°C and -100°C traces. This indicates the production of compounds of different volatilities and in fact this is borne out by SATVA experiments (see below) which show the major volatile products of thermal degradation to be HCl and styrene. Under TVA conditions, HCl is non-condensable at -100°C while styrene is completely condensed. Thus the area
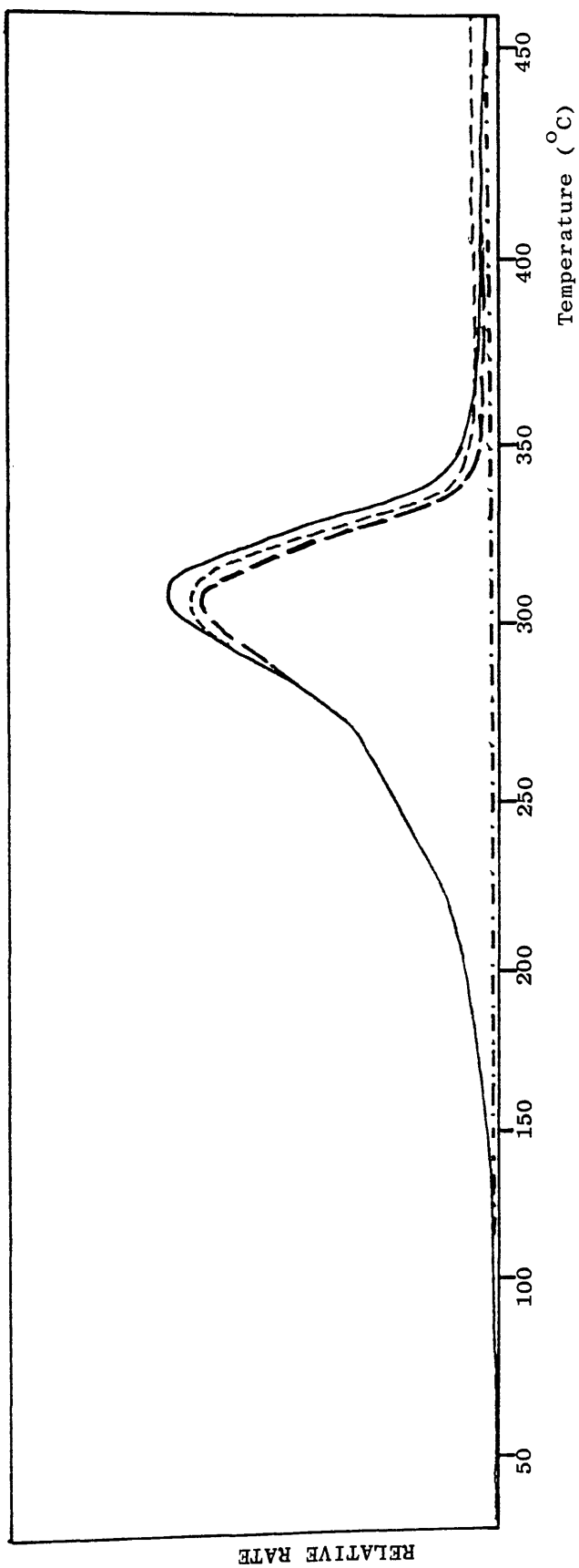
Figure 4.33   TVA curve for CCPS using 50mg powder sample.
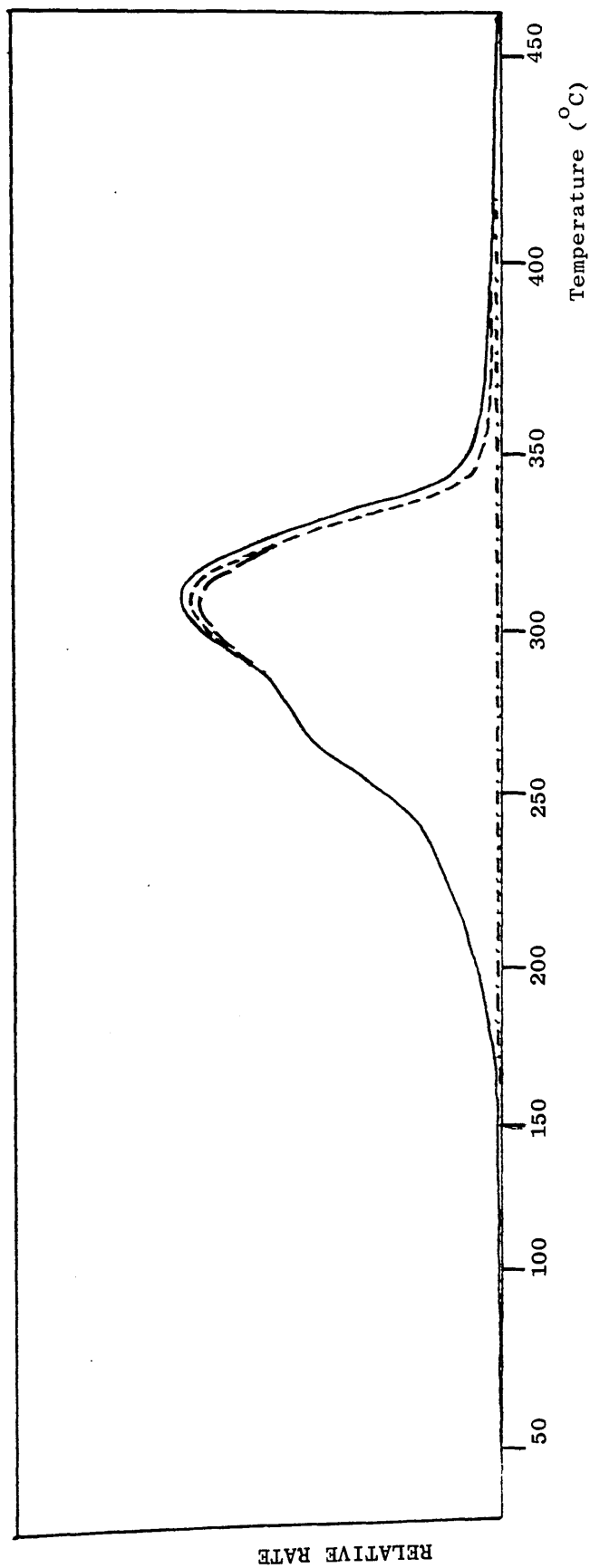
Figure 4.34   TVA curve for 2CCPS using 50mg powder sample.
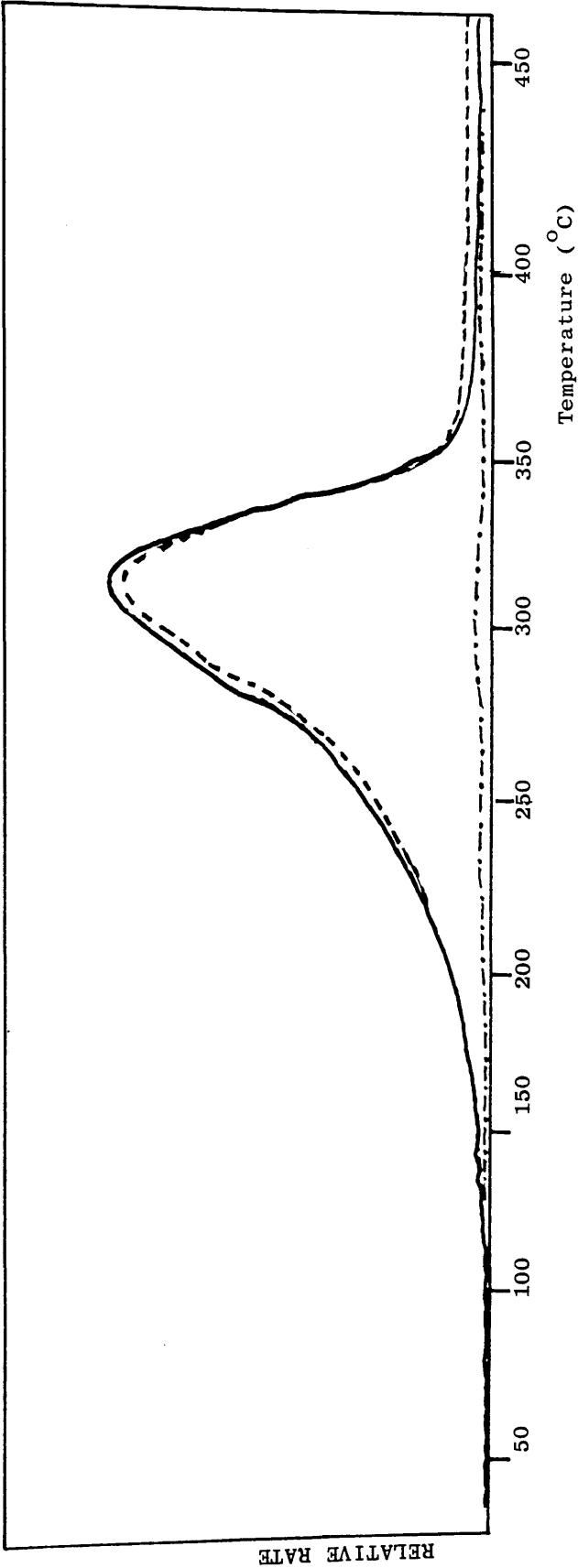
Figure 4.35   TVA curve for 3CCPS using 50mg powder sample
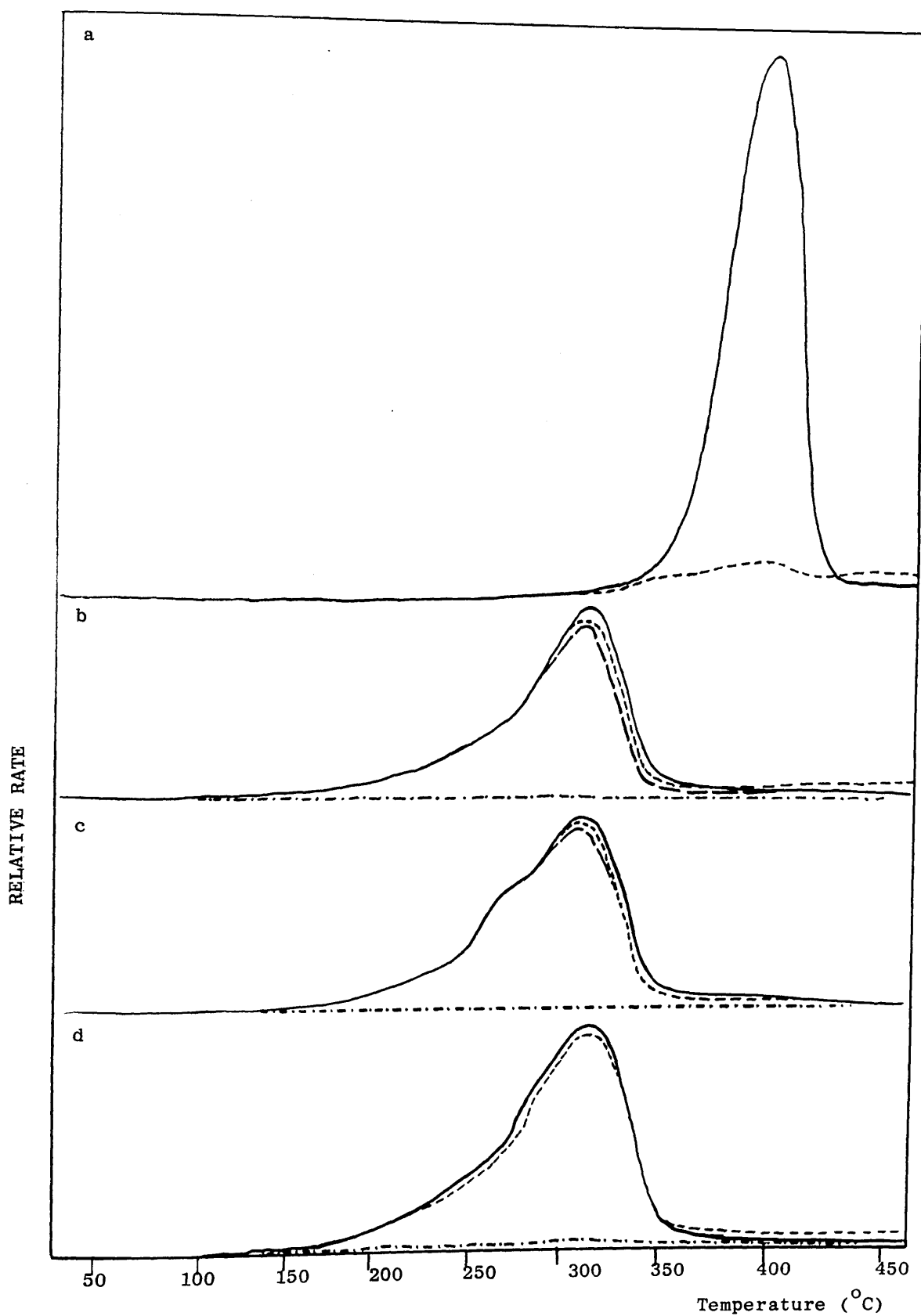
Figure 4.36   TVA curve for a) PS   b) CCPS c) 2CCPS and d) 3CCPS using
50mg powder sample.

Polymer Sample	T onset (^{o}C)	T min(^{o}C) Endotherm 1	T max(^{o}C) Exotherm	T min (^{o}C) Endotherm 2
CPS1	213	292	-	350
2CPS2	237	297	313	391
2CPS3	237	297	305	412

Table 4.12   Differential scanning calorimetry of mono-, di- and tri-chain chlorinated polystyrene.

Polymer Sample	T onset (^{o}C)	T shoulder 1 (^{o}C)	T shoulder 2 (^{o}C)	T max (^{o}C)
CPS1	149	212	269	304
CPS2	173	214	277	306
CPS3	149	215	274	303
CPS4	145	218	276	309
2CPS2	154	279$^{\Delta}$	293*	318
2CPS3	154	276$^{\Delta}$	300*	318
3CPS	158	286$^{\Delta}$	-	300
3CPS4	160	285$^{\Delta}$	-	315
PS	261	-	-	400

Δ onset shoulder

* end shoulder

Table 4.13   TVA Degradation Temperatures for mono-, di- and tri-chain chlorinated polystyrene.

below the -100°C trace indicates the contribution of HCl evolution to the overall production of volatile material.   Taking this into consideration, on regarding the behaviour of the -100°C trace, the initial product evolved on the degradation of CCPS is HCl. When the chlorine content is increased to approximately 2 Cl atoms per monomer unit, the -75°C and -100°C traces are raised to be almost coincident with the 0°C trace (see Figure 4.34).   This indicates an increase in HCl production and that HCl is virtually the sole product on degradation.   The increase in HCl evolution is also seen, to a greater extent, in the TVA trace of the approximately tri-chlorinated polymer as in this case the -100°C is elevated to become coincident with the -75°C trace which in turn is almost coinicdent with the 0°C trace (see Figure 4.35).   As with PS there are no non-condensable products produced from the degradation of the chlorinated polymers.   The onset temperatures and peak maximum temperatures obtained by TVA for the highly chlorinated polymers, do not vary noticeably from those obtained in the monochlorinated polymer and all three compare favourably with TG results.

SATVA Separation and Identification of Degradation Products.

        The condensable products of degradation on heating CCPS to 500°C were separated using SATVA and identified using IR spectroscopy and mass spectrometry.   The SATVA separation illustrated in Figure 4.37, for each of the chain-chlorinated polymers gave four fractions.   The fraction boundaries are diagramatically depicted in Figure 4.38.

Figure 4.37   SATVA trace for Condensable Degradation Products
from heating a) CCPS and b) 2CCPS to 500°C.
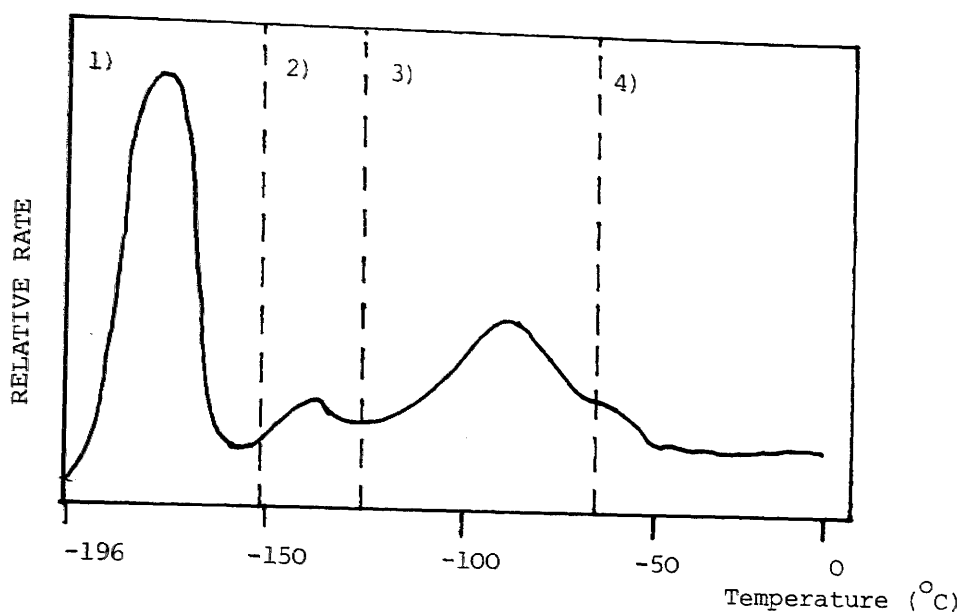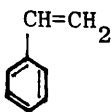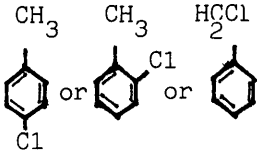
Figure 4.38   SATVA trace for CCPS illustrating fraction boundaries.

The first fraction, the major peak in the SATVA trace, was found from IR and MS data to be due solely to HCl.   In fraction two, the major component was benzene as identified from absorption bands at 3050 cm^{-1}, 3040 cm^{-1} and 640 cm^{-1} in the IR spectrum with toluene also present, observed by MS.   The third fraction was found to consist mainly of styrene with traces of chlorobenzene, dichlorobenzene and chlorotoluene revealed by MS.   The molecular ion peaks from the mass spectra used in the identification of these compounds together with their % base values for the standard compounds are summarised in Table 4.14a-c.   As the fractions tend to consist of mixtures of components they may distort the % base values observed, thus making product identification and the estimation of the relative proportion of each product difficult. A rough estimation of the relative importance of each component was carried out by comparing observed % base values to those of the eight strongest peaks in the spectra of authentic standard compounds.

m/e	% Base Observed	% Base Reference	Structure	Importance
104	100	(100)		
105	9.2	(8)		
102	7.3	(8)		
27	25.4	(7)	$CH=CH_2$ benzene ring	
63	31.4	(7)		major
74	16.5	(5)		
76	10.0	(4)		
103	42.6	(4)		
78	88.5	(100)		
52	24.5	(19)		
51	69.0	(18)		
50	53.4	(16)	benzene radical	secondary
77	35.7	(14)		
39	46.2	(13)		
79	6.1	(6)		
76	10.0	(6)		
91	34.1	(100)		
92	19.9	(75)		
39	46.2	(20)	CH_3 benzene ring	
65	11.0	(14)		minor
51	69.0	(10)		
63	31.4	(10)		
90	1.2	(8)		
50	53.4	(6)		
112	21	(100)		
77	35.7	(45)		
114	0.7	(33)	Cl benzene ring	
51	69.0	(12)		trace
50	53.4	(60)		
113	0.1	(7)		
36	3.1	(6)		
75	10.1	(5)		

m/e	% Base Observed	Reference [†]	Reference [‡]	Reference [‡‡]	Structure	Importance
91	34.1	(100)	,(100)	(100)		
126	0.2	(42)	(25)	(13)		
125	–	(17)	–	–	CH_3 ...Cl or CH_3 ...Cl or H_2CCl	
128	–	(13)	(9)	(7)		
63	31.4	(9)	(6)	(10)		
89	4.8	(8)	(5)	–		
92	19.9	(8)	(8)	(9)		
65	11.0	(7)	(9)	(12)		trace

m/e	% Base Observed	% Base Reference	Structure	Importance
146	0.2	(100)		
148	0.1	(65)		
111	–	(32)	Cl ... Cl	
75	10.1	(19)		
74	16.5	(12)		
150	–	(10)		
113	0.1	(10)		
73	3.9	(8)		

Reference values [101,102] for 4-chlorotoluene [†] 2-chlorotoluene [‡] and α chlorotoluene [‡‡]

Table 4.14a   Mass Spectrum $^m/e$ values of assignments for Fractions 2 and 3 from SATVA of CCPS (heated to 500^oC).
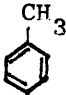
		% Base		
$^m/e$	Observed	Reference	Structure	Importance
78	100	(100)		
52	26.4	(19)		
51	42.5	(18)		
50	43.1	(16)	benzene ring	major
77	24.2	(14)		
39	41.1	(13)		
79	6.4	(6)		
76	5.8	(6)		
91	37.5	(100)		
92	25.0	(75)		
89	41.1	(20)	CH_3-benzene	secondary
65	8.3	(14)		
51	42.5	(10)		
63	19.2	(10)		
90	0.6	(8)		
50	43.1	(6)		
112	3.3	(100)		
77	24.2	(45)		
114	0.6	(33)		
51	42.5	(12)	Cl-benzene	trace
50	43.1	(10)		
113	–	(7)		
36	5.6	(6)		
75	3.6	(5)		

Table 4.14b   Mass spectrum $^m/e$ values and assignments for Fraction 2 from SATVA of 2CCPS (heated to 500^oC)
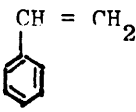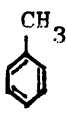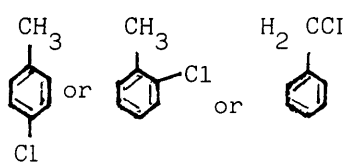
% Base

m/e	Observed	Reference			Structure	Importance
104	100	(100)				
105	9.0	(18)				
102	7.4	(8)			$CH = CH_2$ benzene ring	major
27	28.0	(7)				
63	24.6	(7)				
74	17.1	(5)				
76	9.6	(4)				
103	41.9	(4)				
78	59.4	(100)				
52	16.4	(19)				
51	57.3	(18)				
50	44.5	(16)			benzene ring	secondary
77	35.0	(14)				
39	38.2	(13)				
79	4.1	(6)				
76	9.6	(6)				
91	21.1	(100)				
92	11.2	(75)				
39	38.2	(20)				
65	8.0	(14)			CH_3 benzene ring	
51	57.3	(10)				
63	24.6	(10)				
90	0.9	(8)				
50	44.5	(6)				
						minor
112	11.2	(100)				
77	35.0	(45)				
114	3.4	(33)				
51	57.3	(12)			Cl benzene ring	
50	44.5	(10)				
113	1.2	(7)				
36	2.9	(6)				
75	11.3	(5)				
146	2.2	(100)				
148	1.2	(65)				
111	1.2	(32)			Cl benzene ring Cl	
75	11.3	(19)				
74	17.1	(12)				
150	-	(10)				
113	1.2	(10)				
73	4.3	(8)				trace
91	21.1	(100)†	(100)‡	(100)‡‡		
126	0.3	(42)	(28)	(13)	CH_3 benzene Cl or CH_3 benzene Cl or H_2CCl benzene	
125	-	(17)	-	-		
128	-	(13)	(9)	(7)		
63	24.6	(9)	(6)	(10)		
89	4.4	(8)	(5)	-		
92	11.2	(8)	(8)	(7)		
65	8.0	(7)	(9)	(12)		

Reference values 101,102 for 4-chlorotoluene†, 2-chlorotoluene‡ and α-chlorotoluene‡‡.

Table 4.14c Mass spectrum ^{m}/e values and assignments for Fraction 3 from SATVA of 2CCPS
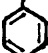
$^m/e$	% Base	Structure
209	7.5	
194	2.5	
105	47.5	$CH = CH - CH - CH_3$
103	27.5	
206	12.5	$CH = CH - C = CH_2$
103	27.5	
91	67.5	
92	17.5	CH_3 (overlap)
65	40.0	
78	12.5	
77	92.5	
52	15.0	(overlap)
51	87.5	
50	97.5	

Table 4.14d   Mass Spectrum $^m/e$ values and assignments for Fraction 4 from SATVA of CCPS.

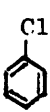| m/e	% Base	Structure
244	1.2	
209	11.2	
141	7.5	
139	6.2	
133	7.5	
127	6.2	
125	6.2	
119	6.2	
113	12.5	
111	31.2	
105	33.7	
104	10.7	
97	28.7	
37	28.7	
35	32.5	
28	30.0	
244	1.2	
209	11.2	
155	2.5	
153	5.0	
141	7.5	
139	6.2	
133	7.5	
118	2.5	
113	12.5	
111	31.2	
105	33.7	
104	10.0	
103	13.7	
91	45.0	
77	88.7	
37	28.7	
35	32.5	

Structures (top group):

Cl
|
HC – CH₂ – CH – CH₃ (phenyl groups attached)

and

CH₂ – CH₂ – CH – CH₃ (para-Cl phenyl and phenyl groups)

Structures (bottom group):

Cl
|
CH₂ – CH₂ – C – CH₃ (phenyl groups)

and

CH₂ – CH₂ – CH – CH₃ (phenyl and para-Cl phenyl)

and

Cl
|
CH₂ – CH – CH – CH₃ (phenyl groups)
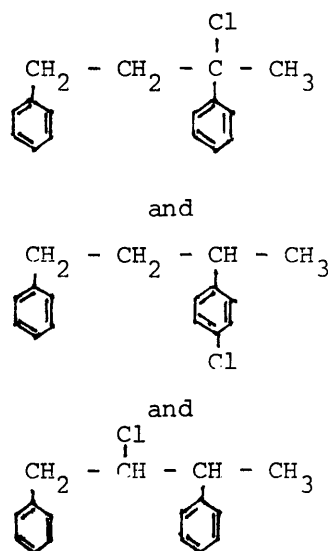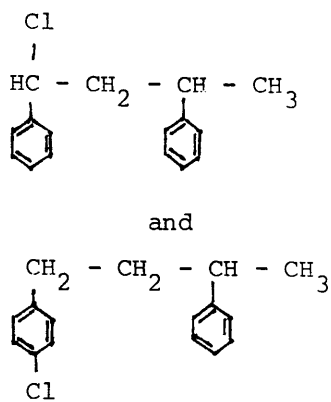
Table 4.14e continued over

$^m/e$	% Base	Structure
244	1.2	
196	2.5	
195	2.5	
155	2.5	
153	5.0	
141	7.5	
139	6.2	
105	33.7	
91	45.0	
77	88.7	
51	96.2	
50	100.0	
49	31.2	
48	7.5	
37	28.7	
35	32.5	

$CH_2-CH_2-CH-CH_2Cl$

$^m/e$	% Base
242	2.5
207	10.0
205	2.5
167	7.5
165	7.5
141	7.5
139	6.2
127	6.2
125	6.2
117	7.5
115	23.7
103	13.7
77	88.7
37	28.7
35	32.5

$HC-CH_2C=CH_2$ with Cl above HC

$^m/e$	% Base
242	2.5
139	6.2
137	8.7
105	33.7
77	88.7
37	28.7
35	32.5

$C = CH - CH - CH_3$ with Cl above first C

$^m/e$	% Base
240	1.2
205	2.5
163	23.7
139	6,2
137	8.7
103	13.7
77	88.7
37	28.7
35	32.5

$C = CH - C = CH_2$ with Cl above first C
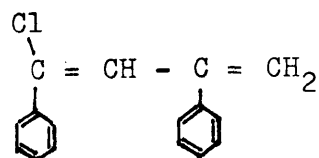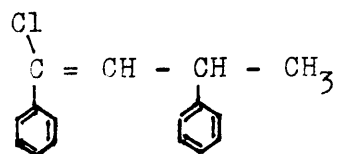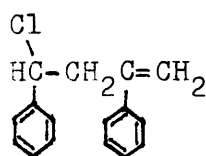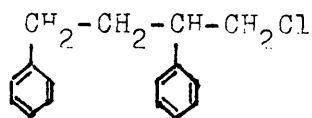
Table 4.14e   continued.

$^m/e$	% Base	Structure
210	10.0	
195	2.5	
133	2.5	
119	6.2	$CH_2-CH_2-CH-CH_3$
105	33.7	
91	45.0	
77	88.7	
208	30.0	
193	3.7	
131	6.2	$CH = CH - CH - CH_3$
105	33.7	
103	13.7	
77	88.7	
206	33.7	
129	15.0	$CH = CH - CH = CH_2$
104	10.0	
102	10.0	
77	88.7	
185	13.7	
184	3.7	
183	40.0	unidentified
182	6.2	
181	45.0	
180	5.0	
178	3.7	
177	5.0	
176	2.5	
175	8.7	
174	5.0	Cl Cl
173	16.2	HC - CH_2
172	13.7	
171	23.7	
143	5.0	
141	7.5	and
139	6.2	
137	8.7	
135	13.7	Cl Cl
101	8.7	$C = CH$
99	16.2	
97	12.5	
95	8.7	
77	88.7	
37	28.7	
35	32.5	

Table 4.14e continued
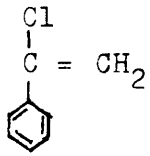
m/e	% Base	Structure
138	10.0	
137	8.7	
136	22.5	
135	13.7	
105	33.7	
103	18.7	
101	8.7	
77	88.7	
63	46.2	
61	32.5	
37	28.7	
35	32.5	

$$\underset{\bigcirc}{\overset{Cl}{\underset{|}{C}}} = CH_2$$

Table 4.14e   Mass Spectrum m/e values and assignments
for Fraction (4) from SATVA of 2CCPS.

The final tailing fraction indicated the slow evolution of one or more compounds of low volatility. The liquid produced was colourless with a pungent odour and was found to contain styrene dimer, partially and fully hydrogenated styrene dimers and their chlorinated analogues, and chlorostyrene. The mass spectral data for the final fraction are given in Table 4.14d and Table 4.14e.

In the more highly chlorinated polymers, the possible production of chlorine gas was investigated by absorbing the products of the first two SATVA fractions into excess KI solution which had been degassed on the SATVA line. On titrating the solution with 0.1M sodium thiosulphate using freshly prepared starch indicator, no iodine was measured and therefore chlorine was not a degradation product.

The CRF in all the CCPS samples consisted of a slim band of dark brown solid near the base of the cold-ring region which spread into a broad band of tacky amber solid. The IR spectra of the CRF samples illustrated in Figure 4.39 differ from that of the starting polymers by broadening of the absorption band at 1580 cm^{-1} to 1520 cm^{-1} indicating conjugated carbon-carbon double bonds. The band at 965 cm^{-1} is due to a trans di-substituted double bond but the CRF does not appear to have a regular structure as there are absorptions at 910 cm^{-1} and 880 cm^{-1}. The band at 910 cm^{-1} is characteristic of the trans structure in polyphenyl acetylene[140] whilst the 880 cm^{-1} absorption is characteristic of the cis conformation.[140] There was no appreciable difference in chlorine content in each region of CRF for a given mono-, di- or tri-chain-chlorinated polymer, the lower region being approximately 0.3 - 0.4% lower in weight % Cl. This
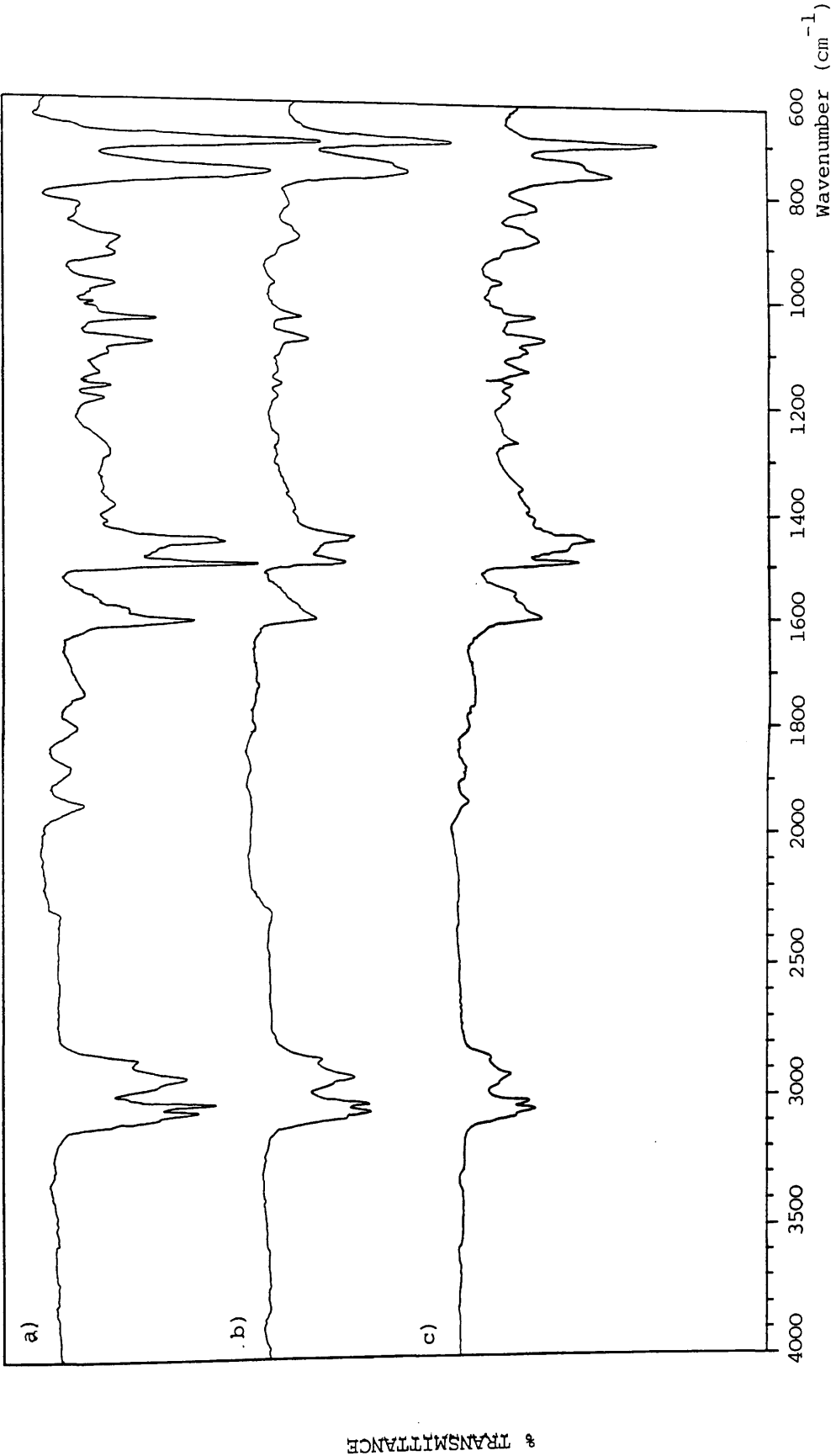
Figure 4.39 IR spectrum of CRF on heating a) CCPS b) 2CCPS and c) 3CCPS to 500°C run as KBr discs.
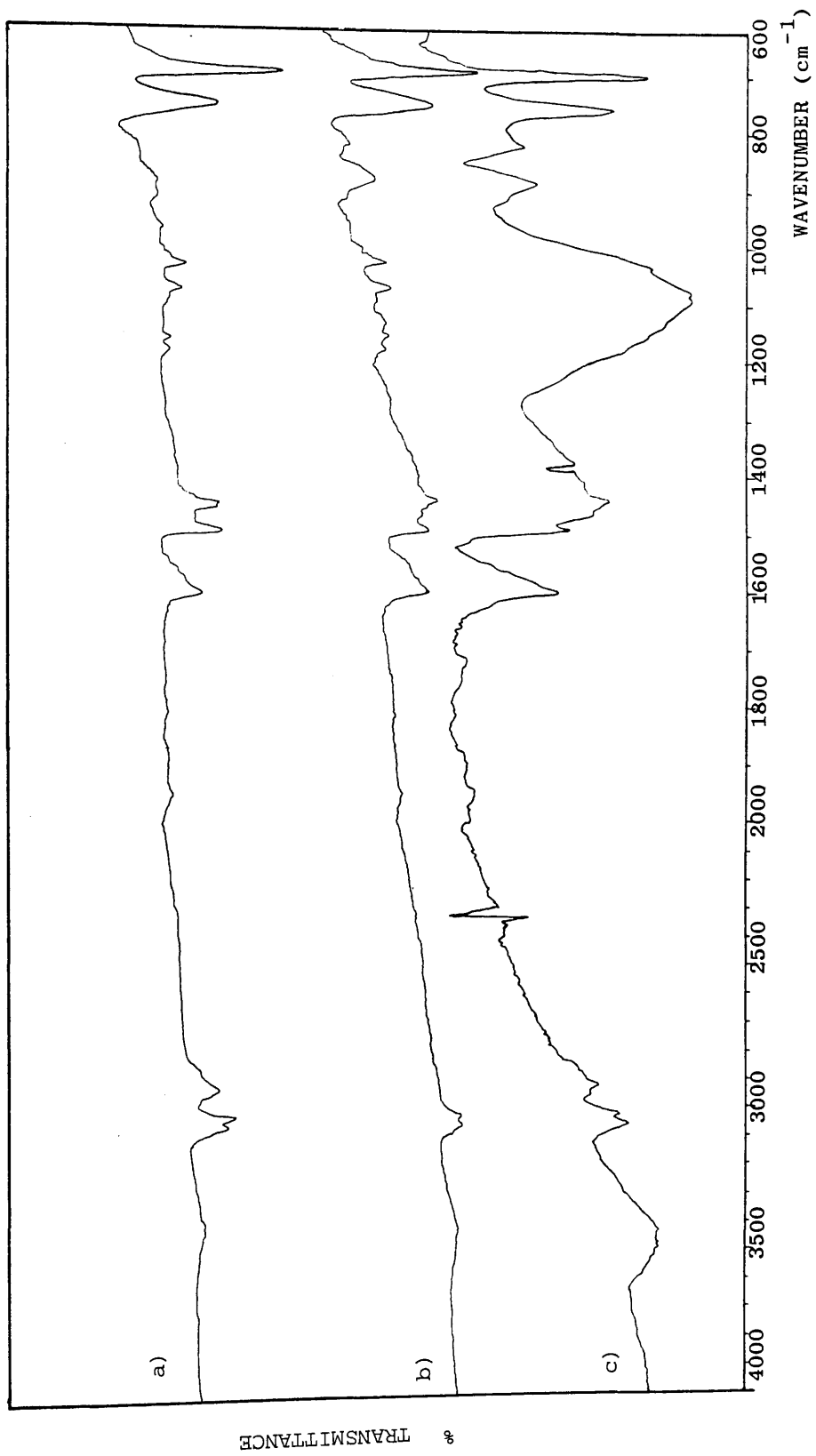
Figure 4.40   IR spectrum of residue on heating a) CCPS   b) 2CCPS   and c) 3CCPS to 500°C run as KBr discs.

suggests that each CRF consists of dehydrohalogenated chain fragments of different lengths and volatility distributing themselves across the water cooled region of the TVA tube.

The residues after degradation to 500°C under TVA conditions were lustrous black solids which were partially soluble in methylene chloride.   In the dichlorinated compounds, the amount of residue produced approximated to 10% of the original polymer weight.   The IR spectra obtained as KBr discs, reproduced in Figure 4.40, show further broadening of the 1580 cm^{-1} band indicating greater conjugation. The absorption bands at 965 cm^{-1} and 880 cm^{-1} in each case are very weak, whereas with the residues from the more highly chlorinated polymer samples the absorption band at 910 cm^{-1} was somewhat stronger. In addition, with the residue obtained from 3CCPS a strong absorption band at $\sim$1185 cm^{-1} was observed.

Quantitative Analysis of HCl and CRF Production.
    The weight % HCl evolved and CRF produced on degrading CCPS samples to 500°C were estimated as previously described in Chapter 2.   These results are shown in Table 4.15.   The chlorine content of the CRF and, where possible, residue were obtained by elemental analysis.   From these results, (reproduced in Table 4.16) the distribution of chlorine in the degradation products was investigated.   This is illustrated in Table 4.17.

From the range of degradation products obtained it can be seen that the major products from the thermal degradation of chain-chlorinated PS are CRF and HCl.   In monochlorinated PS the amount of CRF produced was of the order of 70-74% of the polymer weight,

Polymer Sample	No Cl atoms per monomer unit	mg HCl evolved per 100 mg polymer	mg CRF produced per 100 mg polymer	mg Residue per 100 mg polymer
CPS 1	1.25	25.70	73.73	–
CPS 2	1.54	25.04	70.87	–
CPS 3	1.39	25.70	71.77	–
CPS 4	1.50	25.90	70.52	–
2CPS 1	2.60	31.50	63.56	–
2CPS 2	2.14	32.55	66.31	2.54
2CPS 3	2.04	31.02	66.53	3.01
3CPS 1	2.70	32.00	58.32	–
3CPS 2	2.52	32.94	59.39	–
3CPS 3	2.63	33.55	55.44	10.48
3CPS 4	2.97	30.50	61.55	9.42
PS	0.0	0.0	35.71	–

Table 4.15   Quantitative Analysis of Product Distribution from Degradation to 500°C of Chain-Chlorinated Polystyrenes.

Polymer Sample	mg Cl per 100 mg polymer	mg Cl from HCl per 100 mg polymer	mg Cl per 100 mg CRF	mg Cl per 100 mg Residue
CPS 1	30.79	24.99	9.69	-
CPS 2	34.76	24.34	10.15	-
CPS 3	32.57	24.99	9.71	-
CPS 4	34.19	25.18	11.04	-
2CPS 1	47.77	30.62	21.41	-
2CPS 2	42.62	31.64	19.49	8.67
2CPS 3	41.56	30.16	19.33	8.37
3CPS 1	49.07	31.11	24.37	-
3CPS 2	47.29	32.02	24.88	-
3CPS 3	47.84	32.62	26.21	14.70
3CPS 4	51.00	29.65	32.28	16.51

Table 4.16 Quantitative Analysis of Chlorine Content in Polymer and Degradation Products on heating Chain-Chlorinated Polystyrenes to 500°C.

Polymer Sample	mg Cl per 100 mg polymer	mg Cl in HCl x 100 per 100 mg polymer	mg Cl in CRF x 100 per 100 mg polymer	mg Cl in Residue x 100 per 100 mg polymer
CPS 1	30.19	24.99	7.14	-
CPS 2	34.76	24.34	7.19	-
CPS 3	32.57	24.99	6.99	-
CPS 4	34.19	25.18	7.78	-
2CPS 1	47.77	30.62	13.61	-
2CPS 2	42.62	31.64	12.92	0.22
2CPS 3	41.56	30.16	12.86	0.25
3CPS 1	49.07	31.11	14.21	-
3CPS 2	47.29	32.02	14.78	
3CPS 3	47.84	32.62	14.53	1.54
3CPS 4	51.00	29.65	19.87	1.55

Table 4.17 Quantitative Analysis of Chlorine Distribution in Polymer and Degradation Products on heating Chain-Chlorinated Polystyrenes to 500°C.

which is in agreement with results obtained by Coşkun and McNeill.[125]

This figure is progressively lowered to approximately 63-66% in the

dichlorinated samples and 55-61% in the more highly chlorinated

compounds.

The distribution of chlorine within the degradation products

indicates that approximately 73% of the chlorine present is evolved

as HCl on degradation of samples having a degree of chlorination

(that is, number of Cl atoms per monomer unit) in the range 1.39 -

2.14.   With higher degrees of chlorination (>2.50) this value is

reduced to 64% while lower chlorine content (1.25 Cl atoms per

repeat unit) increases the proportion of chlorine evolved as HCl

to 83%.   Thus in the monochlorinated polymers approximately 20%

of the original chlorine appears in the CRF and in the more highly

chlorinated compounds the value is raised to roughly 30%.

Partial Degradation of Chain-Chlorinated Polystyrenes.

The results obtained by TVA and TG indicate a two stage

degradation process for the thermal degradation of chain chlorinated

PS.   In order to investigate the mode of degradation in greater

detail, partial degradation was carried out on some samples.   Two

methods of partial degradation were used, namely programmed and

isothermal heating.

(a) Programmed Heating

For programmed heating, samples of both monochlorinated PS and

dichlorinated PS were heated to $275^{\circ}C$ at a rate of 10 min^{-1}.   This

temperature corresponds to where the second shoulder in the TVA trace

for the monochlorinated sample ends.   It was found (see Table

4.18) that 8.14% and 10.19% HCl was evolved for mono- and di-
chlorinated samples respectively.   No CRF was produced in each
case and only trace amounts of styrene were observed in the SATVA
trace.

(b) Isothermal Heating

Isothermal experiments were carried out to maximise HCl evolution
with minimal CRF production.   From TVA experiments the CRF begins
to appear around 290°C in monochlorinated samples and approximately
10°C higher (300°C) in dichlorinated samples under programmed
heating conditions.   An isothermal temperature of 275°C was
chosen and the effect of duration considered.   The results are
given in Table 4.19.

Polymer Sample.	Temperature Reached (0°C)	Mg HCl evolved per 100mg polymer	mg CRF produced per 100mg polymer
CPS 3	275	8.14	-
2CPS 3	275	10.19	-

Table 4.18   Quantitative Analysis of HCl evolution and CRF production
on programmed heating of chain-chlorinated PS to 275°C.

Polymer Sample	Isothermal Temperature (^{o}C)	Duration Time (hrs)	mg HCl evolved per 100mg polymer.	mg CRF produced per 100mg polymer.
CPS1	280	1.5	23.08	26.08
CPS1	275	1.5	20.97	18.42
CPS1	273	2.0	21.50	19.97
CPS1	273	3.0	22.69	22.65
2CPS	275	1.5	25.50	11.79

Table 4.19   Quantitative Analysis of HCl evolution and CRF production
on isothermal degradation of chain-chlorinated PS.

4.6.2 Discussion

It can be seen from the TVA and TG results that chain-chlorination of PS to a higher (approximately 2-3 Cl atoms per styrene unit) or a lower (approximately 1 Cl atom per styrene unit) degree thermally destabilises the polymer.

TG indicates a two stage decomposition mechanism for the monochlorinated polymers.   However in more highly chlorinated compounds there is a wide temperature range of breakdown in which a second stage is not distinguished.   The first weight loss, approximately 30%, in the monochlorinated polymers corresponds to the elimination of HCl (26.5% theoretical) while the second stage is due to chain fragmentation resulting in CRF and other degradation products.   Another factor to note is the increase in weight% residue produced in the degradation of chlorinated PS.   This is even more pronounced in the trichlorinated compounds and is of importance when taken in the context of degradation of a polymer in a fire.   The char produced will tend to protect undegraded polymer thus breaking the fire cycle (see Chapter 1).   In addition it has been shown that as the amount of char remaining after combustion of a polymer increases, the level of smoke production should decrease.[25]   This has been observed with chlorinated PVC Thus chain-chlorinated PS may have the potential for a decrease in smoke production during degradation as compared with PS.

Chain-brominated PS[141] shows some resemblance to chain-chlorinated PS in its stability and degradation behaviour.   The monobrominated polymer degrades in two stages, in the regions 150-300°C and above 300°C, respectively.   The first decomposition

result in the formation of HBr and the second produces chain

fragments from the modified polymer structure.   There are however

some differences from the chain-chlorinated polymer.   Halogenation

is more specific to the tertiary H sites when bromine is used, but

the side reactions of ring halogenation and chain scission occur

to a somewhat greater extent.   It is also observed that less HBr

is produced than expected during degradation and some bromine is

present in the major product fraction which consists of chain

fragments.   Finally, the amount of residue remaining after

heating to 500°C is approximately three times that produced from

the corresponding chlorinated polystyrene.

TVA results from chain-chlorinated PS are in agreement with the

above observations from TG results and the clear indications by

TVA of changed product distribution, on altering chlorine content

of the polymer, especially with respect to HCl evolution, are

borne out by quantitative measurements following SATVA.   The

weight % HCl evolved on heating monochlorinated polymers to 500°C

is around 26% of the polymer weight which corresponds to the

evolution of one molecule of HCl per repeat unit.   Thus in this

case, the formation of HCl is due to the simple elimination of HCl

from the polymer backbone.

The resulting polyphenylacetylene (which will contain

chlorine if the degree of chlorination is greater than one) can then,

depending on temperature, undergo main chain scission producing CRF,

smaller volatile products and involatile residue.   Non-uniformity

in the chlorination process is indicated in the minor and trace

products.   Styrene monomer, dimer and hydrogenated dimer arise

from unchlorinated segments in the chain as does toluene. Minute quantities of chlorobenzene, dichlorobenzene and chlorotoluene show that a very small amount of ring chlorination, most probably in the para-position, has taken place but that this side reaction is negligible as it is not detected in the IR spectra of the undegraded polymer and can only be inferred from the degradation products. This emphasises the importance of polymer degradation in structural analysis.

The distribution of the above mentioned minor and trace products can be seen on comparing SATVA traces for identical sample sizes of mono- and di-chain chlorinated PS. In Figure 4.34 it can be seen from the relative peak heights of fractions 2 and 3 that as polymer chlorine content increases, the amount of unchlorinated product (styrene etc) decreases. It must be noted however that due to the variation in sensitivity to different compounds and the limited range of linear response from the Pirani gauge, this type of direct comparison can only be made between peaks containing identical compounds which are below 1.5 mv Pirani output. Both these conditions were satisfied in this case.

CRF is a major product in all the chain-chlorinated samples and accounts for, on average, 72%, 65% and 59% of the polymer weight for mono-, di- and more highly chlorinated PS respectively. The high percentage of CRF produced reflects the lack of monomer production and thus the importance of chain transfer reactions after dehydrochlorination. The reduction in CRF formed as polymer chlorine content increases is balanced by the increase in the evolution of HCl and residue deposited.

The weight % Cl per mg CRF is approximately 10% in monochlorinated PS (see Table 4.16) which corresponds roughly to two Cl atoms per seven phenylacetylene repeat units. The average weight % Cl per mg CRF in the more highly chlorinated compounds was almost twice that for the monochlorinated samples. Although it is known that the CRF consists of oligomeric chains of partially chlorinated polyphenyl acetylene, the absolute structure of the CRF is difficult to determine due to the possibility of cis and trans isomerisation. These would be easy to distinguish for single structures, however in all trans and all cis conjugated unsaturated polymer chains rotation about single C-C bonds is possible. Thus a trans-transoid converts to a trans-cisoid form (and vice versa) by 180° rotation about C-C.

trans-transoid   trans-cisoid
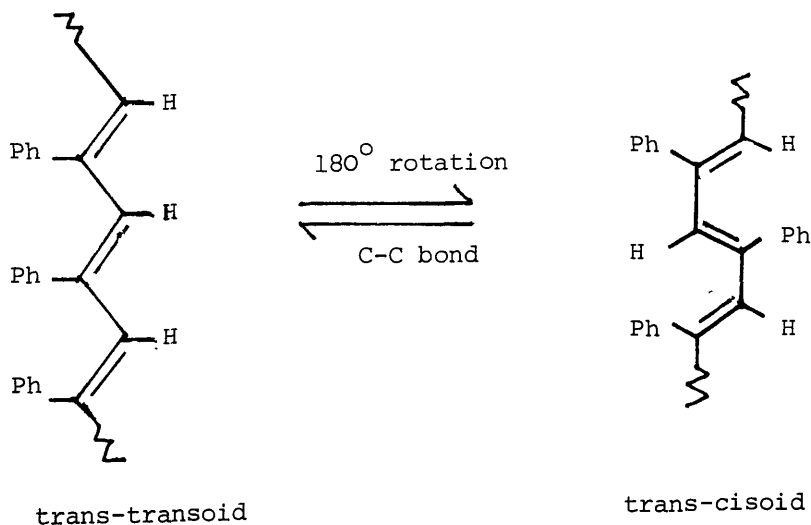
Also the possibility of a structure such as
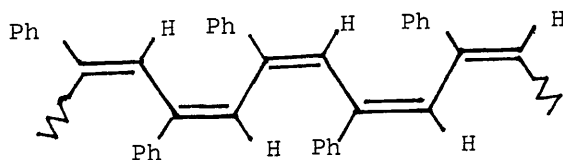
cannot be ruled out.

In reality it is possible that the CRF does not have a
regularly repeating structure and that several conformations may
be present within the chain.   Nevertheless, the preferred
structure will be that which is of lower energy and presents the
least steric hindrance.

Production of HCl in the more highly chlorinated polymers appears
to be the more complex.   The availability of aliphatic H atoms
for dehydrochlorination suggests that only 8% HCl
by weight of polymer should in theory be produced.   However
four times the theoretical amount was obtained.   A possible
explanation for this anomaly is that a cyclisation reaction occurs,
involving two cyclisations per four repeat units with the total
elimination of six molecules of HCl.   The reaction scheme for
the production of HCl from dichlorinated PS is shown below:
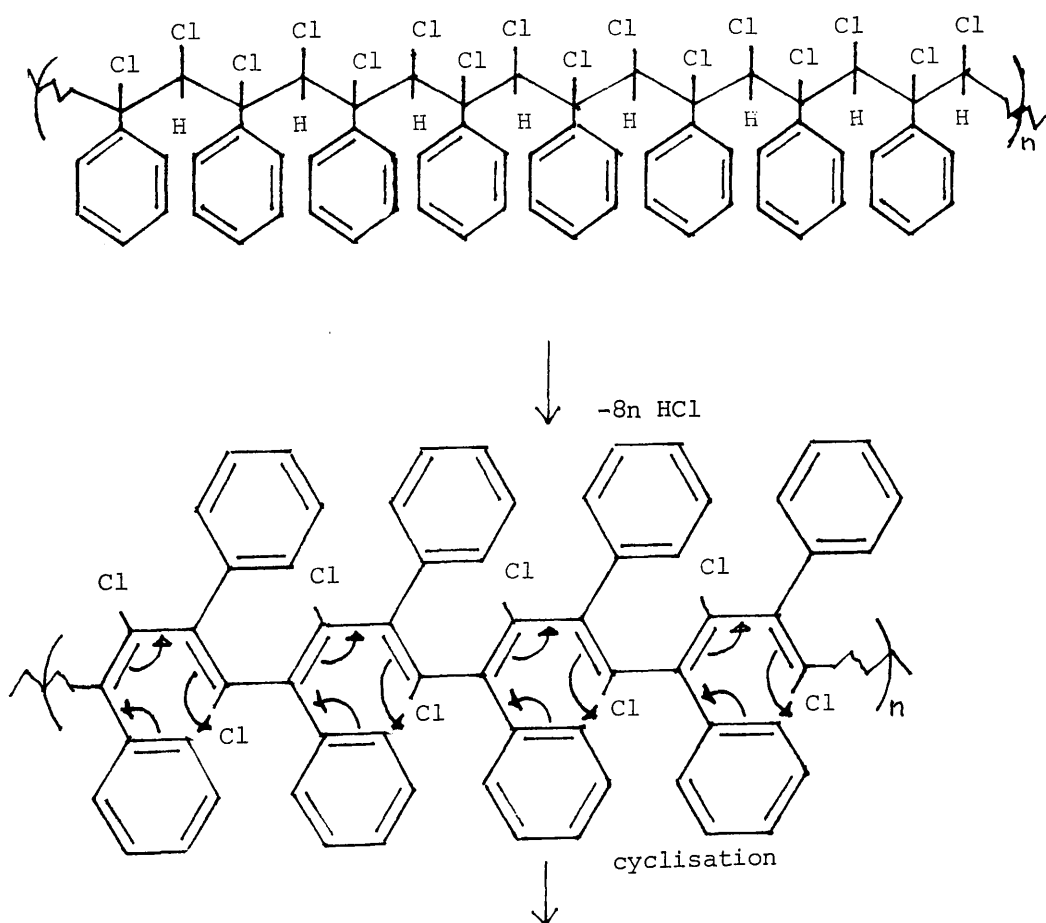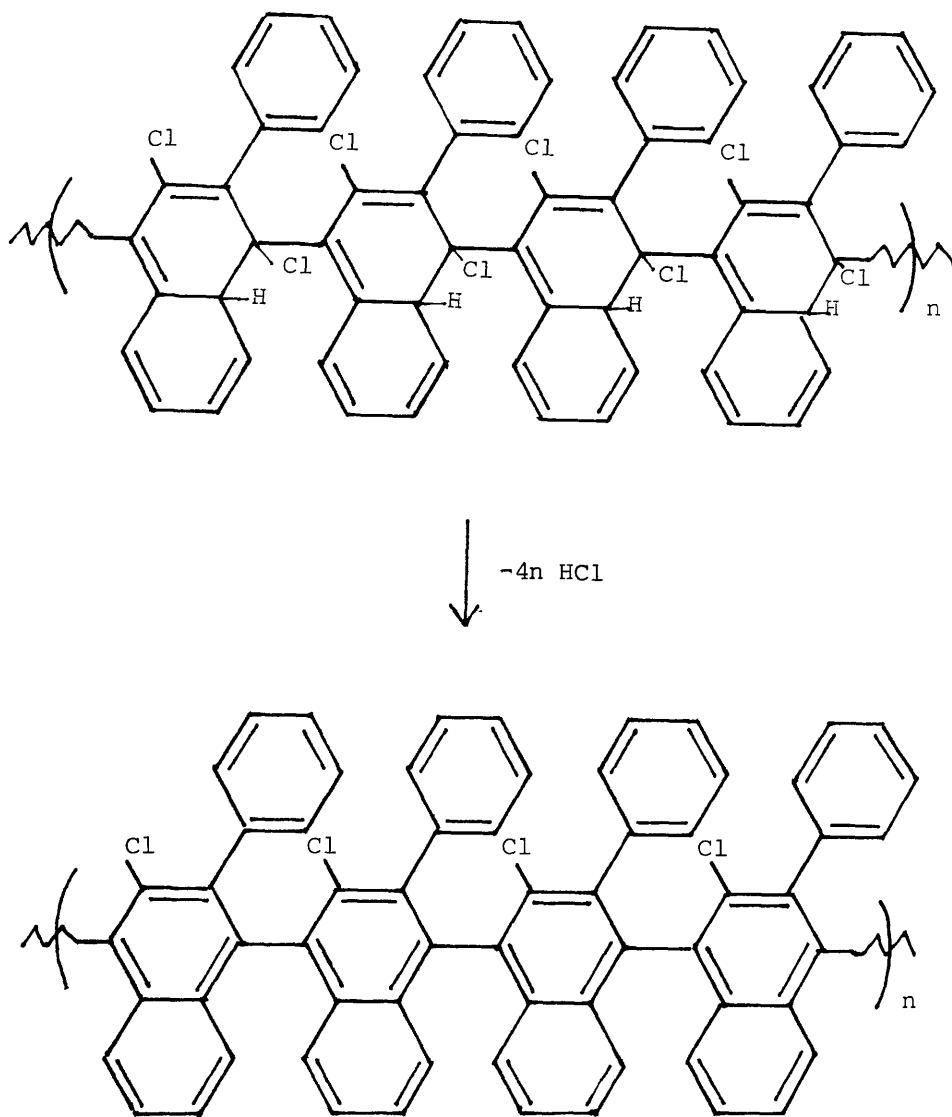
Scheme 4.1   Dehydrochlorination of Dichlorinated Polystyrene.

The theoretical total weight % HCl evolved from this reaction

is 31.65% which is in good agreement with the average observed

value of 31.78% (see Table 4.15).   However, there is some

discrepancy in results when considering the weight % Cl remaining

in the residues.   The observed chlorine content was found to be

just over half the theoretical value (8.37% observed cf. 13.01 %

theoretical).

Nevertheless, the thermal degradation of chain-chlorinated PS, in which the degree of chlorination is greater than or equal to two Cl atoms per monomer unit, may be explained in terms of roughly three deomposition stages which occur over a broad temperature range.   These correspond to initial dehydro-chlorination along the polymer backbone followed by cyclisation of the resultant polyene backbone and finally a second elimination of HCl. This second dehydrochlorination is favoured as it restores aromaticity and also results in a highly conjugated substituted polynaphthalene residue.   Similar cyclisation reactions[142] have been reported during the deompositions of other vinyl polymers including PVC, PVB, PVA and PVAc.   During these degradations several aromatic hydrocarbons were produced, in particular benzene, naphthalene and anthracene.

4.7 CONCLUSIONS

PS which is exclusively ring-chlorinated can be prepared by the polymerisation of o- or p-chlorostyrene.   This is a more satisfactory technique than the reaction of chlorine with PS in the presence of iodine which leads to some chain-chlorination as a side reaction.

Chain-chlorinated PS can be synthesised in vacuo by the reaction of chlorine on PS.   Under these conditions no initiator is necessary and it is possible to prepare polymers which have a chlorine content of 1-3 Cl atoms, per styrene unit.

The site of chlorination has a profound effect on the

degradation behaviour of the polymer both in respect of the temperatures and the mechanism of degradation.   In poly(chloro-styrene), which has exclusively ring-chlorinated substituants, thermal degradation occurs in a single stage with the onset and rate maximum temperatures similar to those for PS.   The depolymerisation process, however, leads to almost 80% monomer production, there being little formation of chain fragmentation products and therefore a much higher ratio of monomer to CRF than for pure PS (monomer : CRF = 5 for PoCS, monomer : CRF = 1.8 for PS).   Virtually no elimination products are produced.

Chain-chlorinated PS is noticeably less stable to heating than PS.   Degradation occurs in two stages in mono-chain-chlorinated PS indicating the presence of a stable partially degraded inter-mediate.   The first stage corresponds to the elimination of HCl while the second stage is due to main chain scission resulting in depolymerisation and a great amount of fragmentation products (CRF). In chain-chlorinated PS where the degree of chlorination is approximately equal to two or three Cl atoms per monomer unit, the thermal decomposition is a more complex process in which, following initial dehydrochlorination, it is proposed that a cyclisation reaction occurs which, together with elivated temperatures, facilitates further HCl elimination resulting in a residue with a highly conjugated partially chlorinated phenyl substituted poly-naphthalene type structure.   The main products of degradation are chain fragments (CRF), HCl and a significant amount of char residue.

Chain-chlorination of PS results in polymers with the potential

of reduced fire hazard when compared to PS due to the alteration in decomposition process. This yields less flammable degradation products and a large amount of residual char which, in addition to reducing thermal feedback to the degrading polymer, may reduce smoke production.

CHAPTER 5.   POLY(ETHYLENE OXIDE) : SALT BLENDS

5.1 INTRODUCTION

5.1.1 History of PEO : Salt Complexes.

It has been known for some time that alkali and alkaline earth metal cations interact with certain neutral organic compounds.   During the past 23 years the complexation of such cations with cyclic ethers[143,144] glymes[144] and crown ethers[145-147] has been studied.   Prior to this dioxanate-metal halide complexes[148,149] had been reported.   It was therefore, not unreasonable to have similar interactions between metal cations and polymeric non-cyclic analogues of the forementioned ethers. Such a complex between PEO and $HgCl_2$ was first reported[150] by Blumberg et al in 1964.   Since then, the complexation between PEO and inorganic salts has been intensely studied although it is only relatively recently that their technological importance has become apparent.   Solvent free complexes of PEO with alkali metal salts have been prepared[151-153] and are potentially useful as polyelectrolytes in high-energy-density battery applications.[154-157]   This function for PEO was first proposed by Armand[154] and his co-workers in 1978 although the conductivity of Na, K and NH_4 salt complexes of PEO had been reported three years earlier by Wright.[152]   Thus, due to their practical and economical importance, most research was carried out on alkali metal salts.   In particular[158] lithium trifluoromethanesulphonate ($LiCF_3SO_3$) and lithium perchlorate ($LiClO_4$) with optimum blend stochiometry 8:1 ethylene oxide (EO) units : salt were studied.   However, PEO-$LiClO_4$ electrolytes have been prepared with EO:salt ratios as high as 2:1[159] which yield improved conductivity to those previously reported.   In addition, the complexation capabilities of PEO towards divalent cations,[160-162] mainly alkaline earths has been investigated and reveal an extraordinarily rich

coordination chemistry for this polymer.   Investigations into the properties of PEO : $MoCl_2$ and $PbBr_2$ complexes,[162] PEO : $CaBr_2$, $CaCl_2$, CaI_2 and $Ca(CF_3SO_3)_2$ complexes[163] and PEO : $ZnCl_2$ complexes[164] (EO:salt, 8:1 and 4:1), indicate that many salts of divalent cations and monovalent anions may form conductive complexes with PEO and thus present a new family of polymer solid electrolytes.

5.1.2   Theory of Polymer : Salt Blends.

In the formation of a polymer-additive blend, it is important that the additive molecule is soluble in the polymer matrix.   If this is so then at certain salt concentrations a homogeneous one phase blend will be formed with the polymer.   Under such conditions, the salt is said to be "compatable" with the polymer forming a "compatable blend". When an excess of salt is added a two phase system results in which one phase consists of salt saturated polymer and the other excess additive. This excess additive may be present as aggregates in discrete zones or be dispersed evenly throughout the polymer matrix.   Such blends are termed "non-compatable" and due to the heterogeneous nature of the system, the additive will be less effective in altering the properties of the polymer.

Four parameters are important for the control of salt-polymer (or neutral molecules in general) interactions namely:

1.   Electron pair donicity (DN)

2.   Acceptor number (AN)

3.   Entropy term

4.   Free energy

DN measures the ability of the polymer to donate electrons to solvate the cation, considered as a Lewis acid.   The acceptor number,

on the other hand, quantifies the possibility for anion (base) solvation.
Ethers are known to be quite strong donors[165] with 1,2-dimethoxyethane
(glyme) having a donor number of 22.   The donicity of PEO therefore
should be similar, i.e. around 20.   However, ethers are poor acceptors
since they lack hydrogen bonding for anion solvation.   Thus favourable
salt forming complexes of PEO are those with large delocalised anions
which require little solvation, typically ClO_4^- and I^-.

The entropy term depends on the optimal spatial configuration of
the solvating units.   The CH_2CH_2O unit is found to have a more
favourable spacing than CH_2O or $CH_2CH_2CH_2O$ units.[166]   The formation of
a complex corresponds to competition between solvation energy and
lattice energy of the salt as shown below[167]:

$$- \left\{ \begin{array}{c} \text{lattice energy of salt} \\ + \\ \text{lattice energy of polymer} \end{array} \right\} + \left\{ \begin{array}{c} \text{solvation energy} \\ + \\ \text{lattice energy of complex} \end{array} \right\}$$

Thus strongly solvated ions such as Li^+ can take smaller anions down
to Cl^- into PEO solution.

Finally the free energy of the system should be considered.
Billingham et al on extending the Flory-Huggins theory of mixing of
liquids with polymers to include non-volatile solutes,[168]   have shown
that in addition to the free energy of mixing ΔG_m, the solubility of
a crystalline additive in a polymer depends upon the free energy of
fusion ΔG_{fus}.

From the Flory-Huggins theory ΔG_m is given by eqn.1.

$$\Delta G_m = RT[\ln\theta_1 + (1 - {}^{V_1}/_{V_2})\theta_2 + X\theta_2^2] \qquad (1)$$

where: θ_1 and θ_2 are the volume fractions of the additive and polymer

respectively.

where : V_1 and V_2 are the molar volumes of additive and polymer

X is the solvent-solute interaction parameter.

With a crystalline additive, ΔG_{fus} is expressed by eqn.2.

$$\Delta G_{fus} = \Delta H_{fus} - T\Delta S_{fus} \tag{2}$$

Now $\Delta S_{fus} = \Delta H_{fus}/Tm$ and thus ΔG_{fus} can be rewritten as eqn.3.

$$\Delta G_{fus} = \Delta H_{fus} (1-T/Tm) \tag{3}$$

For solubility of a crystalline additive in contact with the polymer the following must hold

$$\Delta G_m + \Delta G_f \leqslant 0 \tag{4}$$

Therefore at the limiting value

$$\Delta G_m = RT[\ln\Theta_1 + (1-V_1/V_2)\Theta_2 + X\Theta_2{}^2] + \Delta H_{fus} (1-T/T_m) = 0 \tag{5}$$

Hence assuming $\Theta_2 \simeq 1$

$$-\ln\Theta_1 = (1/RT)H_{fus}(1-T/T_m) + (1-V_1/V_2) + X \tag{6}$$

Thus the solubility, of which Θ_1 is a measure, is dependent upon both the heat of fusion and the melting point of the additive.

5.1.3 Nature of PEO : Salt Complexes

A PEO : salt complex can be looked upon as a salt dissolved in a solvating polymer matrix. Interaction occurs between the positively charged cation and the lone pair of electrons on the oxygen atoms of the polyether and thus the polymer may be thought of as a macromolecular array of Lewis bases of low polarity. In general, the result of this complexation is to reduce the ionic interaction between the cation and its counteranion increasing the nucleophilic nature of the latter which usually brings about enhanced reactivity of the species formed.[169]

PEO : salt complexes are usually mixed-phase mixtures of crystalline PEO : salt complex, crystalline PEO, crystalline salt (if excess added) and amorphous solution of salt in PEO. Depending on the molar ratios of monomer units to salt the relative amounts of the components of the mixture will differ. The maximum complex stoichiometry was thought to be a 4:1 ratio of ether oxygens to salt cation, with small cations i.e. Li^+ and Na^+ forming 3:1 complexes whereas larger cations gave 4:1 adducts. However, microcalometric studies into the complexation between PEO and alkali salt in solution[170] have revealed a 4:1 complex for LiI whilst a 2:1 complex predominates for NaI, and for KI, 4:1, 3:1, 2:1 and 1:1 complexes all seem possible when KI concentration is increased. Moreover, Blumberg et al[150] synthesised a 1:1 $HgCl_2$ complex and 2:1 $ZnCl_2$ complexes[159] have been reported. Thus it appears PEO is capable of high salt density adducts. The stoichiometry is dependent on numerous factors including cationic radius[171] and the lattice energy of the salt. There is however a discrepancy in the literature as to whether the relative binding affinity of the three alkali metal salts to PEO decreases[170,172] or

increases[173] with the cation size following the order $K^+ > Na^+ > Li^+$.

Structure of PEO : Salt Complexes.

The structure of crystalline PEO : salt complexes are not known with certainty. Pristine PEO adopts a helical configuration with seven monomer units and a thread of 19.3Å per unit of quadratic cell[174] as illustrated in Fig 5.1. The conformational assignment to internal rotation[175] about the $O-CH_2$, CH_2-CH_2 and CH_2-O bonds is trans, gauche, trans respectively.
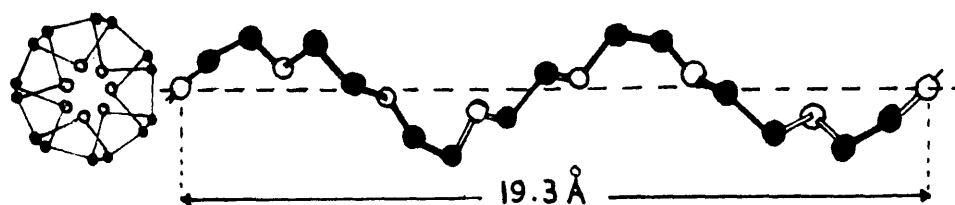
Fig 5.1 The helical structure of PEO.

A reasonable model for PEO:salt complexes assumes that the helical configuration of PEO is retained and the cation involved resides in the centre of the helix.   On the other hand, Humba[176] found that the potassium in the KSCN complex resides outside the PEO spiral.   Also a zig-zag conformation cannot be completely excluded for any ion in a 2:1 or richer complex.

In general, two models have been proposed for PEO:salt complexes.   These involve either single strand helical arrangements[177,153] or double strand helical arrangements[154,178], the variations on which are described below:

1) Cations are enclosed in a single helical unit.

Buschmann[179] on calculating the stability constant of PEO with several K^+, Rb^+, Cs^+ and Ba^{2+} salts in methanol estimated PEO (M.wt. 14000) was able to complex approximately $10K^+$ or $12Ba^+$ ions. As illustrated in Fig 5.2a, some oxygen atoms of PEO are not able to interact with the cation. A certain distance between the complexed ions is necessary due to electrostatic repulsion.

O : cation

o : oxygen
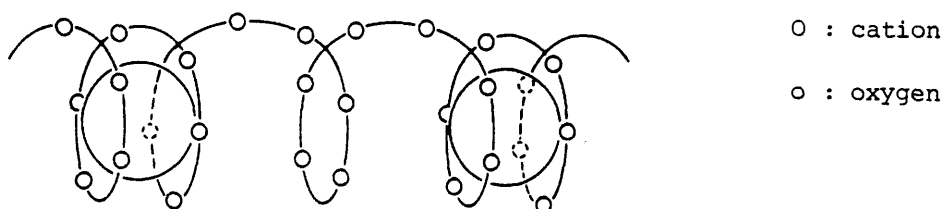
Fig 5.2a. Schematic diagram of PEO:KNO_3 complex.

One of the earliest reported investigations into the structure of PEO:salt complexes was that by Blumberg et al on the PEO:mercuric chloride complex.[150] They identified a complex with the empirical formula $(CH_2CH_2O)_4 \cdot HgCl_2$ and tentatively the unit cell of the complex was orthorhombic with dimensions $\underset{\sim}{a}$ = 13.5 Å, $\underset{\sim}{b}$ = 17.1 Å and $\underset{\sim}{c}$ = 11.6 Å ($\underset{\sim}{c}$, the fibre axis). The IR spectrum of the complex resulted in a more detailed spectrum than for pure PEO suggesting that more rotational states to be present in the former than the latter. This was consistent with a change from trans to gauche state of one O-C bond. Further investigations[180,181] revealed that PEO forms two kinds of crystalline complexes with mercuric chloride, one of which consists of mole ratio of $4CH_2CH_2O$: $1HgCl_2$ and the other consists of mole ratio of $1CH_2CH_2O:1HgCl_2$. The structure of the former crystalline complex, denoted as type I, was determined by X-ray analysis and the conformation of the PEO in type I was found to be the $T_5GT_5\bar{G}$ form

(where T, G and $\bar{G}$ indicate <u>trans</u> and the right- and left-handed

<u>gauche</u> forms respectively). Similar analysis for the type II PEO:

mercuric chloride complex [182] indicated the unit cell to be orthorhombic

of dimensions $\underset{\sim}{a}$ = 7.75 Å, $\underset{\sim}{b}$ = 12.09 Å and $\underset{\sim}{c}$ = 5.88 Å ($\underset{\sim}{c}$, the fibre

axis), and that the conformation of PEO in type II complex was found

to be of form near to $TG_2T\bar{G}_2$. A molecular model of PEO in the

complex of type II is illustrated below:
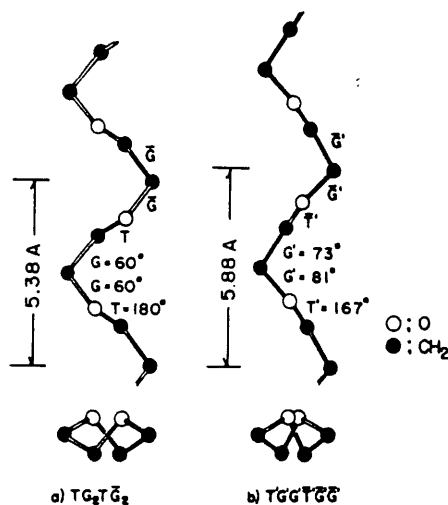
Fig 5.2b. Molecular model of PEO in the complex of type II :
a) starting model, $TG_2T\bar{G}_2$; and b) most plausible
model, $T'G'_2\bar{T}'\bar{G}'_2$

Papke and co-workers [183] using IR and Raman vibrational spectroscopic

analysis to determine structure and ion pairing in complexes of PEO

with Li^+ salts proposed a model in which the PEO chain wraps around

the lithium ions in a $T_2GT_2\bar{G}$ conformation. The PEO chain as

proposed for complexation to lithium (and sodium) cations is shown in

Fig 5.2c.

● : C atoms

◉ : O atoms

○ : H atoms
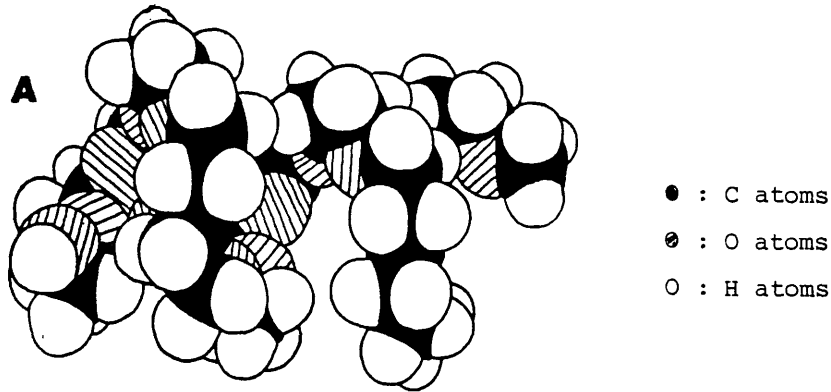
Fig 5.2c. Molecular model of PEO in a $T_2GT_2\bar{G}$ conformation as proposed
for complexation to sodium and lithium cations.

James et al[184] investigated the nature of the complex formed
between poly(propylene oxide)(PPO)and $ZnCl_2$.   The complex was
thought of in terms of an intramolecular chelate ring model involving
the coordination of two adjacent ether oxygen atoms in the polymer
backbone to the zinc cation.   It is not unreasonable to consider
this model to represent the interaction between PEO and $ZnBr_2$.   This
is illustrated below:
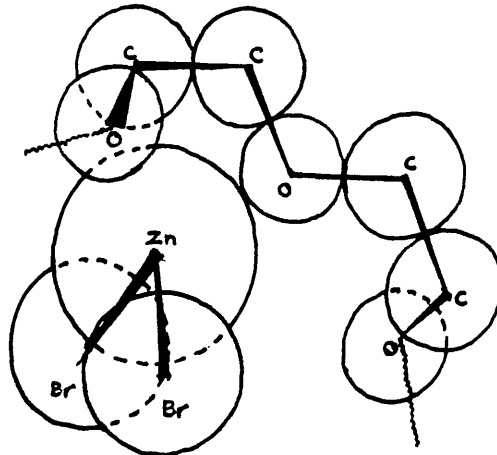
Fig 5.3 Molecular model of PEO:$ZnBr_2$ complex.

The complexation between K^+ ions and adjacent PEO ether oxygen atoms was subsequently reported by Panayotov[185] and his fellow workers when studying alkali metal solutions in organic solvents obtained in the presence of PEO.

2) cations are coordinated by two chains which complex the cations on either side.

A general feature of the complexes described so far is the gauche rotation angle adopted by the CH_2-CH_2 bond while the CH_2-O bond adopts either trans or gauche. Such sequences impart the appropriate radial orientation of the lone pairs towards the central cation. The bond rotation angles may be adjusted to some extent (see PEO : $HgCl_2$ type II complex) to allow optimum interaction with different cations.

Moreover, in the amorphous polymer, coordination of the cations by oxygens from neighbouring chain segments[152] (intermolecular interaction) is possible.

● carbon atom
O oxygen atom
⊘ cation
---- "lone pair" electrons
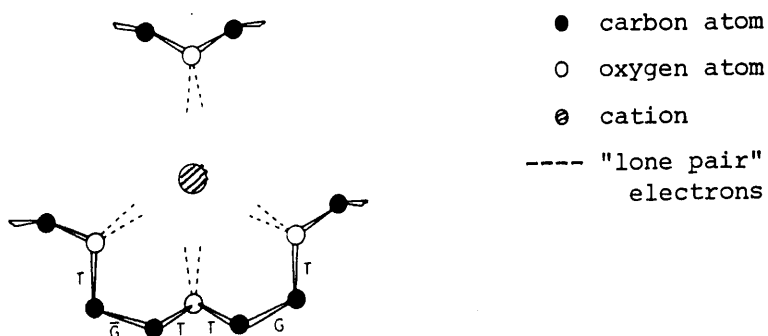
Fig 5.4 Conformation illustrating possible intermolecular interaction between PEO chains and a cation in non-crystalline regions.

3) two PEO chains are mutually intertwined in a double helix which encloses cations along its axis.

Parker et al[177] working on KSCN and NaSCN : PEO complexes have proposed a double helical model. The unit cell contains 8 EO repeating units with 2 cations and anions, PEO is in the $T_2GT_2\bar{G}$ conformation. The molecular model of the complex is reproduced in Figure 5.5.
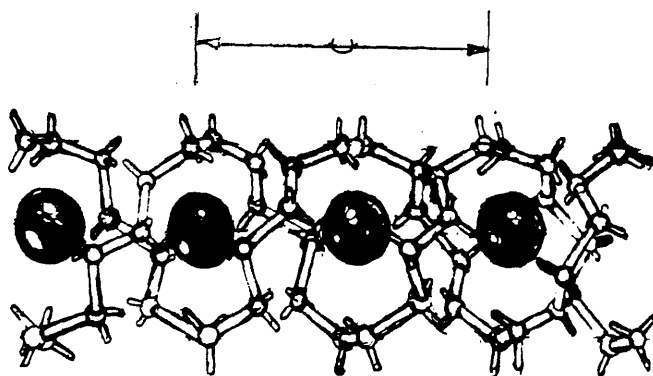
Figure 5.5   Molecular model of proposed double helical structure for alkali metal PEO complexes.

5.1.4   Thermal Analysis of PEO : Salt Blends.

The thermal analysis of PEO : salt blends has mainly focused upon determining the melting point and phase transitions within PEO : salt complexes as these are important thermal parameters for the use of these materials in polymeric electrolytes. The analytical techniques most commonly employed are DTA and DSC.[186,187] Wright[152] using DTA and a polarising microscope fitted with a hot stage, found the melting points of crystalline complexes formed between PEO and NaSCN, NaI, KSCN and NH_4SCN to be 237°, 282°, 177° and $147^{\circ}C$ respectively. He also noticed that at certain temperatures, a

transition from lower to higher conductivity occurred. For Na^+ ion complexes the transition occurred between 127° and $137^{\circ}C$ whereas for the K^+ ion complexes the transition was observed between 177° and $187^{\circ}C$. Lee and Wright[188] first reported order-disorder transformations in a linear polymer-complex system when studying PEO : NaI and PEO : NH_4SCN blends. The transformation occurred at $100^{\circ}C$ in the case of the NaI complex and at $69^{\circ}C$ for the NH_4SCN adduct. It was also noted that the melting point of the pure polymer ($76^{\circ}C$) was enhanced by complexation. The elevation of glass transition temperature (Tg) of PEO (dp 13500) from $-60^{\circ}C$ to $34^{\circ}C$ with the addition of 17 mole % $ZnCl_2$ was observed by Marco[189] and attributed to chelation of adjacent oxygen atoms by $ZnCl_2$. Similar increases in Tg of poly(propylene oxide)(PPO) when complexed by metal salts has been reported.[184] The elevation of Tg depends on the amount of salt added and the type of salt added. The dispersion of ten metal halides in PPO when carried out by solution blending gave single phase polymeric complexes. These amorphous complexes displayed a single Tg at temperatures $\leqslant 140^{\circ}$ greater than that of the pure polymer. The order of effects in the elevation of Tg were $ZnBr_2 > ZnCl_2 > ZnI_2$.

Stainer et al[190] studied the interaction between PEO and the ammonium salts NH_4SCN and $NH_4SO_3CF_3$ in the composition range 10:1 to 2:1 (repeat unit : salt). DSC experiments confirmed the conclusion from X-ray diffraction measurements that a crystalline complex is formed between the salt and polymer with the approximate stoichiometry of PEO_4NH_4SCN. A single sharp endotherm at $68^{\circ}C$ was found for PEO_4NH_4SCN and corresponds to the melting point of the crystalline complex. Decreasing the salt concentration to 5:1 and 6:1 composition gave a relative decrease in magnitude of the $68^{\circ}C$ endotherm and the

appearance of an endotherm at ~42°C. The latter was assigned to

the eutectic melting of a mixture of PEO_4NH_4SCN and PEO. Whereas the

X-ray diffraction pattern for 8:1 EO : NH_4SCN contained reflections

assignable to free PEO, the data for 8:1 $EO:NH_4SO_3CF_3$ did not. The

DSC for this complex showed a single endotherm at 41°C which corresponds

to the crystalline-amorphous phase transition of the polymer:salt

complex. Increasing the salt concentrations to 4:1 composition gave

a second higher temperature endotherm in the DSC curve at 60°C.

This was assigned to the crystalline melt of a second polymer:salt

complex phase corresponding to roughly 4:1 polymer to salt stoichiometry

similar to that formed in the $PEO:NH_4SCN$ system.

There is little reported in the literature on the thermal

degradation of PEO:salt complexes. Yang et al[191] working on $PEO:MgCl_2$

blends of polymer to salt ratios of 4,8,12,16 and 24 revealed, using

DSC, that the composites consist of two crystalline phases corresponding

to pure PEO and the salt rich complex, and coexisting elastomeric phases

having different salt concentrations. The Tg of the $PEO:MgCl_2$ complexes

increased gradually with increasing salt concentration and was in the

range of 148°-160°C. It was incidentally reported that the 16:1

$EO:MgCl_2$ complex decomposed above 290°C as indicated by TGA.

An intensive investigation into the thermal properties of PEO

complexed with NaSCN and KSCN using DSC and optical spectroscopy was

carried out by Robitaille and co-workers.[192] A series of blends were

made having EO:Na molar ratios ranging from 1 to 16. The DSC curves

on heating from ambient temperature to 350°C revealed three sharp

endotherms at 58°, 182° and 309°C respectively. The transition at

58°C occurred for all mixtures having EO:Na ratios greater than 3.

This was close to the endotherm observed for pure PEO.   The same

blends (EO:Na > 3) also exhibited a second and broader endotherm

at higher temperature which increased in relative intensity and

moved from 93° to 186°C with decreasing the EO:Na ratio from 16 to

3.3.   For EO:Na = 3, the endotherm at 58°C disappeared and a sharp

endotherm at 187°C was observed.   With all remaining blends

(EO:Na < 3), a transition at 182°C was obtained which was attributed

to an incongruent melting of the compound having stoichiometry 3:1

EO:NaSCN.   Among these latter blends, only those with EO:Na $\leqslant$ 2

exhibited the third transition at 309°C.   This coincided with the

melting endotherm of pure NaSCN indicating that the salt was not

completely miscible with PEO over the whole range of composition.

When repeat heating-cooling cycles between 100° and 320°C were

performed on a blend of composition EO:Na = 2, a reduction in the

area of the melting-endotherm at 182°C was observed indicating some

thermal degradation.

The effect of K salts on the thermal stability of PEO has been

studied.[193]   DTA was performed in air and the effectiveness of the

stabilising action of the salt was evaluated on the basis of DTA

curves according to differences in melting points and the start of

the exothermic peak corresponding to oxidation.   DTA of pure PEO

showed a melting point at 75°C, a series of exothermic effects at

175°C due to the start of the process of oxidation of the polymer,

followed by decomposition of PEO around 300°C.   The TG curve

indicated a two stage degradation occurred in an oxygen atmosphere

with T_1 onset at approximately 240°C and T_2 onset at roughly 325°C.

In the thermo-oxidative decomposition of PEO blended with KCl and KBr,

no change in degradation behaviour from pure PEO was observed.

With KF, in the 50°-140°C region a three-step endo-effect was observed for the blend which was due to the difference in structure caused by the complexation of PEO by KF. There was no significant shift to higher temperature of the exotherm corresponding to the start of oxidation (210°C) and the temperature of the decomposition of PEO was slightly lowered to approximately 290°C. On the other hand KI and KSCN appeared to be more effective in stabilising PEO to oxidative degradation. DSC results indicated that the decomposition of PEO was in the region 260°-290°C for PEO:KI blends and this temperature was increased to 310°C with KSCN. In addition, the TG curves for both PEO:KI and PEO:KSCN mixtures gave a single stage decomposition with onset temperatures of approximately 330° and 340°C respectively. Blends with the greatest thermal stability were obtained in the presence of 30% K salt. Overall it was concluded from the investigation into the effect of K salts on the thermo-oxidative stability of PEO that effectiveness of stabilisation by the salts depends on the nature of anion and changes KSCN > KI > KF > KCl = KBr and was determined by the specific solvation of the salt by the poly-ether molecules with the formation of intramolecular coordination complexes.

A recent study by Cameron et al[194] into the thermal

degradation of PEO:NaSCN complexes (8:1 EO:NaSCN) has revealed

that NaSCN destabilises PEO. TG results showed that PEO has a peak

maximum at $415^{\circ}C$ whereas the complex has a maximum rate of

decomposition at $406^{\circ}C$. TVA experiments on the PEO:NaSCN blend

revealed an increase in the production of non-condensable products

when compared to the decomposition of pure PEO. Preliminary

investigations into identifying the volatile degradation products

indicated that, in addition, to compounds evolved on the decomposition

of pure PEO (CO, formaldehyde, acetaldehyde and oligomeric fragments),

HCN, chain fragments with some cyanate or thiocyanate groups and a

large amount of CO_2 and ethane were produced on degradation of the

PEO:NaSCN complex. The products of complete degradation up to

$500^{\circ}C$ were accounted for in terms of a radical reaction initiated

by random scission of backbone bonds. Cameron and co-workers

proposed that the effect of the complex on decomposition is dominated

by the influence of the anion rather than the cation as i) replacing

Na^+ with Li^+ produced little if any change; ii) the nature of the

degradation products indicated SCN^- ions reacted chemically with PEO

at elivated temperatures; iii) the onset temperature of degradation

was lowered appreciably ($365^{\circ}C$ cf $320^{\circ}C$) when SCN^- was replaced

by the ClO_4^- anion.

As reviewed above, investigations with the thermal properties of

PEO:salt complexes have mainly concentrated on the effect the additive

has on the value of the Tg of the polymer. The thermal degradation

of PEO:salt blends and in particular, product formation during such

processes has been neglected. The aim of this chapter therefore is

to undertake a general survey into the thermal degradation of

several PEO:salt blends.   In addition to the commercial importance

of the processes occurring whereby PEO:complex based polyelectrolytes

degrade there is also academic interest in the effect of small molecule

additives on polymer degradation.   The effects of such additives

on the thermal decomposition of certain polymers has been reviewed by

McNeill.[16]   Particular interest is focussed on these systems in

which complexation can occur between the polymer and the additive as

in the case of metal halide- PMMA and PVAc blends investigated by

McNeill [195,196], McGuiness [195,196] and Liggat.[38]

5.2 THERMAL DEGRADATION OF PEO:SALT BLENDS

5.2.1 Experimental

Preparative Methods

Purification of Salt.

Zinc bromide (May and Baker Limited) and zinc chloride (B.D.H. Limited, AR grade) were dried by heating in vacuo at 150°C for twelve hours then purified by vacuum sublimation in the apparatus illustrated in Figure 5.6. This arrangement permitted the samples to be dried and sublimed in situ then transferred to a dry box thus keeping the purified salt free from atmospheric moisture.

Lithium perchlorate (B.D.H. Limited, Laboratory reagent) was dried for twelve hours at 200°C in vacuo before use.

Calcium bromide (Hopkin and Williams, Limited, Laboratory reagent), calcium chloride (Hopkin and Williams, Limited, Laboratory reagent), sodium bromide (May and Baker, Limited, analytical reagent), cobalt bromide (Hopkin and Williams, Limited, Laboratory reagent) and sodium thiocyanate (Aldrich) were dried at 100°C for fifteen hours prior to use.

Zinc oxide (Hopkin and Williams Limited, AR grade) was used without further purification.

Purification of Solvent.

Methanol was purified[197] by adding 50ml AR grade methanol to warm, dry magnesium turnings (5g) and iodine (0.5g) under argon. Once the iodine had disappeared and all the magnesium was converted to methoxide, 500ml methanol was added and the solution refluxed for twelve hours. As the system was kept free from moisture in an atmosphere of argon, samples of dry methanol were distilled off when required.
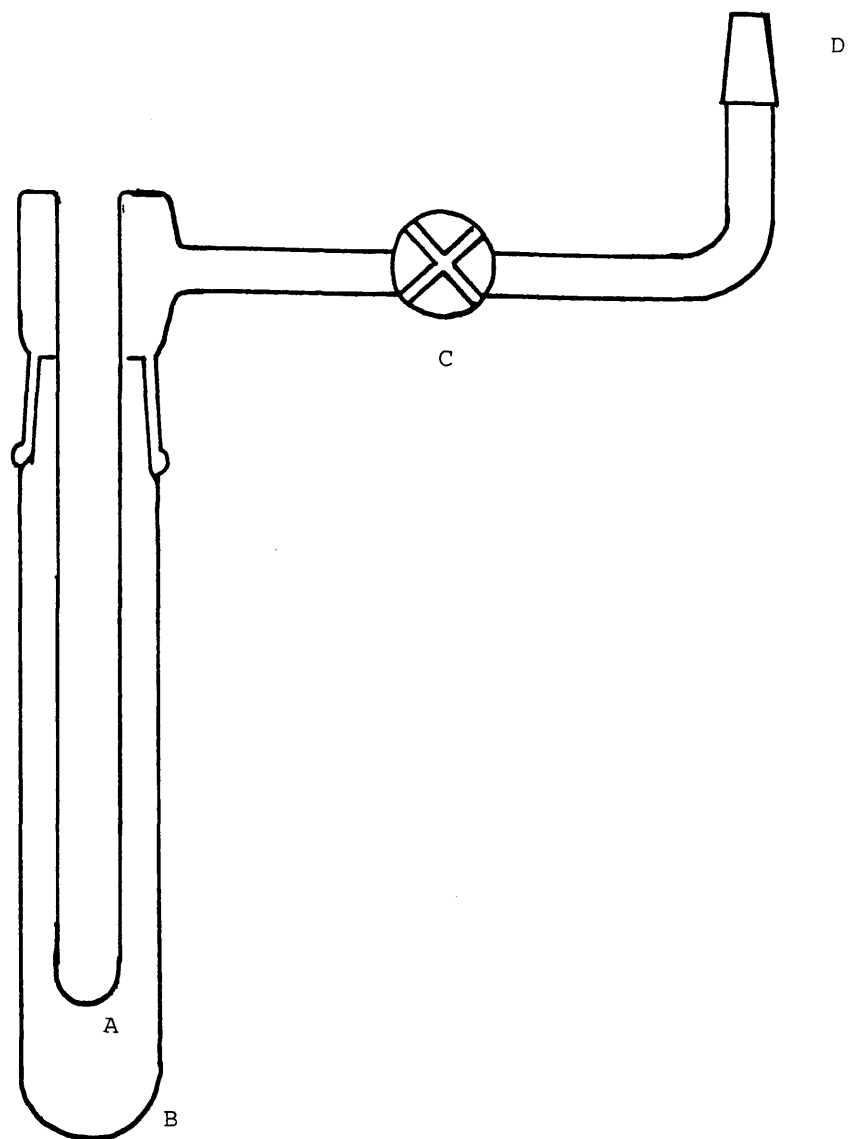
A	Cold Finger
B	Sample Container.
C	B14 Stopcock
D	B14 Cone to allow attachment to vacuum line.

Fig. 5.6   Sublimation Apparatus

Preparation of PEO : Salt Blends.

In the preparation of all PEO : salt blends, PEO was used without further purification, as in powder form it was more suitable for grinding in dry blends and more easily dissolved for casting films. In addition, the results from Chapter 3 indicate that reprecipitation did not affect the thermal degradation behaviour of PEO.

Two methods of blend preparation were employed - either casting a film from a common solvent or preparing a dry-blend by grinding both components together. PEO : salt film blends were prepared by making a standard solution of PEO in dry methanol and similar solutions for each salt. By mixing appropriate volumes of polymer and salt standard solutions the proportion of ethylene oxide units to salt could be varied as well as the sample size required for each analytical technique. A typical standard solution of PEO in methanol contained 0.4g ml of which 1 ml (+ 1 ml salt solution) would be used for a ^{TVA} experiment. Solvent was initially removed in a stream of dry nitrogen followed by pumping in vacuo.

Dry blends were prepared by adding PEO powder to a sample of finely ground additive and then thoroughly grinding the mixture together under a heating lamp. With very hygroscopic salts, the procedure was carried out in a dry-box. The blend was placed in a TVA tube and a special head (see Fig. 2.7) was then fitted. Finally the whole assembly was removed for attachment to a TVA/SATVA line.

Prior to degradation, each blend was heated to 150°C to remove any residual solvent or traces of water.

In every case the composition of the PEO : salt blend was based upon the ratio of the number of moles of ethylene oxide (EO) repeat unit to each mole of salt.

The type and composition of blend degraded is detailed in the thermal analysis section below.

5.2.2 Thermal Analysis of PEO : Salt Blends.

The thermal behaviour of nine PEO:salt blends was investigated using TVA, SATVA and TG techniques. During each analysis a standard heating rate of 10° min^{-1} was employed. The TG experiments were carried out in most cases on cast film samples which were preheated to $150^{\circ}C$ to ensure complete removal of solvent. Both preheat and analysis were carried out in an atmosphere of nitrogen. With PEO: ZnO blends, as there is no common solvent for both the polymer and salt, TG analysis was performed on thoroughly mixed dry powders. TVA and SATVA experiments were carried out using blends prepared as either films or in dry form. This is detailed in the relevant sections. Following SATVA separation, degradation products were identified using both IR spectroscopy and mass spectrometry.

Before the thermal behaviour of each blend was studied the behaviour of the individual component parts of the blend, that is, PEO and salt were examined. The thermal degradation of PEO has been studied in depth as reported in Chapter 3. The thermal behaviour of each salt was investigated by TVA and is considered where appropriate.

THERMAL ANALYSIS OF PEO:$ZnBr_2$ BLENDS

In PEO:$ZnBr_2$ systems, blends in the molar ratio of 10:1 EO to salt was studied initially. This ratio is of the order of those used in the preparation of polymeric electrolytes. As investigations proceeded the ratio was varied.

The thermal behaviour of ZnBr$_2$ was investigated by TVA. It has been shown by Brewer[198] that when ZnBr$_2$ is heated, it does not dissociate to zinc metal at its boiling point or dissociate to the monovalent state but instead sublimation takes place. TVA experiments were carried out on a 50mg dry powder sample of ZnBr$_2$. No volatile products were observed in the TVA trace however ZnBr$_2$ was found to sublime from the base of the TVA tube to the cold-ring-region. The sublimation of ZnBr$_2$ under TVA conditions was first observed at 306°C. This is comparable to the temperature of 323°C obtained by McGuiness[37] using the same method.

TVA Investigation of PEO : ZnBr$_2$ Blends.

The following three blends were studied:-

Blend 1. - was cast as a film from mixed solutions of PEO and ZnBr$_2$ in methanol to give a molar ratio of 10:1 EO:ZnBr$_2$.

Blend 2. - was cast as a film to give a molar ratio of 2:1 EO:ZnBr$_2$.

Blend 3. - was a dry blend prepared to give a molar ratio of 2:1 EO : ZnBr$_2$.

The TVA curves for blend 1, 2 and 3 are illustrated in Fig. 5.7 Fig. 5.8 and Fig. 5.9 respectively. The degradation temperatures are given in Table 5.1.

PEO:ZnBr$_2$ Blend.	Composition EO : ZnBr$_2$	T onset ($^{\circ}$C)	T max 1 ($^{\circ}$C)	Tsh ($^{\circ}$C)	Ts ($^{\circ}$C)	T max 2 ($^{\circ}$C)	T onset CRF ($^{\circ}$C)
1	10 : 1	228	346	373	-	-	323
2	2 : 1	205	252	-	292	316	235
3	2 : 1	183	232	-	287	308	230

Table 5.1 Degradation temperatures obtained by TVA for PEO:ZnBr$_2$ Blend 1, Blend 2 and Blend. 3.

332
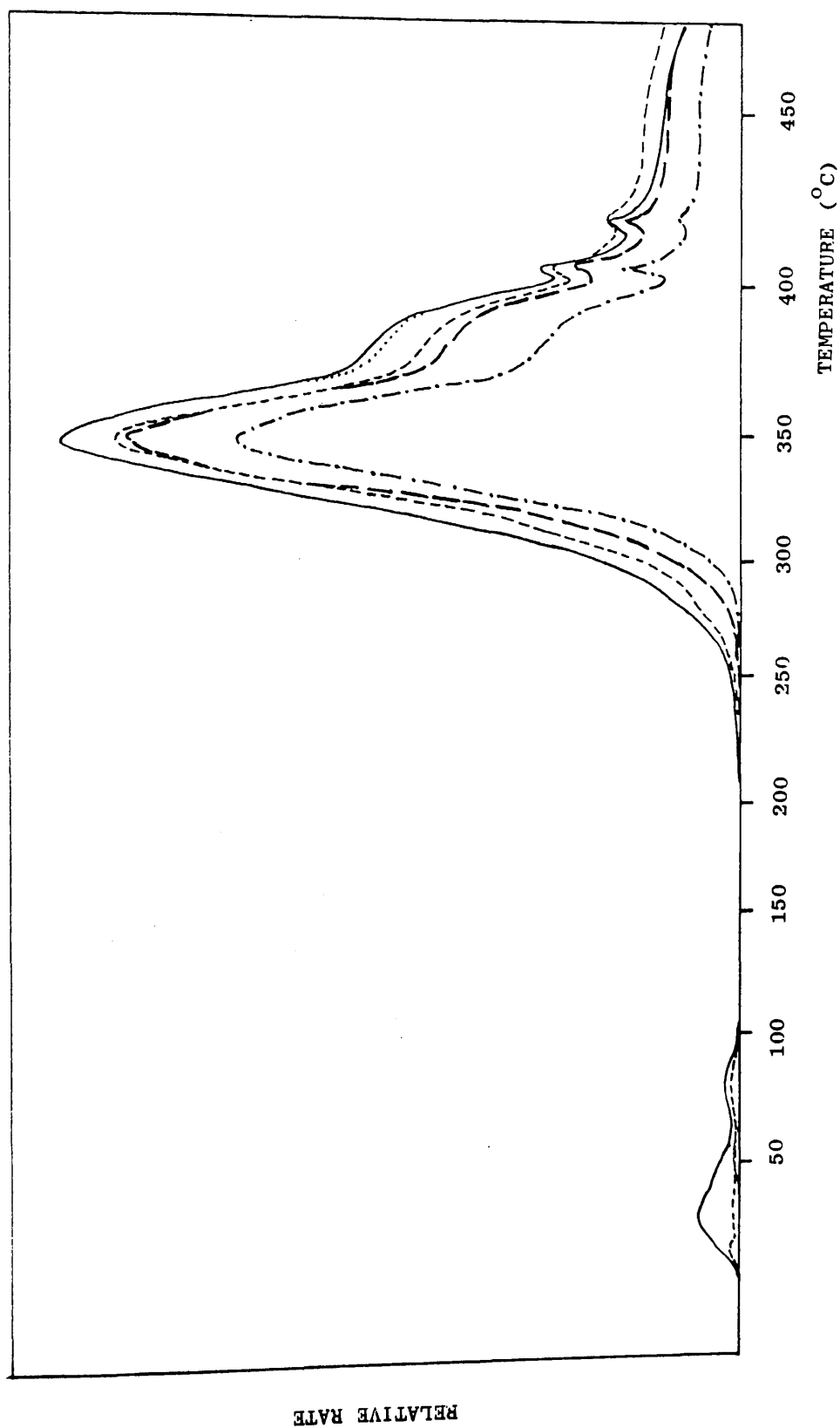
Fig. 5.7 TVA curve for PEO:ZnBr₂ Blend 1 10:1 EO:ZnBr₂ film cast from methanol.
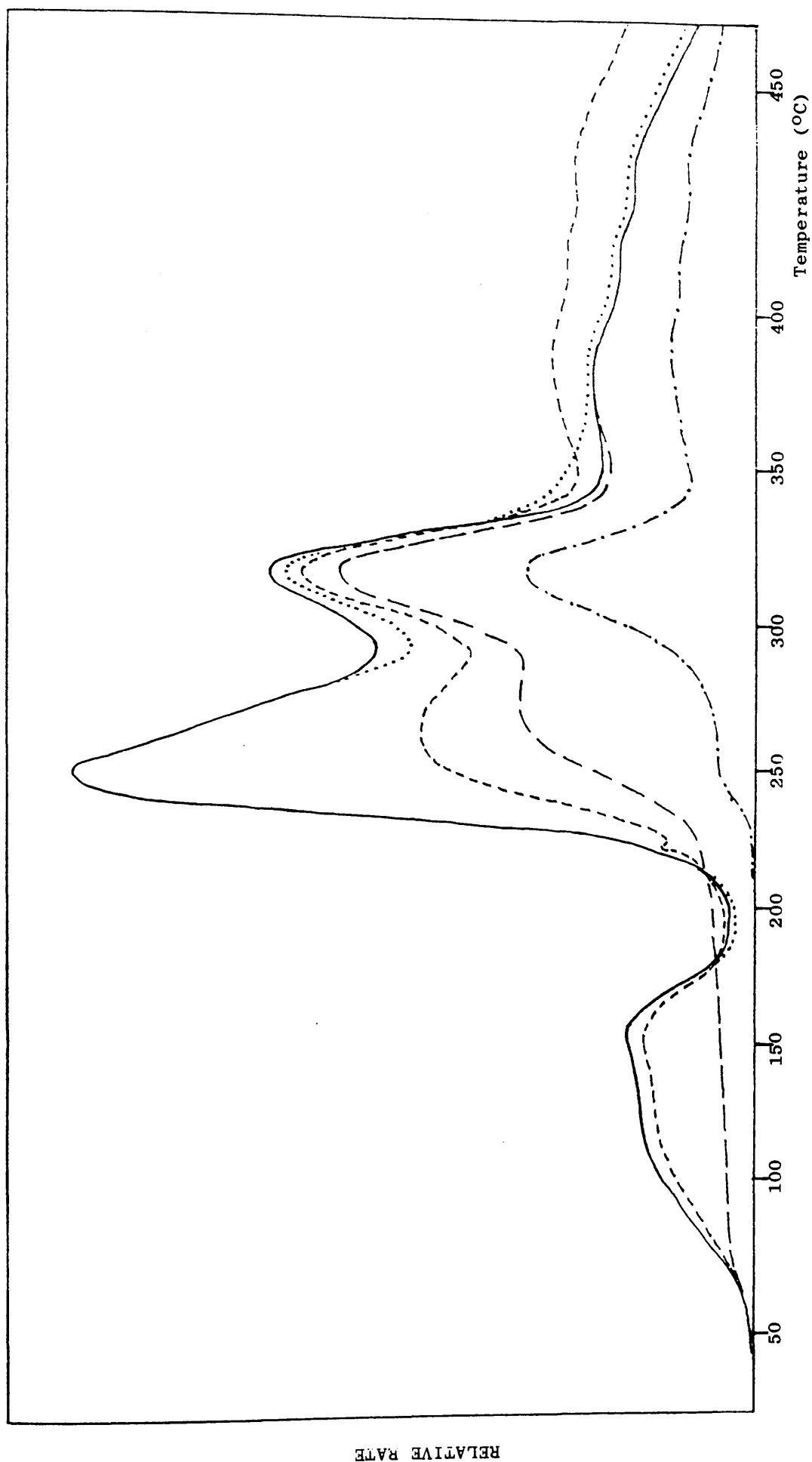
Fig 5.8. TVA curve for PEO:ZnBr$_2$. Blend 2 2:1 EO:ZnBr$_2$ film cast from methanol.
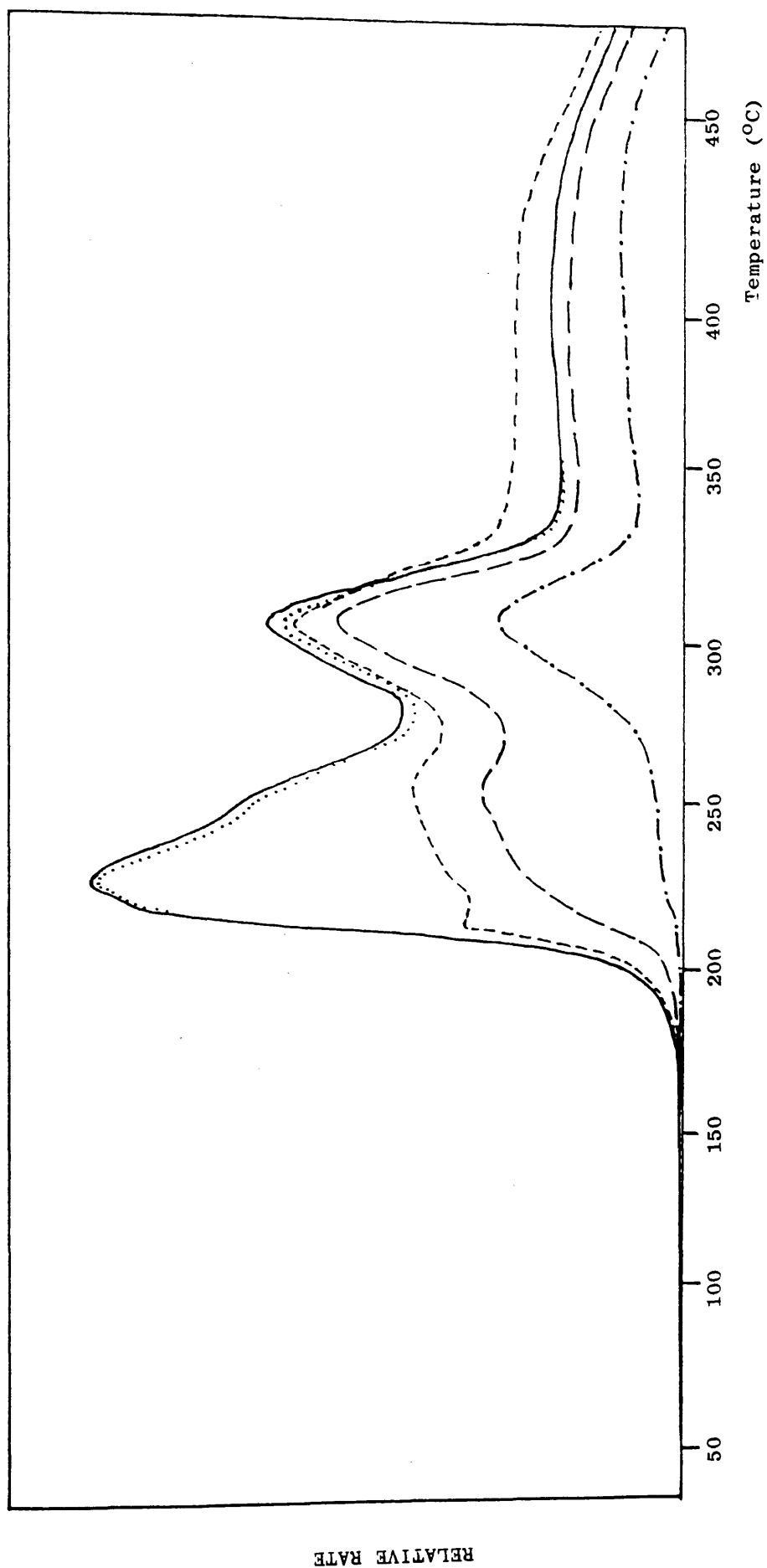
Fig. 5.9   TVA curve for PEO:ZnBr$_2$ Blend 3   2:1   EO:ZnBr$_2$ dry blend.

The TVA curve for Blend 1 (see Fig. 5.7) gave a single peak having a maximum evolution of volatile products at $346^{\circ}C$ and a shoulder following the main peak at $373^{\circ}C$. The small peak at $34^{\circ}C$ is due to traces of trapped solvent being evolved. Individual traces indicate a variety of products being produced on degradation including non-condensable products.

When the $ZnBr_2$ content of the blend is increased (see Fig. 5.8 and Fig. 5.9) a two stage degradation is clearly seen. In Blend 2, the main degradation peak is preceeded by a large solvent peak. The first degradation peak begins around $205^{\circ}C$ with a maximum rate of evolution of volatile compounds at $252^{\circ}C$. At this point the 0° and $-45^{\circ}C$ traces are coincident while the $-75^{\circ}C$ and $-100^{\circ}C$ traces are significantly suppressed relative to them. There is little evolution of non-condensable products which increases to a maximum during the second stage of degradation at $316^{\circ}C$. Towards the end of the decomposition there is a steady evolution of degradation products. There is also a limiting-rate effect seen in the $-75^{\circ}C$ trace.

The TVA trace obtained for the dry Blend 3 is virtually identical to that of solution Blend 2 which has the same composition although the onset temperature and peak maxima temperatures in the dry blend are slightly lower than those observed for the blend cast as a film.

TG of PEO:$ZnBr_2$ Blends

TG analysis was carried out on blends having an approximate ratio of EO:$ZnBr_2$ equal to 10:1 (Blend 1) and 2:1 (Blend 2). The TG and DTG curves obtained for the blends prepared as described in section 5.2.2 are illustrated in Fig. 5.10. A two stage degradation process

Fig 5.10   TG (━◆◆◆━) and DTG (.......) curves for PEO ZnBr$_2$ Blend 1
EO:ZnBr$_2$ 10:1 film cast from methanol.   TG (━━━) and
DTG (━ ━ ━) curves for PEO:ZnBr$_2$ Blend 2   EO:ZnBr$_2$ 2:1 film
cast from methanol.
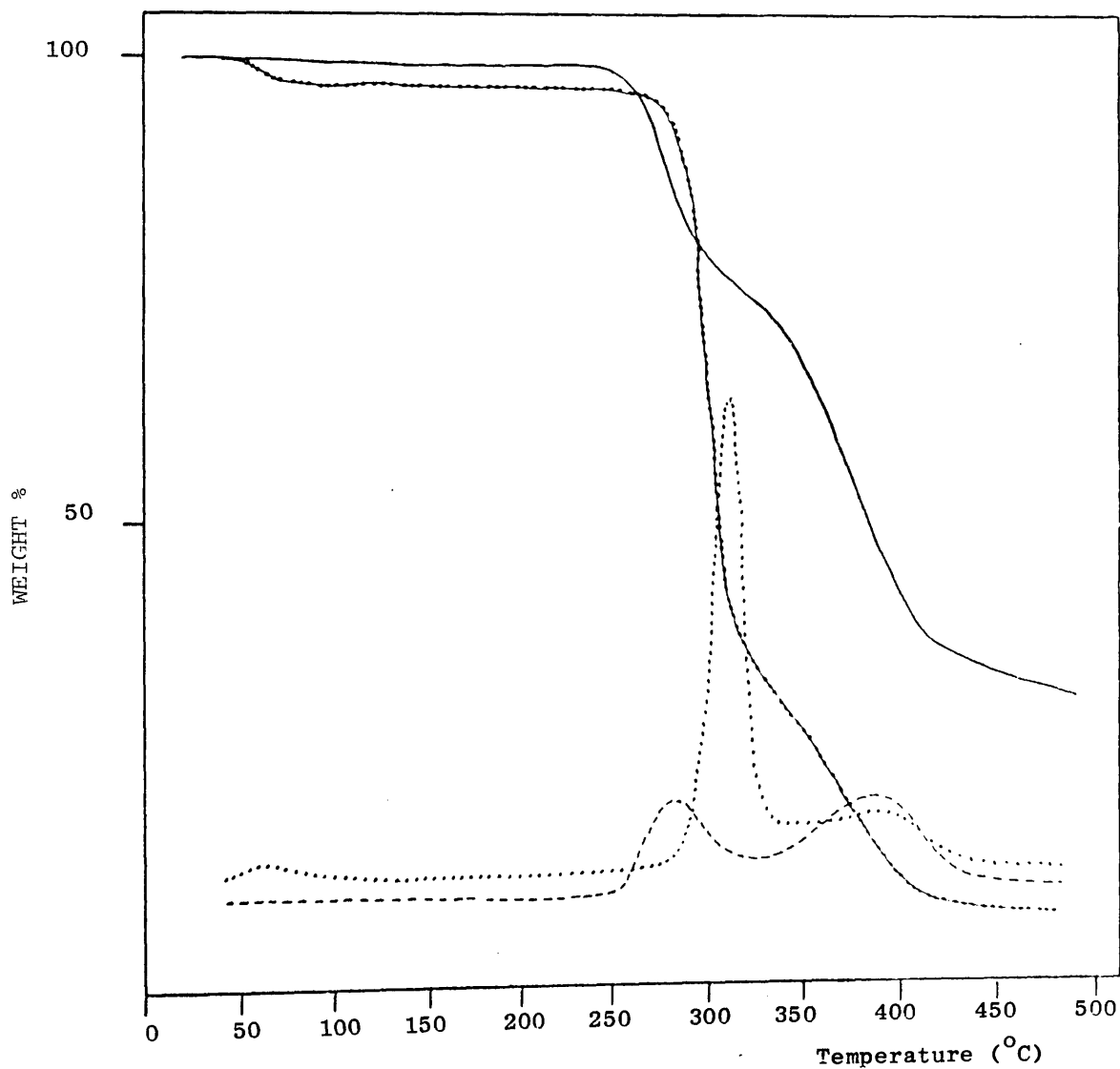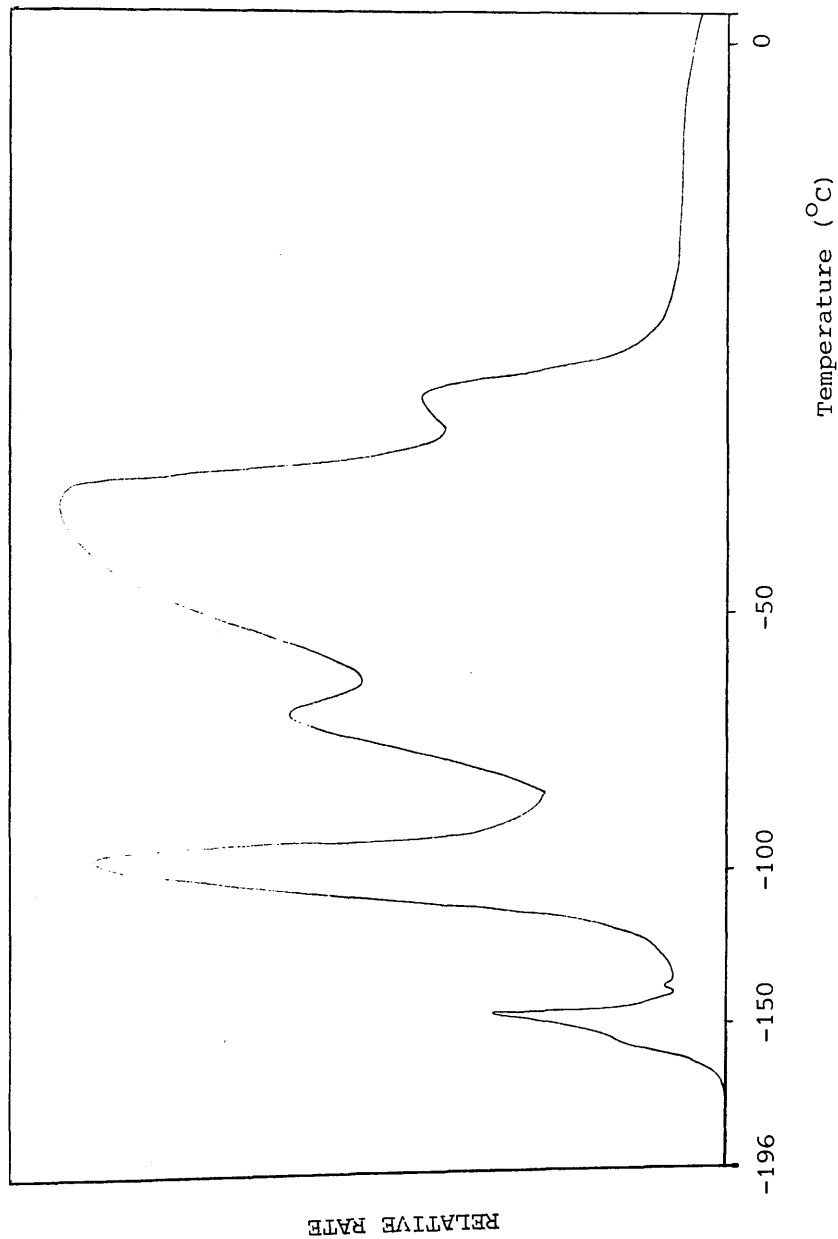
Fig 5.11 SATVA trace for condensable degradation products on heating PEO:ZnBr$_2$ blend (EO:ZnBr$_2$ 10:1, 2:1) to 500°C.

is observed from the TG and DTG curves obtained from Blend 1, the
first decomposition being the dominant stage.   The onset of
degradation occurs at approximately 265°C and has a rate maximum at
309°C.   The residue, after degradation to 500°C amounts to 7.5% by
weight of the original polymer blend.

At higher $ZnBr_2$ content, Blend 2, TG and DTG data reveal the
second stage weight loss degradation process to be more dominant.
The first weight loss occurs at approximately 245°C reaching a maximum
rate at 278°C.   The onset of the second weight loss stage is less
clearly defined but is in the region of 300°C with a maximum evolution of
volatile compounds at 386°C.   After heating to 500°C under nitrogen, 30%
by weight of residue remains.

SATVA Products Separation of PEO:$ZnBr_2$ Blends.

The SATVA traces using 80-100mg PEO samples with the appropriate
weight of $ZnBr_2$ for Blend 1, Blend 2 and Blend 3 were very similar, the
only difference being poorer resolution between the peaks due to the final
three fractions in the blends of high $ZnBr_2$ concentration.   This is
illustrated in Fig. 5.11.   The trace indicates five fractions and is
shown diagramatically in Fig. 5.12 illustrating the fraction boundaries.
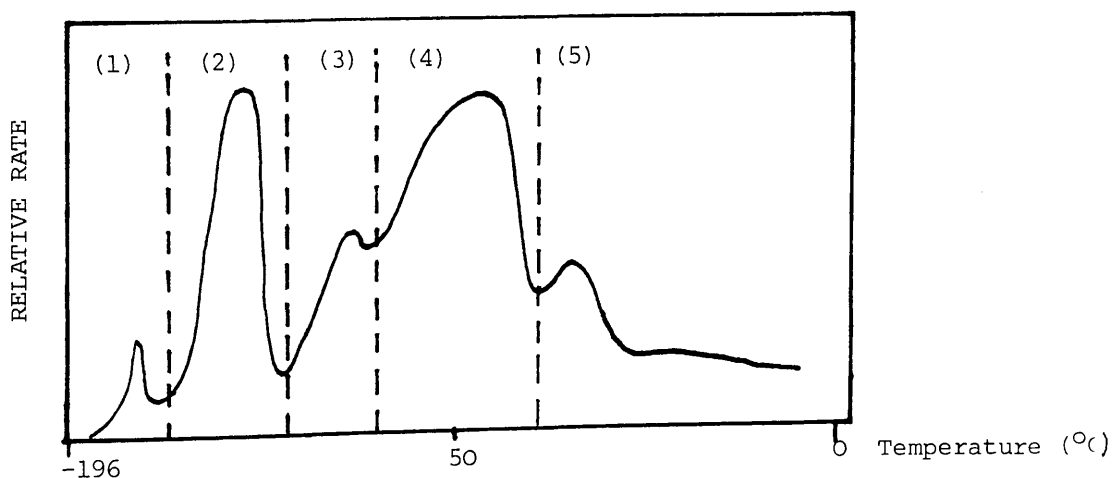
Fig. 5.12   SATVA trace for condensable degradation products from PEO:
$ZnBr_2$ blend indicating fraction boundaries.

The degradation products were identified from IR spectroscopy and MS data. The IR absorption frequencies and MS ^{m}/e values used in product identification are listed in Tables 5.2 to 5.6.

The first fraction was found to comprise CO_2 and ethene with traces of ketene and ethyne. The large peak giving rise to fraction 2 was due to acetaldehyde, however, traces of HBr, methyl- and ethylbromide were also present as revealed by MS (see Table 5.3b). There was also present in the IR spectrum a winged absorption band at 742 cm^{-1} not attributable to acetaldehyde (see Table 5.3a). Identification of the compound(s) in fraction 3 was extremely difficult due to the overlap in SATVA peaks, nevertheless an ether absorption band at 1145 cm^{-1}, CH_2 bending absorptions at 1410 cm^{-1} and a carbonyl stretching band at 1725 cm^{-1} were observed. The mass spectrum gave a base peak at ^{m}/e = 29 with other strong peaks at ^{m}/e = 43 (93.8%), ^{m}/e = 45 (71.0%), ^{m}/e = 28 (57.8%) and ^{m}/e = 15 (49.0%). This confirms the presence of aliphatic aldehyde and ether compounds. The fourth fraction, a colourless liquid, was found to be due to dioxane. Traces of 2-bromo-ethanol however were also present. The final fraction was difficult to identify for the reasons described above, but in addition, the fraction was unstable. It was initially a colourless liquid which, even after removal from the SATVA line using the modified cold finger (see Fig. 2.17) turned yellow through red-brown until finally remained brown during spectral analysis. However water was identified as a major component with ether and aldehyde compounds also present.

IR Absorbance Frequency (cm^{-1})	Product or Band Assignment
2960 (m) 2865 (m)	CH_2 stretching
3720 (w) 3620 (w) 2320 (m) 719 (w) 670 (w)	CO_2
2160 (w) 2140 (w)	H_2CCO
940 (w)	$CH_2=CH_2$
928 (m)	$HC\equiv CH$

Table 5.2a : IR Spectrum of Fraction (1) from SATVA Trace of PEO:ZnBr$_2$ Blend.

$^m/e$ Value.	% Base	Product or Fragmentation Ion.
44	100	CO_2
42	51.16	H_2CCO
41	83.14	
40	17.91	
28	78.38	C_2H_4
27	38.25	
26	22.44	HCCH
39	52.05	unidentified

Table 5.2b : Mass Spectrum of Fraction (1) from SATVA trace of PEO:ZnBr$_2$ Blend.

Absorbance Frequency (cm^{-1})   Product or Band Assignment.

3470 (w)	3070 (w)	3010-2990 (m)	
2940 (m)	2800 (s)	2720 (s)	
1760 (s)	1750 (s)	1735 (s)	CH_3CHO
1410 (s)	1365 (s)	1350 (s)	
1100 (s)	880 (m)		
744 (m)			unidentified

Table 5.3a
IR Spectrum for Fraction (2) from SATVA of PEO:ZnBr$_2$ Blend.

$^m/e$ Value.	% Base	Product or Fragmentation Ion.
29	100.00	
44	94.42	
43	60.66	CH_3CHO
42	18.61	
26	16.19	
41	15.79	
94	8.09	
96	7.52	CH_3Br
79	1.29	
81	1.20	
110	0.99	
108	1.04	
29	100.00	C_2H_5Br
27	14.18	
79	1.29	
81	1.20	
82	0.23	
80	0.21	HBr
81	1.20	
79	1.29	

Table 5.3b
Mass Spectrum of Fraction (2) from SATVA of PEO:ZnBr$_2$ Blend.

Absorbance Frequency (cm^{-1})	Product or Band Assignment
2980 (s) 2885 (s)	CH$_3$CH$_2$ stretching
2730 (m) 2710 (m)	CH stretching
1760 (m) 1748 (m) 1737 (m)	CH$_3$CHO
1725 (s) 1715 (s)	aldehydic C=O stretching
1410 (s)	CH$_2$ bending
1143 (s) 1100 (sh) 1035 (m)	C-O stretching
828 (m)	unidentified
723 (w)	unidentified

Table 5.4a

IR Spectrum Frequencies for Fraction (3) from SATVA of PEO:ZnBr$_2$ Blend

^{m}/e value	% Base	Product or Fragmentation Ion
29	100.0	
88	7.9	
87	8.6	C$_2$H$_5$OCH$_2$CHO
59	4.2	
43	93.8	
29	100.0	
74	4.0	
59	4.2	CH$_3$OCH$_2$CHO
45	71.0	
15	49.0	
58	33.4	
30	8.9	
28	57.8	

Table 5.4b

Mass Spectrum of Fraction (3) from SATVA of PEO:ZnBr$_2$ Blend.

Absorbance Frequency (cm^{-1})   Product or Band Assignment

2970 (s)	2920 (m)	2900 (m)	2865 (s)
2750 (w)	2670 (w)	1453 (w)	1376 (w)
1290 (w)	1255 (m)	1140 (s)	1053 (w)
890 (s)	880 (w)		

Table 5.5a
IR Spectrum for Fraction (4) from SATVA trace of PEO:ZnBr$_2$ Blend.

^{m}/e value	% Base	Product or Fragmentation Ion
28	100.0	
29	19.2	
88	56.3	
58	29.9	
31	10.7	
89	2.1	$CH_3CH_2OCH_2CH_2O\cdot$
91	0.2	unidentified

Table 5.5b
Mass Spectrum of Fraction (4) from SATVA trace of PEO:ZnBr$_2$ Blend.

Absorbance Frequency (cm^{-1})   Product of Band Assignment

| 3400 (s) | 1640 (m) | | | | H_2O |

2965 (m)	2915 (w)	2890 (w)	2860 (m)
2760 (w)	2690 (w)	1445 (m)	1365 (m)
1288 (m)	1254 (m)	1115 (s)	885 (s) 868 (s)

| 1094 (s) | 1080 (s) | 1040 (s) | 1030 (s) | unidentified |

Table 5.6a
IR Spectrum of Fraction (5) from SATVA trace of PEO:ZnBr$_2$ Blend.

$^m/e$ value	% Base	Product or Fragmentation Ion
126	1.9	
124	2.1	
109	0.5	
108	1.2	
107	0.4	
106	1.4	$BrCH_2CH_2OH$
95	12.6	
93	2.4	
81	8.9	
79	3.0	
45	59.7	
31	100.0	
18	91.2	H_2O
96	47.2	unidentified
68	84.7	unidentified
59	29.3	$CH_2 = \overset{+}{O} -C_2H_5$
45	59.7	$CH_3CH=\overset{+}{O}H \quad .CH_2CH_2-OH$ $CH_3\overset{+}{O} = CH_2$
43	48.2	CH_3CO^{+}
44	41.1	CO_2
39	44.8	unidentified
59	29.3	
45	59.7	
31	100.0	$CH_2 = \overset{+}{O} C_2H_5$
29	78.8	
15	36.6	

Table 5.6b
Mass Spectrum of Fraction (5) from SATVA trace of PEO:ZnBr$_2$ Blend.

The CRF of Blend 1 collected in two distinct regions, a lower paler brown band (CRFa) and an upper brown band (CRFb). Both materials were tacky solids. IR spectra were obtained for each of these, run in the form of KBr discs. These are illustrated in Fig. 5.13. The IR spectrum for the lower CRF region was very similar to that for the CRF obtained from pure PEO. Broad absorption bands at 3440 cm^{-1} and 1615cm^{-1} are attributed to H_2O either absorbed on exposure to the atmosphere or present in the KBr.

Strong absorption bands observed at 2900cm^{-1} and 2870cm^{-1} are due to CH_2 stretching vibrations, while the bands at 1480cm^{-1}, 1350cm^{-1}, 1290cm^{-1} and 1240cm^{-1} are assigned to CH_2 bending and twisting deformations. The strongest absorption in the spectrum is at 1100cm^{-1} and is due to a C-O-C stretch.

IR spectra of CRFa of the blend and CRF of pure PEO, differ in the absence of bands at 1323cm^{-1} and 1205cm^{-1} in the spectrum obtained for the blend CRFa. These bands are assigned to CH_2 wagging and CH_2 twisting respectively.

The IR spectrum for the upper region, CRFb, showed much stronger hydroxyl absorptions which is likely to be due to water being absorbed while the previous sample was being prepared for IR analysis. The spectrum for CRFb, although poorer, shows similarities to that for CRFa having strong ether absorptions at 1100cm^{-1} but has an additional broad absorption band at $\approx$500cm^{-1}. This new band is attributed to C-Br bonds.

The CRF for Blend 2 and Blend 3 formed similar brown bands as in Blend 1. The main features in both IR spectra (see Fig. 5.13) are strong absorption bands at $3530cm^{-1}$ and $3465cm^{-1}$ which are assigned to hydroxyl groups, most probably H_2O, and a very sharp band at $1600cm^{-1}$. The latter is attributed to $ZnBr_2$. Other strong absorption bands observed at $538cm^{-1}$ and $518cm^{-1}$ are assigned to C-Br bonds, whilst that at $360cm^{-1}$ remains unidentified. Absorption bands at $1115cm^{-1}$ and $1065cm^{-1}$ indicate ether structures. In all blends, especially when larger sample sizes, i.e. blends containing 100mg PEO were used, a zinc mirror was noticed in the upper region of the cold ring area and occasionally zinc was found to coat regions in the subambient trap. To avoid the latter effect a hollow stopper was inserted into the socket of the TVA tube head assembly.

The residues obtained on heating all three blends to $500^{\circ}C$ under TVA conditions were black lustrous solids. IR spectra for residues produced from Blend 1 and Blend 3 are shown in Fig. 5.14. The major absorptions in both spectra, excluding that for absorbed H_2O ($3420cm^{-1}$) occur at $2920cm^{-1}$ and $2870cm^{-1}$ due to aliphatic CH_2 stretching, $1595cm^{-1}$ from unsaturated CH absorptions, $1100cm^{-1}$ arising from C-O-C stretching and finally a strong absorption band at $460cm^{-1}$ which is attributed to ZnO.
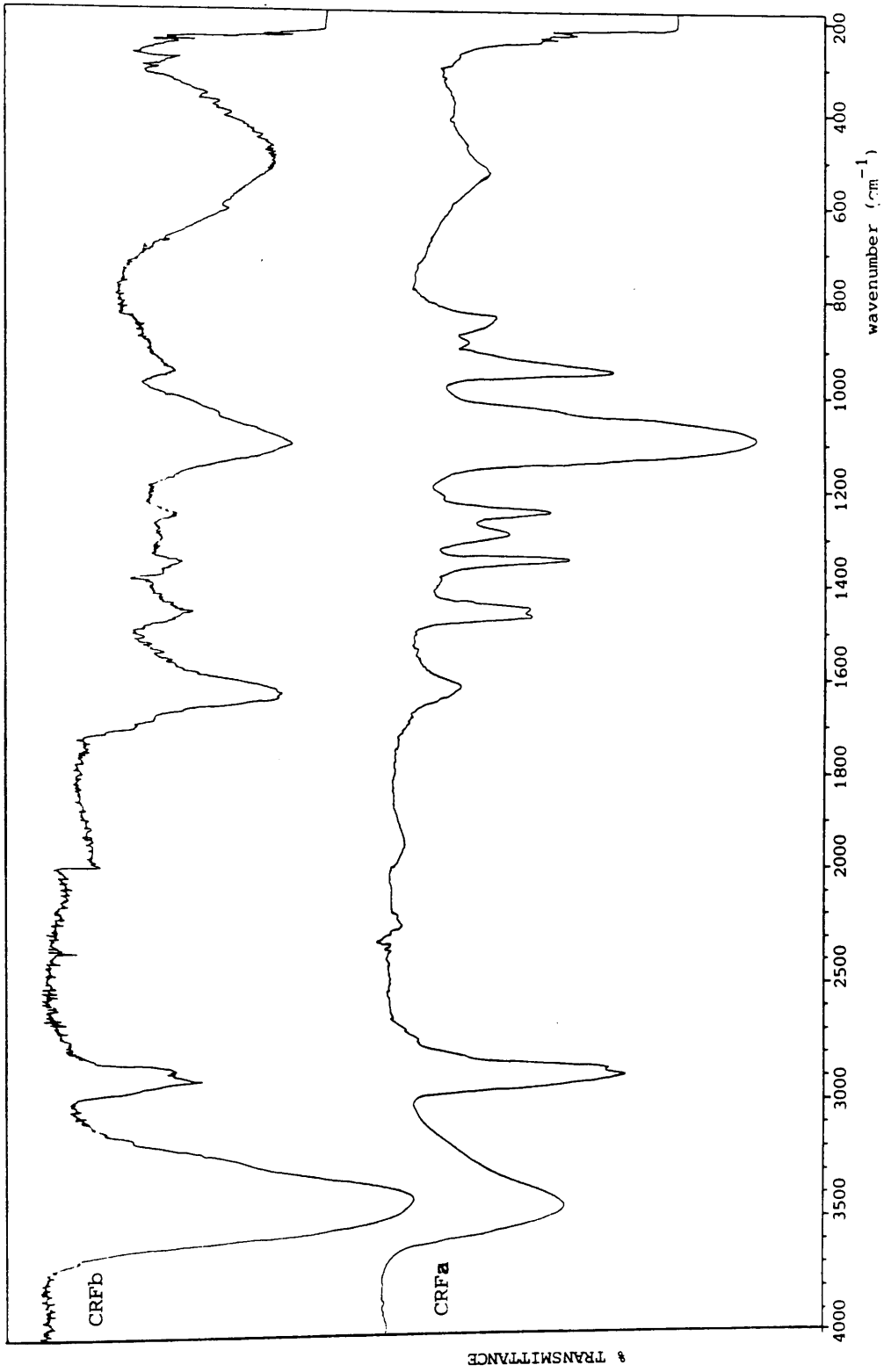
Fig. 5.13   IR spectra of CRFa and CRFb obtained from the degradation of PEO:ZnBr$_2$ Blend 3 run as KBr disc.
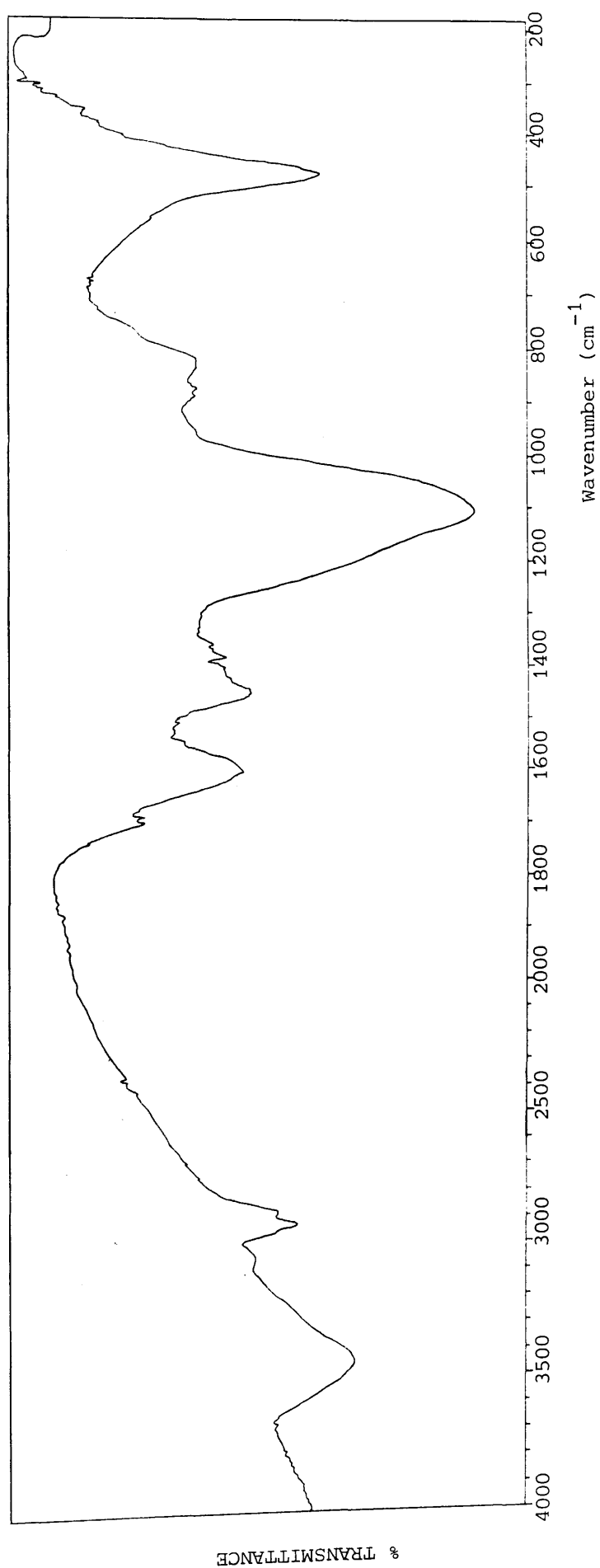
Fig 5.14 IR spectrum for residue obtained on heating PEO:ZnBr$_2$ Blend 1 or 3 to 500°C run as KBr disc.

TVA Product Separation of PEO:ZnBr$_2$ Blend 2.

The TVA and TG results for blends containing a high ZnBr$_2$ content (i.e. 2:1 EO:ZnBr$_2$ ratio) show a multistage degradation process. In order to elucidate the mode of degradation, a TVA experiment was carried out in which the total products contributing to each peak in the TVA trace were collected and analysed by IR spectroscopy. The peak boundaries are illustrated in Fig. 5.15.
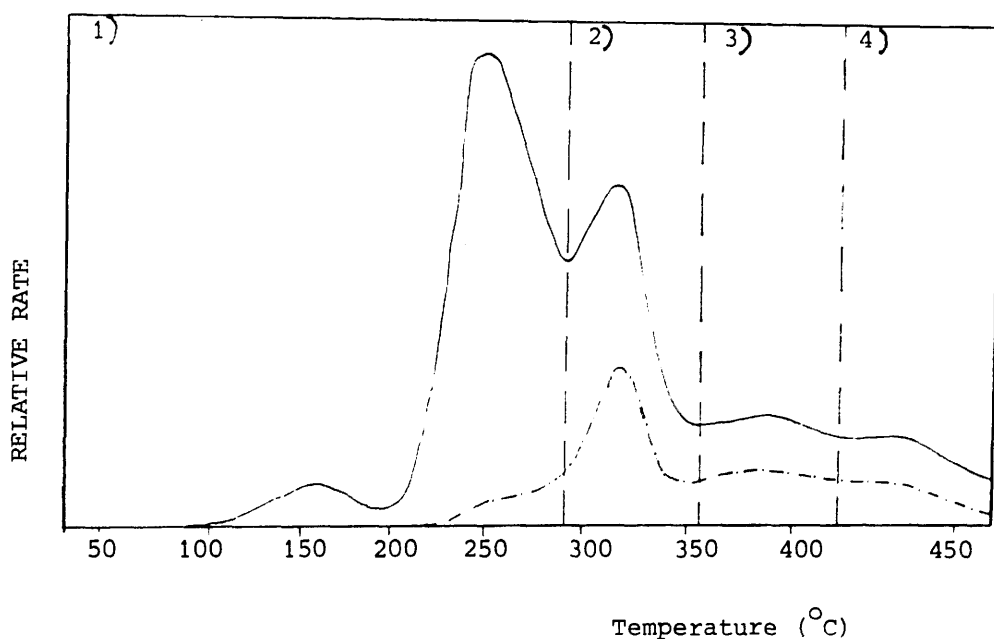
Fig. 5.15 TVA curve for PEO:ZnBr$_2$ 2:1 Blend cast from methanol indicating total product fraction boundaries.

The 2:1 EO:ZnBr$_2$ blend was cast as a film from methanol then the total products from each TVA peak produced on heating to 500°C were isolated. The small peak in the first fraction was due to traces of methanol (solvent) slowly evolving from the film on warming. The products of the first degradation fraction were found to be acetaldehyde, dioxane and carbon dioxide. In the second fraction, acetaldehyde and carbon dioxide were present, however, dioxane production had ceased. There was also an additional unidentified minor product as seen by a winged absorption band at

745cm^{-1} in the IR spectrum.   In the remaining two fractions, only acetaldehyde could be positively identified.

Partial Degradation of PEO:ZnBr$_2$ Blend 1 and Blend 2.

Investigations into the degradation behaviour and product formation in partially degraded blends were carried out.   For these studies programmed heating conditions ($10^\circ \text{ min}^{-1}$) were employed.

a) Product Formation During Stages of Degradation.

Blend 1 was heated to 346°C.   The SATVA trace obtained featured four fractions, the small first peak in the SATVA trace on full degradation of the blend i.e. to 500°C being absent.   On IR analysis, the first fraction in the partial degradation SATVA trace was found to be due to acetaldehyde.   The second fraction was poorly resolved from the third and appeared on a shoulder, however, strong absorption bands in the IR spectrum at 1720cm^{-1} and 1132cm^{-1} suggests compounds having aldehydic and ether type structures to be present.   Due to the small amount of final fraction, the two remaining fractions were collected together. From the resultant spectrum dioxane was clearly identifiable but the presence of an aldehydic compound was also noted, by an absorption band at 1740cm^{-1}.   The IR spectrum obtained for the CRF was identical to that for the CRFa obtained on complete degradation of Blend 1.   The residue remaining after partial degradation was a tacky black solid which gave an IR spectrum very similar to that obtained for the CRF, the only difference being an increase in the absorbance band at 790cm^{-1} and the appearance of a weak absorption at 1598cm^{-1} in the spectrum due to unsaturation.

Blend 2 was heated to 256°C. The resultant TVA trace gave five fractions as in the complete degradation of the blend. The very small first peak was attributed to CO_2 production and acetaldehyde was identified in the second sharp peak. The third and fourth fractions were poorly resolved, the third fraction appearing as a preceding shoulder. This fraction contained a mixture of acetaldehyde and dioxane. The final fraction appeared to be due to carbonyl and ether compounds of low volatility. Negligable CRF was formed. The black shiny residue gave an IR spectrum very similar to that obtained on the partial degradation of Blend 1.

b) PEO:Salt Blend Structural Changes During Stages of Degradation.

To investigate any structural changes occuring in the polymer:salt blend during degradation, partial degradation studies were carried out in thin films cast from methanol on a NaCl plate. A 2:1 EO:$ZnBr_2$ blend was prepared and a film formed in which approximately 8 mg PEO was deposited on the salt plate. This sample size was found to give a good IR spectrum. The total products evolved at each stage of heating were also collected for analysis to assist elucidating the mechanism of degradation of blend. The temperatures reported are oven temperatures which, when taking into account the thermal insulating effect of the base of the TVA tube and the salt plate onto which the blends were cast, are approximately 40°C higher than those for the sample.

The film was left under vacuum (rotary pump) for four days to remove solvent. At this stage, prior to heating, the film was opaque which may be an indication that the components of the

blend at this high salt ratio, were incompatable at room
temperature.

IR analysis of the film resulted in a poorly defined
spectrum on comparison with spectrum obtained from pure PEO cast
in a similar fashion as a film from methanol. The CH and CO band
absorption frequencies in the spectrum of the blend were shifted
slightly in the presence of $ZnBr_2$. The IR spectrum of the blend
showed strong CH_2 antisymmetric and symmetric stretching absorptions
at $2915cm^{-1}$ and $2875cm^{-1}$ compared to shoulder and strong absorptions
at $2950cm^{-1}$ and $2890cm^{-1}$ for these assignments in pure PEO. The
CH_2 bending deformation was slightly lower in frequency in the blend
sample occuring at $1450cm^{-1}$ rather than $1468cm^{-1}$. In the PEO
spectrum the CH_2 wagging deformations appear as a doublet absorption
at $1360cm^{-1}$ and $1345cm^{-1}$ whereas in the case of the blend a single
peak is seen at $1345cm^{-1}$. The intensities of the medium and
weak CH_2 twisting absorptions at $1281cm^{-1}$ and $1244cm^{-1}$ in PEO are
reversed in the spectrum of the blend (1275(w) and 1245(m)). The
presence of weak and medium to strong absorption bands at $1275cm^{-1}$ and
$1245cm^{-1}$ in the IR spectra of PEO:Salt complexes has previously
been reported by Papke et al.[153] The strongest peak in the spectrum
of PEO:$ZnBr_2$ was that due to C-O-C stretching. In PEO, three C-O
stretching absorptions are clearly visible in the IR spectrum at
$1149cm^{-1}$ (asymmetric stretch), $1112cm^{-1}$ (symmetric stretch) and
$1062cm^{-1}$. The blend, however, shows a single peak at $1072cm^{-1}$.
Finally the CH_2 rocking deformations at $966cm^{-1}$ and $845cm^{-1}$ in PEO
are lowered to $940cm^{-1}$ and $825cm^{-1}$ in the blend. The latter of
these rocking deformations is much reduced in the blend. In
addition to the absorption bands assigned to PEO, a strong broad

absorption band at $3400cm^{-1}$ and a sharper band at $1618cm^{-1}$ were present. These were attributed to the presence of residual methanol and water.

The blend was initially heated to $232^{\circ}C$ after which point, the evolution of solvent and any adsorbed water had virtually ceased. The film now appeared transparent. The absorption bands at $3400cm^{-1}$ and $1618cm^{-1}$ in the IR spectrum of the blend were very much reduced and the other spectral bands remained unchanged. The IR spectrum of the blend is shown in Fig. 5.16.

On heating to $333^{\circ}C$, a slight white smear was noted on the cold ring region of the TVA tube. This was attributed to $ZnBr_2$ subliming from the blend. There was no difference in the IR spectrum of the film from that previously obtained and the film remained transparent. The film began to discolour, turning pale brown, when it was heated to $351^{\circ}C$. Up to this temperature no CRF attributable to PEO degradation had formed yet although dioxane and a trace of acetaldehyde were observed as degradation products. The IR spectrum of the "residual" film remained unchanged, but because of the cut-off point in the IR spectral region at $\sim600cm^{-1}$ due to the NaCl plate used in the experiment, it was not possible to observe any C-Br absorptions which occur in the range $750-500cm^{-1}$.

When the film was heated to the temperature of the T(max) of the first degradation peak in the TVA curve ($420^{\circ}C$ oven temperature i.e. sample temperature of $380^{\circ}C$) a dark brown residue was obtained. At this stage in the degradation, the IR spectrum of the remaining film was much weaker however medium intensity C-H absorption
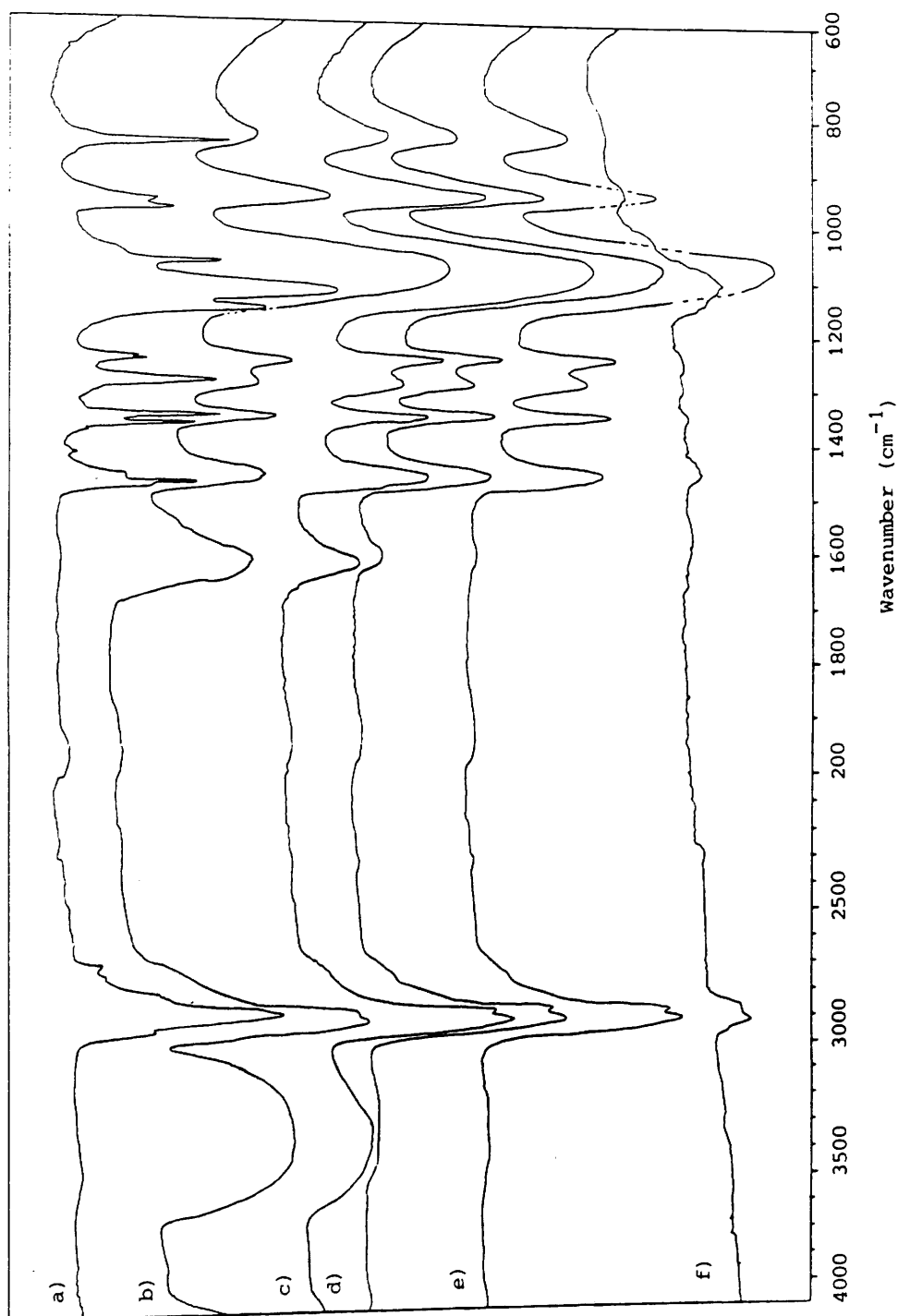
Fig 5.16 IR spectrum of. a)PEO b) PEO:ZnBr$_2$ blend EO:ZnBr$_2$ 2:1 and c)-f) PEO:ZnBr$_2$ blend heated to 232°C, 333°C, 351°C and 500°C.

bands at 2920cm^{-1} and 2850cm^{-1} together with a C-O-C absorption band at 1100cm^{-1} were clearly visible but no signs of any carbonyl group or unsaturation. In addition to dioxane, acetaldehyde was evolved during the decomposition.

On complete degradation, i.e. heating to 500°C a black solid was obtained. There was no indication of dioxane in the degradation products although acetaldehyde was observed.

The IR spectrum of the residues obtained on heating to the various forementioned temperatures are reproduced in Fig. 5.16.

THERMAL ANALYSIS OF PEO:$ZnCl_2$ BLENDS.

Following the results obtained from the thermal degradation of PEO:$ZnBr_2$ blends, interest was focussed on high salt:polymer repeat unit ratios as this had given the most interesting degradation behaviour. Thus in the PEO:$ZnCl_2$ systems a blend of 2:1 EO:salt was chosen. Both dry blends and blends cast as films were used. Dry blends were prepared by mixing and thoroughly grinding freshly sublimed $ZnCl_2$ and dry PEO in a glove box. For film samples appropriate weights of PEO (to give a concentration of 40 mg ml^{-1}) and $ZnCl_2$ were weighed into volumetric flasks in a dry atmosphere and made up to volume with dry methanol. Portions of these solutions were mixed to give sample sizes of 50 mg and 80-100 mg PEO for TVA and SATVA experiments respectively. Similar sample sizes of PEO with the appropriate weight of salt were used in dry blends.

Thermal Behaviour of $ZnCl_2$

A TVA experiment was carried out on 50 mg dry $ZnCl_2$. As for $ZnBr_2$ no volatile decomposition products were evolved, instead $ZnCl_2$ started to sublime to the cold ring region at 289°C under the conditions employed.

TVA Investigation of PEO:$ZnCl_2$ Blend.

The TVA curves for dry blends and blends cast as film from methanol in the molar ratio 2:1 EO:Salt were identical in appearance. Although not as clearly defined as for the PEO:$ZnBr_2$ blends of the same composition, a two stage decomposition was evident. The TVA curve for a typical 2:1 EO:$ZnCl_2$ blend is illustrated in Fig. 5.17. The evolution of volatile products begins at 206°C (on average) and reaches a maximum at 254°C. During this first degradation step the 0°C and -45°C traces are almost coincident and well elevated from the non-coincident 175° and -100°C traces. These latter two traces appear more as a shoulder onto the second peak rather than a distinct peak. There is negligable non-condensable product formation during the first stage of degradation. From the 0°C trace the evolution of volatile products in the second and major stage in the decomposition commences at 269°C with an average peak maximum at 322°C. During this stage the -75°C and -100°C traces are coincident and register a more significant pressure. There is also an evolution of non-condensable products. These features indicate a change in product composition during the degradation. The onset of CRF production is at approximately 253°C.
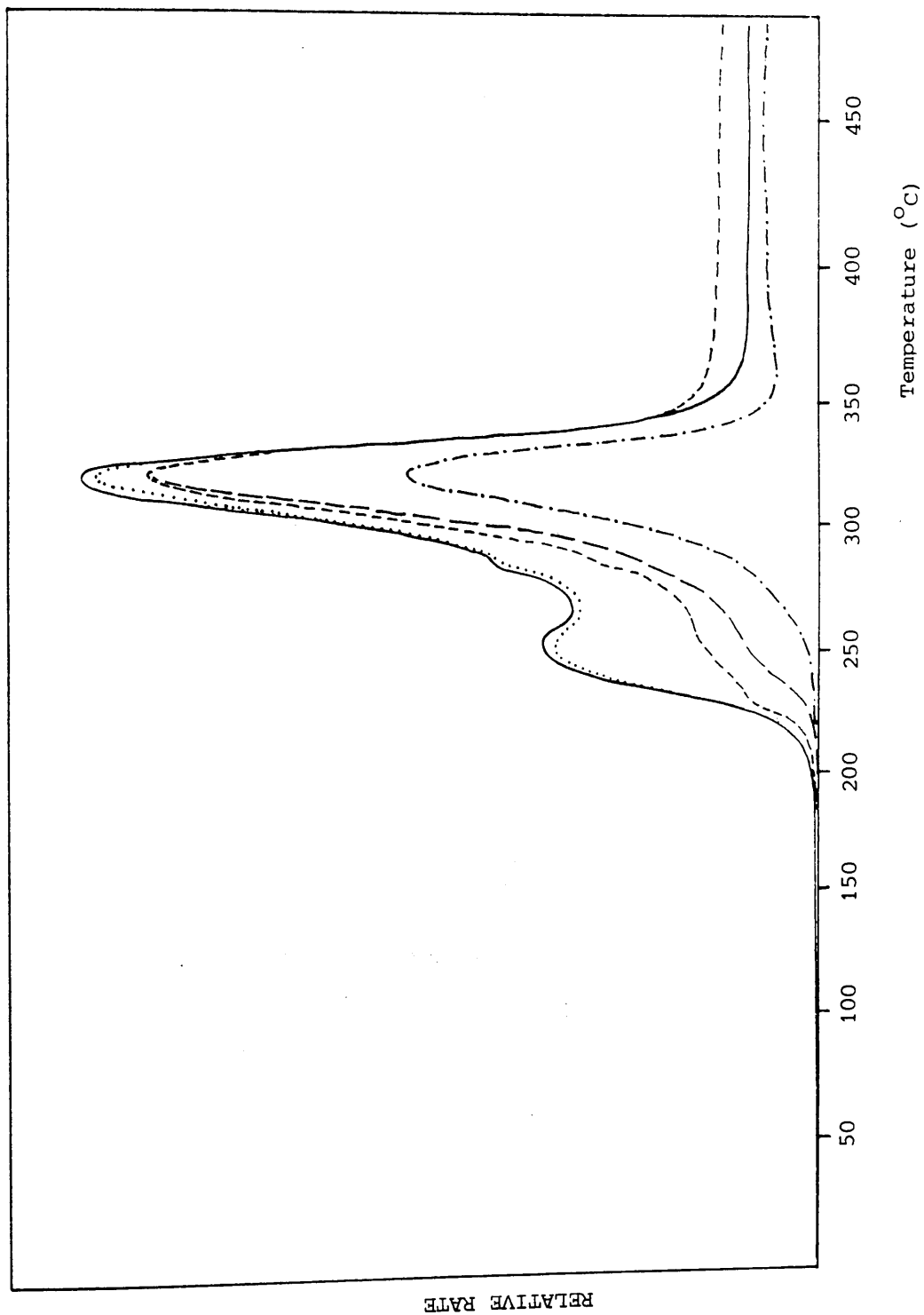
Fig. 5.17   TVA curve for PEO:$ZnCl_2$ Blend   2:1   EO:$ZnCl_2$ dry blend.

TG of PEO:ZnCl$_2$ Blends.

TG was carried out on PEO:ZnCl$_2$ blends having EO:ZnCl$_2$ ratios of both 10:1 (Blend 1) and 2:1 (Blend 2). The blends were cast as films from methanol. The TG and DTG curves for each blend are reproduced in Fig. 5.18. In Blend 1 the initial weight loss around 50°C is due to trapped solvent evolving from the blend. The decomposition of the blend occurs in two stages, with the onset of degradation occurring at 270°C and reaching a rate maximum at 325°C. The first decomposition is a very rapid process and during this, weight loss amounts to 60.93% by weight of the original blend mass. The second weight loss occurs much more gradually over 348°-500°C and accounts for 17.20% w/w of the blend. After heating to 500°C, 21.87% of the blend weight remains as residue.

The TG curve for the PEO:ZnCl$_2$ Blend 2 (EO:ZnCl$_2$, 2:1) shows three stages of weight loss. The first of these stages begins at 277°C and reaches a maximum rate of weight loss at 313°C. This is followed by a less rapid drop in weight in the range 373-445°C with a maximum rate at 426°C. During the final fifty degrees of heating, the rate of evolution of volatiles is further decreased and has a maximum rate at 470°C. After heating to 500°C under nitrogen, the remaining residue constitutes 40% of the original blend weight.

SATVA Product Separation for PEO:ZnCl$_2$ Blend.

The SATVA separation of the products of heating a 2:1 EO:ZnCl$_2$ blend to 500°C gave four fractions as shown in Fig. 5.19. The first fraction was found to consist of ethene and another unidentified compound which gave absorption bands at 2960cm^{-1}, 2920cm^{-1} and 725cm^{-1} (see Table 5.7a). The second fraction was carbon dioxide.

Fig 5.18   TG (———) and DTG (·····) curves for PEO:ZnCl$_2$ Blend
           EO:ZnCl$_2$ 10:1 film cast from methanol.

           TG (———) and DTG (— — —) curves for PEO:ZnCl$_2$ blend
           EO:ZnCl$_2$ 2:1   film cast from methanol.

WEIGHT %

Temperature (^{o}C)

Fig 5.19 SATVA trace for condensable degradation products on heating PEO:$ZnCl_2$ blend EO:$ZnCl_2$ 2:1 to 500°C.
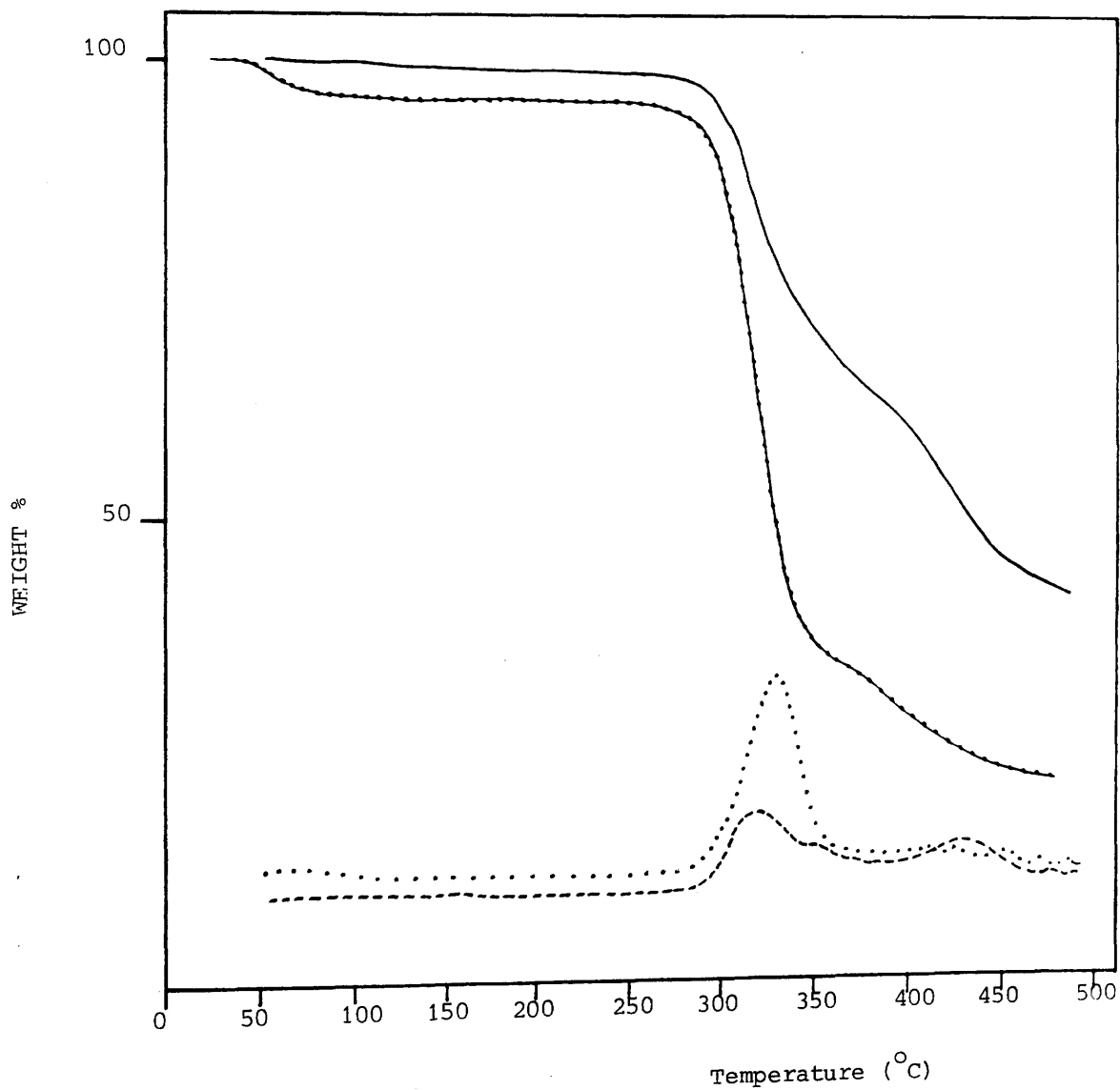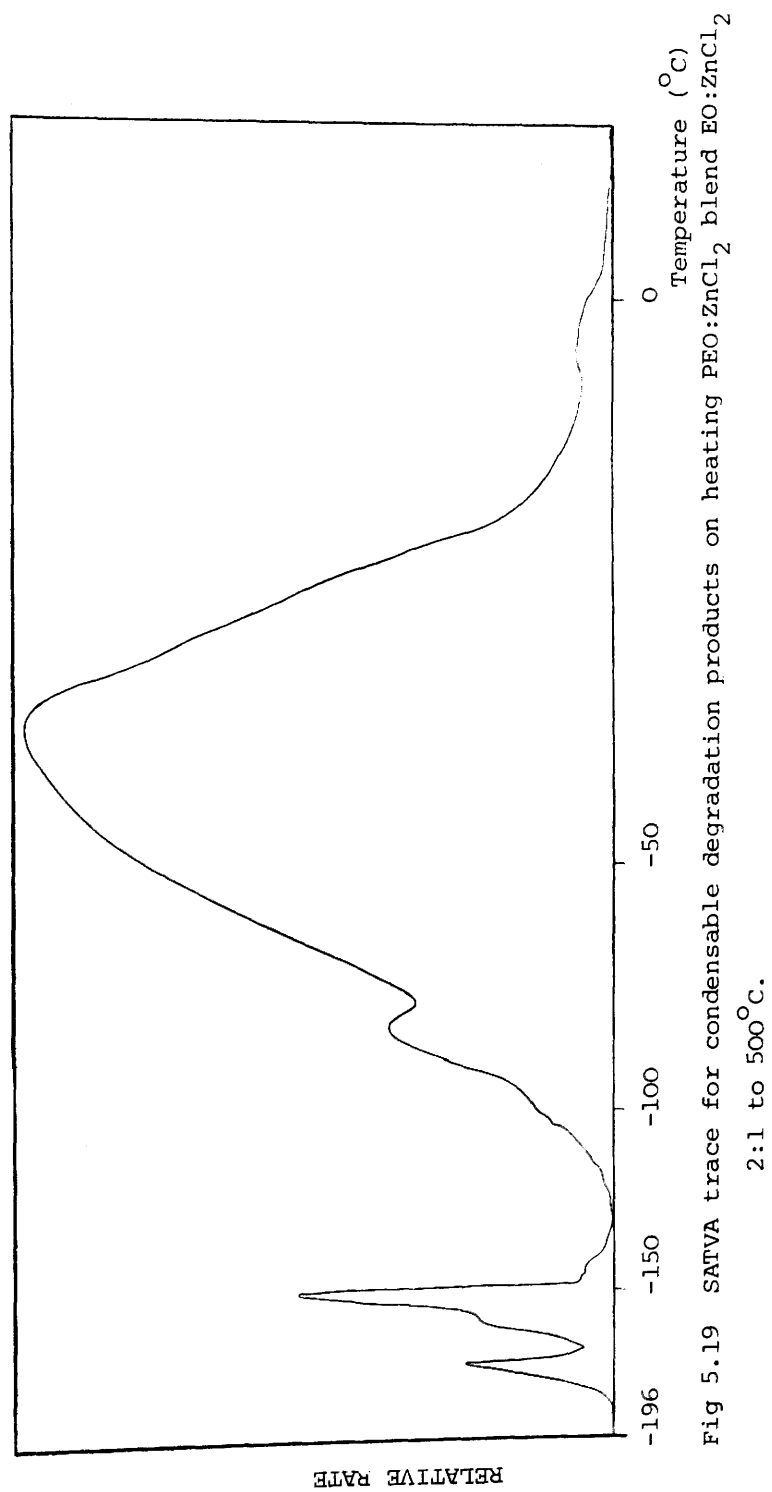
The third SATVA peak was poorly resolved from the final major broad peak. The components of the third fraction were collected in an IR gas cell, fitted with a cold finger which would allow the removal of any less volatile compounds for spectroscopic analysis as a liquid film. Once the fraction had been collected and allowed to warm to room temperature all the components volatilised. The major absorption bands of the gas phase spectrum were in the carbonyl stretching region at $1735cm^{-1}$ and the C-O-C stretching zone at $1185cm^{-1}$ and $1125cm^{-1}$. The base peak in the mass spectrum at $^m/e = 29$ is very characteristic of an aldehyde and is consistent with the IR data. This, in conjunction with the peak at $^m/e = 44$ implies acetaldehyde being present although the position of the fraction in the SATVA trace, $-80^{o}C$ at the peak maximum is high for acetaldehyde which usually gives a peak maximum on distilling from the subambient trap at approximately $-95^{o}C$ - $-102^{o}C$. Thus there may be traces of acetaldehyde present but also higher aldehydic compounds and ethers. Other major bands in the IR spectrum were a winged absorption band at $744cm^{-1}$ and strikingly sharp bands in the range $3000-2700cm^{-1}$.

From experience from previous runs, the final fraction was collected in a gas cell as in the preceeding fraction to permit spectroscopic analysis to be carried out without the compound(s) being exposed to the atmosphere. Unfortunately decomposition still occurred as on warming to room temperature (during the time taken to obtain the IR spectrum), the cell contents turned from light brown to dark brown/black. The IR spectrum of the final fraction clearly showed acetaldehyde with traces of dioxane and water. These compounds were also identified in the mass spectrum

of the more volatile gaseous components of the final fraction. In order to obtain information on the less volatile products in the fraction, the experiment was repeated but collecting the final fraction as a liquid for introduction into the mass spectrometer. However, due to the instability of the compounds analysis was inconclusive and irreproducible. An IR spectrum of the liquid portion could not be obtained.

The CRF was first observed to be produced at approximately 250°C. It took the form of a series of coloured bands ranging from orange to dark brown and was attributed to a mixture of unsaturated chain fragments.

The IR and MS data for each product fraction obtained for the PEO:$ZnCl_2$ blend are presented in Table 5.7 - Table 5.10.

Absorbance Frequency (cm^{-1})			Product or Band Assignment
3120 (w)	1430 (w)	944 (s)	$CH_2=CH_2$
2960 (w)	2920 (w)	725 (s)	unidentified CH_2

Table 5.7a
IR Spectrum of Fraction (1) from SATVA trace of PEO:$ZnCl_2$ Blend.

$^m/e$ value	% Base	Product or Fragmentation Ion.
28	100.0	
27	46.4	H_2CCH_2
26	62.3	
25	10.2	
39	2.4	unidentified

Table 5.7b
Mass Spectrum of Fraction (1) from SATVA trace of PEO:$ZnCl_2$ Blend.

Absorbance Frequency (cm^{-1})			Product or Band Assignment
3720 (w)	3620 (w)	2330 (s)	CO_2
720 (m)	669 (m)		
2960 (w)	2915 (w)		unidentified CH_2

Table 5.8a
IR Spectrum of Fraction (2) from SATVA trace of PEO:$ZnCl_2$ Blend.

$^m/e$ value	% Base	Product or Fragmentation Ion.
44	100.0	CO_2
56	0.7	unidentified no CH_3Cl, C_2H_5Cl,
39	7.1	HCl etc.

Table 5.8b
Mass Spectrum of Fraction (2) from SATVA trace of PEO:$ZnCl_2$ Blend.

Absorbance Frequency (cm^{-1})	Product or Band Assignment
3000-2860, 2700-2850	unidentified
1815 - 1805 (w)	
1755, 1743, 1730 (winged)	CH_3CHO
1450	CH_2 bending
1400 (winged)	
1370	
1342 (m), 1347	
1260	
1186 (s)	
1145 - 1110	
950 (m)	
862 (m)	
744 (s)	
675 (m)	

Table 5.9a
IR Spectrum of Fraction (3) from SATVA trace of PEO:$ZnCl_2$ Blend.

^{m}/e value	% Base	Product or Fragmentation Ion
29	100.00	·CHO, aldehyde CH_3CHO
43	33.9	·CH_2CHO
59	2.9	·OCH_2CHO, $CH_3OCH_2CH_2$
73	8.6	·CH_2OCH_2CHO
87	0.9	·$CH_2CH_2OCH_2CHO$
88	3.1	
36	31.7	
39	27.0	
44	21.0	CH_3CHO
38	15.0	unidentified
15	28.6	CH_3

Table 5.9b
Mass Spectrum of Fraction (3) from SATVA trace of PEO:$ZnCl_2$ Blend.

Absorbance Frequency (cm^{-1})   Product or Band Assignment

3420 (s)				OH, H_2O
2970 (s)	2920 (m)	2900 (m)	2860 (s)	
2750 (w)	2700 (w)	1448 (w)	1290 (w)	(hexagon with 2 O) (?)
1258 (m)	1130 (s)	1052 (w)	890 (s)	
	880 (s)			

2820 (w)	2790 (w)	744 (w)	unidentified
1755 (s)	1743 (s)	1730 (s) 1408 (m)	CH_3CHO
	1365 (m)	1350 (m) 1341 (m)	

Table 5.10a
IR Spectrum of Fraction (4) from SATVA trace of PEO:$ZnCl_2$ Blend.
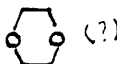
$^m/e$ value	% Base	Product or Fragmentation Ion.
29	100.0	
44	21.4	
43	21.0	
15	25.0	CH_3CHO
42	6.2	
26	9.2	
47	0.1	
28	28.1	
88	5.9	
58	6.8	(hexagon with 2 O) (?)
31	7.8	
91	0.1	unidentified
89	0.3	
38	2.3	HCl
36	6.7	
37	0.9	.Cl
35	2.3	

Table 5.10b (Gas Phase)
Mass Spectrum of Fraction (4) from SATVA trace of PEO:$ZnCl_2$ Blend.

THERMAL ANALYSIS OF PEO:ZnO BLENDS

Degradation studies were performed on two PEO:ZnO blends. Blend 1 had an EO:ZnO molar ratio of 10:1 and Blend 2 was in the ratio 2:1 EO:ZnO. As there is no common solvent for both components the blends were prepared in powder form. Samples were prepared in air and contained 50mg PEO for TVA experiments and 100mg PEO for SATVA runs plus the appropriate weight of ZnO for each blend.

Thermal Behaviour of ZnO.

The behaviour of ZnO under TVA conditions was investigated. On heating 45mg ZnO to 500°C a small peak was obtained (see Fig.5.20). Volatile material began to evolve at 207°C reaching a maximum at 250°C. The 0°C and -45°C traces were coincident and the non-coincident -75°C and -100°C responses were smaller. There were no non-condensable products. The residue exhibited a slight discolouration from white to pale fawn. SATVA experiments showed that the sole product on degradation was carbon dioxide. This was attributed to a slight amount of $ZnCO_3$ impurity being present.

TVA Investigations of PEO:ZnO Blends.

The TVA curve obtained for Blend 1, illustrated in Fig. 5.21, gave a single peak commencing at 298°C and which had a peak maximum at 373°C. The peak was slightly unsymmetrical and exhibited a small shoulder at 383°C. Prior to the onset of the degradation peak there was a hint of slow evolution of volatile products beginning at 230°C. This was accounted for by the degradation of traces of $ZnCO_3$ in the ZnO. From the behaviour of the individual trap traces at the degradation peak, a variety of products of differing volatiles appear to have been produced including non-
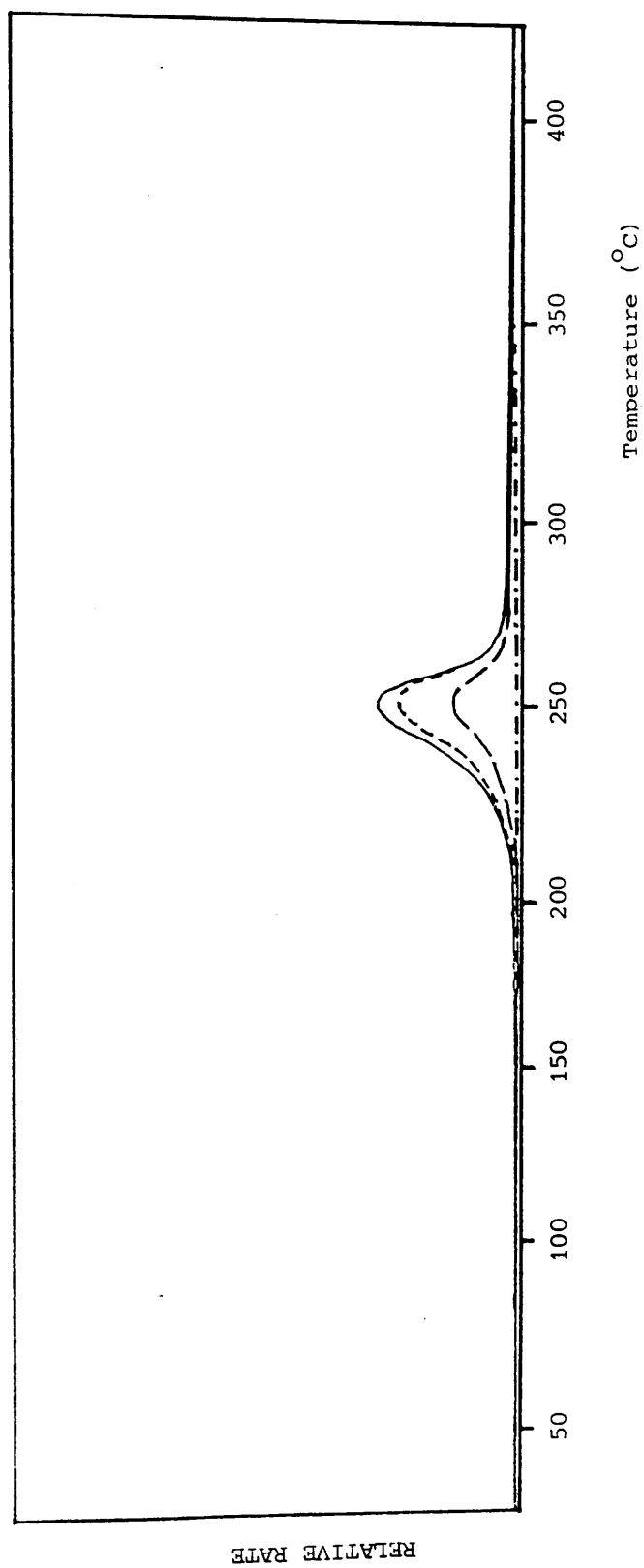
Fig. 5.20   TVA curve for 45 mg ZnO powder sample.
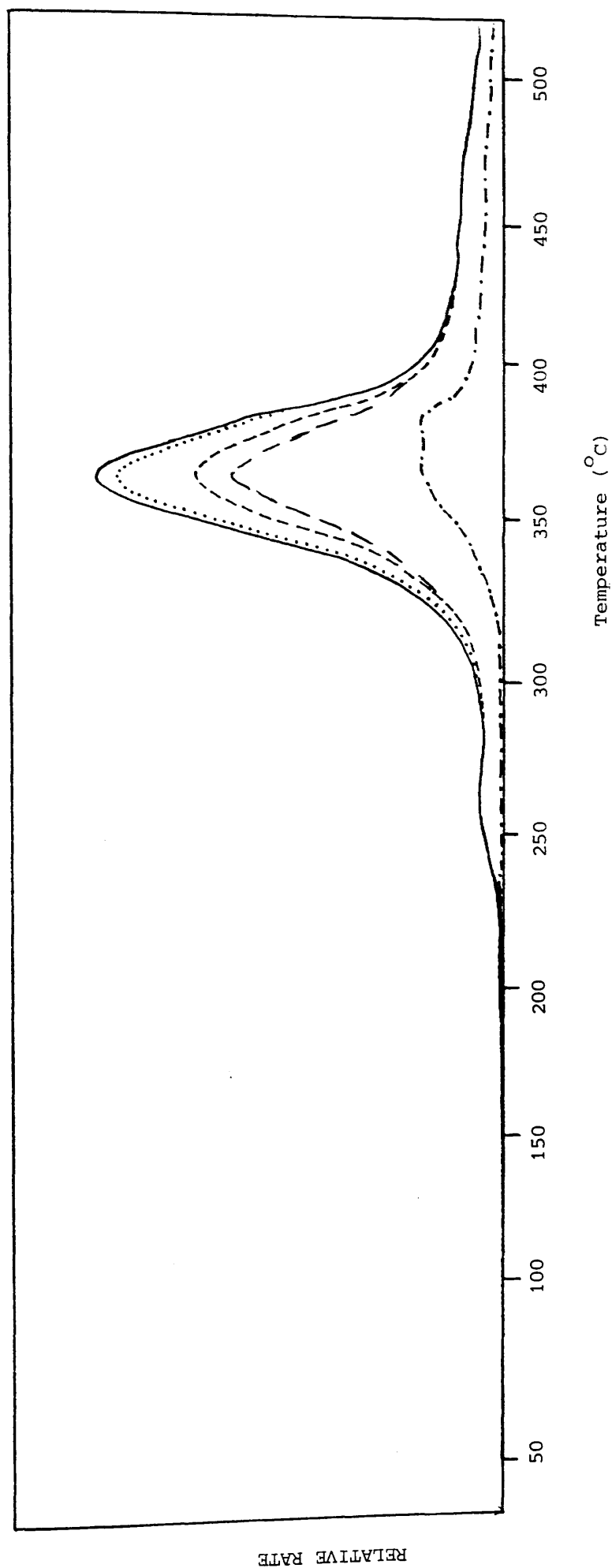
Fig. 5.21 TVA curve for PEO:ZnO Blend 1 EO:ZnO ratio 10:1 powder blend.
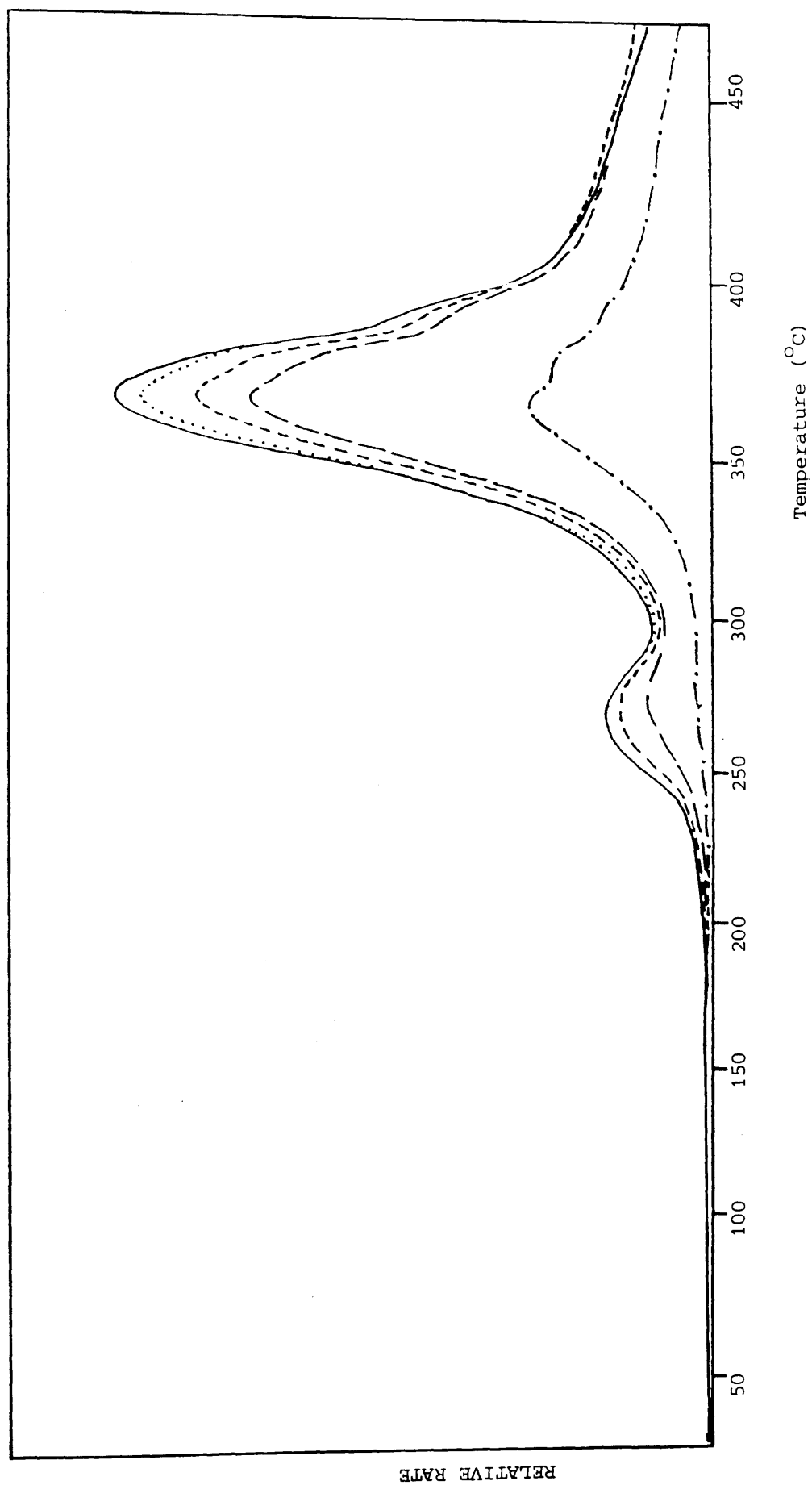
Fig. 5.22 TVA curve for PEO:ZnO Blend 2 EO:ZnO ratio 2:1 powder blend.

Sample	Molar Ratio EO : ZnO	T(onset 1) (^{o}C)	T(max 1) (^{o}C)	T(onset 2) (^{o}C)	T(max 2) (^{o}C)	T(sh) (^{o}C)	T(onset CRF) (^{o}C)
Blend 1	10 : 1	210	261	298	373	383	348
Blend 2	2 : 1	215	272	301	372	388	351
ZnO	-	207	250	-	-	-	-

Table 5.11 Degradation Onset (T(onset)) and Rate Maxima (T(max)) Temperatures for PEO:ZnO Blends and ZnO as obtained by TVA.

condensable products.   The overall appearance of the TVA curve
was very similar to that for pure PEO.   The TVA curve for Blend 2,
shown in Fig. 5.22, is almost identical to that obtained for Blend 1
except that with the higher ZnO concentration the evolution of
decomposition product from $ZnCO_3$ is more pronounced resulting in a
small peak prior to the main degradation.   The formation of CRF
was first observed at approximately $350^{\circ}C$ in each blend.   The
degradation onset and rate maxima temperatures for the PEO:ZnO
Blend 1 and Blend 2 together with those for PEO as obtained by TVA
are summarised in Table 5.11.

TG of PEO:ZnO Blends.

The TG and DTG curves for both Blend 1 and Blend 2,
reproduced in Fig. 5.23 indicate a single stage degradation occurs.
Decomposition begins at approximately $325^{\circ}C$ and $337^{\circ}C$ respectively
for the 10:1 EO:ZnO and 2:1 EO:ZnO blends.   The corresponding rate
maximum temperatures are $388^{\circ}C$ and $392^{\circ}C$.   During the rapid
degradation process, 82.5% w/w of Blend 1 is lost as decomposition
products leaving 17.5% w/w residue.   The corresponding weight
loss and residual deposits for Blend 2 are 51.04% and 48.96%.

Fig. 5.23　TG (━━━━━) and DTG (·····) curves for PEO:ZnO Blend 1
　　　　　　 EO:ZnO　10:1 dry blend.

　　　　　　 TG (━━━━━) and DTG (— — —) curves for PEO:ZnO Blend 2
　　　　　　 EO:ZnO　2:1 dry blend.

Temperature (°C)
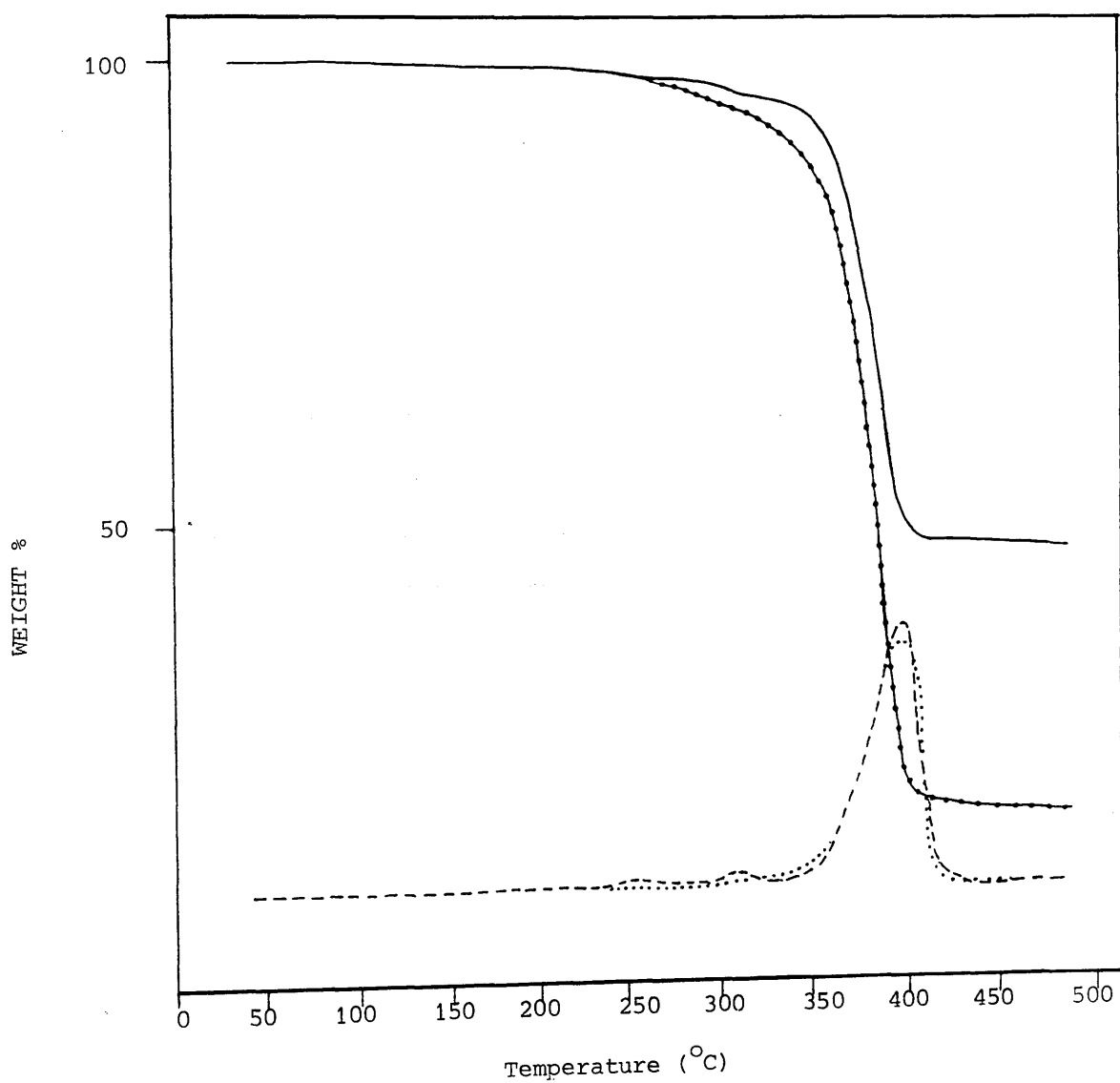
SATVA Product Separation for PEO:ZnO Blend.

In the SATVA traces for Blend 1 and Blend 2, four fractions were clearly visible. This is demonstrated in Fig. 5.24. The overall form of the SATVA trace, in particular the second fraction, resembled that for pure PEO more than any of the previous blends. However, the amount of the first fraction (especially at high ZnO content) was greatly increased in the case of the blend.

The first three fractions were collected in gas cells for identification by IR spectroscopy whilst the final fraction was collected as a liquid. The first fraction was found to contain mostly CO_2 with ketene and ethyne also present. Although there was some overlap between the second and third fractions, the highly characteristic absorption band pattern for formaldehyde was seen in the IR spectrum of fraction 2. Acetaldehyde was identified in the third fraction. The final fraction was a pale yellow/green liquid with a slightly caramelised odour. From the appearance of the SATVA peak, the fraction contained a mixture of products as indicated by the shoulders both preceding and following the main peak. The major component of the fraction identified by IR and MS was to be water. The mass spectrum suggested the presence of methoxy acetaldehyde, ethoxy acetaldehyde, vinyloxy acetaldehyde divinyl ether and ethyl vinyl ether. These compounds were present on the thermal degradation of pure PEO. In addition vinyloxy-diethyl ether may have been produced from the PEO:ZnO blend from the peak at $^m/e = 116$ in the mass spectrum.

The CRF produced by each PEO:ZnO blend was a pale yellow liquid which solidified to form a wax on cooling. The IR spectra
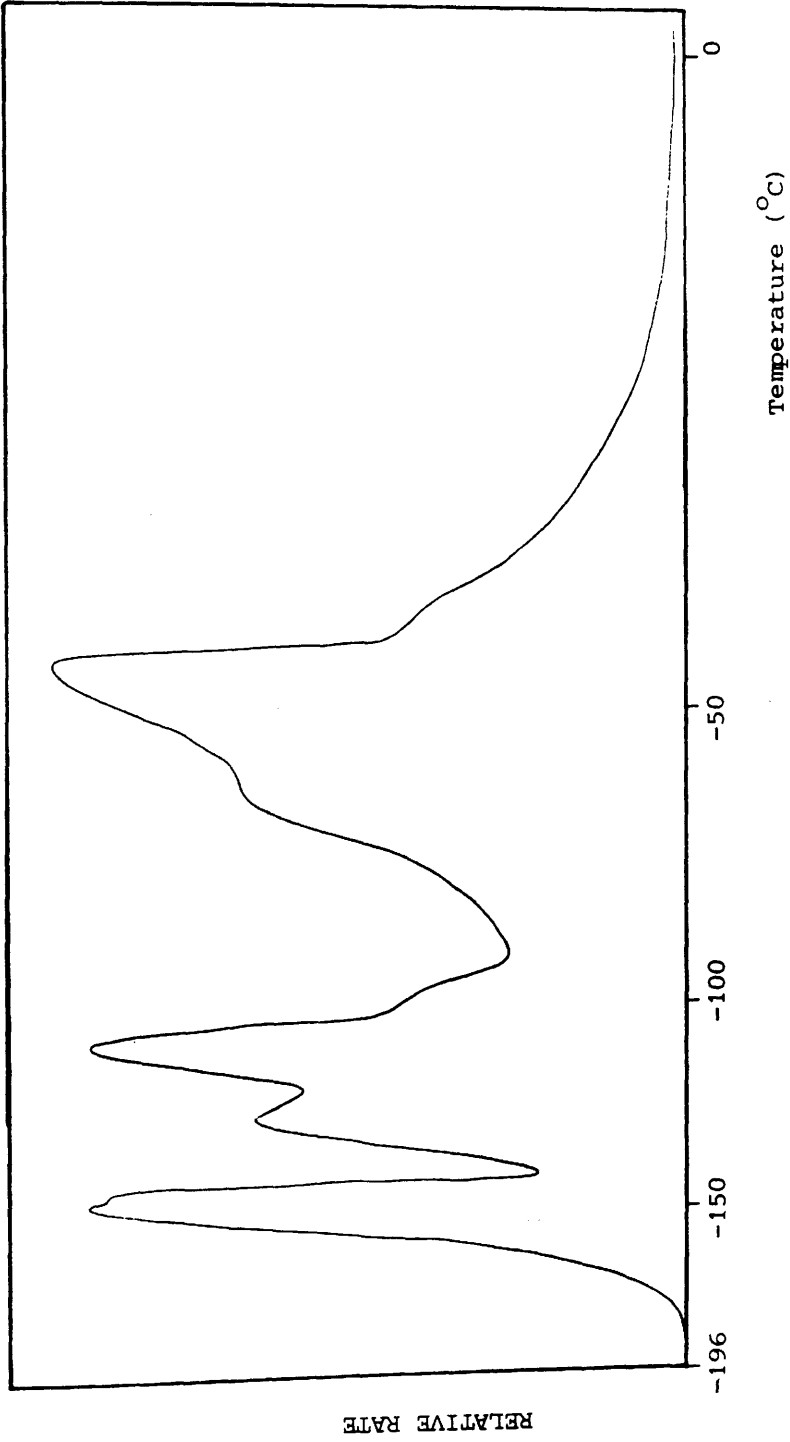
Fig 5.24   SATVA trace for condensable degradation products on heating PEO:ZnO blend   EO:ZnO
2:1 to 500°C.

obtained for both CRF's were identical to that of the CRF produced by pure PEO. Thus the CRF consisted of oligometric chain fragments with predominantly methoxy- and ethoxy end groups and unsaturated groups also present.

The residue after heating the blend to 500°C was a dull grey/biege solid. An IR spectrum revealed a strong absorption band at 480 cm^{-1} which was attributed to ZnO and a weaker absorption at 1080 cm^{-1} due to an ether C-O-C asymmetric stretch.

When degradation of each blend was carried out in a closed system, the non-condensable products were found to be CO and CH$_4$ from bands at 2170 cm^{-1}, 2110 cm^{-1} and 1300 cm^{-1} in the IR spectrum.

The IR and MS data for fractions obtained by SATVA of PEO:ZnO blend are reproduced in Tables 5.12 - 5.15.

Absorption Frequency (cm^{-1})	Product or Band Assignment
3930 (w), 3710 (w), 2310 (s), 730 (s), 720 (w) 680 (w)	CO_2
2160 (m) 2135 (m)	H_2CCO
3310 (m), 3230 (w) 730 (s)	$HC\equiv CH$

Table 5.12
IR Spectrum of Fraction (1) from SATVA trace of PEO:ZnO Blend.

Absorption Frequency (cm^{-1})	Product or Band Assignment
2930 - 2750 (s) 1765 - 1720 (s) 1505 (w)	HCHO

Table 5.13
IR Spectrum of Fraction (2) from SATVA trace of PEO:ZnO Blend

Absorption Frequency (cm^{-1})	Product or Band Assignment
3465 (w) 2980 (m) 2810 (s) 2730 (s) 2710 (s) 1765-1728 (s) 1410 (m) 1365 (m) 1120 (m)	CH_3CHO
1610 (w)	C=C unsaturation
1206 (m) 744 (w)	unidentified

Table 5.14
IR Spectrum of Fraction (3) from SATVA trace of PEO:ZnO Blend.

Absorption Frequency (cm^{-1})	Product or Band Assignment
3520-3230 (s), 1640-1620 (m)	H_2O
1720 (w)	C=O
1020 (w)	C-O
2960-2870 (s)	CH_3 CH_2 stretching
2840 (m)	C-H stretching

Table 5.15a
IR Spectrum of Fraction (4) from SATVA trace of PEO:ZnO Blend.

^{m}/e value	% Base	Product or Band Assignment
72	2.4	
71	0.3	
67	2.5	
44	6.7	$CH_3CH_2OCH=CH_2$
43	15.0	
29	25.4	
15	9.8	
70	0.8	
44	6.7	
43	15.0	$CH_2=CHOCH=CH_2$
42	3.3	
27	11.4	
86	1.4	
59	8.0	
57	2.5	$CH_2=CHOCH_2CHO$
43	15.0	
29	25.4	
27	11.4	
28	24.6	CO
116	0.2	
87	1.4	
71	0.3	$CH_2=CHOCHCHOCH_2CH_3$
57	2.5	
43	15.0	

Table 5.15b
Mass Spectrum of Fraction (4) from SATVA trace of PEO:ZnO Blend.

^{m}/e value	% Base	Product or Fragmentation Ion
18	100.0	H_2O
15	9.8	
29	25.4	
31	30.1	$CH_3CH_2OCH_2CHO$
45	23.5	
59	8.0	
88	0.7	
43	15.0	CH_3CO
45	23.5	$CH_2=OCH_3$, $CH_3CH=OH$
74	10.7	
73	9.1	
59	8.0	
57	2.5	
45	23.5	CH_3OCH_2CHO
43	15.0	
31	30.1	
29	25.4	
15	9.8	

Table 5.15c
Mass Spectrum of Fraction (4) from SATVA trace of PEO:ZnO Blend.

THERMAL ANALYSIS OF PEO:CoBr$_2$ BLENDS.

TG, TVA and SATVA experiments were carried out on a PEO:CoBr$_2$ blend having the ratio 4:1 EO:CoBr$_2$ units.   Dry blends and blends cast as films were used for TVA and SATVA investigations.   CoBr$_2$, a mauve colour in the hexahydrated state, was dried overnight in vacuo at 80°C.   The resultant green CoBr$_2$ was purified by sublimation prior to the formation of the blends.   Dry blends were prepared by thoroughly grinding powdered CoBr$_2$ and PEO under nitrogen. With film samples, standard solutions were prepared in methanol containing 40 mg ml^{-1} PEO and 49.6g mg ml^{-1} CoBr$_2$.   From these, films were cast to give sample sizes of 40 mg and 80 mg PEO for TVA and SATVA experiments.   The blend solutions were bright blue in colour as was obtained for CoBr$_2$ in methanol.   On removal of solvent, the blend remained transparent blue indicating compatability between the components.

Thermal Behaviour of CoBr$_2$

Under TVA conditions CoBr$_2$ was found to sublime at 495°C.

TVA Investigation of PEO:CoBr$_2$ Blend.

Both dry blends and blends cast as film gave identical TVA curves in which there were no differences in degradation temperatures. The TVA curve for a 4:1 EO:CoBr$_2$ blend reproduced in Fig. 5.25 showed a clear two stage degradation although decomposition products continued to evolve slowly after the second degradation peak.   The evolution of volatile products start at 184°C and reaches a maximum rate at 257°C.   The first stage of the degradation appears to be the major process as a larger peak is produced.   In this stage the 0°C and -45°C traces are virtually coincident and well separated from the
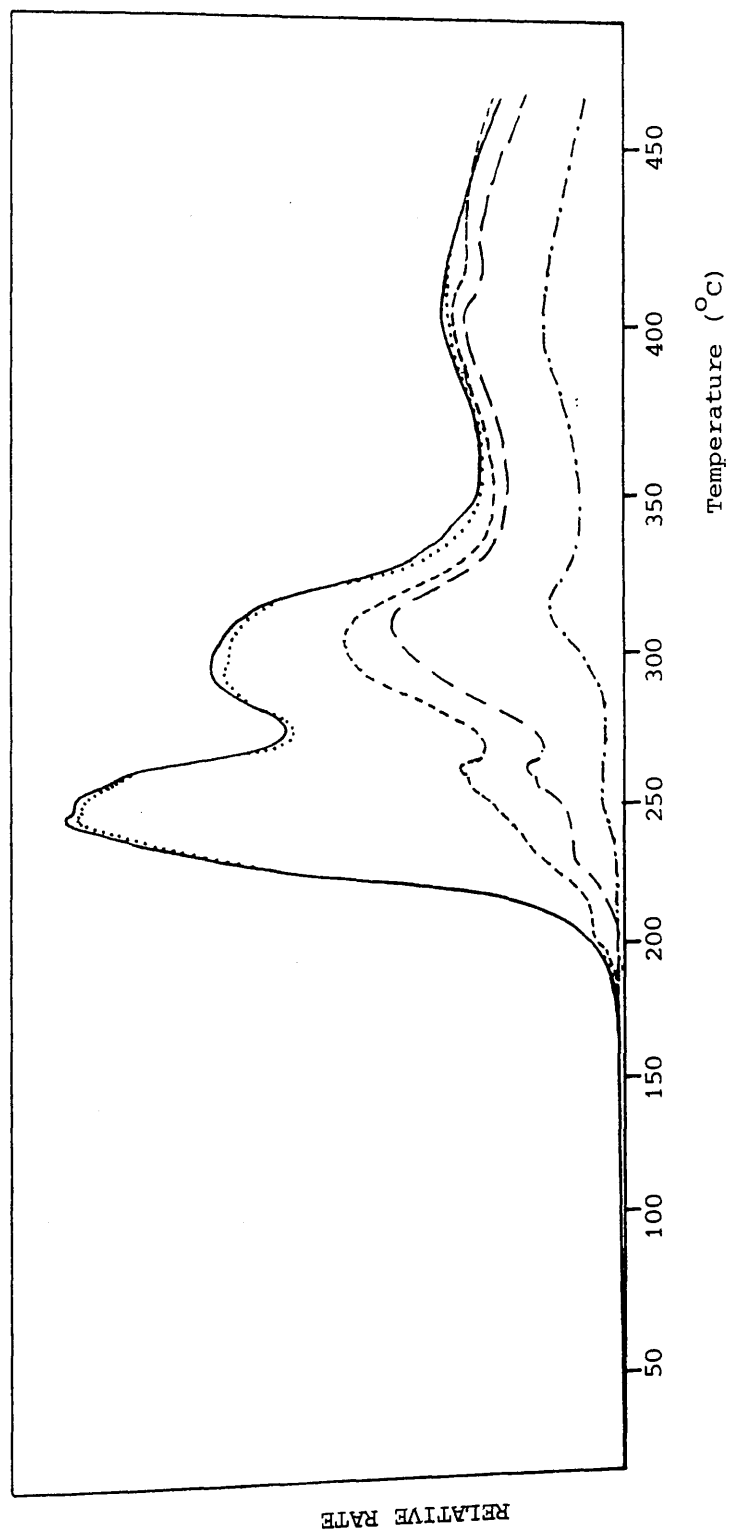
Fig 5.25   TVA curve for PEO:CoBr$_2$ blend EO:CoBr$_2$ ratio 4:1

non-coincident -75°C and -100°C traces. Non-condensable product formation at this point is negligable. The production of volatile compound increases again at 285°C and a maximum rate in this second stage is reached at 300°C. During this stage, there is an increasing in pirani output for the -75°C and -100°C traces whilst in comparison to the first step, the 0°C and -45°C traces are reduced. In the second stage there is the slight evolution of non-condensable products. Thus, as the degradation proceeds an alteration in degradation products occurs. The onset of CRF formation is at approximately 247°C.

TG of PEO:CoBr$_2$ Blends.

TG was performed on PEO:CoBr$_2$ blends cast as film from methanol having the approximate composition 4:1 EO:CoBr$_2$ (Blend 1) and 2:1 EO:CoBr$_2$ units (Blend 2). The TG and DTG curves for each blend are illustrated in Fig. 5.26. Both blends indicate that weight loss occurs in two stages. The degradation temperatures in each case are very similar. In both blends, the onset temperature of degradation occurs at approximately 237°C while the rate maximum temperature is at 281°C in Blend 1 and slightly lower at 277°C in Blend 2. The DTG traces also exhibit a shoulder at 328°C (322°C Blend 2). During this initial degradation stage a rapid weight loss is observed comprising 54.28% and 26.53% of the original polymer weight for Blend 1 and Blend 2 respectively. The second decomposition stage ranging from 393-500°C is a more gradual process. On heating to 500°C 35.90% and 60.71% by weight of original blend remains as residue.

Fig 5.26   TG (———) and DTG (— — —) curves for PEO:CoBr$_2$ Blend 1
           EO:CoBr$_2$ 4:1 film cast from methanol.

           TG (——•——) and DTG (•••••) curves for PEO:CoBr$_2$ Blend 2
           EO:CoBr$_2$ 2:1 film cast from methanol.
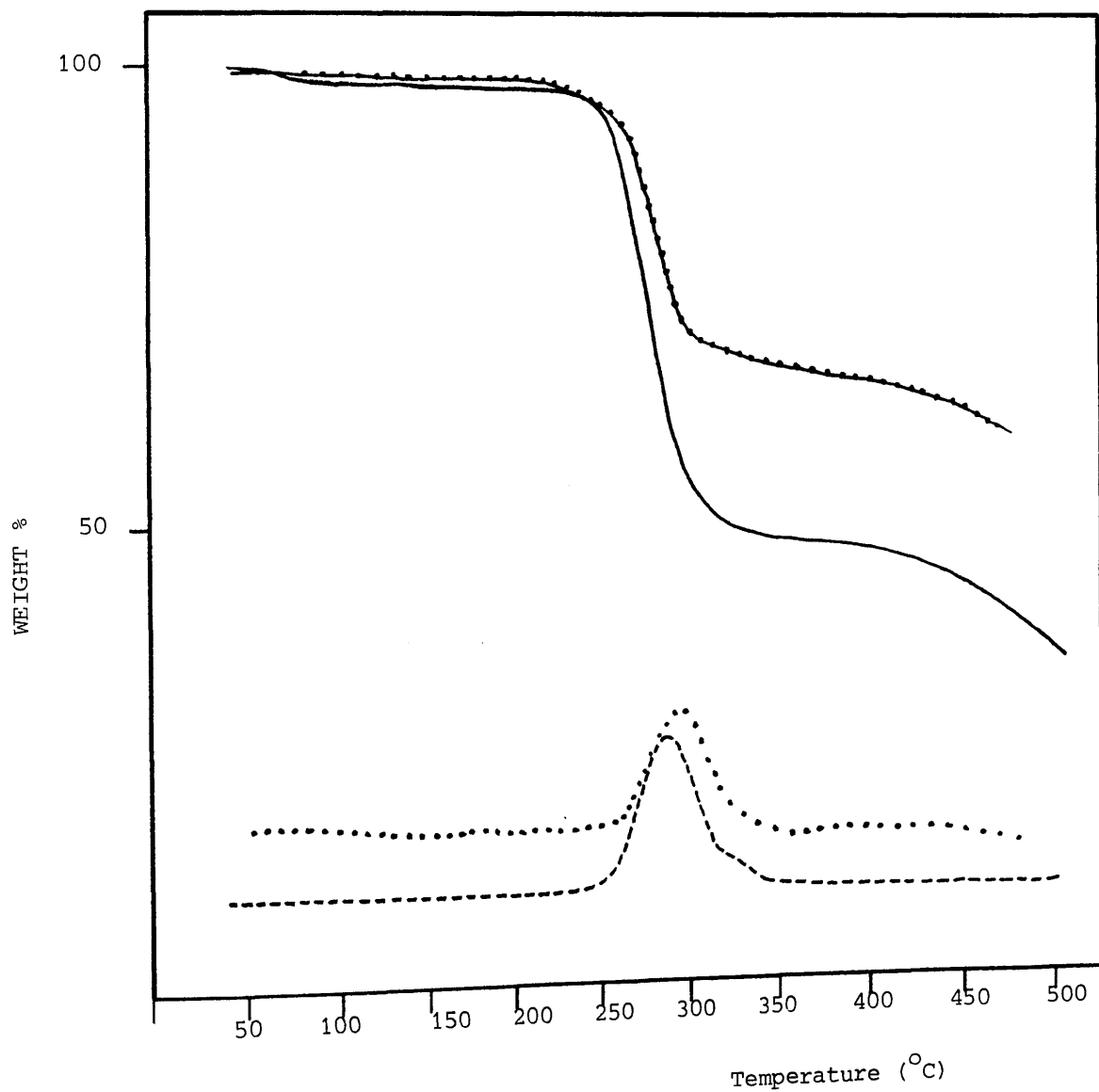
SATVA Product Separation for PEO:CoBr$_2$ Blend.

The SATVA trace for the CoBr$_2$ blend of composition 2:1 EO:CoBr$_2$ units gives four fractions. This is illustrated in Fig. 5.27. The initial highly volatile fraction was due to ethene. In the second fraction CO$_2$ and HBr were readily identified by both IR spectroscopy and mass spectrometry. Additional CH$_2$ absorption bands at 2960-2850 cm^{-1} were also observed and a weak band at 913 cm^{-1} which could possibly be attributed to a vinyl compound. These absorptions may correspond to the unknown compounds giving peaks at $^m/e$ = 117, 119 and 39 in the mass spectrum. The third fraction was poorly resolved from the major final fraction. It was collected as a colourless liquid in a gas cell, from which on IR analysis, acetaldehyde and dioxane were identified. A gas phase mass spectrum of the fraction suggested methyl-bromide and ethyl-bromide also present. The final fraction was collected in a cold finger as a colourless liquid which rapidly discoloured. Due to the decomposition of the fraction it was not possible to obtain an IR spectrum although the running of a mass spectrum before discolouration could be achieved. The fraction was found to be mostly due to dioxane with traces of higher ethers from the $^m/e$ peak at 89. The highest unidentified fragmentation peak was at $^m/e$ = 91.

During heating under TVA conditions, in addition to the formation of a brown CRF, CoBr$_2$ sublimed to the cold ring region forming a green band. The IR spectrum of the brown band obtained as a thin film on a KBr disc was identical to that for the PEO:ZnBr$_2$ blend. The band at 518 cm^{-1} was again present in the PEO:CoBr$_2$ CRF spectrum.
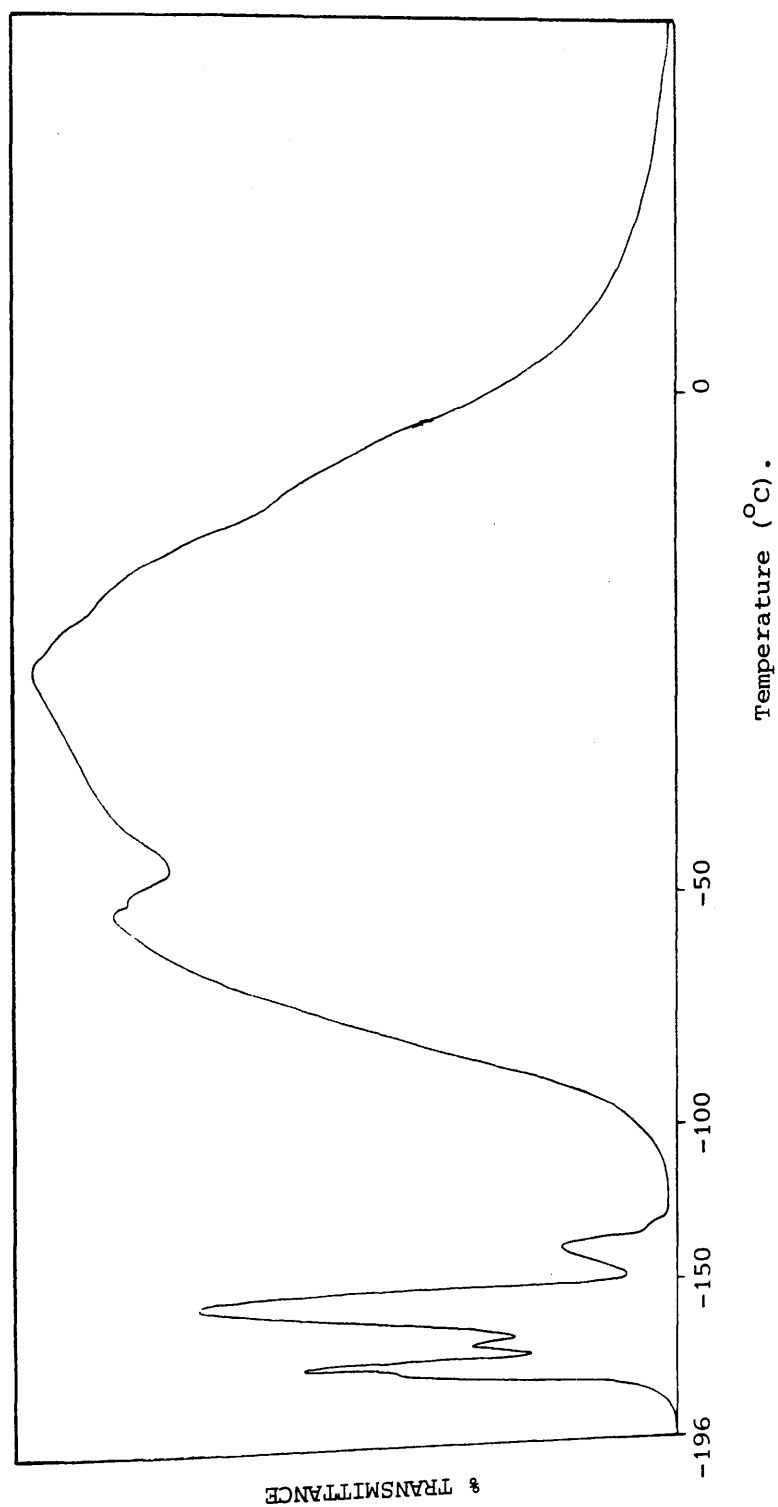
Fig 5.27   SATVA trace for condensable degradation products on heating   PEO:CoBr$_2$ blend
EO:CoBr$_2$ 2:1 to 500°C.

The IR spectrum of the residue obtained from heating the blend to $500^{\circ}C$ gave a broad band over the range 700-450 cm^{-1} centering at approximately 625 cm^{-1}. This was attributed to CoO. A weak band at 1085 cm^{-1} due to a C-O stretch was also present.

Closed system degradation and subsequent IR analysis revealed the non-condensable products to be CO and CH_4.

The IR and MS data for condensable product fractions obtained on SATVA of the $PEO:CoBr_2$ blend are presented in Tables 5.16 - 5.19.

Absorbance Frequency (cm^{-1})		Product or Band Assignment
3120 (w)	3070 (w)	$CH_2=CH_2$
1443 (w)	950 (s)	
3000-2930 (m)	2870 (m)	unidentified

Table 5.16a
IR Spectrum of Fraction (1) from SATVA trace of PEO:CoBr$_2$ Blend.

m/e value	% Base	Product or Fragmentation Ion.
28	100.0	$CH_2=CH_2$
27	56.9	
26	54.4	
15	1.0	
44	2.6	CO_2 (overlap)
43	0.1	
41	0.3	
29	4.6	
15	1.0	

Table 5.16b
Mass Spectrum of Fraction (1) from SATVA trace of PEO:CoBr$_2$ Blend.

Absorbance Frequency (cm^{-1})			Product or Band Assignment
3720 (w)	3700 (w)	3620 (w)	CO_2
3590 (w)	2340 (s)	720 (m)	
668 (m)	648 (w)		
950 (m)			$CH_2=CH_2$ (overlap)
2700-2565 (m)	2540-2400 (m)		HBr
2960 (m)	2920 (m)	2850 (w)	unidentified
2270 (w)	913 (w)	729 (w)	

Table 5.17a
I.R. Spectrum of Fraction (2) from SATVA trace of PEO:CoBr$_2$ Blend.

$^m/e$ value	% Base	Product or Fragmentation Ion.
44	100.0	CO_2
82	0.8	
80	0.8	
81	0.5	HBr
79	0.5	
28	28.7	
27	9.9	$CH_2=CH_2$ (overlap)
26	5.3	

Table 5.17b
Mass Spectrum of Fraction (2) from SATVA trace of PEO:CoBr$_2$ Blend.

$^m/e$	% Base	Product or Fragmentation Ion
39	9.8	
38	14.0	
37	7.0	unidentified
36	35.0	
35	15.7	
57	0.3	
56	0.6	unidentified
119	0.2	
117	0.2	unidentified

Table 5.17c
Mass Spectrum of Fraction (2) from SATVA trace of PEO:CoBr$_2$ Blend.

Absorbance Frequency (cm^{-1})			Product or Band Assignment
3470 (w)	2730 (m)	2725 (m)	
1756 (s)	1742 (s)	1730 (s)	CH_3CHO
1410 (m)	1367 (m)	1356 (m)	
2970 (s)	2920 (m)	2895 (m)	
2865 (s)	2730 (w)	2700 (m)	
1855 (w)	1132 (s)	890 (m)	
882 (m)			
2820 (w)	1036 (w)	674 (m)	unidentified
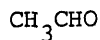
Table 5.18a
IR Spectrum of Fraction (3) from SATVA of PEO:CoBr$_2$ Blend.

$^m/e$ value	% Base	Product or Fragmentation Ion.
29	100.0	
44	19.6	
43	19.3	CH_3CHO
15	25.6	
42	6.9	
88	1.2	
28	12.2	
58	100.0	(dioxane ring structure)
31	3.0	
110	1.4	
108	1.5	
29	100.0	
27	14.9	CH_3CH_2Br
81	0.6	
79	0.6	
96	0.9	CH_3Br
94	1.0	

Table 5.18b
Mass Spectrum of Fraction (3) from SATVA of PEO:CoBr$_2$ Blend.

$^m/e$ value	% Base	Product or Fragmentation Ion
28	100.0	
29	63.1	
88	20.2	
58	20.9	(dioxane ring structure)
31	14.3	
15	15.8	
30	9.8	
26	8.8	
44	20.8	CH_3CHO (overlap)
29	63.1	
89	1.0	
73	2.6	
59	1.4	
45	7.8	$CH_3CH_2OCH_2CH_2O\cdot$
29	63.1	
15	15.8	
38	2.5	
36	8.0	
35	2.0	unidentified
57	6.3	
91	0.4	

Table 5.19
Mass Spectrum of Fraction (4) from SATVA of PEO:CoBr$_2$ Blend.

THERMAL ANALYSIS OF PEO:CaBr$_2$ BLENDS

TVA, SATVA and TG were carried out on a blend having the composition 2:1 EO:CaBr$_2$. In TVA experiments blends were used which contained 50 mg polymer. This was increased to 80 mg for SATVA experiments.

Thermal Behaviour of CaBr$_2$

A dry 50 mg powder sample of CaBr$_2$ was heated to 500°C under TVA conditions whereupon no volatile decomposition products were evolved nor did sublimation of the salt to the cold ring region take place.

TVA Investigation of PEO:CaBr$_2$ Blend

The TVA curve for a dry powder blend of composition 2:1 EO:CaBr$_2$ is illustrated in Fig. 5.28. It can be seen, as for similar PEO:ZnBr$_2$ blends, that a two stage degradation process occurs of which the first stage process appears more important. The onset of evolution of volatile products occurs at 252°C and a small shoulder at 322°C is present on the main degradation peak which reaches a maximum at 339°C. The second peak in the TVA curve begins at approximately 362°C, however due to the overlap between peaks it does not necessarily reflect the temperature at which the decomposition products in the second stage begin to evolve. The peak was a small shoulder at roughly 380°C and reaches a maximum at 409°C. By 478°C the evolution of volatile products is at a minimum. The individual trap traces indicate a range of product volatility and also that product formation or distribution changes as the degradation proceeds. During the first stage of degradation, the 0° and -45°C traces are close together but the -75° and -100°C traces are both well separated from each other and the warmer traps. In the second stage of the degradation, however, there is less separation of the 0°, -45°, -75° and -100° traces, indicating greater volatility in the products.

The -196°C trace indicates the evolution of non-condensable products as it appears slightly elivated from the base line. The evolution of non-condensable products remains fairly constant throughout the whole degradation process unlike the case of PEO:ZnBr$_2$ blends where non-condensable production is considerably increased in the second stage of degradation.
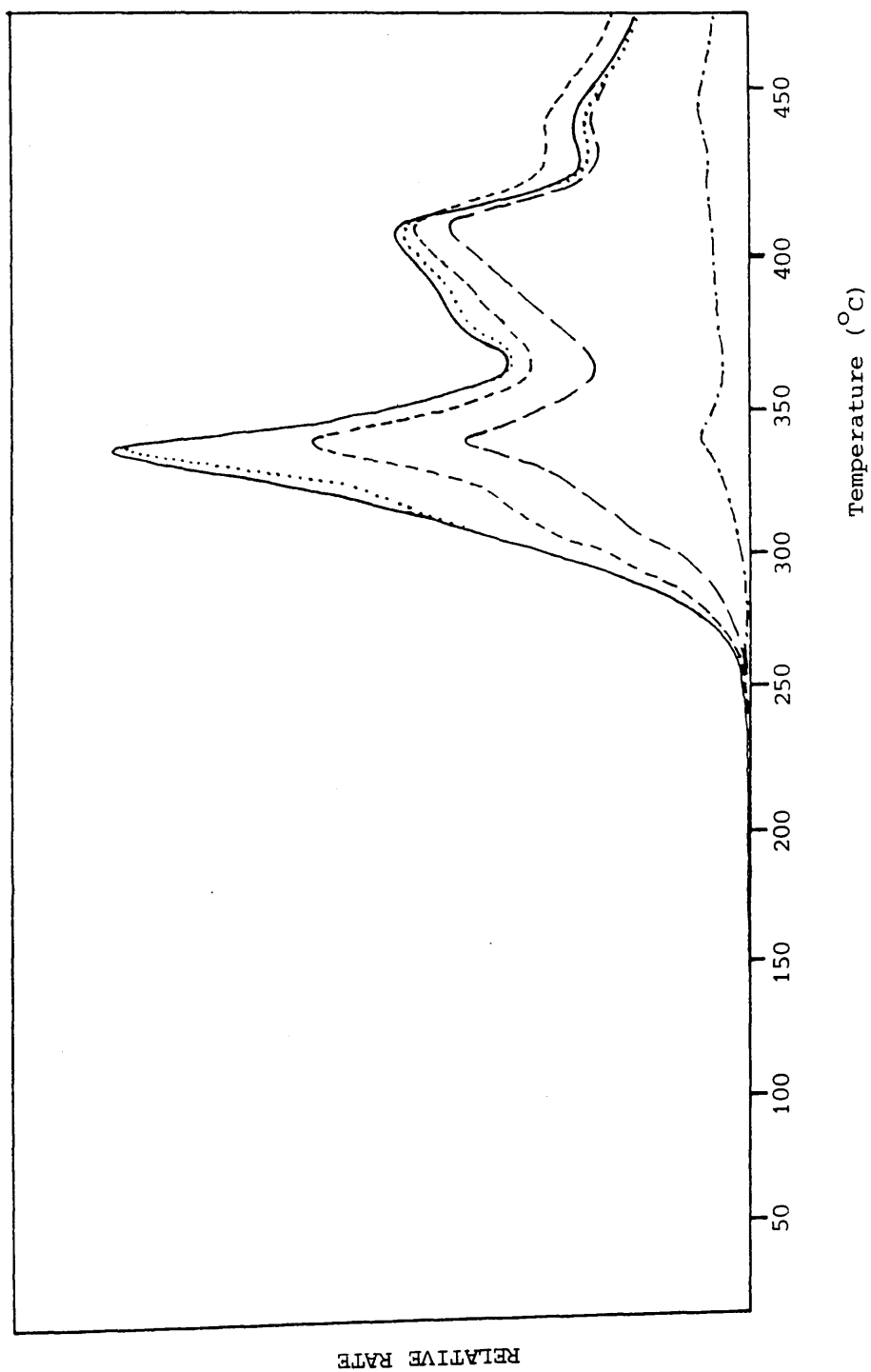
Fig. 5.28   TVA curve for PEO CaBr$_2$ powder blend   EO:CaBr$_2$ ratio   2:1

TG of PEO:CaBr$_2$ Blends.

TG was carried out on two blends. Blend 1 had EO:CaBr$_2$ ratio of 10:1 whilst in Blend 2 the EO:CaBr$_2$ ratio was increased to 2:1. The TG and DTG curves for both blends, which were cast as films from methanol, are reproduced in Fig. 5.29. In Blend 1, the TG curve shows a single stage weight loss. The onset of degradation is at 272°C and reaches a maximum rate at 350°C. The weight loss occurring during decomposition accounts for 78.5% by weight of the original blend sample.

The TG curve for the 2:1 EO:CaBr$_2$ blend (Blend 2) indicates a two stage weight loss. The initial rapid weight loss begins at 273°C and reaches a maximum rate at 336°C. (The weight loss prior to this at approximately 50°C is due to trapped solvent leaching from the warm film). The second weight loss is very gradual and covers a wide temperature range commencing at 370°C with a maximum rate at 385°C. During the second stage of decomposition i.e. from 370-500°C, 5.1% of the original weight is evolved as compared to the weight loss of 44.9% in the first stage. After heating to 500°C under nitrogen the residue comprises 50% of the initial weight.

SATVA Product Separation for PEO:CaBr$_2$ Blends.

The SATVA trace for the condensable products of a dry blend of PEO:CaBr$_2$ in the molar ratio of 2:1 EO:CaBr$_2$ gave four peaks as illustrated in Fig. 5.30. Products giving the first two peaks, an initial small spike and a second more substantial peak, both of which were due to highly volatile compounds, were collected together and found to consist of CO$_2$ (major product) with ketene and ethene

Fig 5.29   TG (————) and DTG (·····) curves for PEO:CaBr$_2$ Blend
            EO:CaBr$_2$ ratio   10:1 film cast from methanol.

            TG (————) and DTG (— — —) curves for PEO:CaBr$_2$ Blend
            EO:CaBr$_2$ ratio   2:1 film cast from methanol.
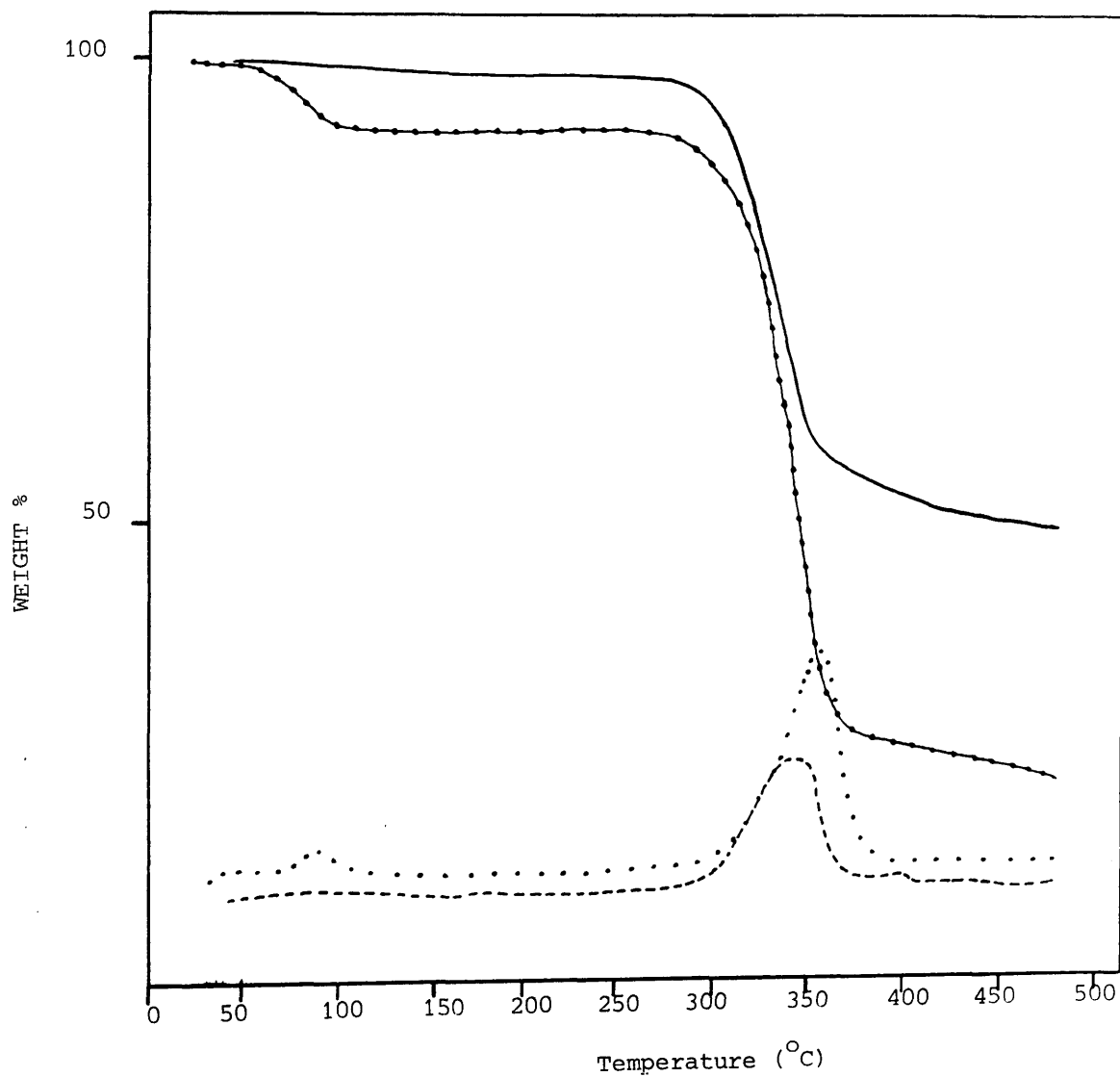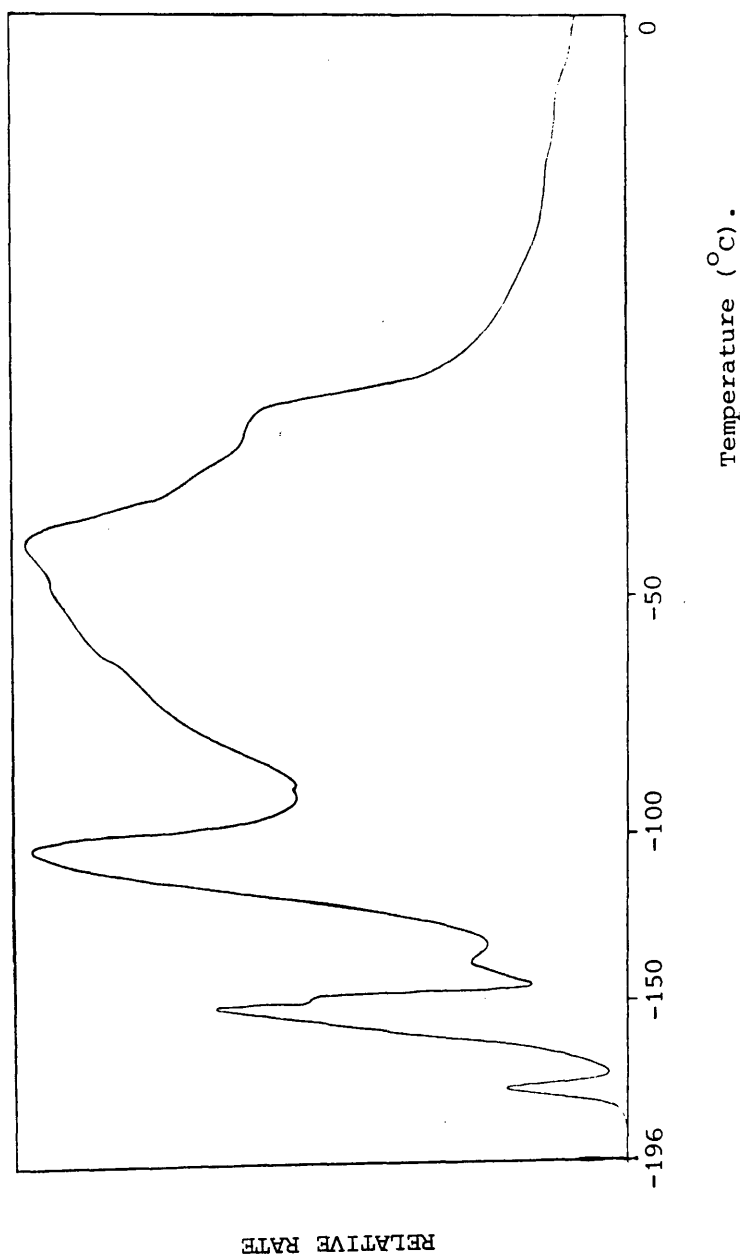
Fig 5.30 SATVA trace for condensable degradation products on heating PEO:CaBr$_2$ powder

blend EO:CaBr$_2$ 2:1 to 500°C.

present to a lesser extent, however, unidentified absorption bands at $\simeq 2960 \text{cm}^{-1}$ due to hydrocarbon and at 990 cm^{-1}, 910 cm^{-1} and 840 cm^{-1} were also observed in the IR spectrum.   IR analysis showed acetaldehyde as the main component of the second fraction with an additional compound which gave a medium intensity absorption band at 744 cm^{-1}.

Mass spectrometry revealed trace amounts of HBr, bromomethane and bromoethane.   The final fraction which produces the largest broadest peak in the trace was further separated into the preceding shoulder, fraction 3 and the remainder of the peak which was collected in the liquid phase as fraction 4.   From the IR spectrum of fraction 3, dioxane and acetaldehyde could clearly be identified although the latter of these compounds will most probably arise from an overlap between fractions 2 and 3.   An absorption band at 675 cm^{-1} not attributable to either dioxane or acetaldehyde appeared in the spectrum. Mass spectral data confirmed these assignments and also indicated the presence of the higher aldehydic compounds methoxy- and ethoxyacetaldehyde together with larger ethers.   Fraction 4 consisted of a milky pale yellow liquid, the mass spectrum of which suggested brominated ether fragments and aldehydic compounds.   Unfortunately due to the instability of the components in this fraction a satisfactory IR spectrum was not obtained, all that was identifiable being absorbed water.

The CRF took the form of a brown band around the cooled portion of the tube.   The IR spectrum of the CRF ran as a liquid film on a freshly prepared thin KBr disc, was very similar to that of the CRF from pure PEO.   Apart from absorbed water (3420 cm^{-1} and 1620 cm^{-1}) the difference between spectra included the disappearance of the
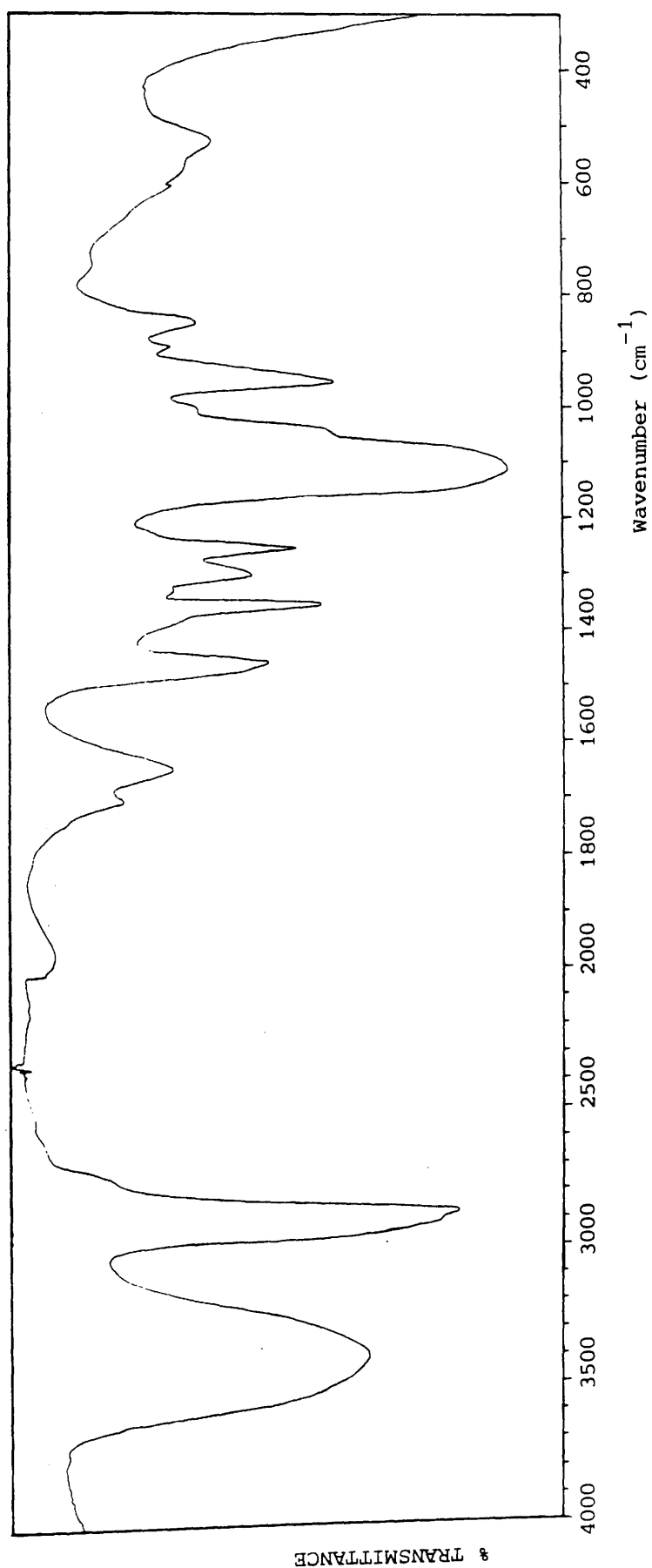
Fig. 5.31 IR spectrum for CRF obtained from the degradation of PEO:CaBr$_2$ blend EO:CaBr$_2$ ratio 2:1 run as liquid film on KBr discs.

% TRANSMITTANCE

Wavenumber (cm^{-1})

Absorbance Frequency (cm^{-1})			Product or Band Assignment
2330 (s)	720 (m)	670 (m)	
2720 (w)	2620 (w)		CO_2
2165 (w)	2130 (w)		H_2CCO
950 (m)			CH_2CH_2
2960 (m)	2880 (sh)		
910 (w)	990 (w)	840 (w)	unidentified

Table 5.19a IR Spectrum of Fraction (1) from SATVA trace of PEO: $CaBr_2$ Blend.

$^m/e$ value	% Base	Product or Fragmentation Ion.
44	100.0	CO_2
42	4.4	
41	11.3	H_2CCO
28	27.7	
27	15.5	
26	10.6	CH_2CH_2

Table 5.19b Mass Spectrum of Fraction (1) from SATVA trace of PEO: $CaBr_2$ Blend.

Absorbance Frequency (cm^{-1})		Product or Band Assignment
3470 (w) 3070 (w) 3070 (w)		
3010 - 2990 (m) 2820 - 2790 (s)		
1755 - 1720 (s) 1409 (s)		
1362 (s) 1350 (s)		
1100 - 1120 (s) 880 - 920 (m)		CH_3CHO
744 (m) 794 (m)		unidentified

Table 5.20a   IR Spectrum of Fraction (2) from SATVA trace of PEO: $CaBr_2$ Blend.

$^m/e$ value	% Base	Product or Fragmentation Ion
29	100.0	
44	45.1	
43	19.7	CH_3CHO
42	8.0	
26	7.9	
41	6.2	
110	0.6	
108	0.5	
29	100.0	
27	8.6	C_2H_5Br
79	0.1	
81	0.1	
96	0.2	
94	0.3	
81	0.1	CH_3Br
79	0.1	
15	17.6	
82	0.2	
80	0.2	
81	0.1	HBr
79	0.1	
121	0.2	
119	0.7	unidentified
117	0.7	

Table 5.20b   Mass Spectrum of Fraction (2) from SATVA trace of PEO:
CaBr$_2$ Blend.

Absorbance Frequency (cm^{-1})			Product or Bond Assignment
2970 (s)	2920 (m)	2895 (m)	
2865 (s)	2730 (w)	1450 (w)	⟨O O⟩
1255 (w)	1132 (s)	890 (m)	
882 (m)			
2730 (w)	1755 (s)	1742 (s)	
1728 (s)	1405 (m)	1368 (m)	CH_3CHO
1350 (m)			
745 (w)	675 (s)		unidentified

Table 5.21a   IR Spectrum of Fraction (3) from SATVA trace of PEO:
CaBr$_2$ Blend.

$^m/e$ value	% Base	Product or Fragmentation Ion
29	100.0	
44	16.4	
43	31.5	CH_3CHO
26	10.8	
42	9.4	
41	8.3	
28	26.8	
88	4.7	
58	9.1	
31	17.9	
89	1.5	$CH_3CH_2OCH_2CH_2O$
96	0.1	
94	0.1	CH_3Br
81	1.3	
79	1.2	
87	1.1	$\cdot CH_2CH_2OCH_2CHO$
78	6.1	unidentified
74	0.8	CH_3OCH_2CHO
73	9.9	$CH_2=O-CH_2CHO$
61	1.9	unidentified
45	16.1	$\cdot CH_2CH_2OH\ CH_3CH=OH$
39	7.6	unidentified
103	0.5	
89	1.5	
73	9.9	$CH_3CH_2OCH_2CH_2\overset{+}{O}=CH_2$
59	7.9	
45	16.1	
29	100.0	

Table 5.21b Mass Spectrum of Fraction 3 from
SATVA trace of PEO:CaBr$_2$ Blends.

$^m/e$ value	% Base	Product or Fragmentation Ion
169	0.8	
167	0.8	
153	1.1	
151	1.1	
139	1.8	
137	1.8	
125	2.5	$BrCH_2CH_2OCH_2CH=\overset{\oplus}{CH}$
123	3.4	
109	7.2	
107	7.8	
95	7.0	
93	5.1	
81	13.5	
79	15.4	
215	0.4	
203	0.7	unidentified
201	0.6	
91	12.3	
92	1.9	unidentified
57	17.8	$CH_3CH=\overset{\oplus}{OH}$
45	100.0	$CH_3C=O$
43	54.1	
41	33.8	HCCO
39	19.0	unidentified
31	41.2	$CH_2=\overset{\oplus}{OH}$
29	49.0	$\cdot C_2H_5 \quad \cdot CHO$
28	20.3	$CO \quad H_2CCH_2$
27	30.0	unidentified
57	17.8	unidentified
55	26.4	" "
18	4.1	H_2O
15	8.0	$\cdot CH_3$

Table 5.22

Mass Spectrum of Fraction (4) from SATVA Trace of PEO:CaBr$_2$ Blend

absorption bands at 1316 cm^{-1} and 1195 cm^{-1} and appearance of band at 1695 cm^{-1} in the spectrum of the CRF produced from the polymer salt blend. There were no obvious C-Br stretching bands in the latter spectrum although a weak band at 520 cm^{-1} was present (see Fig. 5.31).

The residue after heating to 500°C under TVA conditions was a black solid. The IR spectrum of the residue run as a KBr disc, gave strong absorptions at 3400 cm^{-1} and 1630 cm^{-1} due to absorbed water and a strong broad band at 525 cm^{-1}. This latter band was attributed to CaO.

The non-condensable products collected in a closed system were identified from IR spectra as CO and CH_4. The IR and MS data for fractions obtained by SATVA of PEO:$CaBr_2$ blends are reproduced in Tables 5.19 - 5.22.

TVA Product Separation of PEO:$CaBr_2$ Blend.

The TVA curve for the PEO:$CaBr_2$ blend in the ratio 2:1 EO:$CaBr_2$ showed that a multistage degradation was taking place and also that the composition of the degradation product was not the same in each stage. To investigate the change in composition the total products at each stage were isolated during a TVA experiment as previously described for the PEO:$ZnBr_2$ blend, then identified by IR spectroscopy. The TVA curve for the PEO:$CaBr_2$ blend is diagramatically reproduced below indicating the fraction boundaries:
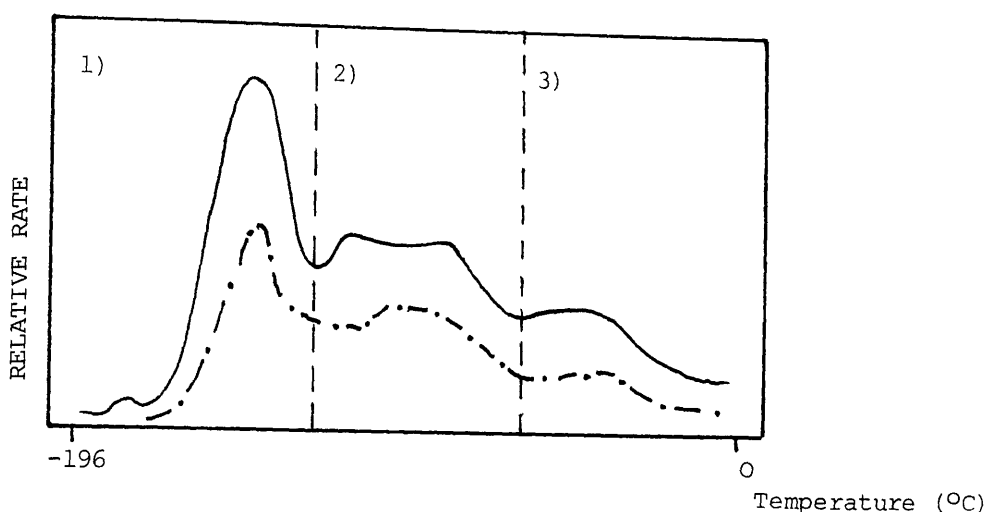
Fig. 5.32   TVA Curve for PEO:CaBr$_2$ 2:1 Dry Blend illustrating
Fraction Boundaries.

The separate fractions were collected in gas cells for IR

analysis.   The small peak in the first fraction, in the TVA curve was

due to traces of absorbed water being evolved.   This was indicated

by the broad band at 3440 cm^{-1} in the IR spectrum.   The compounds

giving rise to the main peak in the fraction were dioxane, acetaldehyde

and carbon dioxide.   An unidentified peak at 744 cm^{-1} was also

present in the spectrum.   A dark brown/green liquid was observed in

the limb of the gas cell.

The second fraction was found to consist of acetaldehyde and

carbon dioxide.   Thus by approximately 366°C, dioxane formation

had ceased.   The peak at 744 cm^{-1} was not present in the spectrum

of the second fraction.

On collecting the final fraction, a colourless liquid was found to

condense in the gas cell.   Acetaldehyde and, to a lesser extent carbon

dioxide were identified as the degradation products although new aliphatic

CH$_2$ absorption bands at 2969 cm^{-1} and 2925 cm^{-1} together with a sharp

band at 730 cm^{-1} were present in the IR spectrum.   A gas phase

mass spectrum was also obtained for this fraction which gave a base

peak at ^{m}/e = 29 (100%) attributed to acetaldehyde with other major

peaks at ^{m}/e = 43 (43.9%) due to CH_3CO fragments, ^{m}/e = 28 (42.1)

arising from CO and ^{m}/e = 15 (24.2%) from methyl radicals.   The

largest fragment was observed at ^{m}/e = 91 (0.3%) while the largest

compound gave a molecular ion peak at ^{m}/e = 86 (0.1%).   This latter

peak plus those at ^{m}/e = 57 (6.5%), ^{m}/e = 43, ^{m}/e 29 may indicate

the presence of vinyl oxy acetaldehyde.

THERMAL ANALYSIS OF PEO:CaCl$_2$ BLEND

TG, TVA and SATVA experiments were performed on a PEO:CaCl$_2$

blend of approximate composition 2:1 EO units:salt.   TVA and SATVA

experiments were carried out on dry blends using 50 mg PEO and 100 mg

PEO plus the appropriate weight of anhydrous CaCl$_2$ respectively.

Thermal Behaviour of CaCl$_2$

A TVA experiment was carried out on 50 mg powdered CaCl$_2$.   No

volatile degradation products were evolved on heating to 500°C nor

did sublimation occur.

TVA Investigation of PEO:CaCl$_2$ Blend.

The TVA curve of a 2:1 EO:CaCl$_2$ blend, illustration Fig. 5.33

gave a single peak.   The onset temperature for the evolution of

volatile product was at 309°C and the production of CRF was first

observed at 344°C.   The evolution of volatile degradation products

was at a maximum at 380°C and a small shoulder on the degradation
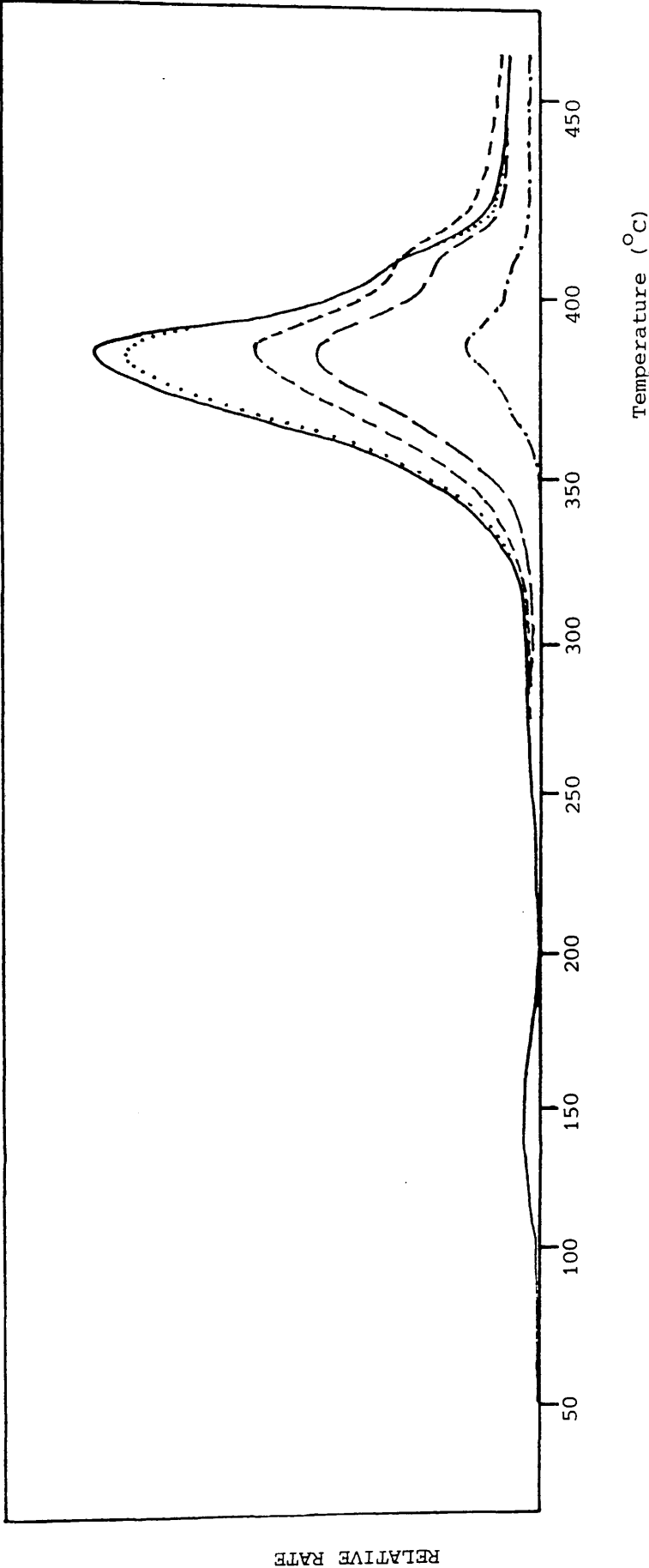
Fig 5. 33 TVA curve for PEO:CaCl$_2$ dry blend EO:CaCl$_2$ ratio 2:1

peak was noted at 405°C. The individual temperature traces were well separated suggesting a variety of products and the production of non-condensable compounds was also indicated. Overall, the appearance of the TVA curve was very similar to that for pure PEO.

TG of PEO:CaCl$_2$ Blends

TG was performed on two blends. Blend 1 had EO:CaCl$_2$ of 10:1 and Blend 2 in which the EO:CaCl$_2$ ratio was increased to 2:1. The blends were cast as a film from methanol. The TG and DTG curves for both blends are shown in Fig. 5.34[34] In both blends a single stage degradation process is observed. With the 10:1 EO: CaCl$_2$ blend, the onset of degradation occurs at 305°C and reaches a maximum rate at 384°C. During the decomposition 77.32% by weight of the original blend is evolved as degradation products leaving 22.68% w/w residue. At higher salt content (EO:CaCl$_2$, 2:1, Blend 2) the decomposition of the blend begins at 320°C and has a maximum rate at 397°C. Weight loss during this process amounts to 44.33% of the initial blend mass and after heating to 500°C, the remaining residue constitutes 55.67% of the original blend weight.

SATVA Product Separation of PEO:CaCl$_2$ Blend.

The SATVA trace for the 2:1 EO:CaCl$_2$ blend, reproduced in Fig. 5.35 shows five fractions with peak positions and shapes resembling those for pure PEO. Due to the small quantity of product evolved in the first fraction, both the first and second fractions were collected together for identification by IR spectroscopy. The IR spectrum revealed three degradation products to be present namely

Fig 5.34 TG (•—•—•) and DTG (......) curves for PEO:CaCl$_2$ Blend 1
EO:CaCl$_2$ 10:1 film cast from methanol.

TG (———) and DTG (— — —) curves for PEO:CaCl$_2$ Blend 2
EO:CaCl$_2$ 2:1 film cast from methanol.
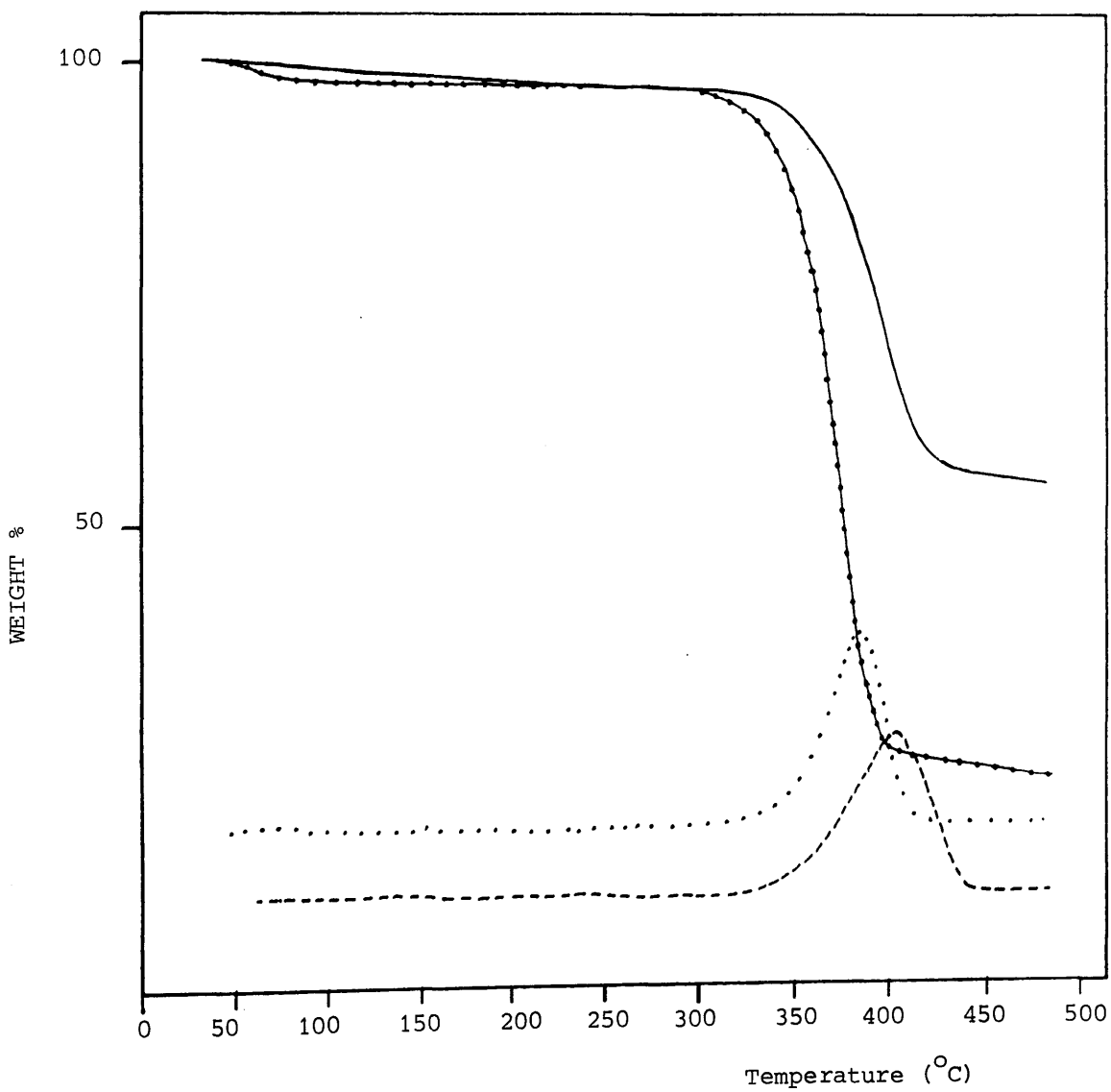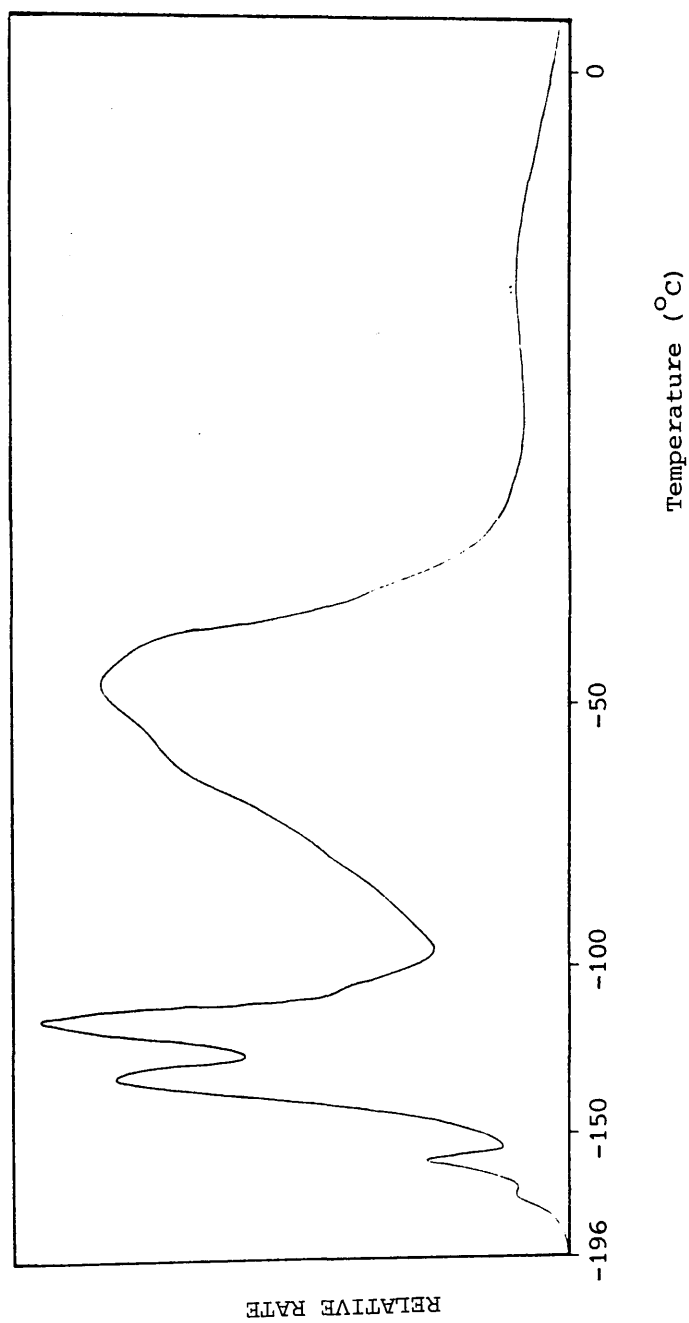
Fig 5. 35   SATVA trace for condensable degradation products on heating

PE O:CaCl$_2$ blend EO:CaCl$_2$ 2:1 to 500°C.

formaldehyde, carbon dioxide and ketene. This was confirmed by mass spectroscopy. The third fraction was found to be mainly due to acetaldehyde with traces of vinyl ethyl ether, vinyl oxy acetaldehyde and methyl ethyl ether identified by mass spectroscopy. The latter of these compounds arising from an overlap with the fourth fraction. The fourth fraction, as for the previous fractions, was collected in a gas cell as a pale brown liquid. A gas phase IR spectrum of the gas cell contents showed only acetaldehyde present although the mass spectrum indicated the presence of higher molecular weight compounds with peaks at $^m/e$ = 87 (0.2%) and the fragmentation peak of highest mass at $^m/e$ = 103 (0.3%). A possible degradation product revealed in the mass spectrum was vinyloxyacetaldehyde. The final fraction consisted of a colourless liquid which had an odour resembling caramelised sugar. The fraction was collected in a cold finger and an IR spectrum obtained of a film cast from methylene chloride on a NaCl plate. The major absorption bands were at 2970 cm^{-1}, 2920 cm^{-1} and 2870 cm^{-1} attributed to CH_2 and OCH_3 stretching bands, 1704 cm^{-1} and 1655 cm^{-1} assigned to an α,β unsaturated carbonyl compound and finally an absorption band at 1110 cm^{-1} due to a C-O stretch. A weak absorption was observed at 3020 cm^{-1} and was assigned to olefinic C-H stretching.

The CRF obtained was a pale yellow oil. When an IR spectrum was run of the CRF as a film cast from methylene chloride on a NaCl plate, the spectrum was found to be identical to that for the CRF of pure PEO.

The residue produced on heating the PEO:$CaCl_2$ blend to 500°C was

a brown powder.   In addition to peaks derived from absorbed water at 3440 cm^{-1} and 1630 cm^{-1} in the IR spectrum of the residue run in the form of a KBr disc, a strong absorption band at 540 cm^{-1} was observed. This absorption was attributed to CaO.

The non-condensable products evolved on degradation were CO and CH_4.   The IR and MS data for condensable product fractions obtained on SATVA of the $PEO:CaCl_2$ blend are presented in Tables 5.23 - Table 5.26.

Absorbance Frequency (cm^{-1})   Product or Band Assignment

3490–3440 (w)	3090–2750 (s)	
1765–1725 (s)	1503 (w)	HCHO
3700 (vw)	2230 (m)	CO_2
2160 (m)	2130 (m)	H_2CCO

Table 5.23a
IR Spectrum of Fraction (1) and (2) from SATVA trace of $PEO:CaCl_2$ Blend.

$^m/e$ value	% Base	Product or Fragmentation Ion
29	78.4	
28	30.1	HCHO
30	6.1	
31	4.6	
42	11.3	
41	12.0	H_2CCO
28	30.1	
14	11.9	
44	100.0	
45	21.7	CO_2
43	25.7	
15	31.8	$.CH_3$
61	3.8	unidentified
60	2.1	$CH_3CH_2OCH_3$

Table 5.23b
Mass Spectrum of Fraction (1) and (2) from SATVA trace of $PEO:CaCl_2$ Blend.

Absorbance Frequency (cm^{-1})	Product or Band Assignment
3470 (w) 2990 (m) 2820 (s) 2730 (s)	
2710 (s) 1760-1730 (s) 1410 (m)	CH_3CHO
1365 (m) 1356 (m) 1122 (m)	
1610 (w) 3130 (w) 3070 (m)	unsaturated C=C
1210 (m)	unidentified

Table 5.24a
I.R. Spectrum of Fraction (3) from SATVA trace of PEO:CaCl$_2$ Blend.

$^{m}/e$ value	% Base	Product or Fragmentation Ion
29	100.0	
44	51.3	
43	22.2	
15	24.5	CH_3CHO
42	6.7	
41	3.1	
26	10.8	
41	3.1	
86	0.1	
57	0.6	$H_2C=CHOCH_2CHO$
43	22.2	
29	100.0	
72	1.6	$CH_3CH_2OCH=CH_2$
60	1.2	$CH_3CH_2OCH_3$

Table 5.24b
Mass Spectrum of Fraction (3) from SATVA trace of PEO:CaCl$_2$ Blend.

Absorbance Frequency (cm^{-1})   Product or Band Assignment

2990 (m)   2820 (s)

2730 (s)   2710 (s)

1758-1733 (s) CH_3CHO

1410 (m)   1365 (m)

1356 (m)   1130-1100 (m)

Table 5.25a
IR Spectrum of Fraction (4) from SATVA trace of PEO:CaCl$_2$

m/e value	% Base	Product or Fragmentation Ion
29	100.0	
44	39.3	
43	29.7	
15	29.3	CH_3CHO
42	8.0	
14	11.3	
26	11.0	
41	4.2	
86	0.6	
57	2.4	
43	29.7	$H_2C{=}CHOCH_2CHO$
29	100.0	
103	0.3	$CH_3CH_2OCH_2CH_2\overset{+}{O} = CH_2$
89	1.5	
87	0.2	$\cdot CH_2CH_2OCH_2CHO$
59	4.3	$CH_3CH_2\overset{+}{O} = CH_2$
60	2.5	
45	10.3	$CH_3CH_2OCH_3$
31	6.9	
29	100.0	
15	29.3	

Table 5.25b
Mass Spectrum of Fraction (4) from SATVA trace of PEO:CaCl$_2$

Absorbance Frequency (cm^{-1})		Product or Band Assignment
3020 (w)		$-C=\overset{|}{C}-H$ C-H unsaturated
2970 (s)	2920 (s)	saturated CH_2 stretching
2870 (s)		$-OCH_3$
1704 (s)	1655 (s)	$\overset{.}{>}C=\overset{|}{C}-O$
1110 (s)		C-O

Table 5.26
IR Spectrum of Fraction (5) from SATVA trace of $PEO:CaCl_2$

THERMAL ANALYSIS OF PEO:NaBr BLENDS.

TG, TVA and SATVA experiments were carried out on PEO:NaBr dry blends and blends cast as a film in which the molar ratio of EO:Salt was 2:1.   Sample sizes of 45 mg PEO (52 mg NaBr) were used in TVA experiments and this was increased to 100 mg PEO in degradations for product separation by SATVA.

Thermal Behaviour of NaBr

Under TVA conditions NaBr was inert as on heating 58 mg NaBr to $500^{\circ}C$ no gaseous decomposition products were evolved nor did sublimation of the salt take place.

TVA Investigations of PEO:NaBr Blend.

The TVA curves for dry and film blends were identical.   A typical TVA curve for a 2:1 EO:NaBr blend is reproduced in Fig. 5.36 The TVA curve gave a single symmetrical peak with an average onset temperature for the evolution of volatile products at $304^{\circ}C$ and a peak maximum at $377^{\circ}C$.   The production of CRF was first observed at $355^{\circ}C$. The behaviour of the individual trap traces was very similar to that for pure PEO.   All the traces were non-coincident and from the $-196^{\circ}C$ trace it could be seen that during the degradation of the blend a small amount of non-condensable products were also evolved.

TG of PEO:NaBr Blends.

TG was carried out on two blends having EO:NaBr ratios of 10:1 (Blend 1) and 2:1 (Blend 2).   The blends were cast as a film from methanol.   The TG and DTG curves for both blends are shown in Fig. 5..37   Degradation in each case occurs in a single stage. The rapid weight loss begins at $300^{\circ}C$ in Blend 1 and occurs slightly
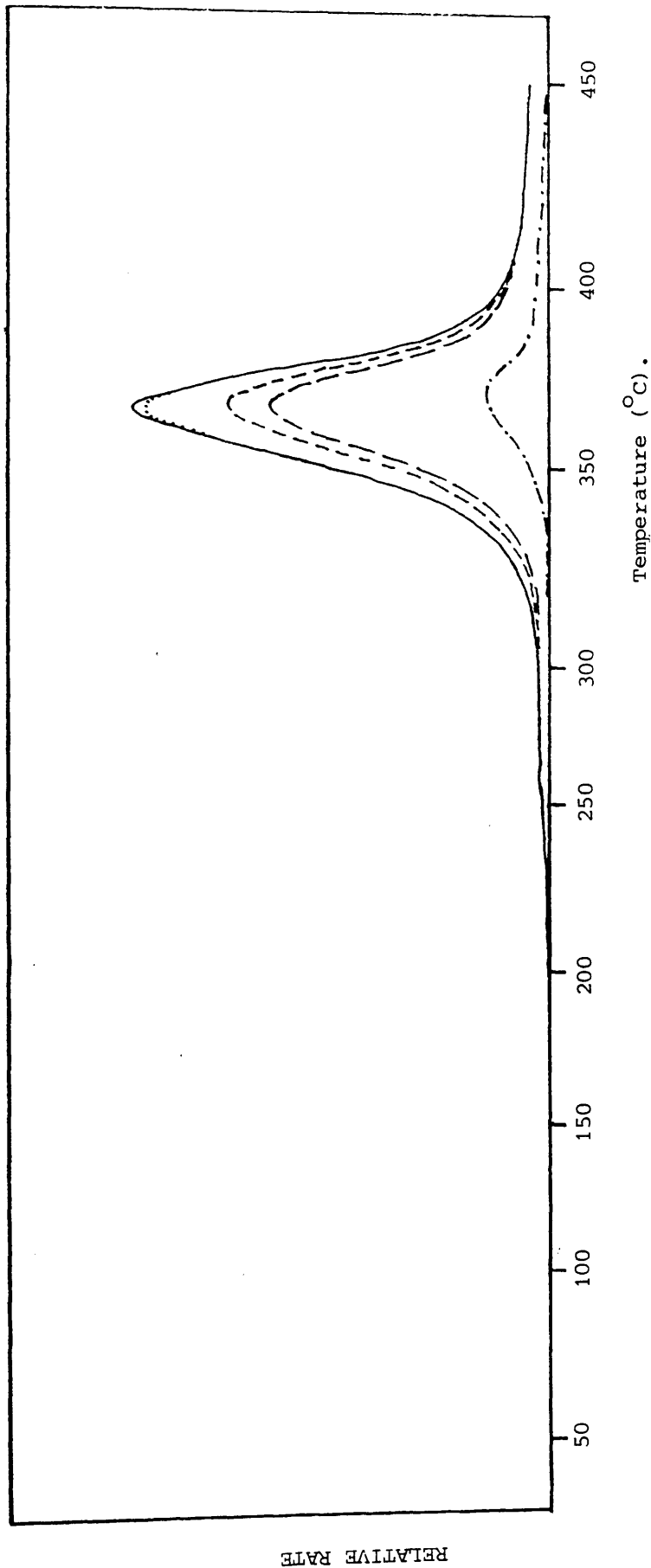
Fig. 5.36   TVA curve for PEO:NaBr blend   EO:NaBr ratio   2:1

Fig 5.37   TG (━•━•) and DTG (·····) curves for PEO:NaBr Blend 1
            EO:NaBr   10:1 film cast from methanol.
            TG (━━━) and DTG (━ ━ ━) curves for PEO:NaBr Blend 2
            EO:NaBr   2:1 film cast from methanol.
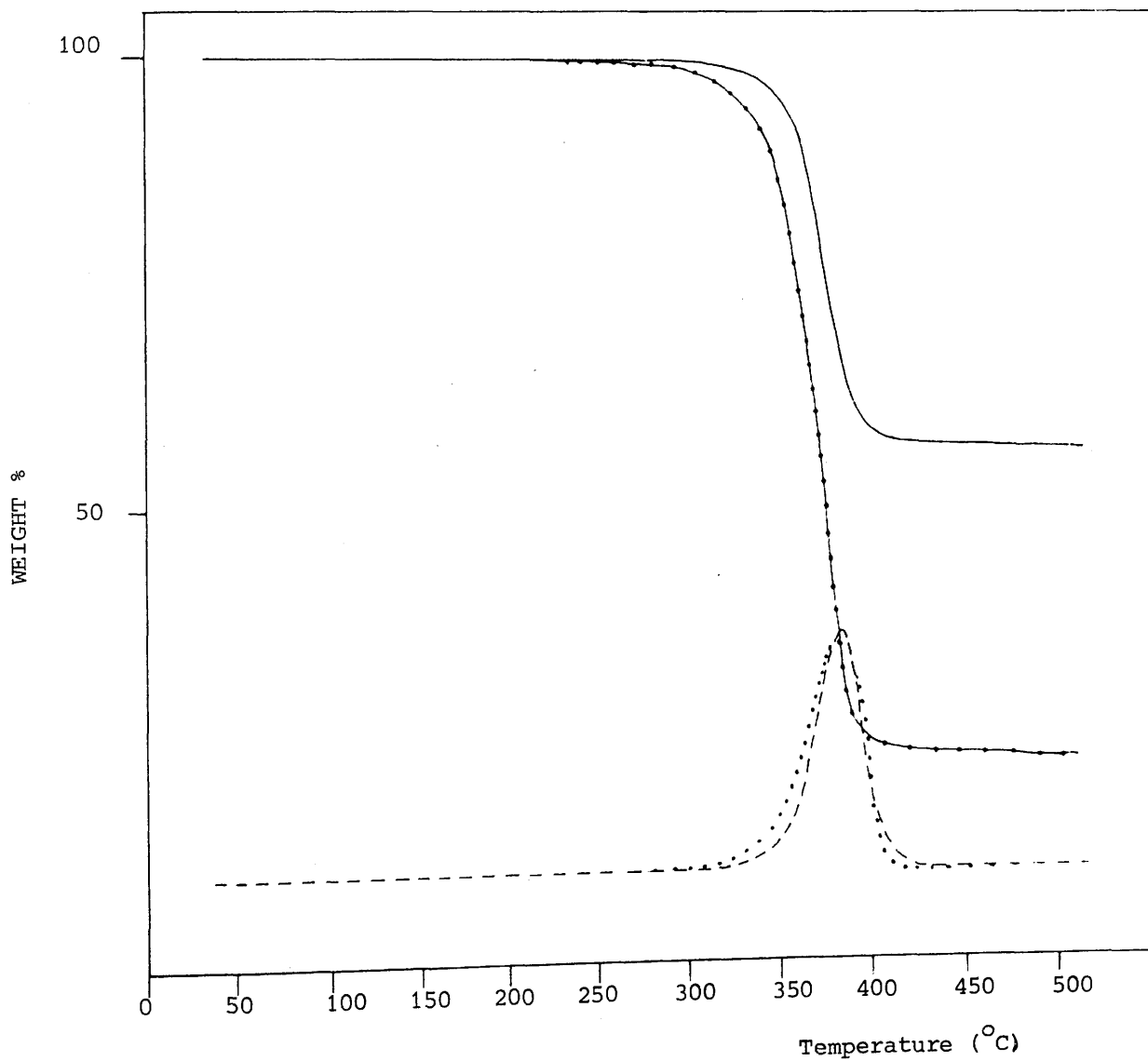
higher at 330°C in the high salt content Blend 2.   The temperatures

at the maximum rate of decomposition in both cases however are

vitrually identical at 378°C and 377°C.   The weight losses

during degradation for the 10:1 EO:NaBr blend and the 2:1 EO:NaBr

blend amount to 77% and 43.5% of the original blend masses respectively.

The corresponding weight % residues remaining after heating to 500°C

are 23% and 56.5%.

SATVA Product Separation of PEO:NaBr Blends.

The SATVA trace obtained for the 2:1 EO:salt blend was

identical to that for pure PEO giving five fractions.   The trace

is illustrated in Fig 5.38.   Due to the small amount of volatile

products in fraction 1, both fraction 1 and fraction 2 were

collected together for spectroscopic analysis, whereupon formaldehyde

carbon dioxide, ketene and traces of methyl ethyl ether were identified.

The major component of the third fraction was acetaldehyde, however

IR evidence suggested the presence of unsaturated compounds.   From

mass spectral data it is possible that vinyl ethyl ether and traces

of vinyl oxyacetaldehyde are also produced during the degradation.

The fourth fraction was separated into the preceding shoulder

(fraction 4a) and the main portion of the peak (fraction 4b) was

collected together with the final fraction.   Fraction 4a was

collected in a gas cell, and with the aid of mass spectrometry

methyl ethyl ether, diethyl ether, methoxyethylene, methoxy

acetaldehyde, ethoxy acetaldehyde and traces of vinyloxyacetaldehyde

are proposed present.   For IR analysis fractions 4b and 5 were

collected in a gas cell.   The IR spectrum of the cell contents

was vitrually identical to that for fraction 4 in pure PEO.   Mass

spectral interpretation revealed ethoxyacetaldehyde,

vinyl oxyacetaldehyde, ethanol and methoxyethanol could be present.
In both liquid and gas phase mass spectra of this blend fraction,
the highest fragmentation ion appeared at $^m/e = 96$ (1.8%) and $^m/e =$
95 (1.5%) in the liquid spectrum which could not be accounted for.

The CRF took the form of a very pale yellow oil.   An IR spectrum
obtained for a neat film on a CsI plate, was identical to that for the
CRF of pure PEO.

The residue, after heating the blend to 500°C under TVA
conditions was a fawn powder.   When a spectrum of the residue, as a
KBr disc, was run the major peaks in the spectrum were at 1100 cm^{-1}
and 472 cm^{-1}.   The former of these bonds is observed in the IR
spectrum of the residue on similar treatment of PEO and is attributed
to residual C-O bonds on the char residue.   The new band in the
blend residue is assigned to NaO.

Degradation in a closed system revealed CO and CH_4 to be the
non-condensable product evolved.   The IR and MS data for condensable
product fractions are presented in Tables 5.27 - 5.30.
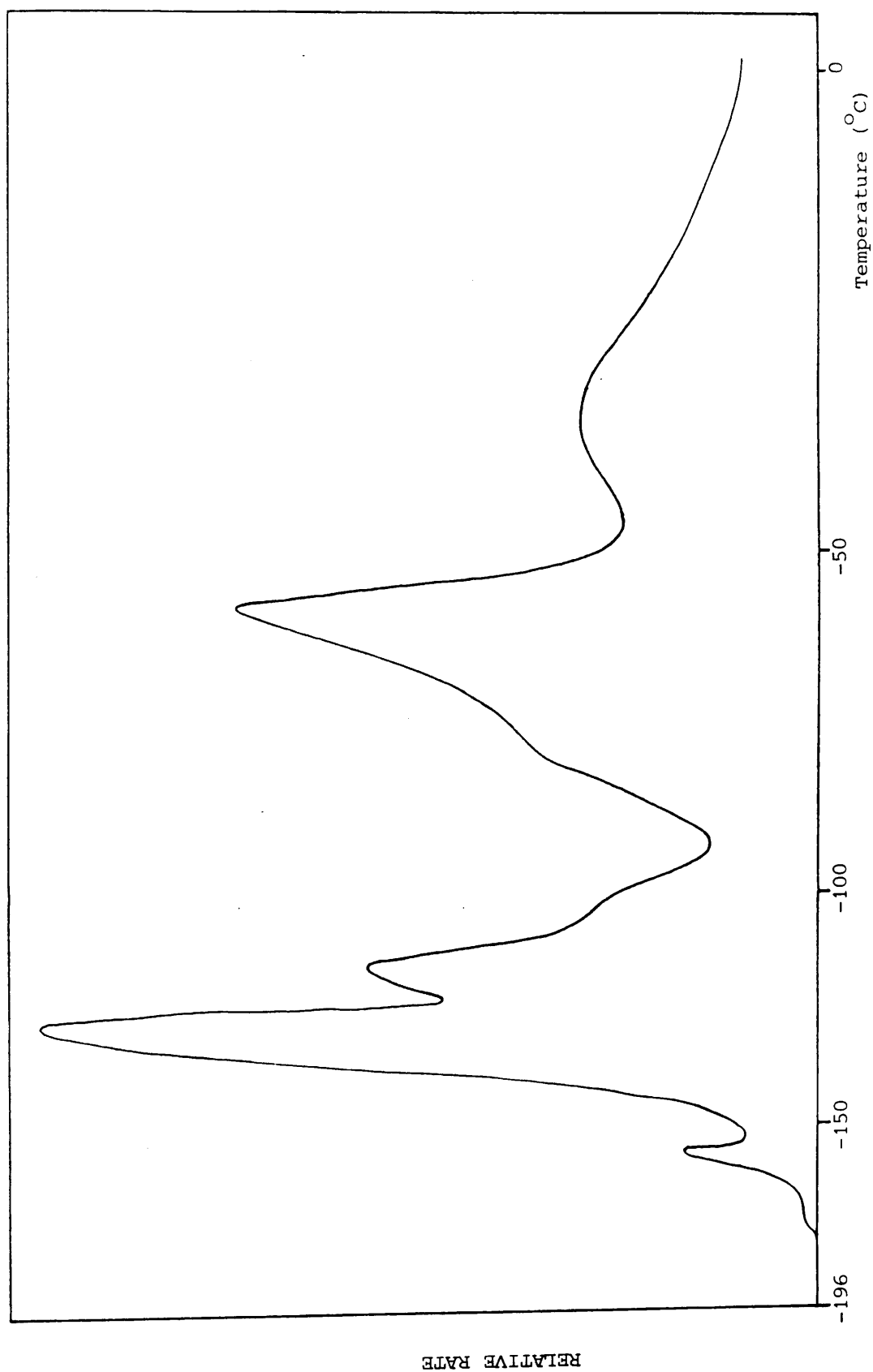
Fig 5.38   SATVA trace for condensable degradation products on heating PEO:NaBr blend

EO:NaBr   2:1   to 500°C.

RELATIVE RATE

Temperature (°C)

Absorbance Frequency (cm^{-1})   Product or Band Assignment

3090-2650 (s) 3490 (w)   3470 (w)

3430 (w)   1765 (s)   1743 (s)   HCHO

1715 (s)   1501 (m)   1468 (m)

3730 (w)   3710 (w)   2314 (s)   668 (w) CO_2

2165 (w)   2135 (w) H_2CCO

Table 5.27a
IR Spectrum of Fractions 1 and 2 from SATVA trace of PEO:NaBr Blend.

^{m}/e value	% Base	Product or Fragmentation Ion.
30	49.4	
29	100.0	HCHO
28	19.2	
44	13.2	CO_2
42	1.6	H_2CCO
41	1.3	
60	1.3	
45	7.8	
31	3.2	$CH_3OCH_2CH_3$
29	100.0	
15	6.8	

Table 5.27b
Mass Spectrum of Fractions 1 and 2 from SATVA trace of PEO:NaBr Blend.

Absorbance Frequency (cm^{-1})   Product or Band Assignment

2765 (m)   2725 (m)   2700 (m)   1754 (s) CH_3CHO
    1407 (m)   1366 (w)   1301 (w)

2985 (m) CH_2 stretch

1726 (s)   1718 (s)   1710 (s)   C=O stretch
1611-1605 (w)   C=C-H unsaturated
1209 (m)   unidentified
1130 (m)   C-O stretch
 959 (m)   C=C
 920 (w)
814 (w)   744 (w)   unidentified

Table 5.28a
IR Spectrum of Fraction (3) from SATVA trace of PEO:NaBr Blend.

$^m/e$ value	% Base	Product or Fragmenation Ion.
29	100.0	
44	23.5	
43	22.4	CH_3CHO
15	20.7	
42	6.3	
26	24.2	
86	0.6	
59	3.4	
57	1.1	$H_2C=CHOCH_2CHO$
43	22.4	
29	100.0	
27	38.8	
72	3.4	
57	1.1	
43	22.4	$CH_3CH_2OCH=CH_2$
29	100.0	
27	38.8	
74	1.3	
59	3.4	
45	7.8	CH_3OCH_2CHO (overlap)
43	22.4	
29	100.0	
74	1.3	
73	2.1	
59	3.4	$CH_3CH_2OCH_2CH_3$ (overlap)
45	7.8	
29	100.0	
89	0.1	$CH_3CH_2OCH_2CH_2O\cdot$
73	2.1	
84	1.0	
58	1.5	$CH_3OCH=CH_2$
56	9.4	unidentified
49	1.9	
39	3.2	
38	2.1	

Table 5.28b
Mass Spectrum of Fraction (3) from SATVA trace of PEO:NaBr Blend.

Absorbance Frequency (cm^{-1})	Product or Bond Assignment
2985 (s) 2965 (s) 2890 (s)	CH_3 CH_2 stretching
1710 (m) 1615 (m)	$C = C - O$
1405 (s)	CH_2 bonding
1250 (m) 1210 (m)	unidentified
1142 (s)	C-O stretch
1050 (s) 1034 (s)	
870 (s)	unidentified

Table 5.29a   IR Spectrum of Fraction (4a) from SATVA trace of PEO:NaBr$_2$ Blend.

^{m}/e value	% Base	Product or Fragmentation Ion.
89	2.7	$CH_3CH_2OCHCH_2O \cdot$
73	82.9	$CH_3CH_2OCH_2CH_2^{\cdot}$
59	36.4	
45	90.0	
29	100.0	
15	50.5	
60	9.3	
45	90.0	
31	89.4	$CH_3CH_2OCH_3$
29	100.0	
89	6.7	
87	9.0	
73	82.9	
59	36.4	$CH_3CH_2OCH_2CHO$
45	90.0	
43	85.9	
29	100.0	
15	50.5	
58	35.8	$CH_3OCH=CH_2$, $CH_2 = \overset{\oplus}{O}H$
31	39.4	
27	50.9	unidentified
39	5.2	
89	5.2	
86	0.4	
59	36.4	$H_2C = CHOCH_2CHO$
57	4.1	
43	85.9	
29	100.0	
27	50.9	
74	2.4	
59	36.4	
45	90.0	CH_3OCH_2CHO
43	85.9	
31	89.4	$CH_3CH_2OCH_2CH_3$ (excl. ^{m}/e 31)
29	100.0	
15	50.5	

Table 5.29b   Mass Spectrum of Fraction 4a from SATVA trace of

PEO:NaBr Blend.

Absorbance Frequency (cm^{-1})	Product or Band Assignment
2990 (s) 2912 (s) 2880 (s) 2850 (sh)	CH_3, CH_2 stretching
1758 (m) 1744 (m) 1738 (m) 1705 (w)	$\rangle C = O$
1640 (m)	$\rangle C = C\langle$ unsaturation
1616 (s)	$\rangle C = C\langle$ unsaturation
1408 (m)	CH_2 stretch bend
1321 (m)	C-H deformation
1212 (s)	unidentified
1143 (s)	C-O-C stretch
858 (w) 718 (w)	unidentified

Table 5.30a   IR Spectrum of Fraction 4b and 5 from
SATVA trace of PEO:NaBr Blend.

^{m}/e value	% Base	Product or Fragmentation Ion
103	0.6	
89	0.3	
73	9.1	$CH_3CH_2OCH_2CH_2\overset{\oplus}{O}=CH_2$
59	5.0	
45	26.3	
29	100.0	
15	22.6	
88	1.9	
73	9.1	
59	5.0	
45	26.3	$CH_3CH_2OCH_2CHO$
43	23.3	
29	100.0	
15	22.6	
86	3.2	
57	4.5	
43	23.3	$H_2C = CHOCH_2CHO$
29	100.0	
27	20.8	
76	0.1	
61	0.3	
45	26.3	CH_3OCHCH_2OH
31	55.1	
18	5.7	
15	22.6	
46	4.3	
45	26.3	
37	55.1	CH_3CH_2OH
29	100.0	
15	22.6	

Table 5.30b   Mass Spectrum of Fraction 4b and 5 from
SATVA trace of PEO:NaBr   Blend.

THERMAL ANALYSIS OF PEO : NaSCN BLENDS

TG, TVA and SATVA experiments were performed on PEO:NaSCN blends in the form of cast films and dry powders. The molar ratio of monomer units : salt initially used was 2:1. In TVA experiment runs sample sizes of 45 mg PEO (41 mg NaSCN) were taken whilst 80 mg PEO (74 mg NaSCN) were used in SATVA product separation experiments.

Thermal Behaviour of NaSCN

TVA and SATVA investigations were carried out on 100 mg sample of NaSCN. From TVA experiments negligible volatile decomposition products were evolved from the salt, however, the subsequent SATVA trace gave three small peaks. The corresponding fractions were found to contain traces of H_2S, HCN and H_2O respectively.

TVA Investigations of PEO : NaSCN Blend.

The TVA curves obtained for both film and dry blends were very similar. In each case, a single peak was obtained. This is illustrated for a 2:1 EO:salt blend in Fig 5.39 The average onset temperature for the evolution of volatile product was $280^{\circ}C$ and the maximum rate of degradation occurred at approximately $343^{\circ}C$.
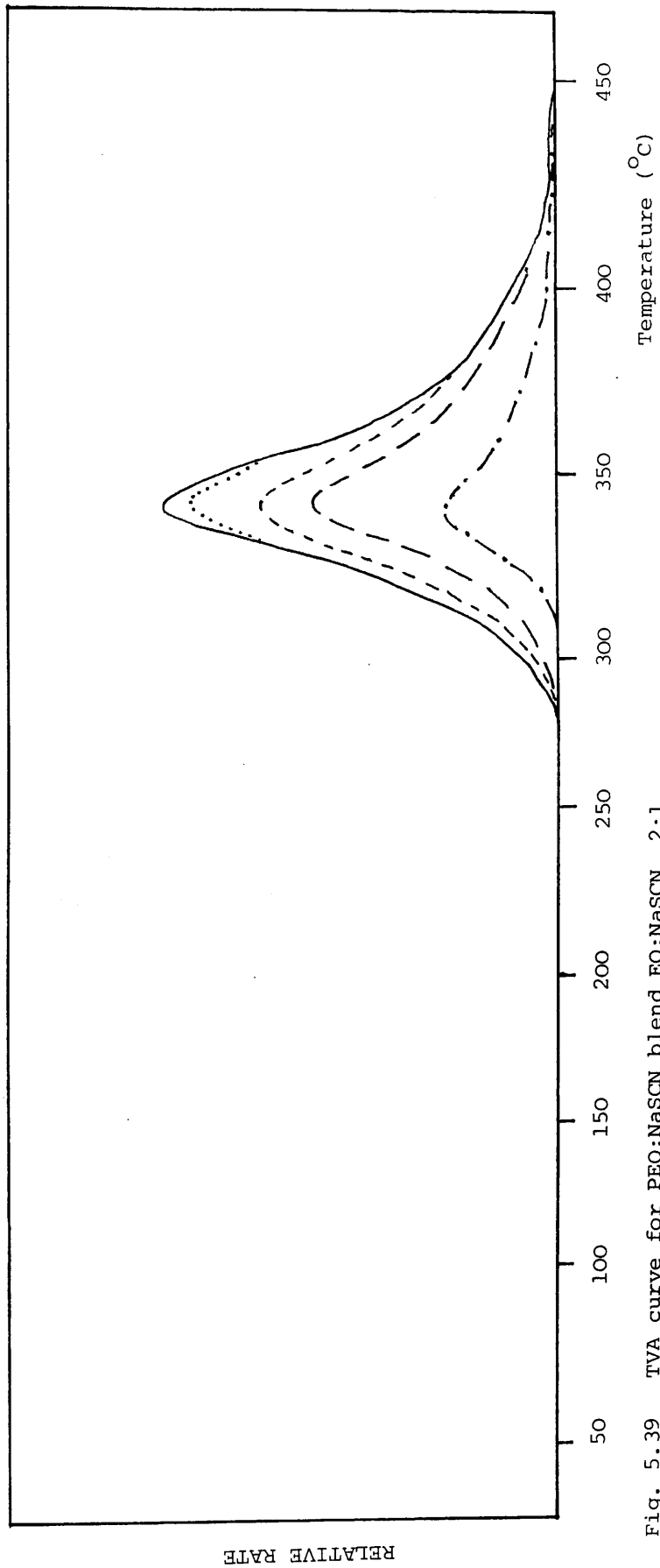
Fig. 5.39   TVA curve for PEO:NaSCN blend EO:NaSCN   2:1

TG of PEO : NaSCN Blends

TG was carried out on two blends having EO : NaSCN ratios of 10:1 (Blend 1) and 2:1 (Blend 2). The blends were cast as a film from methanol. The TG and DTG curves for both blends, reproduced in Fig. 5.40 show that weight loss occurs in a single stage. In Blend 1, the onset of the degradation process leading to the evolution of volatile compounds is at $305^{\circ}C$ and the rate maximum temperature observed at $373^{\circ}C$. During the decomposition, 84.85% of the original blend weight is evolved as degradation products leaving 15.15% weight residue after heating to $500^{\circ}C$.

In Blend 2, (EO : NaSCN 2:1) both the degradation onset and rate maximum temperature are elevated relative to those for Blend 1 (EO : NaSCN 10:1) and occur at $358^{\circ}C$ and $393^{\circ}C$ respectively. The weight loss during degradation accounts for 52.58% of the initial blend

Fig 5.40 TG (——•—) and DTG (·•····) curves for PEO:NaSCN Blend 1
EO:NaSCN 10:1 film cast from methanol.
TG (———) and DTG (——— —) curves for PEO:NaSCN Blend 2
EO:NaSCN 2:1 film cast from methanol.
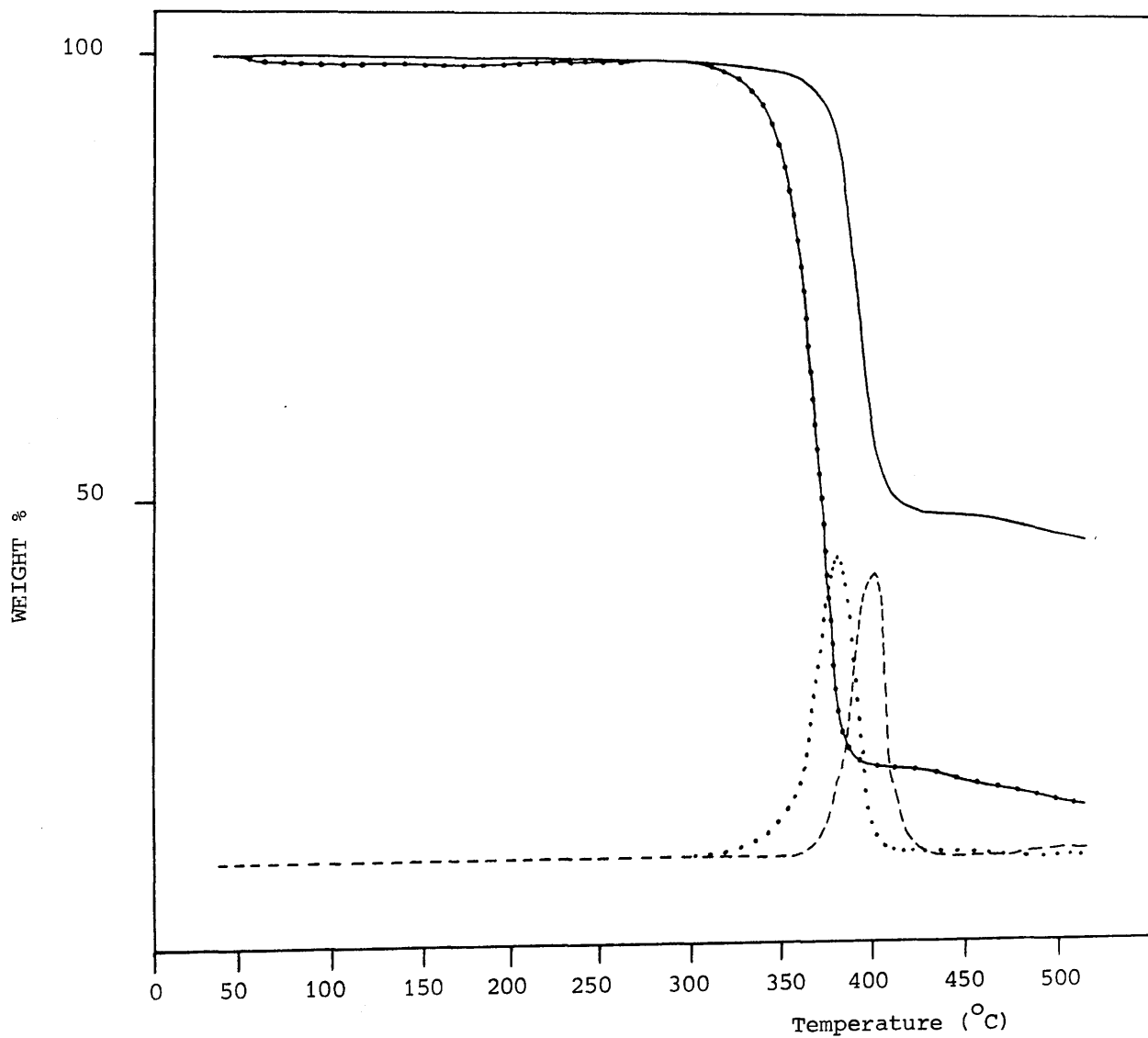
mass, the remaining 47.42% being deposited as residue.

SATVA Product Separation of PEO : NaSCN Blend

The SATVA trace for a 2:1 EO:NaSCN blend, shown in Fig. 5.41 gave four readily separable fractions. The overall appearance of the peaks, a very sharp initial peak followed by three similar broad peaks, was unlike those in any of the previous blends investigated. The first fraction was found to contain mostly ethene with traces of ketene and ethyne present as revealed by IR spectroscopy. In the second fraction CO_2 was identified by IR analysis but the base peak in the corresponding mass spectrum was at $^m/e = 34$ indicating H_2S was a major component in the mixture. Other major peaks on the IR spectrum at 2072 cm^{-1} and 2052 cm^{-1} suggested ketene or thiocyanate or cyanide compounds also to be present. There were also unidentified absorption bands at 1061 cm^{-1} and 1024 cm^{-1}. The third fraction (as for fractions 1 and 2) was collected in a gas cell whereupon a colourless liquid was observed to have condensed in the collection limb. The fraction was found to be almost solely due to HCN with possible traces of ethyl cyanide, ether fragments and unsaturated compounds. In the final fraction, collected as a colourless liquid, water was clearly identified and the remainder of the components, mostly ether structures, chain fragments and possibly dioxone, were only present in trace amounts.

The CRF appeared as a pale yellow viscous liquid. The IR spectrum of the blend CRF obtained as a neat film on a salt plate was very similar to that for pure PEO. The differences are as follows: (i) the reduction of the CH_2 rocking band at ≈1195 cm^{-1} in CRF of PEO to appear as a shoulder in the spectrum of the blend CRF; (ii) the absence of the band at 1317 cm^{-1} in the spectrum of the blend CRF;
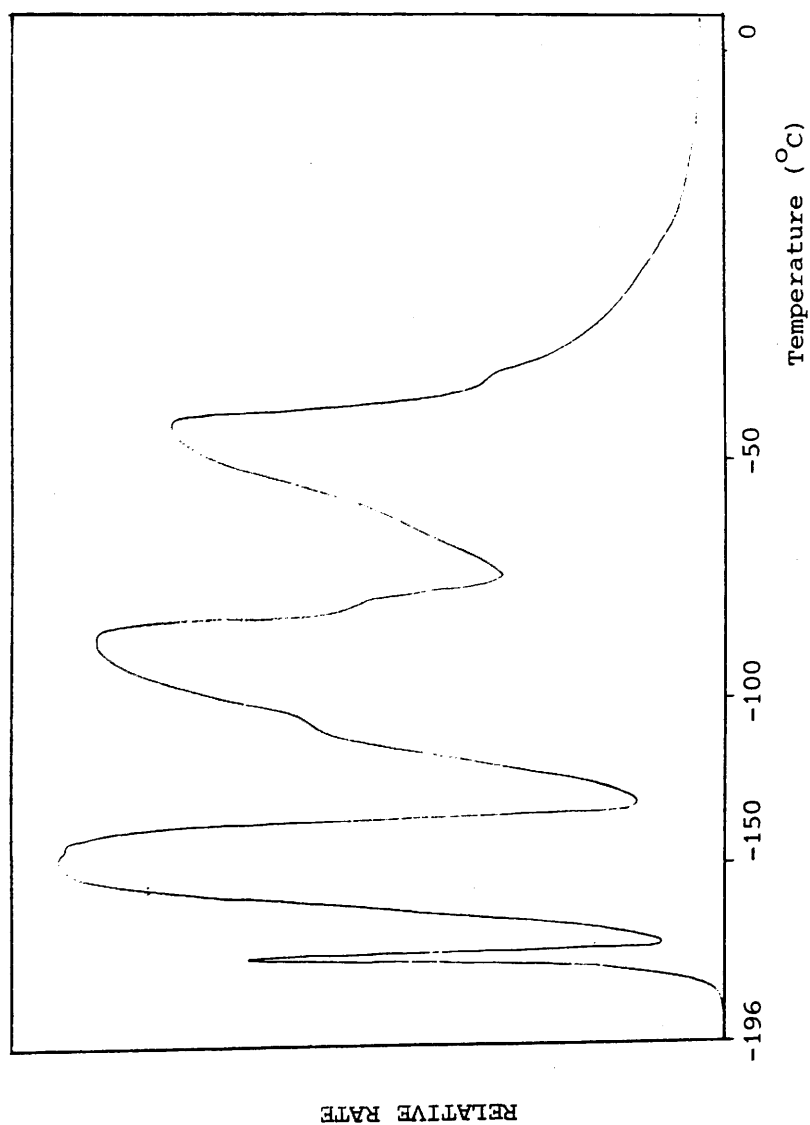
Fig 5. 41 SATVA trace for condensable degradation products on heating PEO:NaSCN blend

EO:NaSCN 2:1 or 10:1 to $500^{o}C$

(iii) the appearance of an absorption band of medium intensity at 1716 cm^{-1} in the spectrum of the blend CRF. This band was attributed to the carbonyl stretch of an α,β unsaturated aldehyde. The IR and MS data for condensable product fractions from 2:1 EO : NaSCN blend are presented in Tables 5.31 - 5.34.

In order to gain further information about the degradation products derived from PEO in the PEO : NaSCN blend TVA and SATVA investigations were carried out on a blend of lower salt concentration. A 10:1 EO:NaSCN blend was prepared (40 mg 1ml PEO : 7.9mg) in methanol and appropriate volumes taken for the required thermal analytical technique.

TVA Investigations of PEO : NaSCN Blend (10:1).

The TVA curve resulting from the 10:1 EO:NaSCN blend gave a single peak with an onset temperature corresponding to the evolution of volatile products at 280°C and a maximum rate of degradation at 360°C. The production of CRF was first observed at 340°C. The appearance of the TVA curve was very similar to that for the 2:1 EO:NaSCN blend. The separation of the individual traces indicate the production of a variety of products of varying volatilities and in particular, a significant amount of non-condensable products.

SATVA Product Separation of PEO:NaSCN Blend (10:1).

The SATVA trace for the 10:1 EO:NaSCN blend was separated into four fractions which were collected in individual gas cells. The first fraction (see Fig. 5.41) contained a small single peak which upon mass spectral and IR analysis was found to be due to ethene. The second fraction, which also consisted of a single peak, contained four compounds. From mass spectral data the main component was H_2S

($^{m}/e$ = 34, see Table 5.36b) with CO_2 a minor product, and ethyne and
ketene as trace products.   In the IR spectrum of the fraction, however,
H_2S could not be traced.   When a standard spectrum for H_2S was run
using the same gas cell (approximate volume 1.18 cm^3) containing over
50 Torr H_2S a very weak spectrum was obtained with absorption bands at
approximately 2690 cm^{-1} and 1251 cm^{-1} in the spectrum.   Thus
identification of H_2S was made solely on mass spectral data with the
assumption that the concentration of H_2S was too low to detect by IR
spectroscopy.   This lack of H_2S IR absorption bands had been
noticed in the spectrum of the 2:1 EO:NaSCN blend.   The third
fraction comprised two poorly resolved peaks.   HCN was the major
component and acetaldehyde a very minor product, was clearly
identifiable from IR and MS data.   Other possible trace products
include ethyl cyanide, methyl ethyl ether and divinyl ether.   The
remaining fraction was found from IR and MS results to contain
methanol traces of water and an aldehydic compound.   The trace
compound derived from polyether chain fragments may be ethyl vinyl
ether, methoxydiethyl ether, methoxy acetaldehyde, ethoxyacetaldehyde,
vinylacetaldehyde and ethanol.

The CRF consisted of a pale yellow viscous liquid and was
attributed to chain fragments.

The IR and MS data for condensable product fractions from
10:1 EO:NaSCN blend are presented in Tables 5.35 - 5.38.

Absorbance Frequency (cm^{-1})			Product or Band Assignment
3110 (w)			
3075 (w)	3010 (w)	2979 (w)	
3760 (m)	1890 (w)	1465 (w)	$CH_2 = CH_2$
1446 (w)	1415 (w)		
949 (s)	729 (m)		$CH \equiv CH$

Table 5.31a   IR Spectrum of Fraction 1 from SATVA trace
of PEO:NaSCN Blend. (2:1)

$^m/e$ value	% Base	Product or Fragmentation Ion
28	100.0	
27	50.9	
26	51.3	$H_2C = CH_2$
25	7.5	
24	2.1	
44	3.7	CO_2 (overlap)
42	0.1	H_2CCO
15	1.0	CH_3
26	51.3	$HC \equiv CH$
60	0.7	
49	0.1	unidentified
39	0.3	

Table 5.31b   Mass Spectrum of Fraction 1 from SATVA trace
of PEO:NaSCN Blend. (2:1)

Absorbance Frequency (cm^{-1})			Product or Band Assignment
3730 (m)	3700 (m)	2312 (s)	CO_2
719 (m)	668 (s)		
2072 (s)	2052 (s)		H_2CCO or CN or SCN?
1061 (s)	1024 (s)	711 (w)	unidentified
730 (w)			$CH \equiv CH$ (overlap)

Table 5.32a   IR Spectrum of Fraction 2 from SATVA trace
of PEO:NaSCN Blend. (2:1)

$^m/e$ value	% Base	Product or Fragmentation Ion
34	100.0	
33	23.6	H_2S
32	24.9	
44	45.3	CO_2
26	0.3	$HC{\equiv}CH$
16	1.8	O
28	3.9	$CH_2{=}CH_2$ (overlap)
36	7.9	
38	1.7	
60	0.8	unidentified
72	0.2	
70	0.1	

Table 5.32b   Mass Spectrum of Fraction 2 from SATVA trace
of PEO:NaSCN Blend. (2:1)

Absorbance Frequency (cm^{-1})			Product or Band Assignment
3330 (s)	3270 (s)	2808 (w)	
2090 (w)	1432 (w)	1378 (s)	HCN
3070 (w)	708 (s)		
2990 (w)			unsaturated C=C
1622 (m)	1520 (m)	1222 (m)	unidentified
1204 (m)	1175 (m)	1038 (m)	

Table 5.33a   IR Spectrum of Fraction 3 from SATVA trace
of PEO:NaSCN Blend. (2:1)

$^m/e$ value	% Base	Product or Fragmentation Ion
27	100.0	
26	11.8	HCN
28	2.9	
55	0.3	
29	0.6	CH_3CH_2CN
26	11.8	
43	0.5	CH_3CO
76	0.2	
72	0.2	unidentified
70	0.2	

Table 5.33b   Gas Phase Mass Spectrum of Fraction 3 from
SATVA trace of PEO:NaSCN Blend. (2:1)

^{m}/e value	% Base	Product or Fragmentation Ion
18	100.0	H_2O
17	12.8	$CH_2=\overset{\oplus}{O}H$
31	13.2	
28	15.7	
29	8.8	
88	0.2	?
58	1.6	
46	1.3	
45	5.7	CH_3CH_2OH
29	8.8	
17	12.8	
59	1.3	$CH_3CH_2\overset{\oplus}{O}=CH_2$
45	5.7	$CH_2=\overset{\oplus}{O}CH_3$
43	4.5	$CH_3CH=\overset{\oplus}{O}H$
90	3.4	$CH_3\ \overset{\oplus}{C}O$
72	1.0	unidentified
225	0.2	
224	0.1	
223	0.2	Chain fragments

Table 5.34   Liquid Phase Mass Spectrum of Fraction (4)
from SATVA trace of PEO:NaSCN Blend. (2:1)

Absorbance Frequency (cm^{-1})	Product or Bond Assignment
950 (m)	$CH_2=CH_2$
731 (w)	$CH{\equiv}CH$ (overlap)
714 (w)	unidentified

Table 5.35a   IR Spectrum of Fraction 1 from SATVA trace
of PEO:NaSCN Blend (10:1)

$^m/e$ value	% Base	Product or Fragmentation Ion
28	100.0	
27	25.6	
26	25.0	$CH_2 = CH_2$
25	5.0	
29	3.1	
24	1.4	
26	25.0	$CH \equiv CH$ (overlap)
44	2.8	CO_2 (overlap)
34	4.2	H_2S (overlap)
33	1.6	
32	15.5	O_2, S
16	1.6	O

Table 5.35b   Mass Spectrum of Fraction 1 from SATVA
trace of PEO:NaSCN Blend (10:1)

Absorbance Frequency (cm^{-1})			Product or Bond Assignment
3735 (w)	3685 (w)	3620 (w)	CO_2
3585 (w)	2322 (s)	714 (m)	
	669 (m)		
2072 (m)	2052 (m)		H_2CCO
1720 (w)			$C=O$
1454 (m)			CH_2 bending
731 (m)			$CH \equiv CH$

Table 5.36a   IR Spectrum of Fraction 2 from SATVA trace
of PEO:NaSCN Blend (10:1)

m/e value	% Base	Product or Fragmentation Ion
34	100.0	
33	26.9	H_2S
32	44.3	
44	15.3	CO_2
26	1.1	$CH{\equiv}CH$
28	2.9	$CH_2 = CH_2$ (overlap)
27	2.2	
42	0.1	H_2CCO
41	0.5	

Table 5.36b   Mass Spectrum of Fraction 2 from SATVA
               trace of PEO:NaSCN Blend (10:1)

Absorbance Frequency (cm^{-1})			Product or Bond Assignment
1756 (s)	1744 (s)	1730 (s)	
2700 (w)	1420 (m)	1372 (m)	CH_3CHO
1350 (w)	1120 (w)	1100 (w)	
3330 (w)	3280 (w)	1438 (m)	HCN
735 (m)	714 (s)	688 (m)	
1632–1618 (m)			unsaturated C=C
1221 (m)	1204 (m)	1180 (m)	unidentified
1072 (m)	1026 (m)		C-O

Table 5.37a   IR Spectrum of Fraction 3 from SATVA trace
               of PEO:NaSCN Blend (10:1)

$^{m}/e$ value	% Base	Product or Fragmentation Ion
27	100.0	
28	33.6	HCN
26	15.1	
29	13.4	
44	8.6	
43	6.3	CH_3CHO
15	7.6	
42	4.1	
41	2.8	
55	0.6	
54	0.4	CH_3CH_2CN
29	13.4	
26	15.1	
72	0.4	
43	6.3	
70	1.8	$H_2C=CH-O-CH=CH_2$
42	4.1	
44	8.6	
27	100.0	
72	0.4	
44	8.6	$CH_3CH_2OCH=CH_2$ (overlap)
43	6.3	
29	13.4	
27	100.0	
60	1.7	
45	3.3	
29	13.4	$CH_3OCH_2CH_3$
15	7.6	
59	2.0	
84		unidentified
62		

Table 5.37b   Mass Spectrum of Fraction 3 from SATVA trace
of PEO:NaSCN Blend (10:1)

Absorbance Frequency (cm^{-1})			Product or Bond Assignment
3640 (w)			unidentified
3500 (w)	2960 (s)	2890 (s)	
1052 (m)	1032 (m)		CH_3OH
2730 (w)	2695 (w)	1755 (m)	
	1725 (m)		aldehyde
1615 (w)			unsaturation
1450 (m)	1405 (w)	1360 (w)	CH_2 CH deformation
1210 (w)	712 (w)		unidentified
2280 (w)	2250 (w)		unidentified

Table 5.38a   IR Spectrum of Fraction 4 from SATVA trace
             of PEO:NaSCN Blend (10:1).

$^m/e$ value	% Base	Product or Fragmentation Ion
31	100.0	
32	7.2	CH_3OH
15	20.0	
18	32.9	
17	8.7	H_2O
55	1.8	
29	54.4	
34	0.4	CH_3CH_2CN
26	9.5	
72	1.0	
44	15.0	
43	25.8	
29	54.9	$CH_3CH_2OCH = CH_2$
27	20.7	
15	20.0	
26	9.5	
103	0.2	
89	6.2	
73	5.4	
59	4.4	$CH_3CH_2OCH_2CH_2\overset{\oplus}{O} = CH$
45	16.9	
29	54.9	
15	20.0	
88	0.8	
73	5.4	
59	4.4	
45	16.9	$CH_3CH_2OCH_2CHO$
43	25.8	
29	54.9	
15	20.0	
86	1.5	
57	5.4	$H_2C = CHOCH_2CHO$
43	25.8	
29	54.9	
27	20.7	
74	0.2	
59	4.4	
45	16.9	
43	25.8	CH_3OCH_2CHO
31	100.0	
29	54.9	
15	20.0	
46	4.8	
45	16.9	
31	100.0	CH_3CH_2CH
29	54.9	
15	20.0	
106		unidentified
100		"
91		"

Table 5.38b   Mass Spectrum of Fraction 4 from SATVA trace
of PEO:NaSCN Blend (10:1)

THERMAL ANALYSIS OF PEO : LiClO$_4$ BLENDS

TG, TVA and SATVA experiments were carried out on PEO:LiClO$_4$ blends having the molar ratios of 10:1 (Blend 1) and 2:1 (Blend 2) EO:salt. Due to the explosive nature of LiClO$_4$ on grinding, blends were cast as films from methanol. Standard solutions were prepared containing either 50 mg PEO ml^{-1} and 18.2 mg LiClO$_4$ ml^{-1} or 50 mg PEO ml^{-1} and 60.3 mg LiClO$_4$ ml^{-1}. From these solutions films were cast to give sample sizes of approximately 50 mg and 100 mg PEO for TVA and SATVA experiments respectively. After removal of solvent, the 2:1 blend was opaque indicating non-compatibility between the components.

Thermal Behaviour of LiClO$_4$

The thermal behaviour of LiClO$_4$ was not investigated using TVA however from the literature DTA experiments[199] reveal LiClO$_4$ melts at 241°C and decomposes with the liberation of oxygen at 489°C. The overall reaction for the decomposition of LiClO$_4$ is

$$LiClO_4 \longrightarrow LiCl + 2O_2$$
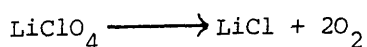
TVA Investigation of PEO:LiClO$_4$ Blends

The TVA curve for Blend 1 (see Fig. 5.42) gave a single peak with the evolution of volatile products commencing at 279°C and reaching a maximum rate at 363°C. Individual traces indicate a variety of products being produced on degradation including non-condensable products. On increasing the LiClO$_4$ content from 10:1 EO:LiClO$_4$ to 2:1 as in Blend 2 (see Fig. 5.43) a two stage decomposition results. The onset of degradation is lowered to 252°C and the maximum rate of evolution of volatile compounds is at 321°C. During this first decomposition stage, all five traces are

Fig. 5.42   TVA curve for PEO:LiClO$_4$ Blend 1   EO:LiClO$_4$ 10:1
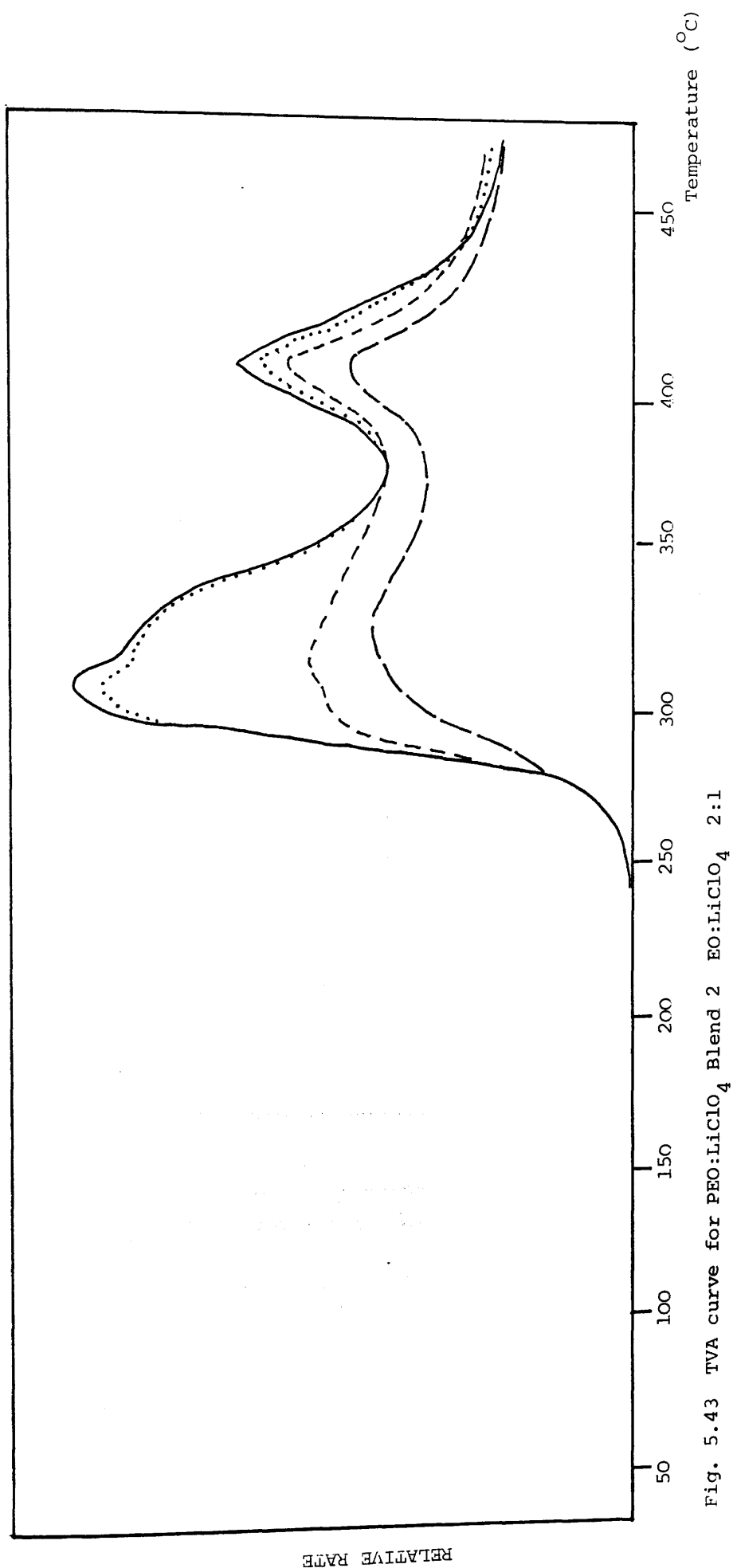
Fig. 5.43 TVA curve for PEO:LiClO$_4$ Blend 2 EO:LiClO$_4$ 2:1

Fig 5.44   TG (•——•) and DTG (••••) curves for PEO:LiClO$_4$ Blend 1
EO:LiClO$_4$ 10:1 film cast from methanol.

TG (——) and DTG (———) curves for PEO:LiClO$_4$ Blend 2
EO:LiClO$_4$ 2:1 film cast from methanol.
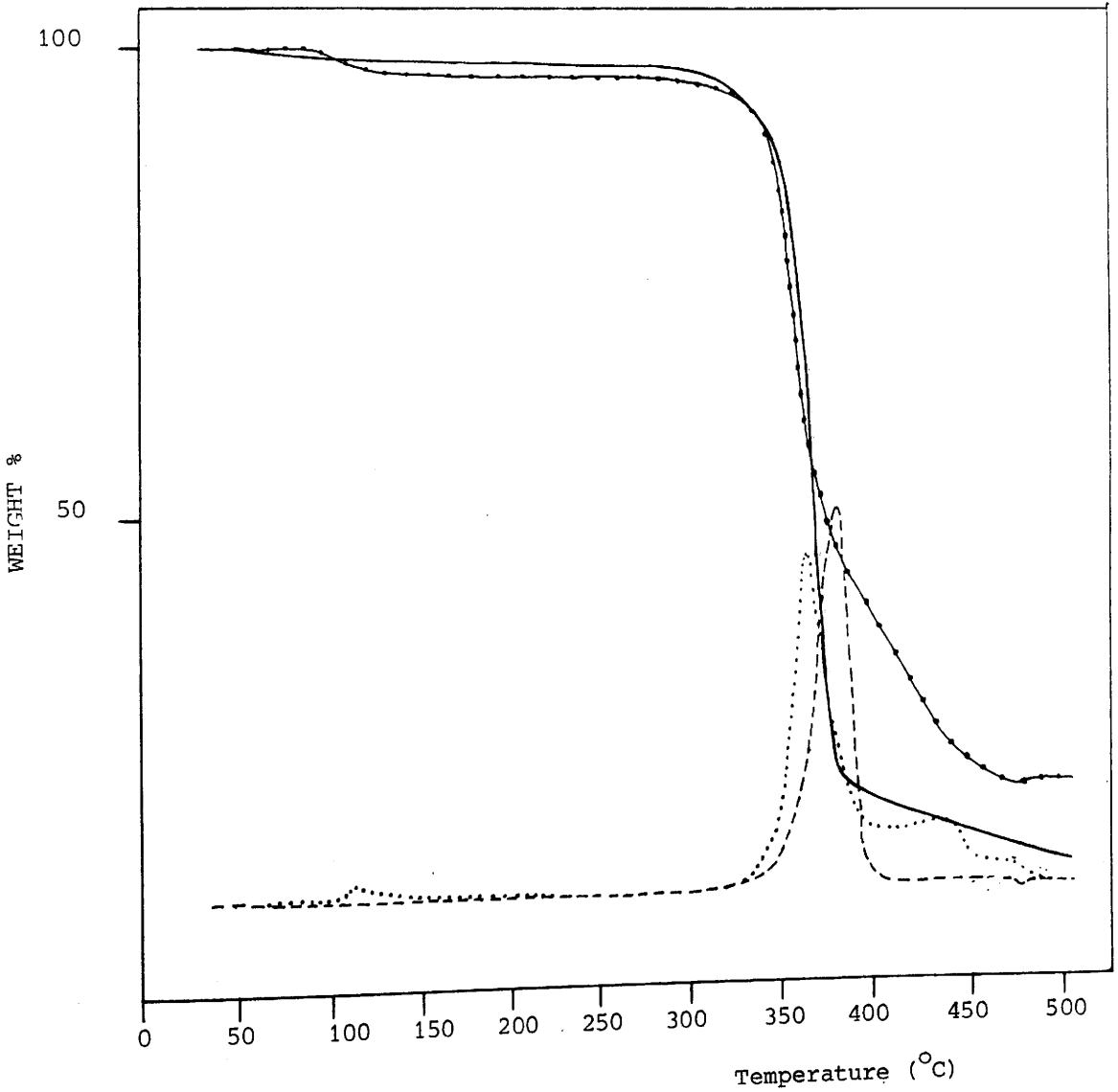
are non-coincident.   There is some evolution of non-condensable
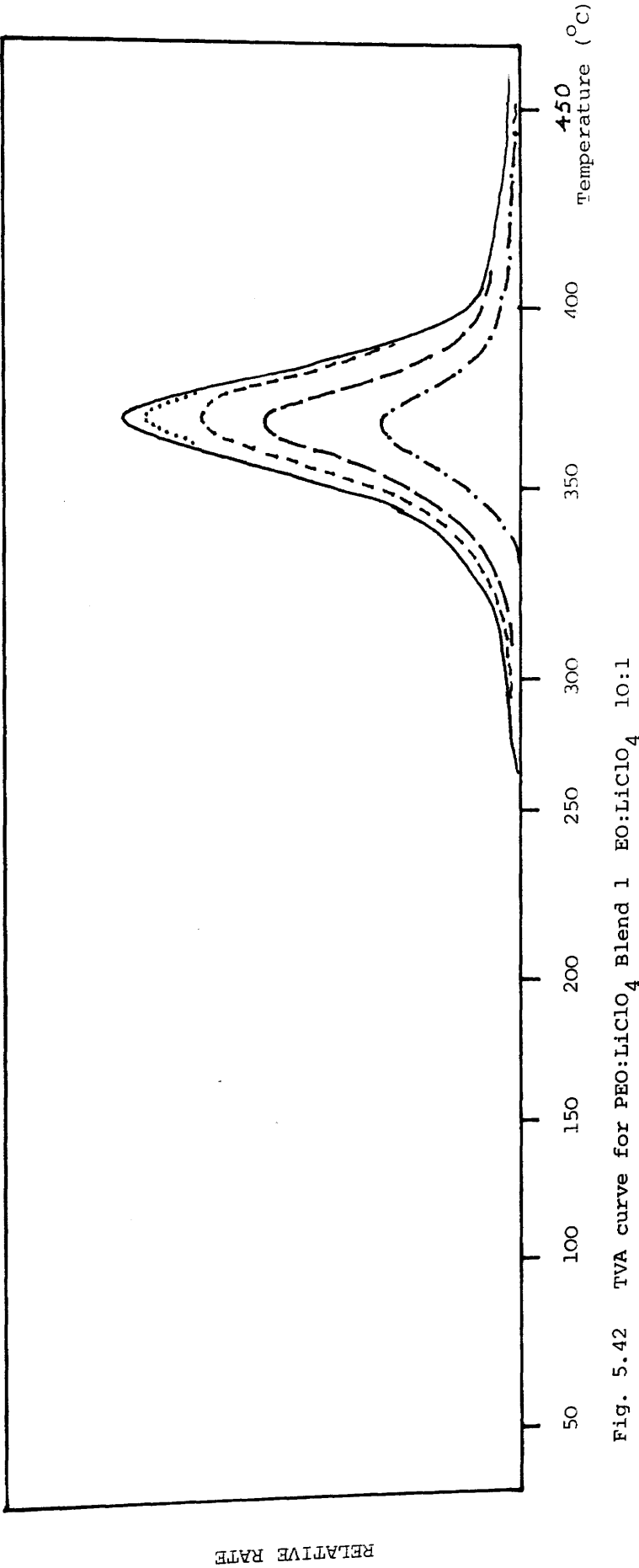
degradation products, however, this increases in the second stage of

decomposition which occurs around 380°C and reaches a maximum rate

at 418°C.

TG of PEO:LiClO$_4$ Blends

The TG and DTG curves, illustrated in Fig. 5.[44] show that for

the 10:1 EO:LiClO$_4$ blend the degradation occurs in a single stage

with the evolution of volatile products commencing at 300°C and

reaching a maximum rate at 374°C.   After heating to 500°C, 13.4%

by weight of blend sample remains as residue.   On increasing the

salt content of the blend, a two stage decomposition is observed.

The onset of degradation beginning at 306°C is virtually identical

to that for the 10:1 blend, however the rate maximum occurs slightly

earlier at 358°C.   During the first stage of decomposition, the

rapid weight loss accounts for 48.45% of the polymer blend.   The

second degradation stage begins at 375°C and reaches a maximum rate

at 431°C.   In this stage 29.89% by weight of the blend decomposes

up to 475°C whereafter no further weight loss is seen and 21.66% by

weight of the original blend remains as residue on heating to 500°C.

SATVA Product Separation for PEO:LiClO$_4$ Blend

The SATVA trace for the condensable products of degradation to

500°C of the 10:1 EO:LiClO$_4$ blend, reproduced in Fig. 5.[45] shows

five fractions.   The initial highly volatile fraction and the

second fraction were collected in the same gas cell for identification.

IR and mass spectral analysis revealed these fractions to contain

predominantly CO$_2$ with ethene (high volatile fraction), ketene and

ethyne also present.   The third fraction was poorly resolved from
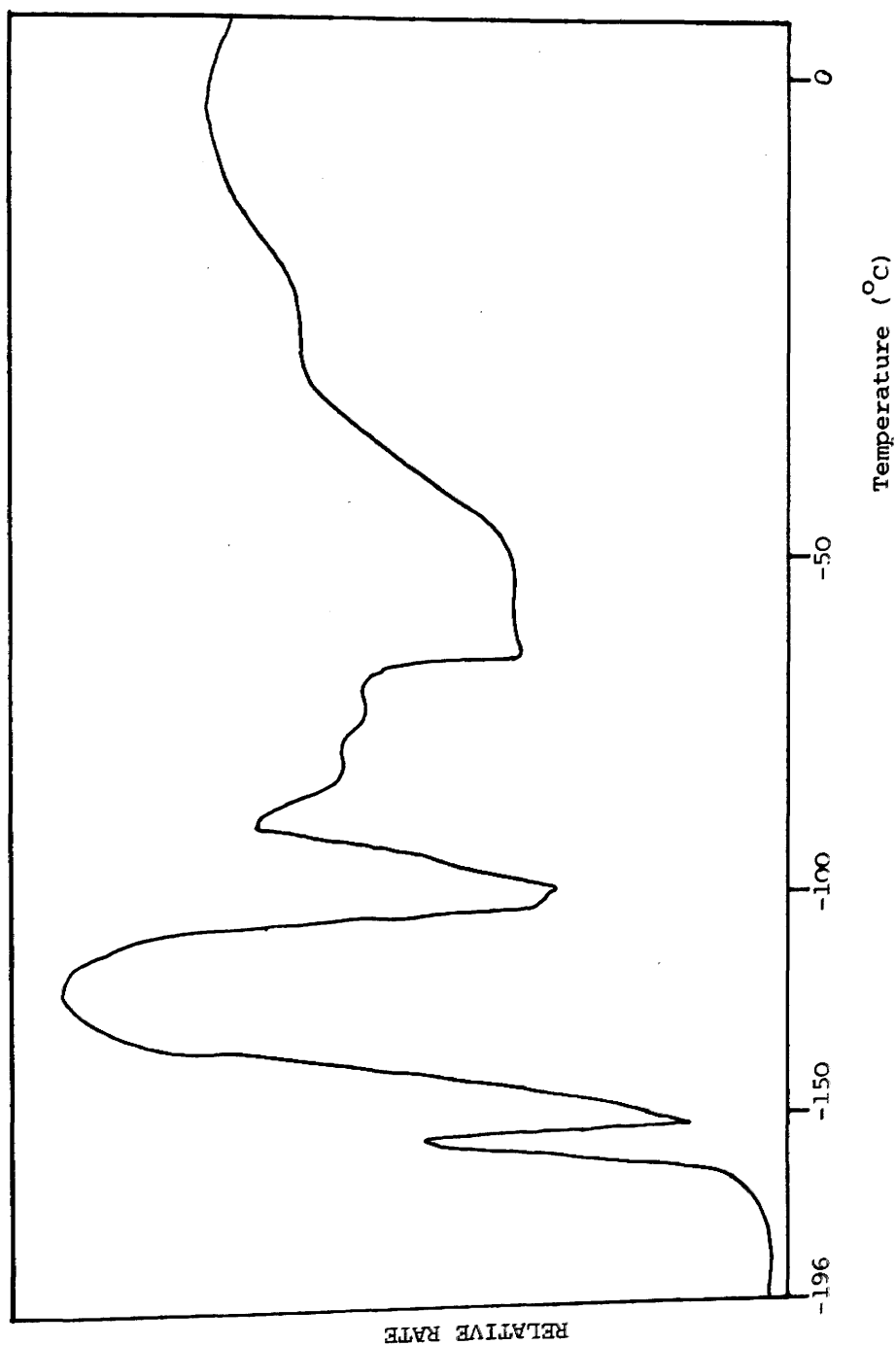
Fig 5.45 SATVA trace for condensable degradation products on heating PEO:LiClO$_4$ blend EO:LiClO$_4$ 10:1 to 500°C.

the fourth fraction which appeared as a shoulder which was itself poorly resolved from its neighbouring peak.   The third and fourth fractions were therefore collected together for spectroscopic analysis.   From the IR and mass spectral results obtained acetaldehyde was identified.   The final fraction, as for the preceding fractions, was collected in a gas cell.   The resultant IR spectrum was very poor and only general stretching CH_2, aldehydic C-H and aldehydic C=O absorption bands could be identified.   The mass spectrum however, indicated the presence of ethoxyacetaldehyde, vinyl oxyacetaldehyde methoxyacetaldehyde, diethyl ether, methyl ether, vinyl ethyl ether, ethanol and chain fragments containing up to two monomer units.

The CRF obtained was a pale yellow wax similar to that for pure PEO.

The IR and MS data for condensable product fractions obtained on SATVA of the PEO:LiClO$_4$ blend are reproduced in Tables 5.39 - 5.41.

The onset temperatures and maximum rate temperatures of degradation of all the blends studied by both TVA and TG are presented in Tables 5.42 and 5.43 respectively.   Finally the condensable and non-condensable degradation products identified on SATVA separation for each PEO:salt blend together with those for pure PEO are reproduced in Table 5.44.

Absorbance Frequency (cm^{-1})   Product or Bond Assignment

			Product or Bond Assignment
3720 (s)	3690 (s)	2380-2270 (s)	CO_2
732 (s)	700-640 (s)		
2170 (m)	2140 (m)		H_2CCO
953 (m)			CH_2CH_2
722 (m)			HCCH

Table 5.39a   IR Spectrum of Fraction 1 and 2 from SATVA trace of $PEO:LiClO_4$ Blend

$^m/e$ value	% Base	Product or Fragmentation Ion
44	100.0	CO_2
45	1.1	
28	12.8	CH_2CH_2
27	0.4	
26	0.6	HCCH
25	0.1	
16	7.4	O

Table 5.39b   Mass Spectrum of Fraction 1 and 2 from SATVA trace of $PEO:LiClO_4$ Blend.

Absorbance Frequency (cm^{-1})   Product or Bond Assignment

			Product or Bond Assignment
3470 (w)	2790 (m)	2820-2700 (s)	CH_3CHO
1760-1715 (s)	1440 (m)	1470 (s)	
1365 (s)	1351 (s)	1120-1100 (s)	
930-855 (w)			
746 (w)			unidentified

Table 5.40a   IR Spectrum Fraction 3 and 4 from SATVA trace of $PEO:LiClO_4$ Blend

$^m/e$ value	% Base	Product or Fragment
29	100.0	
44	51.3	
15	40.9	CH_3CHO
43	31.4	
42	10.6	
26	12.5	

Table 5.40b   Mass Spectrum of Fraction 3 and 4 from SATVA trace of $PEO:LiClO_4$ Blend.

Absorbance Frequency (cm^{-1})	Product or Bond Assignment
2820 (m) 2700 (m)	CH_2, CH stretching
1720 (m)	C=O stretching

Table 5.41a IR Spectrum of Fraction 5 from SATVA trace of $PEO:LiClO_4$ Blend.

^{m}/e value	% Base	Product or Fragmentation Ion
89	0.2	
73	2.2	
59	0.9	$CH_3CH_2OCH_2CH_2O\cdot$
45	5.3	$CH_3CH_2OCH_2CH_2$
29	100.0	
15	38.3	
88	6.8	
87	0.7	
73	2.2	
59	0.9	$CH_3CH_2OCH_2CHO$
45	5.3	
43	30.1	
29	100.0	
15	38.3	
86	2.2	
59	0.9	
57	2.4	$H_2C{=}CHOCH_2CHO$
43	30.1	
29	100.0	
27	14.9	
78	0.4	unidentified
74	0.1	
59	0.9	
45	5.3	CH_3OCH_2CHO
43	30.1	$CH_3CH_2OCH_2CH_3$ (excl ^{m}/e=31)
31	11.8	
29	100.0	
15	38.3	
60	1.1	
45	5.3	
31	11.8	$CH_3CH_2OCH_3$
29	100.0	
58	8.4	$CH_3OCH{=}CH_2$, $CH_2{=}\overset{\oplus}{O}H$
31	11.8	
27	14.9	unidentified
39	3.1	
46	0.3	
45	5.3	
31	11.8	CH_3CH_2OH
29	100.0	
15	38.3	
39	3.1	unidentified

Table 5.41b Mass Spectrum of Fraction 5 from SATVA
trace of PEO:LiClO$_4$ Blend.

Salt Used in PEO Blend	Molar Ratio of Components EO:Salt	Blend Form.	T onset (°C)	T CRF (°C)	T max 1 (°C)	T onset 2 (°C)	T max 2 (°C)
$ZnBr_2$	10:1	film	232		323	376	
$ZnBr_2$	2:1	film	200	240	252	293	315
$ZnBr_2$	2:1	dry	183	230	232	287	308
ZnO	10:1	dry	298	348	373		
ZnO	2:1	dry	301	348	373		
$ZnCl_2$	2:1	film	208	250	252	297	320
$ZnCl_2$	2:1	dry	201	247	255	294	325
$CoBr_2$	4:1	film	181		257	385	300
$CoBr_2$	4:1	dry	184		257	385	301
$CaBr_2$	2:1	dry	203	252	339	366	409
$CaCl_2$	2:1	film	317	354	372		
$CaCl_2$	2:1	dry	309	351	374	405	
NaBr.	2:1	film	281	323	383		
NaBr	2:1	dry	304	355	377		
NaSCN	10:1	film	280	340	360		
NaSCN	2:1	film	283	344	357		
NaSCN	2:1	dry	275	346	361		
$LiClO_4$	10:1	film	279		363		
$LiClO_4$	2:1	dry	252		321	380	418
PEO		dry	310	350	374		

Table 5.42   Degradation Temperatures obtained by TVA for PEO:Salt blends.

Salt used in PEO Blend	molar ratio of components EO:salt	T onset 1 (°C)	T max 1 (°C) (sh °C)	T onset 2 (°C)	T max 2 (°C)	% Wt loss Stage 1(sh)	% Wt loss Stage 2	Wt % residue
$ZnBr_2$	10:1	265	309	320	382	60.94	31.77	7.29
$ZnBr_2$	2:1	245	278	300	386	20.00	50.00	30.00
$ZnCl_2$	10:1	270	325	348	420	60.93	17.20	21.87
$ZnCl_2$	2:1	277	313	373	426	36.00	24.00	40.00
ZnO	10:1	325	388			82.50	–	17.50
ZnO	2:1	337	392			51.04		48.96
$CoBr_2$	4:1	237	281(328)	393		51.28	12.82	35.90
$CoBr_2$	2:1	237	277(322)	395		26.53(2.04)	10.72	60.71
$CaBr_2$	10:1	272	350			78.50		21.50
$CaBr_2$	2:1	273	336	370	385	44.90	5.10	50.00
$CaCl_2$	10:1	305	384			77.32		22.68
$CaCl_2$	2:1	320	397			44.33		55.67
NaBr	10:1	300	378			77.00		23.00
NaBr	2:1	330	377			43.50		56.50
NaSCN	10:1	305	373			84.85		15.15
NaSCN	2:1	358	393			52.58		47.42
$LiClO_4$	10:1	300	374			86.60		13.40
$LiClO_4$	2:1	306	358	375	431	48.45	29.89	21.66
PEO		310	384			98.25		1.95

Table 5.43 Degradation Temperatures and Weight Loss as obtained by TG and DTG for PEO:Salt Blends.
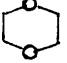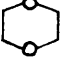
454

SALT USED IN PEO BLEND.

	ZnBr₂	ZnO	ZnCl₂	CoBr₂	CaBr₂	CaCl₂	NaBr	NaSCN	LiClO₄	PEO
Non-condensable Products	CO, CH₄	CO, CH₄	CO, CH₄	CO, CH₄	CO, CH₄	CO, CH₄	CO, CH₄	CO, CH₄		CO, CH₄, CH₃CH₃
Fraction 1	CO_2, $CH_2{=}CH_2$, H_3CCO, $CH{=}CH$	CO_2, $CH_2{=}CH_2$, $CH{=}CH$	CO_2, $CH_2{=}CH_2$	CO_2, $CH_2{=}CH_2$, HBr	CO_2, $CH_2{=}CH_2$, H_2CCO	CO_2, H_2CCO	CO_2, H_2CCO	$CH_2{=}CH_2$	CO_2 $CH_2{=}CH_2$	CO_2, $CH_2{=}CH_2$, H_2CCO
Fraction 2	CH_3CHO, CH_3Br, HBr, CH_3CH_2Br	HCHO	CH_3CHO	CH_3CHO, CH_3CH_2Br, CH_3Br	CH_3CHO, CH_3CH_2Br, CH_3Br	CH_3CHO	HCHO, $CH_3OCH_2CH_3$	CO_2, H_2S, $CH{=}CH$	H_2CCO, $CH{=}CH$	HCHO, $CH_3OCH_2CH_3$
Fraction 3	$CH_3CH_2OCH_2CHO$, CH_3OCH_2CHO, $CH_3OCH{=}CH_2$	CH_3CHO	(ring) (?)	(ring)	(ring)	CH_3CHO	CH_3CHO, $CH_3CH_2OCH_2CHO$, CH_3OCH_2CHO, $CH_2{=}CHOCH_2CHO$, $CH_3CH_2OCH_2CH_3$, $CH_3OCH{=}CH_2$			CH_3CHO
Fraction 4	(ring)	$CH_3CH_2OCH{=}CH_2$, $CH_2{=}CHOCH{=}CH_2$, $CH_2{=}CHOCH_2CHO$, $CH_2{=}CHOCH_2CH_2{-}OCH_2CH_3$			$BrCH_2CH_2OCH_2CH_2$	$CH_3CH_2OCH_3$, $CH_3CH_2OCH{=}CH_2$, $H_2C{=}CHOCH_2CHO$				$CH_3CH_2OCH_2CH_3$, $CH_3CH_2OCH{=}CH_2$, $CH_2{=}CHOCH{=}CH_2$, $CH_2{=}CHOCH_2CHO$, CH_3OCH_2CHO, $CH_3CH_2OCH_2CHO$
Fraction 5	$BrCH_2CH_2OH$, H_2O									H_2O, CH_3CH_2OH, $HOCH_2CH_2OH$, $CH_2{=}CHOCH_2CH_2OH$

CONDENSABLE PRODUCTS

Table 5.44 Non-condensable and Condensable Degradation Products from PEO-Salt Blends.

5.3 DISCUSSION

The addition of $ZnBr_2$ to PEO whether to a lesser (10:1 $EO:ZnBr_2$) or greater (2:1 $EO:ZnBr_2$) extent has a profound effect on the thermal degradation behaviour of PEO with respect to both temperature and mode of decomposition.   In both blends, the thermal stability is lowered relative to that for pure PEO by approximately $100^{\circ}C$ (see Table 5.42 and Table 5.43) suggesting that there is a strong interaction between $ZnBr_2$ and PEO to alter its degradation behaviour.   A two stage decomposition is observed (Fig. 5.9) which is less defined in the low salt content blend (the second stage appears as a shoulder on the TVA curve of the 10:1 $EO:ZnBr_2$ blend).   The second stage becomes more dominant however in the 2:1 $EO:ZnBr_2$ blend.   In this case, the TVA and TG (DTG) results both indicate a clear two stage degradation occurs followed by a less significant slow evolution of degradation products. The onset and rate maxima temperatures shown by these techniques are in reasonable agreement (see Table 5.42 and 5.43).   With the $PEO:ZnBr_2$ system, as the $ZnBr_2$ content of the blend is increased, the blend becomes less stable.   TVA results suggest there is a slight effect due to blend form on the temperature region of degradation which is lowered in the dry blend compared to the blend cast as a film when identical sample compositions are used.   This is contrary to what might have been expected since in a blend which has been cast as a film there is more intimate polymer - additive contact, thus facilitating interaction between the species.

In addition to the observed temperature effects noted by the presence of $ZnBr_2$, the degradation mechanism is changed considerably. This is reflected in both the multistage decomposition process and the additional degradation products formed.   The major new degradation product from both high and low $ZnBr_2$ content blends is dioxane and

traces of HBr, methyl bromide, ethyl bromide and bromoethanol are also produced (see Table 5.2 - Table 5.6). TVA product separation and partial degradation experiments on a 2:1 EO:ZnBr$_2$ blend indicate that on heating the blend the first products of degradation evolved include acetaldehyde, dioxane and carbon dioxide. The formation of CRF is first observed at 235°C on average. Above approximately 280°C, (the onset of the second decomposition) the production of dioxane has ceased although acetaldehyde and carbon dioxide evolution continues. In the final stages of degradation, above 365°C, acetaldehyde is still produced, together with chain fragments of low volatility.

It is proposed that the production of dioxane is a direct consequence of the interaction between ZnBr$_2$ and PEO. The complex formed arises due to coordination of the lone pair of electrons of the ether oxygen with Zn^{2+}. It has been outwith the scope of this investigation, due to limitations in time available, to elucidate the exact structure of the complex involved, although the possible models suggested in the literature[179,152,177] include : a) the cations are enclosed in a single helical unit; b) the cations may be coordinated by two chains which complex the cations on either side; c) the two chains are mutually intertwined in a double helix which encloses cations along its axis. For the purpose of this discussion, the simplest model put forward by Buschmann[179] is considered to represent the interaction between PEO and ZnBr$_2$. Thus the complex is thought of in terms single helical strand of PEO in which zinc cations are enclosed at certain spacings. This is illustrated in Fig. 5.2a. By this model it is possible to consider the complex as a random copolymer consisting of complexed and uncomplexed monomer units. These complexed and uncomplexed regions within the polymer

chain may, on degradation, result in the formation of different
decomposition products.

It appears feasible that the production of dioxane may arise
from a cyclisation reaction in the polymer chain brought about by the
coordination of Zn^{2+} with two non-adjacent oxygen atoms as shown below:
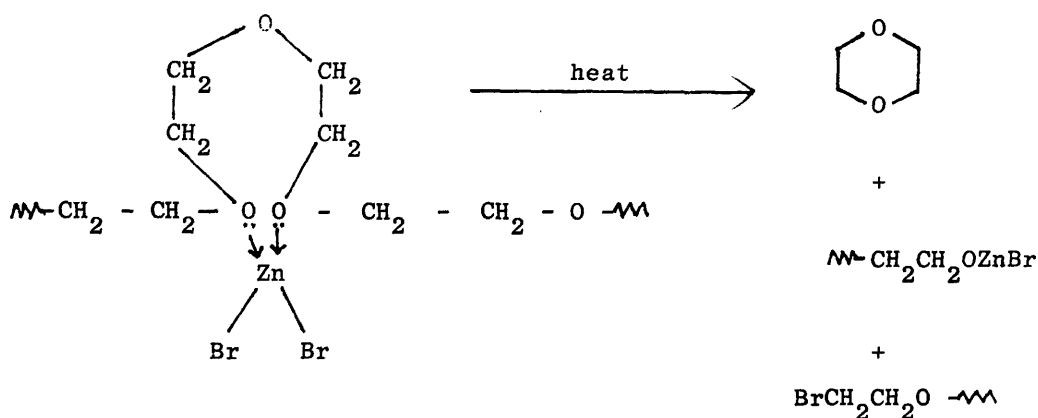
In this mechanism zinc exhibits tetrahedral geometry which is
favoured.   The two bromine terminated macromolecules formed can
then undergo further degradation to produce the brominated products
observed including HBr, methyl bromide, ethyl bromide and bromoethanol.
With the zinc containing macromolecule these processes will result in
the formation of zinc oxide which was found in the residue after
heating PEO : $ZnBr_2$ blends to $500^{\circ}C$.

Acetaldehyde and the products common to those obtained on the
degradation of pure PEO will be produced via the random chain scission
process described in Chapter 3, although the production of these
compounds occurs at a lower temperature due to the destabilising
effect of $ZnBr_2$.

In the high salt content blends (2:1 EO:salt), an excess of ZnBr$_2$ has been added which is above the optimum ratio for complexation observed in practice for some PEO:salt blends (i.e. EO: salt ratio of 4:1). These blends exhibit a two stage degradation. In the first stage up to approximately 280°C, products associated with the interaction between PEO and ZnBr$_2$ are observed. During this stage CRF production commences although sublimation of ZnBr$_2$ occurs at approximately 20°C higher. The second degradation stage (>280°C) is thought to arise from the decomposition of uncomplexed regions within the chain resulting in degradation products obtained for pure PEO. One significant PEO degradation product, formaldehyde is not present in the second stage degradation products. It may be that formaldehyde reacts with the salt residue at higher temperatures, to give hydrogen and carbon monoxide (increase in non-condensable products in TVA trace). Since formaldehyde is observed in the degradation of PEO blends with ZnO and CaCl$_2$ however, it is possible that the degradation mechanism for uncomplexed regions in the PEO:ZnBr$_2$ system has been modified by the preceding degradation processes induced by ZnBr$_2$. Formaldehyde, however, is known[200-202] to form condensation complexes with alkali halide salt molecules in argon at high temperature, in which a species between the halide anion and CH$_2$O is formed, having an ion-dipole interaction between the halide anion and the centre of CH$_2$O resulting in the formation of a CH$_2$XO$^-$ anion. It may be that similar CH$_2$XO$^-$ anion or ion-dipole interactions occur with ZnBr$_2$ and also ZnCl$_2$ and CoBr$_2$ as these salts sublime in the temperature region employed in TVA/SATVA experiments. This would account for the production of formaldehyde from PEO:ZnO and PEO:CaCl$_2$ blends, as neither of these salts undergo sublimation at these temperatures. However no direct evidence for such adducts or

interactions has been found.

The situation with PEO:$ZnCl_2$ appears to be more complex. The TG and DTG results suggest that the PEO:$ZnCl_2$ blends (10:1 EO:$ZnCl_2$ and 2:1 EO:$ZnCl_2$) appear to be slightly more stable than the corresponding PEO:$ZnBr_2$ blend although TVA results indicate that both 2:1 EO:salt blends have virtually identical onset and maximum rate degradation temperatures. As for $ZnBr_2$ blends, a two stage degradation mechanism for both compositions is observed. However on comparing the TVA curve for a 2:1 EO:$ZnCl_2$ blend to that for a 2:1 EO:$ZnBr_2$ blend (see Fig. 5.17 and Fig 5.9)it can be seen that the relative importance of each stage differs between the blends. In the $ZnCl_2$ blend the first decomposition stage giving rise to dioxane is minor in comparison to the second decomposition stage. The TG evidence, on the other hand, indicates a greater weight loss during the initial degradation stage. This discrepancy can however be explained by the formation of cold ring products which would cause a significant weight loss in the TG curve but which would be condensed out during TVA analysis and therefore not make any contribution to the TVA curve obtained from highly volatile degradation products. The difference between TVA curves of equivalent PEO:$ZnCl_2$ and PEO:$ZnBr_2$ blends suggests that perhaps a different mechanism is involved for the degradation of the PEO:$ZnCl_2$ blend to that proposed for PEO:$ZnBr_2$ blend. This may be reflected in the nature of the complexes formed in each case, supporting James et al[184] chelate ring model for the complexation between PPO and $ZnCl_2$ if considered to represent the

interaction between PEO and ZnCl$_2$.   In this model the coordination

of two adjacent ether oxygen atoms in the polymer back bone to the

ZnCl$_2$ could restrict the production of dioxane (formed during the

first degradation stage) whereas complexation involving two non-

adjacent oxygen atoms, as suggested for the PEO:ZnBr$_2$ system, may

readily yield dioxane upon degradation.   From the limited amount of

information on the degradation products (due to their instability)

from the PEO:ZnCl$_2$ blend, it appears that ZnCl$_2$ also destabilises

PEO towards heating and considerably alters the polymer degradation

mechanism resulting in the formation of dioxane and a reduction in

acetaldehyde production, although there are no analogous chlorinated

products to those observed in ZnBr$_2$ blends.   As zinc oxide was

produced in the residue during the degradation of PEO:ZnBr$_2$ and

PEO:ZnCl$_2$ blends, the effect of ZnO on the decomposition of PEO was

investigated.

The presence of ZnO appears to have no effect on the

degradation of PEO.   This is indicated from the onset and rate

maximum decomposition temperatures obtained by TVA as these are

vitrually identical to those for pure PEO.   In addition, a single

stage is obtained for both high (2:1 EO:ZnO) and low (10:1 EO:ZnO)

salt content blends which give an almost identical TVA curve to that

for PEO (see Fig.3.8 and Fig. 5.21).   Finally, the degradation

products on heating the blend to 500°C do not differ from those

produced from PEO.   All this evidence suggests that there is no

interaction between ZnO and PEO and therefore no complex formation.

The presence of $CoBr_2$ markably reduces the thermal stability of PEO. This is clearly seen in the TVA results (see Table 5.42) where the onset of degradation is lowered by approximately $125^{\circ}C$ relative to that for pure PEO. The TVA results also suggest that sample form does not effect the degradation process as both powder and film blends produce virtually identical degradation temperatures. Thermogravimetry results suggest that altering the salt content from 4:1 EO:$CoBr_2$ to 2:1 EO:$CoBr_2$ effects the decomposition of the blend. The lowering in the degradation temperatures is very similar to those obtained in the PEO:$ZnBr_2$ blends indicating a strong interaction between the salt and the polymer enhancing decomposition.

Pomogailo et al[203] attributes the degradation observed between heteroatom containing polymers on their complexation with transition metal chlorides ($TiCl_4$, VCl_4, $VOCl_3$ or $NbCl_5$) to radical formation as the result of partial reduction of the transition metal and to mechanical forces resulting from coordination. In $CoBr_2$ cobalt(II) is a d^7 ion and will therefore have unfilled d orbitals which can readily accept the lone pair of electrons from oxygen (polyether ligand) forming preferentially a tetrahedrally complexed structure similar to that for the $ZnBr_2$:PEO complex. The interaction of $CoBr_2$ with PEO is also reflected in the degradation products. As for $ZnBr_2$ blends, HBr, methyl bromide, ethyl bromide and dioxane are produced upon degradation.

In the PEO:CaBr$_2$ blends it is clearly seen that CaBr$_2$ has a major effect on the thermal degradation of PEO. Both TG and TVA results indicate the destabilising effect of CaBr$_2$ by the lowering of the temperature of the threshold for degradation. The TG results for 10:1 and 2:1 EO:CaBr$_2$ blends indicate 40°C lowering but TVA suggests a lowering of 100°C. At lower CaBr$_2$ content a single stage degradation is observed, but when the salt composition is raised from 10:1 EO:CaBr$_2$ to 2:1 EO:CaBr$_2$, a two stage decomposition occurs. The onset and rate maximum temperatures determined for those successive stages by the two techniques are in reasonable agreement. Furthermore, both techniques indicate that the first

decomposition stage is the dominant process taking place during degradation of the blend.

In addition to destabilising PEO, the interaction between $CaBr_2$ and PEO also causes an alteration in the degradation products evolved from the polymer, which, as observed for PEO:$ZnBr_2$ blends include traces of HBr, bromomethane and a major product, dioxane. The results obtained from SATVA product separation of the PEO:$CaBr_2$ blend indicate that during the initial stage of degradation (203° - $366^{\circ}C$) carbon dioxide, acetaldehyde and dioxane are produced but in the latter stages (>$366^{\circ}C$) although acetaldehyde formation continues, dioxane production stops. Thus similar processes to those postulated for the PEO:$ZnBr_2$ blend are occurring during the degradation of this blend. Comparison of the degradation temperatures in these two systems shows that $ZnBr_2$ has a greater destabilising effect on PEO. It is possible that this may be accounted for by $ZnBr_2$ forming a stronger complex with PEO, having a stronger chelating ability than $CaBr_2$ with PEO.

By analogy with the $ZnBr_2$ and $ZnCl_2$: PEO blends it might be expected that on comparison with the PEO:$CaBr_2$ blend, $CaCl_2$ should induce a more complex degradation process and further destabilise PEO. In fact, on degrading a PEO:$CaCl_2$ blend, it appears that $CaCl_2$ has no effect on the decomposition of PEO. Both TG and TVA results indicate a single stage degradation at low (10:1) and high (2:1) EO:salt content. The onset and rate maximum degradation temperatures obtained by each technique are virtually identical to those for pure PEO (see Table 5.42 and Table 5.43). At high $CaCl_2$

content the TG and DTG results suggest there may in fact be slight

stabilisation of the PEO.   This was also observed in the 2:1

EO:ZnO blend, and it may be that in this case the salt acts as a heat

sink removing the heat from and thus protecting PEO.

The appearance of the SATVA trace for the PEO:CaCl$_2$ blend

is very similar to that for pure PEO and the degradation products

correspond to those evolved on the decomposition of PEO.   There is

no production of dioxane, the compound indicative of the cyclisation

of PEO brought about by coordination with the salt cation, whilst

formaldehyde is produced.   Thus the thermal behaviour shown by the

PEO:CaCl$_2$ and PEO:CaBr$_2$ system is not analogous to that of the PEO:

ZnCl$_2$ and PEO:ZnBr$_2$ system in which substituting the bromide anion for

chloride enhances the interaction between PEO in the zinc salts.   Using

calcium salts, when the bromide ion is replaced by chloride no

interaction between salt and PEO occurs.

From the results obtained on the degradation of PEO:NaBr blends,

it can be seen that NaBr does not alter the decomposition of PEO upon

heating.   TVA and TG indicate that degradation of the blend occurs

in a single stage at both low (10:1) and high (2:1) salt content

(EO:salt molar composition).   The onset and rate maximum degradation

temperatures are very similar to those obtained by each technique for

PEO.   The lack of any brominated degradation products and in

particular the absence of dioxane support the conclusion that NaBr

does not participate in the degradation of PEO although complexation

between the polymer and NaBr has been reported.   All of the

degradation products identified as arising from the blend were

produced upon the thermal decomposition of pure PEO.

In contrast to NaBr, NaSCN has a pronounced effect on the thermal degradation of PEO. Both TG and TVA results indicate that at low (10:1) and high (2:1) salt content a single stage decomposition occurs. TG data suggests slight destabilisation of PEO where the concentration of EO:NaSCN is 10:1 but at higher NaSCN content, 2:1, stabilisation in PEO is observed (see Table 5.43). The degradation temperatures obtained for 2:1 EO:NaSCN blend by TVA however do not illustrate the stabilising effect and in fact show PEO to be slightly destabilised.

The SATVA trace, also demonstrates that NaSCN alters the decomposition of PEO with the formation of H_2S, HCN and trace amounts of ethyl cyanide in addition to degradation products associated with pure PEO including acetaldehyde amongst others.

The presence of $LiClO_4$ has a considerable effect on the degradation of PEO. TG and TVA results show a lowering of both onset and maximum rate decomposition temperatures. The destabilisation of PEO is more pronounced in the blend with higher level of $LiClO_4$ (2:1 EO:$LiClO_4$). In addition, the high salt content blend displays a two stage degradation process in contrast to the single stage decomposition of the 10:1 EO:$LiClO_4$ blend and pure PEO. The second degradation stage commencing at 380°C and reaching a maximum at 418°C may indicate that after the first decomposition

stage, a stable PEO intermediate is formed.

The SATVA trace for the PEO:LiClO$_4$ blend however, was similar to that for pristine PEO, as were the identifiable degradation products. Thus from the variety of products evolved it would appear that a more complex process was occurring between PEO in the presence of LiClO$_4$ than when in dilute benzene solution with butyl lithium where PEO undergoes rapid cleavage via a β-elimination mechanism at ambient temperature to form hydroxyl terminated polyethers.[204]

5.4 CONCLUSION

It has been shown by TVA, SATVA and TG techniques that the thermal degradation of PEO can be greatly effected by certain transition metal, alkaline earth and alkali metal salts. In general, the onset and rate maximum temperatures of degradation for PEO are lowered (in some cases by approximately $125^{\circ}C$ and $120^{\circ}C$ respectively) and decomposition products are formed which are not associated with the pure polymer, in the presence of the above salts. These observations are similar to those noticed by McNeill and McGuiness on investigating the effect of $ZnBr_2$ on the thermal degradation of PVA [196] and PMMA [195] and Liggat [38] studying the effect of several transition metal salts on the thermal decomposition of PMMA. Also, the concentration of salt added can modify the decomposition process in that at high salt content (EO:salt 2:1 or 4:1), a two stage degradation is observed in contrast to the single stage decomposition of low salt content blends (EO:salt 10:1) and pure PEO.

The results indicate that $ZnBr_2$, $ZnCl_2$, $CoBr_2$, $CaBr_2$, NaSCN and $LiClO_4$ thermally destabilise PEO whereas ZnO and $NaBr_2$ appear to have no effect on either the temperature of mechanism of decomposition. $CaCl_2$ on the other hand, may have a slight thermal stabilising effect on the polymer.

It is proposed that as a result of complexation between ether oxygen atoms and the cations of the following salts - $ZnBr_2$, $CoBr_2$ and $CaBr_2$, the decomposition mechanism of PEO is altered resulting in the production of dioxane. With $ZnCl_2$ blends, a more complex process occurs which is difficult to interpret due to the instability of the degradation products. The difference in decomposition behaviour of PEO:$ZnCl_2$ blends to the previously mentioned blends is attributed

to a difference in complex structure between PEO:ZnCl$_2$ and PEO:ZnBr$_2$. In the case where the salt added has no effect on the degradation of PEO i.e. ZnO and CaCl$_2$ it is either assumed that a complex does not form (which may be dependent on the counter anion) or suggested that the complex dissociates prior to decomposition of PEO resulting in the production of degradation products associated with pure PEO.

CHAPTER 6 : CONCLUSIONS

6.1 CONCLUSIONS

Chlorination of poly(ethylene oxide), PEO, initiated by UV irradiation, may be carried out in either air or in an atmosphere of nitrogen to yield polymers, in the form of white powders, which have a chlorine content corresponding to a di-substituted (62.78%Cl) or tri-substituted (72.16%) EO unit. The di-substituted polymer appears to contain a mixture of $-CH_2-CCl_2O-$ and $-CHCl-CHClO-$ structural units rather than a uniform $-CH_2-CCl_2O-$ repeat structure. Chlorination thermally destabilises PEO as the onset and maximum rate degradation temperatures (as determined by TVA) are lowered from $310^{O}C$ and $374^{O}C$ respectively in PEO to approximately $192^{O}-217^{O}$ and $266^{O}-271^{O}C$ in CPEO. The thermal degradation of PEO is initiated via random main chain scission, yielding a range of decomposition products, including carbon dioxide, ketene, formaldehyde, acetaldehyde, methoxyacetaldehyde, ethoxyacetaldehyde, diethyl ether, ethanol and alkyl terminated oligomeric chain fragments (CRF). Vinyl degradation products may also be produced such as ethyl vinyl ether, divinyl ether and vinyl oxyacetaldehyde. The thermal degradation of chlorinated PEO, CPEO, following initiation via C-Cl scission, occurs in a random single stage fashion as for PEO. This process results in a number of decomposition products including carbon monoxide, carbon dioxide, phosgene, HCl and a major amount of acid chloride and carbonyl terminated CRF. Mono-, di- and trichloroacetyl chloride are formed in preference to their aldehydic analogue.

In the case of chlorine-containing polystyrenes the position of chlorine within the styrene repeat units has a profound effect

on the degradation behaviour of the polymer.   Consequently the method of synthesis of polystyrenes with ring chlorine substituents has a fundamental effect on the decomposition mechanism.   Ring chlorinated PS (RCPS) is thermally less stable than PS.   This is attributed, however, to a small amount of chain-chlorination which accompanies ring-substitution and introduces weak sites.   RCPS exhibits a two stage degradation.   The first of these processes is due to dehydrochlorination of the polymer backbone and is followed by the major depolymerisation and transfer reactions which are also observed during the thermal decomposition of PS.   The production of 30% by weight monomer (p-,o-chlorostyrene and styrene) is comparable with that produced from PS and illustrates the simularity to PS degradation in the latter stages of degradation of RCPS.   Poly-p-chlorostyrene (PpCS) and poly-o-chlorostyrene (PoCS), in which chlorination is exclusively in the ring, have thermal properties resembling PS.   The major decomposition process involved is depolymerisation.   Fewer transfer reactions leading to chain fragmentation and CRF production take place than in PS as only approximately 15% CRF is evolved during degradation.   The reduction of transfer reactions is a result of the formation of more stable terminal radicals due to the inductive effect of chlorine enhancing reasonance stabilisation.   Furthermore, chlorine provides steric hindrance thereby impeding chain transfer.   In the thermal degradation of PoCS, a small amount of HCl is produced.   The mechanism proposed for this involves elimination of HCl followed by hydrogen rearrangement.   Chain-chlorination of PS may be carried out readily in solution in an evacuated system to give polymers with chlorine contents approximating to a mono-, di- and trichlorinated

styrene unit. Chain-chlorination thermally destabilises PS. In contrast to the single decomposition process observed in poly(chlorostyrenes), mono-chain-chlorinated PS (CCPS) displays a two stage degradation. The first stage is due to dehydrochlorination along the polymer backbone and the second (which cannot be readily distinguished from the preceding stage in more highly chlorinated polymers) is accounted for by chain fragmentation. Chain-chlorination of PS increases the weight % residue remaining after degradation. This is more pronounced in the trichlorinated polymer and may serve to reduce smoke production on combustion. In highly chlorinated CCPS, large quantities of HCl are produced on decomposition. It is proposed that following the elimination of HCl from the polymer backbone, dehydrochlorination continues via a cyclisation reaction involving chlorine and phenyl side groups on the polyene backbone. This second dehydrochlorination is favoured as it restores aromaticity.

The presence of $ZnBr_2$ whether to a lesser (10:1 EO:$ZnBr_2$) or greater (2:1 EO:$ZnBr_2$) extent has a pronounced effect on the thermal degradation of PEO. The thermal stability of PEO is lowered in the blend by roughly 100°C which implies a strong interaction between PEO and salt. A two stage decomposition occurs in the blend, which is more pronounced at high salt concentrations. In addition, the mechanism of decomposition of PEO is dramatically altered in PEO:$ZnBr_2$ blends with a multi-stage degradation process occurring and the formation of additional decomposition products. The major new degradation product is dioxane, with traces of brominated compounds HBr,

ethyl bromide and bromoethane also produced.   Furthermore, product distribution changes during the various stages in PEO-$ZnBr_2$ blend degradation.   Initial decomposition products include acetaldehyde, dioxane and carbon dioxide.   During the second degradation stage (above $280^{\circ}C$) the production of dioxane ceases.   In the final stage of decomposition acetaldehyde continues to be produced together with chain fragments of low volatility. It is proposed that the production of dioxane may arise from a cyclisation reaction in the polymer chain brought about by the coordination of Zn^{2+} with two non-adjacent oxygen atoms.   At high salt content the blend clearly shows a two stage degradation. The first stage is a result of the decomposition of PEO-$ZnBr_2$ complex and the second stage due to degradation of uncomplexed PEO.   PEO-$ZnCl_2$ blends while showing a two stage decomposition have a more complex thermal behaviour than PEO-$ZnBr_2$ blends. The major TVA peak associated with dioxane formation in PEO-$ZnBr_2$ blends is virtually absent in PEO-$ZnCl_2$ blends.   In addition, the degradation products are much less stable in PEO-$ZnCl_2$ blends. The differences observed between the two blends are attributed to a difference in complex formation with Zn^{2+} coordinating between two adjacent ether oxygen atoms in PEO-$ZnCl_2$ blends and coordinating between two non-adjacent ether oxygen atoms in PEO-$ZnBr_2$ blends. In contrast, ZnO has no effect on the thermal degradation of PEO. $CoBr_2$, however, markedly reduces the thermal stability of PEO and the blends have degradation characteristics similar to that for PEO-$ZnBr_2$ blends.   With PEO-$CaBr_2$ blends the decomposition processes are similar to those in PEO-$ZnBr_2$ blends.   Possibly due to a weaker interaction between PEO and $CaBr_2$, however, $CaBr_2$

does not destabilise PEO as much as $ZnBr_2$ does.   As with ZnO, NaBr has no effect on the thermal degradation of PEO.   In contrast to the destabilising effects of some of the other salts studied, $CaCl_2$ may have a slight stabilising influence on PEO.   NaSCN on the other hand thermally destabilises PEO.   A single stage degradation is observed at high salt content which results in the formation of additional decomposition products including H_2S, HCN and trace amounts of ethyl cyanide plus those products associated with degradation of pure PEO. $LiClO_4$ also thermally destabilises PEO.   This is more evident in high salt content blends which also show a two stage degradation.   The decomposition products identified however, are as for pure PEO.

The major observations and conclusions outlined above are summarised in Table 6.1.

POLYMER SYSTEM	DEGRADATION TYPE	DEGRADATION T(max) BY TVA (°C)	MAJOR DEGRADATION PRODUCTS	DEGRADATION MECHANISM
PEO	single stage	374	formaldehyde acetaldehyde chain fragments	random chain scission
CPEO	single stage	266-271	HCl Mono-, di- trichloroacetyl chloride	HCl elimination random chain scission
PS	single stage	400	styrene chain fragments	depolymerisation
RCPS	two stage	320, 380	chlorostyrene, chain fragments, HCl	depolymerisation HCl elimination
PoCS	single stage	405	o-chlorostyrene chain fragments	depolymerisation
PpCS	single stage	400	p-chlorostyrene chain fragments	depolymerisation
CCPS	two stage	274, 303	HCl, chain fragments residual char	HCl elimination cyclisation
PEO-ZnBr$_2$,	two stage*	252, 316	dioxane	cyclisation
CoBr$_2$, CaBr$_2$		257, 300; 339	acetaldehyde	random chain scission

POLYMER SYSTEM	DEGRADATION TYPE	DEGRADATION T(max) BY TVA (°C)	MAJOR DEGRADATION PRODUCTS	DEGRADATION MECHANISM
PEO-ZnCl$_2$	two stage *	254, 322	chain fragments	random chain scission
PEO-NaSCN	single stage	343	H$_2$S, HCN	random chain scission
PEO-LiClO$_4$	two stage *	321, 418	formaldehyde acetaldehyde chain fragments	random chain scission
PEO-ZnO, CaCl$_2$	single stage	373 380	formaldehyde acetaldehyde chain fragments	random chain scission
PEO-NaBr	single stage	378	formaldehyde acetaldehyde chain fragments	random chain scission

* at high salt content blends i.e. 2:1 EO:Salt

Table 6.1   Thermal Degradation Characteristics of PEO, CPEO, PS, chlorine-containing PS and PEO-salt blends.

6.2 FUTURE WORK

Several interesting features have come to light on the thermal degradation of the chlorine-containing polymers and PEO-salt blends investigated.   However, due to time limitations, they have not been fully explored.

Further experiments on the detection and then identification of chlorinated aldehydes produced on the thermal degradation of CPEO could be carried out.   This could be done using GC-MS on oxime derivatives of chlorinated aldehydes.   It may be of profitable interest to compare the thermal decomposition of CPEO with that of the polymers of mono-, di- and trichloroacetyl aldehyde as they would have a regular repeating structural unit.

In the chlorinated PS systems, the conductivity of partially degraded CCPS samples at various stages of degradation could be investigated.   However, from initial experiments, these systems appear not to be inherently conductive and would require doping, for example, with iodine.

In the PEO-salt blends, it may be feasible to gain further information on the degradation products from PEO-ZnCl$_2$ blends if the products were bled directly from the TVA-SATVA line into the VG Micromass QX200 quadropole mass spectrometer.   In addition much work is required to determine the structure of the complexes formed between PEO and the various salts studied in this investigation. Analytical techniques used for this purpose include several spectroscopic methods (IR, Raman) and X-ray crystallography.

REFERENCES

1.   H.R. ALLCOCK and F.W. LAMPE, "Contemporary Polymer Chemistry", Prentice-Hall, Inc., New Jersey, 1981.

2.   K.J. SAUNDERS, "Organic Polymer Chemistry", Chapman and Hall, London, 1973.

3.   N. GRASSIE and G. SCOTT, "Polymer Degradation and Stabilisation", Cambridge University Press, Cambridge, 1985.

4.   N. GRASSIE and H.W. MELVILLE, Proc. Roy. Soc., 1949, A199, 1, 14, 24.

5.   T. KELEN, "Polymer Degradation", Van Nostrand Reinhold Company Inc., 1983.

6.   F. CHEVASSUS and R.DE BROUTELLES, "The Stabilisation of Poly(vinyl chloride)", Arnold, London, 1963.

7.   "Degradation and Stabilisation of PVC", E.D. Owen (ed.) Elsevier, London, 1984.

8.   N. GRASSIE in "Developments in Polymer Degradation-1", p. 137, N. GRASSIE (ed.) Applied Science, London, 1977.

9.   D.H. GRANT and N. GRASSIE, Polymer, 1960, 1, 445.

10.   N. GRASSIE, Trans. Farad. Soc., 1952, 48, 379.

11.   I.C. McNEILL in "Developments in Polymer Degradation-1" p. 171, N. GRASSIE (ed.), Applied Science, London, 1977.

12.   D.H. RICHARDS and D.A. SALTER, Polymer, 1967, 8, 127.

13.   L.P. BLANCHARD, V. HORNHOF, HONG-LA LAM and S.L. MALHORTA, Eur. Polym. J., 1974, 10, 1057.

14.   B. DODSON and I.C. McNEILL, J. Polym. Sci., A-1, 1976, 14, 353.

15.   A. JAMIESON and I.C. McNEILL, ibid. 603.

16.   N. GRASSIE, A. JAMIESON, I.C. McNEILL, J.N.R. SAMSON and T. STRAITON, J. Macromol. Sci., 1978, A12 (4), 503.

17.   A. JAMIESON and I.C. McNEILL, J. Polym. Sci., A-1, 1974, 12, 387.

18.   R.F. BENDER and D. BRAUN, Eur. Polym. J. Suppl., A-1 1969, 5, 269.

19.   B. DODSON, I.C. McNEILL and T. STRAITON, J. Polym. Sci., A-1, 1974, 12, 2369.

20.   I.C. McNEILL and D. NEIL, Eur. Polym. J., 1970, 6, 143.

21.   I.C. McNEILL and D. NEIL, ibid, 569.

22.   A. JAMIESON and I.C. McNEIL, J. Polym. Sci., A-1, 1976, 14, 1839.

23.   J.N.R. SAMSON, Ph.D. Thesis, University of Glasgow, 1975.

24.   D.W. VAN KREVELEN, Polymer, 1975, 16, 617.

25.   C.F. CULLIS and M.M. HIRSCHLER, Eur. Polym. J., 1982, 20, 53.

26.   R.A. DIPERT, M.J. DREWS and R.G. GANN in "Encyclopedia of Polymer Science and Engineering", 2nd Edit., 7, p. 185;   N.M. BIKALES, H.F. MARK, G. MENGES and C.G. OVERBERGER (eds)., Wiley-Interscience, U.S.A. 1985.

27.   G.L. DRAKE, Jr., in "Encyclopedia of Chemical Technology", 3rd edit., 10, p. 363;   H.F. MARK, D.F. OTHMER, C.G. OVERBERGER and G.T. SEABORG (eds.) Wiley-Interscience, U.S.A., 1978.

28.   N. GRASSIE and M. ZULFIQAR in "Developments in Polymer Stabilisation - 1", p. 197, G. SCOTT (ed.) Applied Science, London, 1979.

29.   N. GRASSIE and G.A.P. MENDOZA, Polym. Deg. Stab., 1985, 11, 145.

30.   N. GRASSIE and G.A.P. MENDOZA, ibid, 359.

31.   G. CAMINO, N. GRASSIE and I.C. McNEILL, J. Polym. Sci., Polym. Chem. Ed., 1978, 16, 95.

32.   C.F. CULLIS and M.M. HIRSCHLER in "The Combustion of Organic Polymers", p. 243, Clarendon Press, Oxford, 1981.

33.   L.S. KOCHNEVA, Yu.D. SEMCHIKOV, L.M. TERMAN and G.A. RAZUVAEV, Vysokomol. Soedin., Ser. B., 1973, 15 (6), 404.

34.   N.A. KOPLOVA, L.S. KOCHNEVA, Yu. D. SEMCHIKOV, L.M. TERMAN and A.V. RYABOV, Tr. Khim. Khim. Tekhnol., 1973, 1, 110.

35. A. JAMIESON, Ph.D. Thesis, University of Glasgow, 1972.

36. A. JAMIESON and I.C. McNEILL, J. Polym. Sci., Polym. Chem. Ed., 1978, 16, 2225.

37. R.C. McGUINESS, Ph.D. Thesis, University of Glasgow, 1977.

38. J.J. LIGGAT, Ph.D. Thesis, University of Glasgow, 1987.

39. I.C. McNEILL in "Comprehensive Polymer Science", 6, p. 474, 1989.

40. F. TÜDŐS, B. IVÀN, T. KELEN and J.P. KENNEDY, Dev. Polym. Deg., 1985, 6, 147.

41. M.M. HIRSCHLER, Eur. Polym. J., 1986, 22, 153.

42. I.C. McNEILL, Eur. Polym. J., 1967, 3, 409.

43. D.L. GARDNER and I.C. McNEILL, J. Thermal. Anal., 1969, 1, 389.

44. T. KELEN, Pure. Appl. Chem., 1974, 38, 201.

45. R.P. LATTIMER and W.J. KROENKE, J. Appl. Polym. Sci., 1980, 25, 101.

46. K.S. MINSKER, R.B. PANCHESHINKOVA and G.E. ZAIKOV, Polym. Deg. Stab., 1978, 19, 1 and references therein.

47. W.H. STARNES, Jr., Polym. Mater. Sci. Eng., 1988, 58, 220.

48. L. DEAN, Z. DAFEI and Z. DEREN, Polym. Deg. Stab., 1988, 22, 31.

49. E.J. ARLMAN, J. Polym. Sci., 1954, 12, 547.

50. C.H. BAMFORD and D.F. FENTON, Polymer, 1969, 10, 63.

51. S.A. LIEBMAN, D.H. AHLSTROM, E.J. QUINN, A.G. GEIGLEY and J.T. MELUSKEY, J. Polym. Sci., A-1, 1971, 9, 1921.

52. L.A. CHANDLER and M.M. HIRSCHLER, Eur. Polym. J., 1987, 23, 677.

53. G.M. BURNETT and R.A. HALDEN, Eur. Polym. J., 1967, 3, 449.

54. G.F. BLOOMFIELD, J. Chem. Soc., 1943, 289.

55. B. DODSON and I.C. McNEILL, J. Polym. Sci., Polym. Chem. Ed., 1974, 12, 2305.

56. H.E. PARKER in "Treatise on Coatings", R.R. MYERS and R.S. LONG (eds.) Dekker, New York, 1967.

57. D.L. GARDNER and I.C. McNEILL, Eur. Polym. J., 1971, 7, 569.

58. D.L. GARDNER and I.C. McNEILL, ibid, 593.

59. D.L. GARDNER and I.C. McNEILL, ibid, 603.

60. Y. MIYATA and M. ATSUMI, J. Polym. Sci., Part A: Polym. Chem. Ed., 1988, 26, 2561.

61. K.S. MINSKER, AL.AL. BERLIN, R.B. PANCHESHNIKOVA and E.D. ANTONOVA, Vysokomolek, Soed., 1987, 29B, 171.

62. D. JAROSZYNSKA, T. KLEPS and D.GDOWSKA-TUTAK, J. Thermal. Anal., 1980, 19, 69.

63. G. CAMINO and L. COSTA, Polym. Deg. Stab., 1980, 2, 23.

64. G. CAMINO and L. COSTA, Polym. Deg. Stab., 1985, 12, 117.

65. G. CAMINO and L. COSTA, ibid, 125.

66. P. BERTICAT, J. Chim. Phys., 1967, 64, 892.

67. M. OKAMOTO, R. YAMADA and O. ISHIZUKA, Bull. Chem. Soc. Jpn., 1981, 54, 1227.

68. N. GRASSIE and R. McGUCHAN, Eur. Polym. J., 1973, 9, 507.

69. V.L. RAO, P.K. DHAL, G.N. BABU and J.C.W. CHIEN, Polym. Deg. Stab., 1987, 18, 19.

70. N. GRASSIE, A. JOHNSON and A. SCOTNEY, Eur. Polym. J., 1981, 17, 589.

71. M.A. DIAB, A.Z. EL-SONBATI and A. EL-DISSOUKY, Eur. Polym. J., 1989, 5, 431.

72. J. DAY and W.W. WRIGHT, Br. Polym. J., 1977, 9, 66.

73. G. IVAN, M. GLURGINCA, R. PITICESCU and E. TAVARU, Mater. Plast. (Bucharest), 1986, 23 (4), 207.

74. P. KUBISA, L.S. CORLEY and O. VOGL, J. Macromol. Sci-Chem., A, 1980, 14 (8), 1145.

75. W. KERN and H. CHERDRON, Makromol. Chem., 1960, 40, 101.

76. D.J. KEMMISH, RAPRA Review Reports, 1989, 2, 2.

77. C.H. KLINE, Chemistry and Industry, 1989, No. 14, 440.

78. C.H. KLINE, Chemistry and Industry, 1989, No. 15, 483.

79. G. DAVID, ibid, 487.

80. J. HELLER, Biomaterials, 1980, _1_, 51.

81. G. SCOTT, J. Polym. Sci., Symp. No. 57, 1976, 357.

82. T.M. KELLER, J. Polym. Sci., A, 1987, _25_ (19), 2569.

83. E. FITZER and M. HEYM, Chem. Ind. 1976, _21_, 663.

84. W. WATT, Carbon, 1972, _10_, 121.

85. H. ASHITAKA, Y. KUSUKI, S. YAMAMOTO, Y. OGATA and
     A. NAGASAKA, J. Appl. Polym. Sci., 1984, _29_, 2763.

86. I.C. McNEILL, J. Polym. Sci., A-1, 1966, _4_, 2479.

87. I.C. McNEILL, Eur. Polym. J., 1967, _3_, 409.

88. I.C. McNEILL and D. NEIL in "Thermal Analysis", p. 353,
     R.F. SCHWENKER and P.D. GARN (eds.), Academic Press, New
     York, 1969.

89. I.C. McNEILL in "Thermal Analysis", p. 417, R.F. SCHWENKER,
     and P.D. GARN (eds.), Academic Press, New York, 1969.

90. I.C. McNEILL, Eur. Polym. J., 1970, _6_, 373.

91. I.C. McNEILL, L. ACKERMAN, S.N. GUPTA, M. ZULFIQAR and
     S. ZULFIQAR, J. Polym. Sci., Polym. Chem. Ed., 1977,
     _15_, 2381.

92. L. ACKERMAN and W.J. McGILL, J.S. Afr. Chem. Inst., 1973,
     _26_, 82.

93. W.J. McGILL, L. PAYNE and J. FOURIE, J. Appl. Polym. Sci.,
     1978, _22_, 2669.

94. W.J. McGILL in "Developments in Polymer Degradation-5",
     p.1, N. GRASSIE (ed.) Applied Science, London, 1984.

95. M.I. POPE and M.D. JUDD, "Differential Thermal Analysis",
     Heyden, London, 1977.

96. D. WELTI, "Infrared Vapour Spectra", Heyden, London 1970.

97. R.H. PIERSON, A.N. FLETCHER and E. ST. CLAIR GANTZ,
     Anal. Chem., 1956, _28_, 1218.

98. "The Aldrich Library of Infrared Spectra", C.J. POUCHERT
     (ed.), Aldrich Chemical Co., Milwaukee, 1981.

99. "The Sadtler Handbook of Infrared Spectra", W.W. SIMONS
     (ed.), Sadtler-Heyden, London, 1978.

100. R.A. NYQUIST and R.O. KAGEL, "Infrared Spectra of Inorganic
     Compounds (3800-45cm^{-1})", Academic Press, New York, 1971.

101.   R.E. ARDREY, C. BROWN, A.R. ALLAN, T.S. BAL and A.C.
        MOFFAT, "An Eight Peak Index of Mass Spectra of
        Compounds of Forensic Interest", Scottish Academic
        Press, Edinburgh, 1983.

102.   "Atlas of Spectral Data and Physical Constants for
        Organic Compounds", J.G. GRASSELLI and W.M. RITCHEY
        (eds.) CRC Press, Ohio. 1975.

103.   N. LINTON and P. MATLOCK in "Encyclopedia of Polymer
        Science and Engineering", 2nd edit., 6, p. 225, N.M.
        BIKALES, H.F. MARK, G. MENGES and C.G. OVERBERGER (eds.)
        Wiley-Interscience, U.S.A., 1985.

104.   S.L. MADORSKY and S. STRAUSS, J. Polym. Sci., 1959,
        36, 183.

105.   E. BORTEL, S. HODOROWICZ and R. LAMONT, Makromol. Chem.,
        1979, 180, 2491.

106.   N. GRASSIE and G.A.P. MENDOZA, Polym. Deg. Stab., 1984,
        9, 155.

107.   "CRC Handbook of Chemistry and Physics", 69th edit.,
        1988-1989, R.C. WEAST (ed.), CRC Press, Inc., Florida,
        1988.

108.   J.A. BORNMANN, J. Polym. Sci., Part C: Polym. Lett.,
        1988, 26 (9), 409.

109.   A. ORZESKO and A. KOLBRECKI, J. Appl. Polym. Sci.,
        1980, 25, 2969.

110.   K. SHIMIZU, Y. MASAOKA and M. TAKAOKA, Patent, Ger.
        Offen. DE 3,412,703 (U.CO8L71/02), Chem. Abstr.,
        1985, 102, P47540.

111.   T. KAGIYA, N. YOKOYAMA and K. TAKEMOTO, Bull. Inst.
        Chem. Res., Kyoto Univ., 1976, 54 (1), 15.

112.   R.J. LAGOW and S. INOUE, U.S. Patent Appl. No.597937.

113.   R.J. LAGOW and S. INOUE, U.S. Patent 4,113,772 (1978).

114.   G.E. GERHARDT and R.J. LAGOW, J. Org. Chem., 1978,
        43 (23), 4505.

115.   R.J. LAGOW and G.E. GERHARDT, U.S. Patent 4,523,039
        (1985).

116. "Dictionary of Organic Compounds", 4th edit., vol. 2, p. 592, 956, 589, J.R.A. POLLOCK and R. STEVENS (eds.) Eyre and Spottiswoode Ltd., London, 1965.

116a. "The Aldrich Catalogue Handbook of Fine Chemicals", p. 321, 488, 1459, United Kingdom, 1988-1989.

117. S. PASARI and S. CHANDRA, Pop. Plast., 1979, 24 (1) 15.

118. G.B. BECKMANN, H. HELLMAN, K.R. ROBINSON, R.W. FINHOLT, E.J. KAHLER, L.J. FINLAR, L.V. HEISEY, L.L. LEWIS and D.D.MICUCCI, J. Org. Chem., 1947, 12, 108.

119. Ph. TEYSSIÉ, M.C. DeWILDE and G. SMETS, J. Polym. Sci., 1955, 16, 429.

120. T. OKUMOTO and T. TAKEUCHI, Makromol. Chem., 1973, 167, 305.

121. M.M. GUSEIVNOV and M.S. SALAKHOV, Plast. Massy., 1982, 1, 9.

122. H. WATANABE, Eur. Patent Appl. EP 73,947 (1983), (Chem. Abstr., 1983, 99, P38974C).

123. R.K. JENKINS, N.R. BYRD and J.L. LISTER, J. Appl. Polym. Sci., 1968, 12, 2059.

124. S. TSUAGE, H. ITO and T. TAKEUCHI, Bull. Chem. Soc., Jpn, 1970, 43, 3341.

125. I.C. McNEILL and M. ĆOŞKUN, Polym. Deg. Stab., 1987, 17, 347.

126. I.C. McNEILL and M. ĆOŞKUN, Polym. Deg. Stab., 1987, 18, 213.

127. K. WINTERSBERGER, F. MEYER and H.E. KNOBLOCH, BASF, Ger. Patent 1,169,122 (1964), (Chem. Abstr., 1964, 61, 2027C).

128. G. MAURA, Chim. Ind. (Milan), 1978, 60, 643.

129. R. GRUNDMAN, Chemische Werke Huels A.-G., Ger. Patent 2,800,013 (1979), (C.A. 91:92280W (1979)).

130. J. KIJI, H. KONISHI, T. OKANO, S. SUGINO and A. IWASA, Makromol. Chem. Rapid Commun., 1985, 6, 49.

131. J. KIJI, H. KONISHI, T. OKANO and E. AJIKI, Appl. Macromol. Chem. and Phys., 1987, 149, 187.

132. G.G. CAMERON and J.R. MacCALLUM, J. Macromol. Sci., 1967, C1, 327.

133.   G.G. CAMERON and G.P. KERR, Eur. Polym. J., 1968
        4, 709.

134.   G.G. CAMERON and G.P. KERR, Eur. Polym. J., 1970,
        6, 423.

135.   G.C. CAMERON, Makromol Chem., 1967, 100, 255.

136.   G.G. CAMERON, J.M. MAYER and I.T. McWALTER,
        Macromolecules, 1978, 11, 696.

137.   I.C. McNEILL and W.T.K. STEVENSON, Polym. Deg. Stab.,
        1985, 10, 247.

138.   A.M. CAMPBELL, B.Sc. Thesis, University of Glasgow,
        1987.

139.   I.C. McNEILL and M. ĆOŞKUN, Polym. Deg. Stab., 1989,
        23, 175.

140.   R.J. KERN, J. Polym. Sci., A-1, 1969, 7, 621.

141.   I.C. McNEILL and M. ĆOŞKUN, Polym. Deg. Stab.,
        1989, 25, 1.

142.   A. BALLISTRERI, S. FOTI, G. MONTAUDO and E. SCAMPORRINO,
        J. Polym. Sci., Polym. Sci. Ed., 1980, 18, 1147.

143.   T.E. HOGEN-ESCH and J. SMID, J. Am. Chem. Soc., 1965,
        87, 669.

144.   J. SMID in "Ions and Ion Pairs in Organic Reactions",
        vol. 1, p. 85, M. SZWARC (ed.), Wiley-Interscience,
        London, 1972.

145.   C.J. PEDERSEN, J. Am. Chem. Soc., 1967, 89, 2495, 7017.

146.   J.M. LEHN, J.P. SAUVAGE and B. DIETRICH, J. Am. Chem.
        Soc., 1970, 92, 2916.

147.   J.M. LEHN, Structure and Bonding (Berlin), 1973, 16, 1.

148.   P.A. LAURENT and E. ARSENIO, Bull. Soc. Chim. France,
        1958, 618.

149.   P.J. HENDRA and D.B. POWELL, J. Chem. Soc., 1960, 4,
        5105.

150.   A.A. BLUMBERG, S.S. POLLACK and C.A.J. HOEVE, J. Polym.
        Sci., A-2, 1964, 2, 2499.

151.   P.E. FENTON, J.M. PARKER and P.V. WRIGHT, Polymer, 1973,
        14, 589.

152.   P.V. WRIGHT, Br. Polym. J., 1975, 7, 319.

153.   B.L. PAPKE, M.A. RATNER and D.F. SHRIVER, J. Phys. Chem. Solids, 1981, 42, 493.

154.   M.B. ARMAND, J.M. CHABAGNO and M.J. DUCLOT, 2nd International Meeting on Solid Electrolytes, St. Andrews, Scotland, 20-22nd Sept., 1978, Extended Abstract, 6.5.

155.   M.B. ARMAND, J.M. CHABAGNO and M.J. DUCLOT in "Fast Ion Transport in Solids", p. 131, P. VASHISTA, N.J. MUNDY and G.K. SHENOY (eds.), Elsevier, North-Holland, New York, 1979.

156.   M.B. ARMAND, M.J. DUCLOT and P. RIGAUD, 3rd International Meeting on Solid Electrolytes-Solid State Ionics and Galvanic Cells, Tokyo, Japan, 15-19th Sept., 1980, Abstract C116.

157.   J.R. OWEN, J. DRENNON, G.E. LAGOS, P.C. SPURDENS and B.C.H. STEELE, Solid State Ionics, 1981, 5, 343.

158.   B. SCROSATI in "Polymer Electrolyte Reviews-1", p. 315, J.R. MacCALLUM and C.A. VINCENT (eds.), Elsevier Applied Science, 1987.

159.   J.R. MacCALLUM, Solid State Ionics, 1984, 11, 307.

160.   M.B. ARMAND, Solid State Ionics, Lake Tahoe, Aug., 1985, Extended Abstract, SSI85.

161.   M.D. GLASSE, R.J. LATHAM, R.G. LINFORD and A.J. PATRICK, Brit. UK. Patent Appl. GB 2,157,066 (1986), (Chem. Abstr., 1986, 104, 158150Z).

162.   L.L. YANG, R. HUQ, G.C. FARRINGTON, G. CHIADELLI and A.R. McGHIE, Solid State Ionics, 1986, 18/19, 291.

163.   A. MORYOUSSET, M. BONNAT, M. FOULETIER and P. HICTER, Transp. Struct. Relat. Fast Ion Mixed Cond., Proc. Risoe Int. Symp. Metall. Mater. Sci., 6th, 1985, 335.

164.   T.M.A. ABRANTES, L.J. ALCACER and C.A.C. SEQUERIA, Solid State Ionics, 1986, 18/19, 315.

165.   V. GUTMANN in "The Donor Acceptor Approach to Molecular Interactions", Plenum Press, New York, 1978.

166.   A.I. SHOTENSHTEIN, E.S. PETROV and A.E. YOKOVLEVA, J. Polym. Sci., 1968, C16, 1799.

167. M.B. ARMAND in "Polymer Electrolyte Reviews-1", p.1, J.R. MacCALLUM and C.A. VINCENT (eds.), Elsevier Applied Science, 1987.

168. N.C. BILLINGHAM, P.D. CALVERT and A.S. MANKE, J. Appl. Polym. Sci., 1981, 26, 3543.

169. "Carbanions, Living Polymers and Electron Transfer Processes", M. SZWARC (ed.), Interscience, New York, 1968.

170. H. DAOUST and B. CLOUTIER, Macromol. Chem. Macromol. Symp., 1988, 20/21, 211.

171. A.E. BEKTUROV, S.E. KUDAIBERGENOV and V. Zh. USHANOV, Vysokonol. Soedin., Ser. A., 1987, 29 (1), 169.

172. F. QUINA, L. SEPULVEDA, R. SARTORI, E.B. ABUIN, C.G. PINO, E.A. LISSI, Macromolecules, 1985, 19, 980.

173. Y. MARCUS, J. Solution Chem., 1988, 15, 291.

174. Y. TAKAHASHI and H. TAKADORO, Macromolecules, 1973, 6, 672.

175. F.E. BAILEY, Jr., J.W. KOLESKA, "Poly(ethylene oxide)", Academic Press, New York, 1976.

176. T. HIMBA, Solid State Ionics, 1983, 9/10, 1101.

177. J.M. PARKER, P.V. WRIGHT and C.C. LEE, Polymer, 1981, 22, 1305.

178. M. YOKOYAMA, H. ISHIHARA, R. IWAMOTO and H. TADOKORO, Macromolecules, 1969, 2, 184.

179. H.J. BUSCHMANN, Makromol. Chem., 1986, 187, 423.

180. H. TADOKORO, T. YOSHIHARA, Y. CHATANI, S. TAHARA and S. MURAHASHI, Makromol. Chem., 1964, 73, 109.

181. R. IWAMOTO, Y. SAITO, H. ISHIHARA and H. TADOKORO, J. Polym. Sci., A-2, 1968, 6, 1509.

182. M. YOKOYAMA, H. ISHIHARA, R. IWAMOTO and H. TADOKORO, Macromolecules, 1969, 2(2), 184.

183. B.L. PAPKE, M.A. RATNER and D.F. SHRIVER, J. Electrochem. Soc., 1982, 129 (7), 1434.

184. D.B. JAMES, R.E. WETTON and D.S. BROWN, Polymer, 1979, 20, 187.

185. I.M. PANAYOTOV, CH.B. TSVETANOV, I.V. BERLIONOVA and R.S. VELICHKOVA, Makromol. Chem., 1970, 134, 313.

186.   C. BERTHIER, W. GORECKI MINIER, M.B. ARMAND, J.M.
        CHABAGNO and P. RIGAUD, Solid State Ionics, 1983,
        11, 91.

187.   R. NEAT, M.D. GLASSE, R.G. LINFORD and A. HOOPER,
        Solid State Ionics, 1986, 18/19, 1088.

188.   C.C. LEE and P.V. WRIGHT, Polymer, 1978, 19, 234.

189.   C. MARCO and J.M. PERENA, An. Quim. Ser. A., 1981,
        77 (2), 247.

190.   M. STAINER, L. CHARLES HARDY, D.H. WHITMORE and D.F.
        SHRIVER, J. Electrochem. Soc., 1984, 131 (4), 784.

191.   L.L. YANG, A.R. McGHIE and G.C. FARRINGTON, J.
        Electrochem. Soc., 1986, 133 (7), 1380.

192.   C. ROBAITAILLE, S. MARQUES, D. BOILS and J. PRUD'HOMME,
        Macromolecules, 1987, 20, 3023.

193.   V.G. SHIBALOVICH, M.V. VINOGRADOV, V.M. BODERENKO and
        A.F. NIKOLAEV, Izv. Vyssh. Uchebn. Zaved., Khim. Khim.
        Tekhnol., 1982, 25 (7), 882.

194.   G.G. CAMERON, M.D. INGRAM, M.Y. QURESHI, H.M. GEARING,
        L. COSTA and G. CAMINO, Eur. Polym. J., 1989, 25 (7/8),
        779.

195.   I.C. McNEILL and R.C. McGUINESS, Polym. Deg. Stab., 1984,
        9, 209.

196.   I.C. McNEILL and R.C. McGUINESS, Polym. Deg. Stab., 1983,
        5, 303.

197.   D.D. PERRIN, W.L.F. ARMAREGO and D.R. PERRIN, "Purification
        of Laboratory Chemicals", 2nd edit., p. 320, Pergamon
        Press, Oxford, 1980.

198.   L. BREWER, Paper No. 7 in "Chemistry of Miscellaneous
        Materials", L.L. QUILL (ed.), McGraw-Hill, New York,
        1950.

199.   B.I. KHORUNZHII, K.G. IL'IN, Izv. Vyssh. Ucheb. Zaved.,
        Khim. Khim. Tekhnol., 1972, 15 (2), 174.

200.   S.B.H. BACH and B.S. AULT, Inorg. Chem., 1984, 23^3 (25),
        4394.

201.   B.S. AULT and L. ANDREWS, Inorg. Chem., 1977, 16^2 (8),
        2024.

202.   B.S. AULT, Inorg. Chem., 1983, 22^2(15), 2221.

203.   A.D. POMOGAILO, A.I. KAZAELI and F.S.D'YACHKOVSKII,
        Dokl. Akad. Nauk. SSSR, 1981, 256 (1), 132.

204.   E.J. VANDENBERG, J. Polym. Sci., Polym. Chem. Ed.,
        1972, 10, 288.